MICROFUNGI ASSOCIATED WITH FOREST PLANTS WITH EMPHASIS ON *THYMELAEACEAE*

XIA TANG

DOCTOR OF PHILOSOPHY

IN

BIOLOGICAL SCIENCE

SCHOOL OF SCIENCE

MAE FAH LUANG UNIVERSITY

2025

MICROFUNGI ASSOCIATED WITH FOREST PLANTS WITH EMPHASIS ON *THYMELAEACEAE*

XIA TANG

THIS DISSERTATION IS A PARTIAL FULFILLMENT OF
THE REQUIREMENTS FOR THE DEGREE OF
DOCTOR OF PHILOSOPHY
IN
BIOLOGICAL SCIENCE

SCHOOL OF SCIENCE
MAE FAH LUANG UNIVERSITY
2025

DISSERTATION APPROVAL

MAE FAH LUANG UNIVERSITY

FOR

DOCTOR OF PHILOSOPHY IN BIOLOGICAL SCIENCE

Dissertation Title: Microfungi Associated with Forest Plants with Emphasis on *Thymelaeaceae*

Author: Xia Tang

Examination Committee:

Associate Professor Rajesh Jeewon, Ph. D.	Chairperson
Adjunct Professor Kevin David Hyde, Ph. D.	Member
Assistant Professor Mahamarakkalage Mary Ruvishika Shehali Jayawardena, Ph. D.	Member
Professor Jichuan Kang, Ph. D.	Member
Chitrabhanu Sharma Bhunjun, Ph. D.	Member
Dan-Feng Bao, Ph. D.	Member

Advisors:

.....Advisor

(Adjunct Professor Kevin David Hyde, Ph. D.)

.....Co-Advisor

(Assistant Professor Mahamarakkalage Mary Ruvishika Shehali Jayawardena, Ph. D.)

.....Co-Advisor

(Professor Jichuan Kang, Ph. D.)

Dean:

.....

(Professor Surat Laphookhieo, Ph. D.)

ACKNOWLEDGEMENTS

In the winter of 2018, I came to Thailand to pursue my studies and embarked on my doctoral journey. In the blink of an eye, seven years have passed. Throughout these years, I have been fortunate to meet many kind and caring people who offered selfless help in both my studies and daily life. Without your support, I can hardly imagine having made it to where I am today. Looking back on the road I have traveled the bewilderment of arriving in a foreign land, uncertainty about my research topic, lack of confidence in experiments, difficulty adjusting to life, even fear of the future and of writing, and frustration with my own clumsiness, these feelings once overwhelmed me. Yet stronger than all of that was the steady care and lift I received from those around me: my advisor's unwavering support and patient guidance, friends' encouragement and companionship, and the efficient assistance of the faculty and laboratory staff—from procuring reagents and maintaining instruments to reminding us of proposal milestones and helping with submissions. They took care of almost all the preparatory work that should have been done by us, solely so we could study with peace of mind and enjoy a comfortable learning environment. Every small act has come together to form the backdrop of these seven years. How fortunate I am to have joined the warm family of Centre of Excellence in Fungal Research, working side by side with everyone as we strive, learn, and move toward our goals. In my PhD research, scholarly outcomes are certainly important; but for personally, you (my colleagues, adivisor and staff at Centre of Excellence in Fungal Research and the teachers and friends at Guizhou University) are an invaluable treasure on my life's journey. Thank you for everything you have done for me; I will remember it and remain deeply grateful.

First and foremost, I would like to express my heartfelt gratitude to my main advisor, Professor Kevin D. Hyde, for giving me the opportunity to pursue a PhD and for leading me into the world of fungal taxonomy, helping me appreciate these tiny yet vital companions in our daily lives. Your rigor, wealth of experience, and professional, patient guidance will benefit me for a lifetime. I still remember the first seminar when I first joined this family of Centre of Excellence in Fungal Research and you gave a talk, that is about research. There is one thing gave me a deep memory. You made a

comment, academically, we need to “think outside the box”. At the time I was rather bewildered, I felt I understood, yet not quite. With the times goes, I gradually realized that the “box” does not refer only to the problems we meet in research; it is everywhere and can be any situation or thing. We often become so entangled that solutions elude us, but once we step outside the problem, clarity dawns and the knot unravel. Your words were a revelation to me, shaping my approach and giving me the ability to solve problems independently in the years that followed. Thank you for this lifelong treasure.

I would like to express my sincere gratitude to my external supervisor, Professor Ji-chuan Kang, for unwavering support and guidance throughout my doctoral studies. Professor Kang’s breadth of expertise and generous mentorship have been indispensable to my research and training. His advice, both academic and personal, helped me navigate challenges inside and outside the laboratory. By sharing learning experiences and experimental insights, he enabled me to avoid many mistakes and learn invaluable lessons. The meticulous work ethic and rigorous, truth-seeking attitude he exemplifies are models I will continue to learn from.

My heartfelt thanks go to my co-advisor, Dr. Mahamarakkalage Mary Ruvishika Shehali Jayawardena, for unwavering support and generous help throughout my doctoral studies. Whenever I faced difficulties, you stood behind me with patience and guidance, never once absent. Like an elder sister, you looked after our well-being, offering comfort and encouragement. From my first days in the program, you taught me laboratory skills from the ground up and carefully revised my first manuscript. With your support, I was able to complete my PhD successfully.

I wish to express my sincere gratitude to my committee chair, Dr. Rajesh Jeewon. Meeting you has been one of the greatest fortunes of my doctoral journey. Your selfless support and good-humored instruction have benefited me immensely. Whenever I felt lost or overwhelmed, you reassured me, “Don’t worry, I will help you”, which encouraged me and renewed my confidence. Thank you for guiding me with both kindness and rigor.

I would like to express my sincere gratitude to my undergraduate teacher, Prof. Yongzhong Lu. Thanks to your recommendation, I was able to join this outstanding academic community for further study. Your humble character and academic attitude

have deeply influenced me. When I was confused about learning methods, you patiently guided me and taught me to construct a system and get out of difficulties. I always remember what you said: "Completing is more important than perfection." This sentence enlightened me and made me stop obsessing over imagined perfection and unnecessary entanglements. Instead, I keep polishing and continuously improving after completion. Your teachings will benefit me for a lifetime.

My heartfelt thanks to my committee members, Dr. Danfeng Bao and Dr. Chitrabhanu Sharma Bhunjun, for joining my defense and for your generous support and guidance. Your feedback significantly improved this dissertation.

I would like to thank Dr. Chuan-Gen Lin, Dr. Jian ma, Dr. Sheng-Nan Zhang, Dr. Junfu Li, Dr. Na Wu, Dr. Xiang-Yu Zeng, Dr. Ning-Guo Liu, Dr. Shaun Pennycook, Dr. Yuan-Pin Xiao, Dr. Hong-Wei Shen, Dr. Rong-Ju Xu, Dr. Xing-Guo Tian, Dr. Jing Yang, Dr. Xing-Yu Zhu, Dr. Fa Zhang, Dr. Ya-Ru Sun, Dr. Hong-Bo Jiang, Dr. Yu-Wei Hu, Dr. Qing Tian, Dr. Jing-Yi Zhang, Dr. Li Lu, Dr. Li-Juang Zhang, Dr. Xiang-Fu Liu, Dr. Ying-Ru Xiong, Dr. Tian-Ye Du, Dr. Ying Gao, Dr. Yu Yang for their assistance with comments on my papers and topic. My special thanks go to Sean for the meticulous review of the Latin nomenclature in this wor, which greatly improved the rigor and consistency of the new taxon names. I am deeply grateful to my classmates. Throughout this journey, we worked hard and learned together; meeting you has been one of the great fortunes of my doctoral life, and you have truly enriched it. My special thanks go to Xue-Mei Chen, Xing-Can Peng, Meng-Lan Chen, Jian-Kang Wang, Yong-Xin Shu, Yan-Yan Yang, Hai-Jun Zhao, Shu-Cheng He, Hong-Li Su, Yun-Hui Yang, Xing-Juan Xiao, Hua Li and so on who stepped forward without hesitation whenever I needed help. I wish you all the very best in the years ahead. I am also grateful to the staff at the Center of Excellence in Fungal Research, Mae Fah Luang University, Guizhou institute of technology and Guizhou University. My special thanks go to P'Pooh and P'Bank for their assistance with university paperwork, and to P'Wi for accompanying me during the collection of coffee samples. I remain deeply appreciative of your help and support.

I am grateful to Mae Fah Luang University for a Thesis Writing Grant and for awarding me a tuition scholarship for my Ph.D. studies in Thailand. I also acknowledge

support from the National Natural Science Foundation of China (NSFC; Grant Nos. 32170019, 31670027, and 31460011); the Open Fund of the Engineering Research Center of Southwest Bio-Pharmaceutical Resources, Ministry of Education, Guizhou University (Grant No. GZUKEY20160702); and the Thailand Research Fund (TRF) grant “Impact of climate change on fungal diversity and biogeography in the Greater Mekong Sub-region” (RDG6130001).

Finally, I am deeply grateful to my family. To my parents, thank you for your unconditional support and for comforting and encouraging me whenever I felt lost. I also thank my younger brother, who has always helped in every way he could. My heartfelt thanks as well to my long-time friend Qian Lu; since we met in 2013, we have been through so much together, and your comfort and support in difficult times have only deepened our friendship. May it endure.

Xia Tang

Dissertation Title	Microfungi Associated with Forest Plants with Emphasis on *Thymelaeaceae*
Author	Xia Tang
Degree	Doctor of Philosophy (Biological Science)
Advisor	Adjunct Professor Kevin David Hyde, Ph. D.
Co-Advisor	Assistant Professor Mahamarakkalage Mary Ruvishika Shehali Jayawardena, Ph. D. Jichuan Kang, Ph. D.

ABSTRACT

Forests are among the most important terrestrial ecosystems on Earth. Composed of trees, soils, microorganisms, animals, and fungi, they form a complex network of energy flow, matter cycling, and multi-scale biotic interactions. Forests fix carbon dioxide, release oxygen, conserve water, stabilize soils, and provide habitat for countless organisms; they also underpin climate regulation, raw-material supply, and cultural and social values for human societies. Forest plants directly serve human needs by supplying timber, medicinal resources, food, and fibers, while vegetation delivers essential ecosystem services, such as air purification, climate regulation, and water retention, that indirectly support social stability and sustainable development.

Against this backdrop, to better understand the relationships between forest plants and fungi, we conducted systematic sampling and analyses targeting saprobic fungi in forest environments and fungi associated with the *Thymelaeaceae*, Sampling covered Guizhou, Hainan, Guangxi, and Yunnan in China, as well as parts of northern Thailand. In total, 706 pure-culture isolates were obtained: 557 endophytic isolates from *Thymelaeaceae*, recovered from diverse tissues (flowers, fruits, roots, stems, and leaves); and 72 saprobic isolates from forest environments, mainly from bamboo, *Dipterocarpaceae*, *Thymelaeaceae*, and unidentified decayed wood. The endophytic isolates belong to 6 classes, 20 orders, 38 families, and 53 genera, spanning six host tissue types. The saprobic isolates are distributed across 33 genera, 19 families, 6 orders, and 3 classes.

In addition, I compiled a checklist documenting the fungal diversity associated with *Thymelaeaceae* in China. The checklist enumerates 117 fungal records, including host (*Thymelaeaceae* genera/species), geographic distribution, updated taxonomic treatments, and references. Through morphological characterization and multi-locus phylogenetic analyses, we provide detailed descriptions, illustration plates, distribution and sampling information, and resolve their taxonomic placements. Collectively, these efforts establish a traceable, comparable, and searchable baseline framework for fungal resources in forest ecosystems, especially lineages associated with *Thymelaeaceae*, and provide standardized data to support subsequent ecological, systematic, and applied research.

Keywords: 72 Saprobic Collections, 31 New Species, 4 New Genera, 557 Endophytic Collection, *Thymelaeaceae* Fungal Checklist, Phylogeny, Taxonomy

TABLE OF CONTENTS

TABLE OF CONTENTS

LIST OF TABLES

LIST OF FIGURES

LIST OF FIGURES

LIST OF FIGURES

LIST OF FIGURES

LIST OF FIGURES

CHAPTER 1

INTRODUCTION

1.1 Definitions and Ecological Value of Forest Plants and *Thymelaeaceae*

Forests are plant communities dominated by trees that account for a considerable proportion of the Earth's biological variation (Hansen, 2013), accounting for 75% of the biosphere's gross primary output and 80% of plant biomass (van der Kamp, 1991). There are hundreds of various definitions of forest, many of which have varied meanings based on where they are planted and how they are managed (Schuck et al., 2002, https://www.cbd.int/forest/definitions.shtml). According to the Food and Agriculture Organization of the United Nations (FAO), a forest is defined as follows: “Trees taller than 5 meters and with a canopy cover of more than 10%, or trees capable of achieving these thresholds in situ, on ground larger than 0.5 hectares in size. It does not include area principally utilized for agricultural or urban development” (FAO, 2023).

As one of the largest terrestrial biological carbon reservoirs and a long-term carbon sink, forest ecosystems contribute to the Earth system and human well-being in five major ways: (1) Climate regulation and carbon sequestration: Forests assimilate CO_2 via photosynthesis and store carbon in vegetation, litter, and soil organic carbon pools; their biophysical effects, evapotranspiration, surface roughness, and albedo, also regulate regional energy and moisture budgets (Bonan, 2008). Syntheses of global inventories and long-term observations indicate that, from 1990 to 2007, forests absorbed 2.4 ± 0.4 Pg C yr^{-1}, making them one of the most important and persistent land carbon sinks (Pan et al., 2011). (2) Hydrological and soil processes: Canopy interception and root-zone infiltration enhance water retention, attenuate flood peaks, and reduce sediment loads; forests also promote soil aggregation and organic matter accumulation, sustaining soil fertility and water quality. Coupling among forests, water, and surface energy is pivotal for regional cooling and precipitation redistribution (Ellison et al., 2017). (3) Biodiversity and ecosystem functioning: Forests form the core

habitat network for terrestrial biodiversity, and global plot-level evidence shows a positive, system-stabilizing relationship between tree species diversity and productivity (Liang et al., 2016). (4) Disaster risk reduction and human well-being: Coastal forests (e.g., mangroves) substantially attenuate wind waves and reduce flood risk from tens of meters to kilometer scales, yielding demonstrable risk-reduction and economic benefits; forests also provide recreational, aesthetic, and cultural values essential to human well-being (Menéndez et al., 2020; IPBES, 2019). (5) Biogeochemical coupling: Forests integrate the C–N–P–S and trace-element cycles and, through vegetation, soil, atmosphere interactions, shape surface energy and material flows, functioning as the backbone of terrestrial ecosystem processes (Bonan, 2008).

Moreover, many forest plants also possess substantial economic value. They contribute to timber/fibers, fragrances and resins, medicinal and functional compounds, ornamental horticulture, and culture and local livelihoods, and in many countries underpin sizeable non-timber forest product (NTFP) sectors and employment. Authoritative sources emphasize that, although NTFPs are often undercounted, their roles in livelihoods and value chains are significant (FAO, 2017, 2023; Shackleton, 2024). Within these groups, the *Thymelaeaceae* are especially illustrative: agarwood (from *Aquilaria* and *Gyrinops*) is a high-value aromatic resin with international trade subject to CITES regulation (CITES, 2022; Lai et al., 2025). *Thymelaeaceae* Antoine Laurent de is important nontimber forest products (NTFPs) to provide NTFPs and timber for the forest community in Southeast Asia, some species in Europe, and parts of South America (Heywood, 1996; Lemmens et al., 1998; Oyen & Dung, 1999). It is a family of flowering plants in the order of *Malvales*, containing 50 genera (Turjaman et al., 2006; Kristanti et al., 2018). *Thymelaeaceae* is mostly trees and shrubs, with a few vines and herbaceous plants, some genera are cultivated for their hardwood. The bark of these trees can be used as raw material for papermaking, and their odorous can be highly resinous wood (agarwood) that is used for incense and perfume production (Turjaman et al., 2006; Kristanti et al., 2018). In addition, many highly diverse secondary metabolites with a wide range of biological activities were found on *Thymelaeaceae* species and numerous applications of extracts in traditional medicine (Kristanti et al., 2018). The bast-fiber species such as *Daphne bholua* and *D. papyracea* provide the primary raw material for Nepal's traditional Lokta handmade paper and

support mountain household industries (Sharma et al., 2017; Aryal et al., 2022); *Edgeworthia chrysantha* (mitsumata) has long been cultivated for washi and as a banknote base paper fiber (MOFA Japan, 2023); additionally, *Daphne* and related genera have well-documented medicinal uses and bioactive constituents supported by modern pharmacological reviews (Moshiashvili et al., 2020; Han et al., 2020). *Aquilaria* species are well-known for it being used extensively as NTFPs and used in the manufacture of incense, perfume, traditional medicine, and other commercial products by Asian Buddhists and Muslims (Turjaman et al., 2006). Agarwood is formed in the heartwood of *Aquilaria* trees, used in the production of agar oil from its infected wood, it is utilized in the pharmaceutical and perfumery industry (Chhipa & Kaushik, 2017). Agarwood is the important raw material of incense, perfumes, drugs, stimulants, cardiac tonics, and carminatives (He et al., 2005), it is widely used in the pharmaceutical industry in many countries such as sedative, analgesic or digestive in Japan; treat injuries such as fractures and bruises with Agarwood leaves in China and as to treatment of cough, asthma, and as a sedative among others in Korea (Kim et al., 1997; Yagura et al., 2003; Zhou et al., 2008).

Fungi are pivotal and ambivalent biological agents in forests. On the one hand, mycorrhizal fungi (including arbuscular (AM), ectomycorrhizal (EcM), and ericoid (ErM) types) expand the root absorptive front and mobilize otherwise inaccessible nutrients, thereby enhancing plant uptake of nitrogen and phosphorus and promoting growth (van der Heijden et al., 2015; Smith & Read, 2008). Endophytic fungi can further improve host stress tolerance by modulating hormones and antioxidant defenses under drought, heat, or salinity (Rodriguez et al., 2009). In addition, extensive fungal hyphae and extracellular polymers help build and stabilize soil aggregates, improving water retention and resistance to erosion (Rillig & Mummey, 2006). On the other hand, fungi can also limit forest growth: host-specific pathogens often increase seedling mortality near conspecific adults and at high conspecific density, generating conspecific negative density dependence (CNDD) that suppresses dominance (Comita et al., 2014); in some EcM-dominated systems, competitive interactions between EcM and saprotrophs can slow litter decomposition and nutrient mineralization, the so-called Gadgil effect, thereby constraining nutrient availability (Fernandez & Kennedy, 2016); moreover, mutualism entails a carbon cost to the host, and under low light or nutrient-

rich conditions the cost–benefit balance can shift toward reduced growth (Johnson et al., 1997).

There are numerous studies indicate a close link between microfungi and agarwood formation. In the resin-producing genera *Aquilaria* and *Gyrinops*, agarwood typically arises via a "wounding → microbial entry → host defense reprogramming" cascade. Mechanical injury provides infection courts for microfungi (commonly *Xylaria*, *Lasiodiplodia*, *Colletotrichum*, *Fusarium*); together with wound cues, infection activates jasmonate-linked defenses and redirects secondary metabolism toward sesquiterpenes and 2-(2-phenylethyl) chromones that accumulate as resinous heartwood. Controlled experiments show that fungal inoculation can trigger agarwood, but efficacy varies markedly with strain, host, environment, and induction method; alternative models also demonstrate that trauma alone or chemical cues can suffice. Thus, fungal infection is best regarded as a common and potent, yet non-exclusive, driver of agarwood formation (Xu et al., 2013; Rasool & Mohamed, 2016; Chhipa et al., 2017; Ngadiran et al., 2023; Fu et al., 2024; Du et al., 2025).

This study is based on both morphology and molecular systematics to investigate the diversity and distribution of microfungi associated with forest plants with emphasis on the family *Thymelaeaceae*. We invested saprobic fungi in forest habitats, saprobes occurring on *Thymelaeaceae*, as well as endophytic and pathogenic fungi. The fungal taxa are delimited and identified by using a combination of morphological characters and DNA evidence, and we provide illustrated plates and detailed descriptions to facilitate future comparative, ecological, and systematic work.

1.2 A Review of Fungi Associated with Forest Plants and *Thymelaeaceae*

Microfungi perform diverse ecological functions in forest ecosystems, including nutrient cycling, food provisioning, promotion of tree growth, and maintenance of soil health, in both native and production forests. They form mycorrhizal associations with vascular plants, cause economically important tree diseases, decompose coarse organic matter (coarse woody debris and litter), and serve as wildlife food resources (Marcot, 2017). Numerous studies have examined the ecology of microfungi in forest litter and documented

many distinct taxa (Subramanian & Vittal, 1974; Rambelli et al., 1983, 1984, 1991; Mercado-Sierra 1984; Bills & Polishook, 1994; Lodge & Cantrell, 1995a, 1995b; Matsushima, 1971, 1975, 1980, 1981, 1996; Polishook et al., 1996; Lodge, 1997; Calduch et al., 2002). Among these contributions, several reported new fungal taxa (Castañeda-Ruiz et al., 1999; Pasqualetti & Rambelli, 1999; Siboe et al., 1999; Calduch et al., 2002), while other investigations addressed possible specialization among saprotrophs (Pirozynski, 1972; Subramanian & Vittal, 1979, 1980; Læssøe & Lodge, 1994; Lodge & Cantrell, 1995a, 1995b; Lodge & Læssøe, 1995; Mulas et al., 1995; Polishook et al., 1996; Lodge, 1997; Pascholati et al., 2001).

Based on the available publications, the earliest record of microfungi associated with forest plants can be traced back to 1729, Micheli (1729) provided systematic descriptions of fungi on substrates such as wood and leaf surfaces. However, for endophytes can be back to 1809, Link (1809) was the first to describe the fungal bodies within plants (later known as “endophytes”) (Hardoim et al., 2015). subsequently, de Bary (1866) formalized the term formalized “endophytes” (Adeleke et al., 2021; Collinge et al., 2022). Frank (1885) introduced the concept of mycorrhiza and demonstrated its prevalence in forest woody plants, thereby laying the modern foundation for research on forest plant-fungus interactions (Frank, 2005).

The association between microfungi and *Thymelaeaceae* plants is firstly report at 1929, when Tunstall explicitly associated fungi with *Aquilaria* and isolated fungi from agarwood, establishing the conceptual basis for fungal induction; this early report has been repeatedly acknowledged by later authors (Gibson, 1977; Liu et al., 2013; Du et al., 2022a, 2022b; Shivanand et al., 2022; Falcon, 2025). Bhattacharyya et al. (1952) explicitly proposed in their study on *Aquilaria agallocha* that microorganisms in the wood were related to the formation of agarwood, which is regarded as an early milestone in the association between "endophytic/wood microorganisms and fragrance production. Subsequent work expanded rapidly: controlled inoculations demonstrated that several genera, such as, *Xylaria*, *Lasiodiplodia* (*L. theobromae*), *Colletotrichum* (*C. gloeosporioides*), *Fusarium* (*F. solani*). Beyond *Aquilaria*, reports on other thymelaeaceous hosts have accumulated: Kim et al. (2005) documented the first occurrence of *Fusarium oxysporum* wilt on *Daphne odora*, and Noshad et al. (2006) reported

Thielaviopsis basicola (current name *Berkeleyomyces*) causing root rot on *D. cneorum*, both first records on these hosts.

To date, a large number of microfungi have been recorded from forest plants (including *Thymelaeaceae* plants), but most of these records are still weak in taxonomic evidence: only a few taxonomic groups have been supported by multi-gene locus phylogenetic analysis, and many remain at the level of pure morphological identification. Moreover, many studies only provide the total number of associated species without verified identification details. Saprophytic and endophytes fungi from these hosts are particularly under-sampled. Meanwhile, relevant information is scattered in regional journals, grey literature, and herbarium entries, and some species lack clear collection location information. As the number of reported species and records increases, systematic integration becomes increasingly difficult. Therefore, it is necessary to carry out targeted re-sampling and systematic organization: supplement standardized molecular data (such as multi-gene sequences) for existing records lacking molecular evidence to clarify their taxonomic status; standardize and complete voucher and geographic information; and compile ecological and pathogenic data under a unified framework. These efforts will provide a solid and reusable foundation for subsequent diversity assessment, phylogenetic, and ecological research.

1.3 Research Objectives

1.3.1 To study the systematics of microfungi (endophytes, pathogens and saprobes) associated with Thymelaeaceae in terms of morphology and multi-gene phylogenies.

1.3.2 To study the systematics of saprobic fungi associated with forest plants in terms of morphology and multi-gene phylogenies.

1.3.3 To provide a checklist of microfungi associated with *Thymelaeaceae* including new host records from all over the world.

1.3.4 To obtain sequence data, construct phylogenetic trees to accurately identify the microfungi.

1.3.5 To provide the identification and supplementation of species that lack

molecular sequences but have morphological characteristics.

1.4 Expected Outcome

1.4.1 To identify and describe novel/known fungal taxa associated with forest plants and *Thymelaeaceae* from China and Thailand based on morphology and multigene phylogeny.

1.4.2 To contribute to tropical fungal diversity with new genera, new species and new records.

1.4.3 To provide an updated checklist of fungi associated with *Thymelaeaceae* worldwide.

1.5 Thesis Outline

1.5.1 A diversity analyses of saprobes associated with forest plants.

1.5.2 Novel species, host/geological records of saprobes associated with forest plants and *Thymelaeacea* from China and Thailand.

1.5.3 Identify *Thymelaeacea*-associated endophytic fungi based on morphology and multigene phylogeny.

1.5.4 A checklist of fungi associated with *Thymelaeacea* in China.

1.6 Research Contents

This study focuses on saprophytic fungi in forest ecosystems and their saprophytic and endophytic diversity on plants of the *Thymelaeaceae*. We combined morphological and molecular systematics methods to identify several fungi, and the results included potential new species, new national/local records of known species, and new habitats. For each taxonomic unit, we provided detailed morphological descriptions, phylogenetic analyses, and compiled a global checklist of microfungi associated with *Thymelaeaceae* plants. The full text consists of six chapters, systematically presenting the research ideas, methods, and main findings.

Chapter 1 mainly provides the general research background, summarizes the basic situation of forest and the *Thymelaeaceae* family, systematically reviews the fungal diversity related to forests and the *Thymelaeaceae* family as reported in previous literature, and discusses the ecological roles and potential application values of these fungi for forest plants and *Thymelaeaceae* plants.

Chapter 2 provides the technical route and methodological framework we employed throughout the entire research process for sample separation, identification, and analysis, including material collection and processing, pure culture and morphological observation, DNA extraction and multi-gene locus amplification sequencing, phylogenetic analysis and species definition procedures.

Chapter 3 Provided the taxonomy and phylogeny of saprobic microfungi related to forests plants collected from China and Thailand, based on the morphological and phylogenetic analysis. The description and illustration of each species are provided here.

Chapter 4 This chapter summarizes the information on endophytic and saproobic fungi on plants of the *Thymelaeaceae*, and provides taxonomic analysis and comparison features based on morphological and molecular evidence. We also provide a fungal checklist of *Thymelaeaceae* plants in China.

Chapter 5 This chapter describes two new genera and one new species of fungi associated with *Dipterocarpaceae* in Thailand, providing detailed illustrations, morphological descriptions, and a phylogenetic tree.

Chapter 6 This chapter provides the overall conclusions of the study, highlights the principal contributions, outlines our methodological and contextual advantages, and discusses future directions. We also list the publications arising from this work.

CHAPTER 2

RESEARCH METHODOLOGY

2.1 Collection, Examination, Isolation, and Deposition of Specimens

2.1.1 Isolation of Endophytes and Pathogens

Symptomatic and healthy fresh specimen tissues (such as leaves, fruits, twigs, roots) will be collected. The collecting sited will be selected in China (mainly from the tropic area of China) and Thailand, during all the seasons of the year. The fresh sample will be taken to the lab by using clean plastic bags and labelled. The sample was kept in the bags with each one host. The surface sterilization technique of endophytes and pathogens mainly followed by Photita et al. (2001) and Zakaria and Aziz (2018). The endophytes were isolated and tested followed by Arnold et al. (2000). The surface sterilization of material will be done by two methods. The first is specializing in twigs and roots. Each material will be taken from the parts that need to be isolated, washed with running tap water, and surface sterilized to eliminate epiphytic microorganisms on a benchtop by dipping in 75% (v/v) ethanol for 3 min, then rinse with sterilized distilled water for 2 min, then in NaClO solution (final concentration of 5% aqueous sodium hypochlorite) for 2 min, and rinse with sterile distilled water three times continuously (Urooj et al., 2018). The second one is for the material of buds, flowers, and leaves. Each material will be washed with running tap water, and surface-sterilized by sequential washes in 0.525% sodium hypochlorite (2 min) and 70% ethanol (2 min), and then rinsed with sterile, distilled water and allowed to surface-dry under sterile conditions. (Schulz et al., 1993; Arnold et al., 2000). Finally, the materials are dried on a new sterilized filter paper and then cut into small cubes (<5 mm2), and placed on fresh potato dextrose agar (PDA) containing antibiotic (50 µg/mL penicillin), five cubes from the same materials were placed in each PDA dish. Samples are incubated in a constant temperature incubator (26°C) for two days until fungi develop. The whole process is completed on the clean bench. Hyphal tips were transferred to fresh PDA plates using a sterilized needle and incubated at room temperature. Asexual or sexual

morphs were checked from the cultures after 14 days using a Motic SMZ-171 Stereo Zoom Microscope. The proceed of the pathogen isolation was the same with the endophytes, but the tissues cubes are the half health and half disease part.

The plates are observed daily and mycelia from the edge of fungal colonies were transferred to fresh PDA to obtain the pure cultures. The obtained fungi will be observed whether Sporulating by using a Motic SMZ-171 Stereo Zoom Microscope. Photographs are taken by using a Nikon ECLIPSE Ni-U compound microscope connected with a Nikon camera series DSRi2. Morphological structures (conidiophores, conidiogenous cells, conidia) were measured by Image Framework software v. 0.9.7. Adobe Photoshop CC 2019 is used for editing the photographic plate. Colonies are described, based on the color charts of Rayner (1970). Living and dry sporulating cultures will be deposited in the Kunming Institute of Botany Culture Collection (KUMCC); the Guizhou Culture Collection (GZCC) and Mae Fah Luang University Culture Collection (MFLUCC) and Mae Fah Luang University Herbarium (MFLU), Chiang Rai, Thailand respectively.

2.1.2 Single Spore Isolation

Single spore isolation was performed by using the following methods of Tang et al. (2020), via sowing conidia suspension onto the surface of PDA media. Single germinating spore is transferred to clean plates under a Stereomicroscope series Motic SMZ-171 with a sterilized needle, and agar plates were incubated at room temperature. All cultures were deposited in the Kunming Institute of Botany Culture Collection (KUMCC); the Guizhou Culture Collection (GZCC) and Mae Fah Luang University Culture Collection, Chiang Rai, Thailand (MFLUCC). Type specimens and herbarium materials will be deposited in the Kunming Institute of Botany, Chinese Academy of Sciences (HKAS), located in Kunming, China; the Guizhou Academy of Agriculture Sciences (GZAAS), situated in Guiyang, China and the herbaria of Mae Fah Luang University, Chiang Rai, Thailand (MFLU). Taxonomic information of the new taxa is deposited in Index Fungorum (Index Fungorum, 2025) and Face of Fungi (https://www.facesoffungi.org/) database (Jayasiri et al., 2015).

2.2 DNA Extraction, PCR Amplification, and Sequencing

Genomic DNA is extracted from fresh mycelia, which are obtained from living cultures that are grown on a PDA petri dish for seven days at room temperature and following the manufacturer's instructions of Biomiga Fungal gDNA Isolation Kits. PCR amplification is done in 50-µl volumes consisting of 2 µl of DNA template, 2 µl of each 10 µl forward and reverse primers, 25 µl of 2 ×Taq PCR Master Mix and 19 µl of deionized water. Thermal cycling conditions are dependent on gene regions are used in the study, and some conditions of the gene regions are provided in table 2.1. PCR products are checked in 1% agarose gels and will be sent to Sangon Biotech (Shanghai) Co. Ltd, China for sequencing.

2.3 Phylogenetic Analyses

The sequences will be combined by using the Contig Express v3.0.0 application. The most similar sequences of related taxa will be found using a BLASTn search (https://blast.ncbi.nlm.nih.gov/Blast.cgi) in GenBank. The MAFFT v. 7 online versions (https://mafft.cbrc.jp/alignment/server/index.html) (Katoh et al., 2017) will be used to align individual gene sequence data by using the 'auto' option and manually improved in BioEdit v. 7.0.5.3. Multiple genes are combined by SequenceMatrix (Vaidya et al., 2011). The alignment will be trimmed using trimAl v 1.2 with the 'gappyout' option (Capella-Gutiérrez et al., 2009). Maximum-parsimony (MP), Maximum Likelihood (ML) and Bayesian Inference (BI) analyses of the combined aligned dataset will be used.

The analysis of maximum likelihood will be processed in the CIPRES web portal (Miller et al., 2010) using the "RAxML-HPC v.8 on XSEDE" tool (Stamatakis et al., 2008). Maximum parsimony analysis will be performed in the CIPRES web portal, and the "PAUP on XSEDE" tool will be used (Swofford, 2002). The heuristic search option with 1000 random taxa addition will be used to infer trees. The value of Maxtrees is set to 5000, with branches of zero length collapsed and all multiple parsimonious trees will be saved. Parsimony score values for tree length (TL), consistency index (CI), retention index (RI) and homoplasy index (HI) will be calculated for trees generated under different optimum

criteria. Bootstrap (BT) analysis of 1000 replicates, each with 100 replicates of random stepwise addition of taxa, will be used to assess the clade stability (Hillis & Bull, 1993).

The BYPP analysis will be performed using the tool “MrBayes on XSEDE” (Huelsenbeck & Ronquist, 2001; Ronquist et al., 2012) in the CIPRES online version. The best fit model of each gene region will be selected by MrModeltest v2. The algorithm of the Markov chain of Monte Carlo (MCMC) will be started with four chains in parallel, from a random tree topology. The operation will be stopped automatically, when the average standard deviation of split frequencies fell below 0.01. The sampling survey of trees will be set up to every 1000th generation and burn-in is set at 25%. The posterior probability (PP) will be calculated for the remaining trees. Trees will be visualized in FigTree v. 1.4.0 and further illustrated using Adobe Illustrator v. 51.1052.0.0 (Adobe Inc., San Jose, California, USA).

2.4 Endophytes Test

2.4.1 Surface-sterilization Validation by Imprint Test

After the moisture on the surface of the sterilized tissues cubes is dried, those will be transferred into a PDA petri dish for 3-5 mins, and then will be transferred into another new PDA petri dish using a sterilized needle. The latter PDA petri dish will keep for getting pure cultures and the previous PDA petri dish will be kept for observing if it is contaminated by surface fungi of the tissue cubes. If it is contaminated, it proves that the tissue cubes have not been sterilized well, and the resulting culture is not an endophyte. Conversely, if the petri dish is not contaminated, it proves that the surface is sterilized well, and the resulting culture is the endophytic fungi (Hyde & Soytong, 2008).

2.4.2 Surface-sterilization Validation by Last-rinse Plating

After the plant tissues are sterilized, keep the last rinsing water, and use sterilized tools sowing the last rinsing water onto a clean PDA petri-dish, keep it for observing. If the PDA gets contaminated, it proves that the tissue cubes don't be sterilized well, and the resulting culture is not reliable to be an endophyte. On the contrary, the tissue cubes are sterilized well. We can confirm that the fungi are endophytic (Sun & Guo, 2012).

Table 2.1 PCR protocols

Locus	Primers (forward/reverse)	PCR amplification conditions	Cycles	Reference(s)
Internal transcribed spacer region of ribosomal DNA (ITS)	ITS5/ITS4	Initial denaturation: 94 °C – 5 min Denaturation: 94 °C – 45 sec Annealing: 52 °C – 1 min Extension: 72 °C – 90 sec Final extension: 72 °C – 10 min Hold: 4 °C – ∞	35	White et al. (1990)
28S large subunit rDNA region (LSU)	LR0R/LR5	Initial denaturation: 94 °C – 5 min Denaturation: 94 °C – 45 sec Annealing: 52 °C – 1 min Extension: 72 °C – 90 sec Final extension: 72 °C – 10 min Hold: 4 °C – ∞	35	Vilgalys and Hester (1990), Cubeta et al. (1991)
RNA polymerase II second largest subunit (*rpb2*)	fRPB2-5F/fRPB2–7cR	Initial denaturation: 94 °C – 3 min Denaturation: 94 °C – 20 sec Annealing: 56 °C – 1 min Extension: 72 °C – 90 sec Final extension: 72 °C – 10 min Hold: 4 °C – ∞	35	Liu et al. (1999)
Small Subunit ribosomal RNA (SSU)	NS1/NS4	Initial denaturation: 94 °C – 5 min Denaturation: 94 °C – 45 sec Annealing: 52 °C – 1 min Extension: 72 °C – 90 sec Final extension: 72 °C – 10 min Hold: 4 °C – ∞	35	White et al. (1990)
Translation elongation factor 1-alpha (*tef1-α*)	983F/2218R	Initial denaturation: 94 °C – 3 min Denaturation: 94 °C – 20 sec Annealing: 56 °C – 1 min Extension: 72 °C – 90 sec Final extension: 72 °C – 10 min Hold: 4 °C – ∞	35	Rehner (2005)
Translation elongation factor 1-alpha (*tef1-α*)	EF1-728F/EF1-986R	Initial denaturation: 94 °C – 3 min Denaturation: 94 °C – 20 sec Annealing: 56 °C – 1 min Extension: 72 °C – 90 sec Final extension: 72 °C – 10 min Hold: 4 °C – ∞	35	Carbone and Kohn (1999)

Table 2.1 (continued)

Locus	Primers (forward/reverse)	PCR amplification conditions	Cycles	Reference(s)
Beta-tubulin (*tub2*)	Bt2a and Bt2b	Initial denaturation: 94 °C – 3 min Denaturation: 94 °C – 20 sec Annealing: 52 °C – 1 min Extension: 72 °C – 90 sec Final extension: 72 °C – 10 min Hold: 4 °C – ∞	35	Glass and Donaldson (1995)

CHAPTER 3

MICROFUNGI ASSOCIATED WITH FOREST PLANTS

3.1 Microfungi: Unravelling New Taxa of *Sordariomycetes* Associated with Forest Plants in China and Thailand

3.1.1 Introduction

Sordariomycetes is one of the largest and most ecologically diverse classes within the *Ascomycota*. The modern placement and usage of the name were consolidated by Eriksson and Winka (1997) who proposed supraordinal taxa for *Ascomycota* and stabilized high-level concepts such as *Sordariomycetes*. This framework was widely adopted and refined in Lumbsch and Huhndorf (2009), which served as a baseline for more than a decade. In recent years, successive editions of the Outline of Fungi have updated the higher-level system based on multi-locus phylogenies, leading to increasingly fine-grained delimitation of orders, families, and genera within *Sordariomycetes* (Zhang et al., 2005; Maharachchikumbura et al., 2015; Hongsanan et al., 2017; Luo et al., 2019; Hyde et al., 2020b; Bao et al., 2023; Hyde et al., 2024).

Morphologically, members of the *Sordariomycetes* are most typically characterized by perithecial ascomata, which are usually ostiolate. The asci are generally inoperculate and unitunicate, often with a distinct apical apparatus, and the ascospores are commonly septate and pigmented. In certain freshwater or hygrophilous lineages, ascospores may bear gelatinous sheaths or appendages as ecological adaptations. Perithecia can be immersed or partially superficial, and both non-stromatic ascomata and a wide range of paraphyses- or pseudoparaphyses-like elements are observed. In a few lineages, near-cleistothecioid conditions and tendencies toward more prototunicate asci have also been reported, indicating substantial plasticity in reproductive structures within the class. These traits are consistent with prior diagnoses of perithecial ascomycetes in *Sordariomycetes* and related orders, which emphasize

ostiolate perithecia, unitunicate asci with an apical apparatus, and pigmented, often septate ascospores. (Réblová et al., 2016a; Luo et al., 2019; Hyde et al., 2024).

Sordariomycetes currently comprises approximately seven subclasses, 46 orders, and 172 families based on the publications (Hyde et al., 2024). These numbers vary slightly among sources because new orders and families continue to be described, but they consistently indicate a rapid expansion compared to the 2009 "Outline of *Ascomycota*," which provided an earlier baseline and a much smaller circumscription of higher taxa within the class. The increase is widely attributed to high-throughput sequencing, phylogenomics, and integrative taxonomy, which have revealed numerous previously unrecognized lineages and reshaped family- and order-level concepts within *Sordariomycetes*. (Lumbsch & Huhndorf, 2009; Wang et al., 2023; Hyde et al., 2024; Nguyen et al., 2024).

Representative orders within the class include *Hypocreales*, *Xylariales*, *Sordariales*, *Diaporthales*, *Glomerellales*, *Ophiostomatales*, *Microascales*, and *Magnaporthales*. These encompass functionally diverse fungal groups ranging from wood-decaying saprotrophs and latent endophytes to major plant pathogens, including lineages responsible for economically important crop diseases such as rice blast. The diversification and continual revision of these orders have been repeatedly highlighted in recent phylogenetic frameworks for *Sordariomycetes*. (Luo et al., 2019; Wang et al., 2023; Hyde et al., 2024).

Sordariomycetes occur across both terrestrial and freshwater systems. They include saprotrophic decomposers, endophytic or mutualistic colonizers of living tissues, plant pathogens, and insect-associated fungi. In freshwater habitats, members of the class are recognized as key agents of organic matter degradation, nutrient cycling, and energy transfer through detrital pathways, and they are frequently cited as prolific sources of chemically diverse and biologically active secondary metabolites. (Luo et al., 2019; El-Elimat et al., 2021). In forest ecosystems, species of Sordariomycetes play an important roles, such as, they participate in the breakdown of woody debris and litter, but they also engage in host interactions that range from asymptomatic colonization to overt pathogenicity. This class is relevant to forest health, wood quality, and disease management, and therefore has both ecological and applied importance in forestry. (Luo et al., 2019; Hyde et al., 2024).

In the present study, we combined detailed morphological observation with multi-locus phylogenetic inference (maximum likelihood and Bayesian analyses) to clarify the placement of our isolates within the *Sordariomycetes*. Based on these data, we describe one new species isolated from bamboo and two new species from unidentified decaying wood in forest habitats, named A*rthrinium bambusicola*, *Cordana guizhouensis*, and *C. liupanshuiensis*, respectively. For each taxon, we provide illustrations, diagnostic morphology, and host/substrate information. These results expand the known diversity of *Sordariomycetes* in saprotrophic niches associated with bamboo culms, decaying twigs, fallen branches, and forest-floor litter. (this study).

3.1.2 Results

3.1.2.1 Phylogenetic Analyses

I retrieved homologous sequences from NCBI GenBank using BLASTn, aligned each locus, manually inspected and trimmed the alignments, and concatenated them into a multi-locus dataset. Phylogenetic relationships were inferred using maximum likelihood and Bayesian approaches to assess the placement of our isolates. The results support the establishment of three new species within *Sordariomycetes*, *Arthrinium bambusicola*, *C. guizhouensis* and *C. liupanshuiensis*. I also provided the taxa table which use in this study.

Table 3.1 List of fungal taxa and their GenBank accession numbers of the sequences used for Arthrinium. The newly generated sequences are indicated in red bold and the type strains are indicated by "T" in superscript

Species	Strain numbers	ITS	LSU	*tub2*	*tef1-α*
Arthrinium aquaticum	S-642	MK828608	MK835806	-	-
A. arundinis	CBS 106.12	KF144883	KF144927	KF144973	KF145015
A. arundinis	CBS 114316	KF144884	KF144928	KF144974	KF145016
A. arundinis	CBS 124788	KF144885	KF144929	KF144975	KF145017
A. arundinis	CBS 133509	KF144886	KF144930	KF144976	KF145018
A. arundinis	CBS 449.92	KF144887	KF144931	KF144977	KF145019
A. aureum	CBS 244.83^{T}	AB220251	KF144935	KF144981	KF145023
A. balearicum	CBS 145129^{T}	MK014869	MK014836	MK017975	MK017946
A. bambusae	LC7106^{T}	KY494718	KY494794	KY705186	KY806204
A. bambusae	LC7124	KY494727	KY494803	KY705195	KY806206
A. bambusae	LC7125	KY494728	KY494804	KY705196	KY705124
A. bambusicola	MFLUCC 20-0144^{T}	MW173030	MW173087	-	MW183262

Table 3.1 (continued)

Species	Strain numbers	ITS	LSU	*tub2*	*tef1-α*
A. camelliaesinensis	LC5007^{T}	KY494704	KY494780	KY705173	KY705103
A. camelliaesinensis	LC8181	KY494761	KY494837	KY705229	KY705157
A. caricicola	CBS 145127	MK014871	MK014838	MK017977	MK017948
A. chinense	CFCC 53036^{T}	MK819291	-	MK818547	MK818545
A. chinense	CFCC 53037	MK819292	-	MK818548	MK818546
A. descalsii	CBS 145130^{T}	MK014870	MK014837	MK017976	MK017947
A. dichotomanthi	LC4950^{T}	KY494697	KY494773	KY705167	KY705096
A. dichotomanthi	LC8175	KY494755	KY494831	KY705223	KY705151
A. esporlense	CBS 145136^{T}	MK014878	MK014845	MK017983	MK017954
A. euphorbiae	IMI 285638b	AB220241	AB220335	AB220288	-
A. gaoyouense	CFCC 52301^{T}	MH197124	-	MH236789	MH236793
A. gaoyouense	CFCC 52302	MH197125	-	MH236790	MH236794
A. garethjonesii	KUMCC 16-0202^{T}	KY356086	KY356091	-	-
A. guizhouense	LC5318	KY494708	KY494784	KY705177	KY705107
A. guizhouense	LC5322^{T}	KY494709	KY494785	KY705178	KY705108
A. gutiae	CBS 135835^{T}	KR011352	MH877577	KR011350	KR011351
A. hispanicum	IMI 326877^{T}	AB220242	AB220336	AB220289	-
A. hydei	CBS 114990^{T}	KF144890	KF144936	KF144982	KF145024
A. hydei	KUMCC 16-0204	KY356087	KY356092	-	-
A. hyphopodii	MFLUCC 15-0003^{T}	KR069110	-	-	-
A. hyphopodii	KUMCC 16-0201	KY356088	KY356093	-	-
A. hysterinum	CBS 145132(AP15318)	MK014873	MK014840	MK017979	MK017950
A. hysterinum	CBS 145133(AP29717)	MK014875	MK014842	MK017981	MK017952
A. hysterinum	ICPM6889^{T}	MK014874	MK014841	MK017980	MK017951
A. ibericum	CBS 145137^{T}	MK014879	MK014846	MK017984	MK017955
A. italicum	CBS 145138^{T}	MK014880	MK014847	MK017985	MK017956
A. italicum	CBS 145139	MK014881	MK014848	MK017986	-
A. japonicum	IFO30500	AB220262	AB220356	AB220309	
A. japonicum	IFO 31098	AB220264	AB220358	AB220311	-
A. jatrophae	AMH-9557^{T}	JQ246355	-	-	-
A. jatrophae	AMH-9556	HE981191	-	-	-
A. jiangxiense	LC4494	KY494690	KY494766	KY705160	KY705089
A. jiangxiense	LC4577^{T}	KY494693	KY494769	KY705163	KY705092
A. kogelbergense	CBS 113332	KF144891	KF144937	KF144983	KF145025
A. kogelbergense	CBS 113333^{T}	KF144892	KF144938	KF144984	KF145026
A. kogelbergense	CBS 113335	KF144893	KF144939	KF144985	KF145027
A. kogelbergense	CBS 117206	KF144895	KF144941	KF144987	KF145029
A. locuta-pollinis	LC11689	MF939597	-	MF939624	MF939617
A. locuta-pollinis	LC11688	MF939596	-	MF939623	MF939618
A. locuta-pollinis	LC11683^{T}	MF939595	-	MF939622	MF939616

Table 3.1 (continued)

Species	Strain numbers	ITS	LSU	*tub2*	*tef1-α*
A. longistromum	MFLUCC 11-0479	KU940142	KU863130	-	-
A. longistromum	MFLUCC 11-0481^{T}	KU940141	KU863129	-	-
A. malaysianum	CBS 102053^{T}	KF144896	KF144942	KF144988	KF145030
A. marii	CBS 497.90^{T}	AB220252	KF144947	KF144993	KF145035
A. mediterranei	IMI 326875^{T}	AB220243	AB220337	AB220290	-
A. minus	AP25418	MK014872	MK014839	MK017978	MK017949
A. minus	CBS 145131	MK014872	MK014839	MK017978	MK017949
A. mytilomorphum	DAOM 214595^{T}	KY494685	-	-	-
A. neogarethjonesii	DQD 2019a^{T}	MK070897	MK070898	-	-
A. neosubglobosa	JHB006	KY356089	KY356094	-	-
A. neosubglobosa	KUMCC 16-0203^{T}	KY356090	KY356095	-	-
A. obovatum	LC4940^{T}	KY494696	KY494772	KY705166	KY705095
A. obovatum	LC8177	KY494757	KY494833	KY705225	KY705153
A. obovatum	LC8178	KY494758	KY494834	KY705226	KY705154
A. ovatum	CBS 115042^{T}	KF144903	KF144950	KF144995	KF145037
A. paraphaeospermum	MFLUCC 13-0644^{T}	KX822128	KX822124	-	-
A. phaeospermum	CBS 114314	KF144904	KF144951	KF144996	KF145038
A. phaeospermum	CBS 114315	KF144905	KF144952	KF144997	KF145039
A. phaeospermum	CBS 114317	KF144906	KF144953	KF144998	KF145040
A. phaeospermum	CBS 114318	KF144907	KF144954	KF144999	KF145041
A. phragmitis	CPC 18900^{T}	KF144909	KF144956	KF145001	KF145043
A. phyllostachium	MFLUCC 18-1101^{T}	MK351842	MH368077	MK291949	MK340918
A. piptatheri	CBS 145149^{T}	MK014893	MK014860	-	MK017969
A. pseudoparenchymaticum	LC7234^{T}	KY494743	KY494819	KY705211	KY705139
A. pseudoparenchymaticum	LC8173	KY494753	KY494829	KY705221	KY705149
A. pseudoparenchymaticum	LC8174	KY494754	KY494830	KY705222	KY705150
A. pseudosinense	CPC 21546^{T}	KF144910	KF144957	-	KF145044
A. pseudospegazzinii	CBS 102052^{T}	KF144911	KF144958	KF145002	KF145045
A. pterospermum	CBS 123185	KF144912	KF144959	KF145003	-
A. pterospermum	CPC 20193^{T}	KF144913	KF144960	KF145004	KF145046
A. puccinioides	CBS 549.86	AB220253	AB220347	AB220300	-
A. qinlingense	CFCC 52303^{T}	MH197120	-	MH236791	MH236795
A. qinlingense	CFCC 52304	MH197121	-	MH236792	MH236796
A. rasikravindrae	MFLUCC 11-0616	KU940144	KU863132	-	-
A. rasikravindrae	MFLUCC 15-0203	KU940143	KU863131	-	-
A. rasikravindrae	LC8179	KY494759	KY494835	KY705227	KY705155
A. rasikravindrae	NFCCI 2144^{T}	JF326454	-	-	-
A. sacchari	CBS 212.30	KF144916	KF144962	KF145005	KF145047
A. sacchari	CBS 301.49	KF144917	KF144963	KF145006	KF145048
A. sacchari	CBS 372.67	KF144918	KF144964	KF145007	KF145049

Table 3.1 (continued)

Species	Strain numbers	ITS	LSU	*tub2*	*tef1-α*
A. sacchari	CBS 664.74	KF144919	KF144965	KF145008	KF145050
A. saccharicola	CBS 191.73	KF144920	KF144966	KF145009	KF145051
A. saccharicola	CBS 463.83	KF144921	KF144968	KF145011	KF145053
A. saccharicola	CBS 831.71	KF144922	KF144969	KF145012	KF145054
A. serenense	IMI 326869^{T}	AB220250	AB220344	AB220297	-
A. setostromum	KUMCC 19-0217^{T}	MN528012	MN528011	-	MN527357
A. sporophleum	CBS 145154	MK014898	MK014865	MK018001	MK017973
A. subglobosum	MFLUCC 11-0397^{T}	KR069112	KR069113	-	-
A. subroseum	LC7215	KY494740	KY494816	KY705208	KY705136
A. subroseum	LC7291	KY494751	KY494827	KY705219	KY705147
A. subroseum	LC7292^{T}	KY494752	KY494828	KY705220	KY705148
A. thailandicum	MFLUCC 15-0199	KU940146	KU863134	-	-
A. thailandicum	MFLUCC 15-0202^{T}	KU940145	KU863133	-	-
A. trachycarpum	CFCC 53038^{T}	MK301098	-	MK303394	MK303396
A. trachycarpum	CFCC 53039	MK301099	-	MK303395	MK303397
A. urticae	IMI 326344	AB220245	AB220339	AB220292	-
A. vietnamense	IMI 99670^{T}	KX986096	KX986111	KY019466	-
A. xenocordella	CBS 478.86^{T}	KF144925	KF144970	KF145013	KF145055
A. xenocordella	CBS 595.66	KF144926	KF144971	-	-
A. yunnanum	DDQ00281	KU940148	KU863136	-	-
A. yunnanum	MFLUCC 15-1002^{T}	KU940147	KU863135	-	-
Seiridium phylicae	CPC 19962^{T}	LT853092	KC005807	LT853239	LT853189
Seiridium phylicae	CPC 19965	LT853093	KC005809	LT853240	LT853190

Notes Ex-type strains are in black bold, and newly generated sequences are in blue bold. Abbreviations: **AMH**: Ajrekar Mycological herbarium, Pune, Maharashtra, India; **CBS**: Westerdijk Fungal Biodiversity Institute, Utrecht, Netherlands; **CFCC**: China Forestry Culture Collection Center, Beijing, China; **CPC**: Culture collection of Pedro Crous, housed at the Westerdijk Fungal Biodiversity Institute; **DAOM**: Canadian Collection of Fungal Cultures, Ottawa, Canada; **DDQ**: D.Q. Dai; **ICMP**: International Collection of Microorganisms from Plants, New Zealand; **IFO**: Institute for Fermentation, Osaka, Japan; **IMI**: Culture collection of CABI Europe UK Centre, Egham, UK; JHB: H.B. Jiang; **KUMCC**: Culture collection of Kunming Institute of Botany, Yunnan, China; **LC**: Working collection of Lei Cai, housed at CAS, China; **MFLUCC:** Mae Fah Luang University Culture Collection, Chiang Rai, Thailand; **NFCCI**: National Fungal Culture Collection of India, **JHB**: J. H. Jiang; **LC**: Working collection of Lei Cai, housed at CAS, China.

Table 3.2 List of fungal taxa and their GenBank accession numbers of the sequences used for *Cordana*. The newly generated sequences are indicated in red bold and the type strains are indicated by "T" in superscript

Species	**Strain no**	**LSU**	**ITS**
Cephalotheca foveolata	UAMH 11631	KC408398	–
Coniochaeta gigantospora	ILLS 60816	JN684909	NR121521
Co. leucoplaca	Jong54	FJ167399	–
Co. ligniaria	C8	AY198388	–
Co. luteoviridis	CBS 206.38^{T}	FR691987	NR154769
Co. velutina	KF428798	KF428798	–
Co. velutina	UAMH10912	EU999180	–
Cordana abramovii	B-98	MK835800	MK828603
C. abramovii	PE0053-24a	KF833358	–
C. aquatica	MFLUCC 16-0954^{T}	MK835799	MK828602
C. bisbyi	CBS 213.65^{T}	MH870183	MH858544
C. confusa	MFLUCC 11–0294	MH236579	MH236576
C. ellipsoidea	IMI 229746	HE672156	HE672145
C. ellipsoidea	IMI 183415	HE672166	HE672155
C. globosa	BCRC FU31796	LC832431	LC832430
C. globosa	HKAS 112622	OP358463	
C. inaequalis	CBS 508.83	HE672157	HE672146
C. lignicola	MFLUCC 17-1332^{T}	MK835797	MK828600
C. lignicola	MFLUCC 17–1323	MK835798	MK828601
C. linzhiensis	KUNCC 10465^{T}	OR674874	OR458380
C. linzhiensis	KUNCC 10466	OR674875	OR674872
C. mercadiana	FMR 11828	HE672165	HE672154
C. oblonga	BCRC FU31890	LC832434	LC832433
C. pauciseptata	IMI 232041a^{T}	HE672159	NR154771
C. pauciseptata	IMI 102120	HE672158	HE672147
C. pauciseptata	CBS 121804	HE672160	HE672149
C. reniformis	KUNCC 24-18024^{T}	PQ152635	PQ168249
C. solitaria	CBS 214.86	HE672161	HE672150
C. taiwanensis	BCRC FU31952	LC832438	LC832437
C. terrestris	FMR 11157	KF771875	HF677173
C. terrestris	CBS 401.52	HF677184	KF733463
C. verruculosa	FMR 11594	HE672164	HE672153
C. verruculosa	CBS 121870	HE672163	HE672152
C. yunnanensis	YMF 1.6947^{T}	MZ267688	MZ265302
C. yunnanensis	YMF 1.6948	MZ265303	MZ265301
Humicola limonispora	LC 5707	KU746719	KU746673
Mirannulata samuelsii	SMH1880	AY578353	–

Table 3.2 (continued)

Species	Strain no	LSU	ITS
Phialemonium atrogriseum	CBS 604.67^{T}	FJ176881	–
Teracosphaeria petroica	ICMP 15111	EF063576	–

Notes Ex-type strains are indicated by "T" in superscript, and newly generated sequences are in red. Abbreviations: **CBS**: Westerdijk Fungal Biodiversity Institute, Utrecht, Netherlands; **GZCC**: Guizhou Culture Collection, Guizhou, China; **KUNCC:** Kunming Institute of Botany Culture Collection; **MFLUCC**: Mae Fah Luang University Culture Collection, Chiang Rai, Thailand; **MFLU**: Mae Fah Luang University Herbarium Collection; **ZHKUCC**: Zhongkai University of Agriculture and Engineering Culture Collection, Guangzhou, China. *K.*: Kirschsteiniothelia; *S.*: Strigula; "–": Not available.

3.1.2.2 Taxonomy

Sordariomycetes O.E. Erikss. & Winka, Myconet 1: 10 (1997)

Amphisphaeriales D. Hawksw. & O.E. Erikss., Syst. Ascomycetum 5: 177 (1986)

Apiosporaceae K.D. Hyde, J. Fröhl., Joanne E. Taylor & M.E. Barr, Sydowia 50 (1): 23 (1998)

Arthrinium Kunze, Mykol. Hefte 1: 9 (1817)

Note: The genus *Arthrinium*, with *A. caricicola* as type species, was established by Schmidt and Kunze (Kunze, 1817). Species of Arthrinium are endophytes, saprobes and important plant pathogens of various hosts, particularly grasses and bamboo (Agut & Calvo, 2004; Li et al., 2016; Dai et al., 2017; Wang et al., 2018; Jiang et al., 2019; Rashmi et al., 2019). The sexual morph is characterised by black, linear, fusiform ascostromata with a long, slit-like opening at the apex. The ascomata are globose to subglobose, with flattened bases and brown to blackish, with or without setae (Jiang et al., 2019; Pintos et al., 2019; Yang et al., 2019). Species of *Arthrinium* produce both hyphomycetous and coelomycetous asexual morphs. The hyphomycetous morph is characterised by septate conidiophores, arising from basal cells or that are reduced to conidiogenous cells. Conidiogenous cells are holoblastic, monoblastic or polyblastic and are hyaline to pale brown, smooth or finely roughened, doliiform, ampulliform or

subcylindrical and conidia are dark brown, brown to pale olivaceous and of various shapes (Hyde et al., 2016). The coelomycetous morph is immersed, black, globose to subglobose, septate, hyphoid conidiomata and hyaline to pale brown conidiophores arising from basal cells or that are reduced to conidiogenous cells. The conidiogenous cells are subhyaline to pale brown, smooth-walled or verrucose, holoblastic, monoblastic or polyblastic and cylindrical., The conidia are dark brown, smooth, globose to subglobose, with or without a germ slit or truncate scar at the base (Senanayake et al., 2015; Dai et al., 2017; Jiang et al., 2018; Yang et al., 2019). The presence of both hyphomycetous and coelomycetous asexual morphs has complicated the taxonomy of *Arthrinium*. There are 92 species epithets for *Arthrinium* in Index Fungorum (2020). A total of 63 species have been introduced, based on the combination of morphological and molecular phylogenetic data (Wijayawardene et al., 2017; Jiang et al., 2018; Wang et al., 2018; Zhao et al., 2018; Jiang et al., 2019; Pintos et al., 2019; Yan et al., 2019; Yang et al., 2019).

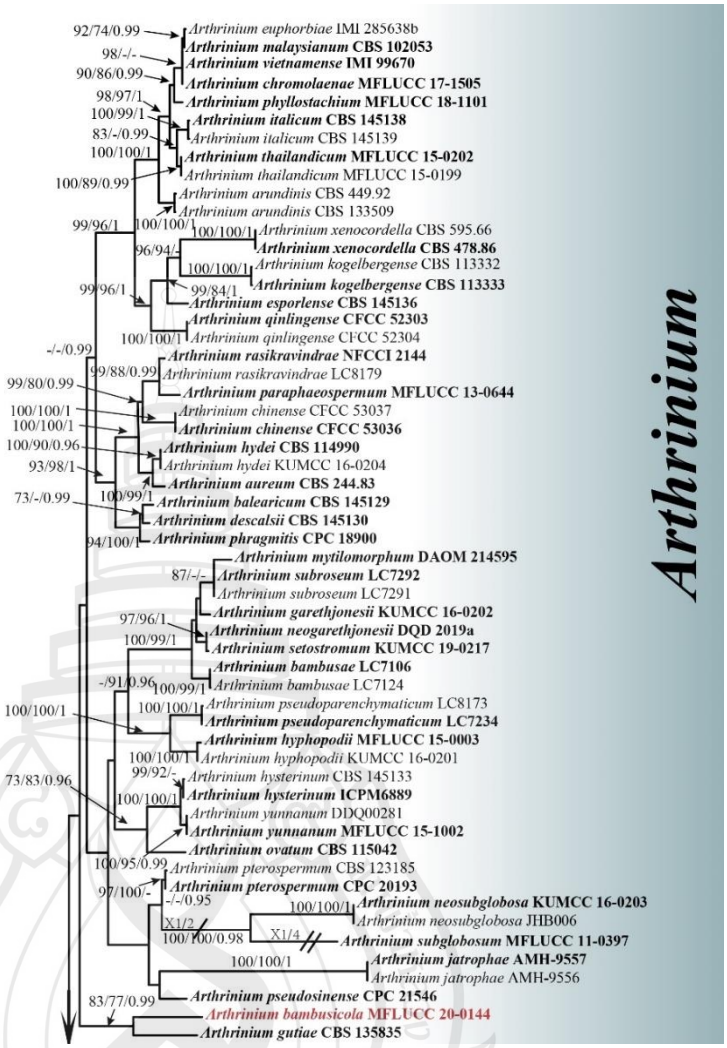

Figure 3.1 Phylogenetic tree of *Arthrinium*

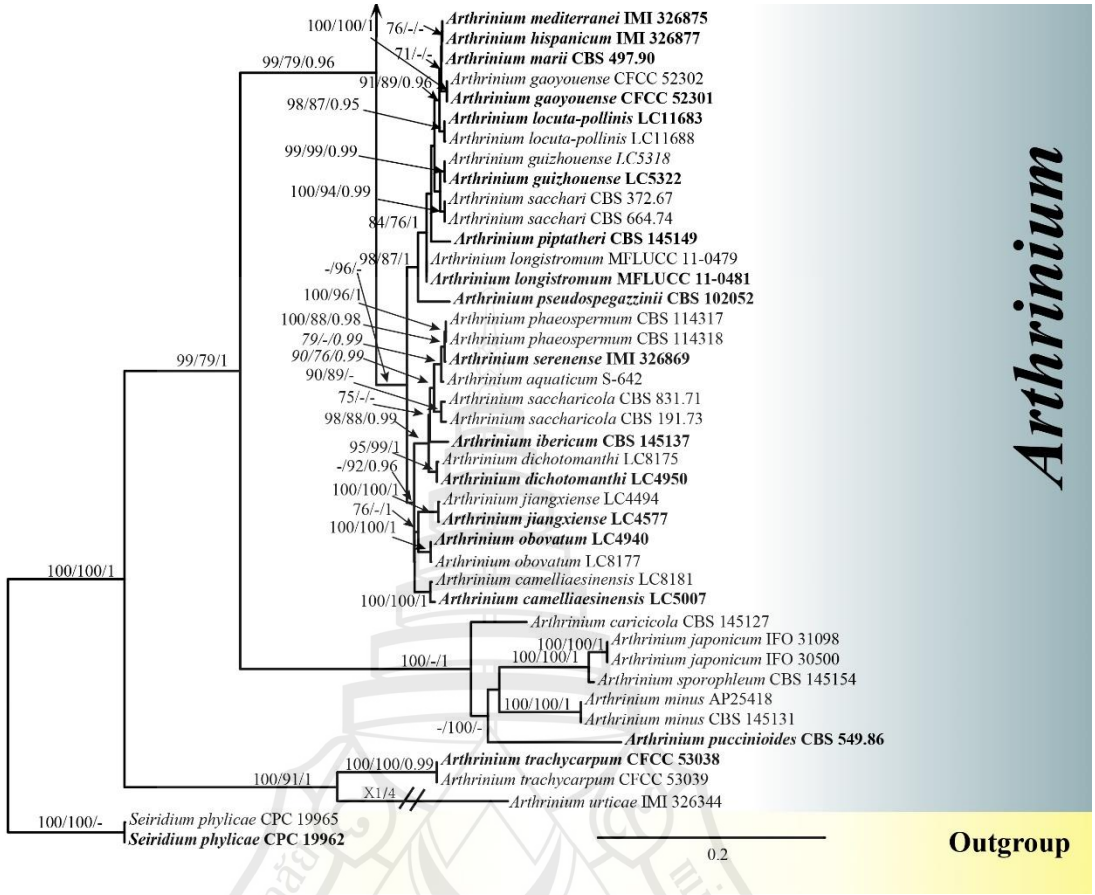

Figure 3.1 (continued)

Figure 3.1 The best-scoring RAxML tree reconstructed from a concatenated ITS, LSU, *tef1-α* and *tub2* dataset. The tree is rooted with *Seiridium phylicae* (strains CPC 19962 and CPC 19965). ML and MP bootstrap values ≥ 70 and Bayesian PP ≥ 0.95 are shown at the nodes (ML/MP/PP). Ex-type strains are in bold; the newly-described species is highlighted in red.

Arthrinium bambusicola X. Tang, K.D. Hyde & J.C. Kang, 2020, sp. nov. Figure 3.2

Etymology: Referring to the host from which the holotype was isolated, a member of the bamboo subfamily (Bambusoideae).

Holotype: MFLU 20-0528

Saprobic on dead culms of *Schizostachyum brachycladum* (*Poales*, *Poaceae*, *Bambusoideae*). **Sexual morph**: Undetermined. **Asexual morph**: *Colonies* on natural substrate, superficial, gregarious, scattered, irregular, dark brown to black. *Mycelium*

consisting of branched, septate, hyaline to dark brown.*Conidiophores* 0.8–3.5 µm diam. semi-micronematous to macronematous, mononematous, solitary, branched, flexuous, smooth, hyaline, aseptate when immature, becoming brown, septate when mature. *Conidiogenous cells* 1.5–4.5 × 1–4 µm, monoblastic or polyblastic, terminal, determinate, cylindrical, hyaline to light brown, smooth, aggregated, ampulliform, in clusters on aerial mycelium. *Conidia* pleurogenous, solitary, oval to broadly round or irregularly round, brown to medium brown, guttulate to roughened, granular, in surface view 6–8 × 6–7.8 µm ($\overline{x}$ = 6.5 × 7 µm, n = 39), in lateral view 3.5–6 × 3.5–6.5 µm ($\overline{x}$ = 4.5 × 5 µm, n = 39), with finely pale slit at outer edge.

Culture characteristics: colonies flat, spreading, with moderate, pale, aerial mycelium. On PDA, surface white, lightly yellow with patches of dirty white, reverse lightly pigmented.

Material examined: Thailand, Chiang Rai Province, Mae Fah Luang University, on dead culms of Schizostachyum brachycladum, 7 May 2019, Xia Tang, M19050706 (MFLU 20-0528, holotype), ex-type living culture MFLUCC 20-0144.

Note: *Arthrinium bambusicola* was retrieved as a sister taxon of *A. gutiae*, with relatively good support (83 ML, 77 MP, 0.99 PP). Morphologically, *A. bambusicola* differs from *A. gutiae* in having larger conidia [surface view: 5.5–8 × 6–8 µm diam., lateral view: 3.5–6 × 3.5–6.5 µm diam. versus surface view: 4.5–6 µm (x = 5.5 µm) diam., lateral view: 2–6 µm (x = 4) diam.] and irregularly rounded, guttulate to roughened conidia (*A. gutiae*: smooth-walled, globose conidia). The conidiogenous cells of *A. bambusicola* are smaller (1.5–4.5 × 1–4 µm versus 3–7× 2–4 µm). Additionally, contrasting morphological features amongst these species are presented in Table 3.1.3. Based on pairwise nucleotide comparisons, *A. bambusicola* is different from *A. gutiae* in 31/ 620 bp (5%) of the ITS, 7/814 (0.98%) of the LSU and 44/342 bp (12%) of *tef1-α*. Based on the combination of morphological characters and sequence data, we consider *A. bambusicola* as a new species.

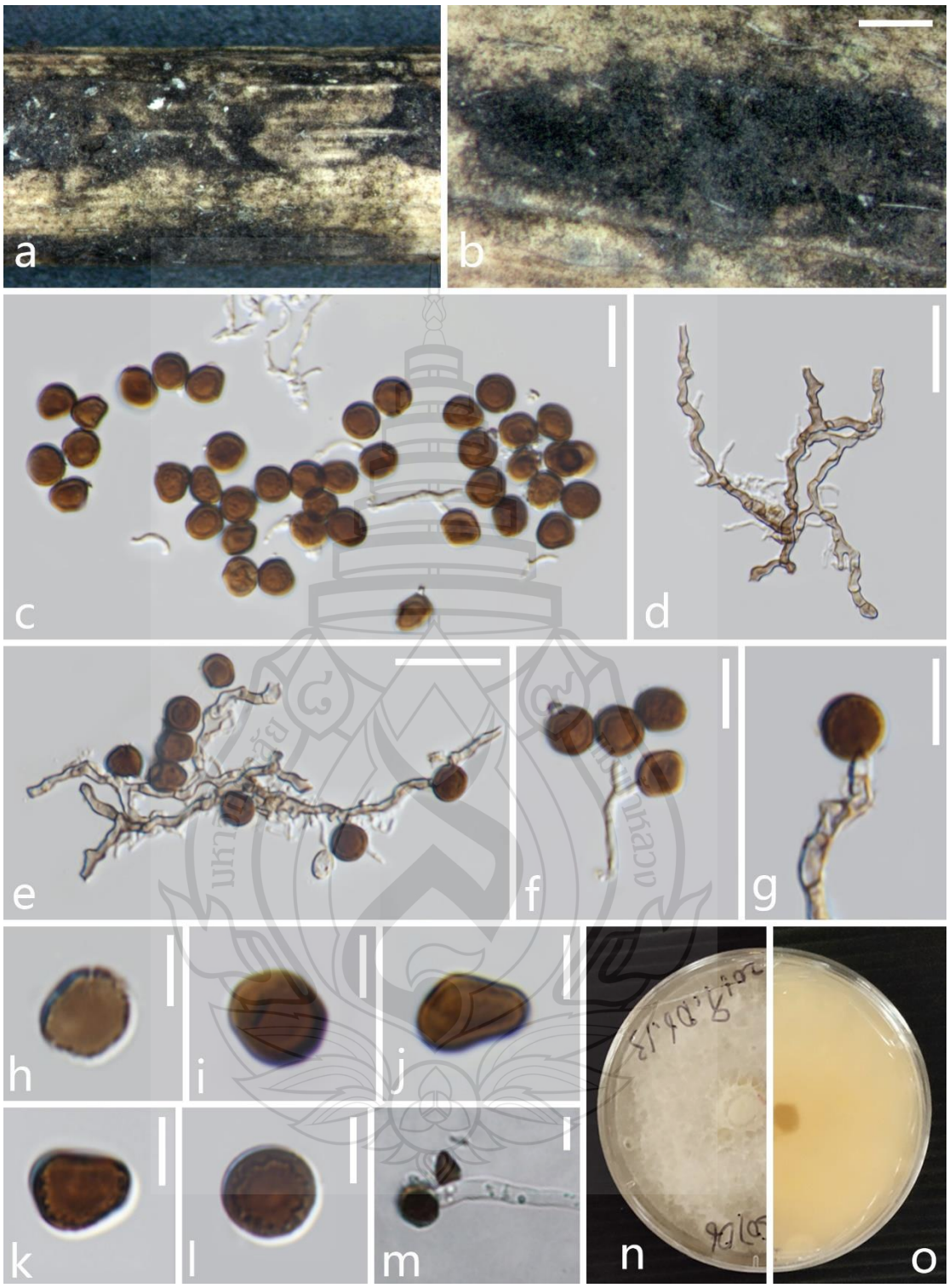

Figure 3.2 *Arthrinium bambusicola* (MFLU 20-0528, holotype)

Figure 3.2 a, b Appearance of the fungus on dead culms of *Schizostachyum brachycladum*. c Conidia with mycelia. d Mycelia. e–f Mycelia bearing conidiogenous cells and conidia. h–l Conidia. m Germinated conidium. n Forward culture. o Reversed culture. Scale bars: b = 500 μm, c–e = 20 μm, f, g = 10 μm, h–m = 5 μm.

Cordanales Hern.-Rest. & Crous, Phytotaxa 205 (4): 233 (2015)

Cordanaceae (Sacc.) Nann., Repertorio sistematico dei miceti dell' uomo e degli animali 4: 498 (1934)

Cordana Preuss, Linnaea 24: 129 (1851)

Note: *Cordana* was established by Preuss (1851) to include three species: *C. polyseptata*, *C. pauciseptata*, and *C. pedunculata*. The genus was later expanded with the addition of *C. parvispora* by Preuss (1852). Saccardo (1877) provided an emended diagnosis of *Cordana*, ultimately recognizing only *C. pauciseptata* as a valid species within the genus (Saccardo, 1886). However, no type species was designated until Hughes (1955) redescribed and illustrated *C. pauciseptata*, which had been found in North American collections on wood and bark, as well as from wood isolations, and subsequently designated it as the lectotype of *Cordana*. The morphological characteristics of *Cordana* hare mainly manifested in the diversity of pellet-producing cells, which can be divided into three different types: (1) the conidogenous cells exhibit polyblastic, terminal and intercalary, cylindrical-subnodose, with tiny prominent denticles at the nodes, such as *Cordana andinopatagonica, C. crassa*, *C. linzhiensis*, *C. lithuanica*, *C. meilingensis*, *C. miniumbonata*, *C. sinensis* and *C. solitaria* (Tóth, 1975; Rao & de Hoog, 1986; Castañeda Ruíz, 1999; Markovskaja, 2003; Ai et al., 2019; Qiu et al., 2021; Xu et al., 2024). (2) integrated, polyblastic, with subhyaline and slightly prominent scars, terminal and intercalary; proliferations percurrent, cylindrical to lageniform, usually inflated at the conidiogenous loci, such as *Cordana abramovii*, *C. aquatica*, *C. boothii*, *C. ellipsoidea*, *C. inaequalis*, *C. lignicola*, *C. lushanensis*, *C. mercadiana*, *C. oblongispora* and *C. verruculosa* (de Hoog, 1973; Matsushima, 1975; Ellis, 1976; Hughes, 1983; Seman & Davydkina, 1983; Hernández-Restrepo et al., 2014; Ai et al., 2019; Luo et al., 2019). (3) polyblastic, subulate, discrete, determinate, denticulate, denticles cylindrical, terminal, hyaline, arranged in a fasciculate cluster over the swollen apex of the stipe, such as *Cordana bisbyi, C. terrestris* and *C. yunnanensis* (Hernández-Restrepo et al., 2014; Yang et al., 2023).

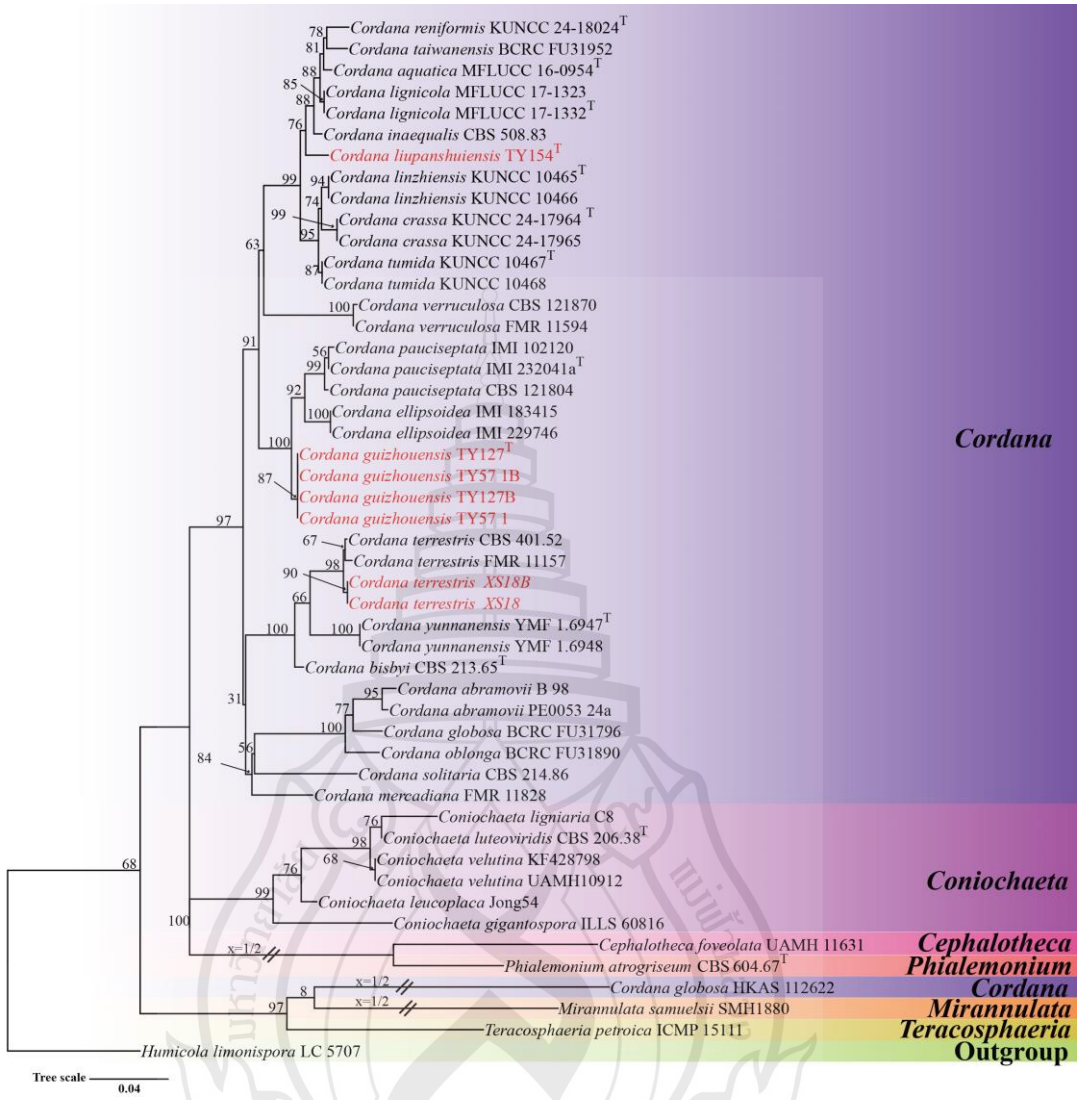

Figure 3.3 Phylogenetic analysis of *Cordana*

Figure 3.3 Phylogenetic analysis of *Cordana* was conducted using RAxML-based maximum likelihood analysis of a combined LSU, and ITS DNA sequence dataset. Bootstrap support values for maximum likelihood (ML) equal to or greater than 70% and Bayesian posterior probabilities (PP) equal to or greater than 0.95 are shown above the nodes. The tree is rooted with *Humicola limonispora* (LC 5707). Newly generated strains are highlighted in red, and type strains are indicated with a superscript 'T'.

Cordana guizhouensis X. Tang, K.D. Hyde, Jayaward & J.C. Kang, sp. nov.; Figure 3.4

Etymology: The specific epithet 'guizhouensis' refers to the place where the fungus was collected.

Holotype: GZAAS25-0652

Saprobic on unidentified decaying wood in the forest. **Sexual morph**: not observed. **Asexual morph**: *Colonies* on the natural substrate superficial, effuse, gregarious, dark brown to black. *Mycelium* immersed, composed of septate, branched, thin-walled, smooth, brown. *Coinidiophores* (–102) 166–298 (–417) × 2–5 (–7) µm ($\overline{x}$ = 227 × 3.8 µm, n = 20), macronematous, mononematous, septate, erect, straight to flexuous, unbranched, with intercalary nodes 3–5 µm wide, swollen at several cells, smooth, brown, paler towards the apex, 5.5–10 µm wider at the swollen base. *Conidiogenous cells* 13–29 × 1.5–4 µm ($\overline{x}$ = 19 × 2.7 µm, n = 20), integrated, polyblastic, with subhyaline and slightly prominent scars, terminal and intercalary; proliferations percurrent, cylindrical to lageniform to spherical, usually inflated at the conidiogenous loci, 3–5 µm wide. *Conidia* 7.5–12.5 × 4–6 µm ($\overline{x}$ = 10.2 × 5.1 µm, n = 20) solitary, acropleurogenous, 1-septate, slightly constricted at the septa, with a darker band surround the septate, ellipsoidal to obovoid, with a subapiculate and dark basal scar, brown. Conidial secession schizolytic.

Culture characteristics: Conidia germinated on PDA within 24 hours, producing germ tubes from both the apex and base. Subsequently, colonies incubated on PDA demonstrated a circular morphology with dense, flat, spreading, and fluffy growth, along with an entire margin. The surface exhibited a blackish-green color with a darker edge, and occasionally milky white mycelium grew randomly on the colonies. The reverse side displayed a circular shape with an entire margin, appearing with a milky white center that transitioned to pale black, ending with a black rim on the margin.

Material examined: China, Guizhou Province, Liupanshui City, Yushe County, saprobic on unidentified decaying branches, 25 February 2023, Xia Tang, TY127 (GZAAS25-0651, holotype); ex-type living culture GZCC 25-0621. China, Guizhou Province, Liupanshui City, Yushe County, saprobic on unidentified decaying branches, 25 February 2023, Xia Tang, TY57.1 (GZAAS25-0652, paratype); living culture GZCC 25-0622.

Note: Blastn results from NCBI indicated that our new collection corresponds to the genus, *Cordana*. Morphologically, our collection is similar to matches the characteristics of *Cordana*, such as macronematous, mononematous coinidiophores with intercalary nodes, swollen at several cells; polyblastic, terminal and intercalary, proliferations percurrent conidiogenous cells, cylindrical to lageniform to spherical, usually inflated at the conidiogenous loci and solitary, acropleurogenous, 1-septate, ellipsoidal to obovoid conidia with a darker band surround the septate and a subapiculate and dark basal scar. Phylogenetic analysis revealed that our collection (GZCC 25-0621, see Figure 3.3) clusters with *C. pauciseptata* (IMI 102120 and IMI 232041a) and *C. ellipsoidea* (IMI 183415 and IMI 229746). Comparisons of ITS and LSU sequences between our collection and *C. pauciseptata* (IMI 232041a) showed 1.3% variation in ITS (7/525 base pairs, excluding gaps) and 2.2% variation in LSU (11/507 base pairs, excluding gaps) There are 2.9% variation in ITS (15/511 base pairs, excluding gaps) and 1.2% variation in LSU (6/507 base pairs, excluding gaps) between our collection and *C. ellipsoidea* (IMI 229746). Based on these findings, we propose our collection as a novel species in *Cordana*, named *Cordana guizhouensis*, in accordance with the guidelines established by Jeewon and Hyde (2016) and Chethana et al. (2021).

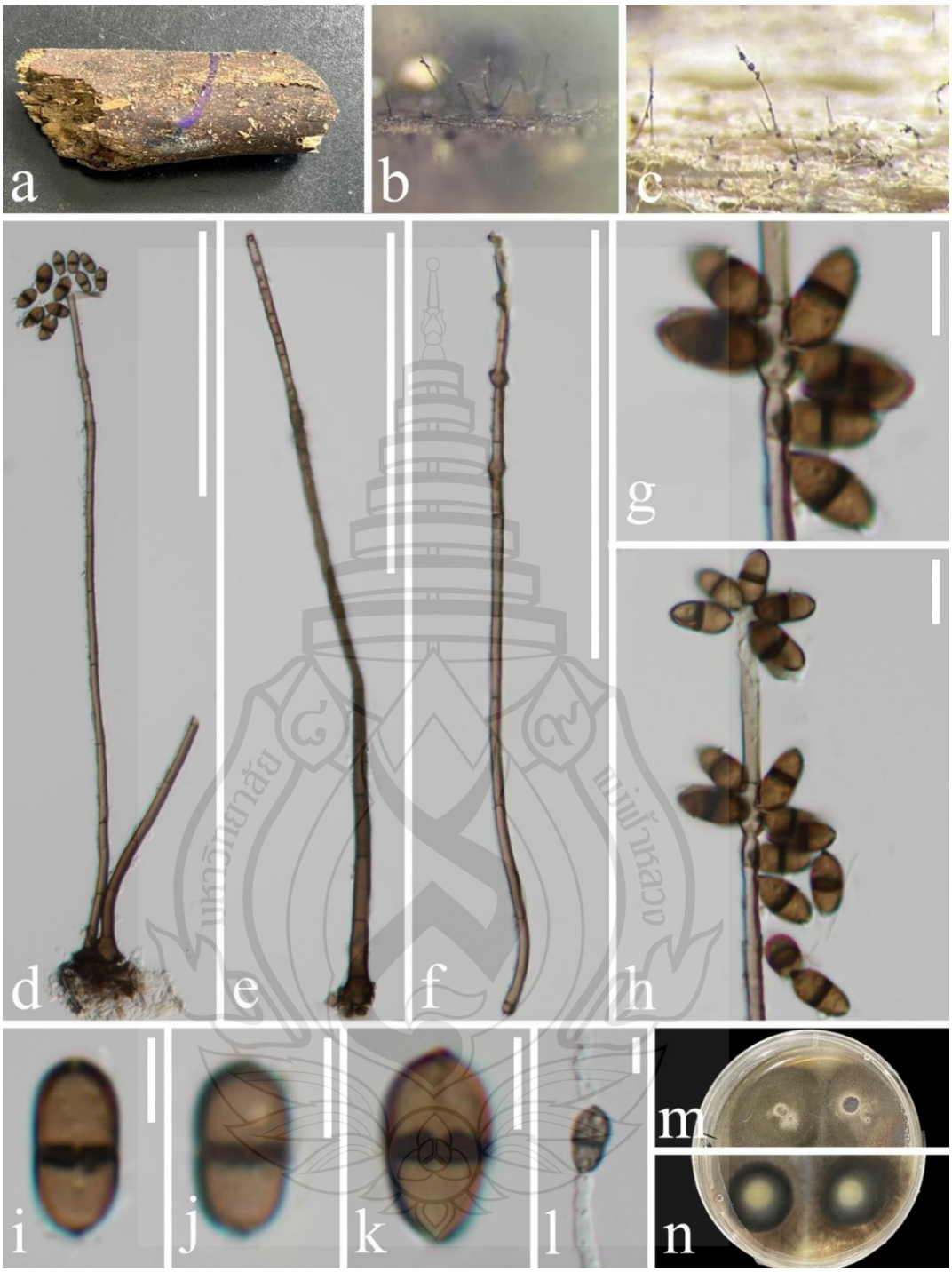

Figure 3.4 *Cordana guizhouensis* (GZAAS25-0651, holotype)

Figure 3.4 a–c Colonies on natural substrate. d–f Conidiophores, conidiogenous cells. g, h conidiogenous cells bearing conidia. i–k Conidia. l Germinated conidium. m Forward culture. n Reversed culture. Scar bar: (d-f) = 100 μm, (g, h) = 20 μm, (i-p) = 50 μm.

Cordana liupanshuiensis X. Tang, K.D. Hyde, Jayaward & J.C. Kang, sp. nov.; Figure 3.5

Etymology: The specific epithet 'liupanshuiensis' refers to the place where the fungus was collected.

Holotype: GZAAS25-0653

Saprobic on unidentified decaying wood. **Sexual morph**: not observed. **Asexual morph**: *Colonies* on the natural substrate superficial, effuse, gregarious, dark brown to black. *Mycelium* immersed, composed of septate, branched, thin-walled, smooth, brown. *Coinidiophores* 127.5–190 × 5–8 µm ($\overline{x}$ = 158 × 6.5 µm, n = 20), macronematous, mononematous, septate, erect, straight to slight flexuous, cylindrical, unbranched, smooth, pale brown to brown, paler towards the apex, wider at the base. *Conidiogenous cells* 28–70 × 5–10 µm ($\overline{x}$ = 55.7 × 6.8 µm, n = 20), integrated, polyblastic, terminal and intercalary; proliferations percurrent, cylindrical, occasionally lageniform. *Conidia* 13.5–21 × 6.5–10 µm ($\overline{x}$ = 17.6 × 8.2 µm, n = 30) solitary, acropleurogenous, 1-septate, slightly constricted at the septa, darker at the septate, ellipsoidal to ovoid, obovoid, rounded to subapiculate at the apex, darker, wider basal scar, with a hyaline mucilaginous sheath surround by apex, pale brown to brown. Conidial secession schizolytic.

Culture characteristics: Conidia germinated on PDA within 24 hours, producing germ tubes from both the apex and lateral sides. Subsequently, colonies incubated at room temperature on PDA exhibited a circular morphology with dense, umbonate, and spreading growth, characterized by an entire margin. The colony surface displayed a reddish-brown color with a paler brown edge. On the reverse side, colonies presented a pale brown circular shape with an entire margin and a dark brown circle embedded within the colony.

Material examined: China, Guizhou Province, Liupanshui City, Yushe County, saprobic on unidentified decaying branches, 25th February 2023, Xia Tang, TY154 (GZAAS25-0653, holotype), ex-type living culture GZCC 25-0623.

Note: Blastn results from NCBI indicated that our new collection corresponds to the genus, *Cordana*. Morphologically, our collection is similar to matches the characteristics of *Cordana*, such as macronematous, mononematous coinidiophores; integrated, polyblastic, terminal and intercalary, proliferations

percurrent, cylindrical conidiogenous cells occasionally lageniform. solitary, acropleurogenous, ellipsoidal to ovoid, obovoid conidia rounded to subapiculate at the apex, with a hyaline mucilaginous sheath surround by apex. Phylogenetic analysis revealed that our collection (GZCC 25-0623, see Figure 3.3) clusters with *C. inaequalis* (CBS 508.83). Comparisons of ITS and LSU sequences between our collection and *C. inaequalis* (CBS 508.83) showed 2.6% variation in ITS (12/462 base pairs, excluding gaps) and 1.6% variation in LSU (8/502 base pairs, excluding gaps). Based on these findings, we propose our collection as a novel species in Cordana, named *Cordana guizhouensis*, in accordance with the guidelines established by Jeewon and Hyde (2016) and Chethana et al. (2021).

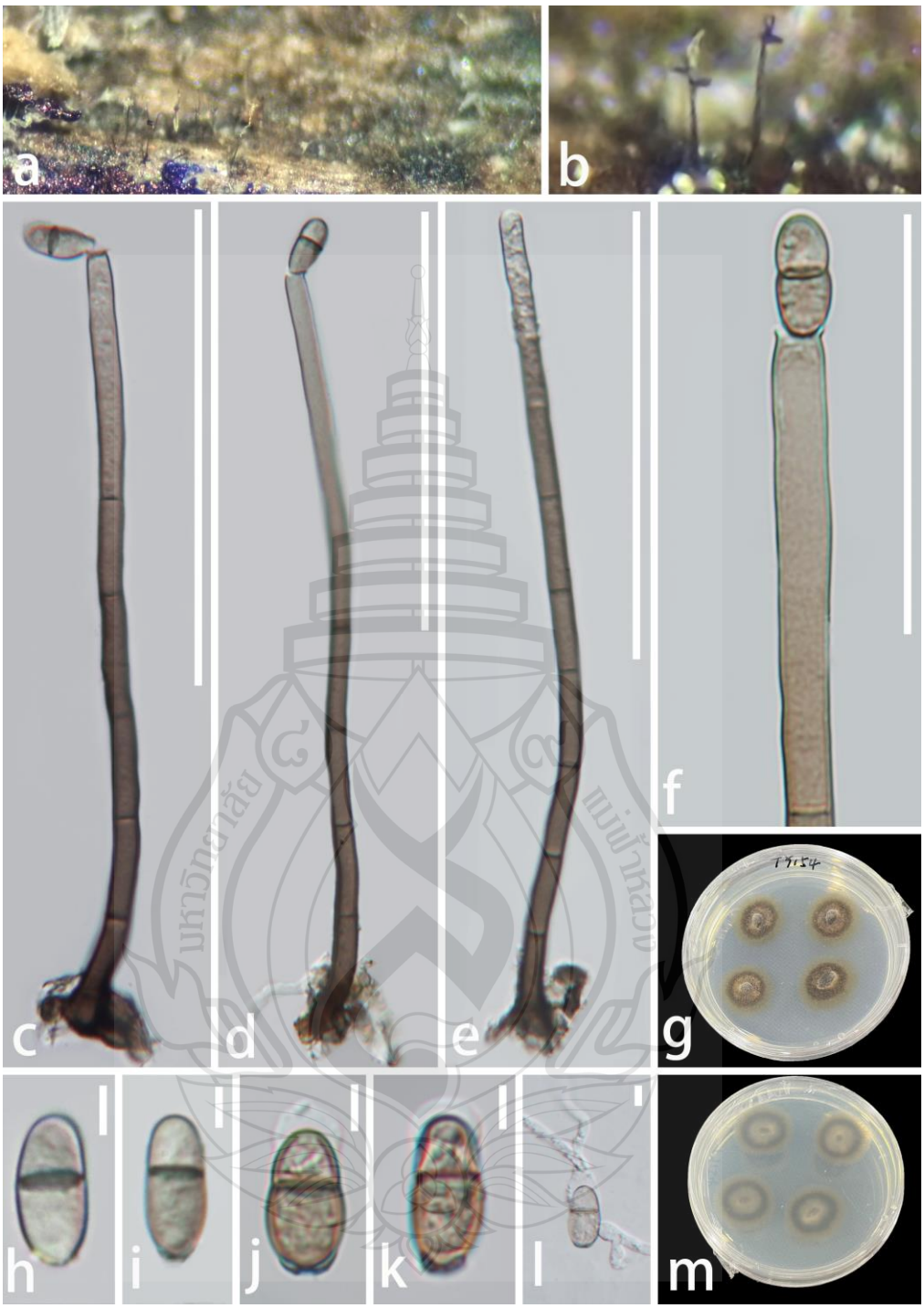

Figure 3.5 *Cordana liupanshuiensis* (GZAAS25-0653, holotype)

Figure 3.5 a, b Colonies on natural substrate. c–e Conidiophores, conidiogenous cells bearing conidia. f conidiogenous cells bearing conidia. h–k Conidia. l Germinated conidium. g Forward culture. m Reversed culture. Scar bar: c-e = 100 μm, f = 50 μm, h-l = 5 μm.

Table 3.3 Morphological comparison of the seven *Arthrinium* species introduced from Thailand

Species name	Substrate	Sexual morph			Asexual morph			Reference
		Stromata (long × high)	Ascomata (long × high)	Asci (µm)	Ascospores (µm)	Conidiogenous cells (µm)	Conidia (µm)	
A. bambusicola	Dead culms of bamboo	NA	NA	NA	NA	1.5–4.5 × 1–4 µm, cylindrical, hyaline to light brown, ampulliform.	Pleurogenous, solitary, oval to broadly round, or irregularly round, brown to medium brown, guttulate to roughened, granular, in surface view 6–8 × 6–7.8 µm ($\bar{x}$ = 6.5 × 7 µm, n = 39), in side view 3.5–6 × 3.5–6.5 µm ($\bar{x}$ = 4.5 × 5 µm, n = 39).	This study

Table 3.3 (continued)

Species name	Substrate	Sexual morph			Asexual morph			Reference
		Stromata (long × high)	Ascomata (long × high)	Asci (µm)	Ascospores (µm)	Conidiogenous cells (µm)	Conidia (µm)	
A. chromolaenae	*Chromolaena odorata*	NA	NA	NA	NA	6.5–12 ?m × 1–2 µm, ($\bar{x}$ = 8.5 × 1.5µm, n = 5). Broadly fliform to ampulliform.	4–6 × 4.5–6.5µm, irregular arrangement in pseudo-chains, pale brown to brown, smooth, globose to subglobose ($\bar{x}$ =5×5.5 µm, n=35).	Mapook et al. (2020)
A. longistromum	Bamboo	5–30 mm× 0.25–0.3 mm regarious, raised, irregularly and sinuously filiform.	140–280 µm diam, 145–265 µm high,10–30 gregarious in one ascostroma.	70–95 × 15.5–20 µm ($\bar{x}$ = 79.7.6 × 18.4 µm, n = 20).	20–30 × 4.5–6.5 µm, without sheath.	NA	NA	Dai et al. (2016)

Table 3.3 (continued)

Species name	Substrate	Sexual morph			Asexual morph			Reference
		Stromata (long × high)	Ascomata (long × high)	Asci (µm)	Ascospores (µm)	Conidiogenous cells (µm)	Conidia (µm)	
A. paraphaeospermum	Bamboo	NA	NA	NA	NA	25–30 × 4–6 µm ($\bar{x}$ = 27 × 4.7µm), basauxic, conical to ampulliform, 3–5 µm diam.	10–19 µm diam, Sterile cells 20–30 × 9–13 µm ($\bar{x}$ = 24 × 11 µm), forming on solitary loci on hyphae, brown, finely roughened, ellipsoid to clavate.	Hyde et al. (2016)
A. rasikravindrii	Rice	0.8–1.7 mm× 0.15–0.2 mm, solitary, fusiform, with a long, broken axis at the top.	100–150 µm high, 200–300 µm diam, 3–5 perithecia immersed within the ascostromata.	70–90 × 15–17.5 µm.	21.5–24.5 × 7–9.5 µm, one large guttule in the centre, surrounded by 3.5–9 µm wide gelatinous sheath attached at both ends.	Basauxic, cylindrical, discrete.	7–10 × 4.5–8.5 µm, lenticular, occasionally elongated to ellipsoidal, dark brown.	Dai et al. (2016)

Table 3.3 (continued)

Species name	Substrate	Sexual morph			Asexual morph			Reference
		Stromata (long × high)	Ascomata (long × high)	Asci (µm)	Ascospores (µm)	Conidiogenous cells (µm)	Conidia (µm)	
A. subglobosum	Bamboo	1000–3000 µm× 150–300 µm, solitary to gregarious, in linear rows, irregular, cells between ascomata and darkened layer above usually 50–200µm thick.	200–350 µm diam, 150–200 µm high, in groups of 3–5.	75–150×27–36 µm.	24–28×8.5–12.5µm, overlapping 1–3-seriate, occasionally at an acute angle from the larger cell at the constricted septum, surrounded by 5–8 µm thick gelatinous sheath.	NA	NA	Senanayake et al. (2015)
A. thailandicum	Bamboo	450–990 µm × 150–200 µm, solitary to gregarious	145–160 µm × 250–280 µm.	80–100 × 16–20 µm, broadly cylindrical to long clavate.	8 22–30 × 8–12.5 µm, surrounded by 3–5 µm wide gelatinous sheath attached, at both ends.	11.5–39 × 2–3.5 µm ($\bar{x}$ = 26.7 × 2.6 µm, n = 20), basauxic, polyblastic, sympodial, cylindrical, discrete.	5–9×5–8 µm, occasionally elongated to ellipsoidal, dark brown.	Dai et al. (2016)

Diaporthomycetidae *families incertae sedis*

Junewangiaceae J.W. Xia & X.G. Zhang, Sci. Rep. 7 (no. 7888): 12 (2017)

Sporidesmiella P.M. Kirk, Trans. Brit. Mycol. Soc. 79 (3): 479 (1982)

*Index Fungorum numbe*r: IF 10023; Facesoffungi number: FoF 06604

Notes: *Sporidesmiella* was established by Kirk (1982), with *S. claviformis* P.M. Kirk designated as the type species, together with five additional species and one variety. Most species of *Sporidesmiella* have been reported as saprobes on decaying wood in both terrestrial and freshwater habitats across from Asia and South America (Holubová-Jechová, 1987; Ma et al., 2012, 2015, 2016; Monteiro et al., 2014; Luo et al. 2019; Crous et al., 2020; Dong et al., 2021; Xiong et al., 2024) To date, only one lichenicolous species, *Sporidesmiella lichenophila,* has been reported, which broadened the ecological scope of the genus (Braun & Heuchert, 2010). Morphologically, *Sporidesmiella* is characterized by macronematous, mononematous, septate conidiophores and monoblastic to polyblastic, terminal, integrated conidiogenous cells that produce numerous enteroblastic percurrent extensions. These may result in false sympodial elongations, giving the conidiophore a geniculate appearance. The genus is further distinguished by annellations near the apex and by basally (sub)truncate, distoseptate conidia (Kirk, 1982). Phylogenetic studies have yielded shifting placements of *Sporidesmiella*, but recent analyses support its affiliation with *Junewangiaceae* (Luo et al., 2019; Dong et al., 2021). Nevertheless, many species remain unresolved due to the lack of molecular data and considerable morphological variation. Further integrative studies combining molecular and morphological evidence are required to clarify the taxonomy of the genus. To date, 46 species of *Sporidesmiella* have been described, of which 18 are supported by molecular data (Luo et al., 2019; Hyde et al., 2020b; Dong et al., 2021; MycoBank 2025; Xu et al., 2025).

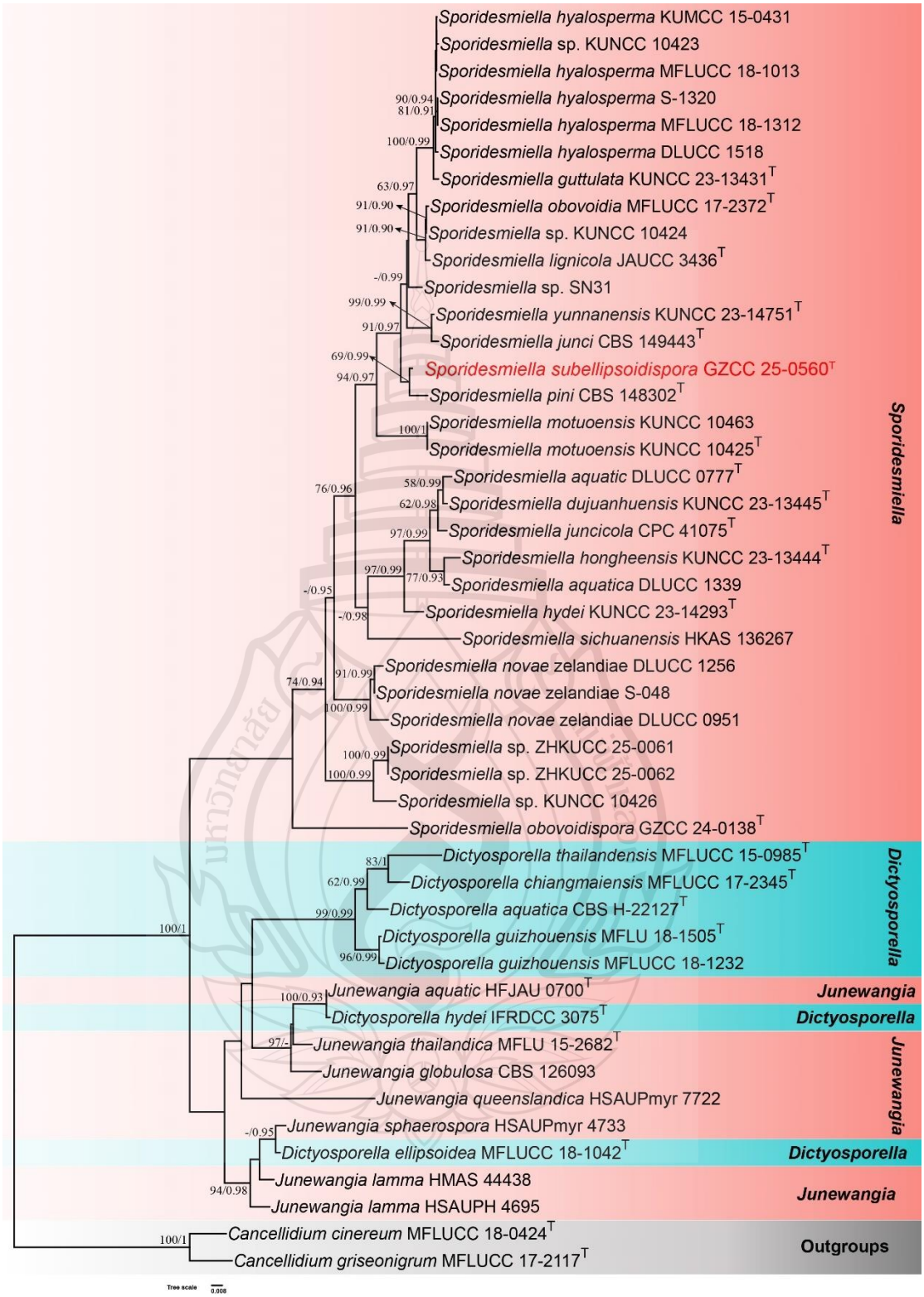

Figure 3.6 Phylogenetic analysis of *Sporidesmiella*

Figure 3.6 Phylogenetic analysis of *Sporidesmiella* was conducted using RAxML-based maximum likelihood analysis of a combined LSU, ITS and *rpb2* DNA sequence dataset. Bootstrap support values for maximum likelihood (ML) equal to or greater than 70% and Bayesian posterior probabilities (PP) equal to or greater than 0.95 are shown above the nodes. The tree is rooted with *Cancellidium cinereum* (MFLUCC 18-0424) and *C. griseonigrum* (MFLUCC 17-2117). Newly generated strains are highlighted in red, and type strains are indicated with a superscript 'T'.

Sporidesmiella subellipsoidispora X. Tang, K.D. Hyde, Jayaward. & J.C. Kang, sp. nov. Figure 3.1.7

Etymology: The specific epithet 'subellipsoidispora' refers to the shape of conidia.

Holotype: GZAAS25-0590

Saprobic on unidentified decaying wood in the forest. **Sexual morph**: Undetermined. **Asexual morph**: *Colonies* on natural substrate effuse, reddish-brown. *Conidiophores* 116–275 × 4–6 µm ($\overline{x}$ = 191.5 × 4.9 µm, n = 20), macronematous, mononematous, unbranched, solitary, erect, cylindrical, guttulate, straight to somewhat flexuous, septate, slightly constricted at septa, reddish-brown, pale toward the apex, 8–15-septate, smooth, thick walled, wide at base. *Conidiogenous cells* 13.5–61 (-70) × 3–6 µm ($\overline{x}$ = 36.1 × 4.4 µm, n = 25), holoblastic, polyblastic, integrated, terminal and intercalary, with several sympodial proliferations, conspicuous denticles, cylindrical, pale brown, smooth. *Conidia* 17–25 × 8.5–13 µm ($\overline{x}$ = 22.2 × 11 µm, n = 32), acrogenous, solitary, subellipsoid to obovoid, occasionally slightly fusiform, rounded at the apex, narrow towards truncate at the base, with hilum truncate, 2–4.5 µm diam, with marginal frill, subhyaline to pale brown, becoming brown at maturity, 3–4-distoseptate, with central pore in septum, guttulate, smooth- and thick-walled.

*Culture characteristic*s: Colonies on PDA at 25°C germinate from the base of conidia, circular, with a flat to slightly raised surface and a dense, velvety to floccose mycelial texture. Mycelium is denser at the center and gradually becomes sparser toward the margin. The colony surface is covered by whitish to pale gray mycelium, sometimes tinged with creamy tones, while the underlying substrate appears reddish-brown. Colonies have a well-defined margin. The reverse is dark brown to nearly black at the center, grading to pale brown toward the periphery. Pigment production is evident

in the colony.

Material examined: China, Guizhou province, Liupanshui City, Yushe National Forest Park, on unidentified decaying wood, 27 November 2024, Xia Tang, LS170 (GZAAS25-0590), holotype, ex-type living culture (GZCC 25-0560).

Notes: Morphologically, our collection conforms to the diagnostic features of *Sporidesmiella*. The conidiophores are macronematous, mononematous, unbranched, septate, and widened at the base. Conidiogenous cells are holoblastic, polyblastic, integrated, terminal or intercalary, and bear conspicuous denticles. Conidia are acrogenous, solitary, subellipsoid to obovoid, guttulate, and distoseptate, tapering towards a truncate base with a distinct hilum. These characters are consistent with the generic concept of *Sporidesmiella*, particularly the combination of denticulate conidiogenous cells and solitary, truncate-hilum conidia.

Compared with congeners, our collection shares the general morphology of *Sporidesmiella*, such as unbranched conidiophores and thick-walled, guttulate conidia. However, subtle differences can be observed in conidial size, shape, and septation. For instance, some species within the genus produce longer or more fusiform conidia, or conidia with more numerous distosepta, whereas our collection exhibits relatively shorter, subellipsoid to obovoid conidia with 3–4 distosepta. These distinctions, though minor, help delineate our material within the morphological spectrum of *Sporidesmiella* and support its identification at the species level.

In the phylogenetic analyses, our collection clusters with *Sporidesmiella pini* (CBS 148302) (Figure 3.6). Morphologically, it resembles *S. pini* in most respects, but differs by having larger conidiophores (116–275 × 4–6 μm vs. 30–70 × 3.5–5 μm), larger conidiogenous cells (35–61(–70) × 3–6 μm vs. 11–25 × 3–4 μm), and subellipsoid to obovoid, occasionally slightly fusiform, guttulate conidia, whereas *S. pini* has predominantly obovoid conidia. Based on these morphological and phylogenetic differences, we identify our isolate as a novel species, *Sporidesmiella subellipsoidispora*, following the guidelines of Jeewon and Hyde (2016) and Maharachchikumbura et al. (2021).

Figure 3.7 *Sporidesmiella subellipsoidispora* (GZAAS25-0590, holotype)

Figure 3.7 a, b Colonies on substrate. c–f Condiophores, conidiogenous cells, conidiogenous cells bearing conidia. g–n Conidia. o Germinated conidium. p Colony on PDA (from front). q Colony on PDA (from reverse). Scale bars: c–f = 50 µm, g–o = 20 µm.

3.2 Microfungi Unravelling New Taxa of *Dothideomycetes* Associated with Forest Plants in China

3.2.1 Introduction

Fungi represent one of the most diverse groups of organisms on the planet, and distributed worldwide in various habitats, such as forest ecosystems, terrestrial, freshwater and marine environments, wetlands and swamps, as well as some extreme environments (Taylor et al., 2010; Glass et al., 2014; Luo et al., 2019; Dong et al., 2020; Lofgren & Stajich, 2021;Tennakoon et al., 2022a,2022b; Barnés-Guirado et al., 2024; Gao et al., 2024; Hyde et al., 2024; Shen et al., 2024 Bao et al., 2025; Habib et al., 2025; Isola & Prenafeta-Boldú, 2025; Karimi et al., 2025; Yang et al., 2025). With the emergence of new sequencing technologies, it has been predicted through high-throughput sequencing methods that there are approximately 11.7 to 13.2 million species in the world (Hyde, 2022).

Forests are among the largest ecosystems on Earth, and their stability not only determines the continuity of ecological processes but also exerts profound impacts on economic development and social well-being (Mongabay, 2025; European Environment Agency, n.d.; Food and Agriculture Organization of the United Nations, 2022; Kumar & Muradian, 2021). The stability of forest ecosystems generally depends on the interactions between multiple biotic and abiotic factors, including species diversity, community structure, key ecological functions, and environmental adaptability (Gottschall et al., 2022). Among these factors, fungi act as crucial regulators of forest stability, performing multiple roles in maintaining forest health. They promote species coexistence, accelerate and optimize nutrient cycling, enhance community resilience, and contribute to carbon fixation and storage, thereby supporting and strengthening ecosystem functions. In forests, fungi occupy diverse ecological niches, ranging from decomposers of litter, soil and root symbionts (such as mycorrhizal fungi), to plant endophytes and potential pathogens, functional groups that can exert both positive (e.g., decomposition and symbiosis) and negative (e.g., disease causation) effects on forest stability (Liu et al., 2022). Therefore, investigating the diversity and functional distribution of forest fungi is essential for understanding and

maintaining the stability of forest ecosystems (Yang et al., 2022; Tennakoon et al., 2022a, 2022b; Hyde et al., 2024). To date, forest-associated fungi span numerous phyla, with major lineages including *Ascomycota*, *Basidiomycota*, *Mucoromycota*, *Zoopagomycota*, *Chytridiomycota*, *Glomeromycota* (and additional early-diverging groups such as *Blastocladiomycota*, *Monoblepharomycota*, *Neocallimastigomycota*, *Olpidiomycota*, *Rozellomycota*). Dominant forest classes frequently reported are *Agaricomycetes*, *Dothideomycetes*, *Eurotiomycetes*, *Leotiomycetes*, *Pezizomycetes*, *Sordariomycetes*, *Tremellomycetes*, and *Glomeromycetes* (Hyde et al., 2024; Naranjo-Ortiz & Gabaldón, 2019; Hibbett et al., 2007; Smith & Read, 2008; Tedersoo et al., 2014; Sheng et al., 2019).

As the largest class within *Ascomycota*, *Dothideomycetes* exhibits a global distribution and occupies diverse ecological niches in forest ecosystems. These fungi form close associations with forest plants and animals, functioning Mainly as endophytes, such as *Alternaria* spp., *Asperisporium* spp., *Phyllosticta* spp., *Botryosphaeria* spp., *Diaporthe* spp., *Paraconiothyrium* spp., *Zasmidium* spp., and so on (Aschehoug et al., 2014; Sandberg et al., 2014; Hardoim et al., 2015; Katoch et al., 2015; Luo et al., 2024); pathogens, such as *Mycosphaerella* spp., *Venturia* spp., *Botryosphaeria* spp., *Hysterium pulicare* and *Dothistroma* spp. (Wingfield et al., 2001; Slippers & Wingfield, 2007; Crous et al., 2009; Quaedvlieg et al., 2013). Many members of *Dothideomycetes* are saprobic fungi, integral to key processes in forest ecosystem. They drive critical ecological functions such as organic matter decomposition, nutrient cycling, and host interactions, such as *Aureobasidium* sp., *Astrosphaeriella* spp., *Cladosporium* spp., *Leptosphaeria* spp., *Lophiostoma* spp., and members from *Pleosporales* (Johnston et al., 2012; Voglmayr et al., 2016; Tennakoon et al., 2022a, 2022b, 2024). Moreover, they can be biotrophs, epiphytes, hemibiotrophs, lichenized and lichenicolous fungi, and mycoparasites (Jones et al., 2019; Hongsanan et al., 2020a, 2022b; Pem et al., 2019, 2021; Calabon et al., 2022; Gao et al., 2023).

The identification of *Dothideomycetes* species was initially based on morphological characteristics, and known by their ascolocular ascoma and fissitunicate (bitunicate) ascus (Nannfeldt, 1932; Luttrell, 1955; Eriksson, 1981; Barr & Huhndorf, 2001; Hyde et al., 2013; Pem et al., 2021). However, subsequent research revealed that these morphological features are not unique to *Dothideomycetes*, as they are also found

in other classes such as *Arthoniomycetes* and *Eurotiomycetes*. Therefore, they are not solely reliable for distinguishing *Dothideomycetes* from other classes (Hyde et al., 2013).

In this study, we investigate saprotrophic fungi within *Dothideomycetes* associated with forest plants in Guizhou, Guangxi and Hainan provinces, China. Based on integrated morphological and phylogenetic analyses, we aim to: (1) describe new taxa collected from these regions; (2) report new habitats, national records, and host associations for known species; and (3) provide additional collections of known species to extend their documented distribution and support the accuracy of previous identifications.

3.2.2 Results and Disscussion

3.2.2.1 Taxonomy

Coniosporiales Crous, Spatafora, Haridas & I.V. Grig., Stud. Mycol. 96: 151 (2020)

Coniosporiaceae Crous, Spatafora, Haridas & I.V. Grig., Stud. Mycol. 96: 151 (2020)

Saprosporodochifer N.G. Liu, Jian K. Liu & K.D. Hyde, Fungal Diversity 129: 196 (2024)

Index Fungorum number: IF 901980; *Facesoffungi number*: FoF 15696;

Notes: *Saprosporodochife*r was established by Liu et al. (2024), with *S. fuscus* designated as the type species, collected from decaying wood in Thailand. Species of *Saprosporodochifer* are characterized by black sporodochial colonies, micronematous conidiophores, and variously shaped, olivaceous brown to brown, muriform and constricted at the septa conidia with verrucose (Liu et al., 2024). Currently, only two species is accepted within this genus (including this study), and its sexual morph remains unknown.

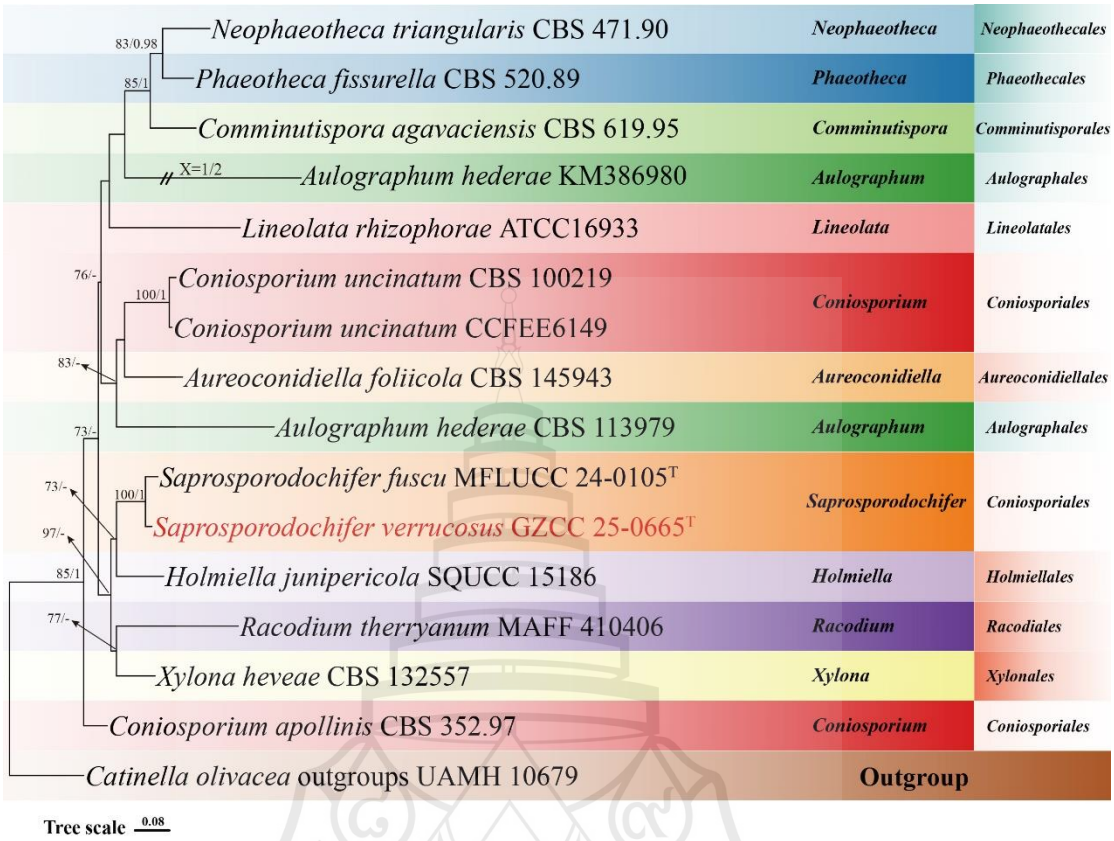

Figure 3.8 Phylogentic tree of *Saprosporodochifer*

Figure 3.8 Phylogenetic analysis of *Saprosporodochifer* was conducted using RAxML-based maximum likelihood analysis of a combined LSU, and ITS DNA sequence dataset. Bootstrap support values for maximum likelihood (ML) equal to or greater than 70% and Bayesian posterior probabilities (PP) equal to or greater than 0.95 are shown above the nodes. The tree is rooted with *Catinella olivacea* (UAMH 10679). Newly generated strains are highlighted in red, and type strains are indicated with a superscript 'T'.

Saprosporodochifer verrucosus X. Tang, Jayaward, J.C. Kang & K.D. Hyde, sp. nov.; Figure 3.9

Etymology: The "verrucosus" is refer to the verrucose ornamentation of the conidia.

Holotype: GZAAS25-0693

Saprobic on unidentified decaying wood in terrestrial habitat. **Sexual morph**: Unknown. **Asexual morph**: Hyphomycetous. *Colonies* on natural substrate

superficial, effuse, black, sparse, scattered. *Mycelium* partly immersed, partly superficial, composed of pale brown to brown, branched, septate hyphae. *Conidiophores* micronematous, mononematous, pale brown to brown, erect, cylindrical, unbranched. *Conidiogenous cells* monoblastic, integrated, cylindrical, terminal, determinate. *Conidia* 9–15 × 10–16 µm ($\overline{x}$ = 11.5 × 12.6 µm, n =40), solitary, various shaped, globose to obovoid, ellipsoidal, cuneiform, or quadrate, pale brown to brown, aseptate when young, muriform or sometimes phragmosporous when mature, constricted at the septa, verrucose.

Culture characteristics: Colonies on PDA at 25°C germinate from the base of conidia, circular, with a flat to slightly raised surface and a dense, velvety to floccose mycelial texture. Mycelium is denser at the center and gradually becomes sparser toward the margin. The colony surface is white to greyish white, becoming pale grey with age; surface velvety to thinly floccose. An internal circular ring, delimited by a sparse hyphal network, gives the colony a distinctly zonate appearance with sharp contrast to the surrounding areas. Margin filiform to weakly fimbriate, reddish-brown; a soluble pigment diffuses into the agar, forming a beige to light-brown halo. Reverse beige to light brown, becoming medium to olivaceous brown with age. Conspicuously zonate: a dark-brown central disc surrounded by 1–2 darker brown rings, with paler, semi-translucent interzones. Colour halos approach yet remain discrete near the plate center. Periphery paler, with a beige to light-brown halo diffusing into the agar; no exudate droplets observed. Margin filiform.

Material examined: China, Guizhou Province, Tongren City, Jiangkou County, Mamagou, on decaying wood in a terrestrial habitat, 6 December 2024, Xia Tang, X7 (GZAAS25-0693, holotype, ex-type living culture GZCC 25-0665).

Notes: In the phylogenetic analysis, our collection formed a clade as sister to *Saprosporodochifer fuscus* (MELCC 24-0105) (Figure 3.8). Our collection displays a similar character with S. fuscus such as micronematous, mononematous, unbranched conidiophores; monoblastic, integrated conidiogenous cells and solitary, various shaped muriform, phragmosporous, verrucose conidia (Liu et al., 2024). However, our collection can be distinct with S. fuscus by its larger conidia (9–15 × 10–16 µm, L/W = 0.91) vs. (7–11 × 5.5–9.5 µm, L/W = 1.2). Nucleotide comparison between our collection and *S. fuscus* revealed differences of 6.1% (28/456 bp) in the ITS region and

1.1% (9/803 bp) in the LSU region, excluding gaps. Based on the distinctive morphological characteristics of our specimen and the phylogenetic distinctiveness, we propose our collection as a novel species, named *S. verrucosus* in accordance with the taxonomic guidelines of Jeewon and Hyde (2016) and Maharachchikumbura et al. (2021).

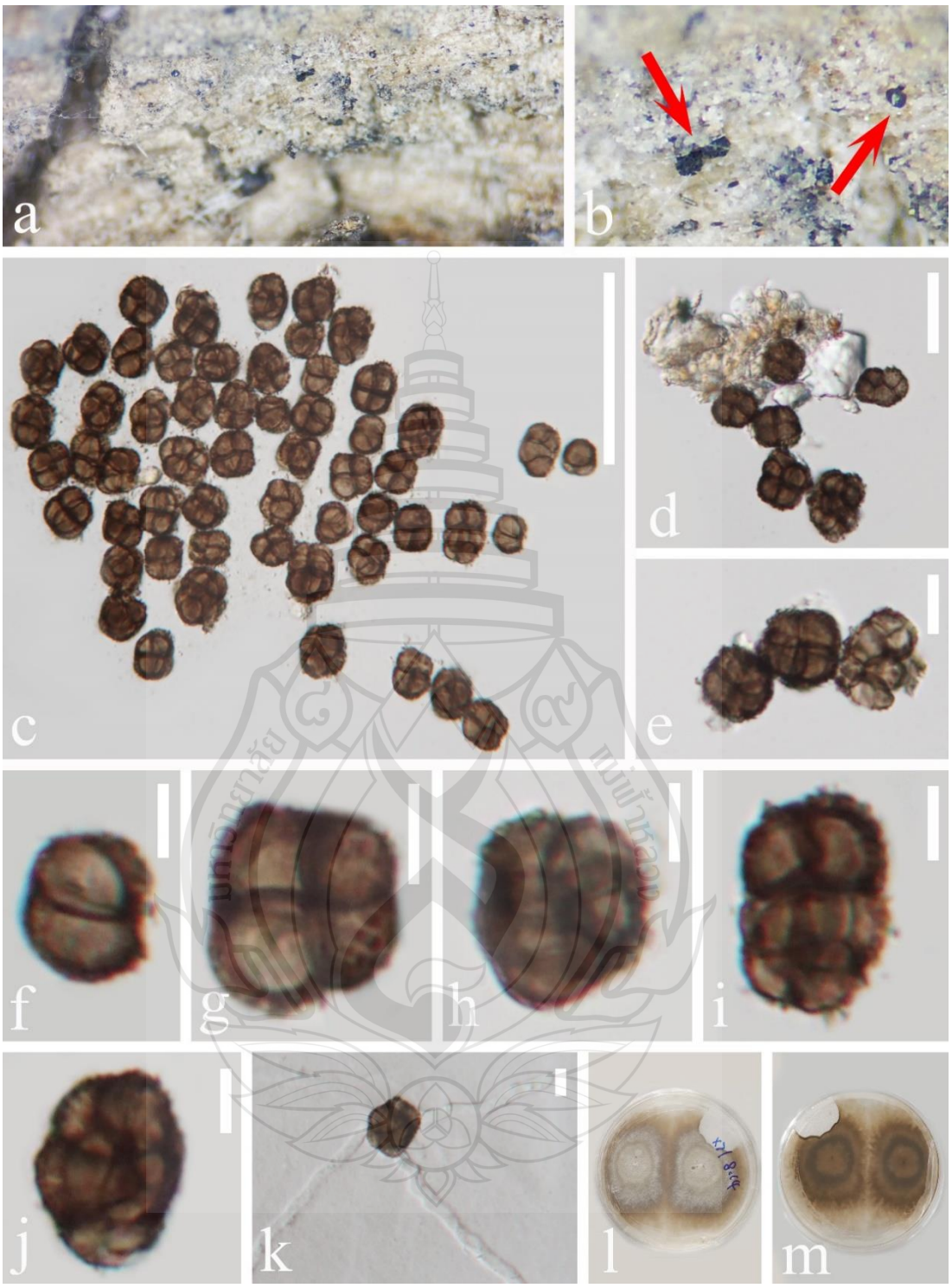

Figure 3.9 *Saprosporodochifer verrucosus* (GZAAS25-0594, holotype)

Figure 3.9 a, b Colonies on host substrate. c, e–j Conida. d Conidiogenous cells and conidia. k Germinated conidium. l Colony on PDA (from front). m Colony on PDA (from reverse). Scale bars: c = 50 μm, d = 20 μm, e = 10 μm, f–k = 5 μm.

Jahnulales K.L. Pang, Abdel-Wahab, El-Shar., E.B.G. Jones & Sivichai, Mycol. Res. 106 (9): 1033 (2002)

Aliquandostipitaceae Inderb., Amer. J. Bot. 88 (1): 54 (2001)

Xylomyces Goos, R.D. Brooks & Lamore, Mycologia 69 (2): 282 (1977)

*Index Fungorum numbe*r: IF 10460; *Facesoffungi number*: FoF 07690;

Notes: *Xylomyces* was established by Goos et al. (1977), with *X. chlamydosporus* designated as the type species. Members of this genus are primarily distributed in freshwater habitats worldwide, though a few occur in terrestrial environments. They are typically associated with plants as saprobes (Castañeda & Kendrick, 1990; Goos et al., 1977; Goh et al., 1997; Kohlmeyer & Volkmann-Kohlmeyer, 1998; Hyde & Goh, 1999; Oliveira et al., 2015; Alves & Gusmão, 2024; this study). Species of *Xylomyces* was characterized by multiseptate, cylindrical to fusiform, spindle-shaped, unbranched, solitary or catenate intercalary or terminal, truncated base, brown to dark brown chlamydospores with lacking of conidiophores and conidia (Goos et al., 1977; Oliveira et al., 2015; Alves & Gusmão, 2024). To date, nine species are currently accepted within this genus, and its sexual morph remains unobserved (Goh et al., 1997; Kohlmeyer & Volkmann-Kohlmeyer, 1998; Hyde & Goh, 1999; Oliveira et al., 2015; Alves & Gusmão, 2024; this study).

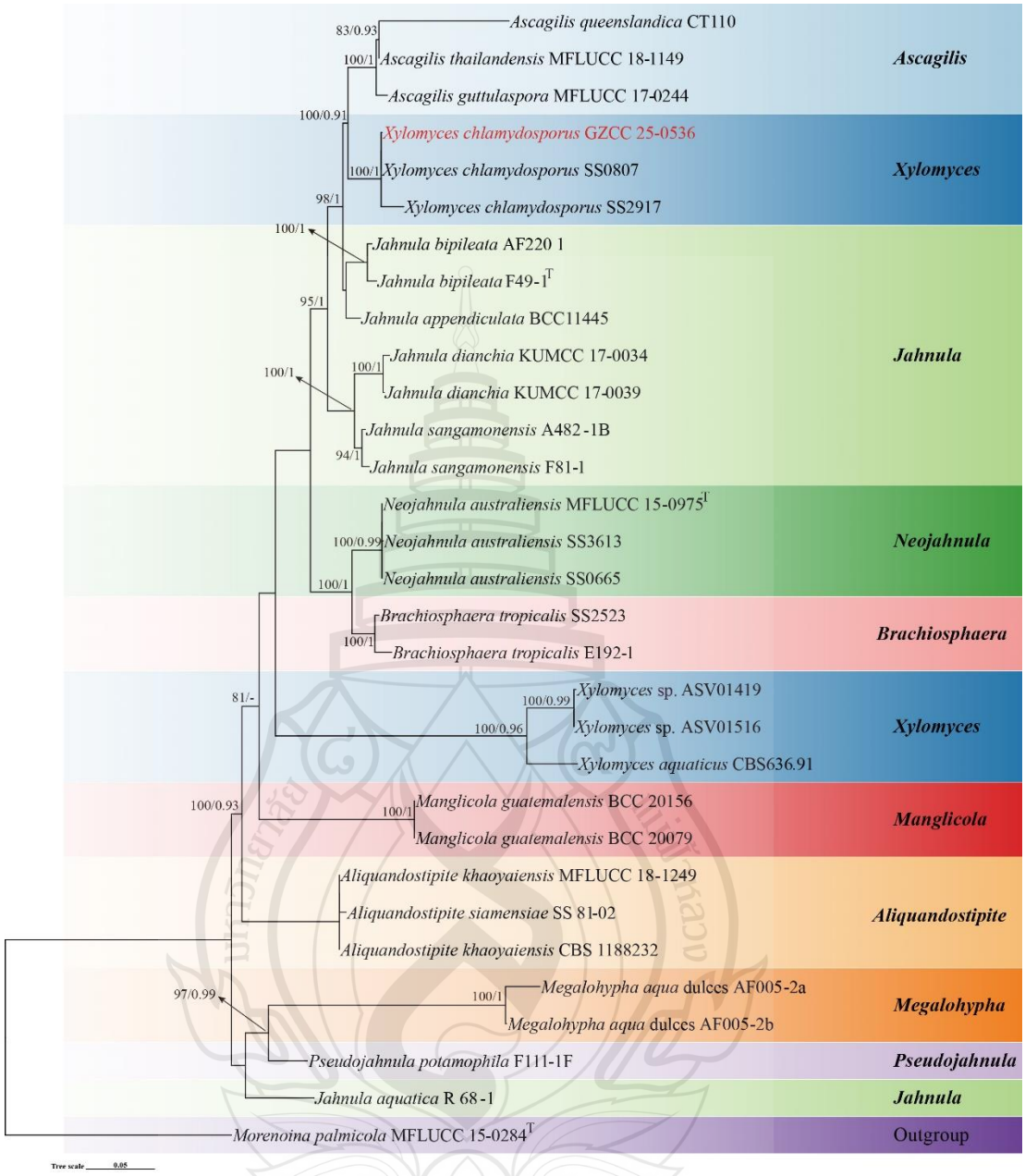

Figure 3.10 Phylogenetic analysis of *Xylomyces*

Figure 3.10 Phylogenetic analysis of *Xylomyces* was conducted using RAxML-based maximum likelihood analysis of a combined LSU, and ITS DNA sequence dataset. Bootstrap support values for maximum likelihood (ML) equal to or greater than 70% and Bayesian posterior probabilities (PP) equal to or greater than 0.95 are shown above the nodes. The tree is rooted with *Morenoina palmicola* (MFLUCC 15-0284). Newly generated strains are highlighted in red, and type strains are indicated with a superscript 'T'.

Xylomyces chlamydosporus Goos, R.D. Brooks & Lamore, Mycologia 69 (2): 282 (1977); Figure 3.11

Saprobic on unidentified decaying wood in the forest. **Sexual morph**: Undetermined. **Asexual morph**: *Colonies* on natural substrate effuse, reddish-brown to blackish. *Mycelium* mostly partly superficial, composed of branched, septate, 5–18(–24) μm wide, dematiaceous, anastomosing hyphae. *Conidiophore* inconspicuous. conidia not developed. *Chlamydospores* abundant, fusiform, intercalary, straight or curved, solitary, 278.5–694 × 26.5–47 μm ($\overline{x}$ = 427.8 × 35.2 μm, n = 20), with 7–14 septa, constricted at the septa, dark brown to blackish, gradually paler toward both ends.

Culture characteristics: Colonies incubate at 25°C, circular, rough, cottony, dry, umbonate, reddish brown with a filiform margin. The colony exhibits concentric zonation, with mycelial density decreasing centrifugally, forming a distinct marginal ring due to abrupt thinning of peripheral hyphae. Colony reverse exhibits uniform reddish-brown pigmentation, discrete, circular, with a distinct darker ring at periphery. Colonies surrounded by a diffuse halo of sparse mycelium.

Material examined: China, Hainan province, Wuzhishan National Nature Reserve, saprobic on unidentified decaying wood, 27th November 2024, Zili Li, W6 (GZAAS25-0566), living culture GZCC 25-0536.

Known distribution: Brunei Darussalam (Goh et al., 1997); China (Goh et al.,1997; Lu et al., 2000; Zhuang 2001; this study); Seychelles (Goh et al., 1997); Thailand (Suetrong et al., 2011); USA (Goh et al., 1997).

Known hosts: *Bauhinia purpurea* (Lu et al., 2000; Zhuang et al., 2001); *Phragmites* sp. (Goh et al., 1997); *Pinus massoniana* (Lu et al., 2000; Zhuang et al., 2001); Submerged wood in freshwater streams (Goh et al.,1997; Suetrong et al., 2011); Unidentified decaying wood (this study).

Notes: Morphologically, our collection conforms to the diagnostic features of *Xylomyces chlamydosporus*, characterized by macronematous, mononematous conidiophores with numerous short branches; tretic, doliiform to lageniform conidiogenous cells that proliferate from the apical or subapical parts of the subtending cells; and cylindrical to occasionally clavate conidia that are 3–4-septate, distinctly constricted and darkened at the septa, and rounded at the apex (Su et al., 2016). In phylogenetic analyses, our collection (GZCC 23-0731) clustered with *X. chlamydosporus* (SS0807 and SS2917)

(Figure 3.11). Excluding gaps, sequence comparison revealed only 0.2% difference (1/502 bp) in the ITS region between our isolate and *X. chlamydosporus* (SS0807). Based on these morphological and molecular data, we identify our isolate as *Xylomyces chlamydosporus*, following the guidelines of Jeewon and Hyde (2016) and Maharachchikumbura et al. (2021). This study represents the first report of *X. chlamydosporus* from China supported by morphological characters and sequence data.

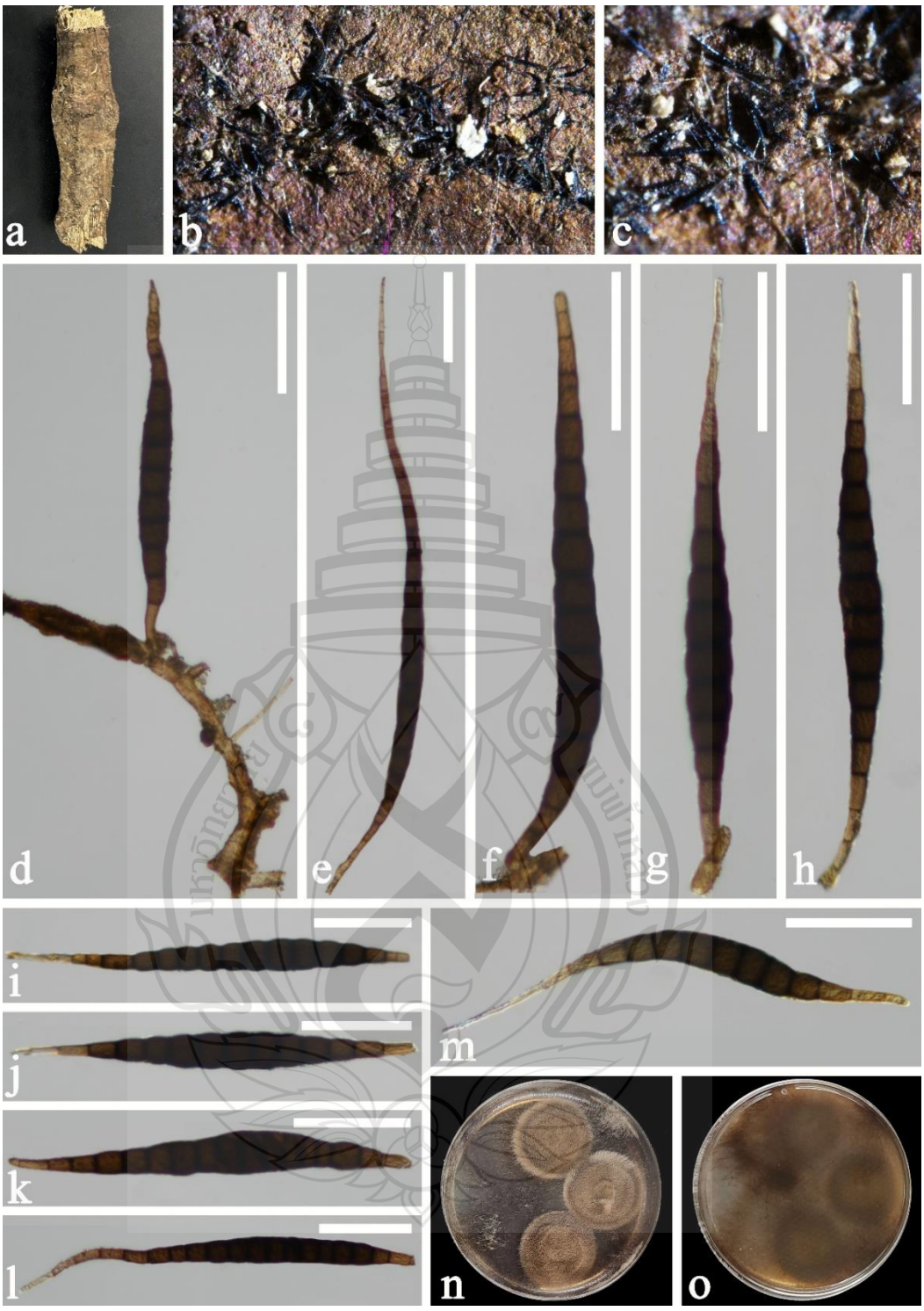

Figure 3.11 *Xylomyces chlamydosporus* (GZAAS25-0566, new collection)

Figure 3.11 a Specimen. b, c Colonies on substrate. d–h Condiophores, conidiogenous cells, conidiogenous cells bearing conidia. i–m Conidia. n Colony on PDA (from front). o Colony on PDA (from reverse). Scale bars: d–m = 100 μm.

Kirschsteiniotheliales Hern.-Restr., R.F. Castañeda, Gené & Crous, Stud. Mycol. 86: 72 (2017)

Kirschsteiniotheliaceae Boonmee & K.D. Hyde, Mycologia 104 (3): 705 (2012)

Kirschsteiniothelia D. Hawksw., Bot. J. Linn. Soc. 91: 182 (1985)

Index Fungorum number: IF 25723; *Facesoffungi number*: FoF 08040;

Notes: *Kirschsteiniothelia* was introduced by Hawksworth (1985) and typified by *K. aethiops*, based on morphological observation, linking it to its asexual genus, *Dendryphiopsis* S. Hughes. Later, the type species was reclassified with its asexual morph, *K. atra* (Hyde et al., 2011; Wijayawardene et al., 2014). The connection between the sexual morphs of *Kirschsteiniothelia atra* (characterised by cylindrical-clavate, bitunicate, 8-spored or rarely 4-spored asci and ellipsoidal verruculose or smooth ascospores with 1–2 septa, lacking a distinct gelatinous sheath) and the asexual morphs (characterised by macronematous, mononematous and branched conidiophores, monotretic, terminal or intercalary, cylindrical, doliiform conidiogenous cells and acrogenous, solitary, cylindrical, oblong, septate conidia with obtuse ends) were previously established by Hughes (1978). This connection was confirmed from cultures obtained from fragments of the ascomata, based on morphological examination. Schoch et al. (2006) further confirmed the connection between the sexual and asexual morphs of *Kirschsteiniothelia*, based on both morphology and phylogenetic analysis of SSU, LSU, *tef1-α* and *rpb2*. Boonmee et al. (2012) established a novel family, *Kirschsteiniotheliaceae*, based on the connection between the sexual and asexual morph of *Kirschsteiniothelia* and multiple gene (LSU, SSU and ITS) phylogeny. Wijayawardene et al. (2014) suggested the use of *Kirschsteiniothelia* as the updated genus to accommodate *Dendryphiopsis* species. To date, there are 59 species of *Kirschsteiniothelia*, amongst which 18 have been reported only in their sexual morph, 32 reported in their asexual morph and six species documented in both morphs (Boonmee et al., 2012; Su et al., 2016; Sun et al., 2021; Xu et al., 2023; Zhang et al., 2023a; de Farias et al., 2024; Sruthi et al., 2024; this study). Amongst the two asexual morphs that have been described so far, only the dendryphi-opsis-like morph is linked to the sexual morph, while the sporidesmium-like state has not been associated with the sexual morph (Hawksworth, 1985; Wang et al., 2004; Mulenko et al., 2008; Boonmee et al., 2012; Su et al., 2016; Sun et al., 2021; Xu et al.,2023; de Farias et al., 2024).

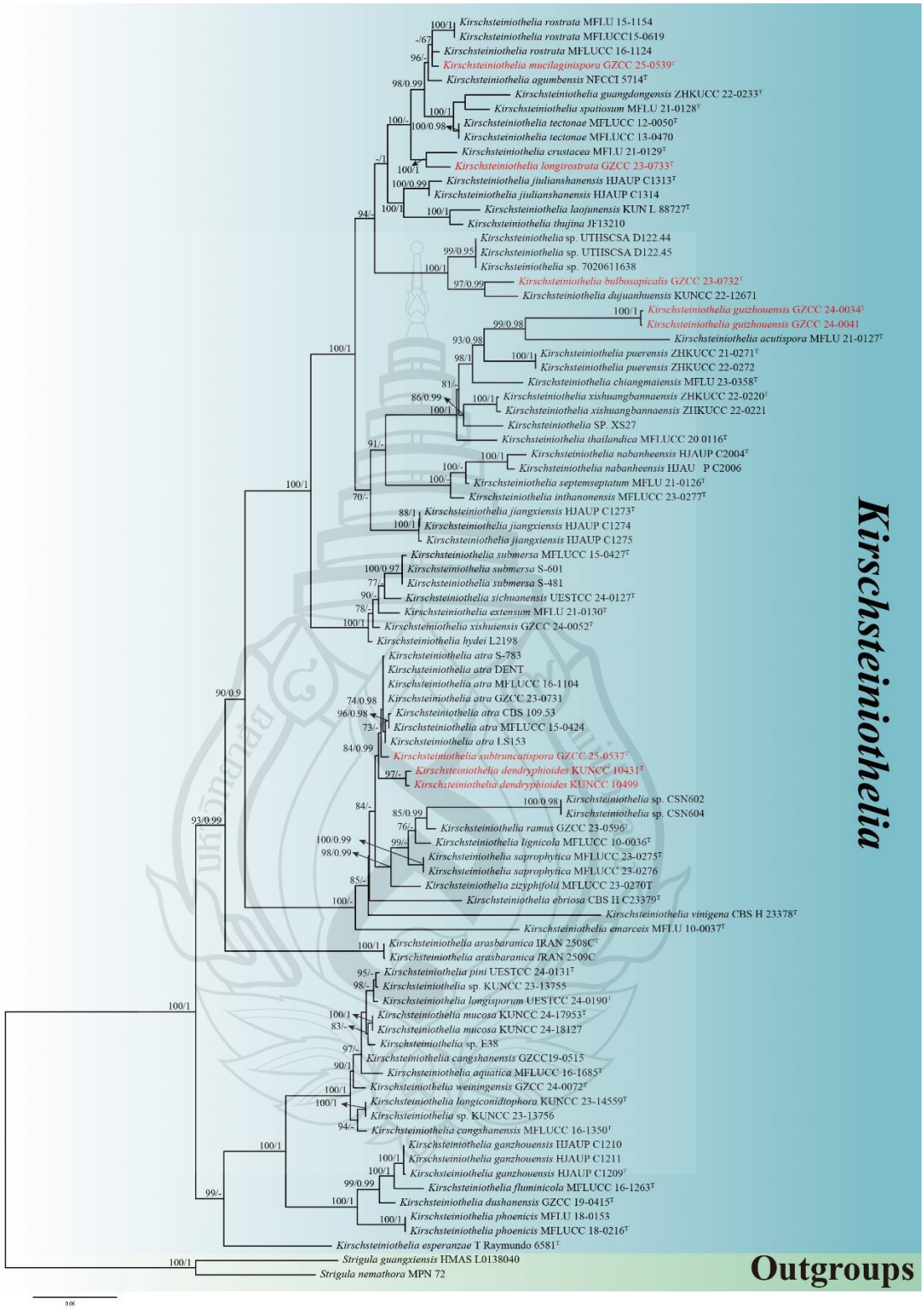

Figure 3.12 The Phylogenetic tree of *Kirschsteiniothelia*

Figure 3.12 Phylogenetic analysis of *Kirschsteiniothelia* was conducted

using RAxML-based maximum likelihood analysis of a combined ITS, LSU, and SSU sequence dataset. Bootstrap support values for maximum likelihood (ML) equal to or greater than 70% and Bayesian posterior probabilities (PP) equal to or greater than 0.95 are shown above the nodes. The tree is rooted with *Strigula guangxiensis* (HMAS-L0138040) and *S. nemathora* (MPN 72). Newly generated strains are highlighted in red, and type strains are indicated with a superscript 'T'.

Kirschsteiniothelia bulbosapicalis X. Tang, K.D. Hyde, Jayaward. & J.C. Kang, sp. nov.; Figure 3.13

Etymology: The specific epithet 'bulbosapicalis' refers to the bulbous area of the conidia at the apex.

Holotype: GZAAS 23-0808

Saprobic on unidentified decaying wood. **Sexual morph**: Undetermined. **Asexual morph**: *Colonies* on the natural substrate superficial, effuse, gregarious, hairy, black, glistening. *Mycelium* semi-immersed, on the substrate, pale brown to dark brown. *Conidiophores* (–47)58–128(–199) µm × 7.5–12.5(–16.5) µm ($\overline{x}$= 86.7 × 10.6 µm, n = 15), macronematous, mononematous, solitary, straight or slightly flexuous, cylindrical, unbranched, septate, smooth, brown to dark brown, truncate at the apex and wider at the base. *Conidiogenous cells* 6–17 µm × 7–10.5 µm ($\overline{x}$= 10.6 × 8.6 µm, n = 15), monoblastic, holoblastic, terminal, determinate, proliferating, cylindrical, brown to dark brown. *Conidia* 118–236.5 µm × 15–27 µm ($\overline{x}$ = 174.8 × 21 µm, n = 30), solitary, acrogenous, cylindrical, ovoid to obclavate, rostrate, smooth, straight or slightly curved, 8–13-septate, slightly constricted at the septa, olivaceous to reddish-brown to dark brown, bulbous at the apex and/or third or fourth cell, truncate at the base, with a spherical hyaline muci-laginous sheath.

Culture characteristics: Conidia germinating on PDA within 24 hours, producing germ tubes from the apex. Colonies displayed a circular morphology with an umbonate elevation, dense growth and a filiform margin. The surface appeared greyish-green, occasionally exhibiting paler mycelium in the bulge region. The reverse colonies exhibited a circular shape with a filiform margin, displaying a dark brown colour, becoming olivaceous towards the periphery.

Material examined: China, Hainan Province, Jianfengling National Forest Park, saprobic on unidentified decaying wood, 23 August 2021, Zili Li, JBT04

(GZAAS 23-0808, holotype), ex-type living culture GZCC 23-0732.

Note: *Kirschsteiniothelia bulbosapicalis* exhibits sporidesmium-like characteristics and shares similar morphologies with other *Kirschsteiniothelia* species. However, *K. bulbosapicalis* can be distinguished from other *Kirschsteiniothelia* species in having different sizes of conidiophores, conidiogenous cells and the unique feature of its conidia, which comprises one or two bulbous structures at or near the apex, with a spherical hyaline mucilaginous sheath. Phylogenetically, *K. bulbosapicalis* is sister to *K. dujuanhuensis* (KUNCC 22-12671) with 85% ML and 0.99 PP support (Figure 3.14). Similar to our new species, *K. dujuanhuensis* also comprises a spherical hyaline mucilaginous sheath. *Kirschsteiniothelia bulbosapicalis* is characterised by larger conidiophores [(–47)58.5–128(–199) µm × 7.5–12.5(–16.5) µm, L/W ratio = 8.2] compared to *K. dujuanhuensis* [29–74(–119) × 9–11 µm, L/W ratio = 5.1] and larger conidia (118–236.5 µm × 15–27 µm, L/W ratio = 8.3) compared to *K. dujuanhuensis* [(114–)122–155(–170) × 10–13(–16) µm, L/W ratio = 11.5]. In addition, *K. bulbosapicalis* exhibits cylindrical to ovoid or obclavate conidia with 8–13 septa and often consist of bulbous structures at the apex and/or the third or fourth cell, as well as a spherical hyaline mucilaginous sheath. In contrast, *K. dujuanhuensis* typically contains obclavate to subcylindrical conidia that are 6–15 septate.

In addition, the comparison of the nucleotides between the sequences of *K. bulbosapicalis* and *K. dujuanhuensis* showed differences of 9% (47/512 bp) across ITS, 1% (8/812 bp) across LSU and 0.1% (2/1003 bp) across SSU, excluding gaps. Based on these findings, we introduce *K. bulbosapicalis* as a novel species, in accordance with the guidelines established by Jeewon and Hyde (2016) and Maharachchikumbura et al. (2021).

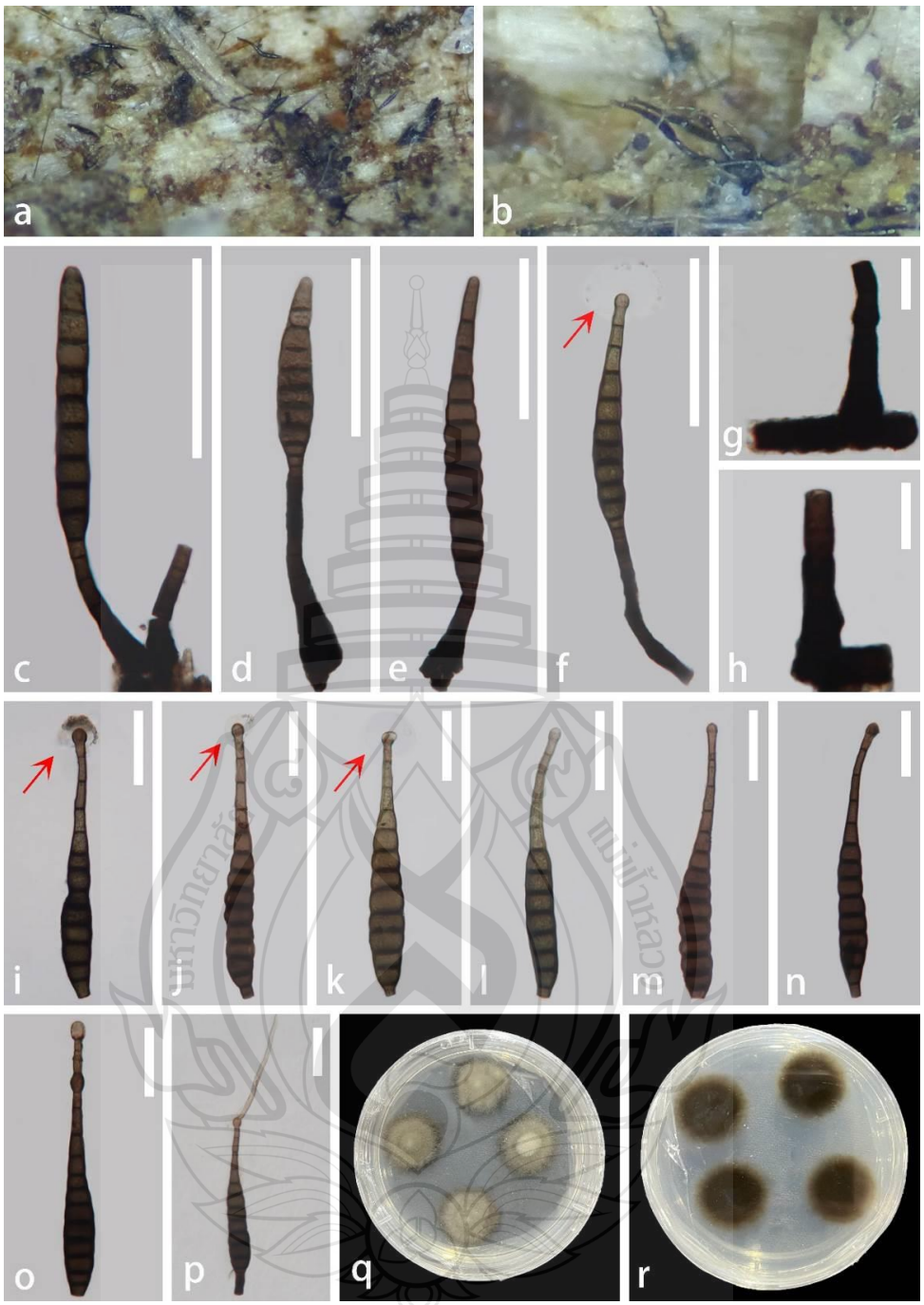

Figure 3.13 *Kirschsteiniothelia bulbosapicalis* (GZCC 23-0732, holotype)

Figure 3.13 a, b Colonies natural substrate. c–f Conidiophores, conidiogenous cells bearing conidia (red arrows indicate mucilaginous sheaths). g, h Conidiophores. i–o Conidia (red arrows indicate mucilaginous sheaths). p A germinated conidium. q Upper surface view of culture. r Lower surface view of culture. Scale bars: c–f = 100 µm, g, h = 20 µm, (i–p) = 50 µm.

Kirschsteiniothelia dendryphioides X. Tang, K.D. Hyde, Jayaward. & J.C. Kang, sp. nov.; Figures 3.14 and Figure 3.15

Etymology: The specific epithet "dendryphioides" is derived from the resemblance to the dendryphiopsis-like features.

Holotype: HKAS 136930

Saprobic on an unidentified decaying wood. **Sexual morph**: Undetermined. **Asexual morph**: *Colonies* on the natural substrate superficial, effuse, scattered, hairy, black, glistening. *Mycelium* partly immersed, on the substrate, pale brown to dark brown. *Conidiophores* 179–467 × 4.5–8 μm ($\overline{x}$ = 318.2 × 6.1 μm, n = 10), macronematous, mononematous, erect, subscorpioid branched, straight or flexuous, cylindrical, septate, smooth, brown to dark brown, becoming paler towards the apex. *Conidiogenous cells* 9–19 × 4–8 μm ($\overline{x}$ = 13.3 × 6.1 μm, n = 30), monotretic, terminal or intercalary, integrated, sometimes percurrent, cylindrical, doliiform, mostly discrete, determinate, smooth, pale brown to brown, both ends appearing darker, with new cells developing from the apical or subapical part of the subtending cells. *Conidia* 30–55 × 9–13.5 μm ($\overline{x}$ = 40 × 11.1 μm, n = 30), solitary, acrogenous, cylindrical, oblong and occasionally clavate, smooth, guttulate, 2–4-septate, slightly or deeply constricted and darker at the septa, brown, rounded at the apex and sometimes truncate at the base, exhibiting obtuse ends.

Culture characteristics: Conidia germinating on PDA within 24 hours. Colonies circular, characterised by dense, flat, spreading and fluffy growth, with an entire margin. The surface displayed a dark brown hue, while the reverse colonies exhibited a circular shape with an entire margin, also appearing dark brown.

Material examined: China, Yunnan Province, Lushui City, Sanhe Village, Gaoligong Mountain, saprobic on decaying wood in a freshwater stream, 5 May 2021, Rong-ju Xu, XS17 (HKAS 136930, holotype), ex-type living culture, KUNCC 10431; China, Yunnan Province, Lushui City, Sanhe Village, Gaoligong Mountain, saprobic on submerged decaying wood in freshwater habitats, 22 August 2021, Rong-ju Xu, SYC-05 (HKAS 135651, paratype), living culture, KUNCC 10499.

Notes: *Kirschsteiniothelia dendryphioides* exhibits dendryphiopsis-like characteristics and shares sim-ilar morphologies with other *Kirschsteiniothelia* species. However, *K. dendryphioides* differs from other species in the size of its conidiophores,

conidiogenous cells and conidia. *Kirschsteiniothelia dendryphioides* is distinct from *K. atra* in having larger conidiophores (179–467 × 4.5–8 µm, L/W ratio = 52.2 vs. 148–228 µm × 6–8 µm, L/W ratio = 27), shorter conidiogenous cells (9–19 × 4–8 µm, L/W ratio = 2.2 vs. 25–33 µm × 5–7 µm, L/W ratio = 4.8) and smaller conidia (30–55 × 9–13.5 µm, L/W ratio = 3.6 vs. 54–63 ×14–18 µm, L/W ratio = 3.4).

The establishment of *Kirschsteiniothelia dendryphioides* as a new species is further supported by molecular data. Based on our phylogenetic analyses, *K. dendryphioides* strains (KUNCC 10431 and KUNCC 10499) form a subclade sister to the strains of *Kirschsteiniothelia atra* (CBS 109.53, DEN, MFLUCC 15-0424, MFLUCC 16-1104 and S-783) with 83% ML and 0.99 PP support (Figure 3.2.5). The comparison of the nucleotides between the sequences of *K. dendryphioides* and *K. atra* (MFLUCC 16-1104) shows a difference of 1.9% (9/481 bp) across ITS and 2.4% (11/458 bp) across SSU, but no difference was observed across LSU (777 bp), excluding gaps. Based on these findings, we introduce *Kirschsteiniothelia dendryphioides* as a novel species, following guidelines outlined in Jeewon and Hyde (2016) and Maharachchikumbura et al. (2021). We were unable to compare the nucleotide differences across LSU and SSU of KUNCC 10499 as it lacks sequence data for these loci.

Figure 3.14 *Kirschsteiniothelia dendryphioides* (HKAS 136930, holotype)

Figure 3.14 a, b Colonies on natural substrate. c, d Conidiophores, conidiogenous cells bearing conidia. e–g Conidiogenous cells bearing conidia. h–o Conidia. p Upper surface view of culture. q Lower surface view of culture. Scale bars: c, d = 100 μm, e = 50 μm, f–o = 20 μm.

Figure 3.15 *Kirschsteiniothelia dendryphioides* (HKAS 135651, paratype)

Figure 3.15 a, b Colonies on natural substrate. c, d Conidiophores, conidiogenous cells bearing conidia. e–g Conidiogenous cells bearing conidia. h–l Conidia. m Upper surface view of culture. n Lower surface view of culture. Scale bars: c, d = 100 μm, (e–l) = 20 μm.

Kirschsteiniothelia longirostrata X. Tang, K.D. Hyde, Jayaward. & J.C. Kang, sp. nov.; Figure 3.16

Etymology: The specific epithet 'longirostrata' refers to the conidia containing a long rostrate.

Holotype: GZAAS 23-0809

Saprobic on an unidentified submerged decaying wood. **Sexual morph**: Undetermined. **Asexual morph**: *Colonies* on the natural substrate superficial, effuse, gregarious, hairy, black, glistening. *Mycelium* partly immersed on the substrate, composed of branched, septate, smooth-walled hyphae, pale to dark brown. *Conidiophores* 80–252 × 4.5–9.5 μm ($\bar{x}$= 161.3 × 6.8 μm, n = 20), macronematous, mononematous, solitary, cylindrical, straight, or slightly flexuous, unbranched, percurrent, smooth, guttulate, 4–13-septate, sometimes slightly constricted at the septa, brown to dark brown tapering towards the apex and wider at the base. *Conidiogenous cells* 6.5–16 × 5–9 μm ($\bar{x}$= 13× 7 μm, n = 20), monoblastic, terminal or indeterminate, percurrently proliferating, cylindrical, pale brown to brown. *Conidia* 36.5–109(–160) × 8–16 μm ($\bar{x}$= 71× 12 μm, n = 30), solitary, acrogenous, cylindrical, obpyriform to obclavate, rostrate 15–100(–120) × 2.5–6 μm ($\bar{x}$= 48 × 4.3 μm, n = 30), smooth, straight or curved, guttulate, 6–18-septate, slightly constricted and darker at the septa, proliferating, pale brown to brown, becoming paler towards the apex, with a truncate base and a mucilaginous sheath surrounding the upper part of the apex.

Culture characteristics: Conidia germinating on PDA within 24 hours, producing germ tubes from the apex. Colonies displayed a circular morphology with dense, flat, spreading and fluffy growth, with an entire margin. The surface exhibited an olivaceous-green hue with a darker edge, while the reverse colonies displayed a circular shape with an entire margin, appearing blackish-green.

Material examined: China, Hainan Province, Jianfengling National Forest Park, saprobic on submerged unidentified decaying wood, 23 August 2021, Zili Li, T10 (GZAAS 23-0809, holotype) ex-type living culture GZCC 23-0733.

Notes: *Kirschsteiniothelia longirostrata* exhibits sporidesmium-like characteristics and shares similar features with other *Kirschsteiniothelia* species. *Kirschsteiniothelia longirostrata* can be distinguished from other *Kirschsteiniothelia* species in having different sizes and shapes of conidiophores, conidiogenous cells and

unique features of conidia, such as obpyriform to obclavate, long rostrate, proliferating, with a mucilaginous sheath surrounding the upper part of the apex. Unlike *K. crustacea*, *K. longirostrata* has cylindrical, proliferating conidiogenous cells and obpyriform to obclavate conidia, with longer (15–100(–120) × 2.5–6 μm), guttulate, proliferating rostrate structures and a mucilaginous sheath surrounding the upper part of the apex.

Molecular data further supports the establishment of *Kirschsteiniothelia longirostrata* as a novel taxon. Based on our phylogenetic analyses, *K. longirostrata* is sister to *K. crustacea* (MFLU 21-0129) with 94% ML and 1.00 PP support (Figure 3.2.5). The comparison of the nucleotides between the sequences of *K. longirostrata* (GZCC 23-0733) and *K. crustacea* (MFLU 21-0129) shows differences of 8.4% (39/467 bp) across ITS and 0.7% (5/718 bp) across LSU, excluding gaps. However, we were unable to compare the nucleotide differences across SSU as *K. crustacea* lacks sequence data for this locus. Based on these findings, we introduce *Kirschsteiniothelia longirostrata* as a novel species, following guidelines outlined in Jeewon and Hyde (2016) and Maharachchikumbura et al. (2021).

Figure 3.16 *Kirschsteiniothelia longirosrata* (GZCC 23-0733, holotype)

Figure 3.16 a Unidentified submerged wood. b Colonies on natural substrate. c, d Conidiophores, conidiogenous cells. e–g Conidiophores, conidiogenous cells bearing conidia. h–p Conidia (red arrows indicate mucilaginous sheaths). q A germinated conidium. r Upper surface view of culture. s Lower surface view of culture. Scale bars: (c–g) = 100 µm, (h–q) = 20 µm.

Kirschsteiniothelia mucilaginispora X. Tang, Jayaward, J.C. Kang & K.D. Hyde, sp. nov.; Figure 3.17

Etymology: The specific epithet 'mucilaginispora' refers to the conidia contain a mucilaginous sheath surrounding the upper part of the conidia with clavate shape.

Holotype: GZAAS25-0569

Saprobic on an unidentified decaying wood in the forest. **Sexual morph**: Undetermined. **Asexual morph**: *Colonies* on the natural substrate superficial, effuse, gregarious, hairy, black. *Mycelium* partly immersed on the substrate, composed of branched, septate, smooth-walled hyphae, pale brown to dark brown. *Conidiophores* 37.5–98 × 5.5–10 μm ($\overline{x}$ = 78 × 8 μm, n = 15), macronematous, mononematous, solitary, cylindrical, straight, or slightly flexuous, unbranched, smooth, 4–6-septate, brown to dark brown, slightly tapering towards the apex and wider at the base. *Conidiogenous cells* 7.5–16 × 5–6.5 μm ($\overline{x}$ = 11.7 × 6.3 μm, n = 15), monoblastic, terminal or indeterminate, percurrently proliferating, cylindrical, sometimes lageniform, brown. *Conidia* 55–203 × 8–20.5 μm ($\overline{x}$ = 125.5× 14.7 μm, n = 25), solitary, acrogenous, cylindrical, obclavate with a distinct, long rostrate 93–279 × 2.5–3.5 μm ($\overline{x}$ = 166.6 × 3.1 μm, n = 6), sometimes secondary conidia developed from the rostrate apices of primary conidia, smooth, straight or curved, 10–19-septate, constricted and darker at the septa, brown to dark brown, becoming paler towards the apex, with a truncate base and with a mucilaginous sheath surrounding the upper part of the conidia with clavate shape.

Culture characteristics: Colonies on PDA at 25°C, circular, umbonate, and dry with an entire margin. Surface rough and cottony, fluffy, gray with a circular, grayish-white ring at the edge; reverse uniformly dark brown with a circular, grayish-white ring at the edge.

Material examined: CHINA, Hainan Province, Wuzhishan City, Wuzhishan National Nature Reserve, on unidentified decaying wood, 27 November 2024, Zili Li, L2 (GZAAS25-0569, holotype, ex-type living culture GZCC 25-0539.

Notes: *Kirschsteiniothelia mucilaginispora* is characterized by macronematous, mononematous conidiophores, monoblastic and terminal (or occasionally indeterminate) conidiogenous cells, and solitary, acrogenous, cylindrical

to obclavate conidia. The conidia are brown to dark brown, with a distinct rostrate apex and a mucilaginous sheath surrounding the upper part, conforming to the generic concept of Kirschsteiniothelia. However, *Kirschsteiniothelia mucilaginispora* can be distinct with other *Kirschsteiniothelia* species by having secondary conidia developed from the rostrate apices of primary conidia and with a mucilaginous sheath only in the upper part of the conidia with clavate shape and longer rostrate.

Phylogenetic analysis revealed a close relationship between *Kirschsteiniothelia mucilaginispora* and *K. rostrata* (MFLU 15-1154, MFLUCC 15-0619, and MFLUCC 16-1124). However, *K. mucilaginispora* differs with the hoplotype of K. rostrata morphologically by its shorter conidiophores (37.5–98 × 5.5–10 μm, L/W = 9.75 vs. 190–450 × 9–15 μm, L/W = 23.3), larger conidia (55–203 × 8–20.5 μm, L/W = 8.5 vs. 80–150 × 10–20 μm, L/W = 7.7), and notably longer rostrate (93–279 × 2.5–3.5 μm, L/W = 53.7), which sometimes produce secondary conidia from their apices. Additionally, nucleotide comparisons with *K. rostrata* (MFLUCC 15-0619) reveal 5% difference (25/496 bp) in ITS and 0.6% difference (5/824 bp) in LSU (gaps excluded), further supporting its distinction.

In our phylogenetic analysis, *K. rostrata* (MFLUCC 16-1124) clusters with our new species. However, morphologically, it differs from *K. rostrata* (MFLU 15-1154 and MFLUCC 15-0619) in having solitary conidiophores (vs. caespitose), longer conidiophores (190–450 × 9–15 μm, L/W ratio = 23.3 vs. 90–120 × 7.5–8.5 μm, L/W ratio = 13.1), and longer, narrower conidia (80–150 × 10–20 μm, L/W ratio = 8.5 vs. 77.5–108.5 × 17.5–20.5 μm, L/W ratio = 4.89). Since only LSU sequence data are available for *K. rostrata* (MFLUCC 16-1124), we could not compare other gene regions. However, when using our new species, K. mucilaginispora, as reference, it differs from *K. rostrata* (MFLU 15-1154 and MFLUCC 15-0619) but shows similarity to *K. rostrata* (MFLUCC 16-1124). Based on these genetic and morphological distinctions along with differences from all examined existing species, we propose the new species *K. mucilaginispora*. This taxonomic delineation follows the species recognition criteria established by Jeewon and Hyde (2016) and Maharachchikumbura et al. (2021).

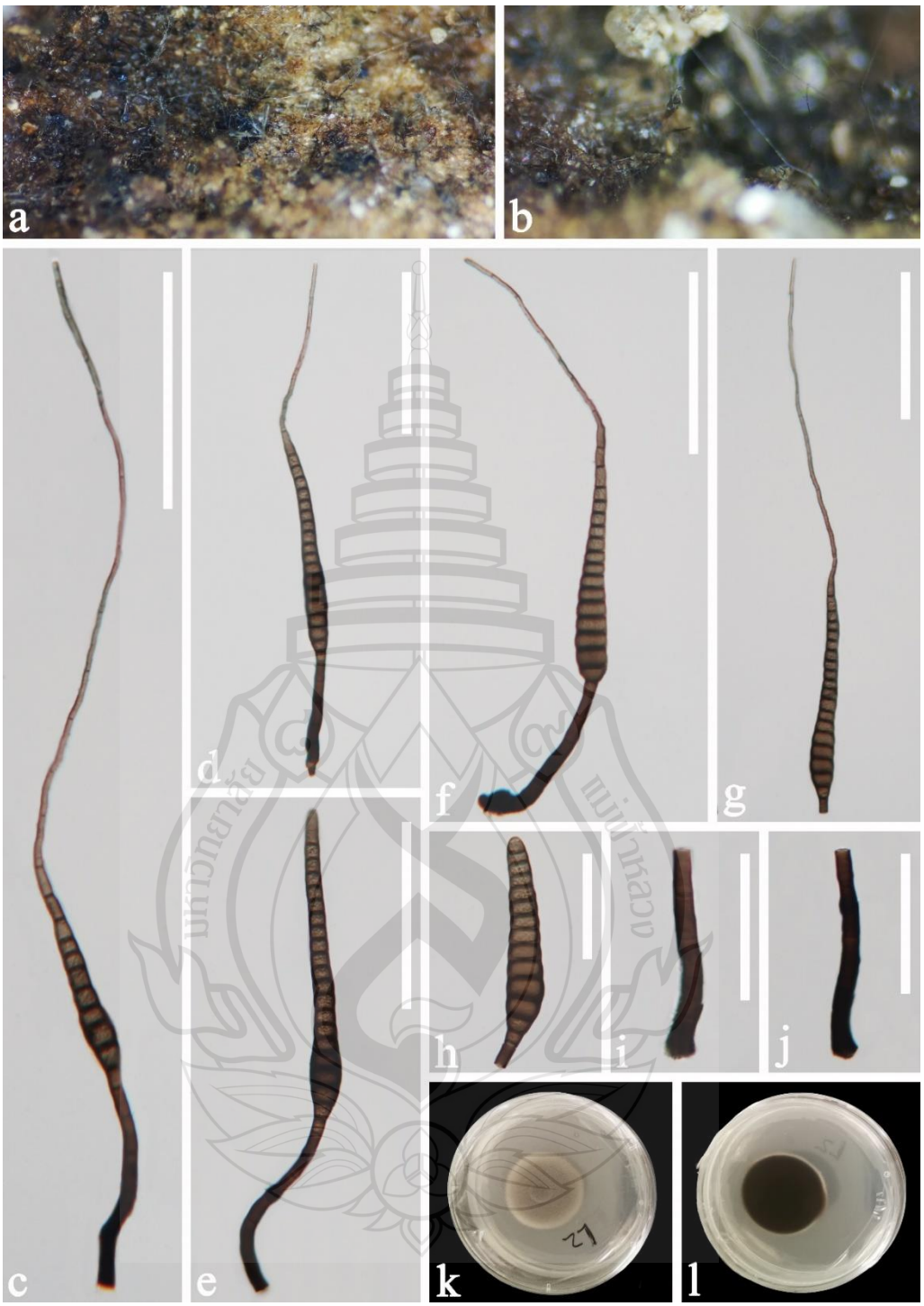

Figure 3.17 *Kirschsteiniothelia mucilaginispora* (GZAAS25-056, holotype)

Figure 3.17 a, b Colonies on substrate. c–f Condiophores, conidiogenous cells, conidiogenous cells bearing conidia. g, h Conidia. i, j Condiophores. k Colony on PDA (from front). l Colony on PDA (from reverse). Scale bars: c–g = 100 μm, h–j = 50 μm.

Kirschsteiniothelia subtruncatispora X. Tang, Jayaward, J.C. Kang & K.D. Hyde, sp. nov.; Figure 3.18

Etymology: The specific epithet 'subtruncatispora' refers to the subtruncate morphology of the conidial base.

Holotype: GZAAS25-0567

Saprobic on unidentified decaying wood in the forest. **Sexual morph**: Undetermined. **Asexual morph**: *Colonies* on the natural substrate superficial, effuse, scattered, hairy, black, glistening. *Mycelium* mostly partly superficial, composed of branched, septate, brown to dark brown. *Conidiophores* 95–438 × 6–13 μm ($\overline{x}$ = 253.2 × 9.5 μm, n = 30), macronematous, mononematous, erect, subscorpioid branched, straight or flexuous, cylindrical, septate, smooth, brown, dark brown at septate, becoming paler towards the apex. *Conidiogenous cells* 13.5–28.5 × 3.5–9 μm ($\overline{x}$ = 20.5 × 6.4 μm, n = 55), monotretic, terminal or intercalary, integrated, sometimes percurrent, cylindrical, doliiform, mostly discrete, determinate, smooth, brown, both ends appearing darker, with new cells developing from the apical or subapical part of the subtending cells. *Conidia* 34–59 × 13–19.5 μm ($\overline{x}$ = 46.81 × 15.65 μm, n = 55), solitary, acrogenous, cylindrical, oblong and occasionally clavate, rarely reniform, smooth, guttulate, 3–4-septate, slightly or deeply constricted and darker at the septa, brown, rounded at the apex, subtruncate at the base, exhibiting obtuse ends.

Culture characteristics: Colonies on PDA at 25°C, circular, flat, and dry with a filamentous margin. Surface rough and cottony, brown with a gray-white center; reverse uniformly dark brown. Surrounded by a diffuse halo of sparse, light-colored mycelium.

*Material examine*d: China, Guizhou province, Xingyi City, on unidentified decaying wood, 27 November 2024, Xia Tang, GC04 (GZAAS25-0567, holotype, ex-type living culture GZCC 25-0537.

Notes: The asexual morph of *Kirschsteiniothelia subtruncatispora* exhibits typical dendryphiopsis-like features. Phylogenetic analysis revealed a close relationship with *K. atra* (KUNCC 10431) and *K. dendryphioides* (KUNCC 10499). However, the new species can be distinguished by the following key morphological differences: *K. subtruncatispora* differs from *K. atra* in the size of its conidiophores, conidiogenous cells and conidia. *Kirschsteiniothelia subtruncatispora* is distinct from

K. atra in having longer conidiophores (95–438 × 6–13 µm, L/W ratio = 26.65 vs. 148–228 µm × 6–8 µm, L/W ratio = 27), shorter conidiogenous cells (13.5–28.5 × 3.5–9 µm, L/W ratio = 3.2 vs. 25–33 µm × 5–7 µm, L/W ratio = 4.8) and smaller conidia (34–59 × 13–19.5 µm, L/W ratio = 3.0 vs. 54–63 ×14–18 µm, L/W ratio = 3.4). While, *K. subtruncatispora* differs from *K. dendryphioides* in having shorter and broader conidiophores (95–438 × 6–13 µm, L/W ratio = 26.65 vs. 179–467 × 4.5–8 µm, L/W ratio = 52.2), longer conidiogenous cells (13.5–28.5 × 3.5–9 µm, L/W ratio = 3.2 vs. 9–19 × 4–8 µm, L/W ratio = 2.2) and larger conidia (34–59 × 13–19.5 µm, L/W ratio = 3.0 vs. 30–55 × 9–13.5 µm, L/W ratio = 3.6).

Phylogenetic analyses provide robust support for the establishment of *Kirschsteiniothelia subtruncatispora* as a novel species. Our strain (GZCC 25-0537) forms a well-supported subclade (80% ML bootstrap/xxx PP) sister to *K. atra* (CBS 109.53, DEN, MFLUCC 15-0424, MFLUCC 16-1104, S-783) and *K. dendryphioides* (KUNCC 10431, KUNCC 10499) in the concatenated ITS, LSU and SSU phylogeny (Figure 3.2.5). The comparison of the nucleotides between the sequences of *K. subtruncatispora* and *K. atra* (MFLUCC 16-1104) shows a difference of 1.6% (8/490 bp) across ITS and 0.1% (1/789 bp) across LSU, excluding gaps. The comparison of the nucleotides between the sequences of *K. subtruncatispora* and *K. dendryphioides* (KUNCC 10431) shows a difference of 3.2% (16/500 bp) across ITS and 0.1% (1/778 bp) across LSU, excluding gaps. These genetic distances, combined with distinct morphological characters, satisfy the species delineation criteria proposed by Jeewon and Hyde (2016) and Maharachchikumbura et al. (2021). The congruent molecular and phenotypic evidence supports the recognition of *K. subtruncatispora* as a new taxon within *Kirschsteiniothelia*.

Figure 3.18 *Kirschsteiniothelia subtruncatispora* (GZAAS25-0567, holotype)

Figure 3.18 a Specimen. b, c Colonies on substrate. d, e Condiophore, conidiogenous cells, conidiogenous cells bearing conidia. f–l Conidia. m Germinated conidium. n Colony on PDA (from front). o Colony on PDA (from reverse). Scale bars: d = 100 μm; e = 50 μm. f–m = 20 μm.

Mytilinidiales E. Boehm, C.L. Schoch & Spatafora, Mycol. Res. 113(4): 468 (2009)

Mytilinidiaceae Kirschst. [as 'Mytilidiaceae'], Verh. bot. Ver. Prov. Brandenb. 66: 28 (1924)

Lophium Fr., Observ. mycol. (Havniae) 2: 345 (1818)

Index Fungorum number: IF 2936; *Facesoffungi number*: FoF 08103

Notes: *Lophium* was described by Fries (1818), and *Lophium mytilinum* was assigned as the type species. Initially, Fries (1823) included this genus in *Pyrenomycetes*. Later, several studies based on morphology and phylogenetic analyses accepted *Lophium* in *Mytilinidiaceae* (Boehm et al., 2009a, 2009b; Hyde et al., 2017). The genus is characterized by having carbonaceous, conchate ascocarps, seated on a foot-like base, or sessile on the substrate, cylindrical, bitunicate, short stiped asci with spirally arranged, multiseptated, filiform, yellowish hyaline ascospores with tapered at ends (Boehm et al., 2009a, 2009b; Pem et al., 2019; https://dothideomycetes.org/). Asexual morph of the genus has been less documented (Hernandez-Restrepo et al., 2016; Hyde et al., 2017). Currently, 15 species are accepted under *Lophium* (Species Fungorum, 2025). This study presents a new record of *Lophium arboricola* collected from Yunnan, China.

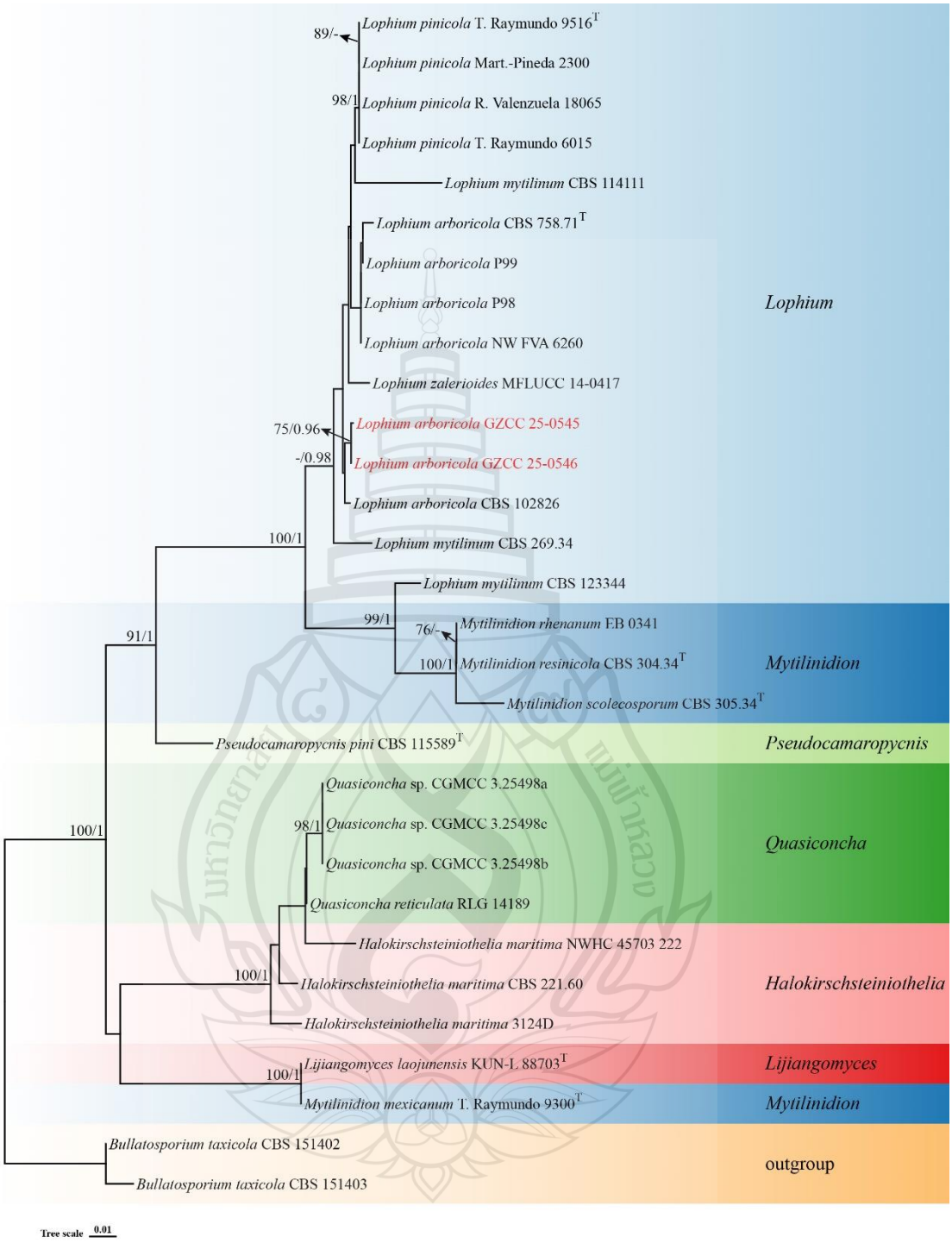

Figure 3.19 Phylogenetic analysis of *Lophium*

Figure 3.19 Phylogenetic analysis of *Lophium* was conducted using RAxML-based maximum likelihood analysis of a combined LSU and ITS sequence dataset. Bootstrap support values for maximum likelihood (ML) equal to or greater than 70% and Bayesian posterior probabilities (PP) equal to or greater than 0.95 are shown

above the nodes. The tree is rooted with *Bullatosporium taxicola* (CBS 151402 and CBS 151403). Newly generated strains are highlighted in red, and type strains are indicated with a superscript 'T'.

Lophium arboricola (Buczacki) Madrid & Gené 2016; Figure 3.20

Basionym: Zalerion arboricola Buczacki 1972

Saprobic on decaying wood in a terrestrial habitat. **Sexual morph**: Unknown. *Asexual morph*: Hyphomycetous, *Colonies* on natural substrate superficial, effuse, gregarious, with masses of crowded, glistening conidia, balck. *Mycelium* partly immersed, partly superficial, composed of hyaline to pale brown, branched, septate, smooth hyphae. *Conidiophores* reduced to conidiogenous cells. *Conidiogenous cells* 3.5–6 × 4.5–5.5 μm ($\bar{x}$ = 4.5× 4.8 μm, n = 30), short-cylindrical, monoblastic, integrated, terminal on hyphae, determinate, pale brown. *Conidia* 16–31 × 14–25 μm ($\bar{x}$ = 22 × 17 μm, n = 30), solitary, irregular, coiled in several planes, multi-cellular, thick-walled, verrucose, rounded at the base, dark brown.

Culture characteristics: Conidia germinated on PDA media within 12 h. Several germ tubes are produced. Colonies are irregular, with filamentous margin, raised and flat at the center, smooth, grey to pale brown from above, brown to black brown from below.

Material examined: China, Guizhou province, Liupanshui City, Yushe National Forest Park, on unidentified decaying wood, 27 November 2024, Xia Tang, LS138 (GZAAS25-0576), living culture (GZCC 25-0546). China, Guizhou province, Liupanshui City, Yushe National Forest Park, on unidentified decaying wood, 27 November 2024, Xia Tang, LS71 (GZAAS25-0575), living culture (GZCC 25-0545).

Notes: In the phylogenetic analysis, strains of our isolates (GZCC 25-0545 and GZCC 25-0546) are grouped within *Lophium*, sister to the strain of *L. arboricola* (CBS 102826), with 46% ML bootstrap support (Figure 3.2.12). However, the type material of *L. arboricola* (CBS 758.71) grouped distinct to our strains and CBS 102826. In comparison of the base pair differences in ITS our strains show 0.9% (4/444) difference with CBS 102826, while 1.8% (9/498) difference with CBS 758.71. Morphologically, characteristics of our collection fits with the characters of *L. arboricola* collection (Czachura & Janik, 2023). Based on the strong morphological evidence and results of phylogeny, we identify our isolates as another record of *Lophium arboricola*.

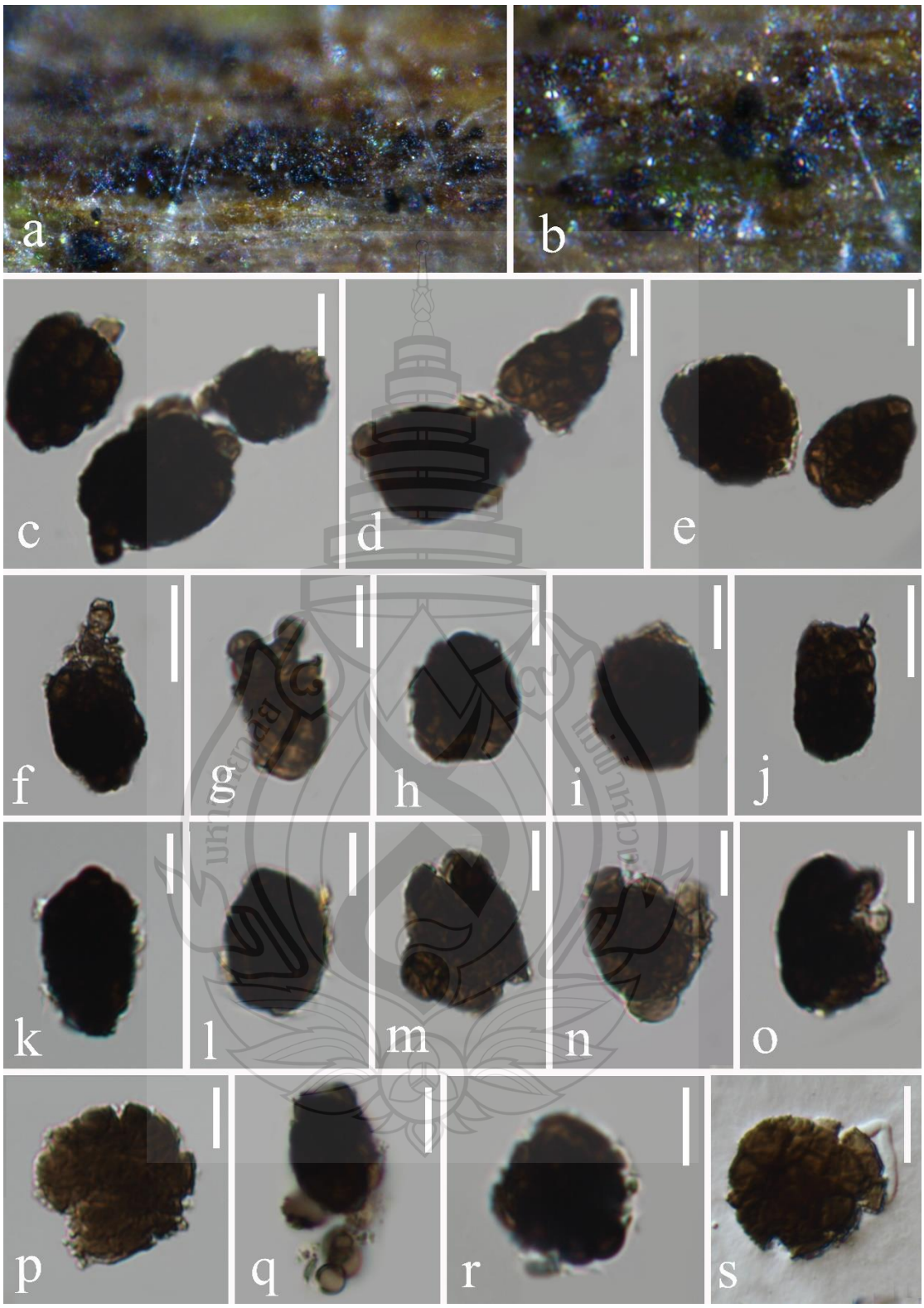

Figure 3.20 *Lophium arboricola* (GZAAS25-0575, new collection)

Figure 3.20 a, b Colonies on the natural substrate. c, d, f, g Conidia with conidiogenous cells. e, h-p Conidia. q A germinated conidium. Scale bars: e, j = 20 µm, c, d, f-i, k-p, r, s = 10 µm, q = 5 µm.

Pleosporales Luttr. ex M.E. Barr, Prodr. Cl. Loculoasc. (Amherst): 67 (1987)

Anteagloniaceae K.D. Hyde, Jian K. Liu & A. Mapook, in Hyde et al.,, Fungal Diversity 63: 33 (2013)

Anteaglonium Mugambi & Huhndorf, Syst. Biodiv. 7(4): 460 (2009)

Index Fungorum number: IF 541631; *Facesoffungi number*: FoF 06701;

Notes: *Anteaglonium* was introduced by Mugambi and Huhndorf (2009) to accommodate hysterothecial taxa outside of *Hysteriales*, *viz. A. abbreviatum* (= *Glonium abbreviatum*) as the type species, and three other species. Later, Hyde et al. (2013) placed this genus within *Anteagloniaceae*. Sexual morph of *Anteaglonium* is characterized by globose to subglobose or elongate, fusiform to oblong, erumpent to superficial brown to black, hysterothecial ascomata with pronounced or longitudinal slit, with or without KOH extractable pigments; cylindrical, 8-spored, uni- or biseriate asci with short pedicle; fusiform to oblong, septate, hyaline or pigmented ascospores (Mugambi & Huhndorf, 2009; Suwannarach et al., 2023). Coelomycetous asexual morphs developed on the culture media such as *A. parvulum* and *A. thailandicum* and *A. soli* have been reported in different studies (Jayasiri et al., 2016; Suwannarach et al., 2023; Yasanthika et al., 2025). The key characteristics of asexual morphs of *Anteaglonium* are pycnidial, uniloculate or multi-loculate conidiomata with long, unbranched conidiophores, with globose, hyaline conidiogenous cells and oval to globose, aseptate conidia with rounded ends. Species in this genus are reported on dead or decaying woody, cupule, culms, or leaf substrates rocks and soils in different regions *viz*. Australia, China, Greece, Kenya, Spain, Thailand, and the USA (Jayasiri et al., 2016; Yasanthika et al., 2025). To date, 14 species are accepted under *Anteaglonium* in Index Fungorum (2025) and molecular data are available for all species. This study presents a new species of *Anteaglonium*, where collected on unidentified decaying wood from China.

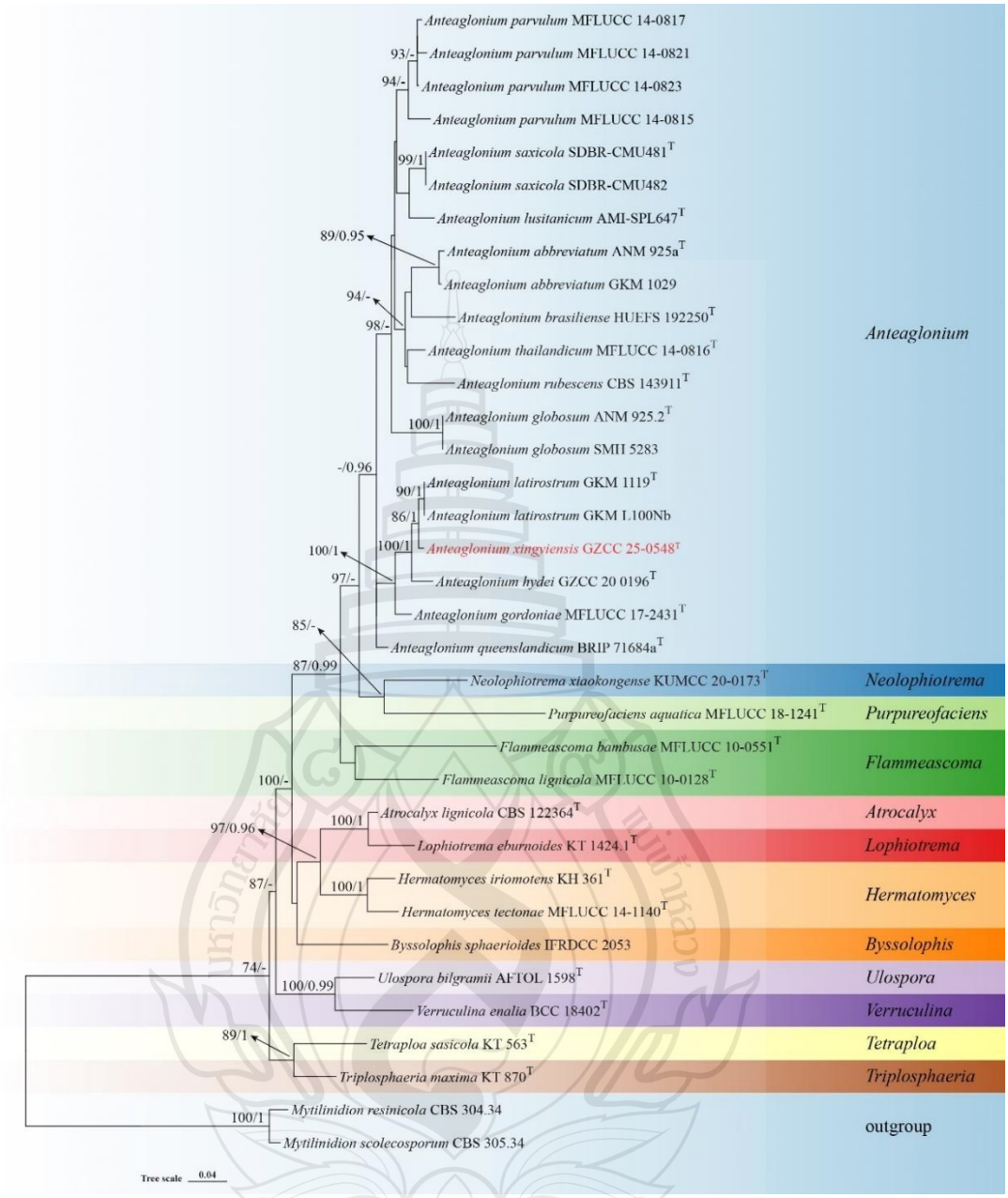

Figure 3.21 Phylogenetic analysis of *Anteaglonium*

Figure 3.21 Phylogenetic analysis of *Anteaglonium* was conducted using RAxML-based maximum likelihood analysis of a combined SSU, LSU ITS, *tef1-α* and *rpb2* sequence dataset. Bootstrap support values for maximum likelihood (ML) equal to or greater than 70% and Bayesian posterior probabilities (PP) equal to or greater than 0.95 are shown above the nodes. The tree is rooted with *Mytilinidion resinicola* (CBS 304.34) and *M. scolecosporum* (CBS 305.34). Newly generated strains are highlighted in red, and type strains are indicated with a superscript 'T'.

Anteaglonium xingyiensis X. Tang, Jayaward., R. & K.D. Hyde sp. nov. Figure 3.22

Etymology: The specific epithet 'xingyiensis' refers to the place where the sample collected.

Holotype: GZAAS25-0578

Saprobic on decaying wood in a terrestrial habitat. **Sexual morph**: Unknown. **Asexual morph**: Hyphomycetous. *Colonies* on natural substrate effuse, dark brown to black. *Mycelium* consist branched, septate, brown hyphae. *Conidiophores* 198–277 × 8.5–10.5 μm ($\bar{x}$ = 225.5 × 9.2 μm, n = 25), macronematous, mononematous, erect, straight to slightly curved, apically branched, cylindrical, tapering towards the apex, dark brown, multi-septate, thick-walled. *Conidiogenous cells* 6.5–9 × 5–6 μm ($\bar{x}$ = 8 × 5.5 μm, n = 25), monoblastic, integrated and discrete, terminal at the apex of the stem and branches, subcylindrical, light to dark brown. *Conidia* 15–25 × 6–7 μm ($\bar{x}$ = 20 × 6.5 μm, n = 25), acrogenous, solitary, dry, olivaceous brown to brown, pale brown at the apex, obclavate, rostrate, sometimes chains, straight or curved, truncate at base, septate, slightly constricted at septa.

Culture characteristics: Conidia germinated on PDA media within 10 h. Several germ tubes are produced. Colonies are irregular, with filamentous margin, raised and flat at the center, smooth, whitish-pale brown from above, greenish-black brown from below.

Material examined: China, Guizhou province, Liupanshui City, Yushe National Forest Park, on unidentified decaying wood, 27 November 2024, Xia Tang, LS27 (GZAAS25-0578, holotype), ex-type living culture (GZCC 25-0548).

*Note*s: Morphologically, *Anteaglonium* is the most similar to *Kirschsteiniothelia* as it has macronematous, mononematous, erect, straight to slightly curved, apically branched, cylindrical conidiophores, monoblastic, subcylindrical conidiogenous cells, acrogenous, solitary, dry, olivaceous brown to brown, pale brown at the apex, obclavate, rostrate conidia (Xiao et al., 2025). However, the phylogenetic analysis result showed that our isolates has a close affinity with the species *Anteaglonium latirostrum* with 100% ML/1.00 PP support (Figure 3.2.14), and indicating that it is distinct species. Therefore, based on morphology and phylogeny, we identified our isolate as a new species, *Anteaglonium xingyiensis*.

Figure 3.22 *Anteaglonium xingyiensis* (GZAAS25-0578, holotype)

Figure 3.22 a, b Colonies on the natural substrate. c–e Conidiophores, conidiogenous cells and conidia. f–l Conidia. m A germinated conidium. n, o Colonies on culture media from above and below. Scale bars: c–e = 50 μm, f–n = 10 μm.

Astrosphaeriellaceae Phookamsak & K.D. Hyde, Fungal Diversity 74: 161 (2015)

Astrosphaeriella Syd. & P. Syd., Ann. Mycol. 11: 260 (1913)

Index Fungorum number: IF 441; *Facesoffungi number*: FoF 01222;

Notes: *Astrosphaeriella* was introduced by Sydow and Sydow (1913), with *A. fusispora* designated as the type species. Members of this genus are widely distributed in tropical to subtropical regions and are mostly associated with monocotyledons such as bamboo, palms and stout grasses, and occasionally occur in freshwater substrates (Shen et al., 2024). They typically act as saprobes or pathogens in both terrestrial and aquatic ecosystems (Hyde & Fröhlich, 1998; Phookamsak et al., 2015). Species of *Astrosphaeriella* are mainly known from their sexual morphs, which are characterized by carbonaceous, dark, erumpent to superficial, conical to mammiform ascomata with ruptured, reflexed, stellate host remnants at the base, trabeculate pseudoparaphyses, bitunicate cylindric to cylindric-clavate asci containing eight spores, and pale brown to brown fusiform ascospores with septate (Sydow & Sydow, 1913; Phookamsak et al. 2015). Asexual morphs may also be produced on natural substrates and are characterized by pycnidial, immersed to superficial, conical or hemisphaerical to globose conidiomata with ostiolate, phialidic, cylindrical or cylindric clavate or ampulliform conidiogenous cells, and globose to subglobose, or oblong aseptate conidia (Phookamsak et al., 2015). Currently, 55 species are listed in Species Fungorum (Habib et al., 2025).

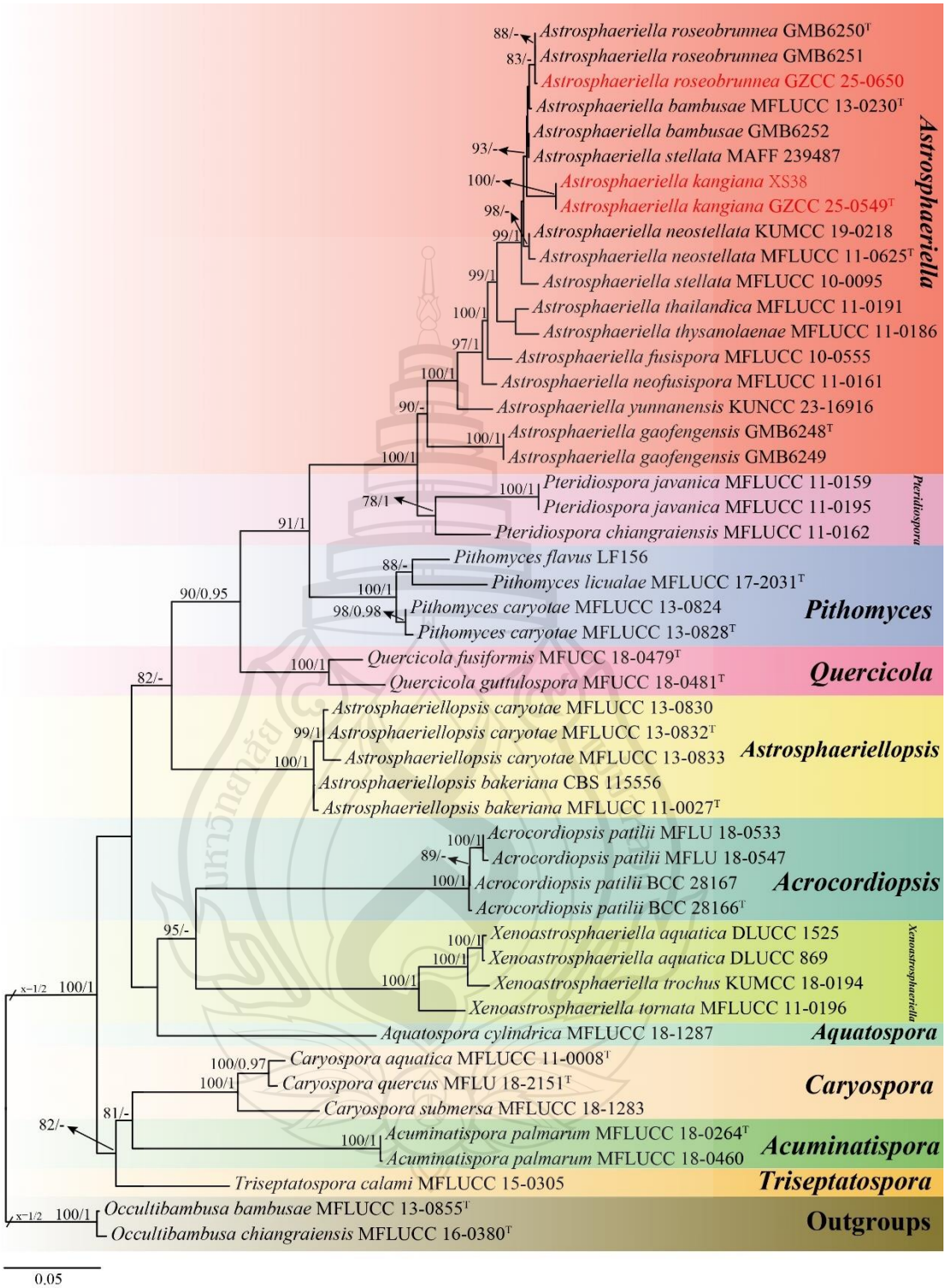

Figure 3.23 Phylogenetic analysis of *Astrosphaeriella*

Figure 3.23 Phylogenetic analysis of *Astrosphaeriella* was conducted using RAxML-based maximum likelihood analysis of a combined ITS, LSU, SSU, *tef1-α* and *rpb2* sequence dataset. Bootstrap support values for maximum likelihood (ML) equal to or greater than 70% and Bayesian posterior probabilities (PP) equal to or greater than 0.95 are shown above the nodes. The tree is rooted with *Occultibambusa bambusae* (MFLUCC 13-0855) and *O. chiangraiensis* (MFLUCC 16-0380). Newly generated strains are highlighted in red, and type strains are indicated with a superscript 'T'.

Astrosphaeriella kangiana X. Tang, K.D. Hyde & Jayaward, sp. nov.; Figure 3.24

Etymology: The specific epithet "kangiana" honours Prof. Ji-Chuan Kang for his contributions to fungal taxonomy.

Holotype: GZAAS25-0579

Saprobic on decaying culms of bamboo in the forest. **Sexual morph**: *Ascostromata* black, erumpent, superficial to slightly erumpent, solitary to gregarious, brittle, carbonaceous, conical to papilla, flattened at the base, with ruptured, reflexed, host remnants, around the base, surface smooth. *Peridium* thick-walled, outer layers of dark, thick-walled cells; base thinner. Internal cavity gelatinized; trabeculate pseudoparaphyses present and anastomosing between the asci. *Ostiole* papillate, conspicuous. *Hamathecium* pseudoparaphyses up to 1–2 µm ($\bar{x}$ = 1.6 µm, n = 30) wide, anastomosing, frequently branched, embedded in a hyaline gelatinous matrix. *Asci* 119–180 × 8–11.5 µm ($\bar{x}$ = 145.2 × 9.7 µm, n = 20), 8-spored, bitunicate (fissitunicate), cylindrical to cylindro-clavate, short pedicellate, apically rounded with a distinct anocular chamber. *Ascospores* 34.5–47 × 3.5–7 µm ($\bar{x}$ = 40.4 × 5 µm, n = 30), uniseriate to biseriate, 1-septate, fusiform to subfusiform, pale brown to brown, with small guttulate, disappear when it matures, smooth, thick walled, slightly constricted at the septum, surrounded by a distinct mucilaginous sheath. **Asexual morph**: Undetermined.

*Culture characteristic*s: Colonies on PDA at 25°C germinate from the base of conidia, floccose to cottony, dense at the center and looser toward the margin, circular, umbonate with an entire margin. The colony surface initially white to pale grey, becoming greyish brown to dark brown with age, and showing distinct concentric zonation. Margin entire to slightly crenulate. The reverse is dark brown to blackish brown at the center, surrounded by a pale to yellowish brown halo, corresponding to

the concentric bands of the surface.

Material examined: China, Guizhou province, Zunyi City, Xishui County, Xishui Nature Reserve, saprobic on decaying culms of bamboo, 14th April 2023, Xia Tang, XS38 (GZAAS25-0579), living culture GZCC 25-0549.

Notes: In our phylogenetic analyses, our collection clusters with *Astrosphaeriella stellata* (MAFF 239487) and *A. bambusae* (MFLUCC 13-0230) (Figure 3.23). Morphologically,our collection can be distinct with other speceis of *Astrosphaeriella* in size, shape of ascospore and asci. Based on these morphological and phylogenetic differences, we identify our isolate as a novel species, *Astrosphaeriella kangiana*, following the guidelines of Jeewon and Hyde (2016) and Maharachchikumbura et al. (2021).

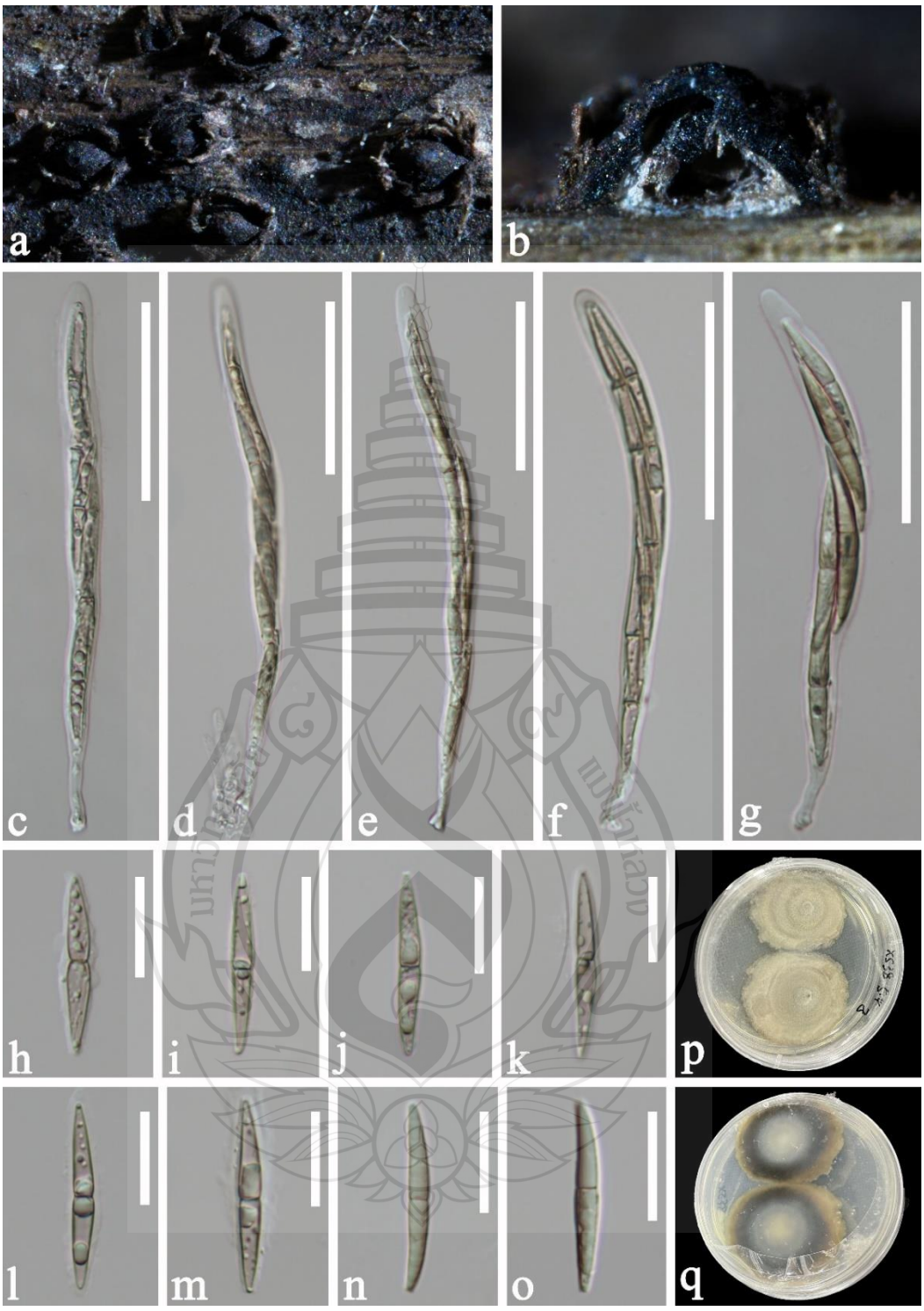

Figure 3.24 *Astrosphaeriella kangiana* (GZAAS25-0579, holotype)

Figure 3.24 a Ascomata on substrate. b longitudinal section of ascomata. c–g Asci. h–o Ascospores. p Colony on PDA (from front). q Colony on PDA (from reverse). Scale bars: c–g = 50 μm; h–o = 20 μm.

Astrosphaeriella roseobrunnea K. Habib, W. Hao Li & Q.R. Li, Mycosphere 16: 1437 (2025); Figure 3.25

Saprobic on decaying culms of bamboo in the forest. **Sexual morph**: *Ascostromata* black, erumpent, solitary to rarely gregarious, brittle, carbonaceous, conical to papilla, flattened at the base, with ruptured, reflexed, host remnants, around the base, surface smooth. *Peridium* thick-walled, outer layers of dark, thick-walled cells; base thinner. Internal cavity gelatinized; trabeculate pseudoparaphyses present and anastomosing between the asci. *Ostiole* papillate, conspicuous. *Hamathecium* pseudoparaphyses 1–2.5 µm ($\bar{x}$ = 1.7 µm, n = 30) wide, trabeculate, anastomosing, frequently branched, embedded in a hyaline gelatinous matrix. *Asci* 140–272 (291-) × 7.5–13 µm ($\bar{x}$ = 192.5 × 10.3 µm, n = 30), 8-spored, cylindrical, short pedicellate, apically rounded with anocular chamber. *Ascospores* 37.5–51 × 3.5–6 µm ($\bar{x}$ = 44.3 × 4.9 µm, n = 30), uniseriate to biseriate, 1-septate, elongate-fusiform, truncated to rounded at ends, pinkish brown, with small guttules, smooth thick walled, deeply constricted at the septum, surrounded by a distinct thick 0.9–2.5 µm ($\bar{x}$ = 1.5 µm, n = 30) wide mucilaginous sheath, truncated with a central depression at the apex. **Asexual morph**: Undetermined.

Material examined: China, Guizhou Province, Xingyi City, Xianheping National Forest Park, saprobic on decaying culms of bamboo, 25 September 2021, Xia Tang, xhp37 (GZAAS25-0680), ex-type culture GZCC 25-0650.

Known distribution: China (Habib et al., 2025; this study).

Known hosts: on dead culm of bamboo (Habib et al., 2025; this study); on dead branch of palm tree (Habib et al., 2025).

Notes: Morphologically, our collection (GZCC 25-0650) exhibit the similar character with the species of *Astrosphaeriella*, such as black, erumpent, brittle, carbonaceous, conical to papilla ascostromata with ruptured, reflexed, host remnants, around the base; papillate, conspicuous ostiole; 8-spored, cylindrical, short pedicellate asci with apical anocular chamber; uniseriate to biseriate, 1-septate, elongate-fusiform, ascospores and surrounded by mucilaginous sheath. However, our collection was resembling to *A. roseobrunnea* with the shape, size and color of asci and ascospores.

In phylogenetic analyses, our collection (GZCC 25-0650) clustered with *A. roseobrunnea* (GMB6250 and GMB6251) with support of 83% ML (Figure 3.23).

Pairwise comparison of our collection and *A. roseobrunnea* (GMB6250, type species) shows less difference in ITS and LSU with 0.3% (2/682 bp) and 0.1% (1/861 bp), respectively. Based on the evidence of both morphology and phylogeny with the guidelines of Jeewon and Hyde (2016) and Maharachchikumbura et al. (2021). We described our collection (GZCC 25-0650) as a known species, *A. roseobrunnea* which previously find on dead culm of bamboo and dead branch of palm tree in China (Habib et al., 2025). This was expending the finding of *A. roseobrunnea* from China and sequence data.

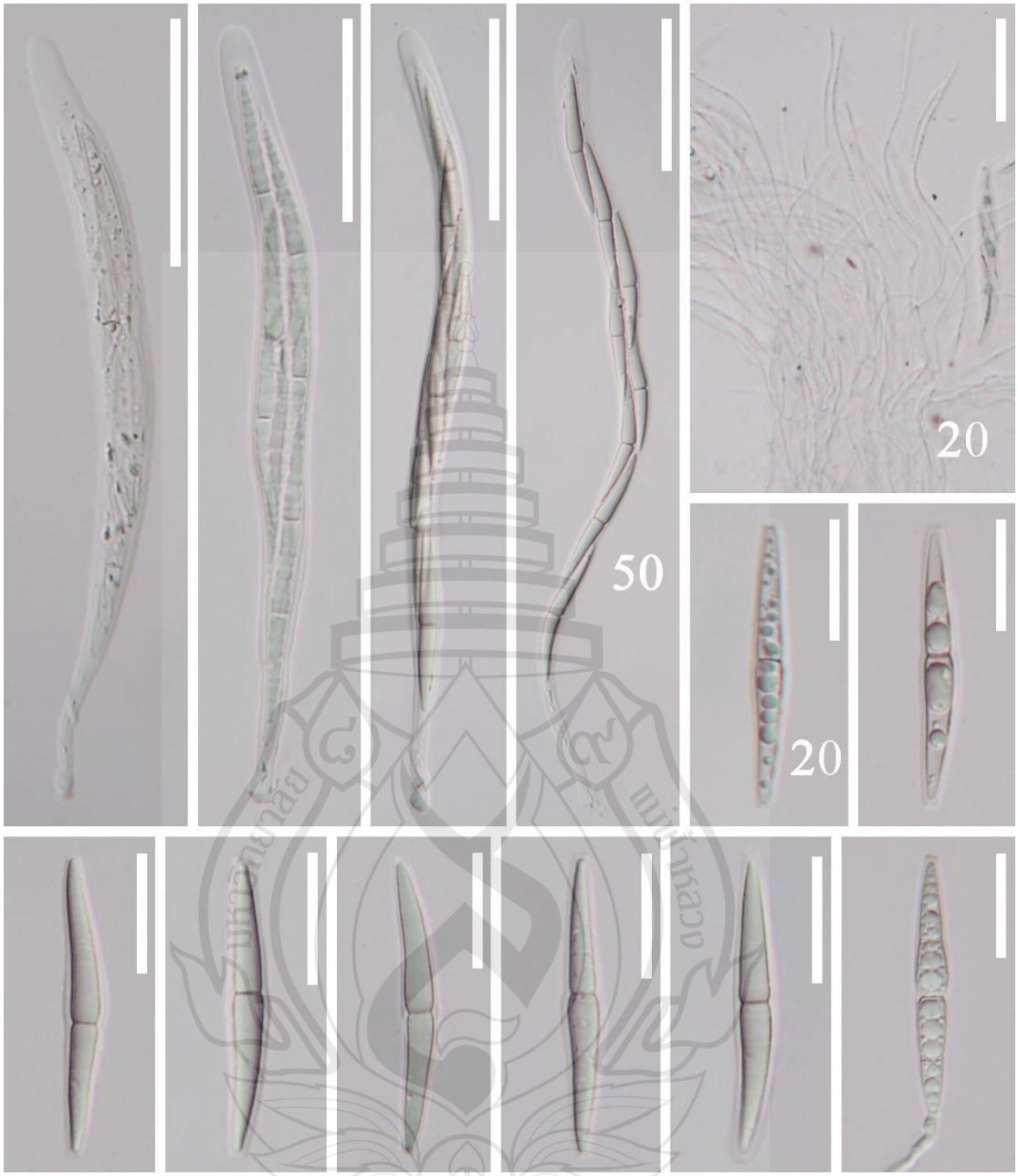

Figure 3.25 *Astrosphaeriella roseobrunnea* (GZAAS25-0680, new collection)

Figure 3.25 a Ascomata on substrate. b longitudinal section of ascomata. c–g Asci. h–o Ascospores. p Colony on PDA (from front). q Colony on PDA (from reverse). Scale bars: c–g = 50 μm; h–o = 20 μm.

Dictyosporiaceae Boonmee & K.D. Hyde, in Boonmee et al., Fungal Diversity 80: 462 (2016)

Dictyosporium Corda, Weitenweber's Beitr. Nat. 1: 87 (1837)

Index Fungorum number: IF 8001; *Facesoffungi number*: FoF 08210

Notes: The type genus of *Dictyosporiaceae*, *Dictyosporium* was introduced by Corda in Witenweber (1836) including *D. elegans* as the type species. This genus is characterized by superficial and subglobose ascomata with cylindrical, bitunicate asci consist of fusiform, hyaline, uniseptate ascospores with or without a sheath. The asexual morph is characterized by sporodochial colonies consist of micronematous to macronematous conidiophores, and cheiroid, digitate complanate conidia with several parallel rows of cells (Boonmee et al., 2016; Tennakoon et al., 2023). Members of this genus have been reported as saprobes on dead or decaying wood in terrestrial and aquatic habitats, worldwide (Boonmee et al., 2016; Nóbrega et al., 2021; Tennakoon et al., 2023; Shu et al., 2024). Currently, 82 species are listed under this genus. Based on morphology and phylogeny, this study presents two new records of *D. digitatum* and *D. tratense* found in China.

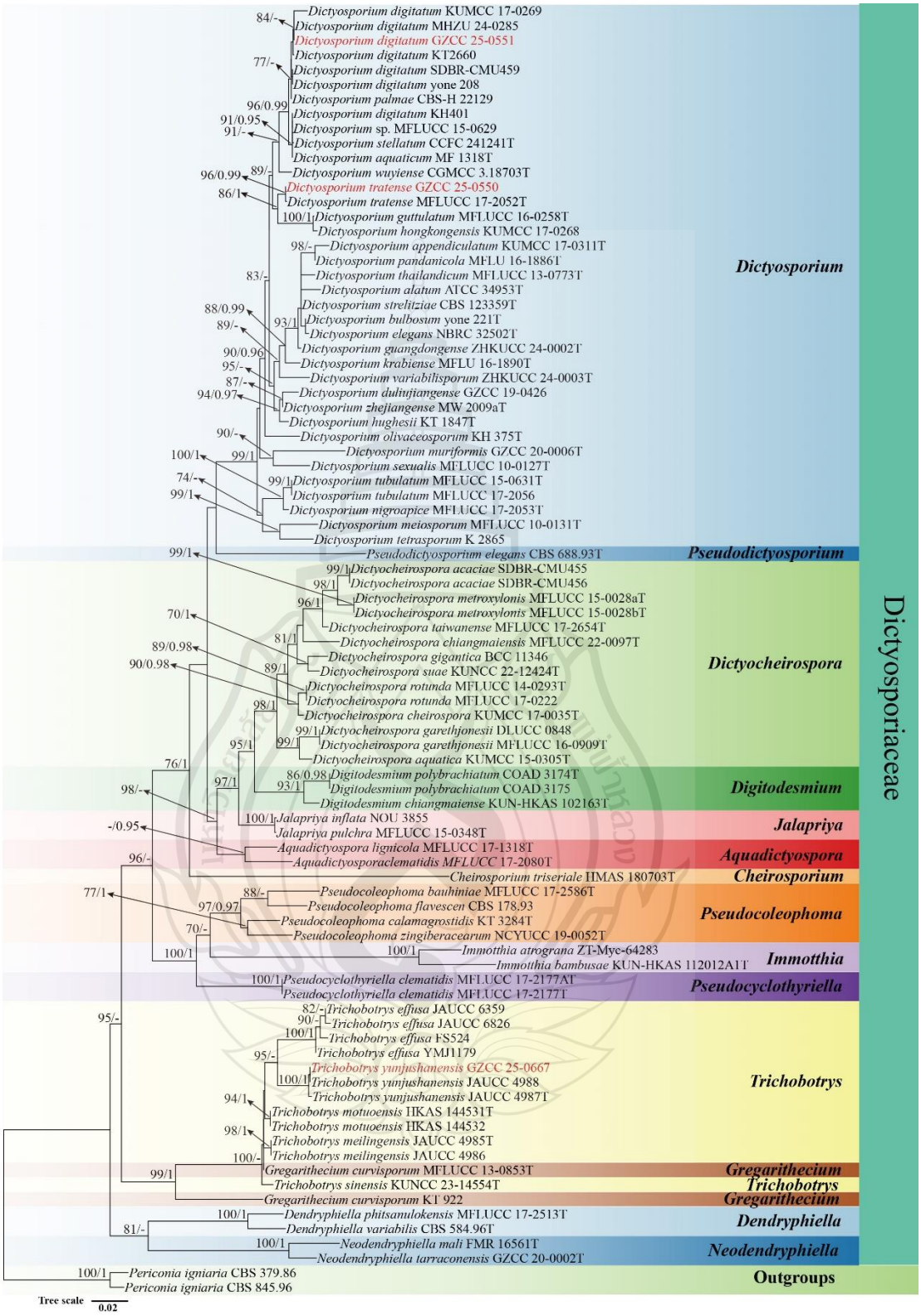

Figure 3.26 Phylogenetic analysis of *Dictyosporiaceae*

Figure 3.26 Phylogenetic analysis of *Dictyosporiaceae* was conducted using RAxML-based maximum likelihood analysis of a combined ITS, LSU and *tef1-α* sequence dataset. Bootstrap support values for maximum likelihood (ML) equal to or greater than 70% and Bayesian posterior probabilities (PP) equal to or greater than 0.95 are shown above the nodes. The tree is rooted with *Periconia igniaria* (CBS 379.86 and CBS 845.96). Newly generated strains are highlighted in red, and type strains are indicated with a superscript 'T'.

Dictyosporium digitatum J.L. Chen, C.H. Hwang & Tzean Mycol. Res. 95: 1145 (1991); Figure 3.27

Saprobic on decaying wood in a terrestrial habitat. **Sexual morph**: Unknown. **Asexual morph**: Hyphomycetes. *Colonies* on natural substrate superficial, effuse, gregarious, with masses of crowded, glistening conidia, balck. *Mycelium* partly immersed, partly superficial, composed of hyaline to pale brown, branched, septate, smooth hyphae. *Sporodochia* on the natural substrate, punctiform or spindle, aggregated, scattered on the substrate, black. *Conidiophores* reduced to conidiogenous cells. *Conidiogenous cells* holoblastic, monoblastic, terminal, cylindrical, pale brown. *Conidia* 89–137 × 23–36.5 μm ($\bar{x}$ = 115 × 30 μm, n = 30), cheiroid, consist with 4–8 parallel arms, tightly packed, complanate, 18–26 cells arranged within one arm, with rounded arm apex, yellowish-brown, digitate terminal cells, straight or slightly curved, thin- and smooth-walled, basal cell cuneiform, guttulate, with schizolytic conidial secession.

Culture characteristics: Conidia germinated on PDA media within 15 h. Several germ tubes are produced. Colonies are irregualr, with filamentous margin, raised and flat at the center, smooth, white to brown from above, reddish yellow to black brown from below.

Material examined: China, Hainan Province, Jianfengling National Forest Park, on unidentified decaying wood, 24 September 2024, Xia Tang, D37 (GZAAS25-0581), living culture GZCC 25-0551.

Known distribution: Australia (Goh et al., 1999), Brunei (Goh et al., 1999), Japan (Tanaka et al., 2015), Mauritius (Whitton et al., 2012), Philippines (Whitton et al., 2012), Seychelles (Goh et al., 1999), China (Chen et al., 1991; Lu et al. 2000; Zhuang 2001; Whitton et al., 2012; this study); Thailand (Pinruan et al., 2007;

Tennakoon et al., 2023)

Known hosts: *Archontophoenix alexandrae* (Goh et al., 1999), *Castanopsis sieboldii* (Tanaka et al., 2015), *Cyperus aggregatus* (Tennakoon et al., 2023); fallen decaying herbaceous stem (Chen et al., 1991); decaying wood (Zhuang 2001), *Licuala longicalycata* (Pinruan et al., 2007), *Machilus velutina* (Lu et al., 2000; Zhuang 2001), *Pandanus* spp. (Lu et al., 2000; Zhuang, 2001; Whitton et al., 2012), *Phoenix hanceana* (Lu et al., 2000; Zhuang, 2001), and *Pinus massoniana* (Lu et al., 2000; Zhuang, 2001).

Notes: In the phylogenetic analysis, the strain of our isolates (GZCC 25-0551) is grouped within *Dictyosporium*, sister to the strain of *D. digitatum* (KUMCC17-0269, MHZU 24-0285, KT2660, yone 208, and SDBR CMU459), with 84% ML bootstrap support (Figure 3.26). In comparison of the base pair differences in ITS our strain is mostly identical to KUMCC17-0269, MHZU 24-0285 strains. Morphological characteristics of our collection fits with the characters of *D. digitatum* collection provided by Chen et al., (1991) and Shu et al., (2024). Based on the morphological and phylogenetic analyses, we conclude our collection is another record of *D. digitatum*. This is the frst record of this species in a terrestrial habitat in China.

Figure 3.27 *Dictyosporium digitatum* (GZAAS25-0581, new habitat record)

Figure 3.27 a Natural host substrate. b, c Sporodochia on the substrate. d Conidiogenous cells and conidia. e–n Conidia. o A Germinating conidium. p Colony on PDA (from front). q Colony on PDA (from reverse). Scalebars: d-o = 20 µm.

Dictyosporium tratense Jing Yang & K.D. Hyde, MycoKeys 36: 96 (2018); Figure 3.28

Saprobic on decaying wood in a freshwater habitat. **Sexual morph**: Unknown. **Asexual morph**: Hyphomycetes. *Colonies* on natural substrate superficial, effuse, gregarious, with masses of crowded, glistening conidia, balck. Mycelium partly immersed, partly superficial, composed of hyaline to pale brown, branched, septate, smooth hyphae. *Sporodochia* on the natural substrate, punctiform or spindle, aggregated, scattered on the substrate, black. Conidiophores reduced to conidiogenous cells. *Conidiogenous cells* holoblastic, monoblastic, terminal, cylindrical, pale brown. *Conidia* 33–37 × 14–22 μm ($\bar{x}$ = 35 × 18 μm, n = 30), cheiroid, consist with 3–4 parallel arms, tightly packed, complanate, with rounded arm apex, yellowish-brown, digitate terminal cells, straight or slightly curved, thin- and smooth-walled, basal cell cuneiform, guttulate, with schizolytic conidial secession.

Culture characteristics: Conidia germinated on PDA media within 15 h. Several germ tubes are produced. Colonies are irregualr, with filamentous margin, raised and flat at the center, smooth, white to brown from above, reddish yellow to black brown from below.

Material examined: China, Hainan Province, Jianfengling National Forest Park, on submerge unidentified decaying wood, 24 September 2024, Xia Tang, D27 (GZAAS25-0580), living culture GZCC 25-0550.

Known distribution: China (this study), Thailand (Yang et al., 2018).

Known hosts: on decaying wood submerged in a freshwater stream (Yang et al., 2018); Unidentified decaying wood (this study).

Notes: In the phylogenetic analysis, strains of our isolate (GZCC 25-0550) are grouped within *Dictyosporium*, sister to the strain of *D. tratense* (MFLUCC 17-2052), with 96% ML bootstrap support and 0.99 BYPP (Figure 3.26), indicating that they are the same species. Morphologically, characteristics of our collection fits with the characters of *D. tratense* (Yang et al., 2018). Based on the strong morphological evidence and results of phylogeny, we identify our isolates as *D. tratense*. This is the frst record of this species in a freshwater habitat in China.

Figure 3.28 *Dictyosporium tratense* (GZAAS25-0580, new habitat record)

Figure 3.28 a Colonies on natural host substrate. b, c Sporodochia on the substrate. d Squashmount of a sporodochium. e Conidiogenous cells and conidia. f–k Conidia. l Colony on PDA (from front). m Colony on PDA (from reverse). Scalebars: d = 50 µm, e-k = 20 µm.

Trichobotrys Penz. & Sacc., Malpighia 15 (7-9): 245 (1902)

Index Fungorum number: IF 10275;

Notes: *Trichobotrys* was established by Penzig and Saccardo (1902) with *Trichobotrys effusa* as the type species. *Trichobotrys* is characterised in having mononematous conidiophores producing catenate, dark brown, spherical and echinulate conidia on fertile, smooth, short, lateral branches with polyblastic conidiogenous cells. Currently, only nine species are recognised in this genus namely *T. effusa*, *T. ipomoeae*, *T. meilingensis*, *T. motuoensis*, *T. pannosa*, *T. ramosa*, *T. sinensis*, *T. trechispora*, and *T. yunjushanensis* (Zhang et al., 2024; He et al., 2025).

Trichobotrys yunjushanensis W.J. Zhang & Z.J. Zhai, MycoKeys 106: 124 (2024); Figure 3.29

Saprobic on decaying wood in a terrestrial habitat. **Sexual morph**: Undetermined. **Asexual morph**: Hyphomycetous. *Colonies* on natural substrate superficial, effuse, gregarious, with masses of crowded, glistening conidia, balck. Mycelium partly immersed, partly superficial, composed of hyaline to pale brown, branched, septate, smooth hyphae. *Conidiophores* 2–3.5 μm wide ($\bar{x}$ = 3 μm, n = 20), up to 750 μm long, mononematous, erect, straight or flexous, septate, with fertile dichotomously branched, pale brown to olivaceous, verruculose, echinulate, thick-walled. *Conidiogenous cells* 7–12 × 2–3 μm ($\bar{x}$ = 9 × 2.5 μm, n = 15), integrated, polyblastic, terminal to subterminal on fertile branches, with several denticulate conidiogenous loci, hyaline to dark brown. *Conidia* 3–4 μm diam ($\bar{x}$ = 3.5 μm, n = 30), catenate, usually acrogenous or lateral, aseptate, spherical, verrucose, echinulate, sometimes guttulate, yellowish brown to dark brown when mature.

Culture characteristics: Conidia germinated on PDA media within 12 h. Several germ tubes are produced. Colonies are irregular, with filamentous margin, raised at the center, smooth, white from above, whitr to reddish from below.

Material examined: China, Guizhou province, Zunyi City, Chishui Bamboo Sea National Forest Park, on decaying branches of bamboo, 07 May 2023, Xia Tang, CS16 (GZAAS25-0695), living culture GZCC 25-0667.

Known distribution: China (Zhang et al.,2024; this study).

Known hosts: the stems of bamboo in freshwater habitats (Zhang et al., 2024); on decaying branches of bamboo in terrestrial habitat (this study).

Notes: Our new isolate (GZCC 25-0667) formed a sister clade with *Trichobotrys yunjushanensis* (JAUCC 4987 and JAUCC 4988), and the phylogeny indicates that they belong to the same species (Figure 3.26). Our collection (GZCC 25-0667) difers from *Trichobotrys yunjushanensis* (HFJAU 10044) only by its shorter conidial diameter (3–4 μm vs. 7–12 μm) (Zhang et al., 2024). Therefore, we identify Our collection (GZCC 25-0667) as *Trichobotrys yunjushanensis* based on morphology and molecular evidence. *Trichobotrys yunjushanensis* was previously found on the stems of bamboo in a freshwater habitat in China (Zhang et al., 2024), and this is the frst record of this species on decaying branches of bamboo in terrestrial habitat from China.

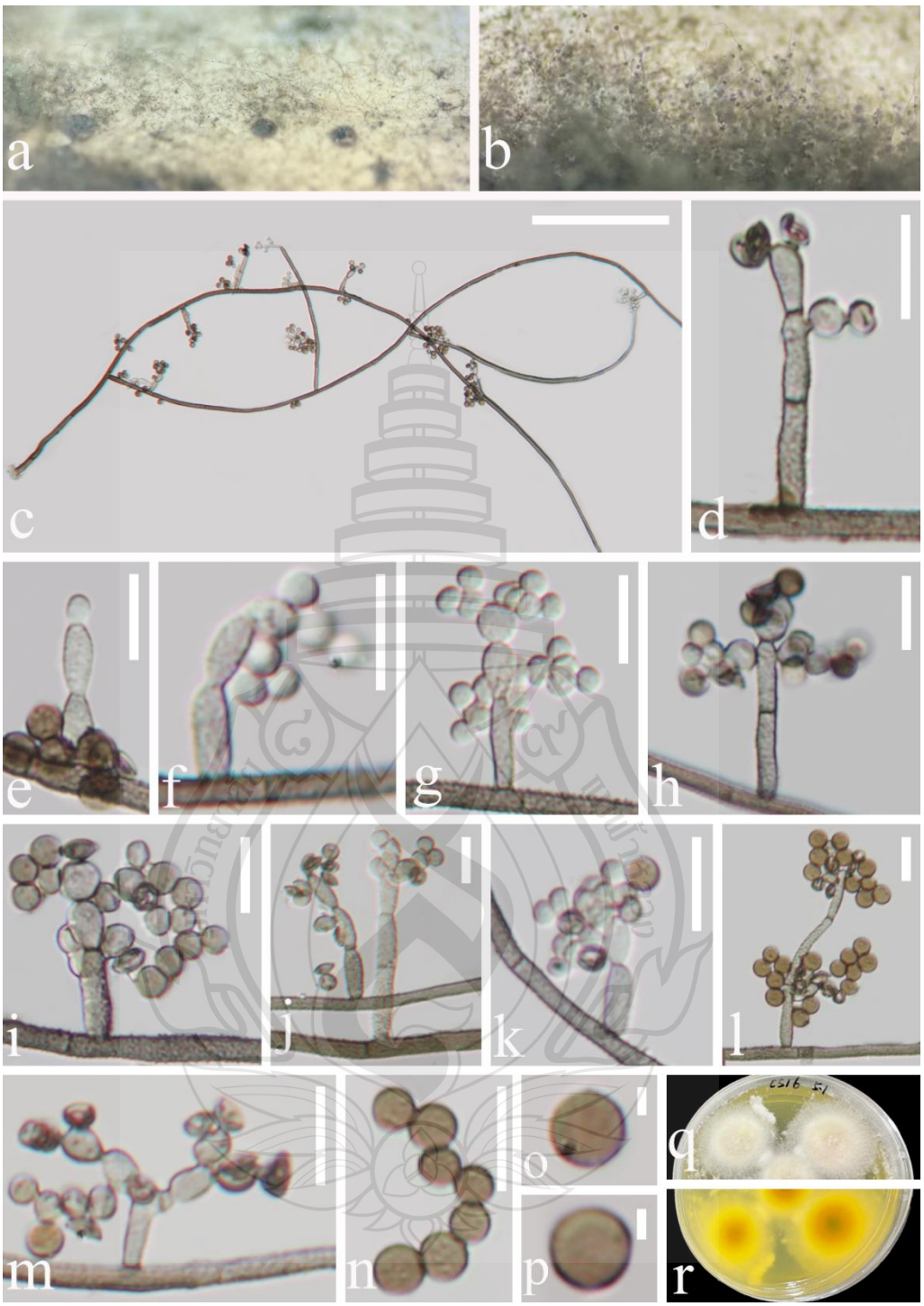

Figure 3.29 *Trichobotrys yunjushanensis* (GZCC 25-0667, new habitat record)

Figure 3.29 a, b Natural host substrate. c–l Mycelium, conidiophores, conidiogenous cells and conidia. n Conidia in chain. o, p Conidia. q Colony on PDA (from front). r Colony on PDA (from reverse). Scalebars: c = 100 µm, e-n = 10 µm, o, p = 2 µm.

Hermatomycetaceae Locq. ex A. Hashim. & Kaz. Tanaka, in Hashimoto, Matsumura, Hirayama & Tanaka, Persoonia 39: 56 (2017)

Hermatomyces Speg., Anal., Mus. nac. B. Aires, Ser. 3 13: 445 (1910) [1911]

Index Fungorum number: IF 8517; *Facesoffungi number*: FoF 08251;

Notes: *Hermatomyces* was established by Spegazzini (1910) to accommodate *H. tucumanensis* found on rotten branches of *Smilax campestris* and Celtis from Tucumán as the type species. Initially, the genus included into *Lophiotremataceae* based on the phylogenetic analyses (Doilom et al., 2016; Tibpromma et al., 2016). Later, Hashimoto et al. (2017) introduced a new family *Hermatomycetaceae* to accommodate *Hermatomyces* as the type genus. The asexual morph of *Hermatomyces* is chacarterized by having sporodochial conidiomata, monoblastic, terminal and cylindrical conidiogenous cells which arising dimorphic conidia such as lenticular conidia (muriform and brown) and cylindrical conidia (hyaline) (Chang, 1995; Hashimoto et al., 2017; de Silva et al., 2022; Zhang et al., 2023a; Shen et al., 2024). Sexual morph is characterized by having dark brown to black ascomata, 8-spored, bitunicate asci, and broadly fusiform, hyaline, 1-septate ascospores which constricted at the septum (de Silva et al., 2022; Zhang et al., 2023a). Members of *Hermatomyces* have cosmopolitan distribution and most are saprobic on different dead and decaying plant hosts in both aquatic and terrestrial habitats (de Silva et al., 2022; Shen et al., 2024). Currently, 34 species are accepted under *Hermatomyces* in Species Fungorum (2025).

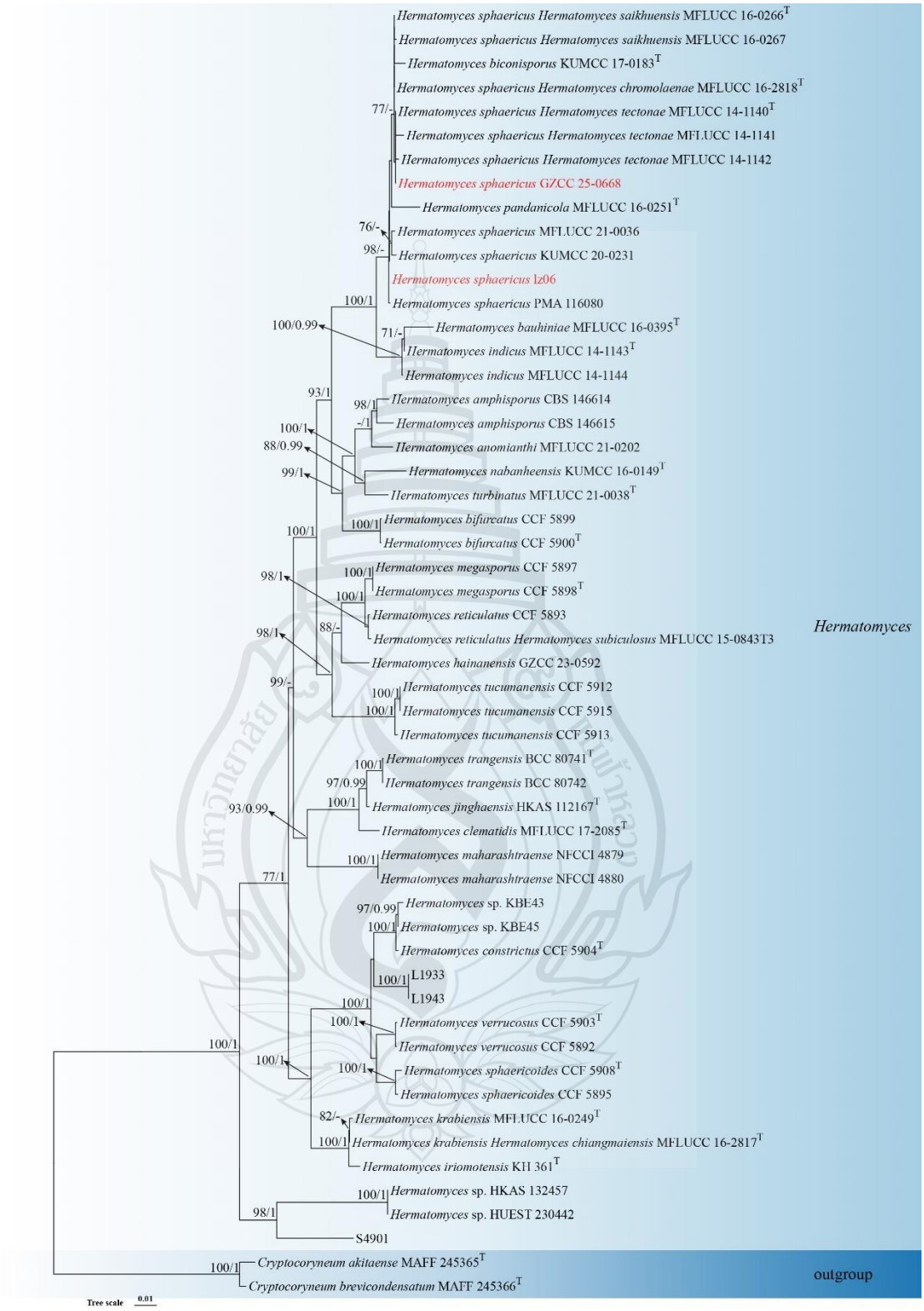

Figure 3.30 Phylogenetic analysis of *Hermatomyces*

Figure 3.30 Phylogenetic analysis of *Hermatomyces* was conducted using RAxML-based maximum likelihood analysis of a combined ITS, LSU, SSU and *tef1-α* sequence dataset. Bootstrap support values for maximum likelihood (ML) equal to or greater than 70% and Bayesian posterior probabilities (PP) equal to or greater than 0.95 are shown above the nodes. The tree is rooted with *Aquasubmersa japonica* (MAFF 245218 and MAFF 245219). Newly generated strains are highlighted in red, and type strains are indicated with a superscript 'T'.

Hermatomyces sphaericus S. Hughes, Mycol. Pap. 50: 100 (1953); Figure 3.31

Basionym: Stemphylium sphaericum Sacc., Atti Accad. Sci. Veneto-Trentino-Istriana 10: 86 (1917)

Saprobic on decaying wood in a terrestrial habitat. **Sexual morph**: Undetermined. **Asexual morph**: Hyphomycetous. *Colonies* on natural substrate superficial, effuse, gregarious, with masses of crowded, glistening conidia, balck. *Mycelium* partly immersed, partly superficial, composed of hyaline to pale brown, branched, septate, smooth hyphae. *Conidiophores* 23–26 × 3–4 μm ($\bar{x}$ = 24.5 × 3.5 μm, n = 20), micronematous, cylindrical or forked, smooth, hyaline or pale brown, often corresponding to conidiogenous cells. *Conidiogenous cells* 5–9 × 3–3.5 μm ($\bar{x}$ = 7 × 3.3 μm, n = 20), monoblastic, integrated, terminal, cylindrical, hyaline to pale brown, smooth or finely verruculose. *Conidia* 21.5–28 × 20.5–25.5 μm ($\bar{x}$ = 24.5 × 22.5 μm, n = 30), solitary, lenticular, globose, subglobose in front view, muriform, smooth, central cells brown, dark brown, outer ring of peripheral cells narrow, pale brown to brown, often constricted at septa, disk-shaped in lateral view.

Culture characteristics: Conidia germinated on PDA media within 10 h. Several germ tubes are produced. Colonies are circular, with filamentous margin, raised and flat at the center, smooth, white to grey from above, reddish yellow to black brown from below.

Material examined: China, Hainan Province, Wuzhishan City, Wuzhishan National Nature Reserve, on unidentified decaying wood, 27 November 2024, Zili Li, S26 (GZAAS25-0696), living culture GZCC 25-0668.

Known distribution: Central and South America, Africa, Asia, Oceania and North America. China (Zhang et al., 2009; Koukol et al., 2018, 2019; Ren et al., 2021;

this study).

Known hosts: *Acanthaceae*, *Apocynaceae*, *Arecaceae*, *Asteraceae*, *Dipterocarpaceae*, *Euphorbiaceae*, *Fabaceae*, *Lamiaceae*, *Leguminosae*, *Mimosaceae*, *Nyctaginaceae*, *Oxalidaceae*, *Pandanaceae*, *Pinaceae*, *Rhamnaceae*, *Sterculiaceae* and on unidentified decaying wood terrestrial habitat (Zhang et al., 2009; Koukol et al., 2018, 2019; Ren et al., 2021; this study).

Notes: In the phylogenetic analysis, strains of our isolates (GZCC 25-0668) are grouped within *Hermatomyces*, sister to the strain of *Hermatomyces sphaericus* (CBS 102826), with 73% ML bootstrap support (Figure 3.30), indicating that they are the same species. Morphologically, characteristics of our collection fits with the characters of *H. sphaericus* (Hughes, 1953). Based on the strong morphological evidence and results of phylogeny, we identify our isolates (GZCC 25-0668) as a new record of *Hermatomyces sphaericus*.

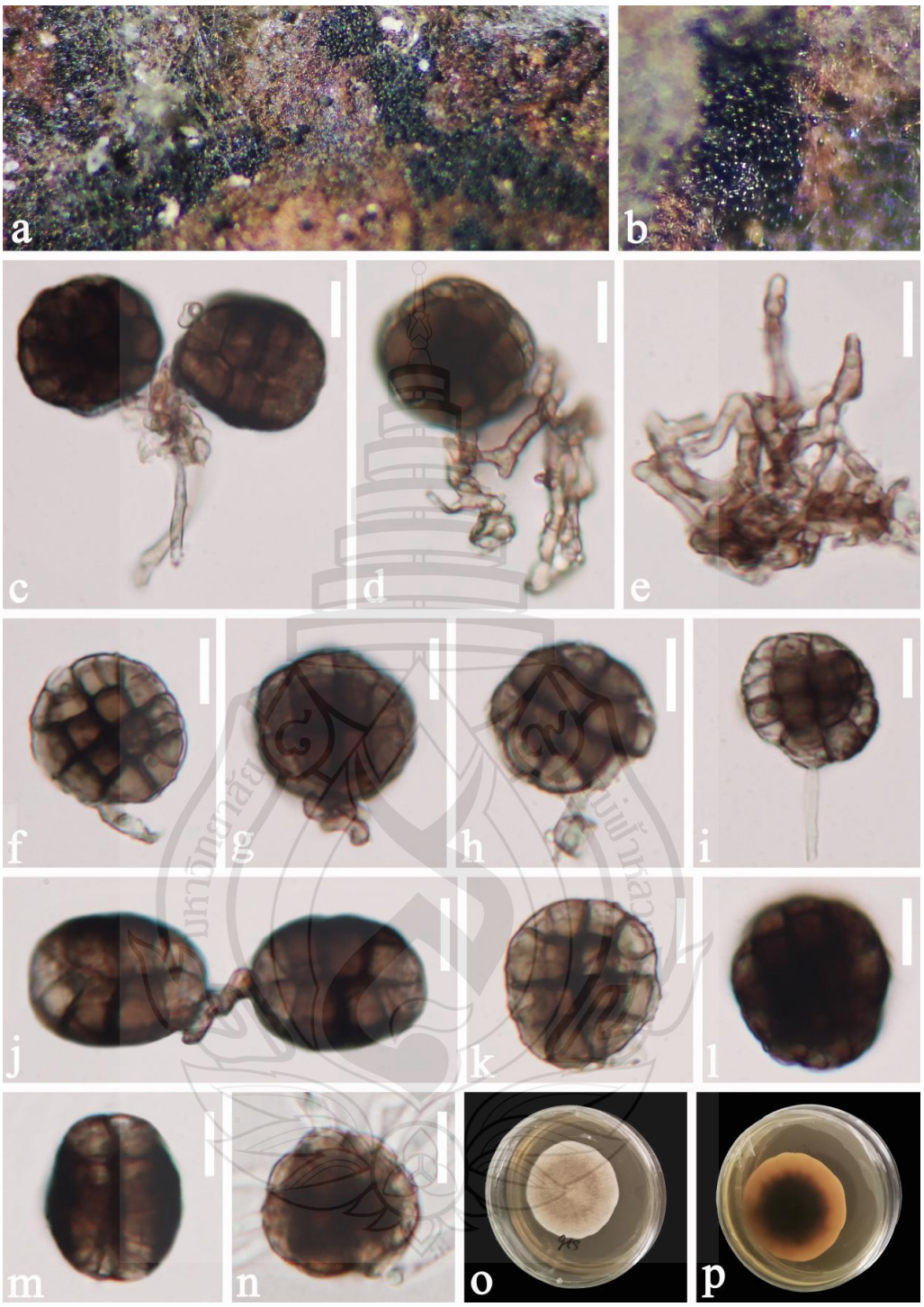

Figure 3.31 *Hermatomyces sphaericu* (GZAAS25-0696, new collection)

Figure 3.31 a, b Colonies on the natural substrate. c–e Conidiophores, conidiogenous cells, and conidia. f–m Conidiogenous cells and conidia. n A germinated conidium. o, p Colonies on culture media from above and below. Scale bars: c–n = 20 μm.

Lophiotremataceae K. Hiray. & Kaz. Tanaka, Mycoscience 52(6): 405 (2011)

Lophiotrema Sacc., Michelia 1(no. 3): 338 (1878)

Index Fungorum number: IF 2934; *Facesoffungi number*: FoF 08285;

Notes: *Lophiotrema* was established by Saccardo (1878) to accommodate a fungal group comprises lophiostomataceous species which are characterized by immersed ascomata with a crest-like ostiolar neck, cylindrical asci and hyaline, multiseptated ascospores (Hashimoto et al., 2017; Boonmee et al., 2021). Initially, this fungal group was placed in *Lophiostomataceae*, however, Hirayama and Tanaka (2011) established *Lophiotremataceae* to accommodate *Lophiotrema* based on morphology and phylogenetic analysis of LSU and SSU sequence data. The coelomycetous asexual morph of this genus is characterized by pycnidial, semi-immersed, long necked conidiomata, blastic, phialidic, cylindrical to lageniform conidiogenous cells, and oblong, aseptate or 1-septate, hyaline conidia (Sun et al., 2025). Species of this genus have been reported as saprobes on plant-based substrates in terrestrial, freshwater and Marine habitats (Boonmee et al., 2021). To date, more than 50 species are accepted under Lophiotrema (Hyde et al., 2024). This study presents, two new records of *Lophiotrema hydei* and *L. neohysterioides* collected from China.

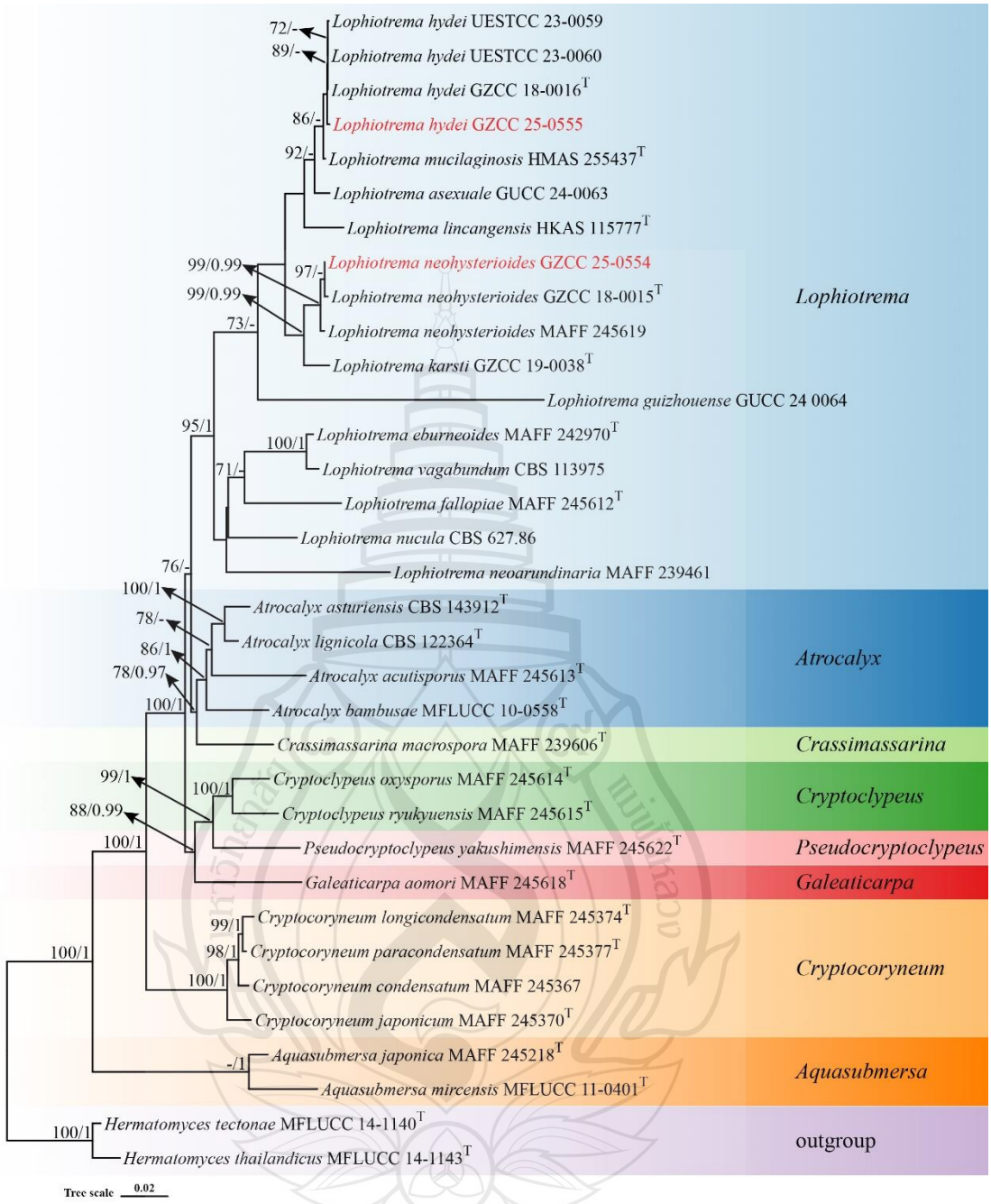

Figure 3.32 Phylogenetic analysis of *Lophiotrema*

Figure 3.32 Phylogenetic analysis of *Lophiotrema* was conducted using RAxML-based maximum likelihood analysis of a combined LSU, ITS, SSU, *rpb2* and *tef1-α* sequence dataset. Bootstrap support values for maximum likelihood (ML) equal to or greater than 70% and Bayesian posterior probabilities (PP) equal to or greater than 0.95 are shown above the nodes. The tree is rooted with *Hermatomyces tectonae* (MFLUCC 14-

1140) and *H. thailandicus* (MFLUCC 14-1143). Newly generated strains are highlighted in red, and type strains are indicated with a superscript 'T'.

Lophiotrema hydei Jin F. Zhang, Jian K. Liu & Z.Y. Liu 2018; Figure 3.33

Saprobic on unidentified decaying wood in forest substrate. **Sexual morph**: *Ascomata* 173–316 (-356.5)× 126 –172 µm ($\bar{x}$ = 265.3 × 154.1 µm, n = 7), solitary, scattered, sometimes aggregated, immersed to erumpent, coriaceous, globose to subglobose, brown to dark brown, uni-loculate, with a distinct ostiolar neck. *Ostiole* central, carbonaceous. *Peridium* 25–40 µm wide, composed of dark brown outer layers mostly fusing with host tissue and hyaline inner layers with the cells of textura angularis, at the base several cells of textura globulosa. *Hamathecium* composed of numerous, 1–2 µm wide, filamentous, septate, cellular pseudoparaphyses embedded in a gelatinous matrix. *Asci* 79.5–101 × 7–9 µm ($\bar{x}$ = 91 × 8.2 µm, n = 30), 8-spored, bitunicate, fissitunicate, cylindrical to cylindric-clavate, with a short pedicel, apically rounded, with a minute ocular chamber. *Ascospores* 20–27 × 3.5–5 µm ($\bar{x}$ = 24 × 4.3 µm, n = 30), overlapping, biseriate, fusiform, straight or slightly curved, 1-3- septate, constricted at the middle septum, slightly constricted at the other septa, acute at the both ends, smooth-walled, with prominent guttules, hyaline. **Asexual morph**: Undetermined.

Material examined: China, Guizhou province, Liupanshui City, Yushe National Forest Park, on unidentified decaying wood, 27 November 2024, Xia Tang, LS1 (GZAAS25-0585), living culture (GZCC 25-0555).

Known distribution: China (Zhang et al., 2018; Boonmee et al., 2021; Li et al., 2023; this study).

Known hosts: on dead wood of *Rosa* sp. (Boonmee et al., 2021); on decaying branches of *Vernicia fordii* (Li et al., 2023); on unidentified decaying wood (Zhang et al., 2018; this study).

Notes: In the phylogenetic analysis, the strain of our isolate (GZCC 25-0555) is grouped within *Lophiotrema*, together with the strains of *L. hydei* (UESTCC 23-0059, UESTCC 23-0060, GZCC 18-0016), with 87% ML bootstrap support (Figure 3.32). In comparison of the base pair differences in ITS, our strain is identical to the type stain of *Lophiotrema hydei* (GZCC 18-0016). Morphologically, the characteristics of our collection fits with the characters of *Lophiotrema hydei* collection provided by (Zhang et al., 2018). Based on the morphology and phylogenetic evidence, we conclude our collection is another

record of *Lophiotrema hydei*.

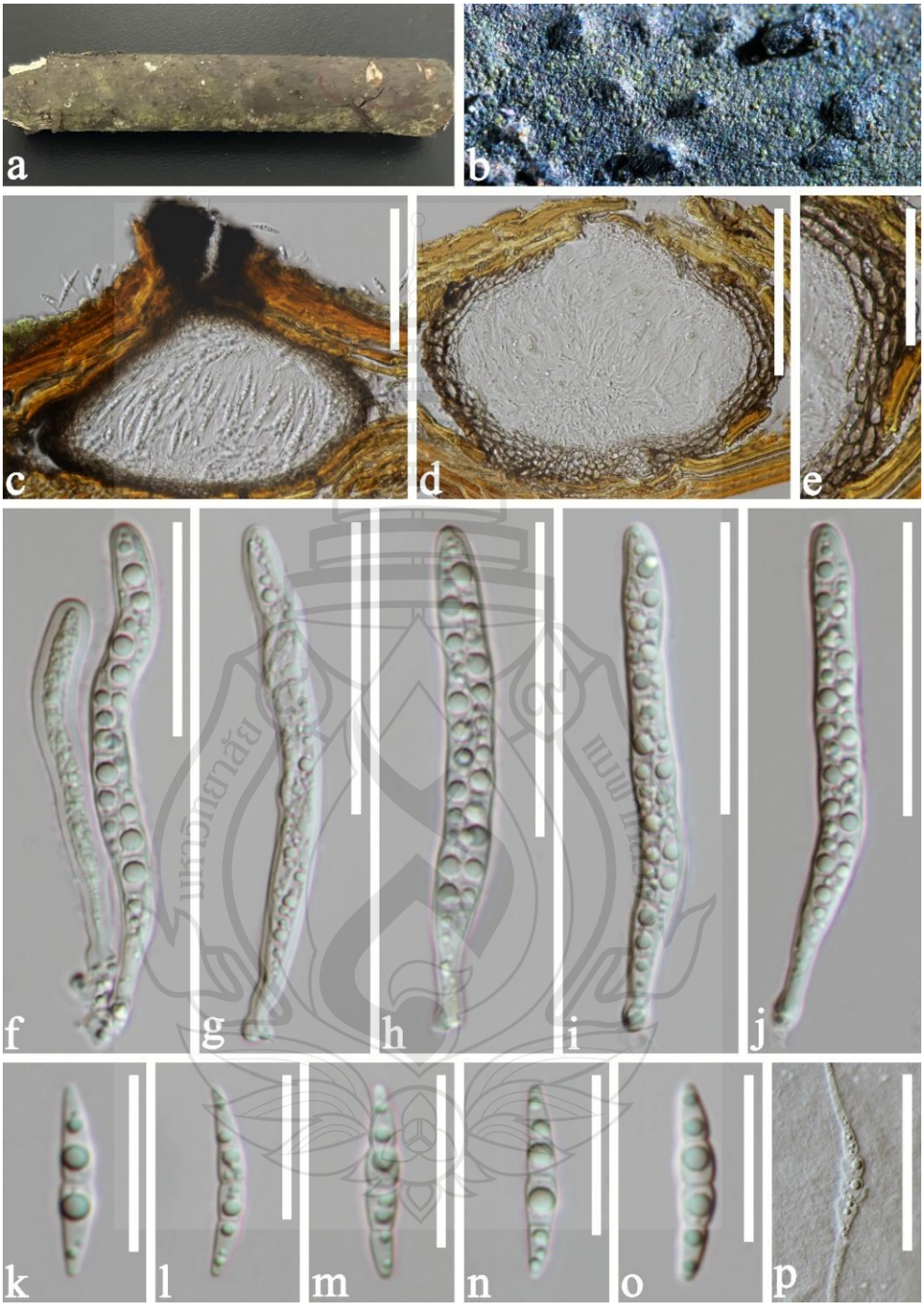

Figure 3.33 *Lophiotrema hydei* (GZCC 25-0555, new collection)

Figure 3.33 a The natural host substrate. b Ascomata on the natural substrate. c,d Longitudinal sections of ascomata. e Peridium. f-j Asci. k-o Ascospores. p A germinating ascospore. Scale bars: c,d = 100 µm, e-j = 50 µm, k-p = 20 µm.

Lophiotrema neohysterioides M.E. Barr 1992; Figure 3.34

≡*Sphaeria hysterioides* Schwein., Trans. Am. Philos. Soc. 4: 216, 1832.

≡*Lophiostoma hysterioides* (Schwein.) Sacc., Syll. Fung. 2: 709, 1883.

≡*Lophiostoma hysterioides* Ellis & Langl., J. Mycol. 4: 76, 1888.

≡*Lophiotrema hysterioides* (Ellis & Everhart.) Berl., Icon. Pyrenomyc. 1: 4, 1890.

Saprobic on unidentified decaying wood in forest substrate. **Sexual morph**: *Ascomata* 119–227.5 µm × 65–143 µm ($\bar{x}$ = 169 × 105, n = 9), immersed to erumpent, coriaceous, visible as black scars on the substrate, solitary, scattered, globose to subglobose, uni-loculate, ostiolate. *Ostioles* 57–104 µm wide, central, carbonaceous, with periphysate, narrowly cylindrical neck. *Peridium* 14–36 µm wide, composed of several layers, outer layers mostly fusing with host tissue, with brown to dark brown cells of textura angularis and inner layers with hyaline cells of textura angularis. *Hamathecium* comprising numerous, dense, 1–2 µm wide, branched, hyaline, cellular pseudoparaphyses embedded in a gelatinous matrix. *Asci* 69–105 µm × 8–10 µm ($\bar{x}$ = 86.3 × 9, n = 20), 8-spored, bitunicate, fissitunicate, cylindric-clavate, apically rounded, with a minute ocular chamber and a short pedicel. *Ascospores* 22.5–28.5 µm × 4–6 µm ($\bar{x}$ = 25.3 × 4.6, n = 30), overlapping, biseriate, fusiform, 2-3-septate, considerably constricted at the median septum, slightly constricted at other septa, straight or slightly curved, smooth-walled, guttulate. **Asexual morph**: Undetermined.

Culture characteristics: Ascospores germinated within 24h in PDA. Colonies on PDA, Tobacco-Brown, with somewhat irregular margin, reverse similar, no pigment is reduced.

Material examined: China, Guizhou province, Liupanshui City, Yushe National Forest Park, on unidentified decaying wood, 27 November 2024, Xia Tang, LS212 (GZAAS25-0584), living culture (GZCC 25-0554).

Known distribution: China (Zhang et al., 2018; this study), Japan (Hashimoto et al., 2017).

Known hosts: on dead branch of unidentified woody plant (Zhang et al., 2018; this study), *Phyllostachys bambusoides* (Hashimoto et al., 2017), *Pinus* sp. (Capital & Lao, 2020).

Notes: In the phylogenetic analysis, the strain of our isolate (GZCC 25-0554) is grouped within *Lophiotrema*, together with the strains of *L. neohysterioides* (GZCC 18-0015 and MAFF 245619), with 97 % ML bootstrap support (Figure 3.32). In comparison of the base pair differences of ITS region, our strain shows 0.1% (1/521) bp difference with the type stain of *L. neohysterioides* (GZCC 18-0015). Morphologically, the characteristics of our collection fits with the characters of *L. neohysterioides* collection provided by (Du et al., 2025). Based on the morphology and phylogenetic evidence, we conclude our collection is another record of *L. neohysterioide*s.

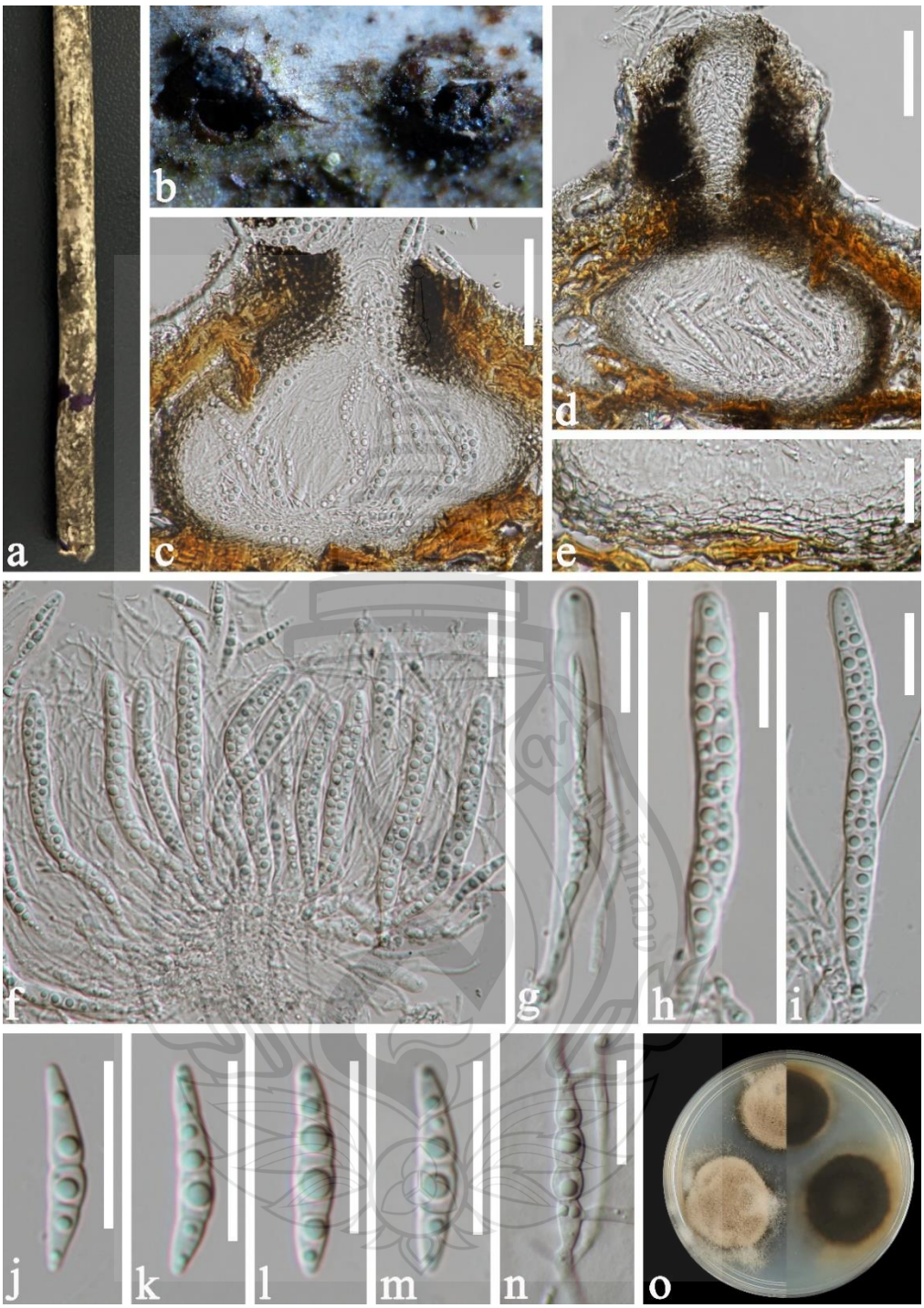

Figure 3.34 *Lophiotrema neohysterioides* (GZCC 25-0554, new collection)

Figure 3.34 a The natural host substrate. b Ascomata on the natural substrate. c,d Longitudinal sections of ascomata. e Peridium. f Asci and pseudoparaphyses. g-i Asci. j-m Ascospores. n A germinating ascospore. o Colonies on PDA media (left: surface: right: lower). Scale bars: c,d = 50 μm, e-n = 20 μm.

Massarinaceae Munk, Friesia 5 (3-5): 305 (1956)

Helminthosporium Link, Mag. Neuesten Entdeck. Gesammten Naturk. Ges. Naturf. Freunde Berlin 3 (1): 10 (1809)

Index Fungorum number: IF 8495; *Facesoffungi number*: FoF 06499;

Notes: *Helminthosporium*, a hyphomycetous genus in the *Massarinaceae* (*Pleosporales*), was established by Link (1809) with *H. velutinum* as the type species. This species-rich genus has a long and complex taxonomic history. Although more than 770 epithets have been recorded for *Helminthosporium*, only about 60 species are currently accepted following successive taxonomic revisions (Link, 1809; Hughes, 1958; Shoemaker, 1959; Ellis, 1961; Tsuda, 1977; Sivanesan, 1987; Siboe et al., 1999; Castañeda-Ruíz et al., 2017; Xu et al., 2020; Zhang et al., 2004, 2007, 2020; Tanaka et al., 2015; Zhu et al., 2016; Voglmayr & Jaklitsch, 2017; Chen et al., 2022; Hu et al., 2023; Index Fungorum, 2025).

Helminthosporium contains both sexual and asexual morph. The asexual is characterized by macronematous, conidiophores with polytretic conidiogenous cells and clavate or obclavate, distoseptate conidia with a flat, ringed pore at the base (Luttrell, 1964; Voglmayr & Jaklitsch, 2017). The sexual morph is characterized by immersed ascomata in pseudostromata with central ostioles and a pseudoparenchymatous peridium; hamathecium of septate, branched, and anastomosing pseudoparaphyses; clavate, 8-spored asci; and subellipsoid to obovoid, 1-septate, asymmetric ascospores that are hyaline when young, becoming brown at maturity, often with inner wall thickenings and a gelatinous sheath (Tanaka et al., 2015; Voglmayr & Jaklitsch, 2017). To date, only six species, *viz.*, *H. tiliae*, *H. microsorum*, *H. oligosporum*, *H. massarinum*, *H. quercicola*, and *H. quercinum*, were characterized based on both morphs (Tanaka et al., 2015; Voglmayr & Jaklitsch, 2017).

Members of *Helminthosporium* are predominantly saprobes on dead or decaying wood, occurring worldwide on diverse hosts in terrestrial habitats (Konta et al., 2021; Voglmayr & Jaklitsch 2017; Tanaka et al., 2015), with only rare records from freshwater environments (Zhu et al., 2016). Among them, *H. solani* is the only notable pathogen, causing potato silver scurf globally (Errampalli et al., 2001; Tian et al., 2007).

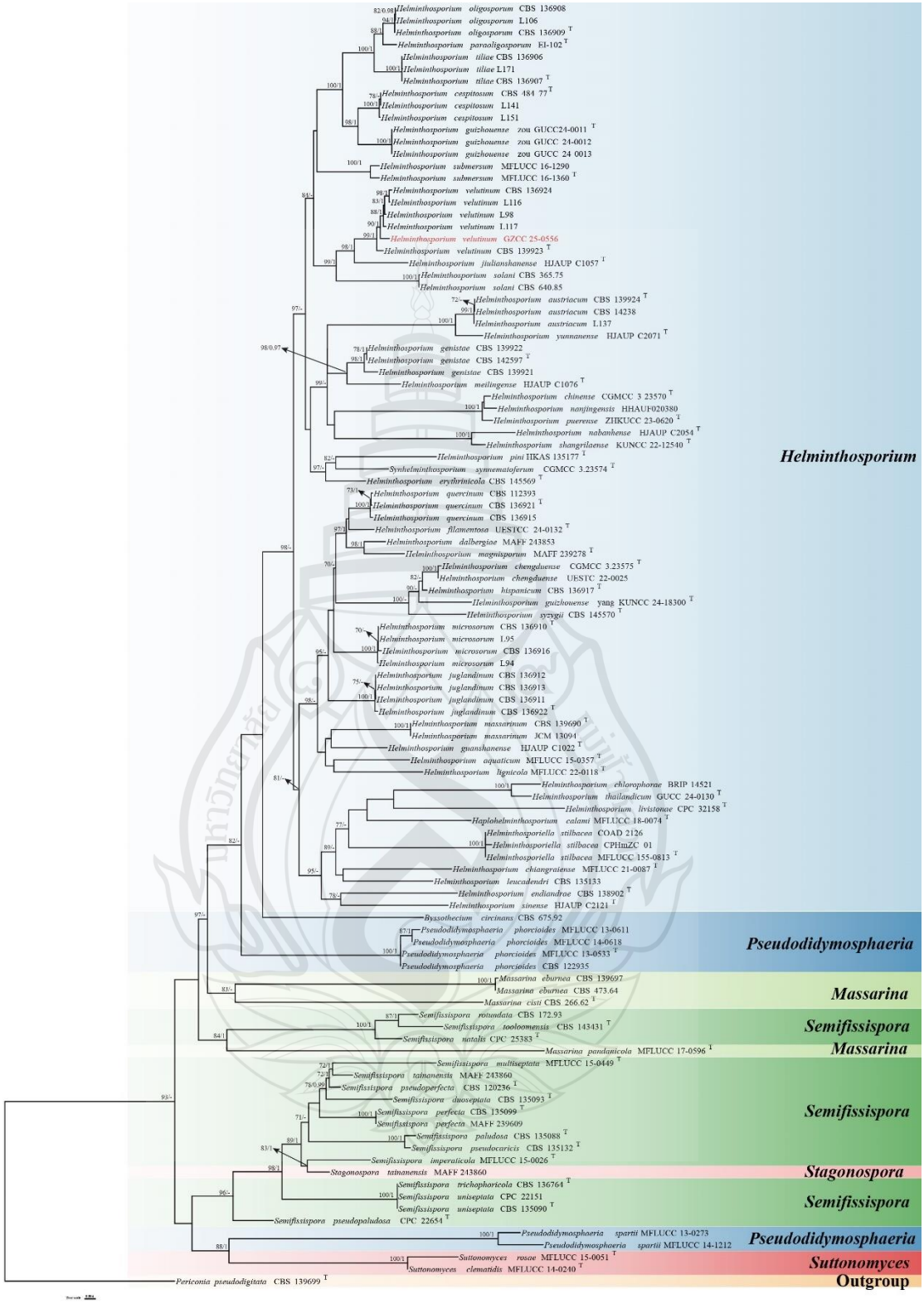

Figure 3.35 Phylogenetic analysis of *Helminthosporium*

Figure 3.35 Phylogenetic analysis of *Helminthosporium* was conducted using RAxML-based maximum likelihood analysis of a combined ITS, LSU, SSU, *rpb2* and *tef-1α* sequence dataset. Bootstrap support values for maximum likelihood (ML) equal to or greater than 70% and Bayesian posterior probabilities (PP) equal to or greater than 0.95 are shown above the nodes. The tree is rooted with *Periconia pseudodigitata* (CBS 139699). Newly generated strains are highlighted in red, and type strains are indicated with a superscript 'T'.

Helminthosporium velutinum Link, Mag. Neuesten Entdeck. Gesammten Naturk. Ges. Naturf. Freunde Berlin 3 (1): 47 (1809) Figure 3.36

Saprobic on decaying wood of *Juglans* sp.. **Sexual morph**: Undetermined. **Asexual morph**: *Colonies* on natural substrate effuse, velvety, brown to dark brown. *Mycelium* mostly immersed, composed of branched, septate. *Conidiophore* 345–932 µm × 12.5–23 (-38) µm wide (($\bar{x}$ = 564.5 µm × 18 µm, n=25), macronematous, mononematous, unbranched, proliferating, dark brown, 15–24-septate, erect or flexuous, tapering towards apex, wider at base. *Conidiogenous cells* 17.5–38 µm × 6.5–14.5 µm (($\bar{x}$ = 26.1 µm × 10.5 µm, n=30), polytretic integrated, cylindrical, intercalary and terminal, brown to dark brown. *Conidia* 51.5–95 µm × 13–22 µm wide (($\bar{x}$ = 75.5–18 µm, n=30), single, obclavate to rostrate with ellipsoidal lumina, pale brown to brown, 7–9-distoseptate, guttulate, smooth, straight or curved, base slightly truncate, cicatrized and wider than apex, dark brown, apical cell paler, rounded at apex. Conidial secession schizolytic.

Culture characteristics: Colonies incubated at 25°C, irregularly circular, flat, and velvety on the surface, with denser mycelium at the center that becomes progressively sparser towards the margin. The colony color ranges from creamy white to pale gray, with a distinct ring of suspected spore-producing secretions at the central region and a well-defined margin. The reverse side is circular, black at the center fading to pale black, and further outward to pale brown, also with a clear margin.

Material examined: China, Guizhou Province, Xingyi City, Xianheping National Forest Park, on decaying wood of Juglans sp., 27 November 2024, Xia Tang, XY19 (GZAAS25-0586), living culture GZCC 25-0556.

Known distribution: Austria (Voglmayr & Jaklitsch, 2017); China (Zhu et al., 2016; Chen et al., 2022; Xu et al., 2022; Tian et al., 2024; Liao et al., 2025; this

study); Germany (Voglmayr & Jaklitsch, 2017); Italy (Voglmayr & Jaklitsch, 2017); Japan (Diene et al., 2010); Spain (Voglmayr & Jaklitsch, 2017); Sweden (Voglmayr & Jaklitsch, 2017).

Known hosts: endophyte in sweet sorghum (Diene et al., 2010), Submerged wood in freshwater streams (Zhu et al., 2016); *Acer campestre* (Voglmayr & Jaklitsch, 2017); *Corylus avellana* (Voglmayr & Jaklitsch, 2017); *Cytisus scoparius* (Voglmayr & Jaklitsch, 2017); *Euonymus europaeus* (Voglmayr & Jaklitsch, 2017); *Gesnouinia arborea* (Voglmayr & Jaklitsch, 2017); *Genista tinctoria* (Voglmayr & Jaklitsch, 2017); *Juglans regia* (Voglmayr & Jaklitsch, 2017, Xu et al., 2022; this study); *Prunus lusitanica* (Voglmayr & Jaklitsch, 2017); *Ribes rubrum* (Voglmayr & Jaklitsch, 2017); *Sambucus nigra* (Voglmayr & Jaklitsch, 2017); on dead branch of an unidentified host (Chen et al., 2022); dead branches of *Pinus* sp. (Tian et al., 2024); on dead branches of unidentified plants under broad-leaved forest (Liao et al., 2025).

Notes: Morphologically, our collection is consistent with the diagnostic features of *Helminthosporium velutinum*, including macronematous, mononematous, unbranched, proliferating conidiophores; polytretic, integrated, intercalary conidiogenous cells; and obclavate to rostrate, guttulate conidia with ellipsoidal lumina. In phylogenetic analyses, our isolate (GZCC 25-0556) clustered with *H. velutinum* (CBS 136924, L116, L98, L117, and CBS 139923) (Figure 3.35). Nucleotide sequence comparisons between our isolate and the type strain of *H. velutinum* (CBS 139923) revealed minimal differences: 0.7% (4/564 bp) in ITS, 0.1% (1/831 bp) in LSU, none in SSU, 1.4% (12/819 bp) in rpb2, and 1% (7/726 bp) in *tef1-α*, excluding gaps. Based on these morphological and molecular data, and following the guidelines of Jeewon and Hyde (2016) and Maharachchikumbura et al. (2021), we identify our collection as the known species *H. velutinum*.

Helminthosporium velutinum is reported from a wide range of hosts worldwide; our collection further extends its known distribution, habitat, and host range, reinforcing its cosmopolitan nature (Voglmayr & Jaklitsch, 2017; Farr & Rossman, 2025).

Figure 3.36 *Helminthosporium velutinum* (GZAAS25-0586, new collection)

Figure 3.36 a Colonies on substrate. b–f Condiophores, conidiogenous cells, conidiogenous cells bearing conidia. g–j, l–n Conidia. o Germinated conidium. k Colony on PDA (from front). p Colony on PDA (from reverse). Scale bars: b–f = 100 μm, g–o = 20 μm.

Megacapitulaceae Rajeshk., Paraparath, Hongsanan, Jeewon, Karun. & Harikr., Kavaka 60 (4): 6 (2024)

Megacapitula J.L. Chen & Tzean, Mycol. Res. 97(3): 347 (1993)

Index Fungorum number: IF 25546; *Facesoffungi number*: FoF 11816;

Notes: *Megacapitula* was introduces by Chen and Tzean (1993), to accommodate the type species *M. villosa* assocoiated with fallen, decaying petioles of a broad-leaf from Taiwan, China based on morphology. Asexual morph is known for this genus with characterized by having branched, septate, verrucose, hyaline or pigmented mycelium; simple or branched, micronematous, semimacronematous, mononematous, terminal conidiogenous cells, and large, ellipsoidal, obclavate, or obpyriform, holoblastic, pigmented, and muriform conidia with hairy apical appendages (Chen & Tzean, 1993; Pem et al., 2019; Rajeshkumar et al., 2024). With the uncertainty of the fungal family *Megacapitula* assigned under *Pleosporales* genera incertae sedis by Boonmee et al. (2021). Later, Rajeshkumar et al. (2024) established a new family *Megacapitulaceae* to accommodate this genus with an epitypication. However, single species is still included in *Megacapitula* (*M. villosa*), and it has been reported as a saprobe on decaying, submerged wood in freshwater habitats from Thailand, decaying fronds of *Caryota urensfrom* hosts and decating wood from India (Prabhugaonkar & Bhat, 2011; Boonmee et al., 2021; Rajeshkumar et al., 2024). More taxon sampling and molecular data are required for the better taxonomic resolution of *Megacapitula* and further studies are suggested. This study presents a new species, *Megacapitula guizhouensis* collected from Guizhou, China.

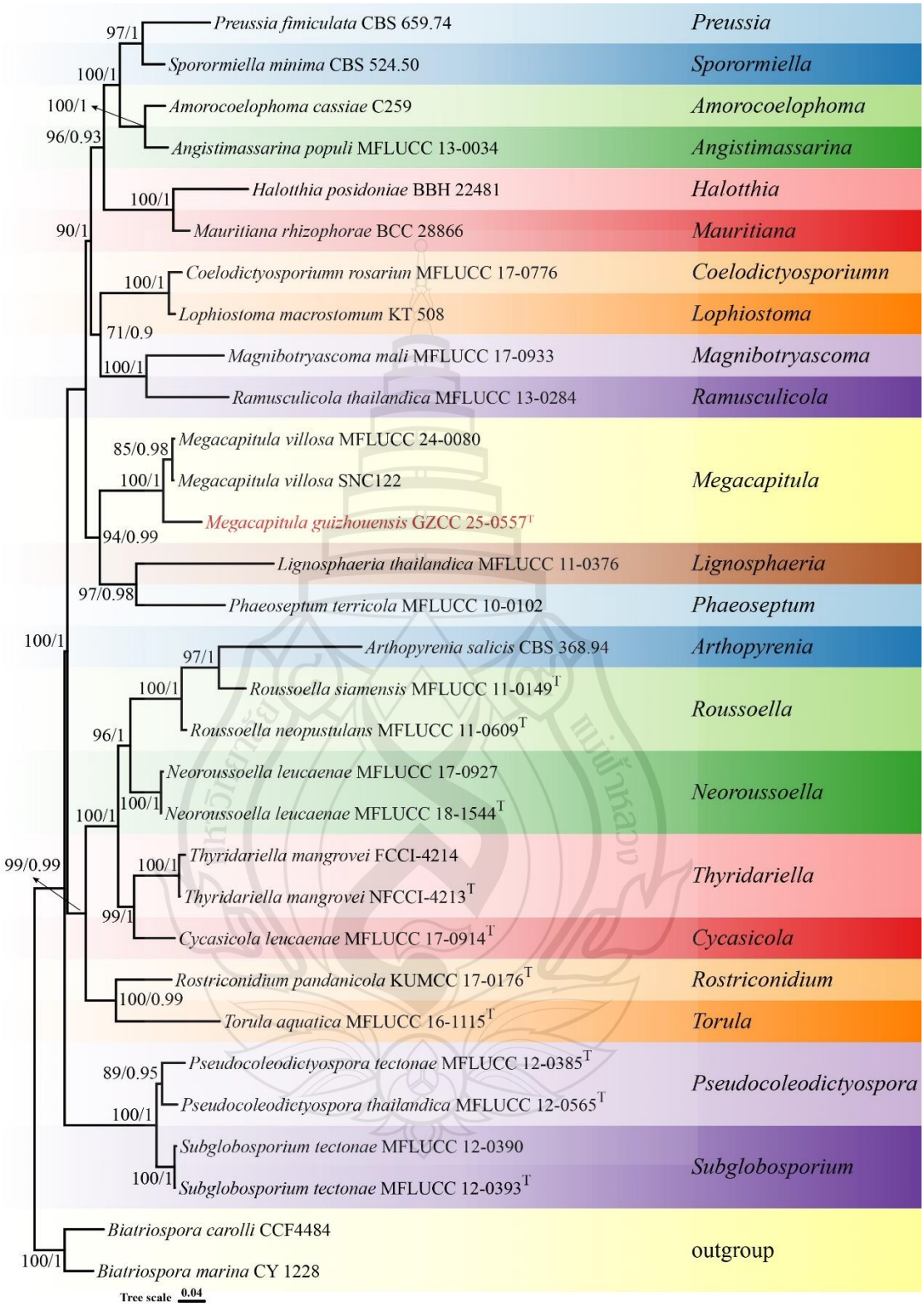

Figure 3.37 Phylogenetic analysis of *Megacapitula*

Figure 3.37 Phylogenetic analysis of *Megacapitula* was conducted using RAxML-based maximum likelihood analysis of a combined LSU, SSU, ITS, *tef-1α* and *rpb2* sequence dataset. Bootstrap support values for maximum likelihood (ML) equal to or greater than 70% and Bayesian posterior probabilities (PP) equal to or greater than 0.95 are shown above the nodes. The tree is rooted with *Biatriospora carolli* (CCF4484) and *B. marina* (CY 1228). Newly generated strains are highlighted in red, and type strains are indicated with a superscript 'T'.

Megacapitula guizhouensis X. Tang, Jayaward., R. & K.D. Hyde sp. nov.; Figure 3.38

Etymology: The specific epithet 'guizhouensis' refers to the place where the sample collected.

Holotype: GZAAS25-0587

Saprobic on decaying wood in a terrestrial habitat. **Sexual morph**: Unknown. **Asexual morph**: Hyphomycetous. *Colonies* on natural substrate superficial, effuse, gregarious, with masses of crowded, glistening conidia, brown to balck. Mycelium partly immersed, partly superficial, composed of hyaline to pale brown, branched, septate, smooth hyphae. *Conidiophores* absent. *Conidiogenous cells* terminal on mycelial extensions. *Conidia* 40–225 × 34–80.5 μm ($\bar{x}$ = 152 × 56 μm, n = 30), subglobose to pyriform or obovoid, solitary, holoblastic, with hairy, septate, unbranched, hyaline to pale brown apical appendages, reticulate outer wall, brown to dark brown, pale brown to hyaline at the apex.

Culture characteristics: Conidia germinated on PDA media within 18 h. Several germ tubes are produced. Colonies are irregular, with filamentous margin, raised and flat at the center, smooth, grey to pale brown from above, brown to black brown from below.

Material examined: China, Guizhou province, Xingyi City, on unidentified decaying wood, 27 November 2024, Xia Tang, GC48 (GZAAS25-0587, holotype, ex-type living culture GZCC 25-0557.

Notes: In our phylogenetic analysis (Figure 3.37), our collection (GZCC 25-0557) grouped with *Megacapitula villosa* (MFLUCC 24-0080, SNC122) forming a separate lineage, with 100% ML bootstrap support. In comparison of bp differences between our collection (GZCC 25-0557) and *M. villosa* MFLUCC 24-0080 revealed 9.44% (46/487 bp) difference in ITS region and 2.31% (19/819 bp) difference in LSU.

Morphologically, our collection fits with the generic characters of *Megacapitula* in having mycelium with pigmented hyphae, terminal conidiogenous cells, holoblastic, solitary conidia with hairy, apical appendages (Rajeshkumar et al., 2024). However, *Megacapitula villosa* can be easily distinguished from *M. guizhouensis* by its densely packed, apically arranged hairy appendages (Chen & Tzean, 1993). Therefore, based on morphological differences and phylogenetic analysis, we conclude our collection represent a new species, *Megacapitula guizhouensis* collected from China.

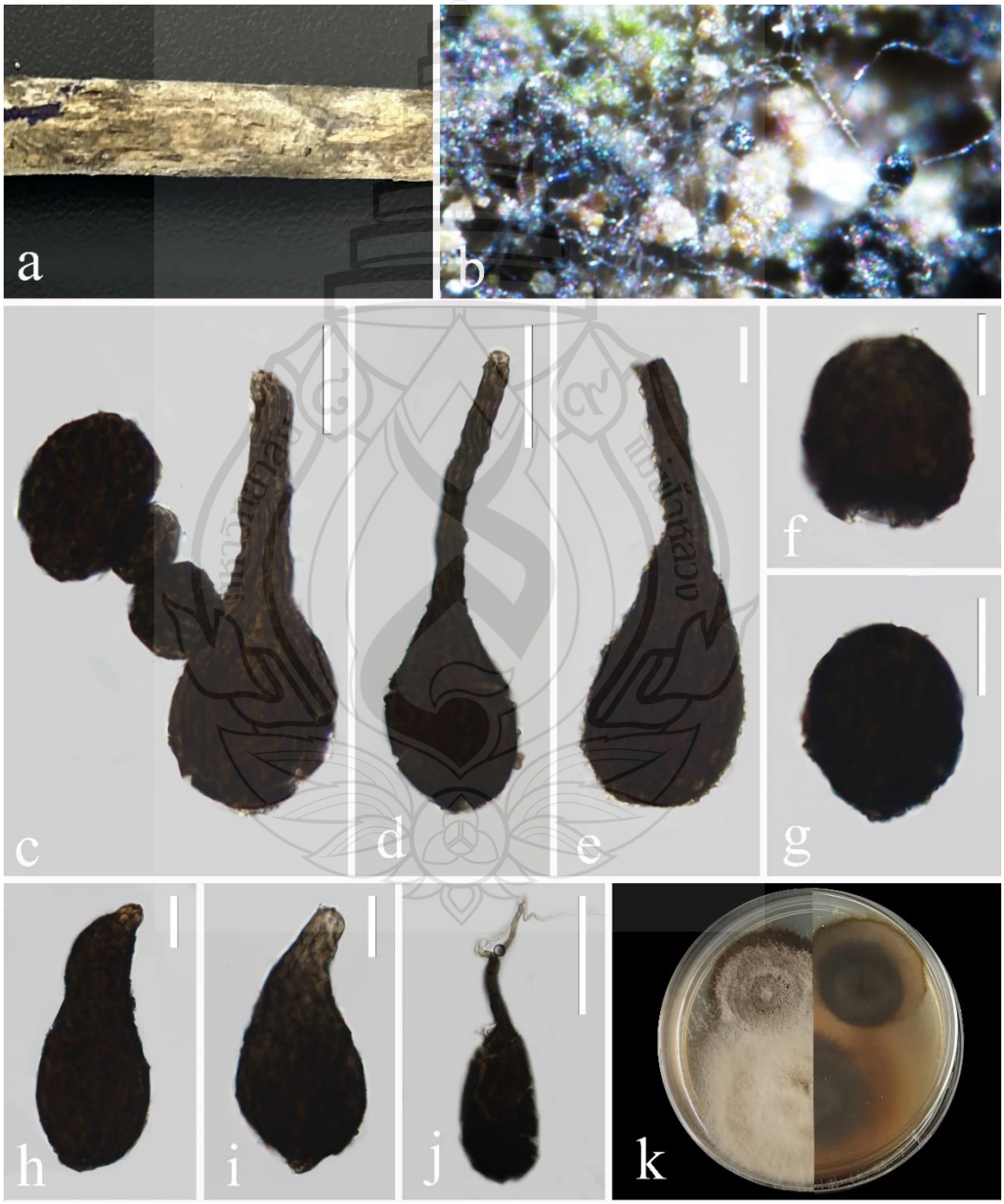

Figure 3.38 *Megacapitula guizhouensis* (GZCC 25-0557, holotype)

Figure 3.38 a Host substrate. b Colonies on natural substrate. c–j Conidia with conidiogenous cells (j, a conidium with apical appendages). k Colonies on culture media (left-above and right-below). Scale bars: j = 100 μm, d = 50 μm, e–i = 20 μm, c = 10 μm.

Melanommataceae G. Winter [as 'Melanommeae'], Rabenh. Krypt.-Fl., Edn 2 (Leipzig) 1.2: 220 (1885)

Byssosphaeria Cooke, Grevillea 7(no. 43): 84 (1879)

Index Fungorum number: IF 711; Facesoffungi number: FoF 00765

Notes: *Byssosphaeria* was introduced by Cooke and Plowright (1879) and *Byssosphaeria keithii* was assigned as the type species. Sexual morph of this genus is characterized by globose, sub-globose, ovoid, and turbinate ascomata that are smaller than 1000 μm with a well-developed subiculum, flat ostiole with yellow, orange or reddish-brown surrounding, hamathecium with long trabeculated pseudoparaphyses, cylindrical–clavate-to-clavate asci consist of fusiform, hyaline-to-brown ascospores with one or more septa (Cobos-Villagrán et al., 2025; Yu et al., 2025). Asexual morph is coelomycetous with pycnidia consist of phialidic conidiogenous cells and ellipsoidal or subglobose, hyaline conidia (Pem et al., 2019; Yu et al., 2025; Cobos-Villagrán et al., 2025). *Byssosphaeria* species have been reported as saprobes, endophytes, or parasites associated with woody angiosperms, on various substrates such as debarked wood bark, fallen branches, decaying leaves, as well as on petioles and pericarps in terrestrial, freshwater, and marine habitats (Yu et al., 2025; Cobos-Villagrán et al., 2025). Currently, 27 *Byssosphaeria* species are accepted in the Index Fungorum (2025). In this study, we introduced a new species *Byssosphaeria guizhouensis* found on unidentified decaying wood in China.

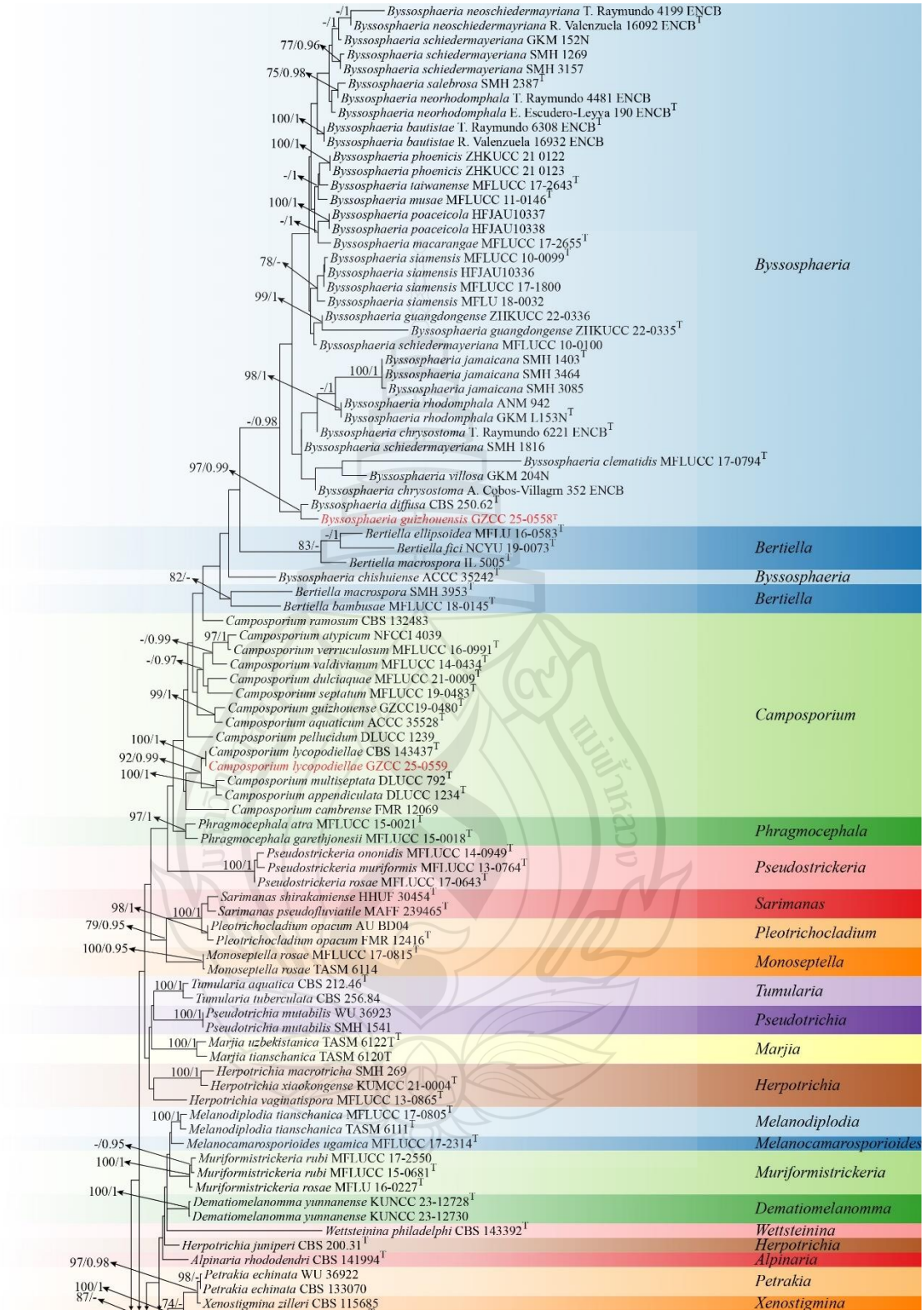

Figure 3.39 Phylogenetic analysis of *Melanommataceae*

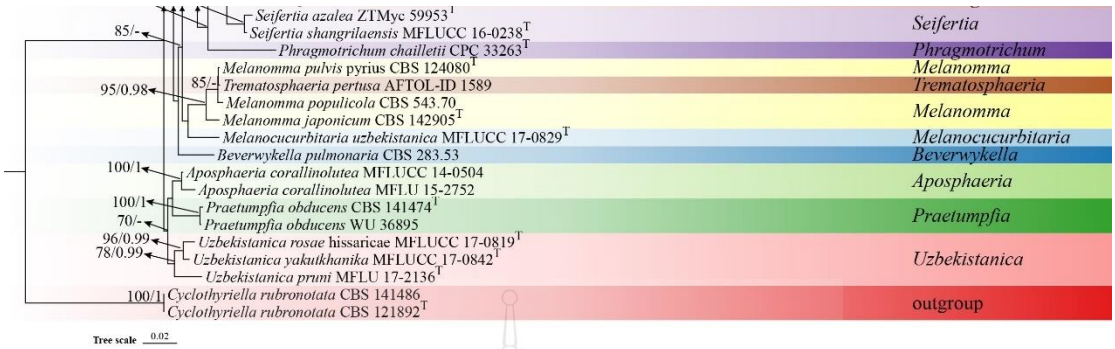

Figure 3.39 (continued)

Figure 3.39 Phylogenetic analysis of *Melanommataceae* was conducted using RAxML-based maximum likelihood analysis of a combined ITS, LSU, SSU and tef-1α sequence dataset. Bootstrap support values for maximum likelihood (ML) equal to or greater than 70% and Bayesian posterior probabilities (PP) equal to or greater than 0.95 are shown above the nodes. The tree is rooted with *Cyclothyriella rubronotata* (CBS 141486 and CBS 121892). Newly generated strains are highlighted in red, and type strains are indicated with a superscript 'T'.

Byssosphaeria guizhouensis X. Tang, Jayaward., R. J.C. Kang & K.D. Hyde sp. nov. Figure 3.40

Etymology: guizhouensis refers to Guizhou Province, China, where the type specimen was collected.

Holotype: GZAAS25-0588

Saprobic on unidentified decaying woodin the forest. **Sexual morph**: *Ascomata* globose to subglobose, superficial, mostly gregarious, occasionally scattered, unilocular, coriaceous, black, shiny, papillate, ostiolate. *Ostiole* single, central, *Peridium* consists of thick, black outermost wall and thin, brown innermost wall. *Hamathecium* composed with dense, trabeculate, anastomosing, hyaline pseudo paraphyses embedded in the hyaline gelatinous matrix. *Asci* 148.5–231× 10–13 diam. µm (($\bar{x}$ = 190 × 11.3 µm; n = 22) cylindric-clavate, 8-spored, apically round, short pedicellate. *Ascospores* 20–30 × 7–9 µm (($\bar{x}$ = 26 × 8 µm; n = 35), fusiform, slightly curved, tapering towards the both ends, uniseriately arranged, aseptate, grayish to pale brown at maturity, becoming brown to dark brown at the maturity, smooth-walled, with a germ slit and 2–4 guttules, surrounded by a thin sheath. **Asexual morph**: Undetermined.

Material examined: China, Guizhou province, Liupanshui City, Yushe National Forest Park, on unidentified decaying wood, 27 November 2024, Xia Tang, LS175 (GZAAS25-0588, holotype), ex-type living culture (GZCC 25-0558).

Notes: Morphologically, characteristics of our collection fit with *Byssosphaeria* by having globose to subglobose, superficial, unilocular, coriaceous, black, shiny, papillate, ostiolate ascomata; dense, trabeculate, anastomosing, hyaline pseudoparaphyses embedded in the hyaline gelatinous matrix. cylindric-clavate, 8-spored, apically round, short pedicellate asci and fusiform, slightly curved, tapering towards the both ends, aseptate, guttules ascospores with a germ slit surrounded by a thin sheath (Chen & Hsieh, 2004; Liu et al., 2025). In the phylogenetic analysis, our isolate (GZCC 25-0558) is grouped within *Byssosphaeria*, sister to the type strain of *B. diffusa* (CBS 250.62), with 97% ML bootstrap support and 0.99 BYPP (Figure 3.39). Excluding gaps, sequence comparison revealed 0.7% (6/807 bp) differences in the LSU, 0.3% (3/890 bp) differences in the SSU and 1.5 % (6/807 bp) differences in the *Tef1-α*. Based on these morphological and molecular data, we identify our isolate as a novel species, *B. guizhouensi*, following the guidelines of Jeewon and Hyde (2016) and Maharachchikumbura et al. (2021).

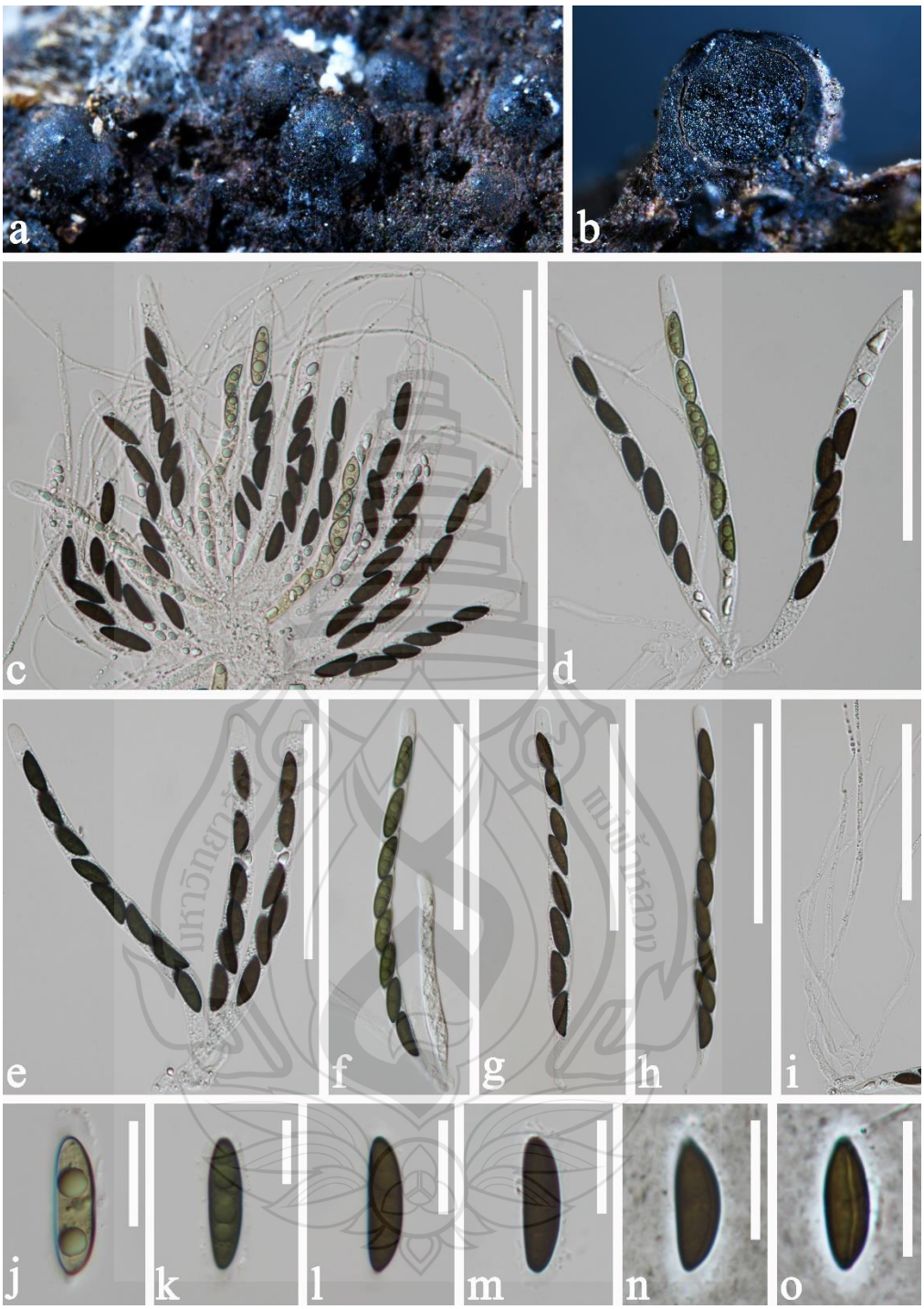

Figure 3.40 *Byssosphaeria guizhouensis* (GZAAS25-0588, holotype)

Figure 3.40 a, b ascomata on the host substrate. c Arrangement of the hamathecium including asci, ascospores and pseudoparaphyses. d–h Asci. i Pseudoparaphyses. j–m Ascospores. n, o Ascospores in indian ink. Scale bars: c–i = 100 µm, j–o = 20 µm.

Camposporium Harkn., Bull. Calif. Acad. Sci. 1(no. 1): 37 (1884)

Index Fungorum number: IF 7479; *Facesoffungi number*: FoF 08296;

Notes: *Camposporium* was introduced by Harkness (1884) with *C. antennatum* as the type species. This polymorphic genus is characterized by dematiaceous conidiophores, terminal, denticulate conidiogenous cells, and cylindrical to elongate, multi-septate conidia rounded at the both ends, with one or more cylindrical appendages at the apex (Pem et al., 2019; Hongsanan et al., 2020a,2020b; Liu et al., 2025). A polygenetic analysis conducted by Crous et al., (2018a) revealed that *Camposporium antennatum* and *Fusiconidium mackenziei* grouped together within *Melanommataceae*. However, based on the differences of conidiogenesis, conidial shapes and the presence of apical appendages these genera are distinct (Hyde et al., 2020). Hyde et al. (2020) placed *Camposporium* in *Melanommataceae* based on the phylogenetic analysis. Later, Koukol and Delgado (2021) synonymized *Fusiconidium* under *Camposporium* based on morphology and multigene phylogeny. *Camposporium* species have a cosmopolitan distribution ranged from freshwater to terrestrial habitats in the world (Hyde et al., 2020b; Liu et al., 2025). 33 species are accepted under *Camposporium* in Index Fungorum (2025).

Camposporium lycopodiellae (Crous & R.K. Schumach.) Tibpromma & K.D. Hyde, Fungal Diversity 100: 81 (2020); Figure 3.41

≡ *Fusiconidium lycopodiellae* Crous & R.K. Schumach., Fungal Systematics and Evolution 1: 188 (2018)

Saprobic on unidentified decaying wood. **Sexual morph**: Undetermined. **Asexual morph**: *Colonies* on natural substrate effuse, blackish-brown. *Conidiophores* solitary, erect, subcylindrical, geniculate-sinuous, brown, smooth. *Conidiogenous cells* terminal, subcylindrical, brown, smooth, proliferating sympodially, holoblastically; scars unthickened, undarkened. *Conidia* 62–94.5× 8–10.5 µm ($\bar{x}$ = 86.5 × 9.3 µm; n = 30), cylindrical, elongate, solitary, rounded or narrowly acute at the both ends, end cells slightly paler, grayish to pale olivaceous green when young, becoming pale brown at maturity, 9–12-septate, slightly constricted at the septa, smooth-walled, sometimes basal cell slightly conical with an appendage.

Cultural characteristics: Conidia germinated on PDA media within 24 h. Germ tubes were produced by both ends . Colonies are circular, raised towards the

center, with filamentous margin, smooth, pale brown at the edge and whitish at the center from above, pale-brown to orange from below.

Material examined: CHINA, Guizhou province, Liupanshui City, Yushe National Forest Park, on unidentified decaying wood, 27 November 2024, Xia Tang, LS199 (GZAAS25-0589), living culture (GZCC 25-0559).

Known distribution: China (this study); Germany (Crous et al., 2018a).

Known host: on unidentified decaying wood (this study); on stems of *Lycopodiella inundata* (Lycopodiaceae) (Crous et al., 2018a).

Note: Morphologically, our collection conforms to the diagnostic features of *Camposporium lycopodiellae*, characterized by solitary, subcylindrical, geniculate-sinuous, brown, smooth conidiophores. terminal, subcylindrical, brown, smooth, proliferating sympodially, holoblastic conidiogenous cells and the conidia perfomed cylindrical, elongate, solitary, rounded or narrowly acute at the both ends, end cells slightly paler, grayish to pale olivaceous green when young, becoming pale brown at maturity, 9–12-septate, slightly constricted at the septa, sometimes basal cell slightly conical with an appendage (Crous et al., 2018). In phylogenetic analyses(Figure 3.39), our collection (GZCC 25-0559) clustered with *Camposporium lycopodiellae* (CBS 143437), with 100% ML bootstrap support. Excluding gaps, sequence comparison revealed no differences (502 bp) in the ITS and LSU (804 bp) region between our isolate and *C. lycopodiellae* (CBS 143437). Based on these morphological and molecular data, we identify our isolate as *C. lycopodiellae*, following the guidelines of Jeewon and Hyde (2016) and Maharachchikumbura et al. (2021). This study represents the first report of *C. lycopodiellae* from China.

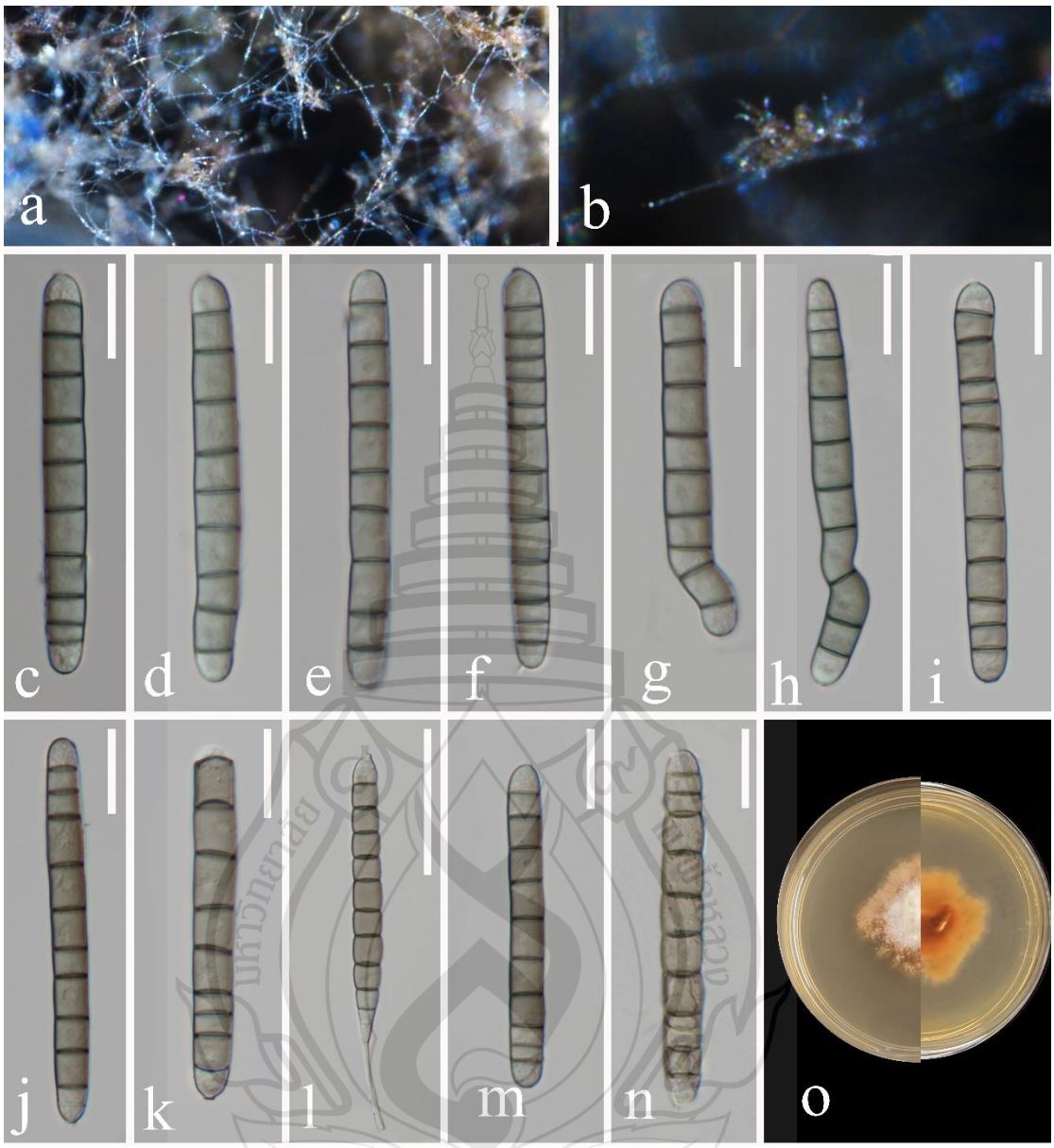

Figure 3.41 *Camposporium lycopodiellae* (GZCC 25-0559, new geographical record)

Figure 3.41 a, b Colonies on the natural substrate. c–n Conidia. o Colony on culture media (left-above and right-below). Scale bars: b–d = 100 µm, e–h = 50 µm, i–n = 20 µm.

Pleosporaceae Nitschke, Verh. naturh. Ver. preuss. Rheinl. 26: 74 (1869)

Pleocatenata Y.R. Sun, Yong Wang bis & K.D. Hyde, in Sun, Liu, Hyde, Jayawardena & Wang, MycoKeys 87: 85 (2022)

Index Fungorum number: IF 559457; *Facesoffungi number*: FoF 10630

Notes: *Pleocatenata* was introduced by Sun et al. (2022) to accommodate a sporidesmium-like fungus, *P. chiangraiensis* as the type species, found on medicinal plants in northern Thailand. The key morphologies of the genus are macronematous, mononematous, septate, unbranched, brown to dark brown conidiophores, terminal, monotretic, cylindrical conidiogenous cells, and catenate, obclavate, multi-euseptate, olivaceous to dark brown conidia in acropetal chain arrangement (Sun et al., 2022; Liu et al., 2024). Liu et al. (2024) transferred *Taeniolella robusta*, originally introduced by Sierra (1984), to the genus *Pleocatenata*. *Taeniolella robusta* shows a closer morphological resemblance to species of *Pleocatenata* than to the type species, *T. exilis*. Phylogenetically *T. exilis* was confirmed within *Kirschsteiniotheliales* (Hongsanan et al., 2020a, 2020b; Liu et al., 2024). However, due to the lack molecular data of *T. robusta*, Liu et al. (2024) kept it as a distinct taxon in *Pleocatenata*. The species of *Pleocatenata* have been reported as saprobes of decaying wood substrates from Cuba and Thailand. Currently, three species are accepted under *Pleocatenata*. In this study, we introduce a new species by expanding the taxonomic framework of the genus, based on morphology and phylogenetic evidence.

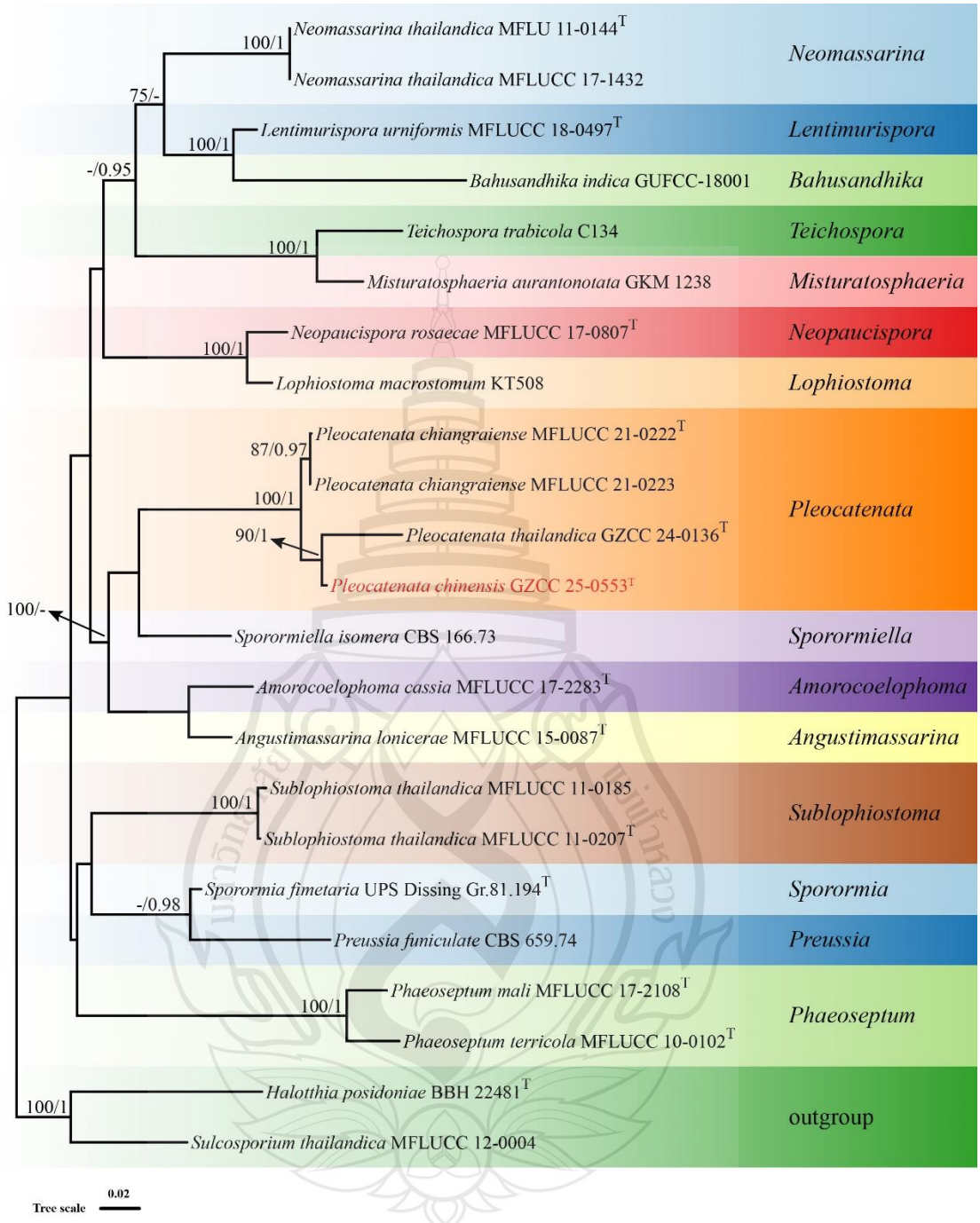

Figure 3.42 Phylogenetic analysis of *Pleocatenata*

Figure 3.42 Phylogenetic analysis of *Pleocatenata* was conducted using RAxML-based maximum likelihood analysis of a combined ITS, LSU, SSU, *tef-1α* and *rpb2* sequence dataset. Bootstrap support values for maximum likelihood (ML) equal to or greater than 70% and Bayesian posterior probabilities (PP) equal to or greater than 0.95 are shown above the nodes. The tree is rooted with *Halotthia posidoniae* (BBH 22481) and

Sulcosporium thailandica (MFLUCC 12-0004) Newly generated strains are highlighted in red, and type strains are indicated with a superscript 'T'.

Pleocatenata chinensis X. Tang, Jayaward., R. & K.D. Hyde sp. nov. Figure 3.2.36

Etymology: "chinensis" refers to China, where the type specimen was collected.

Holotype: GZAAS25-0583

Saprobic on decaying wood in a terrestrial habitat. **Sexual morph**: Unddetermined. **Asexual morph**: Hyphomycetous. *Colonies* on natural substrate effuse, dark brown to black. Mycelium consist branched, septate, brown hyphae. *Conidiophores* 68–151 × 8.5–11 μm ($\bar{x}$ = 100.5 × 9.5 μm, n = 25), macronematous, mononematous, cylindrical, septate, darkened and thickened at the septa, unbranched, straight, truncate at the apex, brown to dark brown, thick-walled. *Conidiogenous cells* 8–11.5 × 5.5–6 μm ($\bar{x}$ = 9.5 × 5.7 μm, n = 25), terminal, monoblastic, cylindrical, integrated brown. *Conidia* 25–53 × 9.5–13 μm ($\bar{x}$ = 38 × 5.7 μm, n = 25), obclavate, straight or slightly curved, guttulate, multi-euseptate, terminal, rounded at the apex, truncate at the base, brown to dark brown.

Culture characteristics: Conidia germinated on PDA media within 24 h. Several germ tubes are produced. Colonies are irregular, with filamentous margin, raised and flat at the center, smooth, whitish-pale brown from above, greenish-black brown from below.

Material examined: China, Hainan Province, Jianfengling National Forest Park, on unidentified decaying wood, 24 September 2024, Xia Tang, D28.1 (GZAAS25-0583), ex-type living culture GZCC 25-0553.

Notes: In the phylogeny, strain of our isolate (GZCC 25-0553) is grouped within *Pleocatenata*, sister to the type strain of *P. thailandica* (GZCC 24-0136), with 90% ML bootstrap support (Figure 3.42). Morphologically, characteristics of our collection fit with *Pleocatenata* by having macronematous, mononematous, cylindrical, unbranched, dark brown conidiophores with septa, terminal, cylindrical, dark brown conidiogenous cells, obclavate, dark brown, multi-euseptate conidia slightly constricted at septa (Sun et al., 2022). However, it differs to *P. thailandica* (GZCC 24-0136) by having longer conidiophores (68–151 × 8.5–11 μm vs. 22–61 × 4–7.5 μm) (Liu et al., 2024). In base pair comparison between these two strains have 1.6% bp (8/483) in ITS

region. Thus, based on morphology and phylogeny, we identified our isolate as a new species, *Pleocatenata chinensis*, collected from China.

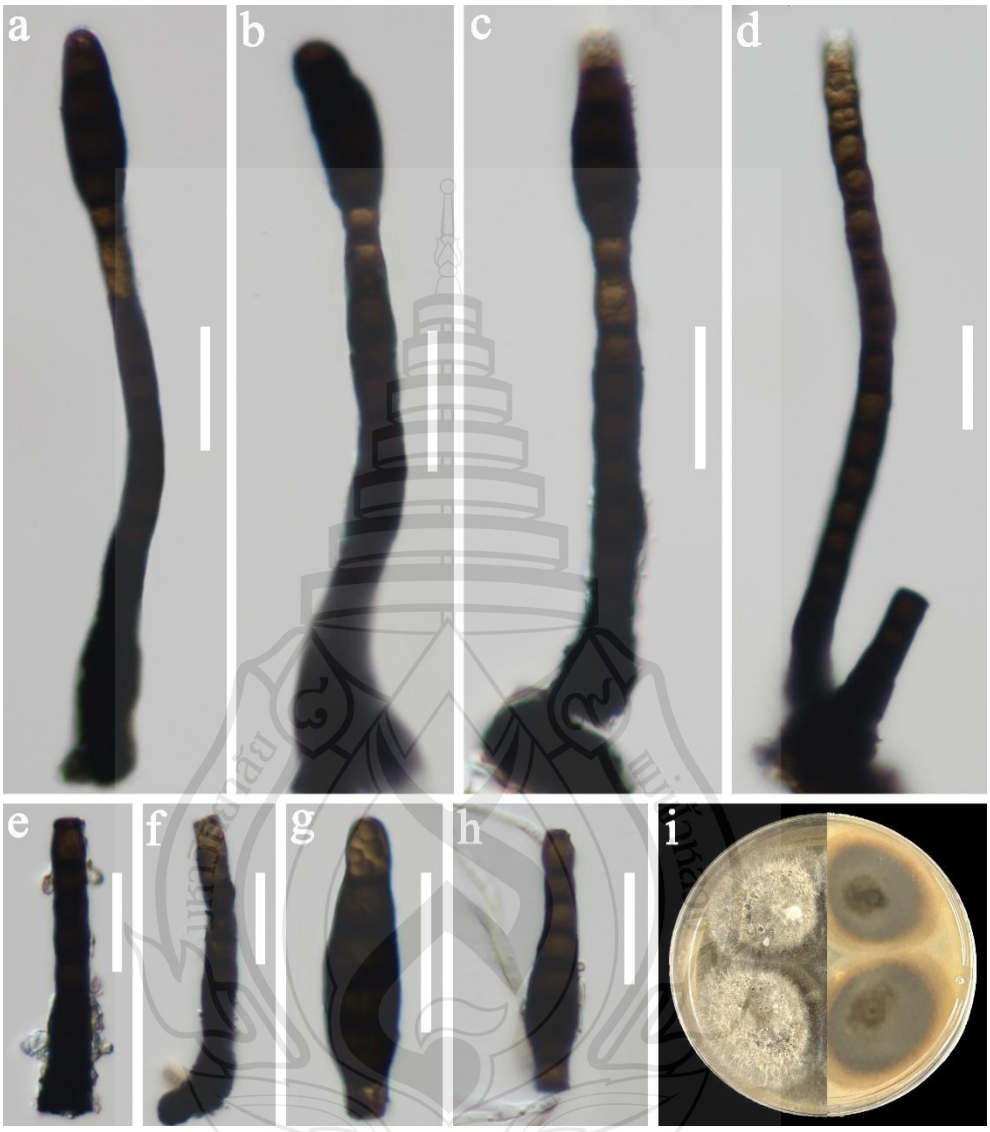

Figure 3.43 *Pleocatenata chinensis* (GZAAS25-0583, holotype)

Figure 3.43 a–c Conidiophores and conidia. d–f Conidiophores and conidiogenous cells. g Conidium. h A germinating conidium. i Colonies on culture media (left-above and right-below). Scale bars: a–h = 20 μm.

Roussoellaceae J.K. Liu, Phookamsak, D.Q. Dai & K.D. Hyde, Phytotaxa 181 (1): 7 (2014)

Roussoella Sacc., Atti Ist. Veneto Sci. Lett. Arti ser. 6, 6: 410 (1888)

Index Fungorum number: IF 4799; *Facesoffungi number*: FoF 06604

Notes: *Roussoella* is the type genus of *Roussoellaceae*, originally introduced by Saccardo and Paoletti (1888) based on the type species *R. nitidula*, which was first collected from bamboo in Malaysia. Species of *Roussoella* are predominantly saprobic on monocotyledons, especially bamboo and palms, although a few species have been reported on dicotyledonous hosts (Dai et al., 2022; Hongsanan et al., 2025). They inhabit mainly terrestrial environments, with occasional occurrences in freshwater habitats (Dong et al., 2020). The sexual morph of *Roussoella* is characterized by immersed, black, uni- to multi-loculate ascostromata; bitunicate, cylindrical to cylindric-clavate asci; and pale brown to dark brown, ellipsoidal to fusiform, 1-septate, ornamented ascospores with or without a mucilaginous sheath (Dong et al., 2020). The asexual morph has been observed both in nature and in culture (Hyde et al., 2023). It is cytospora-like, forming pycnidial, semi-immersed to superficial conidiomata with enteroblastic, phialidic, cylindrical to ampulliform conidiogenous cells, and hyaline to brown, globose to ellipsoidal, aseptate or septate conidia (Dai et al., 2017; Dong et al., 2020). Currently, 58 species are accepted in the genus *Roussoella* (Hongsanan et al., 2025; Sun et al., 2025).

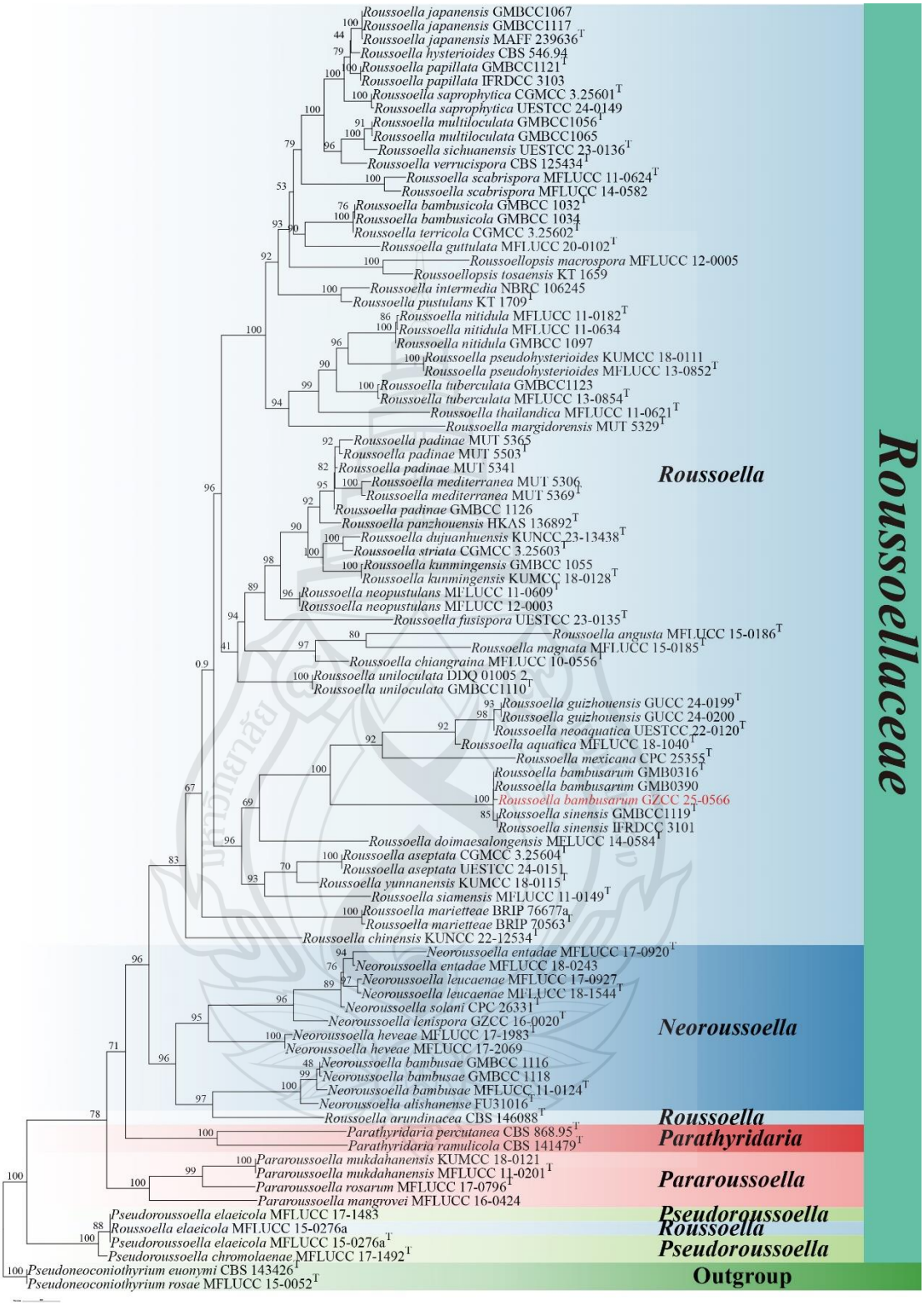

Figure 3.44 Phylogenetic analysis of *Roussoellaceae*

Figure 3.44 Phylogenetic analysis of *Roussoellaceae* was conducted using RAxML-based maximum likelihood analysis of a combined ITS, LSU, *rpb2* and *tef-1α* sequence dataset. Bootstrap support values for maximum likelihood (ML) equal to or greater than 70% and Bayesian posterior probabilities (PP) equal to or greater than 0.95 are shown above the nodes. The tree is rooted with *Parathyridaria percutanea* (CBS 868.95) and *Pa. ramulicola* (CBS 141479). Newly generated strains are highlighted in red, and type strains are indicated with a superscript 'T'.

Roussoella bambusarum H.M. Hu & Q.R. Li, MycoKeys 93: 178 (2022); Figure 3.45

Saprobic on decaying culms of bamboo. **Sexual morph**: *Ascostromata* immersed under a clypeus, solitary or scattered, raised hemispherical or dome-shaped on host epidermis, black, coriaceous, glabrous, uni-loculate. *Locules* 393.5–547 × 200.5–337 μm ($\bar{x}$ = 468.2 × 265 μm, n = 3), immersed within ascostromata, black, globose to subglobose. *Ostioles* with minute papillate. *Peridium* composed of dark brown thin-walled cells of textura angularis. *Hamathecium* comprised of 1–3.5 μm ($\bar{x}$ = 2.2 μm, n = 30) wide, numerous, septate, branched, anastomosing, filiform, hyaline, *pseudoparaphyses*. *Asci* 138–166 × 6–12 μm ($\bar{x}$ = 151 × 9.7 μm, n = 30), 8-spored, bitunicate, cylindrical, straight to curved, short pedicellate with knob-like pedicel, apically rounded with an indistinct ocular chamber. *Ascospores* 17–23 × 6–9.5 μm ($\bar{x}$ = 19.4 × 8 μm, n = 30), 1-seriate, sometimes overlapping, ellipsoidal to fusiform, 2-celled, 1-septata with a visible as transverse dark bands, slightly constricted at the septum, straight, rough-walled, guttulate, pale brown to brown, conically rounded ends, with longitudinal striations. **Asexual morph**: Undetermined.

Culture characteristics: Colonies on PDA at 25°C germinate from the base of ascospore, circular, with a flat to slightly raised surface and a dense, velvety to floccose. Mycelium is expansive, covering all over of the dish. The colony surface is dull to slightly lustrous, floccose–cottony in patches with dense aerial mycelium centrally, locally appressed, white to pale buff, becoming isabelline to grey-olivaceous in mottled patches; amber exudate droplets present. The colony reverse is dark olivaceous-brown to black, with scattered ochraceous punctae/stromatic spots.

Material examined: CHINA, Guizhou province, Xingyi City, Xianheping National Forest Park, on decaying culms of bamboo, 27 November 2024, Xia Tang,

XY03 (GZAAS25-0596), living culture (GZCC 25-0566).

Known distribution: China (Hu et al., 2022; this study).

Known hosts: on decaying culms of *Bambusa bambusarum* (Hu et al., 2022); on dead culm of bamboo (this study).

Notes: In phylogenetic analyses, our isolate (GZCC 25-0566) clustered with *R. bambusarum* (GMB0316 and GMB0390) (Figure 3.44). Nucleotide sequence comparisons between our isolate and the type strain of *R. bambusarum* (GMB0316) revealed minimal differences: 0.2% (1/4478 bp) in ITS and no difference (0/804 bp) in LSU, excluding gaps. Based on these morphological and molecular data, and following the guidelines of Jeewon and Hyde (2016) and Maharachchikumbura et al. (2021), we identify our collection as the known species, *R. bambusarum*.

Roussoella bambusarum was established by Hu et al. (2022) from decaying culms of *Bambusa bambusarum* in China. Our collection, also from bamboo in China, provides an additional record and broadens the ecological notes on this species by documenting its substrate/host association (Hu et al., 2022).

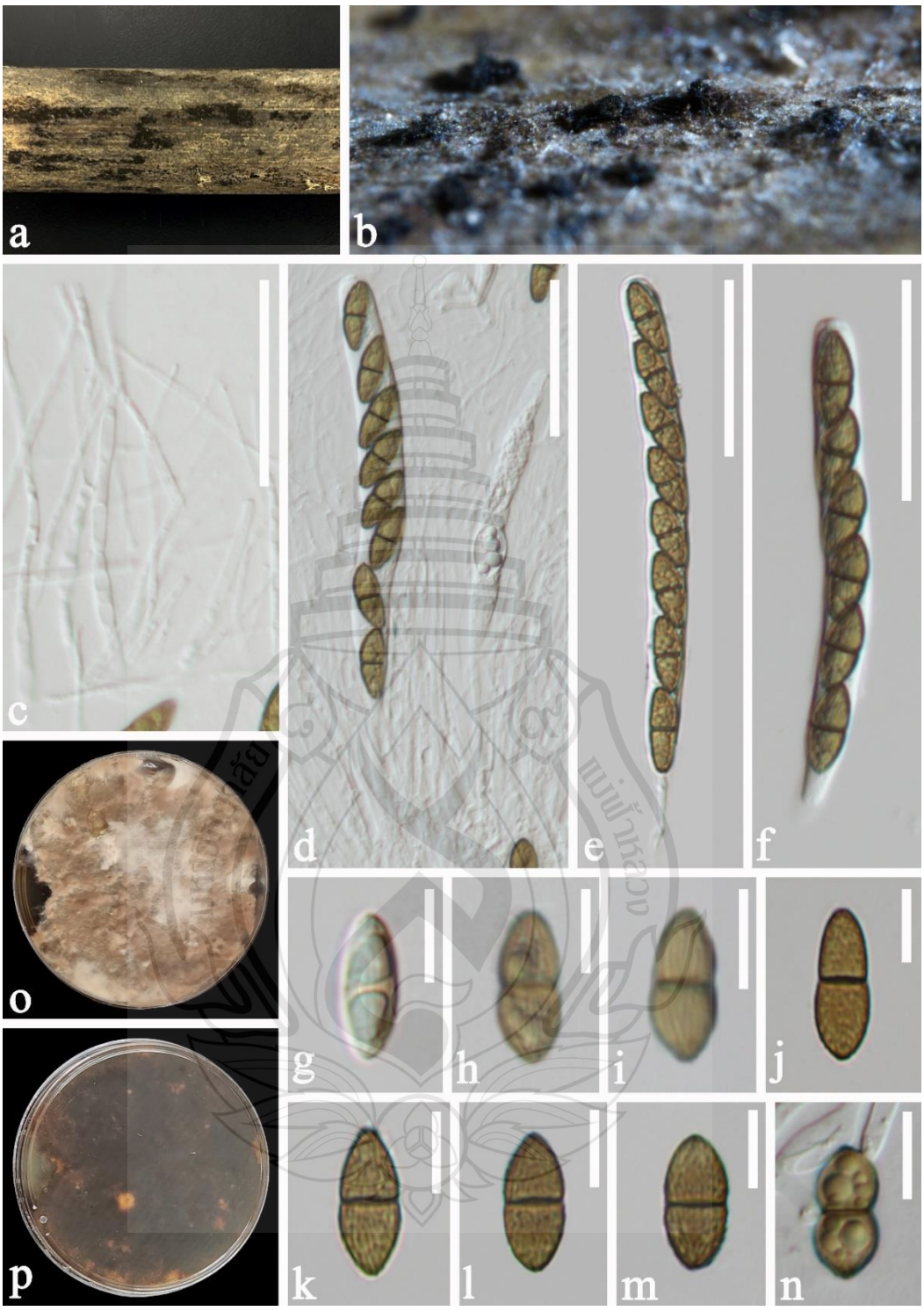

Figure 3.45 *Roussoella bambusarum* (GZAAS25-0596, new collection)

Figure 3.45 a Host. b Ascostromata on substrate. c Pseudoparaphyses. d–f Asci. g–m Ascospore. n Germinated ascospore. o Colony on PDA (from front). p Colony on PDA (from reverse). Scale bars: c–f = 40 μm, g–n = 10 μm.

Pseudomassarinaceae Phukhams. & K.D. Hyde, Fungal Diversity 102: 99 (2020)

Neopleopunctum X. Tang, Jayaward, J.C. Kang & K.D. Hyde, gen. nov.

Etymology: To refers this genus morphologically similar to *Pleopunctum*.

Saprobic on unidentified decaying wood in the forest. **Sexual morph**: Undetermined. **Asexual morph**: *Colonies* on the natural substrate superficial, effuse, solitary, scattered, dark brown to black. *Mycelium* mostly partly superficial, composed of branched, septate, brown to dark brown. *Conidiophores* macronematous, mononematous, erect, straight or flexuous, cylindrical, septate, smooth, subhyaline to pale brown. *Conidiogenous cells* monoblastic terminal, cylindrical, smooth, subhyaline to pale brown. *Conidia* solitary, acrogenous, muriform, oval, ellipsoidal, clavate, sometimes pyramidal, rarely irregular, smooth, slightly or deeply constricted, brown to dark brown, broadly obtuse at the apex with a pale brown elliptical to globose basal cell, sometimes infundibuliform or absent.

Type species: *Neopleopunctum hydeanum* X. Tang, Jayaward, J.C. Kang & K.D. Hyde

Notes: Phylogenetic analyses using Maximum Likelihood (ML) and Bayesian Inference (BYPP) robustly place *Neopleopunctum* as a distinct lineage sister to Pseudomassarina (ML bootstrap support = 97%; Bayesian posterior probability = X.XX) within *Pseudomassarinaceae* (*Pleosporales*) (Figure 3.2.39).

Previously, the family Pseudomassarinaceae comprised only a single genus, *Pseudomassarina* Phukhams. & K.D. Hyde, which was described from sexual morphs on dead stems of *Clematis vitalba* in Italy. In contrast, *Neopleopunctum* exhibits an asexual morph. Following the taxonomic guidelines of Jeewon and Hyde (2016) and Maharachchikumbura et al. (2021), which emphasize the integration of molecular divergence and phenotypic distinctness in genus delimitation, we propose *Neopleopunctum* as a novel genus within *Pseudomassarinaceae*, with *N. hydeanum* designated as the type species, rather than treating it as a new species of *Pseudomassarina*. The observed ITS/LSU sequence divergence (exceeding genus-level thresholds in fungi) together with differences in reproductive mode further support its recognition as a distinct genus.

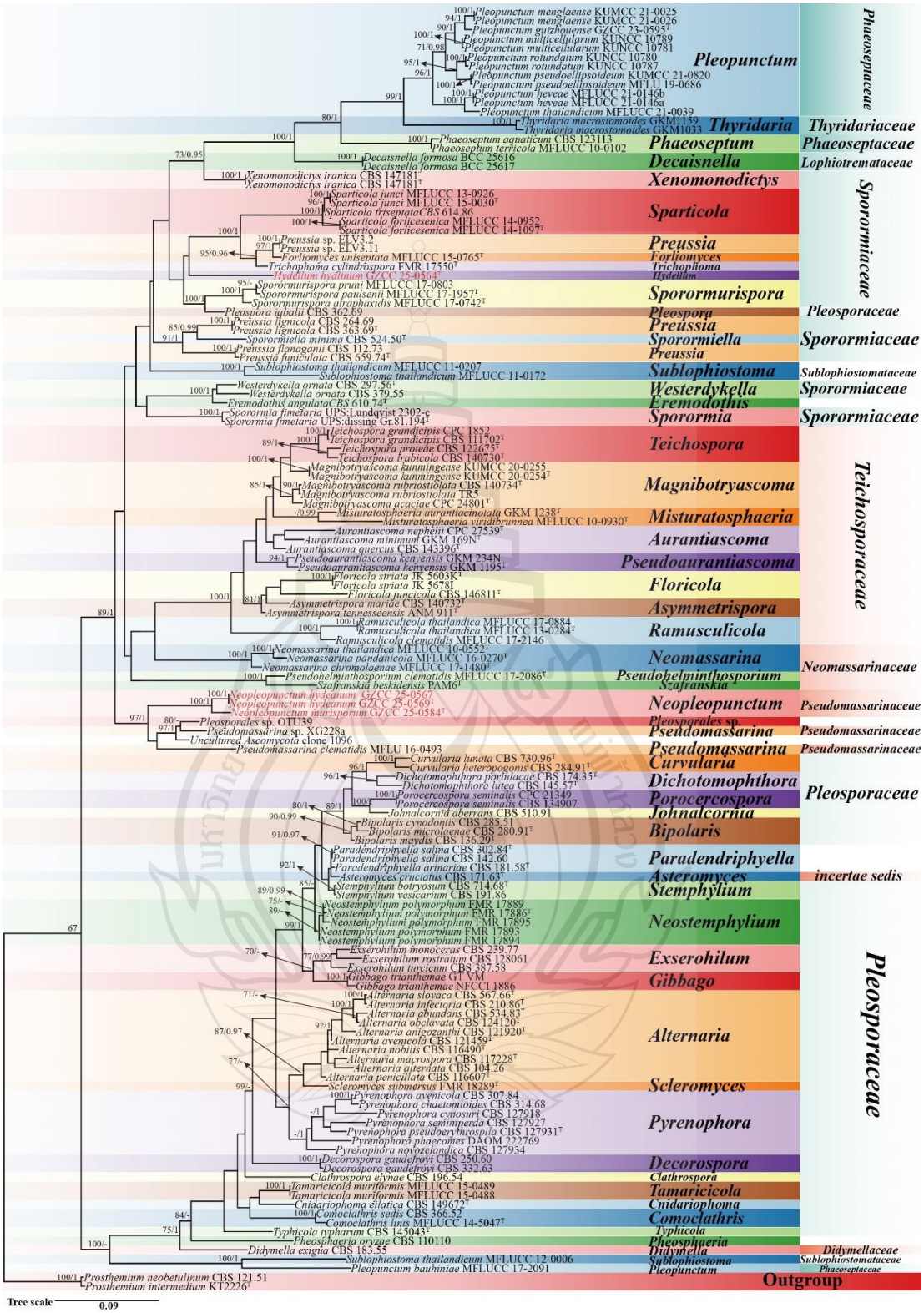

Figure 3.46 Phylogenetic analysis of *Pseudomassarinaceae*

Figure 3.46 Phylogenetic analysis of *Pseudomassarinaceae* was conducted using RAxML-based maximum likelihood analysis of a combined LSU and ITS sequence dataset. Bootstrap support values for maximum likelihood (ML) equal to or greater than 70% and Bayesian posterior probabilities (PP) equal to or greater than 0.95 are shown above the nodes. The tree is rooted with *Prosthemium neobetulinum* (CBS 121.51) and *P. intermedium* (KT2226). Newly generated strains are highlighted in red, and type strains are indicated with a superscript 'T'.

Neopleopunctum hydeanum X. Tang, Jayaward, J.C. Kang & K.D. Hyde, sp. nov.; Figure 3.47

Etymology: Named in honor of Professor Kevin D. Hyde, recognizing his outstanding contributions to mycology and commemorating his 70th birthday.

Holotype: GZAAS25-0598

Saprobic on unidentified decaying wood in the forest. **Sexual morph**: Undetermined. **Asexual morph**: *Colonies* on the natural substrate superficial, effuse, solitary, scattered, dark brown to black, glistening. *Mycelium* mostly partly superficial, composed of branched, septate, brown to dark brown. *Conidiophores* macronematous, mononematous, erect, straight or flexuous, cylindrical, septate, smooth, subhyaline to pale brown. *Conidiogenous cells* 5–11 × 2–3 μm ($\bar{x}$ = 8.9 × 2.7 μm, n = 5), monoblastic terminal, cylindrical, smooth, subhyaline to pale brown. *Conidia* 30–65 × 19–36 μm ($\bar{x}$ = 49.7 × 28.8 μm, n = 30), solitary, acrogenous, muriform with 10–13 transverse-septate, 6–9 longitudinal septa, oval, ellipsoidal, clavate, sometimes pyramidal, rarely irregular, smooth, slightly or deeply constricted, brown to dark brown, broadly obtuse at the apex with a pale brown elliptical to globose basal cell, sometimes infundibuliform or absent.

Culture characteristics: Colonies on PDA at 25°C, circular, umbonate, and dry, with an entire margin. The surface exhibits a veined texture and cottony (floccose) mycelium, appearing brown overall but with a distinct olive-green central disc. A very fine, sparse mycelial fringe is present at the periphery. The reverse is brown, with paler coloration corresponding to the surface patterning. The colony is surrounded by a diffuse halo of light-colored, sparse hyphae.

Material examined: China, Guizhou province, Liupanshui City, Yushe National Forest Park, on unidentified decaying wood, 15 March 2023, Xia Tang, TY32 (GZAAS25-0598, holotype, ex-type living culture GZCC 25-0568, GZCC 25-0569.

CHINA, Guizhou province, Zunyi City, Chishui Bamboo Sea National Forest Park, on decaying branches of bamboo, 07 May 2023, Xia Tang, CS66 (GZAAS25-0597, paratype, living culture GZCC 25-0567.

Notes: Phylogenetic analyses, Maximum Likelihood (ML) and Bayesian Inference (BYPP), robustly place *Neopleopunctum hydeanum* as a sister to species of *Pseudomassarina* (ML bootstrap support = 97%, Bayesian posterior probability = 1) within *Pseudomassarinaceae* (*Pleosporales*) (Figure 3.46). The nucleotide comparison revealed differences of 8.9% (36/403 bp) in the ITS region and 3.2% (26/804 bp) in the LSU region (excluding gaps) between *N. hydeanum* (GZCC 25-0568) and *P. clematidis* (MFLU 16–0493). Similarly, comparisons between *N. hydeanum* (GZCC 25-0568) and *Pseudomassarina* sp. (XG228a) showed 10% (50/515 bp) divergence in ITS and 3% (23/806 bp) in LSU, also excluding gaps. Crucially, *Neopleopunctum* exhibits asexual morph such as macronematous, mononematous conidiophores; monoblastic terminal, cylindrical conidiogenous cell; solitary, acrogenous, muriform, brown to dark brown conidia with a pale brown elliptical to globose basal cell, consistent with morphological traits observed in other pleosporalean taxa, whereas species of *Pseudomassarina* is characterized by sexual morphs. Due to this reproductive disparity, direct morphological comparisons were unfeasible.

Following the taxonomic guidelines of Jeewon and Hyde (2016) and Maharachchikumbura et al. (2021), which emphasize combined molecular divergence and phenotypic distinctness for species delimitation, we propose *Neopleopunctum hydeanum* as a new species of *Neopleopunctum* within *Pseudomassarinaceae*.

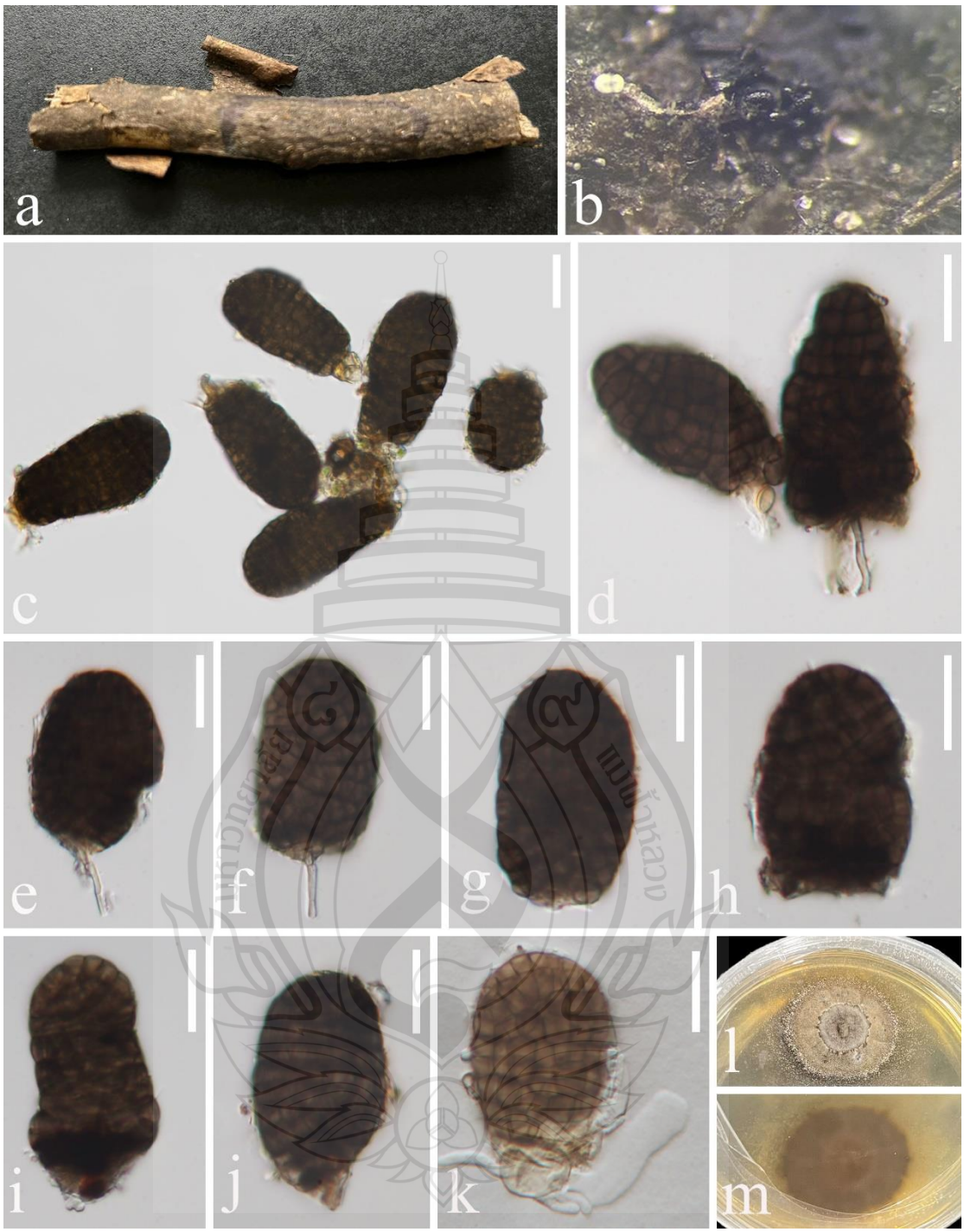

Figure 3.47 *Neopleopunctum hydeanum* (GZAAS25-0598, holotype)

Figure 3.47 a Specimen. b Colonies on substrate. c– f Conidiogenous cells, conidiogenous cells bearing conidia. g–j Conidia. k Germinated conidium. l Colony on PDA (from front). m Colony on PDA (from reverse). Scale bars: c–k = 20 μm.

Neopleopunctum murisporum X. Tang, Jayaward, J.C. Kang & K.D. Hyde, sp. nov.; Figure 3.48

Etymology: The specific epithet 'murisporum' refers to the muriform conidia.

Holotype: GZAAS25-0614

Saprobic on unidentified decaying wood in the forest. **Sexual morph**: Undetermined. **Asexual morph**: *Colonies* on the natural substrate superficial, effuse, solitary, scattered, dark brown to black, glistening. *Mycelium* mostly partly superficial, composed of branched, septate, brown to dark brown. *Conidiophores* reduce to conidiogenous cells. *Conidiogenous cells* monoblastic terminal, cylindrical, smooth, subhyaline to pale brown. *Conidia* 30–52 × 20–32 µm ($\bar{x}$ = 43.4 × 25.4 µm, n = 30), solitary, acrogenous, murifor with 6–8 transverse-septate, 4–5 longitudinal septa, oval, ellipsoidal, clavate, smooth, slightly constricted at the septate, brown to dark brown, broadly obtuse at the apex with a pale brown elliptical to globose basal cell 5.5–13 × 7.5–15 µm ($\bar{x}$ = 9.8 × 10.5 µm, n = 15), sometimes retraction causes the basal cell to shrink.

Culture characteristics: Colonies on PDA at 25°C, circular, raised, and dry with an entire margin. Surface rough and cottony, fluffy, creamy with a brown, very thin mycelia ring at the edge; reverse uniformly reddish brown with a circular, pale brown ring at the edge, some darker spots scattered all over the colony.

Material examined: China, Xingyi City, Xianheping National Forest Park, on decaying branches of Juglans, 27 November 2024, Xia Tang, XY14 (GZAAS25-0614, holotype, ex-type living culture GZCC 25-0584.

Notes: Phylogenetic analyses (Maximum Likelihood (ML) and Bayesian Inference BYPP), our new species is sister to *Neopleopunctum hydeanum* with a stable support (ML bootstrap support = 100%, Bayesian posterior probability = 1) within the genus, *Neopleopunctum* (Figure 3.46). The comparison of the nucleotides between *N. murisporum* (GZCC 25-0584) and *N. hydeanum* (GZCC 25-0568) shows differences of 4.5% (25/552 bp) across ITS and 0.6% (5/807 bp) across LSU, excluding gaps. Morphologically, *N. murisporum* differs with *N. hydeanum* by its reduced conidiophores and oval, ellipsoidal, clavate, sparsely septate (transverse-septate and longitudinal septa) (6–8 transverse-septate vs. 10–13 transverse-septate and 4–5 longitudinal septa vs. 6–9 longitudinal septa) and smaller conidia (30–52 × 20–32 µm, L/W ratio = 1.71 vs. 30–65 × 19–36, L/W ratio = 1.73) with a retraction causes the basal cell to shrink basal cell, whereas,

N. hydeanum has pyramidal conidia with an infundibuliform or absent basal cell.

Based on both differences of Phylogenetic and morphological analysis, we introduced our new taxon, *N. murisporum* as a new species under *Neopleopunctum* with following the taxonomic guidelines of Jeewon and Hyde (2016) and Maharachchikumbura et al. (2021).

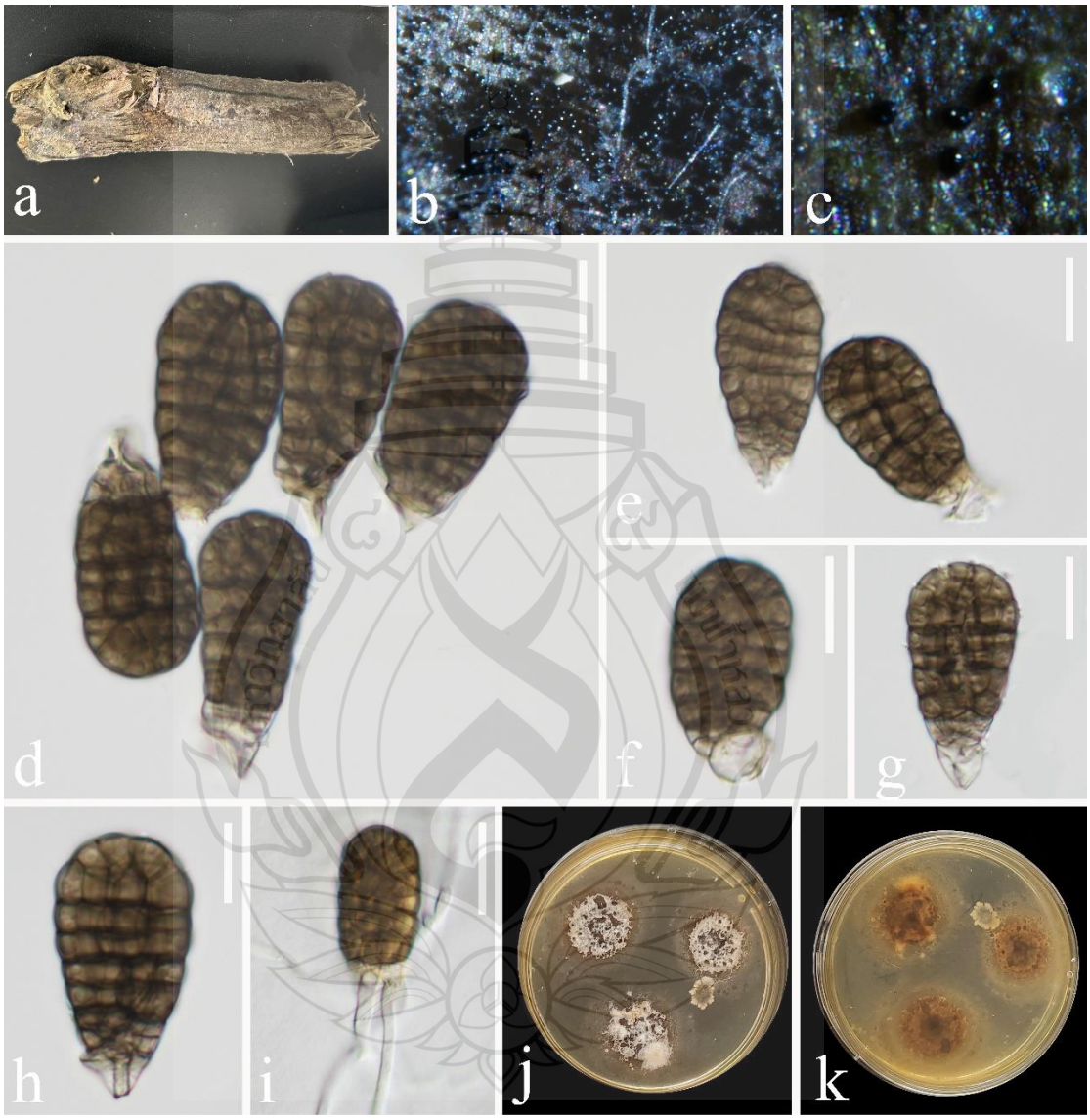

Figure 3.48 *Neopleopunctum murisporum* (GZAAS25-0614, holotype)

Figure 3.48 a Specimen. b, c Colonies on substrate. d–h Conidia. i Germinated conidium. j Colony on PDA (from front). k Colony on PDA (from reverse). Scale bars: d–i= 20 μm.

Sporormiaceae Phukhams. & K.D. Hyde, Fungal Diversity 102: 99 (2020)

Hydellum X. Tang, Jayaward & J.C. Kang, gen. nov.

Etymology: Named in honor of Professor Kevin D. Hyde, recognizing his outstanding contributions to mycology and commemorating his 70th birthday.

Saprobic on an unidentified decaying wood in the forest. **Sexual morph**: *Ascomata* perithecial, erumpent, scattered, solitary, coriaceous, immersed, globose to subglobose, centrally ostiolate, with a minute papilla, dark brown to black. *Peridium* is composed of brown, compressed cells of textura angularis. *Hamathecium* consisting of cylindrical, unbranched, smooth, hyaline, septate, straight to flexuous, constricted at the septa, tapering toward the apex, *pseudoparaphyses*. *Asci* 8-spored, bitunicate, fissitunicate, clavate to broadly fusoid, short-pedicellate, with a blunt, apically rounded apex bearing an ocular chamber. *Ascospores* biseriate, fusiform, acutely to bluntly rounded at both ends, 4-celled, guttulate, 3-septate, constricted at the septa, most strongly at the median septum, straight to slightly curved, smooth-walled, hyaline, becoming dark olive-green upon germination with walls and septa turning dark brown, surrounded by a prominent mucilaginous sheath. **Asexual morph**: Undetermined.

Type species: *Hydellum hyalinum* X. Tang, Jayaward, J.C. Kang & K.D. Hyde

Notes: *Hydellum* shares morphological characteristics with other members of the family *Sporormiaceae*, including the formation of pseudothecia with fissitunicate asci (Kruys & Wedin, 2009; Hyde et al., 2013), and typically 4-celled ascospores that are constricted at the septa and often disarticulate into part-spores at maturity, each surrounded by a mucilaginous sheath (Barr, 2000; Hyde et al., 2013).

The family *Sporormiaceae* currently comprises 11 genera: *Chaetopreussia* Locq.-Lin., *Forliomyces* Phukhams., *Camporesi* & K.D. Hyde, *Pleophragmia* Fuckel, *Preussia* Fuckel, *Sparticola* Phukhams., Ariyaw., Camporesi & K.D. Hyde, *Sporormia* De Not., *Sporormiella* Ellis & Everh., *Sporormurispora* Wanas., Bulgakov, Gafforov & K.D. Hyde, *Trichophoma* Magaña-Dueñas, Cano & Stchigel, *Westerdykella* Stolk, and *Xenomonodictys* Hern.-Restr., Karimi, Alizadeh & T. Ghanbary. Among these, *Forliomyces*, *Trichophoma*, and *Xenomonodictys* are known only by their asexual morphs; *Preussia*, *Sparticola*, and *Westerdykella* exhibit both sexual and asexual morphs (Eisvand & Mehrabi-Koushki, 2025; Phurbu et al., 2025), whereas *Chaetopreussia*, *Pleophragmia*, *Sporormia*, *Sporormiella*, *Sporormurispora*, and the taxon examined in this study are

known solely from their sexual morph (Grove, 1886; Viégas, 1943; Pawar et al., 1967; Locquin-Linard, 1977; Wanasinghe et al., 2018; Crous et al., 2020; Yuan et al., 2020; Song et al., 2020; this study).

However, the collection examined here can be distinguished from other sexually reproducing genera in *Sporormiaceae* by a combination of characteristics, including the type, size, and structure of the ascomata and asci, and particularly by ascospore features such as colour, size, shape, and number of cells.

In the phylogenetic analysis, *Hydellum* is resolved within *Sporormiaceae*, where it forms a distinct lineage sister to a clade comprising *Preussia*, *Sporormurispora*, *Forliomyces*, and *Trichophoma* (Figure 3.46). Based on its unique morphological characteristics (Figure 3.49) and robust phylogenetic placement (Figure 3.46), *Hydellum* is proposed as a new genus with type species, *Hydellum hyalinum* in the *Sporormiaceae*. In this study, we describe its sexual morph; its asexual morph remains to be discovered.

Hydellum hyalinum X. Tang, Jayaward, J.C. Kang & K.D. Hyde, sp. nov.; Figure 3.49

Etymology: The epithet refers to the hyaline ascospores.

Holotype: GZAAS25-0594

Saprobic on an unidentified decaying wood in the forest. **Sexual morph**: *Ascomata* 330–817 × 254–673 μm ($\bar{x}$ = 622.8 × 429 μm, n = 20), perithecial, erumpent, scattered, solitary, coriaceous, immersed, globose to subglobose, centrally ostiolate, with a minute papilla, dark brown to black. *Ostioles* central, papillate, with a short canal., *Peridium* 22–84 μm ($\bar{x}$ = 45.2, n = 30) composed of brown, compressed cells of textura angularis. *Hamathecium* consisting of cylindrical, unbranched, smooth, hyaline, septate, straight to flexuous, constricted at the septa, tapering toward the apex, exceeding the asci, *pseudoparaphyses* with anastomosing hyphae 1.5–4 μm ($\bar{x}$ = 2.7, n = 30) wide. *Asci* 132.5–174 × 25.5–33 μm ($\bar{x}$ = 150.8 × 29 μm, n = 10), 8-spored, bitunicate, fissitunicate, clavate to broadly fusoid, short-pedicellate, with a blunt, apically rounded apex bearing an ocular chamber. *Ascospores* 25–43 × 9–15 μm ($\bar{x}$ = 36.1 × 11.8 μm, n = 30), biseriate, fusiform, acutely to bluntly rounded at both ends, 4-celled, guttulate, 3-septate without germ slits, constricted at the septa, most strongly at the median septum, straight to slightly curved, smooth-walled, hyaline, becoming dark olive-green upon germination with walls and septa turning dark brown, surrounded by a prominent mucilaginous sheath. **Asexual morph**:

Undetermined.

Culture characteristics: Colonies on PDA at 25°C, and germinated bipolarly from ascospores, appearing circular, raised, and dry with a filiform margin. The surface is cottony and fluffy, exhibiting a beige colouration, while the reverse is uniformly dark brown to black, circular with an entire margin.

Material examined: China, Guizhou province, Liupanshui City, Yushe National Forest Park, on unidentified decaying wood, 27 November 2024, Xia Tang, LS16 (GZAAS25-0594, holotype, ex-type living culture GZCC 25-0564.)

Notes: In the phylogenetic analysis, *Hydellum hyalinum* formed a clade as sister to *Forliomyces uniseptata* (MFLUCC 15-0765) and *Torliomyces cylindrospora* (FMR 17550) (Figure 3.46). *Hydellum hyalinum* exhibits a sexual morph, whereas *F. uniseptata* and *T. cylindrospora* represent asexual morphs. Nucleotide comparison between *Hydellum hyalinum* and *F. uniseptata* revealed differences of 11.4% (55/482 bp) in the ITS region and 4.3% (36/834 bp) in the LSU region, excluding gaps. Between *Hydellum hyalinum* and *T. cylindrospora*, the differences were 11% (52/484 bp) in ITS and 5.3% (8/817 bp) in LSU, also excluding gaps. Based on the distinctive morphological characteristics of our specimen and the phylogenetic distinctiveness, we propose *Hydellum hyalinum* as a novel species, in accordance with the taxonomic guidelines of Jeewon and Hyde (2016) and Maharachchikumbura et al. (2021).

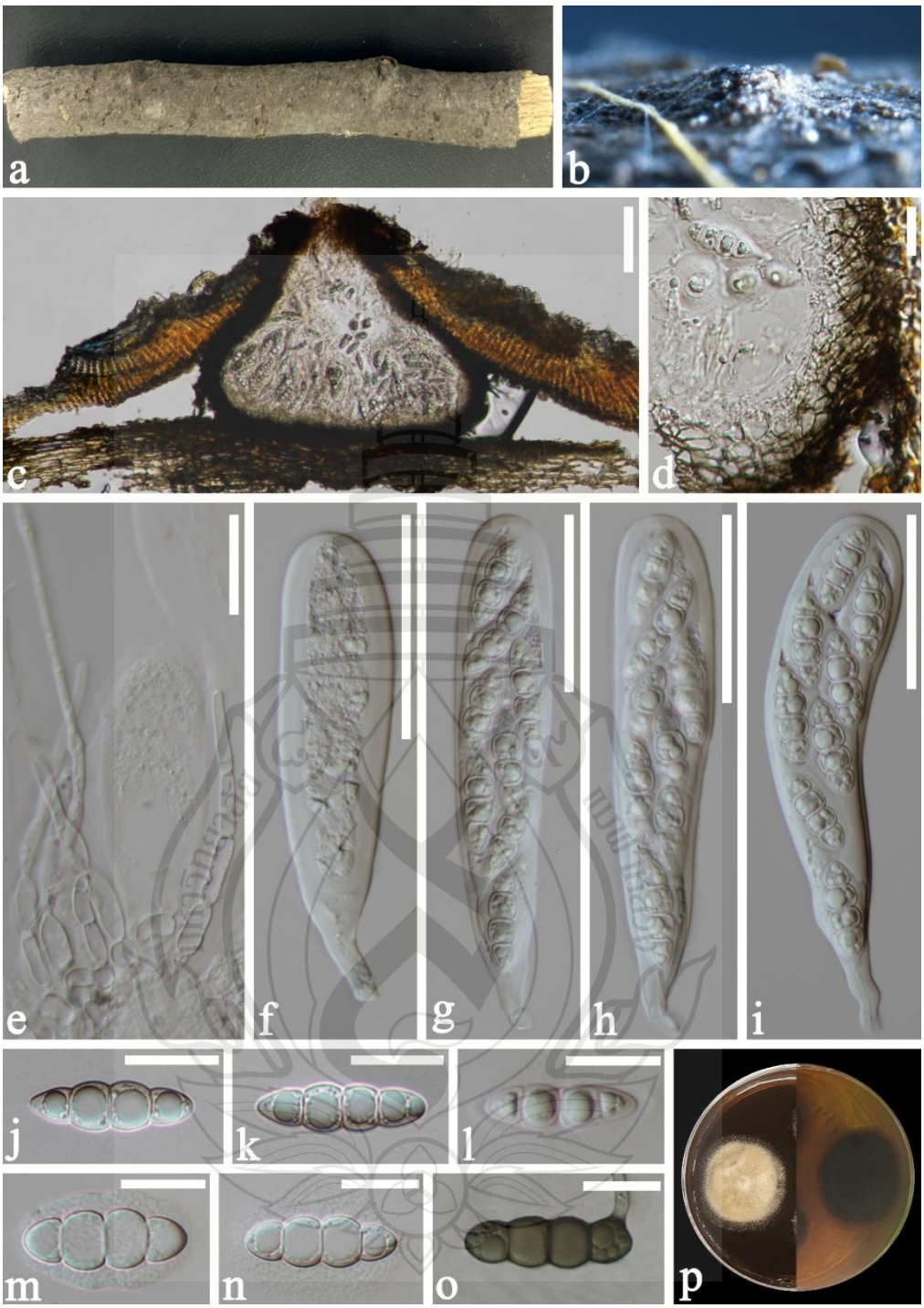

Figure 3.49 *Hydellum hyalinum* (GZAAS25-0594, holotype)

Figure 3.49 a Specimen. b Appearance of ascomata on host substrate. c Section of an ascoma. d Peridium. e Pseudoparaphyses. f–i Asci in different stage. j–n Ascospores. o Germinated conidium. p Colony on PDA (from front). q Colony on PDA (from reverse). Scale bars: c = 100 μm, d, e, j–o = 20 μm, f–i = 50 μm.

Tetraplosphaeriaceae Kaz. Tanaka & K. Hiray, Studies in Mycology 64: 177 (2009)

Polyplosphaeria Kaz. Tanaka & K. Hiray., Stud. Mycol. 64: 192 (2009)

Index Fungorum number: IF 515257; *Facesoffungi number*: FoF 06669;

Notes: Tanaka et al. (2009) established *Polyplosphaeria* and typified with *Po. fusca* based on a combined SSU and LSU DNA sequence data. All the members of *Polyplosphaeria* were reported as saprobes from various plant hosts, such as *Pleioblastus chino*, *Phyllostachys bambusoides* and *Pandanaceae* (Tananka et al., 2009; Li et al., 2016; Tibpromma et al., 2018). *Polyplosphaeria* is distributed in Japan, China and Thailand in terrestrial habitats (Tananka et al., 2009; Li et al., 2016; Tibpromma et al., 2018). Dong et al. (2020) transferred *Po. xishuangbannaensis* into *Ernakulamia* based on phylogenetic analyses and differences in morphology. The genus contains eight species *viz. Polyplosphaeria appendiculata*, *Po. fusca*, *Po. guizhouensis*, *Po. hainanensis*, *Po. nabanheensis*, *Po. nigrospora*, *Po. pandanicola* and *Po. thailandica* (Tanaka et al., 2009; Li et al., 2016; Tibpromma et al., 2018; Senanayake et al., 2023; Liu et al., 2024; This study).

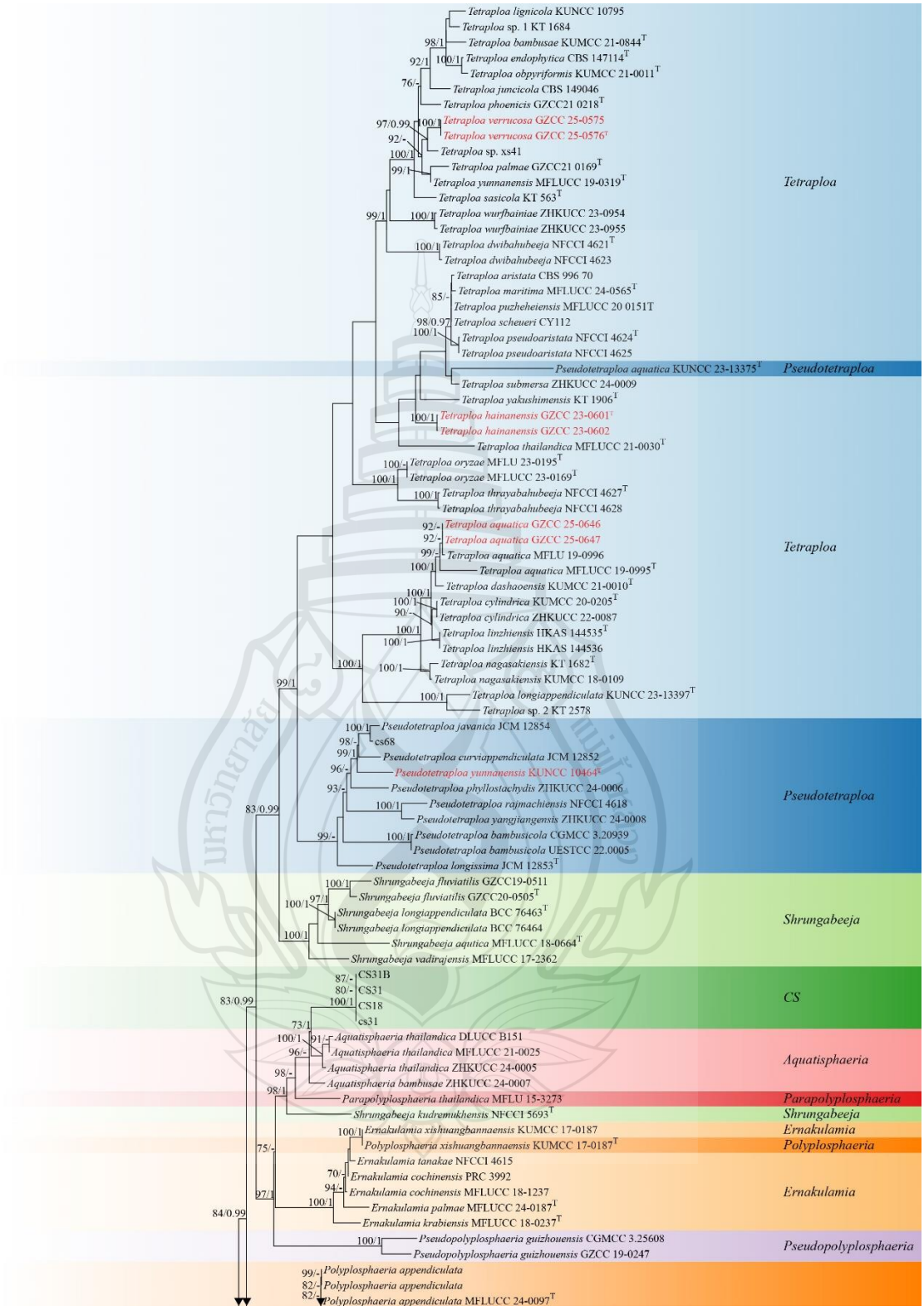

Figure 3.50 Phylogenetic analysis of *Tetraplosphaeriaceae*

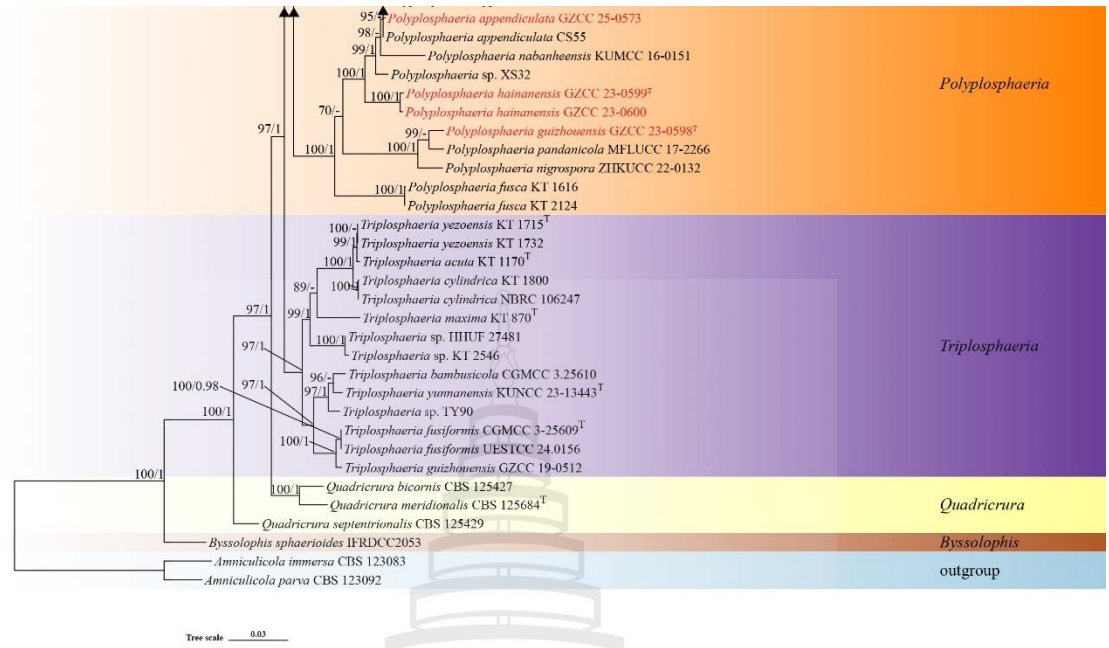

Figure 3.50 (continued)

Figure 3.50 Phylogenetic analysis of *Tetraplosphaeriaceae* was conducted using RAxML-based maximum likelihood analysis of a combined LSU, ITS, SSU and *tub2* sequence dataset. Bootstrap support values for maximum likelihood (ML) equal to or greater than 70% and Bayesian posterior probabilities (PP) equal to or greater than 0.95 are shown above the nodes. The tree is rooted with *Amniculicola immersa* (CBS 123083) and *Am. Parva* (CBS 123092). Newly generated strains are highlighted in red, and type strains are indicated with a superscript 'T'.

Polyplosphaeria appendiculata Y.R. Sun, N.G. Liu & K.D. Hyde, Fungal Diversity 129: 174 (2024) Figure 3.51

Saprobic on unidentified decaying wood in terrestrial habitat. **Sexual morph**: Undetermined. **Asexual morph**: Hyphomycetous. *Colonies* on natural substrate superficial, solitary, dark brown to black. *Mycelium* superficial to semi-immersed, composed of pale brown to brown, branched, septate, smooth hyphae. *Conidiophores* micronematous. *Conidiogenous cells* forming directly on creeping hyphae, integrated, monoblastic, determinate. *Conidia* 90.5–169 (-205) × 60–165 µm ($\bar{x}$ = 135.5 × 118.4 µm, n = 20), solitary, acrogenous, subglobose to ellipsoidal or irregular, pale brown when it immature, brown when it matures, darker at base, with thin peel-like outer wall and numerous internal hyphae. *Appendages* 25.5–79.5 × 2.5–

7 μm ($\bar{x}$ = 42.7 × 5 μm, n = 30) cylindrical, brown, unbranched, septate, arising randomly from conidia.

Culture characteristics: Colonies incubate at 25°C, circular, rough, cottony, flat, reddish brown with an entire margin. The surface of colony floccose to velvety, centrally dense, gray-white to pale gray-green, with distinct concentric zones; margin regular, slightly raised, becoming thinner towards the periphery. The reverse dark brown to blackish at the center, lighter brown towards the edge, showing concentric zonation. Colonies thin and appressed in profile, without prominent aerial tufts.

Material examined: China, Guizhou province, Xingyi City, on unidentified decaying wood, 27 November 2024, Xia Tang, GC40 (GZAAS25-0603, holotype, ex-type living culture GZCC 25-0573.

Known distribution: China (study); Thailand (Liu et al., 2024)

Known hosts: Unidentified decaying wood (Liu et al., 2024; this study).

Notes: Morphologically, our collection conforms to the diagnostic features of *Polyplosphaeria appendiculata*: micronematous conidiophores; monoblastic conidiogenous cells produced directly on creeping hyphae; and solitary, acrogenous conidia that are subglobose to ellipsoidal or irregular and darker at the base. Overall, it closely matches *P. appendiculata*. In the phylogenetic analyses, our isolate (GZCC 25-0573) clustered with *P. appendiculata* (MFLUCC 24-0097) with 84% ML bootstrap support (Figure 3.50). Excluding gaps, ITS sequences differed by only 0.6% (5/832 bp) between our isolate and *P. appendiculata* MFLUCC 24-0097. Integrating these morphological and molecular data, and following the species-delimitation guidelines of Jeewon and Hyde (2016) and Maharachchikumbura et al. (2021), we identify our isolate as *P. appendiculata*. To our knowledge, this represents the first record of *P. appendiculata* from terrestrial habitats in China, supported by both morphology and sequence data.

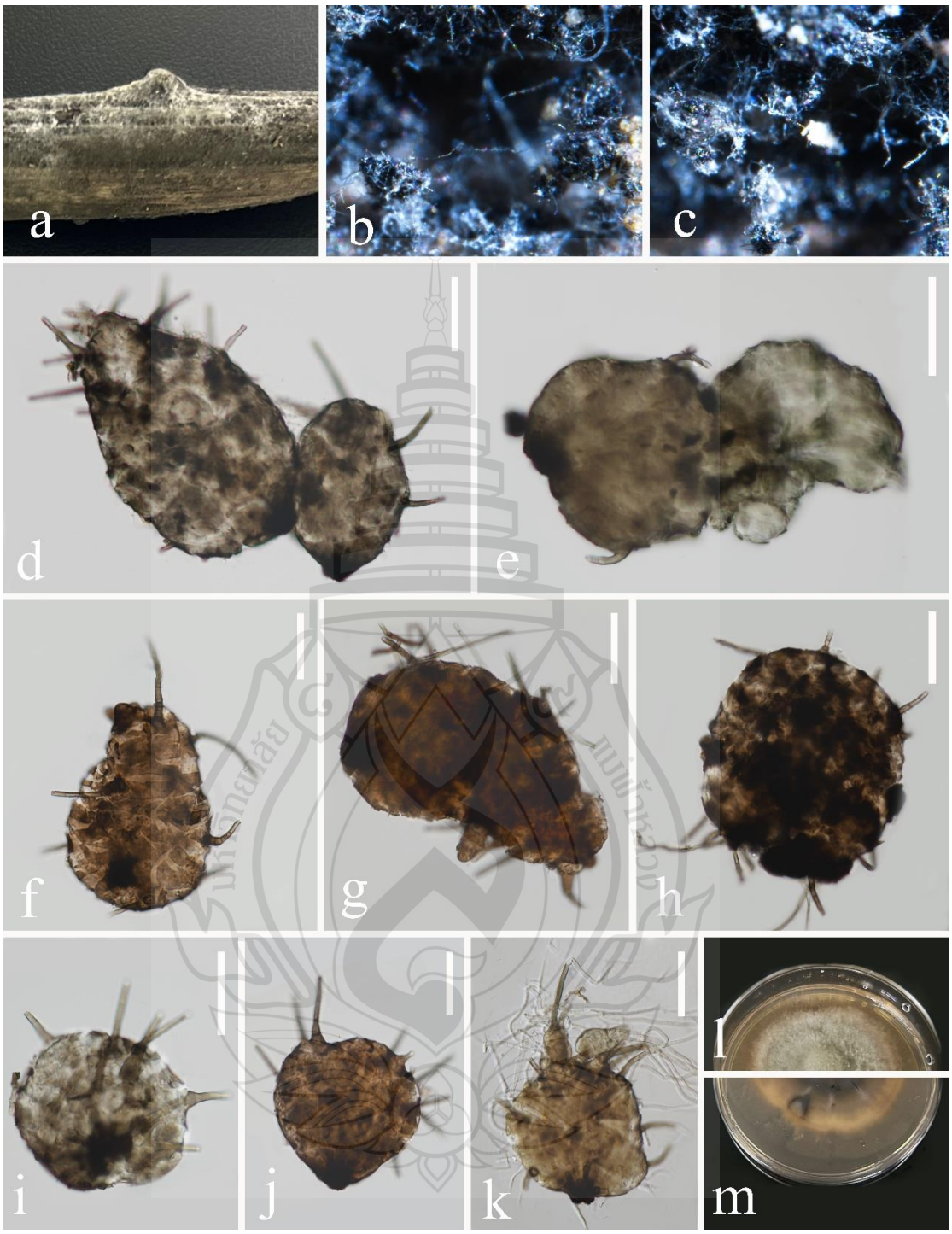

Figure 3.51 *Polyplosphaeria appendiculata* (GZAAS25-0603, new geographical record)

Figure 3.51 a Host. b, c Colonies on substrate. d–j Conidia. k Germinated conidium. l Colony on PDA (from front). m Colony on PDA (from reverse). Scale bars: d–k = 50 μm.

Polyplosphaeria guizhouensis X. Tang, Jayaward., R. Jeewon & J.C. Kang, sp. nov. Figure 3.52

Etymology: The specific epithet 'guizhouensis' refers to the place where the fungus was collected, Guizhou Province, China.

Holotype: GZAAS 23–0600

Saprobic on unidentified decaying wood in the forest. **Sexual morph**: not observed. **Asexual morph**: Hyphomycetous. *Colonies* effuse, gregarious on host substrate, brown to dark brown. *Mycelium* semi-immersed or immersed, pale brown, branched, septate. *Conidiophores* absent. *Conidiogenous cells* forming directly on creeping hyphae, integrated, monoblastic,determinate. *Conidia* 34–61 × 41–63 µm ($\bar{x}$ = 51 × 51 µm, n = 20), globose to subglobose to turbinate, solitary, olivaceous-green to brown, verrucose and darker at base, with setose appendages on surface. *Appendages* with two forms, solitary, cylindrical, unbranched, septate, smooth, brown at base and paler towards to apex, long appendages 51–152 × 3–5 µm ($\bar{x}$ = 89 × 4.0 µm, n = 20), wide at the base, 2–6-septate, arising from apical part of conidia; short appendages 13–38 × 2.5–6 µm ($\bar{x}$ = 25 × 4 µm, n = 20), wide at the base, 0–3-septate, arising randomly from conidial apex.

Culture characteristics: Conidia germinated on PDA and incubate at room temperature (25˚C). Colonies circular, cottony, flat, slightly grey with an undulate margin, forming three concentric zonation, margin regular, brownish grey. The reverse side is a greenish grey in the centre, with a dark brown margin and pigment.

Material examined: China, Guizhou Province, Xingyi City, Xianheping National Forest Park, on unidentified decaying wood, 25 September 2021, Xia Tang, xhp08 (GZAAS 23–0600, holotype), ex-type culture GZCC 23–0598.

Notes: The phylogenetic results (Figure 3.50) showed that *Polyplosphaeria guizhouensis* is sister to *Po. pandanicola* within *Polyplosphaeria* with support (ML = 100). The comparison of pairwise nucleotides showed that *Polyplosphaeria guizhouensis* is different from *Po. pandanicola* in 2/801 bp (0.2%) in LSU and 11/460 (2.5%) in ITS. Thus, we describe *Polyplosphaeria guizhouensis* herein as a novel species in *Polyplosphaeria* following recommendations proposed by Jeewon and Hyde (2016) and Chethana et al. (2021).

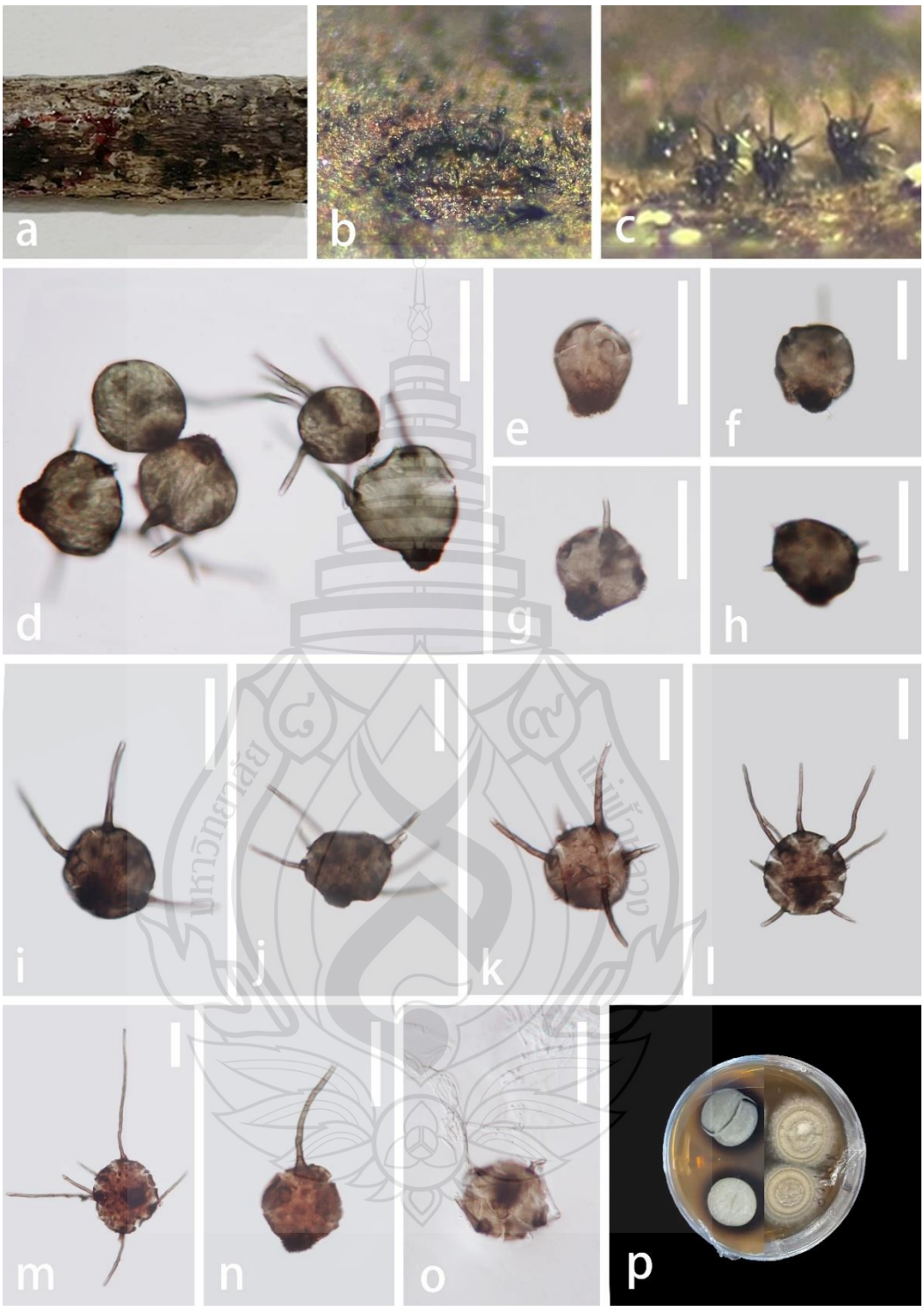

Figure 3.52 *Polyplosphaeria guizhouensis* (GZAAS 23–0600, holotype)

Figure 3.52 a Colonies on decaying wood. b, c Colonies on natural substrates. d–n Conidia bearing appendages. o Germinating conidium. p Colony on PDA (front at right, reverse at left). Scale bars: d–o = 50 μm.

Polyplosphaeria hainanensis X. Tang, Jayaward., R. Jeewon & J.C. Kang, sp. nov.; Figure 3.53, 3.54

Etymology: The specific epithet 'hainanensis' refers to the place where the fungus was collected, Hainan Province, China.

Holotype: GZAAS 23–0601

Saprobic on unidentified decaying wood in the forest. **Sexual morph**: not observed. **Asexual morph**: Hyphomycetous. *Colonies* effuse, gregarious on host substrate, brown to blackish brown. *Mycelium* semi-immersed or immersed, dark brown, branched, septate. *Conidiophores* absent. *Conidiogenous cells* indistinguishable from creeping hyphae, integrated, monoblastic, determinate. *Conidia* 49–134.5 × 52–90.5 μm ($\bar{x}$ = 86 × 71 μm, n = 20), globose, subglobose, obconical, broadly ellipsoidal to broadly pyriform, variable in shape, sometimes with thin peel on the outer wall of conidia, internally filled with a mass of hyaline, solitary, brown to dark brown, smooth. *Appendages* 36–58 × 3–5.5 μm ($\bar{x}$= 44.5 × 4 μm, n = 20), cylindrical, solitary, straight or flexuous, unbranched and almost hyaline at the apex, 0–4-septate, smooth, round at apex, pervasive.

Culture characteristics: Conidia germinated from both ends on PDA and incubate at room temperature (25˚C). Colonies circular, cottony, flat, olivaceous with a slightly grey entire margin. The reverse side is an olive drab, which gradually extends outwards to form a deep colour ring in the centre with a pale grey margin and no pigment.

Material examined: China, Hainan Province, Wuzhishan City, Wuzhishan National Nature Reserve, on unidentified decaying wood, 25 September 2021, Zili Li, WZS27 (GZAAS 23–0601, holotype), ex-type living culture GZCC 23–0599; WZS31 (GZAAS 23–0602, paratype), living culture GZCC 23–0600.

Notes: Based on the phylogenetic analysis (Figure 3.50), two of our *Polyplosphaeria* collections share similar morphology and clustered together with support (ML = 100, and BPP = 1). The base pair differences between the two strains (GZCC 23–0599 and GZCC 23–0600) were: LSU = 0.2% (2/834), ITS = 0.1% (1/840), respectively, therefore, we considered them as the same species according to the guidelines for species delineation proposed by Jeewon and Hyde (2016). The phylogenetic result (Figure 3.50) showed that *Polyplosphaeria hainanensis* is sister to

Po. nabanheensis within *Polyplosphaeria*. Based on the comparison of the morphological characters with other species in *Polyplosphaeria*, our collection can be distinct in having obconical, broadly ellipsoidal to broadly pyriform, variable conidial shape (without verrucose at the base) and pervasive appendages. The comparison of pairwise nucleotides showed that *Polyplosphaeria hainanensis* is different from *Po. nabanheensis* in 24/826 bp (3%) in LSU, 20/758 (2.6%) in SSU, 17/472 (3.6%) in ITS and 16/344 (5%) in *tub2*. Thus, we describe *Polyplosphaeria hainanensis* herein as a novel species in *Polyplosphaeria* according to the guidelines of Jeewon and Hyde (2016) and Chethana et al. (2021).

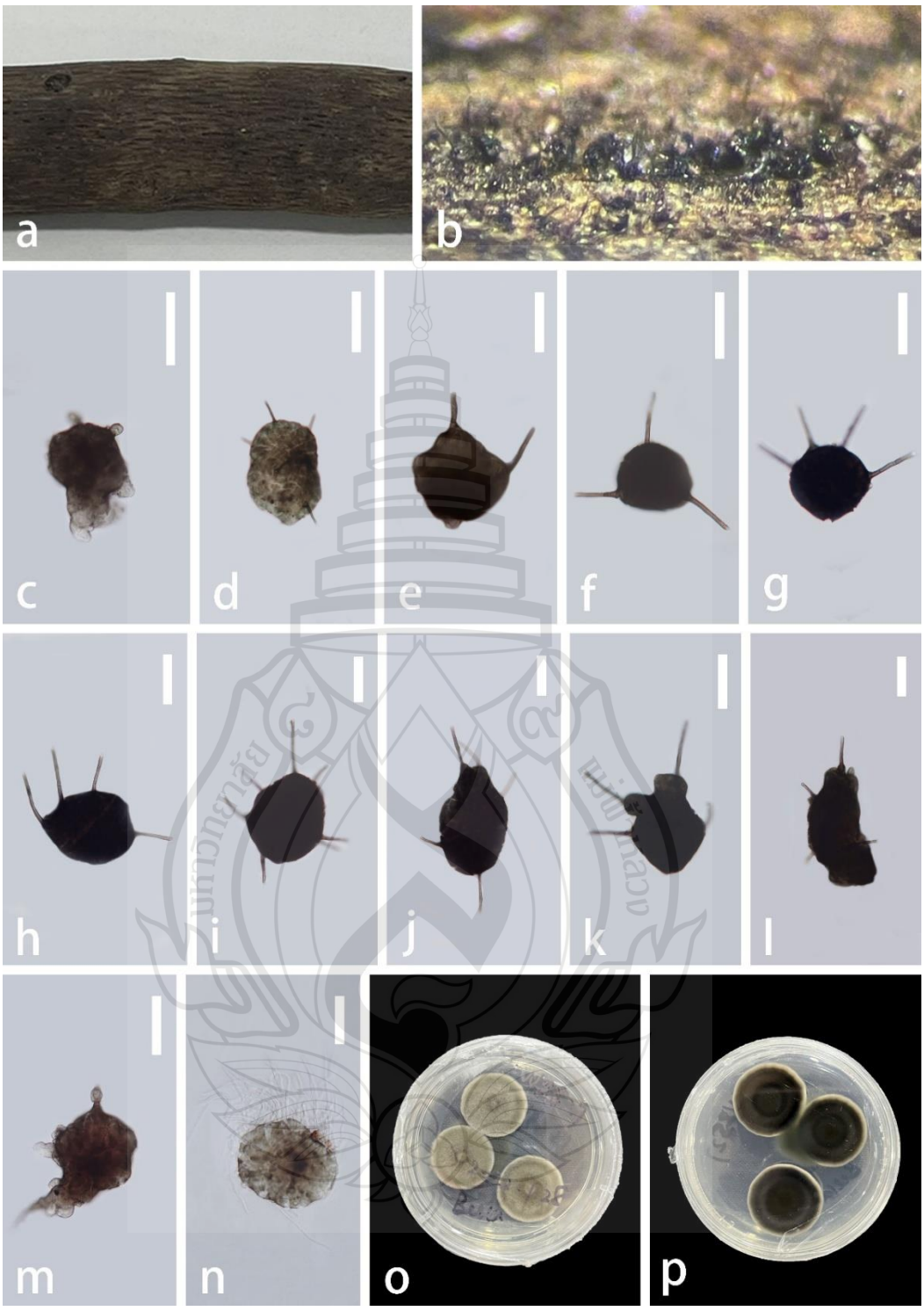

Figure 3.53 *Polyplosphaeria hainanensis* (GZAAS 23–0601, holotype)

Figure 3.53 a Colonies on decay wood. b Colonies on natural substrates. c–m Conidia bearing appendages. n Germinating conidium. o Colony on PDA (from front). p Colony on PDA (from reverse). Scale bars: c–n = 50 µm.

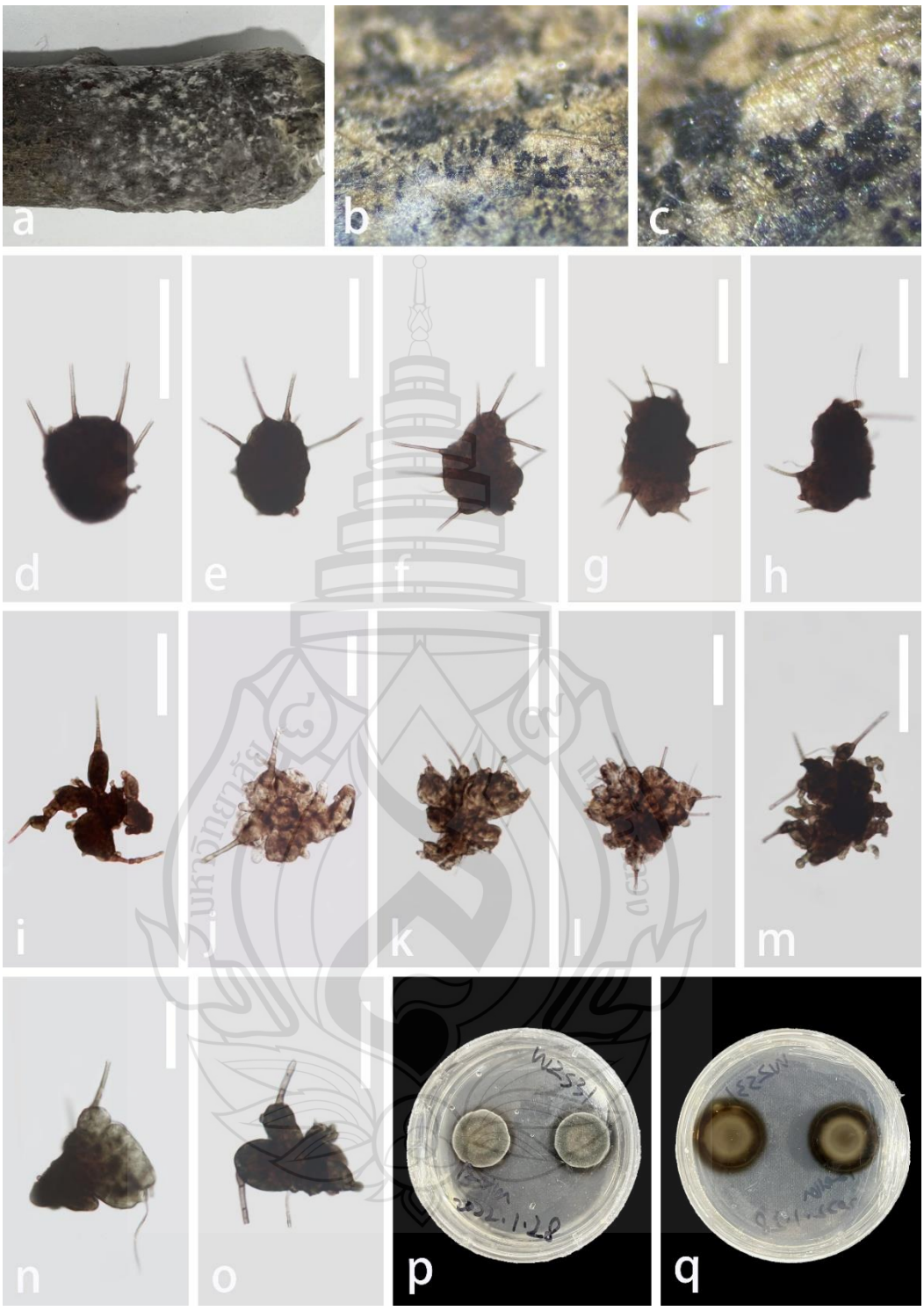

Figure 3.54 *Polyplosphaeria hainanensis* (GZAAS 23–0602, paratype)

Figure 3.54 a Colonies on decay wood. b, c Colonies on natural substrates. d–o Conidia bearing appendages. p Colony on PDA (from front). q Colony on PDA (from reverse). Scale bars: d–i, k–m = 100 μm, j, n, o = 50 μm.

Pseudotetraploa Kaz. Tanaka & K. Hiray., Stud. Mycol. 64: 193 (2009)

Index Fungorum number: IF 515257; *Facesoffungi number*: FoF 06669

Notes: Tanaka et al. (2009) established *Pseudotetraploa* (*Ps.*) with three species, which were previously described in Tetraploa and typified by *Ps. curviappendiculata* based on a combined SSU and LSU DNA sequence data. *Pseudotetraploa* species are reported as saprobes on bamboo, dead bark of the broad-leaved tree, and unidentified herbaceous plants in Japan, China, and India (Hatakeyama et al., 2005; Tanaka et al., 2009; Hyde et al., 2020a; Yu et al., 2022). *Pseudotetraploa* is only known in its anamorphic state and dwell in terrestrial habitats and contains six species *viz. Ps. bambusicola*, *Ps. curviappendiculata*, *Ps. javanica*, *Ps. longissima*, *Ps. Rajmachiensis*, and *Ps. yunnanensis* (Hatakeyama et al., 2005; Tanaka et al., 2009; Hyde et al., 2020a; Yu et al., 2022; this study).

Pseudotetraploa yunnanensis X. Tang, Jayaward., R. Jeewon & J.C. Kang, sp. nov. Figure 3.55

Etymology: The specific epithet 'yunnanensis' refers to the place where the fungus was collected, Yunnan Province, China.

Holotype: HKAS 129442

Saprobic on bamboo. **Sexual morph**: not observed. **Asexual morph**: Hyphomycetous. *Colonies* effuse, gregarious on host substrate, brown to dark brown. Mycelium superficial, hyaline to pale brown. *Conidiophores* absent. *Conidiogenous cells* micronematous, mononematous, monoblastic, integrated, usually undistinguishable from superficial hyphae. *Conidia* 67–120 × 16.5–35 µm ($\bar{x}$ = 95 × 24 µm, n = 20), solitary, septate, brown to dark brown, ovoid to obclavate or narrowly obpyriform, consisting of 3–6 columns of cells, rounded at the base 19–36 µm wide ($\bar{x}$ = 26 µm, n = 20), slightly constricted at septa, rarely branched and make V-shaped conidia; setose appendages at the apical part 15–87 × 3.5–7 µm ($\bar{x}$ = 37 × 5 µm, n = 20), appendages 3–6 in number, 1–8-septate, brown at the base and almost hyaline at the apex, smooth, unbranched, shorter appendage is straight and longer appendage is curved.

Culture characteristics: Conidia germinated from both ends on PDA and incubate at room temperature (25˚C). Colonies circular, cottony, flat, slightly grey with an entire margin, containing a circular white mycelium in the centre. The reverse side

is a pale brown in the centre that gradually extends outwards while the colour changes to pale grey, with a brown margin and no pigment.

Material examined: China, Yunnan Province, Puer City, Ailao mountains, on bamboo, May 23, 2022, Rong-Ju Xu, ALS 29 (HKAS 129442, holotype), ex-type culture KUNCC 10464.

Notes: *Pseudotetraploa yunnanensis* is similar to *Ps. curviappendiculata* and *Ps. longissima*. However, *Pseudotetraploa yunnanensis* differs from *Ps. curviappendiculata* in having branched and V-shaped conidia, consisting of 3–6 columns of cells with 3–6 apical appendages, larger conidia [67–120 µm vs. 52–67(–75) µm] in length and [16–35 µm vs. 15–22 µm] in width, while *Ps. curviappendiculata* consists of 4–5 columns of cells with 4 apical appendages; *Pseudotetraploa yunnanensis* differs from *Ps. longissima* in having smaller conidia [67–120 µm vs. (98–)110–148(–155) µm] in length and [16–35 µm vs. 18–25 µm] in width, without verrucose at the base. The phylogenetic analysis showed that *Pseudotetraploa yunnanensis* is sister to *Ps. rajmachiensis* and *Ps. javanica*. The comparison of pairwise nucleotides showed that *Pseudotetraploa yunnanensis* is different from *Ps. rajmachiensis* in 27/1021 bp (2.6%) in LSU and 30/560 (6%) in ITS; *Pseudotetraploa yunnanensis* is different from *Ps. javanica* in 11/1020 bp (1.1%) in LSU and 17/538 (3.2%) in ITS. Thus, we describe *Pseudotetraploa yunnanensis* herein as a novel species in *Pseudotetraploa* according to the guidelines Jeewon and Hyde (2016) and Chethana et al. (2021).

Figure 3.55 *Pseudotetraploa yunnanensis* (HKAS 129442, holotype)

Figure 3.55 a, b Colonies on natural substrates. c–n Conidia. Scale bars: c = 20 µm, d–n = 50 µm.

Tetraploa Berk. & Broome, Ann. Mag. Nat. Hist. 5: 459, t. 11:6 (1850)

Index Fungorum number: IF 10199; *Facesoffungi number*: FoF 06666

Notes: Tanaka et al. (2009) established *Tetraplosphaeria* to accommodate pleosporalean species that have massarina/lophiostoma-like teleomorph and anamorphs belonging to Tetraploa sensu stricto based on a combined SSU and LSU DNA sequence data. Later, Hyde et al. (2013) treated *Tetraploa* as a synonym of *Tetraplosphaeria*, which has been applied previously to anamorphic species and used Tetraploa instead of *Tetraplosphaeria*. Species of *Tetraploa* are mainly reported as saprobes, distributed in freshwater and terrestrial habitats, and only *T. aristata* has been reported as a pathogen on various plants and human pathogen that cause cysts (Markham et al., 1990; Tanaka et al., 2009; Hyde et al., 2013; Liao et al., 2022). *Tetraploa* has been recovered from more than 80 plants, such as bamboo culms, submerged wood, palms, and *Poaceae*, on the leaves of Acer and liverworts (Ellis, 1949; Ando, 1992; Hyde et al., 2013; Liao et al., 2022). Saxena et al. (2021) mentioned that *Frasnacritetrus* is probably a fossil of *Tetraploa*. Nuñez Otaño et al. (2022) considered *Frasnacritetrus* as a synonym of *Tetraploa* and transferred five *Frasnacritetrus* fossil species into *Tetraploa viz. Tetraploa conata*, *T. indica*, *T. josettae*, *T. siwalika* and *T. taugourdeaui* based on the observation that the spores of both fossil and contemporary species exhibit identical morphological characteristics. To date, there are 36 species accepted in *Tetraploa* (Wijayawardene et al., 2022; Jayawardena et al., 2023; this study). In this study, a new *Tetraploa* species is introduced.

Tetraploa aquatica W.L. Li & H.Y. Su, Phytotaxa 459 (2): 184 (2020); Figure 3.56

Saprobic on decaying wood of bamboo in terrestrial habitat. **Sexual morph**: Undetermined. **Asexual morph**: Hyphomycetous. *Colonies* effuse, scattered, dark brown to black with pale brown appendages. *Mycelium* 1.3–4 μm wide, superficial to semi-immersed, composed of pale brown to brown, flexuous, septate hyphae. *Conidiophores* micronematous, indistinct. *Conidiogenous cells* holoblastic, monoblastic or polyblastic, integrated, determinate, cylindrical. *Conidia* solitary, acrogenous, unbranched, ovoid, rounded, verruculate at the base, consisted of 4 columns of cells with 3-4 apical appendages. Conidial body17–34 × 17–28 μm ($\bar{x}$ = 25.5 × 21 μm, n = 30), pale brown to brown, smooth, narrowly ovate or ovate, composed of 4 closely-adhered vertical columns of cells, with each column 2–3-septate. *Appendages* 85.5–182 × 3.5–7.5 μm ($\bar{x}$ = 139.3 × 4.9 μm, n =

30), brown at the base, almost hyaline at the apex, 6–15-pseudoseptate. Mature conidia with shallow furrows between 4-columns of cells which develop independently and later get compacted and tend to remain vertically to one another apically.

Culture characteristics: Colonies incubate at 25°C, circular, rough, cottony, umbonate, sharply delimited, with a thick, dome-shaped central umbo and 1–2 concentric zone with an entire margin. Colony surface velvety to finely floccose, with aerial mycelium dense at the center and thinning toward the edge; umbo pale grey to mouse-grey, grading to grey-olivaceous in the middle ring; the outermost rim is narrow and paler, nearly hyaline. Margin entire to slightly crenulate, low and appressed. On the reverse, colonies show a light-brown to pale-yellow central disc surrounded by a broad, sharply defined blackish-brown ring forming a clear concentric band, lobate margin with a narrow, pale outer halo toward the margin.

Material examined: China, Guizhou province, Zunyi City, Xishui County, Xishui Nature Reserve, on unidentified decaying wood, 15 March 2023, Xia Tang, XS39 (GZAAS25-0676), living culture GZCC 25-0646, GZCC 25-0647.

Known distribution: China (Li et al., 2020; this study).

Known hosts: on submerged decayed wood (Li et al., 2020); on decaying wood in terrestrial habitats (this study).

Notes: Morphologically, our collection conforms to the diagnostic features of *Tetraploa aquatica*: micronematous and indistinct conidiophores; monoblastic or polyblastic conidiogenous cells; and solitary, acrogenous, unbranched, ovoid conidia, composed of four closely adherent vertical columns of cells, each column being 2–3-septate and verruculate at the base. Conidia bear four cylindrical, pseudoseptate appendages, brown at the base and almost hyaline toward the apex.

In the phylogenetic analyses, our isolate GZCC 25-0646 clustered with *T. aquatica* (MFLUCC 19-0995), supported by 76% ML bootstrap (Figure 3.50). Excluding gaps, ITS sequences differed by only 0.1% (1/796 bp), and LSU sequences differed by only 0.2% (1/438 bp) between our isolate and *T. aquatica* (MFLUCC 19-0995). Based on these morphological and molecular data, and following the species delimitation guidelines of Jeewon and Hyde (2016) and Maharachchikumbura et al. (2021), we identify our isolate as *T. aquatica*. To our knowledge, this represents the first record of *T. aquatica* from terrestrial habitats in China, supported by both morphology and sequence data.

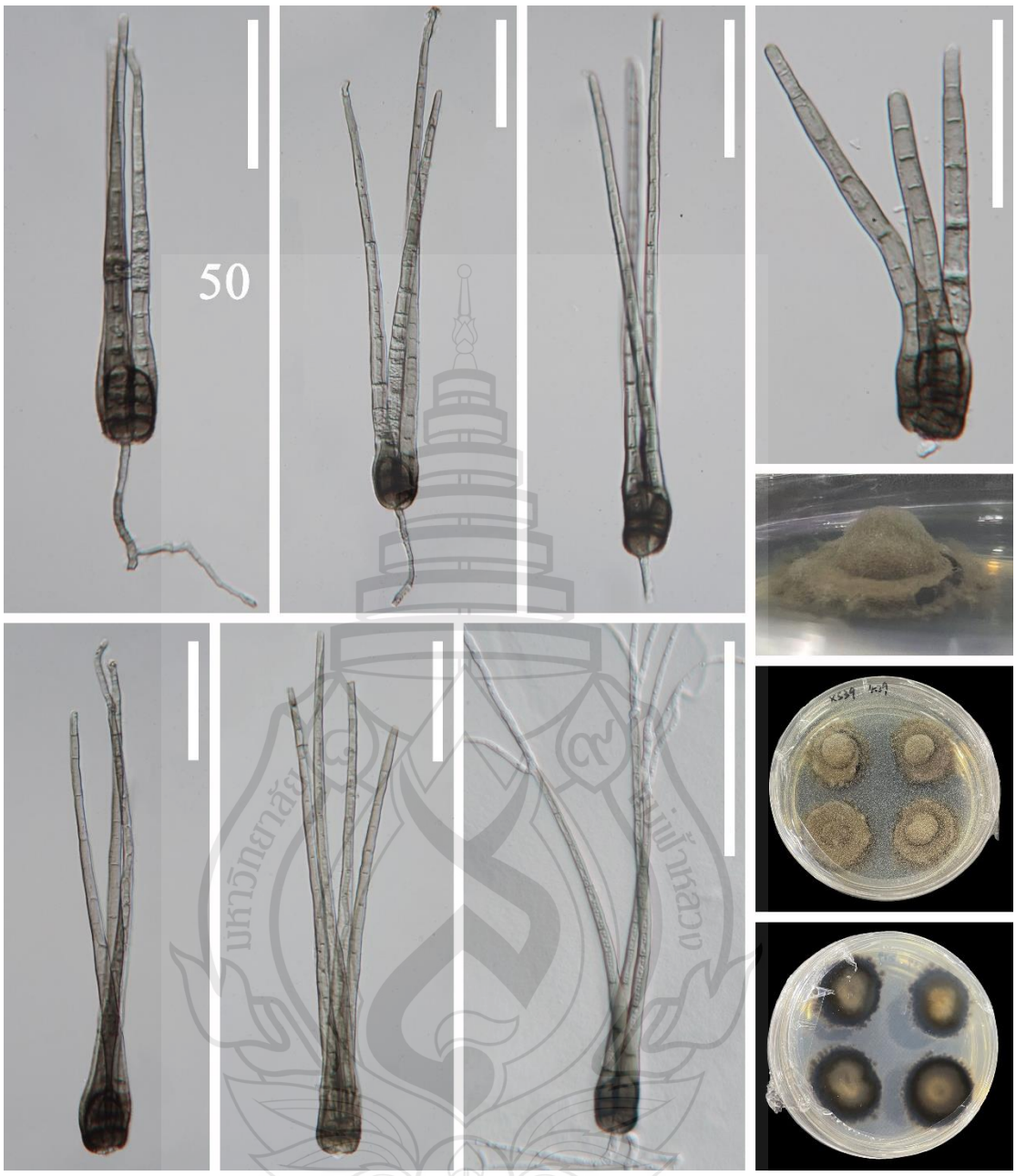

Figure 3.56 *Tetraploa aquatica* (GZAAS25-0676, new habitat record)

Figure 3.56 a, b Colonies on substrate. c–f Condiophores, conidiogenous cells, conidiogenous cells bearing conidia. g–n Conidia. o Germinated conidium. p Colony on PDA (from front). q Colony on PDA (from reverse). Scale bars: c–f = 50 μm, g–o = 20 μm.

Tetraploa hainanensis X. Tang, Jayaward., R. Jeewon & J.C. Kang, sp. nov.; Figure 3.57, 3.58

Etymology: The specific epithet 'hainanensis' refers to the place where the fungus was collected, Hainan Province, China.

Holotype: GZAAS 23–0603

Saprobic on unidentified decaying wood in forest. **Sexual morph**: Not observed. **Asexual morph**: Hyphomycetous. *Colonies* effuse, gregarious on host substrate, brown to dark brown. *Mycelium* semi-immersed or immersed, pale brown, branched, septate. *Conidiophores* absent. *Conidiogenous cells* integrated, monoblastic, determinate. *Conidia* 30–46 × 18–36 μm ($\bar{x}$ = 38 × 27 μm, n = 20), cylindrical with obtuse ends, pale brown to brown, verrucose, composed of four columns of cells, sometimes five columns of cells, 4–5-septate in each column, smooth, mostly with four apical appendages, some with one or two or five appendages. *Appendages* 52–209 × 3–6 μm ($\bar{x}$ = 140 × 4 μm, n = 20) cylindrical, solitary, unbranched, guttulate, septate, wide at the base, divergent, pale brown to brown, 5–16-septate, straight or slightly flexuous, smooth-walled.

Culture characteristics: Conidia germinated from both ends on PDA and incubate at room temperature (25˚C). Colonies circular, cottony, flat, slightly grey with an entire margin, contain a circular white mycelium in the centre. The reverse side is a pale brown in the centre that gradually extends outwards while the colour changes to pale grey, with a brown margin and no pigment.

Material examined: China, Hainan Province, Wuzhishan City, Wuzhishan National Nature Reserve, on unidentified decaying wood, 25 September 2021, Zili Li, WZS59 (GZAAS 23–0603, holotype), ex-type living culture GZCC 23–0601; WZS66.2 (GZAAS 23–0604, paratype), living culture GZCC 23–0602.

Notes: *Tetraploa hainanensis* is morphologically similar to *T. pseudoaristata*. However, *Tetraploa hainanensis* can be distinguished from *T. pseudoaristata* in having larger conidia (30.5–46 × 18–36 μm vs. 22–31 × 15–20 μm) with four columns of cells, sometimes five columns of cells, and longer appendages (52–209 × 3–6 μm vs. 23–107 × 2–5 μm), commonly four in number, sometimes five. Based on the phylogenetic analysis, two of our *Tetraploa* collections which share similar morphology clustered together with high support (ML = 100, and BPP = 1 (Figure 3.2.46)). The base pair

differences between the two strains were: LSU = 0.1% (1/806), ITS = 0% (0/516), and tub2 = 0% (1/633), respectively. Therefore, we considered them as the same species according to the guidelines for species delineation proposed by Jeewon and Hyde (2016). *Tetraploa hainanensis* forms a distinct lineage but close to *T. yakushimensis* and *T. tetraploa*. However, *Tetraploa hainanensis* differs from *T. yakushimensis* by having four or five columns and appendages, while *T. yakushimensis* has only four columns and appendages; *Tetraploa hainanensis* differs from *T. tetraploa* in having four or five columns and shorter appendages (52–209 × 3–6 μm vs. 263–350 × 2–3 μm), while *T. tetraploa* has only four columns and slender appendages. The comparison of pairwise nucleotide showed that *Tetraploa hainanensis* is different from *T. yakushimensis* in 31/620 bp (3%) in LSU, 7/814 (0.98%) in ITS, and 87/450 (19%) in *tub2* and *Tetraploa hainanensis* is different from *T. tetraploa* in 31/620 bp (3%) in LSU, 7/814 (0.98%) in ITS, and 87/450 (19%) in tub2. Based on the combination of morphological characters and multigene phylogeny, we describe *Tetraploa hainanensis* herein as a distinct species according to the guidelines of Jeewon and Hyde (2016) and Chethana et al. (2021).

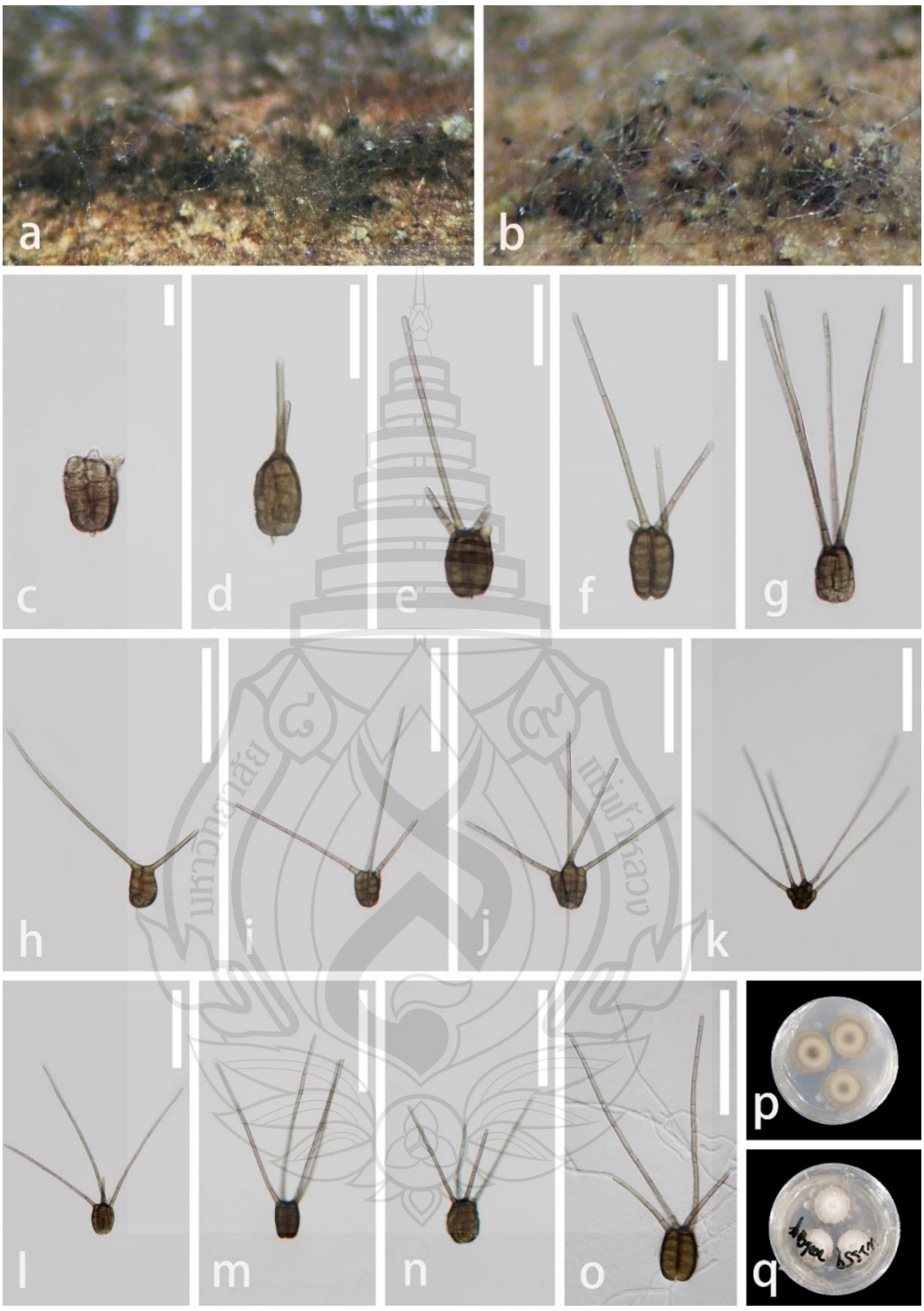

Figure 3.57 *Tetraploa hainanensis* (GZAAS 23–0603, holotype)

Figure 3.57 a, b Colonies on natural substrates. c–n Conidia bearing 1–5 appendages. o Germinating conidium. p Colony on PDA (from reverse). q Colony on PDA (from front). Scale bars c = 20 μm, d–g = 50 μm, h–o = 100 μm.

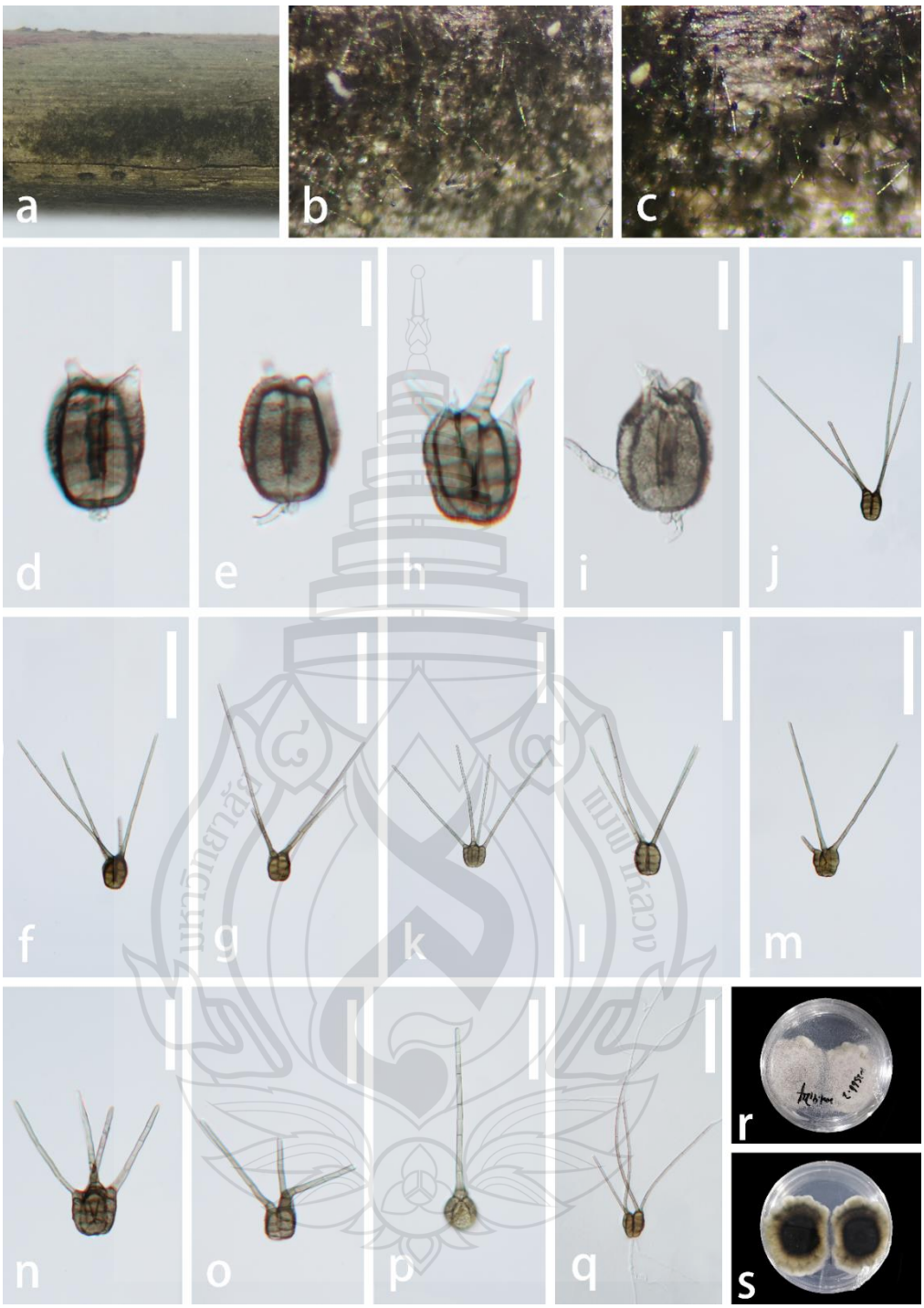

Figure 3.58 *Tetraploa hainanensis* (GZAAS 23–0604, paratype)

Figure 3.58 a Colonies on decay wood. b, c Colonies on natural substrates. d–p Conidia bearing 1–4 appendages. q Germinating conidium. r Colony on PDA (from front). s Colony on PDA (from reverse). Scale bars: d–g = 20 μm, h–l, o, q = 100 μm, m, n, p = 50 μm.

Tetraploa verrucosa X. Tang, K.D. Hyde, Jayaward. & J.C. Kang, sp. nov.; Figure 3.59

Etymology: The specific epithet 'verrucosa' refers to this fungus containing verrucose conidia.

Holotype: GZAAS25-0606

Saprobic on decaying wood of bamboo in terrestrial habitat. **Sexual morph**: Unknown. **Asexual morph**: Hyphomycetous. *Colonies* effuse, scattered, dark brown to black with brown appendages. *Mycelium* superficial to semi-immersed, composed of pale brown to brown, flexuous, septate hyphae. *Conidiophores* micronematous, septate, smooth-walled, pale to mid brown, often reduced or indistinct, sometimes giving rise to conidia directly. *Conidiogenous cells* holoblastic, monoblastic to polyblastic, integrated, terminal, determinate, cylindrical. *Conidia* 15–27 × 12–27 µm ($\bar{x}$ = 21.6 × 19.3 µm, n = 30), solitary, acrogenous, unbranched, broadly ellipsoid to subglobose, 2-4 transverse septate, rounded, verrucose, dark brown to olivaceous brown, composed of 4 closely-adhered vertical columns of cells, with each column 2–3-septate and with 2-4 apical appendages, radiating outward. *Appendages* (-15.5) 18.5–41 (-49) × 2–4 µm ($\bar{x}$ = 27 × 3 µm, n = 45), cylindrical, arising from the apical region of the conidial body, brown to olivaceous brown, unbranched, basal part of each appendage slightly swollen, distinctly demarcated from the conidial wall, tapering toward the apex, almost hyaline and verrucose at the apex, smooth at base part, 1–4-septate. *Mature conidia* with shallow furrows between 4-columns of cells which develop independently and later get compacted and tend to remain vertically to one another apically.

Culture characteristics: Colonies on PDA at 25°C germinate from the base of conidia and apical appendage, circular, with a umbonate surface and a dense, velvety to floccose mycelial texture with an entire margin. Mycelium is denser at the center and gradually becomes sparser toward the margin. The colony of surface floccose to velvety, dense, pale grey to olivaceous-grey at the center, gradually becoming darker toward the margin; concentric ring-like zones visible with age. Texture cottony to powdery, raised centrally forming dome-like elevations, flatter toward the edges.

Material examined: China, Guizhou province, Zunyi City, Chishui Bamboo Sea, on decaying branches of bamboo, 15 March 2023, Xia Tang, CS65.1 (GZAAS25-0606, holotype), ex-type living culture GZCC 25-0576; CS64 (GZAAS25-0605,

paratype), living culture GZCC 25-0575.

Notes: Morphologically, our collection (GZCC 25-0576) is similar to *Tetraploa bambusae*, but differs from it by having micronematous conidiophores and smaller conidia (15–27 × 12–27 µm; L/W ratio = 1.1 vs. (21–)23–30(–33) × (17–)18–23(–26) µm; L/W ratio = 1.2), which are broadly ellipsoid to subglobose, with 2–4 transverse septa, and appendages that are verrucose at the apex. In contrast, *T. bambusae* has macronematous conidiophores and smooth-walled appendages without verrucose ornamentation at the apex.

In the phylogenetic analyses, our isolate (GZCC 25-0576) clustered with *T. palmae* (GZCC 21-0169), supported by 100% ML bootstrap and 1 Bayesian PP (Figure 4.2.43). Morphological comparison indicates that *T. palmae* exhibits the sexual morph, whereas our collection exhibits only the asexual morph. Comparison of nucleotide sequences shows 1.1% (9/806 bp) divergence in LSU and 0.2% (2/989 bp) divergence in SSU between our isolate and *T. palmae* (GZCC 21-0169), excluding gaps. Based on these morphological and molecular data, and following the species delimitation guidelines of Jeewon and Hyde (2016) and Maharachchikumbura et al. (2021), we identify our isolate as a novel species, *T. verrucosa*, supported by both morphology and sequence data.

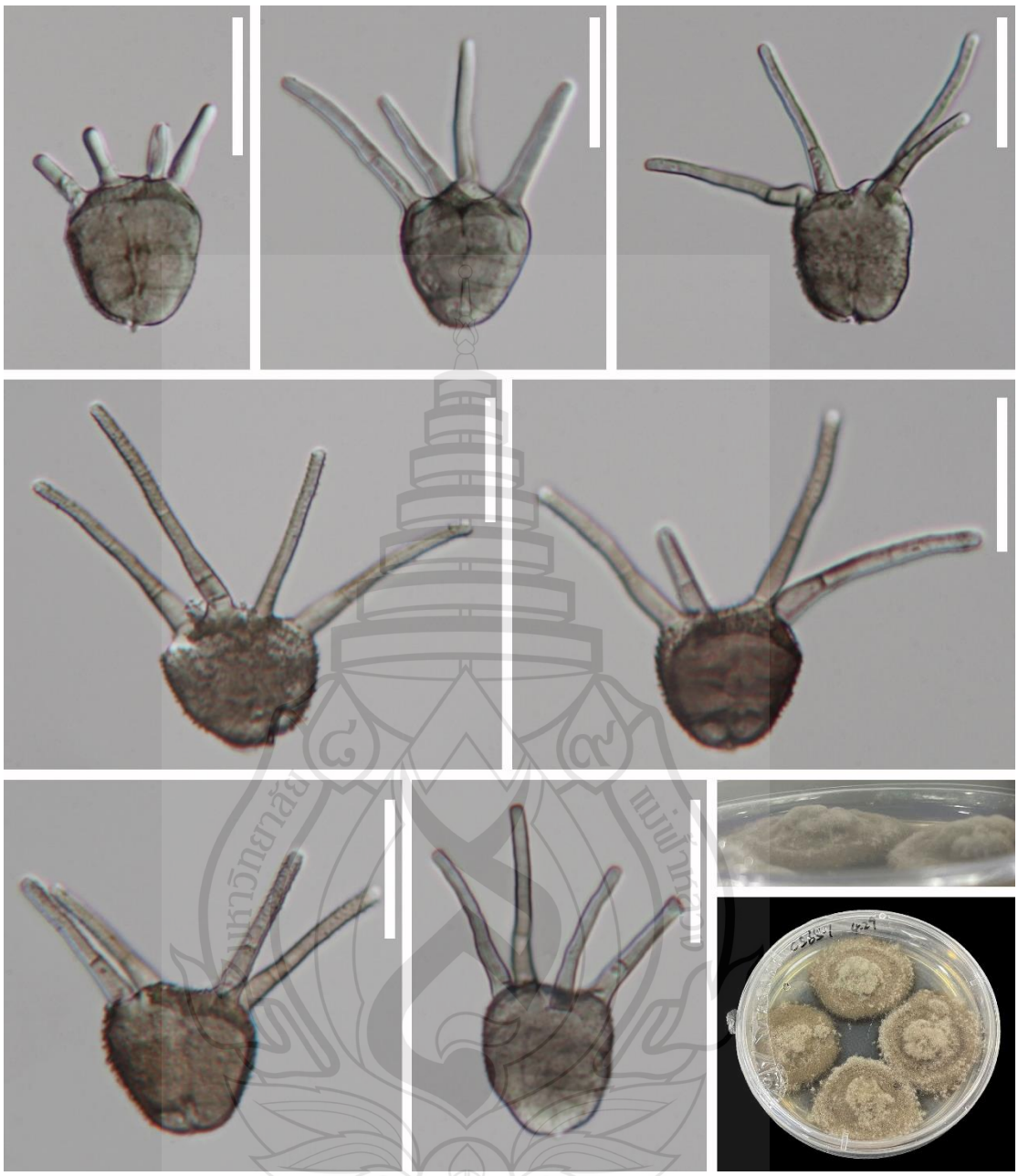

Figure 3.59 *Tetraploa verrucosa* (GZAAS25-0606, holotype)

Figure 3.59 a, b Colonies on substrate. c–i Conidia. o Germinated conidium. j the side of the colony. k Colony on PDA (from front). Scale bars: c–i = 20 μm.

Torulaceae Corda, Deutschlands Flora, Abt. III. Die Pilze Deutschlands 2: 71 (1829)

Torula Pers., Ann. Bot. (Usteri) 15: 25 (1794)

Index Fungorum number: IF 10248; *Facesoffungi number*: FoF 01740

Notes: *Torula* is the type genus of *Torulaceae*, originally introduced by Persoon (1794), and is currently typified by *T. herbarum* following the treatment of Crous et al. (2015) based on multilocus phylogeny. Species of *Torula* are widely distributed on dead branches and submerged wood in terrestrial and freshwater ecosystems worldwide, including Asia, Europe, North America, and South America (Li et al., 2024; He et al., 2025, Wu et al., 2025). Although most species are saprobic on angiosperms, a few species have also been recorded from ferns (Kirk & Spooner, 1984; Zhang et al., 2025). The genus is known only from its asexual morph, characterized by dark brown to black, effuse, velvety colonies; micronematous conidiophores that may be reduced to the conidiogenous cells or supported by a single brown basal cell; terminal or lateral, doliiform to ellipsoid or clavate, mono- or polyblastic, intact or cupulate conidiogenous cells; and brown, phragmosporous, moniliform, smooth to verrucose conidia that are frequently strongly constricted at the septa and form branched chains (Crous et al., 2015; Tian et al., 2023; Zhang et al., 2025). *Torula* is the largest genus in *Torulaceae*, with about 500 epithets listed in Index Fungorum (2025). However, only approximately 60 species are currently accepted in Species Fungorum (2025) due to the lack of molecular data for historically described taxa (Zhang et al., 2025).

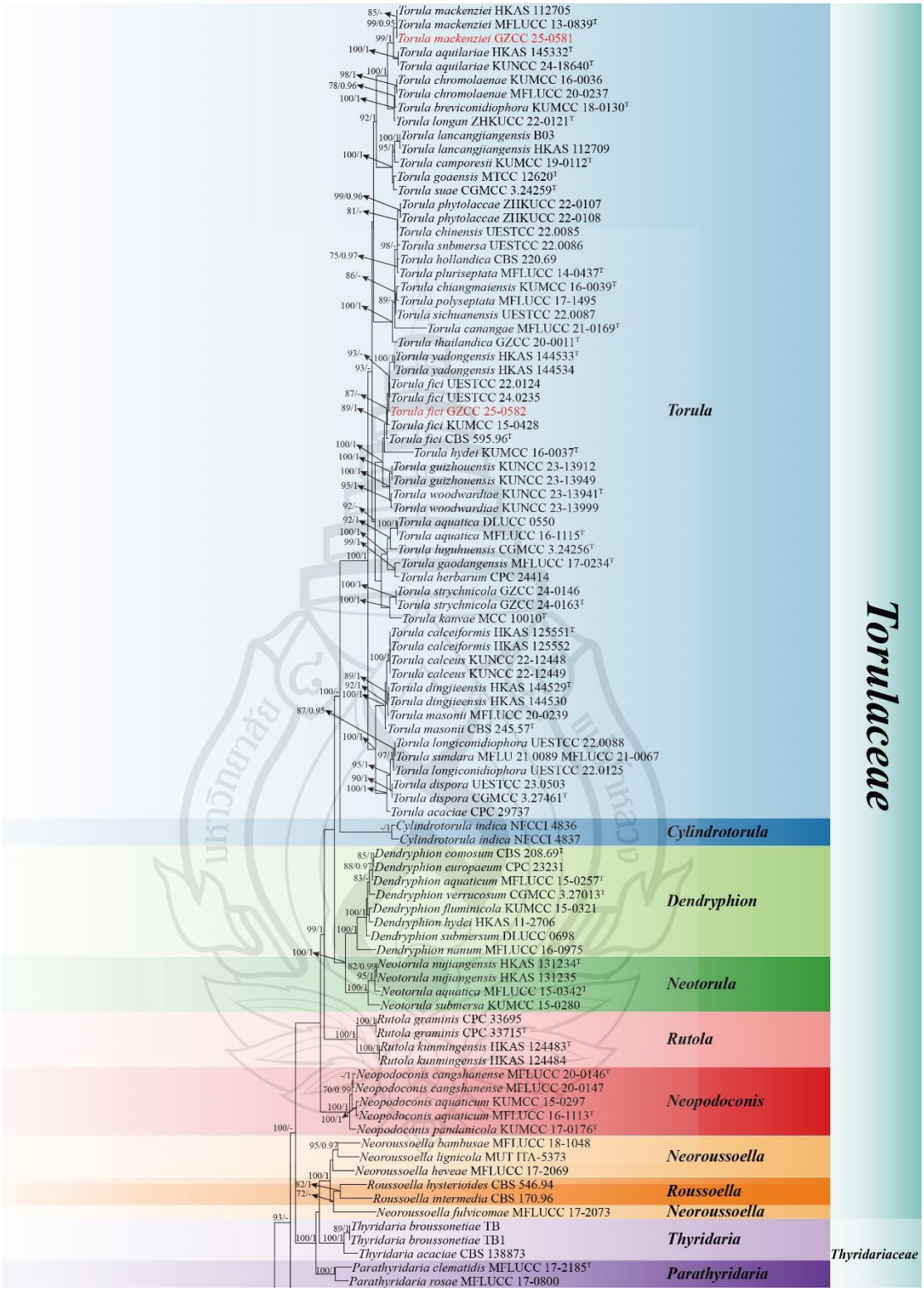

Figure 3.60 Phylogenetic analysis of *Torulaceae*

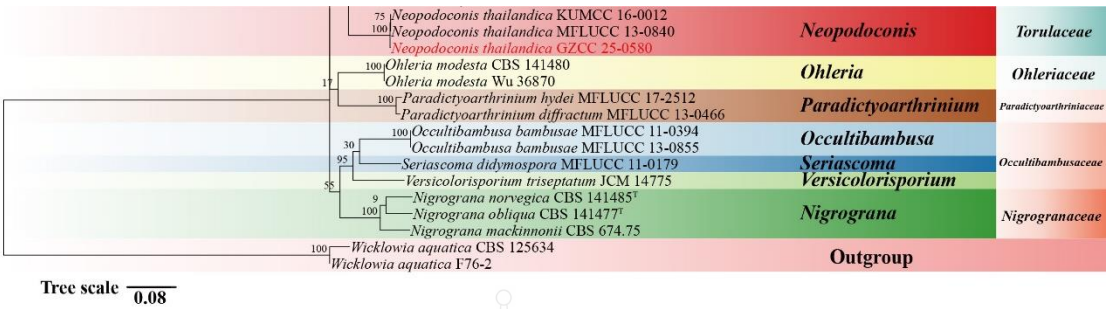

Figure 3.60 (continued)

Figure 3.60 Phylogenetic analysis of *Torulaceae* was conducted using RAxML-based maximum likelihood analysis of a combined LSU, SSU, ITS, *rpb2* and *tef1-α* sequence dataset. Bootstrap support values for maximum likelihood (ML) equal to or greater than 70% and Bayesian posterior probabilities (PP) equal to or greater than 0.95 are shown above the nodes. The tree is rooted with *Wicklowia aquatica* (CBS 125634 and F76-2). Newly generated strains are highlighted in red, and type strains are indicated with a superscript 'T'.

Torula fici Crous (2015); Figure 3.61

Saprobic on unidentified decaying wood. **Sexual morph**: Undetermined. **Asexual morph**: *Colonies* effuse on host, black, gregarious, powdery. *Mycelium* partly immersed to superficial on the substrate, composed of septate, branched, minutely verrucose, subhyaline to pale brown hyphae. *Conidiophores* 8–19.5 × 2.5–4 µm ($\bar{x}$ = 12.4 × 3.3 µm, n = 6), macronematous, mononematous, solitary, erect, paler brown to brown, ampulliform, minutely verrucose, consisting of 1–2 cells, arising from hypha. *Conidiogenous cells* 4–8.5 × 4–7 µm ($\bar{x}$ = 6× 5.4 µm, n = 15), mono- to polyblastic, terminal, pale brown to brown, smooth to minutely verruculose, thick walled, ellipsoid to coronal. *Conidia* 4–8.5 × 4–7 µm ($\bar{x}$ = 6× 5.4 µm, n = 15), acrogenous, catenate, light brown to greyish-brown, smooth to distinctly verrucose, phragmosporous, 1–3-septate, slightly constricted at septa, chiefly subcylindrical with rounded and paler colored at ends. Conidial secession schizolytic.

Culture characteristics: Colonies on PDA at 25 °C germinate from both end and mid of conidia, circular, umbonate, with entire margins and conspicuous concentric zoning; mycelium compact in the center, becoming progressively looser towards the margin, thick, floccose to cottony, and soft in texture. The colony surface is white to pale grey, floccose to cottony with abundant aerial mycelium; the center is denser, almost felted,

with a narrow light-colored peripheral band. Margin even to slightly fimbriate. The colony reverse is dark olivaceous-brown to almost black in the center, conspicuously zonate with a paler ochraceous ring and an outer umber band; a narrow pale marginal halo.

Material examined: China, Guizhou province, Xingyi City, on unidentified decaying wood, 27 November 2024, Xia Tang, GC46 (GZAAS25-0612), living culture GZCC 25-0582.

Known distribution: China (Su et al., 2018; Samarakoon et al., 2021; Yang et al., 2022; Wu et al., 2025; this study); Cuba (Crous et al., 2015); Thailand (Li et al., 2017; Tibpromma et al., 2018).

Known hosts: on dead branch of *Chromolaena odorata* (Li et al., 2017); on dead vines of *Lonicera japonica* (Wu et al., 2025); on decayed branch of *Mangifera indica* (Yang et al., 2022); on dead leaf vein of *Musa* sp. (Samarakoon et al., 2021); on dead leaf of *Pandanus* sp. (Tibpromma et al., 2018); on *Ficus religiosa* (Crous et al., 2015); on submerged decaying wood (Su et al., 2018); on unidentified decaying wood (this study).

Notes: Morphologically, our collection exhibits the asexual morph of *Torula* and closely resembles *T. fici*, having macronematous, mononematous conidiophores, mono- to polyblastic, terminal conidiogenous cells. Especially size, color, shape of Conidia which is catenate, phragmosporous, 1–3-septate. The observed size variation does not exceed the reported intraspecific limits for *T. fici*.

In the phylogenetic analysis, our collection formed a clade as sister to *Torula fici* (CBS 595.96, KUMCC 15-0428, UESTCC 22-0124 and UESTCC 24-0235) (Figure 3.60). Pairwise comparisons showed no nucleotide differences between our collection and Torula fici in the ITS region and LSU region, excluding gaps. Few differences in *rpb2* and *tef1-α*, all within the reported intraspecific range for *T. fici*. Based on the distinctive morphological characteristics of our specimen and the phylogenetic evidence, we propose our collection as a known species, *T. fici* in accordance with the taxonomic guidelines of Jeewon and Hyde (2016) and Maharachchikumbura et al. (2021). This record extends the distribution of *T. fici* in subtropic area of China.

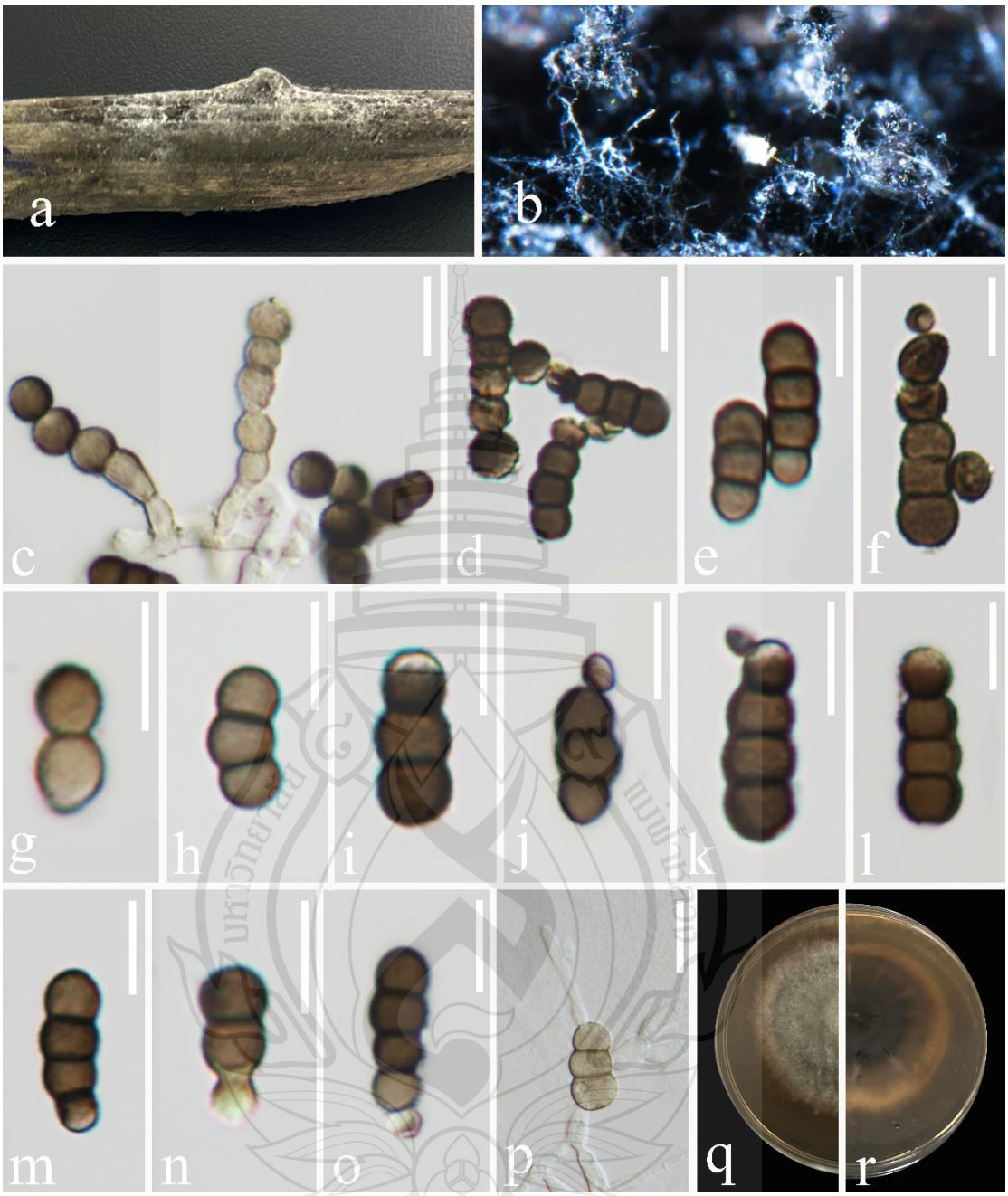

Figure 3.61 *Torula fici* (GZAAS25-0612, new collection)

Figure 3.61 a Specimen. b Colonies on substrate. c Conidiophores, conidiogenous cells bearing conidia. d–o Conidia. p Germinated conidium. q Colony on PDA (from front). r Colony on PDA (from reverse). Scale bars: c–p = 10 μm.

Torula mackenziei J.F. Li, Phookamsak & K.D. Hyde, Mycol. Progr. 16 (4): 455 (2017); Figure 3.62

Saprobic on unidentified decaying wood in the forest. **Sexual morph**: Undetermined. **Asexual morph**: *Colonies* on the natural substrate superficial, effuse, crowded, gregarious, powdery, dark brown to black. *Mycelium* mostly partly superficial, composed of branched, septate, pale brown to brown. *Conidiophores* macronematous, mononematous, solitary, erect, minutely verrucose, brown, branched, septate, ellipsoidal to subglobose cells at the apex. *Conidiogenous cells* monoblastic or polyblastic, terminal and intercalary, brow paler at apex, dry, ellipsoidal to subglobose. *Conidia* 11–16.5 ×5.5–7.5 μm ($\bar{x}$ = 13.3 × 7 μm, n = 30), acrogenous, catenate, formed in branched chains, monilioid composed of subglobose cells, rounded at both ends, brown to dark brown, sometimes paler at the apex, minutely verrucose, 1–3-septate, slightly constricted at septum. Conidial secession schizolytic.

Culture characteristics: Colonies on PDA at 25°C, circular, slight umbonate, and dry with a lobate margin. The surface is white to off-white, velvety to floccose with abundant aerial mycelium; centers more compact with faint concentric zoning. Margins fimbriate/feathery with a narrow pale buff halo. The reverse is pale straw to honey-yellow, forming a darker gray- to olivaceous-brown circular pigmented disc in the center with paler margins. The colony is surrounded by a diffuse halo of light-colored, sparse hyphae.

Material examined: China, Guizhou province, Xingyi City, on unidentified decaying wood, 27 November 2024, Xia Tang, GC06 (GZAAS25-0611), living culture GZCC 25-0581.

Known distribution: China (Boonmee et al.,2021; Wang et al., 2024; Xu et al., 2025; this study); Thailand (Li et al., 2017).

Known hosts: on a dead branch of *Bidens pilosa* (Li et al., 2017); on decaying branches of *Xanthoceras sorbifolium* (Xu et al., 2025); on submerged decaying wood (Boonmee et al., 2021; Wang et al., 2024); on decaying wood in the forest (this study).

Notes: Morphologically, our collection exhibits the asexual morph of *Torula* and closely resembles *T. mackenziei*, having macronematous, mononematous minutely verrucose, conidiophores, mono- to polyblastic, terminal, ellipsoidal to subglobose conidiogenous cells and the size, color, shape of Conidia which formed branched chains, monilioid composed of subglobose cells, minutely verrucose. The observed size variation

does not exceed the reported intraspecific limits for *T. mackenziei*.

In the phylogenetic analysis, our collection formed a clade as sister to *Torula mackenzie* (HKAS 112705 and MFLUCC 13-0839) (Figure 3.60). Pairwise comparisons showed no nucleotide differences between our collection and *Torula mackenziei* in the ITS, LSU SSU, *rpb2* and *tef1-α*. Based on the distinctive morphological characteristics of our specimen and the phylogenetic evidence, we propose our collection as a known species, *T. mackenziei* in accordance with the taxonomic guidelines of Jeewon and Hyde (2016) and Maharachchikumbura et al. (2021). This record extends the distribution of *T. mackenziei* in subtropic area of China.

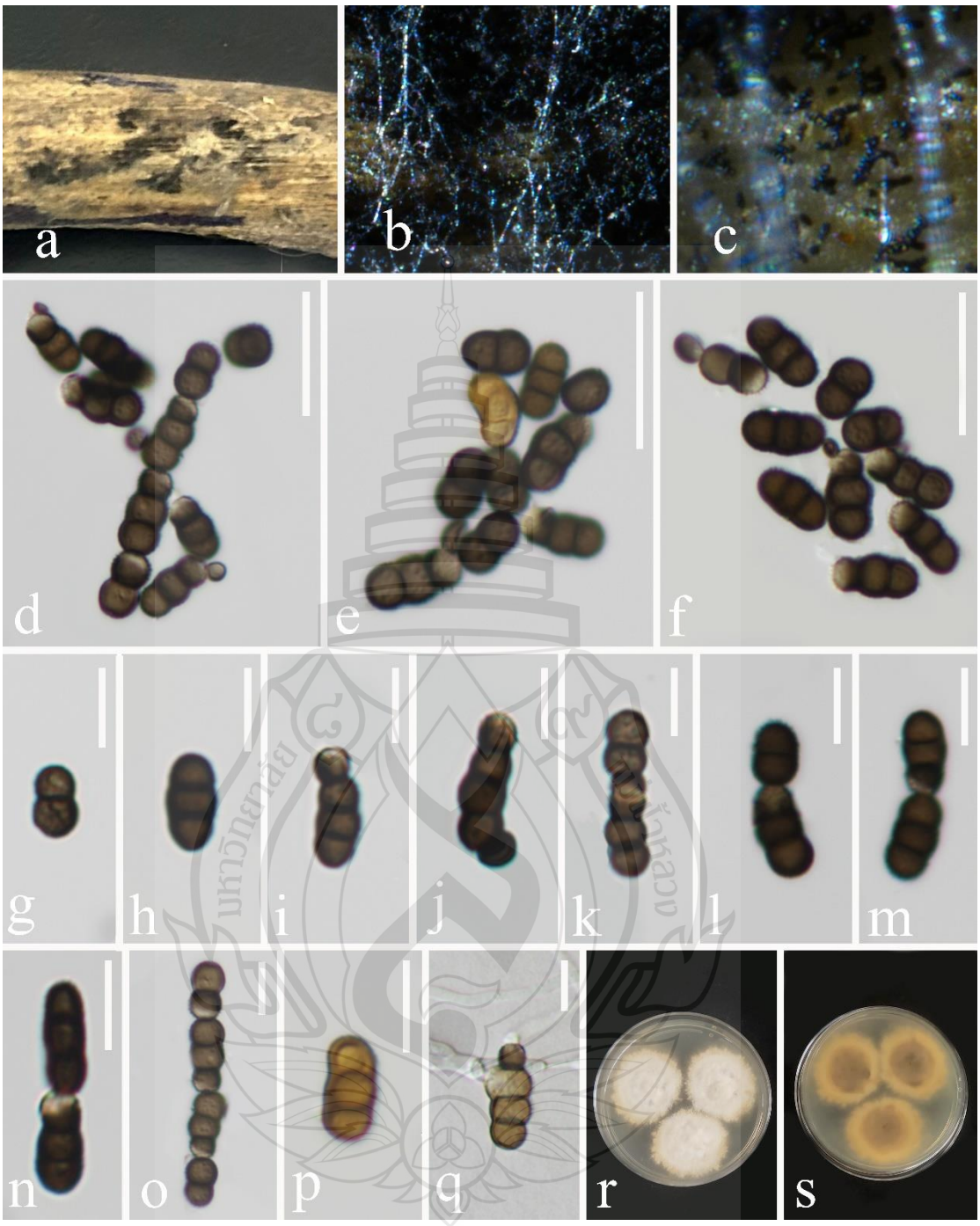

Figure 3.62 *Torula mackenziei* (GZAAS25-0611, new collection)

Figure 3.62 a Specimen. b, c Colonies on substrate. d, e, k–o Branched or chains of conidia. f–j, p Conidia. q Germinated conidium. r Colony on PDA (from front). s Colony on PDA (from reverse). Scale bars: d–f = 20 μm, g–q = 10 μm.

Neopodoconis Rifai, Reinwardtia 12 (4): 277 (2008)

Index Fungorum number: IF 569714; *Facesoffungi number*: FoF 17030

Notes: *Neopodoconis* was established by Rifai (2008) to accommodate two exosporium-like species. *Neopodoconis ampullacea* is the type species (Rifai, 2008). The genus is characterized by macronematous, mononematous, unbranched, smooth-walled, septate conidiophores, integrated, elongated sympodially conidiogenous cells that are terminal and monotretic or polytretic, and acropleurogenous, obclavate, fusiform to pyriform, smooth walled or verrucous conidia with euseptate and a truncate dark scar at the base (Rifai, 2008; Li et al., 2016; Su et al., 2018; Tibpromma et al., 2018; Shen et al., 2021; Qiu et al., 2022).

Previously two genera, *Sporidesmioides* and *Rostriconidium*, were introduced based on DNA sequence data without morphological comparison with the similar genus *Neopodoconis* (Li et al., 2016; Su et al., 2018). However, subsequent studies undertook a morpho-phylogenetic approach and synonymized *Sporidesmioides* and *Rostriconidium* under *Neopodoconis* (Qiu et al., 2022). Qiu et al. (2022) also clarified the taxonomic placement of *Neopodoconis* within *Torulaceae* (*Pleosporales*, *Dothideomycetes*, *Ascomycota*); however, it was found to be paraphyletic. The type species of the genus thus needs to be re-analysed. Species of *Neopodoconis* occur in both freshwater and terrestrial habitats as saprobes, and with a wide geographical distribution, including China, Ghana, Java, Sierra Leone, Sri Lanka and Thailand (Rifai, 2008; Li et al., 2016; Qiu et al., 2022; Wang et al., 2023; Zhang et al., 2025). There are currently 13 species in the genus (Zhang et al., 2025).

Neopodoconis thailandica (Jun F. Li, Phook. & K.D. Hyde) Y.F. Hu, L. Qiu, R.F. Castañeda & Jian Ma, Res Sq. (2022); Figure 3.63

= *Sporidesmioides thailandica* J.F. Li, Phookamsak & K.D. Hyde, Mycol. Progr. 15 (10): 1171 (2016)

Saprobic on unidentified decaying wood. **Sexual morph**: Undetermined. **Asexual morph**: *Colonies* on the natural substrate superficial, effuse, scattered, gregarious, glistening, dark brown to black. *Mycelium* semi-immersed on the substrate, composed of septate, branched, brown, smooth hyphae. *Conidiophores* 108–280 × 9–15 µm ($\bar{x}$ = 194.5 × 11.5 µm, n = 30), macronematous, mononematous, erect, solitary to fasciculate, dark brown to black, paler towards the apex, straight to slight flexuous, cylindrical, septate,

4–13-septa, unbranched, wider at base, sometimes percurrently proliferating, smooth, thick-walled. *Conidiogenous cells* 12–31 × 11–17 µm ($\bar{x}$ = 20.2 × 13.4 µm, n = 20), polyblastic, integrated, terminal, later becoming intercalary, cicatrized, determinate, cylindrical, brown to dark brown, smooth, with enlarged, thickened, protuberant, melanized, lenticular conidiogenous loci. *Conidia* 103.5–165 × 19–33 µm ($\bar{x}$ = 142 × 25.4 µm, n = 30), solitary, dark brown to black, obclavate to lageniform, rostrate, percurrently proliferating, septate, 8–14-septate, slightly constricted at septa, minutely verrucose, basal cell pale brown with a thick, black, truncate hilum; with a mucilaginous sheath at the apex.

Culture characteristics: Colonies on PDA at 25°C, circular, flat, and dry with an entire margin. Surface is olivaceous, with a white to pale grey circle at the center, floccose to cottony with abundant aerial mycelium and a slightly raised center showing faint concentric zoning. Reverse is pale honey to olivaceous-brown, usually with a dark brown to nearly black central patch, with scattered minute black puncta.

Material examined: China, Guizhou Province, Qiandongnan Miao and Dong Autonomous Prefecture, Liping County, Yongcong Township, on unidentified decaying wood, 27 November 2024, Xia Tang, LP23 (GZAAS25-0610), living culture GZCC 25-0580.

Known distribution: China (this study); Thailand (Li et al., 2016).

Known hosts: on stem of a dead herb (Li et al., 2016; this study).

Notes: Our collection (GZCC 25-0580) exhibits the asexual morph of exosporium-like. Morphologically, it resembles to *Neopodoconis* thailandica in having macronematous, mononematous, erect, solitary to fasciculate conidiophores, sometimes percurrently proliferating; polyblastic, integrated, terminal, cicatrized, conidiogenous cells with enlarged, thickened, protuberant, melanized, lenticular conidiogenous loci and solitary, obclavate to lageniform, minutely verrucose, percurrently proliferating conidia with basal cell pale brown with a thick, black, truncate hilum and mucilaginous sheath at the apex. The observed size variation does not exceed the reported intraspecific limits for *N. thailandica*.

The evidence of phylogenetic analysis showed that our collection formed a clade as sister to *N. thailandica* (KUMCC 16-0012 and MFLUCC 13-0840) (Figure 3.60). The pairwise comparisons showed no nucleotide differences between our collection and *N. thailandica* (MFLUCC 13-0840) in the LSU and SSU gene region, 0.4% (3/801) in *rpb2*

gene region and 0.1% (1/673) in *tef1-α* gene region; *N. thailandica* (KUMCC 16-0012) in the LSU and SSU gene region, 0.4% (3/801) in *rpb2* gene region and 0.2% (1/646) in *tef1-α* gene region. Based on the distinctive morphological characteristics of our specimen and the phylogenetic evidence, we propose our collection as a known species, *N. thailandica* in accordance with the taxonomic guidelines of Jeewon and Hyde (2016) and Maharachchikumbura et al. (2021). *Neopodoconis* thailandica was originally established by Li et al. (2016) as *Sporidesmioides thailandica*, which was collected from the stem of a dead herb in Thailand. Later, Qiu et al. (2022) transferred this species to the genus *Neopodoconis* based on both morphological and phylogenetic analyses, giving taxonomic priority to the latter genus. Our collection was obtained from decaying wood in a forest in China. This represents the first record of this species in China and expands the current knowledge of the genus in this region.

Figure 3.63 *Neopodoconis thailandica* (GZAAS25-0610, new geographical record)

Figure 3.63 a Host. b, c Colonies on substrate. d–g Conidiophores, conidiogenous cells. h–m Conidia. n Germinated conidium. o Colony on PDA (from front). p Colony on PDA (from reverse). Scale bars: d–g = 100 µm; h–n = 50 µm.

Tubeufiales Boonmee & K.D. Hyde, Fungal Diversity 68 (1): 245 (2014)

Tubeufiaceae M.E. Barr, Mycologia 71: 948 (1979)

Acanthostigmina Höhn., Sitzungsberichte der Kaiserlichen Akademie der Wissenschaften Math.-naturw. Klasse Abt. I 118: 1499 (1909)

Index Fungorum number: IF 19; *Facesoffungi number*: FoF 06814

Notes: *Acanthostigmina* was introduced by Von Höhnel (1909) with *A. minuta* as the type species. Currently, the genus comprises two recognized species *A. minuta* and *A. multiseptatum* (Lu et al., 2018b; Yang et al., 2024). The asexual morph of *Acanthostigmina* is characterized by macronematous, mononematous, erect, cylindrical, short, straight or slightly flexuous, branched or unbranched, septate conidiophores, holoblastic, monoblastic, integrated, determinate, terminal, cylindrical conidiogenous cells, and solitary, acrogenous, helicoid conidia (Ma et al., 2024). The sexual morph of *Acanthostigmina* is characterized by superficial, solitary, gregarious, subglobose, obovoid, black ascomata, 8-spored, bitunicate, fissitunicate, cylindrical, short pedicellate, apically rounded asci, and subfusiform, elongate, tapering at the ends, curved, multi-septate, hyaline ascospores (Ma et al., 2024).

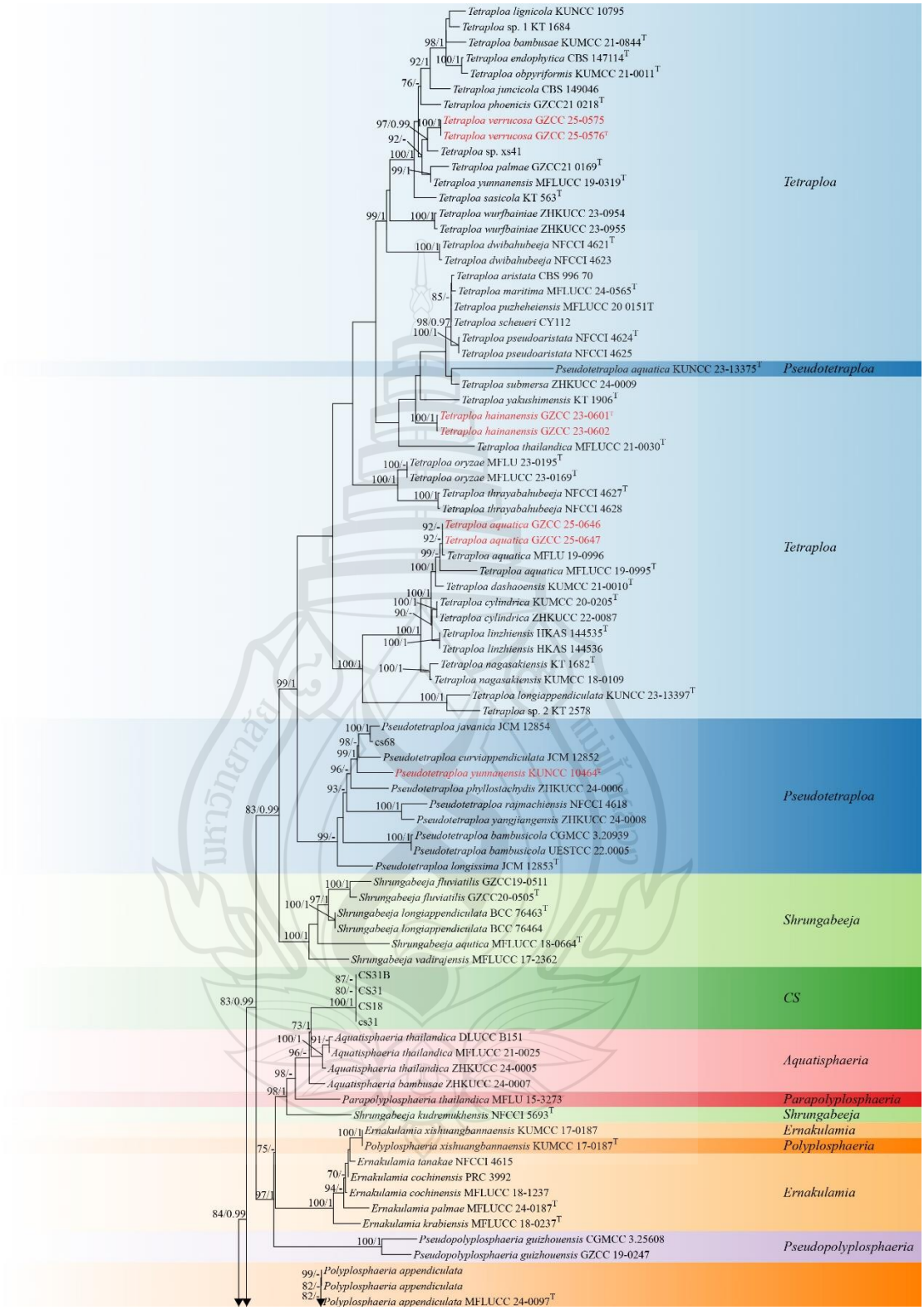

Figure 3.64 Phylogenetic analysis of *Tubeufiaceae*

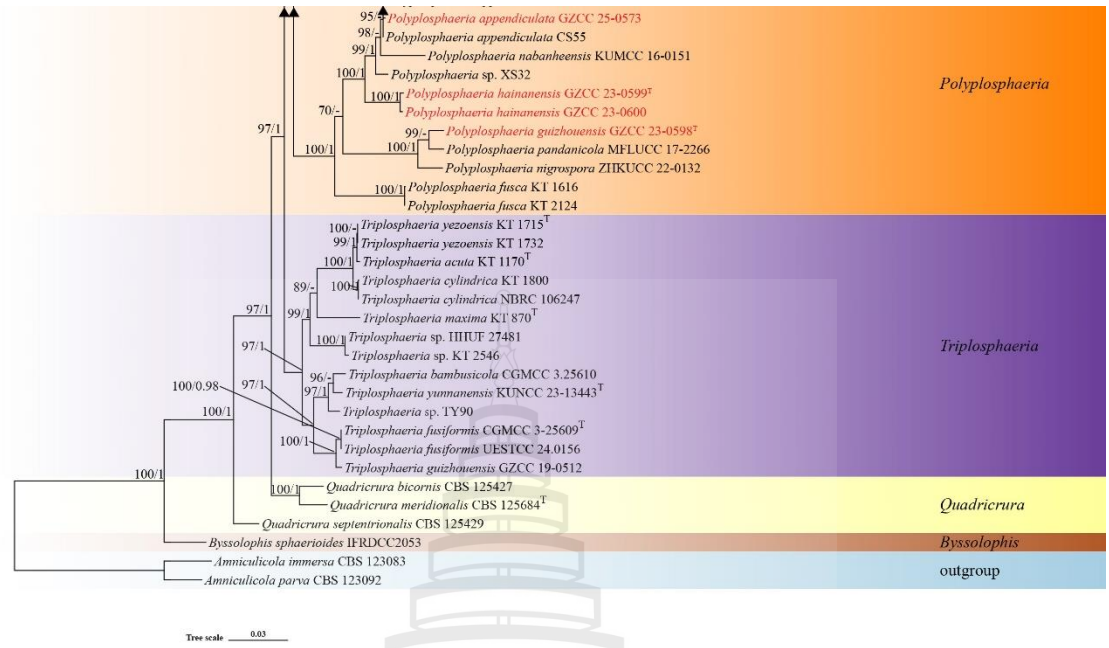

Figure 3.64 (continued)

Figure 3.64 Phylogenetic analysis of *Tubeufiaceae* was conducted using RAxML-based maximum likelihood analysis of a combined ITS, LSU, *tef1-α* and *rpb2* sequence dataset. Bootstrap support values for maximum likelihood (ML) equal to or greater than 70% and Bayesian posterior probabilities (PP) equal to or greater than 0.95 are shown above the nodes. The tree is rooted with *Botryosphaeria agaves* (MFLUCC 10-0051) and *B. dothidea* (CBS 115476). Newly generated strains are highlighted in red, and type strains are indicated with a superscript 'T'.

Acanthostigmina multiseptatum (Promp. & A.N. Mill.) Boonmee & K.D Hyde, Fungal Diversity 68 (1): 256 (2014); Figure 3.65

Saprobic on decaying leaves of *Camptotheca acuminata*. **Sexual morph**: see Promputtha and Miller (2010). **Asexual morph**: Hyphomycetous, helicosporous. *Colonies* on natural substrate superficial, effuse, gregarious, with masses of crowded, glistening conidia, white to pale brown. *Mycelium* partly immersed, partly superficial, composed of hyaline to pale brown, branched, septate, guttulate, smooth hyphae. *Conidiophores* 39–44.5 × 4.5–5.5 µm ($\bar{x}$ = 41.5 × 5 µm, n = 20), macronematous, mononematous, erect, cylindrical, short, straight or slightly flexuous, unbranched, septate, subhyaline to pale brown, smooth-walled, thick-walled. *Conidiogenous cells* 10.5–16 × 4–5 µm ($\bar{x}$ = 13 × 4.5 µm, n = 20), holoblastic, monoblastic, integrated,

determinate, terminal, cylindrical, rounded at apex after conidial secession, subhyaline to pale brown, smooth-walled. *Conidia* solitary, acrogenous, helicoid, tapering towards the rounded ends, 56–59 µm diam. and conidial filament 8.5–10 µm wide ($\bar{x}$ = 57.5 × 9 µm, n = 20), 387–424 µm long ($\bar{x}$ = 402 µm, n = 20), tightly coiled 23/4–41/2 times, not becoming loose in water, multi-septate, slightly constricted at septa, hyaline to pale brown, smooth-walled.

Culture characteristics: Conidia germinated on PDA and produced germ tubes within 12 hrs. Colonies on PDA reached 26 mm diam. after 39 days of incubation at 25 ℃ and had a circular shape with a flat surface and entire margin, hyaline to brown; the reverse side is hyaline to pale brown.

Material examined: China, Guizhou Province, Tongren City, on decaying leaves of Camptotheca acuminata, 10 October 2024, Xia Tang, XS17 (GZAAS 25-0681), living culture GZCC 25-0651.

Known distribution: China (Ma et al., 2024; this study); USA (Promputtha & Miller 2010).

Known hosts: on rotting wood in a freshwater habitat (Ma et al., 2024); on rotting wood in a terrestrial habitat (Ma et al., 2024); on decaying leaves of *Camptotheca acuminata* (this study).

Notes: In the phylogenetic tree (Figure 3.64), our isolation (GZCC 25-0651) formed a sister clade to *Acanthostigmina multiseptatum* (ANM 475) with weak support, indicating that they belong to the same species. Our new isolate shares the same conidiophores and conidial characteristics with the specimen of *Acanthostigmina multiseptatum* (GZAAS 22-2157) (Promputtha & Miller, 2010; Boonmee et al., 2014; Ma et al., 2024). Therefore, based on both morphological and molecular data, we identify our new isolate as *Acanthostigmina multiseptatum*. This is the first report of *A. multiseptatum* associated with *Camptotheca acuminata* from China.

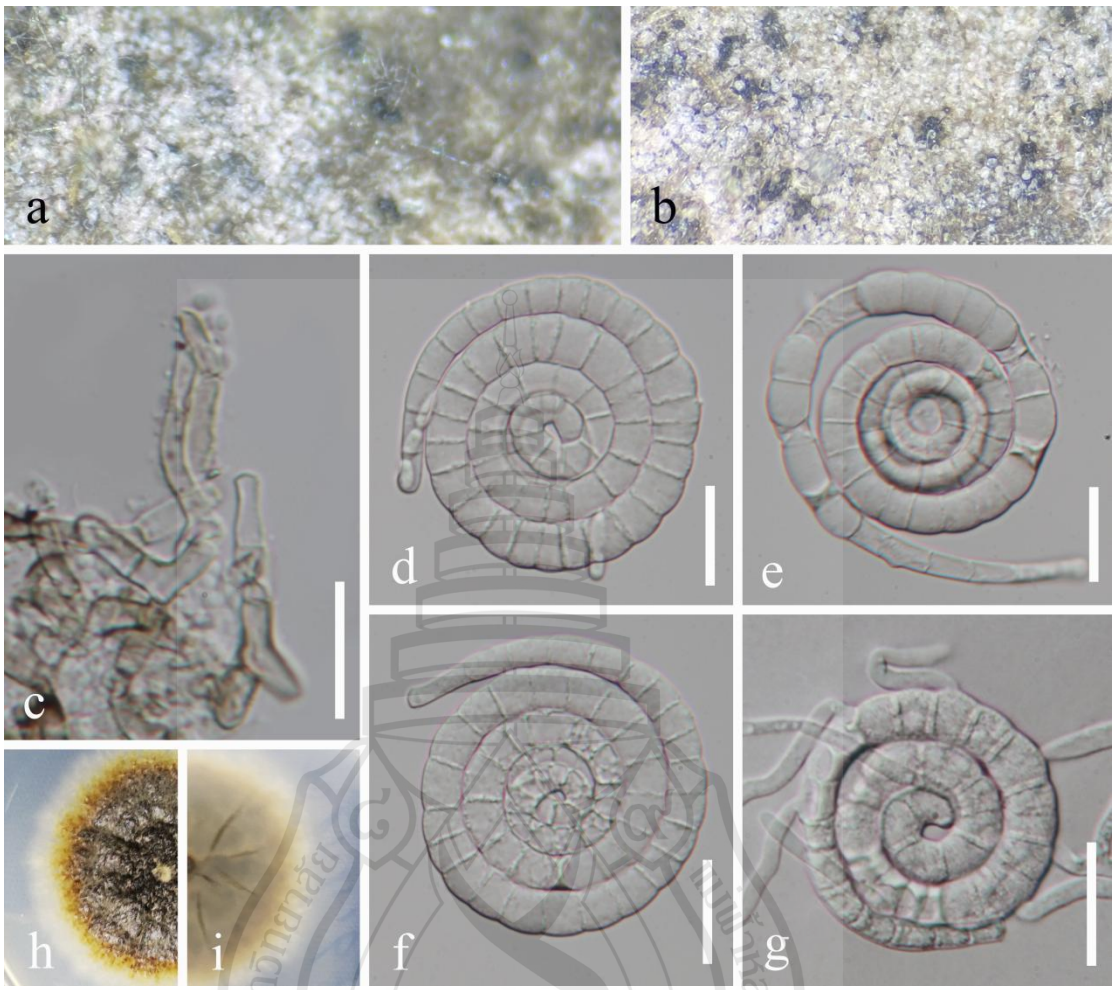

Figure 3.65 *Acanthostigmina multiseptatum* (GZAAS 25-0681, new host record)

Figure 3.65 a, b Colonies on substrate. c Conidiophores and conidiogenous cells. d–f Conidia. g Germinating conidium. h, i Colonies on PDA from above and below. Scale bars: c–g = 20 µm.

Aquaphila Goh, K.D. Hyde & W.H. Ho, Mycol. Res. 102 (5): 588 (1998)

Index Fungorum number: IF 22719; *Facesoffungi number*: FoF 02356

Notes: *Aquaphila* (*Tubeufiaceae*) was established by Goh et al. (1998) with *A. albicans* as the type species. Currently, *Aquaphila* comprises two species: *A. albicans* and *A. edentata* (Lu et al., 2018b). *Aquaphila albicans* is characterized by semi-macronematous, mononematous, hyaline, delicate, septate, simple or branched, flexuous and geniculate conidiophores; integrated, terminal or intercalary, denticulate, monoblastic or polyblastic, proliferation sympodial conidiogenous cells; acrogenous, proliferation, hyaline, fusoid to falcate or sigmoid conidia (Goh et al., 1998).

Aquaphila albicans Goh, K.D. Hyde & W.H. Ho, Mycol. Res. 102(5): 588 (1998); Figure 3.66

Saprobic on unidentified decaying wood in a terrestrial habitat. **Asexual morph**: Colonies superficial, hairy, velvety, white, conidia arising from aerial hyphae. *Mycelium* partly immersed in the woody substratum and partly superficial, consisting of septate, branched, hyaline, smooth, repent hyphae. *Conidiophores* 7.5–41 × 3–4 μm ($\bar{x}$ = 15.5 × 3.5 μm, n = 20), semi-macronematous, arising singly as lateral branches from the procumbent hyphae, cylindrical, simple or branched, septate, thin-walled, smooth, indistinctly septate, hyaline, flexuous or geniculate. Conidiogenous cells monoblastic or polyblastic, denticulate, sympodial proliferations, cylindrical, Conidia 56–66 × 7–9 μm ($\bar{x}$ = 61 × 8 μm, n = 30), holoblastic, solitary, borne acrogenously on conidiogenous denticles, becoming lateral after proliferation of the conidiophore, hyaline or very pale yellowish, predominantly fusoid to sickle-shaped, sometimes sigmoid, very rarely straight and obclavate, thin-walled, smooth, euseptate, slightly constricted at the septa, heavily guttulate, conically rounded at both ends slightly broaded at the base, basal cell obconical but not pedicellate.

Culture characteristics: Conidia germinated on PDA and produced germ tubes within 8 hrs. Colonies on PDA reached 5 mm diam. after 21 days of incubation at 25℃ and had a circular shape with a flat surface and entire margin, grey to pale brown; the reverse side is grey to brown.

Material examined: China, Hainan Province, Wuzhishan City, on decaying wood in a terrestrial habitat, 24 September 2024, Xia Tang, S21 (GZAAS 25-0623), living culture GZCC 25-0593.

Known distribution: Australia (Goh et al., 1998), Brunei Darussalam (Goh et al., 1998), Malaysia (Goh et al., 1998), Philippines (Goh et al., 1998); China (this study).

Known hosts: on submerged decaying wood (Goh et al., 1998); on decaying wood in a terrestrial habitat (this study).

Notes: Goh et al. (1998) described *Aquaphila albicans* from submerged, decaying wood in a tropical habitat. Our newly isolated strain (GZCC 25-0593) clustered with *A. albicans* (BCC 3520 and MFLUCC 16-0020) with 100% ML bootstrap support and 1.00 Bayesian posterior probability, indicating that they belong

to the same species. Morphologically, the new isolate is indistinguishable from the holotype of *A. albicans*. Therefore, based on both molecular and morphological evidence, we identify our isolate as *Aquaphila albicans*. This represents the first record of this species from a terrestrial habitat in China.

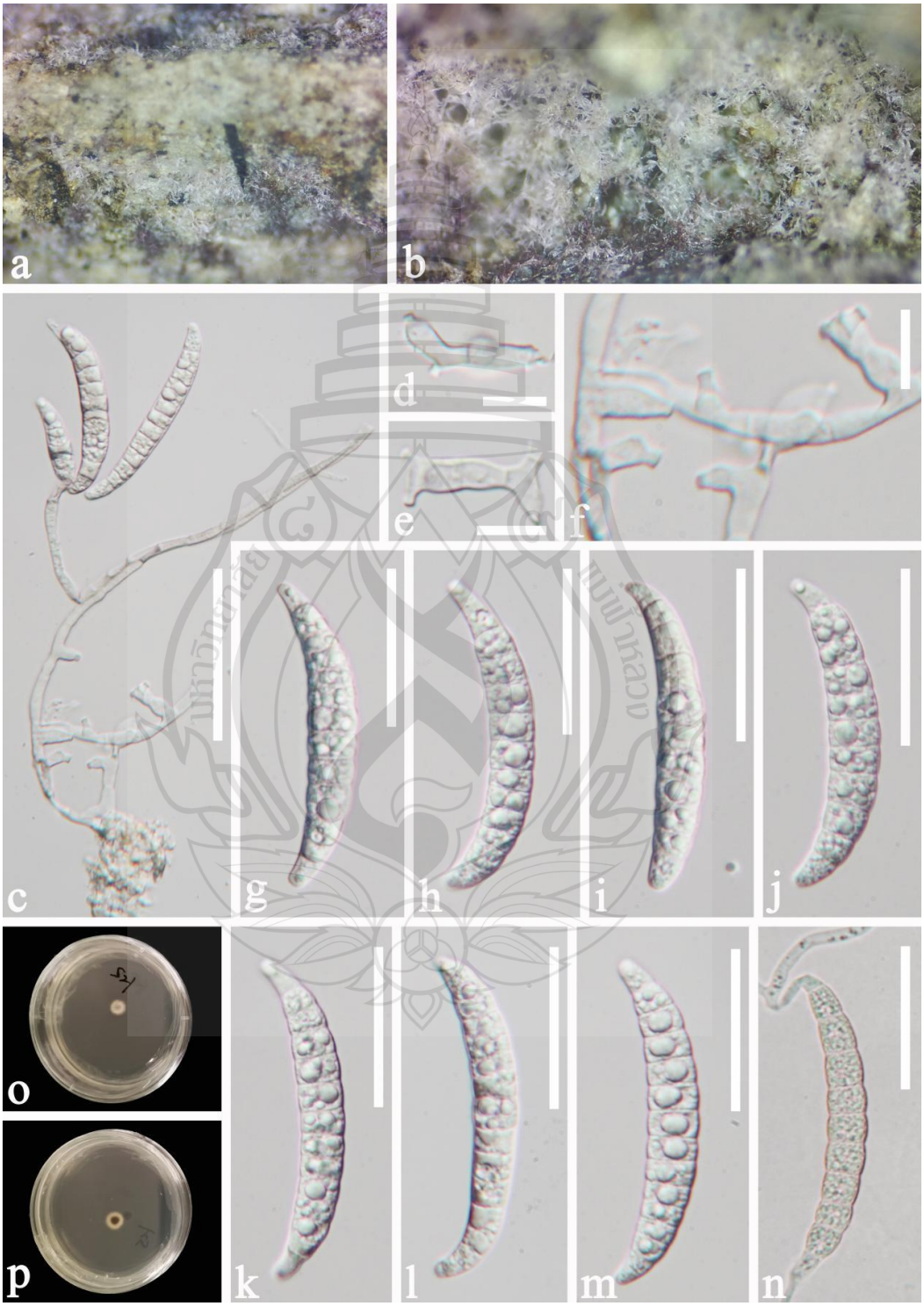

Figure 3.66 *Aquaphila albicans* (GZAAS 25-0623, new geographical record)

Figure 3.66 a, b Colonies on decaying wood. c–f Conidiophores and conidiogenous cells. g–m Conidia. n Germinating conidium. o, p Colonies on PDA from above and below. Scale bars: c = 50 µm, g–n = 30 µm, d–f = 10 µm.

Berkleasmium Zobel, Icones fungorum hucusque cognitorum 6: 4 (1854)

Index Fungorum number: IF 7362; *Facesoffungi number*: FoF 01879

Notes: *Berkleasmium* was established by Corda (1854), with *B. concinnum* as the type species. The type species, *B. concinnum*, is characterized by dictyoconidia and helicosporous asexual conidia, as supported by molecular evidence (Lu et al., 2018b). Currently, Berkleasmium comprises 10 species: *B. aquaticum*, *B. concinnum*, *B. fusiforme*, *B. guangxiense*, *B. hainanense*, *B. hydei*, *B. latisporum*, *B. longisporum*, *B. macrofilamentosus*, and *B. thailandicum* (Ma et al., 2024; Xiao et al., 2025). These species have been reported from dead wood in both freshwater and terrestrial habitats across diverse regions, including Canada, China, Russia, the USA, and Thailand (Lu et al., 2018b; Ma et al., 2024; Xiao et al., 2025).

Berkleasmium hydei X.J. Xiao, N.G. Liu & Y.Z. Lu, Mycosphere (2025); Figure 3.2.67

Saprobic on decaying wood in a terrestrial habitat. **Sexual morph**: Undetermined. **Asexual morph**: Hyphomycetous, helicosporous. *Colonies* on natural substrate superficial, effuse, gregarious, with masses of crowded, glistening conidia, pale brown. *Mycelium* partly immersed, partly superficial, composed of pale brown to brown, branched, septate, guttulate, smooth hyphae. *Conidiophores* 26–63 × 5.5–7 µm ($\bar{x}$ = 40 × 6 µm, n = 30), micronematous to semi-macronematous, mononematous, erect, cylindrical, flexuous, simple, septate, pale brown, smooth-walled, thick-walled. *Conidiogenous cells* 8.5–22 × 4–5 µm ($\bar{x}$ = 14 × 4.4 µm, n = 20), holoblastic, monoblastic, integrated, determinate, terminal, cylindrical, truncate at apex after conidial secession, pale brown, smooth-walled. *Conidia* solitary, acrogenous, helicoid, tapering towards the rounded ends, 81–87.5 µm diam. and conidial filament 10–11.5 µm wide ($\bar{x}$ = 85 × 10.5 µm, n = 20), 506–584 µm long ($\bar{x}$ = 542 µm, n = 20), tightly coiled 21/2–3 times, becoming loosely coiled in water, multi-septate, slightly constricted at septa, pale brown, smooth-walled.

Culture characteristics: Conidia germinated on PDA and produced germ tubes within 12 hrs. Colonies on PDA reached 42 mm diam. after 49 days of incubation

at 25℃ and had a circular with a flat surface and entire margin, pale brown to brown; the reverse side is pale brown to brown.

Material examined: China, Hainan Province, Wuzhishan City, Wuzhishan National Nature Reserve, on unidentified decaying wood in a terrestrial habitat, 24 September 2024, Xia Tang, MM5 (GZAAS 25-0624), living culture GZCC 25-0594.

Known distribution: China (Xiao et al., 2025; this study).

Known hosts: on submerged rotting wood in freshwater habitat (Xiao et al., 2025); on decaying wood in a terrestrial habitat (this study).

Notes: *Berkleasmium hydei* (GZAAS 25-0536) was collected from freshwater habitats in southern China (Xiao et al., 2025). Morphologically, our new isolate (GZCC 25-0594) is indistinguishable from the holotype of *B. hydei* (GZAAS 25-0536) (Xiao et al., 2025). Phylogenetic analyses further confirmed that the new isolate belongs to the same species as *B. hydei*, with 100% ML bootstrap support and xx BYPP (Figure 3.2.57). Therefore, we identify our isolation (GZCC 25-0594) as *Berkleasmium hydei*. This represents the first record of this species from a terrestrial habitat in China.

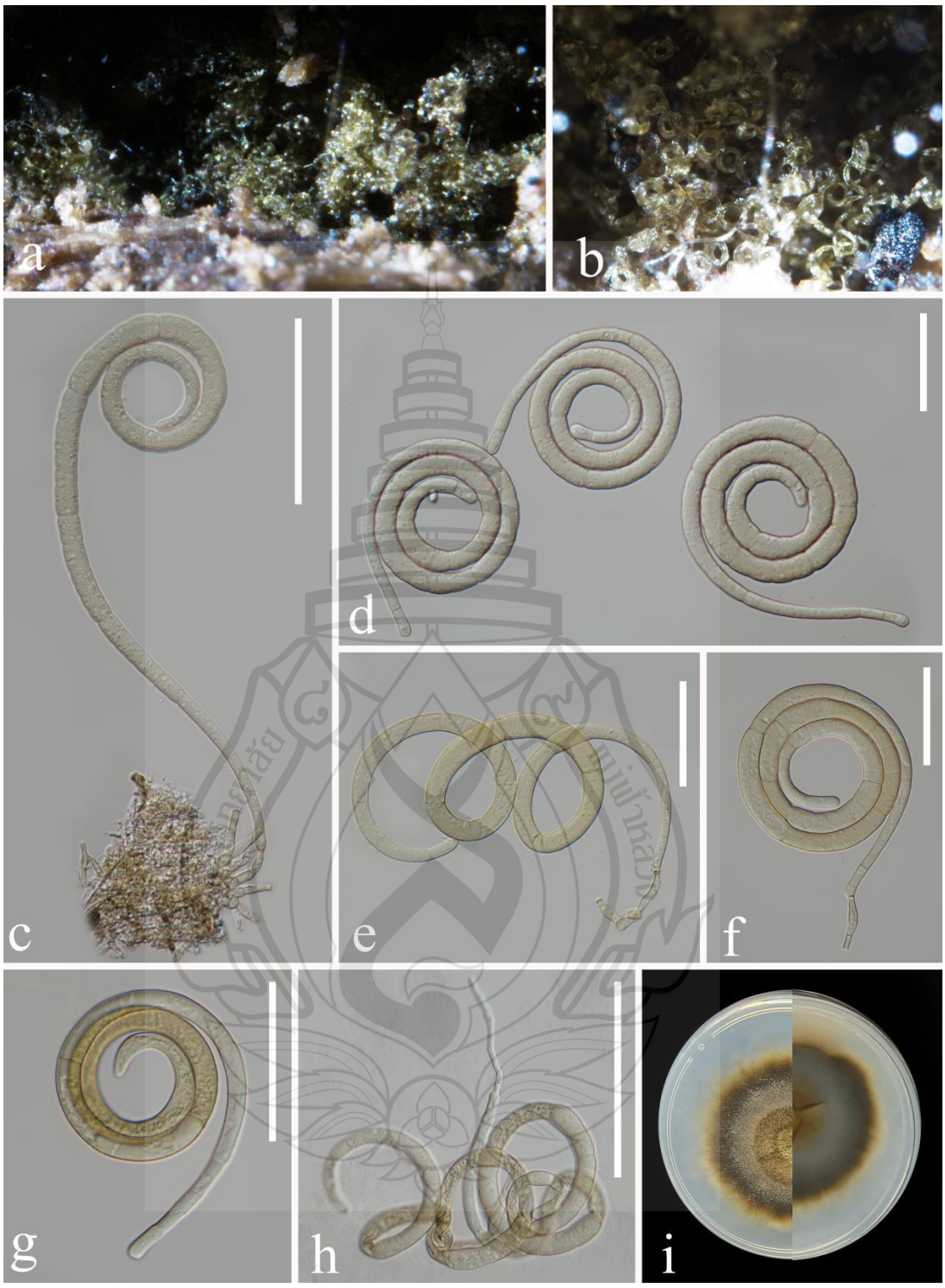

Figure 3.67 *Berkleasmium hydei* (GZAAS 25-0624, new habitat record)

Figure 3.67 a, b Colonies on submerged decaying wood. c Conidiophores, conidiogenous cells, and conidia. d–g Conidia. h Germinating conidium. i Colonies on PDA from above and below. Scale bars: c = 100 µm, d–h = 50 µm.

Helicoma Corda, Icones fungorum hucusque cognitorum 1: 15 (1837)

Index Fungorum number: IF 8473; *Facesoffungi number*: FoF 00211

Notes: Helicoma was introduced by Corda (1837) with *Helicoma muelleri* as the type species. Currently, 70 species are accepted in the genus based on combined molecular data and morphological evidence (Lu et al., 2018b; Ma et al., 2024). Multi-gene phylogenetic analyses indicate that *Helicoma* encompasses three distinct asexual morphs of helicosporous hyphomycetes (Lu et al., 2018b; Ma et al., 2024). Eight sexual species of *Helicoma* have been described based on molecular evidence (Lu et al., 2018b; Ma et al., 2024). Among them, only *H. fusiforme* and *H. miscanthi* remain without corresponding asexual morphs (Lu et al., 2018b; Ma et al., 2024).

Helicoma hydei N.G. Liu, Y.Z. Lu & J.K. Liu, Mycological Progress 18: 678 (2018); Figure 3.68

Saprobic on decaying fruit of *Entada* sp.. **Sexual morph**: Undetermined. **Asexual morph**: Hyphomycetous, helicosporous. *Colonies* on natural substrate superficial, effuse, gregarious, pale brown. *Mycelium* partly immersed, partly superficial, composed of hyaline to pale brown, branched, septate, guttulate, smooth hyphae. *Conidiophores* 166–233 × 6–97 μm ($\bar{x}$ = 204 × 6.5 μm, n = 20), macronematous, mononematous, erect, cylindrical, straight or slightly flexuous, branched, septate, brown or dark brown at base, paler towards apex, smooth-walled, thick-walled. *Conidiogenous cells* 12–16 × 6–7.5 μm ($\bar{x}$ = 14 × 6.5 μm, n = 25), holoblastic, monoblastic or polyblastic, integrated, sympodial, terminal, cylindrical, with denticles, truncate at apex after conidial secession, pale brown, smooth-walled. *Conidia* solitary, acropleurogenous, helicoid, dry, tapering towards the ends, developing on tooth-like protrusion, 10–22 μm diam. and conidial filament 6–8 μm wide ($\bar{x}$ = 16 × 7 μm, n = 20), 36.5–48 μm long ($\bar{x}$ = 42 μm, n = 20), tightly coiled up to 13/4 times, not becoming loose in water, multi-septate, slightly constricted at septa, guttulate, pale brown, smooth-walled.

Culture characteristics: Conidia germinated on PDA and produced germ tubes within 11 hrs. Colonies on PDA reached 29 mm diam. after 42 days of incubation at 25℃.

Material examined: China, Hainan Province, Jianfengling National Forest Park, on decaying fruit of *Entada* sp., 24 September 2024, Xia Tang, D17B (GZAAS

25-0626), living culture GZCC 25-0596.

Known distribution: China (this study); Thailand (Liu et al., 2019).

Known hosts: on decaying wood in a freshwater stream (Liu et al., 2019); on decaying fruit of *Entada* sp. (this study).

Notes: In the phylogenetic tree (Figure 3.64), GZCC 25-0596 formed a sister clade to *Helicoma hydei* (GZCC 23-0374 and HKAS 102204) with 80% ML support, indicating that they belong to the same species. Our new isolate shares the same conidiophores and conidial characteristics with the holotype of *H. hydei* (MFLU 18-1508) (Liu et al., 2019). Therefore, based on both morphological and molecular data, we identify our new isolate as *Helicoma hydei*. This is the first report of *H. hydei* associated with a *Entada* sp. from China.

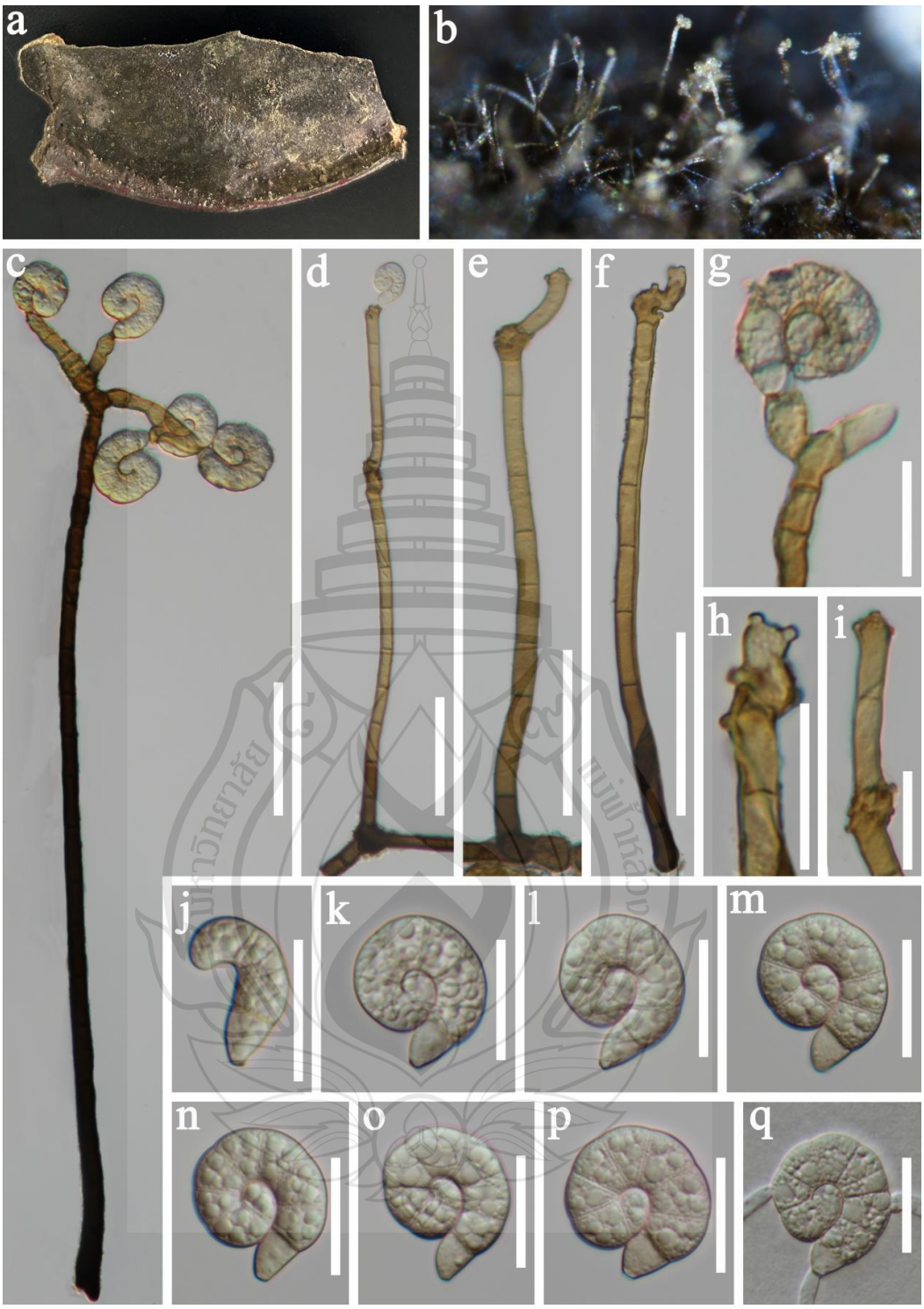

Figure 3.68 *Helicoma hydei* (GZAAS 25-0626, new host record)

Figure 3.68 a, b Colonies on decaying wood. c–f Conidiophores with attached conidia. g–i Conidiogenous cells and conidia. j–p Conidia. q Germinating conidium. Scale bars: c–f = 50 µm, g–q = 20 µm.

Helicoma rugosa (C. Booth) Boonmee & K.D. Hyde, Fungal Diversity 68 (1): 266 (2014); Figure 3.69

Saprobic on decaying fruit of *Entada* sp.. **Sexual morph**: Undetermined. **Asexual morph**: Hyphomycetous, helicosporous. *Colonies* on natural substrate superficial, effuse, gregarious, glistening, pale brown. Mycelium partly immersed, partly superficial, composed of hyaline to pale brown, branched, septate, smooth hyphae. *Conidiophores* 155–211 × 8.5–13 μm ($\bar{x}$ = 175 × 10 μm, n = 25), macronematous, mononematous, erect, cylindrical, tapering at tip, straight or slightly flexuous, occasionally branched, septate, the lower brown and the upper part subhyaline to brown, thick-walled. *Conidiogenous cells* 10–16.5 × 6.5–8 μm ($\bar{x}$ = 12.5 × 7.5 μm, n = 25), holoblastic, monoblastic, integrated, determinate, intercalary, cylindrical, with tiny tooth-like protrusions, truncate at apex after conidial secession, pale brown to brown, smooth-walled. *Conidia* solitary, pleurogenous, helicoid, dry, tapering towards the rounded ends, developing on tooth-like protrusion, 61–74 μm diam. and conidial filament 4–8 μm wide, 278–438 μm long ($\bar{x}$ = 359 μm, n = 25), loosely coiled 2–3 times, becoming loosely coiled in water, multi-septate, slightly constricted at septa, pale brown, guttulate, smooth-walled.

Culture characteristics: Conidia germinated on PDA and produced germ tubes within 10 hrs. Colonies on PDA reached 45 mm diam. after 51 days of incubation at 25℃ and had an irregular shape with a raise surface and undulate margin, pale brown to brown; the reverse side is brown to dark brown.

Material examined: China, Hainan Province, Jianfengling National Forest Park, on decaying fruit of *Entada* sp., 24 September 2024, Xia Tang, D16 (GZAAS 25-0628), living culture GZCC 25-0598; Ibid. D19.1 (GZAAS 25-0629), living culture GZCC 25-0599.

Known distribution: Bermuda (Boonmee et al., 2014); China (Li et al., 2022a; Lu et al., 2023; Ma et al., 2024; this study).

Known hosts: on submerged decaying wood (Li et al., 2022a; Lu et al., 2023); on leaves of *Sabal bermudiana* (Boonmee et al., 2014); on decaying wood in a terrestrial habitat (Ma et al., 2024); on decaying fruit of *Entada* sp. (this study).

Notes: *Helicoma rugosa* was introduced by Boonmee et al. (2014) based on morphology and molecular data. The asexual morphological description of *H. rugosa*

in freshwater and terrestrial habitats in China was further clarified by Li et al. (2022a), Lu et al. (2023), and Ma et al. (2024). Our new isolate shares the same conidiophores and conidial characteristics with the holotype of *H. rugosa*. In our phylogenetic analyses (Figure 3.64), the new isolates (GZCC 25-0598 and GZCC 25-0599) cluster with *H. rugosa* (GZCC 22-2034) with 100% ML/1.00 MP support, indicating that they belong to the same species. Therefore, based on both morphological and molecular data, we identify our new isolate as *Helicoma rugosa*. This is the first report of *H. rugosa* associated with *Entada* sp. from China.

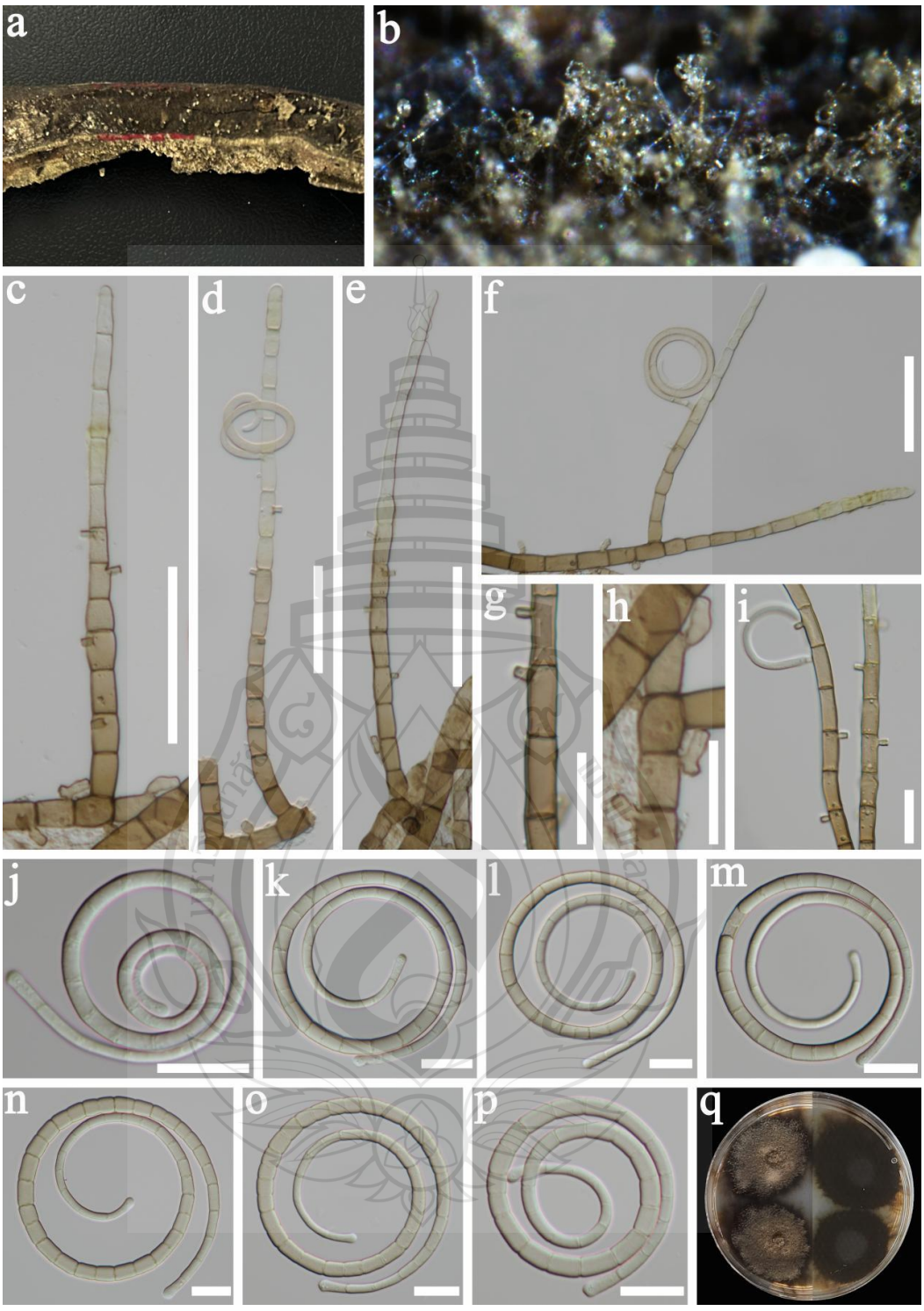

Figure 3.69 *Helicoma rugosa* (GZAAS 25-0628, new host record)

Figure 3.69 a, b Colonies on decaying wood. c–f Conidiophores and conidia. g–i Conidiogenous cells. j–p Conidia. q Colonies on PDA from above and below. Scale bars: c–f = 50 μm, g–p = 20 μm.

Neohelicomyces Z.L. Luo, D.J. Bhat & K.D. Hyde, Cryptogamie Mycologie 38 (1): 39 (2017)

Index Fungorum number: IF 818820; *Facesoffungi number*: FoF 02643

Notes: *Neohelicomyces* was introduced by Luo et al. (2017) with *N. aquaticus* as the type species. Currently, *Neohelicomyces* comprises 30 species (Ma et al., 2025a). Members of *Neohelicomyces* occur in both freshwater and terrestrial habitats across diverse regions, including China, the Czech Republic, Germany, Italy, Japan, the Netherlands, Thailand, and the USA (Ma et al., 2025a). The asexual morph of *Neohelicomyces* is characterized by macronematous, mononematous, erect, septate, sparsely branched, pale brown, glistening, and smooth-walled conidiophores that arise directly on the substrates, monoblastic, holoblastic, and integrated conidiogenous cells consisting of denticles, and helicoid, acropleurogenous, hyaline, indistinctly multi-septate, smooth-walled, and guttulate conidia that are tightly or loosely coiled, and rounded at the apical end (Luo et al., 2017; Lu et al., 2018b).

Neohelicomyces congjiangensis X. Tang, K.D. Hyde & J.C. Kang, sp. nov.; Figure 3.2.70

Etymology: ‘‘congjiangensis” refers to the ‘‘Congjiang County” where the holotype was collected.

Holotype: GZAAS25-0682

Saprobic on submerged decaying wood in a freshwater habitat. **Sexual morph**: Undetermined. **Asexual morph**: Hyphomycetous, helicosporous. *Colonies* on natural substrate superficial, effuse, gregarious, with a little of crowded, glistening conidia, white. *Mycelium* partly immersed, partly superficial, composed of hyaline to pale brown, branched, septate, smooth hyphae. *Conidiophores* 150–247 × 3–5 μm ($\bar{x}$ = 177 × 4.5 μm, n = 20), macronematous, mononematous, arising from creeping hyphae, erect, cylindrical, straight or slightly flexuous, simple, septate, subhyaline to pale brown, thick-walled. *Conidiogenous cells* 11–17.5 × 3.5–5.5 μm ($\bar{x}$ = 14 × 4 μm, n = 25), holoblastic, monoblastic or polyblastic, integrated, terminal or intercalary, cylindrical, with denticles, subhyaline to pale brown, smooth-walled. *Conidia* solitary, acropleurogenous, helicoid, tapering towards the rounded ends, developing on tooth-like protrusion, 15–17 μm diam. and conidial filament 2–3.5 μm wide ($\bar{x}$ = 16 × 3 μm, n = 20), 90–125 μm long ($\bar{x}$ = 110.5 μm, n = 30), tightly coiled up to 3 times, becoming

loosely coiled in water, aseptate, guttulate, hyaline, smooth-walled.

Culture characteristics: Conidia germinated on PDA and produced germ tubes within 12 hrs. Colonies on PDA reached 27 mm diam. after 37 days of incubation at 25℃ and had a circular shape with a raise surface and entire margin. They are pale yellowish brown to dark brown in PDA medium.

Material examined: China, Guizhou Province, Qiandongnan Miao and Dong Autonomous Prefecture, Congjiang County, on submerged decaying wood in a freshwater habitat, 24 August 2020, Xia Tang, ZLC4 (GZAAS 25-0682, holotype), ex-type living culture GZCC 25-0652.

Notes: In our phylogenetic tree (Figure 3.64), our isolates (GZCC 25-0652) formed a sister clade to *N. liuzhouensis* (GZCC 25-0653) with 100% ML and 1.00 BYPP support. *Neohelicomyces congjiangensis* can be distinguished from *N. liuzhouensis* by its shorter conidiophores (90–125 μm long vs. 136–155 μm long). Moreover, base pair comparison of *Neohelicomyces congjiangensis* and *N. liuzhouensis* shows 31/523 bp differences in ITS (5.9%, gaps 3 bp), 3/835 bp differences in LSU (0.3%, without gap), and 3/848 bp differences in *tef1-α* (0.4%, without gap). Therefore, based on DNA molecular data and morphological characteristics, we introduce our collection as a novel species, *Neohelicomyces congjiangensis*.

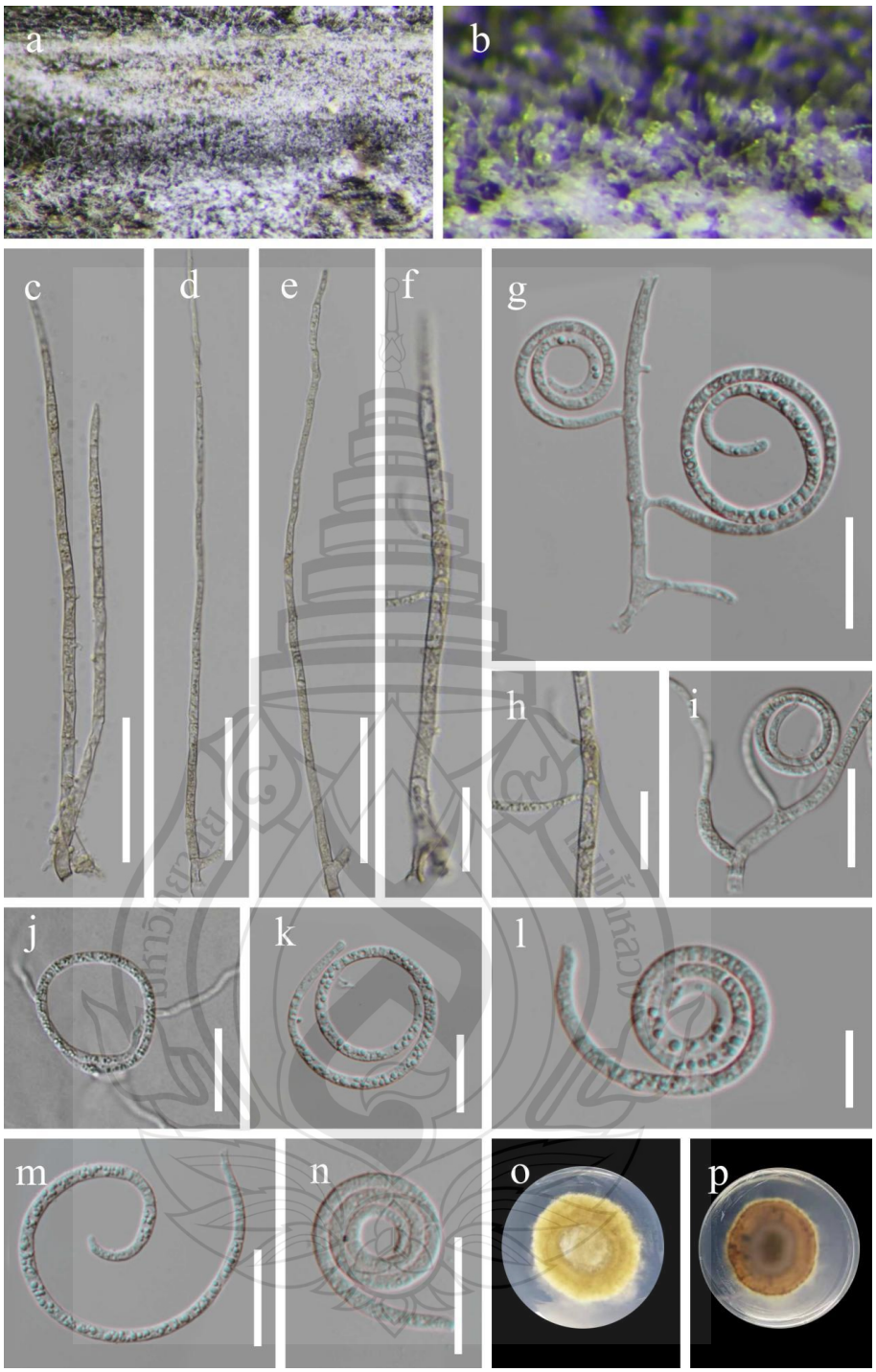

Figure 3.70 *Neohelicomyces congjiangensis* (GZAAS 25-0682, holotype)

Figure 3.70 a, b Colonies on submerged decaying wood. c–f Conidiophores and conidiogenous cells. g–i Conidiogenous cells. k–n Conidia. j Germinating conidium. o, p Colonies on PDA from above and below. Scale bars: c–e = 50 µm, f–i, k, m, n = 20 µm, j, l = 10 µm.

Neohelicomyces liuzhouensis X. Tang, K.D. Hyde & J.C. Kang, sp. nov.; Figure 3.71

Etymology: "liuzhouensis" refers to the "Liuzhou City" where the holotype was collected.

Holotype: GZAAS25-0683

Saprobic on submerged decaying wood in a freshwater habitat. **Sexual morph**: Undetermined. **Asexual morph**: Hyphomycetous, helicosporous. *Colonies* on natural substrate superficial, effuse, gregarious, with a little of crowded, glistening conidia, white. *Mycelium* partly immersed, partly superficial, composed of hyaline to pale brown, branched, septate, smooth hyphae. *Conidiophores* 218–312 × 4.5–7.5 μm ($\bar{x}$ = 270 × 5.5 μm, n = 20), macronematous, mononematous, erect, cylindrical, straight or slightly flexuous, branched, septate, subhyaline to pale brown, thick-walled. *Conidiogenous cells* 11–19 × 3.5–5 μm ($\bar{x}$ = 14.5 × 4 μm, n = 25), holoblastic, monoblastic or polyblastic, integrated, terminal or intercalary, cylindrical, with denticles, subhyaline to pale brown, smooth-walled. *Conidia* solitary, acropleurogenous, helicoid, tapering towards the rounded ends, developing on tooth-like protrusion, 18–19.5 μm diam. and conidial filament 2–2.5 μm wide ($\bar{x}$ = 18.5 × 2.3 μm, n = 20), 136–155 μm long ($\bar{x}$ = 145.5 μm, n = 30), tightly coiled up to 4 times, not becoming loose in water, aseptate, guttulate, hyaline, smooth-walled.

Culture characteristics: Conidia germinated on PDA and produced germ tubes within 14 hrs. Colonies on PDA reached 30 mm diam. after 39 days of incubation at 25°C and had a circular shape with a raise surface and entire margin. They are pale brown to black brown in PDA medium.

Material examined: China, Guangxi Zhuang Autonomous Region, Liuzhou City, Luzhai County, on submerged decaying wood in a freshwater habitat, 2 May 2021, Xia Tang, LZ14 (GZAAS 25-0683, holotype), ex-type living culture GZCC 25-0653.

Notes: Our new isolate (GZCC 25-0653), formed a sister clade with *Neohelicomyces congjiangensis* (GZAAS 25-0682), and the phylogeny indicates that they belong to the different species (Figure 3.2.57). Our collection (GZCC 25-0653) differs from *Neohelicomyces congjiangensi* (GZAAS 25-0682) by its longer conidiophores (90–125 μm long vs. 136–155 μm long). Therefore, based on morphology and molecular evidence, we identify our collection as a novel species, named *Neohelicomyces liuzhouensis*.

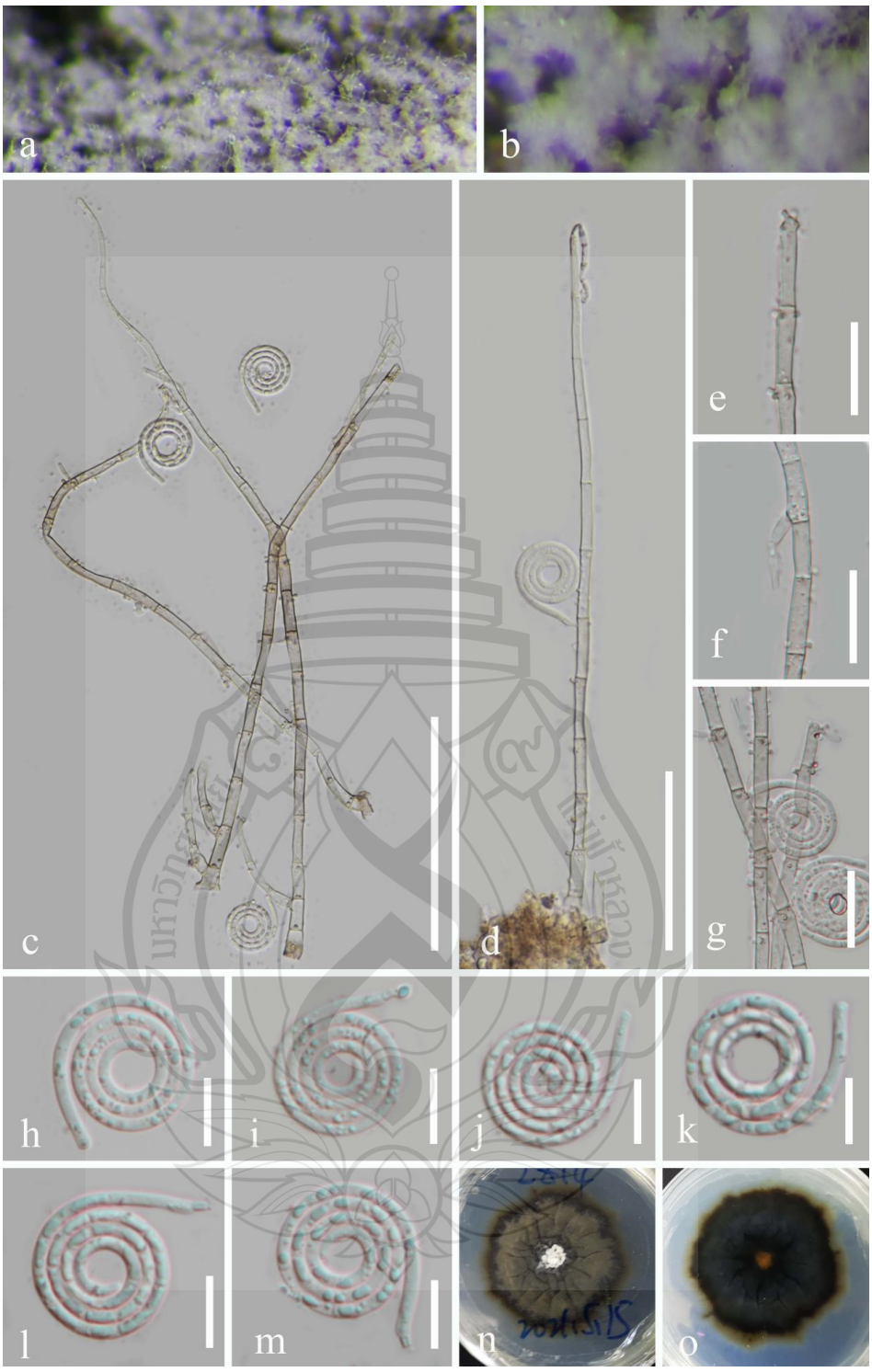

Figure 3.71 *Neohelicomyces liuzhouensis* (GZAAS25-0683, holotype)

Figure 3.71 a, b Colonies on submerged decaying wood. c, d Conidiophores, conidiogenous cells, and conidia. e–g Conidiogenous cells. h–m Conidia. n, o Colonies on PDA from above and below. Scale bars: c = 100 µm, d = 50 µm, e–g = 20 µm, h–m = 10 µm.

Neohelicosporium Y.Z. Lu, J.C. Kang & K.D. Hyde, Mycol. Progr. 17 (5): 637 (2017)

Index Fungorum number: IF 822045; *Facesoffungi number*: FoF 03570

Notes: *Neohelicosporiu*m was introduced by Lu et al. (2018a) with *N. parvisporum* as the type species based on morphological and phylogenetic evidence. Currently, *Neohelicosporium* comprises 35 species (Ma et al., 2025b). Members of *Neohelicosporium* occur in both freshwater and terrestrial habitats across diverse regions, including Australia, Belgium, Brazil, Canada, China, Cuba, Germany, Honduras, India, Indonesia, Japan, New Zealand, Panama, Peru, the Solomon Islands, South Africa, Thailand, Venezuela, and the USA (Ma et al., 2025b). The asexual morph of *Neohelicosporium* is characterized by white, light pink, or pale brown colonies; short and solitary conidiophores that are mostly branched and gregarious; mono- to polyblastic conidiogenous cells; and guttulate, hyaline, helicoid conidia (Ma et al., 2025b). Its sexual morph is depicted by globose to subglobose, spherical or ellipsoidal-ovate, pale brown to yellow or dark brown to black ascomata, 8-spored or 2-4–6-spored, bitunicate asci, and fusiform, hyaline ascospores (Ma et al., 2025b).

Neohelicosporium diaoluoshanense X. Tang, K.D. Hyde & J.C. Kang, sp. nov.; Figure 3.72

Etymology: ‘‘diaoluoshanense” refers to the ‘‘Diaoluoshan National Forest Park” where the holotype was collected.

Holotype: GZAAS 25-0639

Saprobic on submerged decaying wood in a freshwater stream. **Sexual morph**: Undetermined. **Asexual morph**: Hyphomycetous, helicosporous. *Colonies* on natural substrate superficial, effuse, gregarious, with masses of crowded, glistening conidia, white to pale brown. *Mycelium* partly immersed, partly superficial, composed of hyaline to pale brown, branched, septate, guttulate, smooth hyphae. *Conidiophores* macronematous, mononematous, erect, cylindrical, flexuous, branched, septate, pale brown, smooth-walled, thick-walled. *Conidiogenous cells* 11–16.5 × 4–6 μm ($\bar{x}$ = 13 × 4.8 μm, n = 25), holoblastic, monoblastic or polyblastic, integrated, intercalary, cylindrical, with denticles, pale brown, smooth-walled. *Conidia* solitary, pleurogenous, helicoid, dry, tapering towards the rounded ends, developing on tooth-like protrusion, 14.5–18.5 μm diam. and conidial filament 2–3 μm wide ($\bar{x}$ = 16.5 × 2.5 μm, n = 20),

114–121 μm long ($\bar{x}$ = 118 μm, n = 30), tightly coiled up to 31/2 times, becoming loosely coiled when the conidia are young and not becoming loose when mature in water, guttulate, aseptate, hyaline, smooth-walled.

Culture characteristics: Conidia germinated on PDA and produced germ tubes within 8 hrs. Colonies on PDA reached 25 mm diam. after 30 days of incubation at 25℃ and had a circular shape with a flat surface and entire margin. They are pale brown to brown in PDA medium.

Material examined: China, Hainan Province, Wuzhishan City, Diaoluoshan National Forest Park, on decaying wood in freshwater habitat, 24 September 2024, Xia Tang, S29.1 (GZAAS 25-0639, holotype), ex-type living culture GZCC 25-0609.

Notes: *Neohelicosporium diaoluoshanense* is morphologically similar to *N. aurantiellum* (GZAAS 23-0137) in having macronematous, mononematous, erect, cylindrical, flexuous, branched conidiophores, holoblastic, monoblastic or polyblastic, integrated, intercalary, cylindrical, with denticles, pale brown conidiogenous cells, and solitary, pleurogenous, helicoid, dry, guttulate, aseptate, hyaline conidia (Ma et al., 2024). However, *Neohelicosporium diaoluoshanense* differs from *N. aurantiellum* by its smaller conidial diameter (14.5–18.5 μm vs. 19–24 μm) (Ma et al., 2024). Phylogenetically, *N. diaoluoshanense* (GZCC 25-0609), a newly identified species, is closely related to other members of *Neohelicosporium* with 89% ML and 0.95 BYPP support (Figure 3.64), but forms a distinct and independent lineage within *Neohelicosporium*. Therefore, based on combined molecular evidence and morphological characteristics, we introduce *Neohelicosporium diaoluoshanense* as a new species.

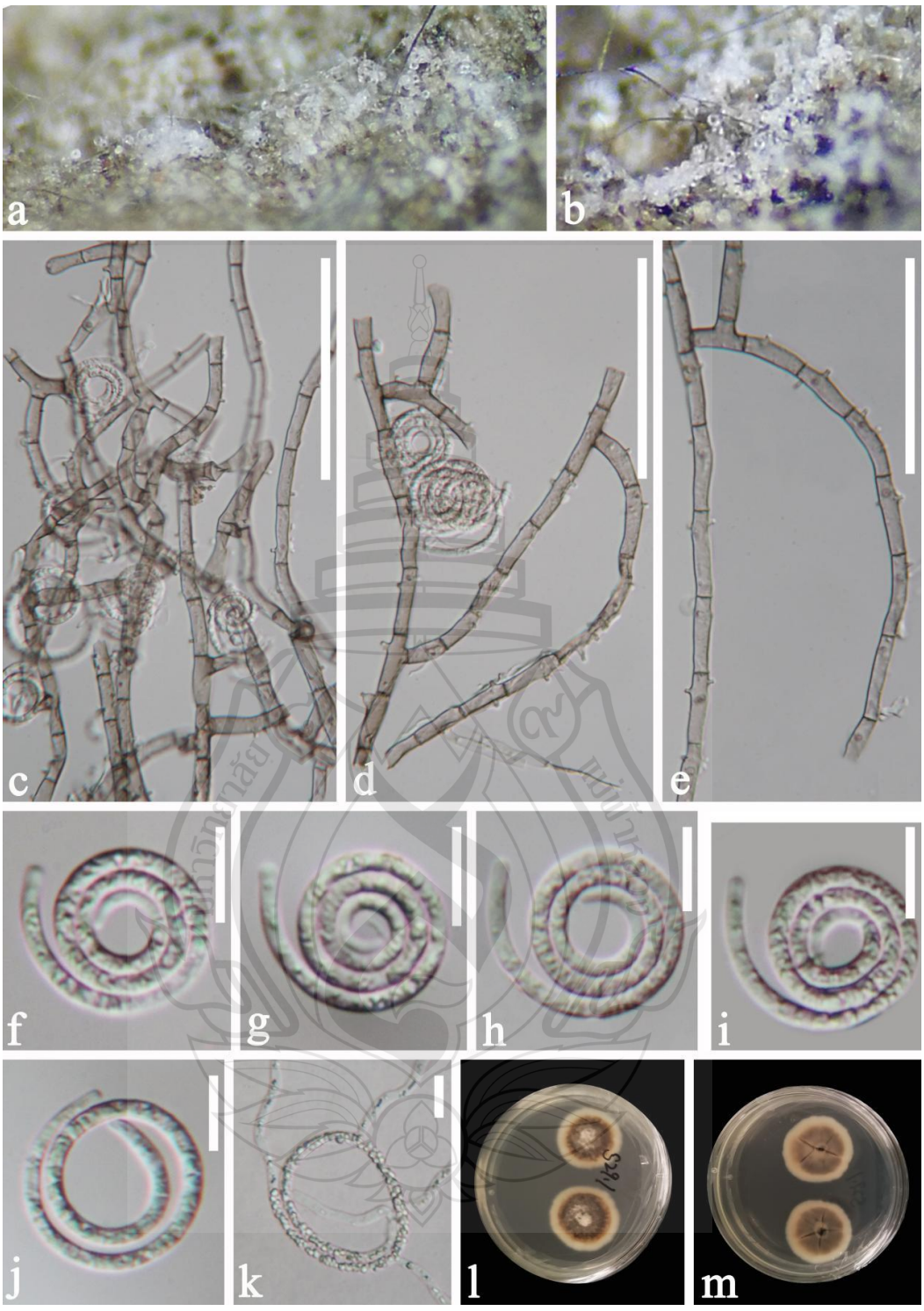

Figure 3.72 *Neohelicosporium diaoluoshanense* (GZAAS 25-0639, holotype)

Figure 3.72 a, b Colonies on submerged decaying wood. c–e Conidiophores and conidia. f–h Conidia. k Germinating conidium. l, m Colonies on PDA from above and below. Scale bars: c–e = 50 µm, f–k = 10 µm.

Neohelicosporium griseum (Berk. & M.A. Curtis) Y.Z. Lu & K.D. Hyde, Fungal Diversity 92: 241 (2018); Figure 3.73

Saprobic on submerged decaying wood of *Camptotheca acuminata* in a freshwater stream. **Sexual morph**: Undetermined. **Asexual morph**: Hyphomycetous, helicosporous. *Colonies* on natural substrate superficial, effuse, gregarious, with masses of crowded, glistening conidia, white to pale brown. *Mycelium* partly immersed, partly superficial, composed of hyaline to pale brown, branched, septate, guttulate, smooth hyphae. *Conidiophores* macronematous, mononematous, erect, cylindrical, flexuous, branched, septate, pale brown, smooth-walled, thick-walled. *Conidiogenous cells* 11–17.5 × 4–5 μm ($\bar{x}$ = 15 × 4.5 μm, n = 25), holoblastic, monoblastic or polyblastic, integrated, terminal or intercalary, cylindrical, with denticles, pale brown, smooth-walled. *Conidia* solitary, acropleurogenous, helicoid, dry, tapering towards the rounded ends, developing on tooth-like protrusion, 16–22.5 μm diam. and conidial filament 2.5–3 μm wide ($\bar{x}$ = 20 × 2.6 μm, n = 20), 115–165 μm long ($\bar{x}$ = 140 μm, n = 30), tightly coiled up to 31/4 times, becoming loosely coiled when the conidia are young and not becoming loose when mature in water, guttulate, aseptate, hyaline, smooth-walled.

Culture characteristics: Conidia germinated on PDA and produced germ tubes within 9 hrs. Colonies on PDA reached 48 mm diam. after 50 days of incubation at 25℃ and had a circular shape with a raised surface and entire margin. They are brown to dark brown in PDA medium.

Material examined: China, Guizhou Province, Tongren City, Jiangkou County, Mamagou, on submerged decaying wood of *Camptotheca acuminata* in a freshwater habitat, 6 December 2024, Xia Tang, JK113 (GZAAS 25-0684), living culture GZCC 25-0654.

Known distribution: Austria, Belgium, Brazil, Britain, Canada, China (Lu et al., 2018b; Ma et al., 2024; this study); Cook Islands (Lu et al., 2018b), Cuba, Czechia, Germany, Italy, Japan, Mexico, Morocco, New Guinea, New Zealand, Panama, Puerto Rico, South Africa, Switzerland, USA.

Known hosts: on submerged decaying wood in a freshwater stream (Ma et al., 2024); on submerged decaying wood of *Camptotheca acuminata* (this study).

Notes: In our phylogenetic tree (Figure 3.64), our isolates (GZCC 25-0654) formed a sister clade to *Neohelicosporium griseum* (CBS 961.69 and GZCC 23-0424) with 94% ML and 1.00 BYPP support. Our new isolate shares the same conidiophores and conidial characteristics with the specimen of *Neohelicosporium griseum* (Ma et al., 2024). Therefore, based on both morphological and molecular data, we identify our new isolate as *Neohelicosporium griseum*. This is the first report of *N. griseum* associated with a *Camptotheca acuminata* from China.

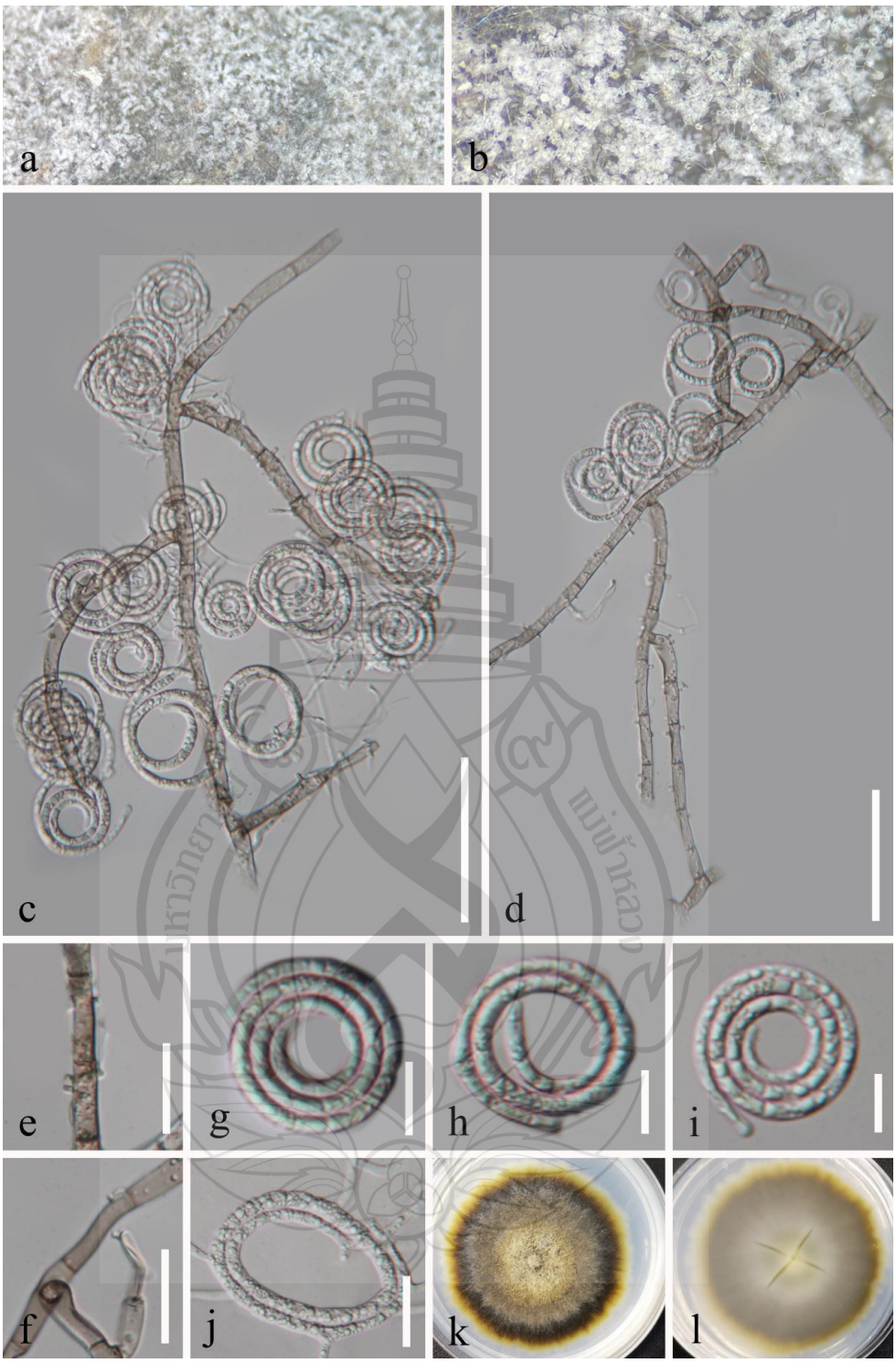

Figure 3.73 *Neohelicosporium griseum* (GZAAS 25-0684, new host record)

Figure 3.73 a, b Colonies on submerged decaying wood. c, d Conidiophores and conidia. e, f Conidiogenous cells. j Germinating conidium. g–i Conidia. k, l Colonies on PDA from above and below. Scale bars: c, d = 50 µm, e, f, j = 20 µm, g–i = 10 µm

Neohelicosporium xianhepingense X. Tang, K.D. Hyde & J.C. Kang, sp. nov.; Figure 3.74

Etymology: ‘‘xianhepingense” refers to the ‘‘Xianheping National Forest Park” where the holotype was collected.

Holotype: GZAAS25-0685

Saprobic on submerged decaying wood in a freshwater stream. **Sexual morph**: Undetermined. **Asexual morph**: Hyphomycetous, helicosporous. *Colonies* on natural substrate superficial, effuse, gregarious, with masses of crowded, glistening conidia, white to pale brown. *Mycelium* partly immersed, partly superficial, composed of hyaline to pale brown, branched, septate, guttulate, smooth hyphae. *Conidiophores* macronematous, mononematous, erect, cylindrical, flexuous, branched, septate, pale brown, smooth-walled, thick-walled. *Conidiogenous cells* 10–13 × 3.5–5 μm ($\bar{x}$ = 12 × 4 μm, n = 25), holoblastic, monoblastic or polyblastic, integrated, terminal or intercalary, cylindrical, with denticles, pale brown, smooth-walled. *Conidia* solitary, acropleurogenous, helicoid, dry, tapering towards the rounded ends, developing on tooth-like protrusion, 17–18.5 μm diam. and conidial filament 2.5–3.5 μm wide ($\bar{x}$ = 18 × 2.2 μm, n = 20), 74.5–101.5 μm long ($\bar{x}$ = 93 μm, n = 30), tightly coiled up to 21/2 times, becoming loosely coiled when the conidia are young and not becoming loose when mature in water, guttulate, aseptate, hyaline, smooth-walled.

Culture characteristics: Conidia germinated on PDA and produced germ tubes within 15 hrs. Colonies on PDA reached 23 mm diam. after 31 days of incubation at 25℃ and had a circular shape with a flat surface and entire margin. They are pale brown to brown in PDA medium.

Material examined: China, Guizhou Province, Qianxinan Buyi and Miao Autonomous Prefecture, Xianheping National Forest Park, 24°97′ N, 105°63′ E, on submerged decaying wood in a freshwater stream, 16 March 2022, Xia Tang, XHP23.6 (GZAAS 25-0685, holotype), ex-type living culture GZCC 25-0655.

Notes: In our phylogenetic tree (Figure 3.64), our isolates (GZCC 25-0655) formed a sister clade to *Neohelicosporium guineensis* (MHZU 23-0153) with 94% ML and 1.00 BYPP support. Our isolates (GZCC 25-0655) can be distinguished from *N. guineensis* (MHZU 23-0153) by its shorter conidiogenous cells (10–13 × 3.5–5 μm vs. up to 20 × 3.5–5.5 μm long). Moreover, base pair comparison of *Neohelicomyces*

xianhepingense and *N. guineensis* shows 10/489 bp differences in ITS (2.0%, gaps 2 bp), and 0/840 bp differences in LSU (0%, without gap). Therefore, based on DNA molecular data and morphological characteristics, we introduce our collection as a novel species, *Neohelicomyces xianhepingense*.

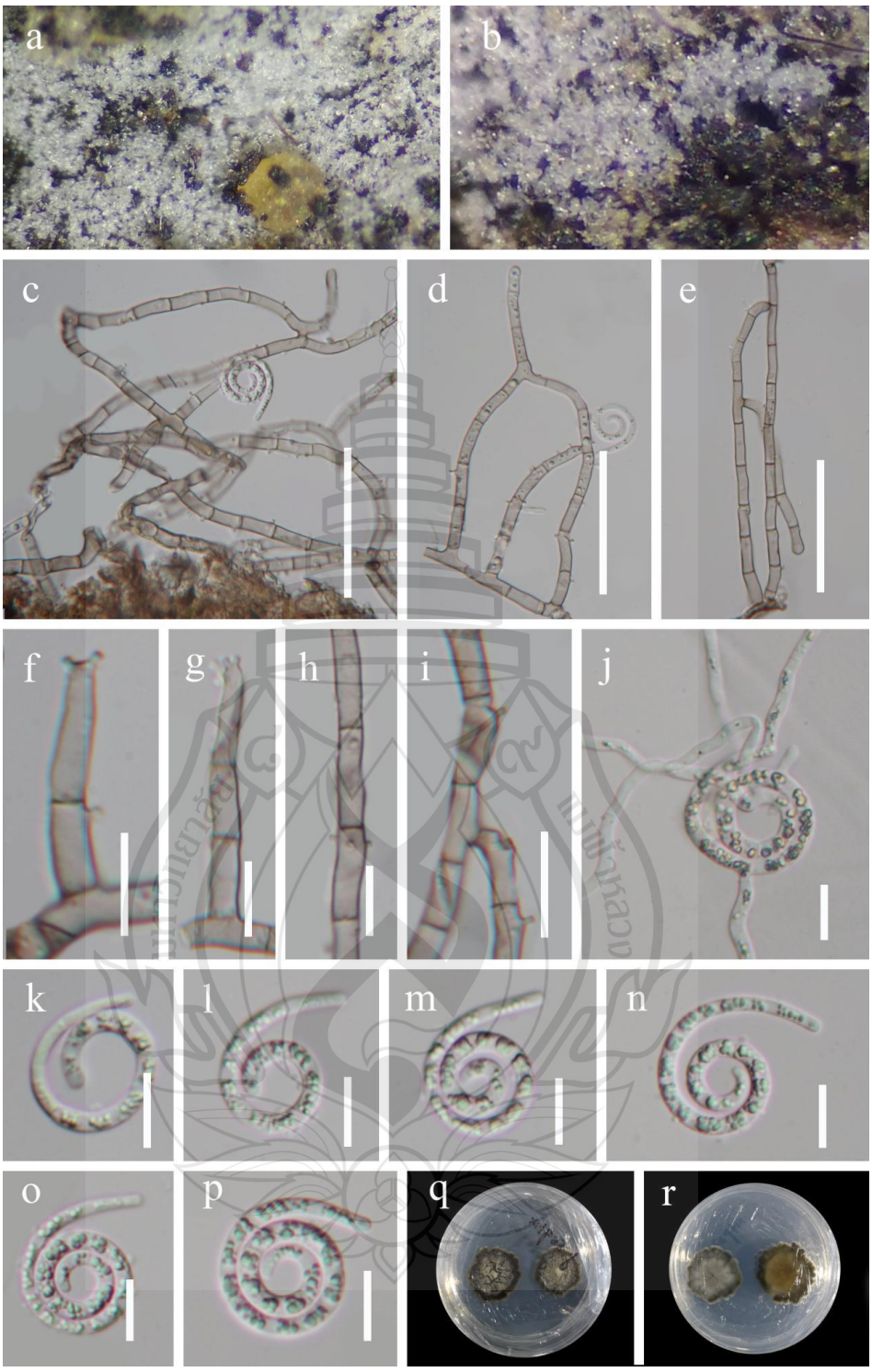

Figure 3.74 *Neohelicosporium xianhepingense* (GZAAS 25-0685, holotype)

Figure 3.74 a, b Colonies on submerged decaying wood. c–e Conidiophores and conidia. f–i Conidiogenous cells. j Germinating conidium. k–p Conidia. q, r Colonies on PDA from above and below. Scale bars: c–e = 50 μm, f–p = 10 μm.

Parahelicomyces Goh, Mycol. Progr. 20 (2): 182 (2021)

Index Fungorum number: IF 837332; *Facesoffungi number*: FoF 12026

Notes: *Parahelicomyces* was introduced by Hsieh et al. (2021) with *Pa. talbotii* as the type species. At present, the genus comprises 13 species (Ma et al., 2024), which are primarily saprobic on woody substrates in both terrestrial and freshwater habitats (Lu et al., 2018b; Ma et al., 2024). The helicosporous asexual morphs of *Parahelicomyces* exhibit considerable morphological diversity: some species produce loosely coiled, elongated conidia with thin filaments, whereas others develop extremely tightly coiled, short conidia with comparatively wider filaments (Lu et al., 2018b; Ma et al., 2024).

Parahelicomyces suae L.L. Li, H.W. Shen & Z.L. Luo, Frontier in Microbiology 13 (no. 1056669): 18 (2022); Figure 3.75

Saprobic on decaying wood in a terrestrial habitat. **Sexual morph**: Undetermined. **Asexual morph**: Hyphomycetous, helicosporous. *Colonies* on natural substrate superficial, effuse, gregarious, with masses of crowded, glistening conidia, white. *Mycelium* partly immersed, partly superficial, composed of hyaline to pale brown, branched, septate, smooth hyphae. *Conidiophores* 80–103 × 4.5–5 μm ($\bar{x}$ = 91 × 4.7 μm, n = 30), macronematous, mononematous, erect, cylindrical, flexuous, widest at the base, tapering toward narrow apex, unbranched, septate, subhyaline to pale brown, thick-walled. *Conidiogenous cells* 10–12 × 3–4.5 μm ($\bar{x}$ = 11 × 4 μm, n = 25), holoblastic, monoblastic or polyblastic, integrated, terminal or intercalary, cylindrical, with denticles, truncate at apex after conidial secession, subhyaline to pale brown, smooth-walled. *Conidia* solitary, acropleurogenous, helicoid, developing on tooth-like protrusion, 14–16 μm diam. and conidial filament 1.7–2 μm wide ($\bar{x}$ = 15 × 1.8 μm, n = 20), 111.5–118 μm long ($\bar{x}$ = 115 μm, n = 30), tightly coiled up to 31/2 times, not becoming loose in water, multi-septate, guttulate, hyaline, smooth-walled.

Culture characteristics: Conidia germinated on PDA and produced germ tubes within 9 hrs. Colonies on PDA reached 25 mm diam. after 42 days of incubation at 25℃ and had a circular shape with a flat surface and entire margin. They are pale brown to dark brown in PDA medium.

Material examined: China, Guizhou Province, Tongren City, Jiangkou County, Mamagou, on decaying wood in a terrestrial habitat, 6 December 2024, Xia

Tang, jk15 (GZAAS 25-0686), ex-type living culture GZCC 25-0656.

Known distribution: China (Li et al., 2022; this study).

Known hosts: on submerged decaying wood in the lake (Li et al., 2022a); on decaying wood in a terrestrial habitat (this study).

Notes: Li et al. (2022a) introduced *Parahelicomyces* suae from submerged decaying wood in a freshwater habitat in China. Our collection (GZCC 25-0656) has similar features with the holotype of *Pa. suae* (HKAS 124604) (Li et al., 2022a). However, our collection (GZCC 25-0656) differs from *Pa. suae* (HKAS 124604) by its shorter conidiophores (80–103 μm vs. 114.8–173.5 μm), and shorter conidiogenous cells (10–12 μm vs. 12–18 μm) (Li et al., 2022a). In our phylogenetic tree (Figure 3.64), our collection (GZCC 25-0656) and *Pa. suae* (CGMCC 3.23534) cluster together, indicating that they belong to the same species. Therefore, we introduce our collection (GZCC 25-0656) as a known species, *Parahelicomyces suae*. This is the first time we report this species in a terrestrial habitat in China.

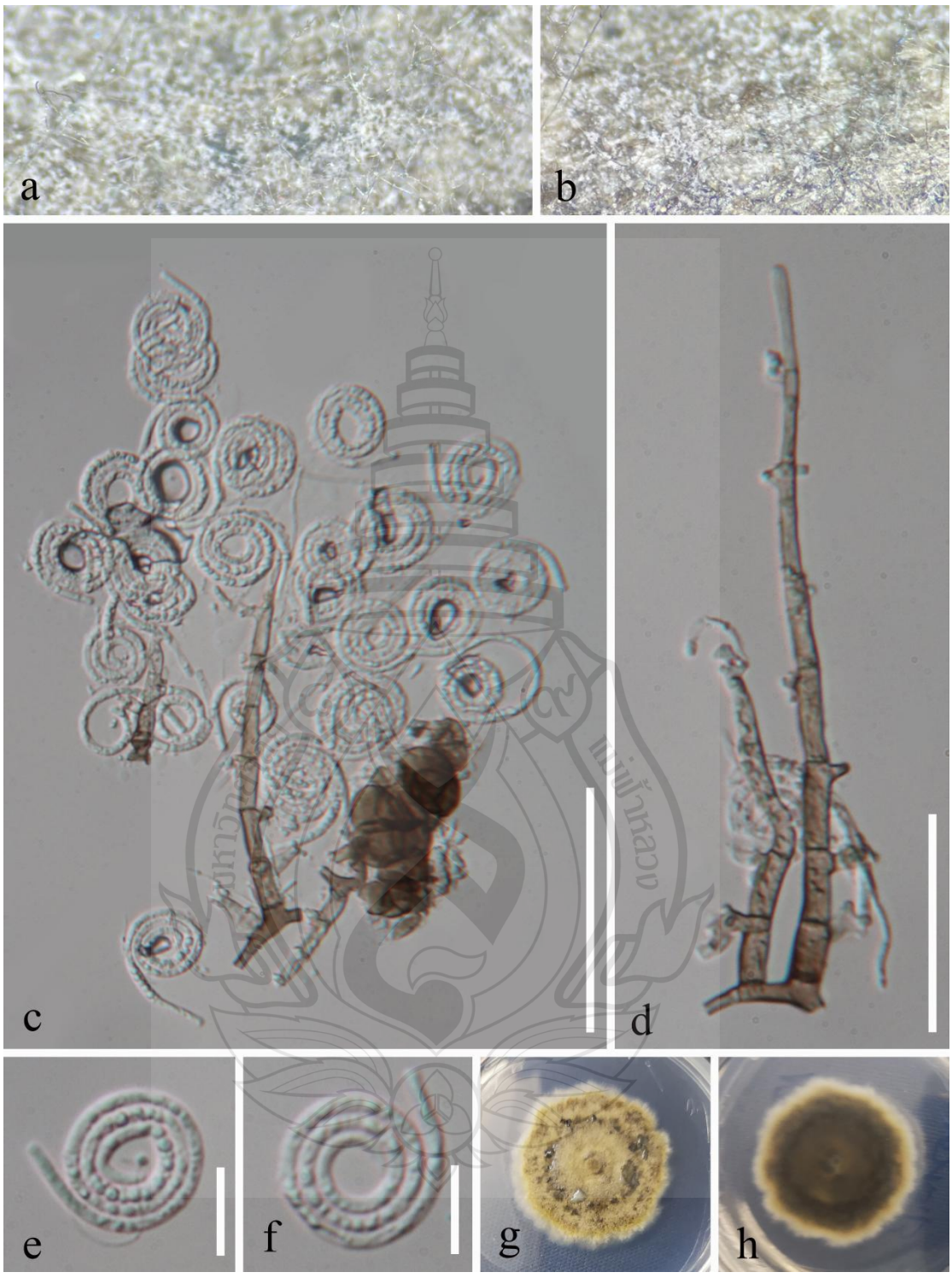

Figure 3.75 *Parahelicomyces suae* (GZAAS 25-0686, new habitat record)

Figure 3.75 a, b Colonies on submerged decaying wood. c, d Conidiophores, conidiogenous cells, and conidia. e, f Conidia. g, h Colonies on PDA from above and below. Scale bars: c = 50 µm, d = 30 µm, e, f = 10 µm.

Pseudotubeufia Jian Ma & Y.Z. Lu, J. Fungi 9 (7, no. 742): 5 (2023)

Index Fungorum number: IF 900553; *Facesoffungi number*: FoF 03700

Notes: *Pseudotubeufia* was introduced by Ma et al. (2023) to accommodate *Ps. hyalospora* and *Ps. laxispora* based on multi-gene phylogenetic analyses and morphological evidence. Currently, *Pseudotubeufia* comprises three species, *Ps. dematiolaxispora*, *Ps. hyalospora*, and *Ps. laxispora*, which were found from freshwater and terrestrial habitat in China (Ma et al., 2024). *Pseudotubeufia* is characterized by macronematous, mononematous, erect or procumbent, flexuous, cylindrical, branched or unbranched, septate conidiophores, holoblastic, mono- to polyblastic, integrated, sympodial, repeatedly geniculate, intercalary or terminal, irregularly cylindrical, denticulate, hyaline to pale brown conidiogenous cells, solitary, acropleurogenous, helicoid, rounded guttulate, hyaline conidia (Ma et al., 2023).

Pseudotubeufia laxispora Jian Ma & Y.Z. Lu, J. Fungi 9 (7, no. 742): 8 (2023); Figure 3.76

Saprobic on decaying wood in a terrestrial habitat. **Sexual morph**: Undetermined. **Asexual morph**: Hyphomycetous, helicosporous. *Colonies* on natural substrate superficial, effuse, gregarious, with a little of crowded, glistening conidia, white to pale brown. *Mycelium* partly immersed, partly superficial, composed of hyaline to pale brown, branched, septate, guttulate, smooth hyphae. *Conidiophores* 30–44 × 4.5–5.5 μm ($\bar{x}$ = 37 × 5 μm, n = 30), macronematous, mononematous, erect, cylindrical, straight or slightly flexuous, unbranched, septate, hyaline to brown, thick-walled. *Conidiogenous cells* 12–21 × 4–5 μm ($\bar{x}$ = 16.5 × 4.5 μm, n = 25), holoblastic, monoblastic or polyblastic, integrated, terminal, cylindrical, truncate at apex after conidial secession, pale brown, smooth-walled. *Conidia* solitary, acrogenous, helicoid, 47–54 μm diam. and conidial filament 4.5–5.5 μm wide ($\bar{x}$ = 50 × 5 μm, n = 20), 261–265.5μm long ($\bar{x}$ = 263.5 μm, n = 30), tightly coiled up to 21/2 times, becoming loosely coiled when the conidia are young and not becoming loose in water, multi-septate, slightly constricted at septa, guttulate, hyaline, smooth-walled.

Culture characteristics: Conidia germinated on PDA and produced germ tubes within 11 hrs. Colonies on PDA reached 31 mm diam. after 40 days of incubation at 25°C and had a circular shape with a flat surface and entire margin. They are pale brown to brown in PDA medium.

Material examined: China, Guizhou Province, Tongren City, Jiangkou County, Mamagou, on decaying wood in a terrestrial habitat, 6 December 2024, Xia Tang, jk2 (GZAAS 25-0687), living culture GZCC 25-0657.

Known distribution: China (Ma et al., 2023; this study).

Known hosts: on dead bamboo culms in a freshwater stream (Ma et al., 2023); on decaying wood in a terrestrial habitat (Ma et al., 2023; this study).

Notes: In the phylogenetic tree (Figure 3.64), our collection (GZCC 25-0657) formed a sister clade to *Pseudotubeufia laxispora* (GZCC 22-2011 and GZCC 22-2012) with 85% ML support, indicating that they belong to the same species. Our new isolate shares the same conidiophores and conidial characteristics with the specimen of *Ps. laxispora* (HKAS 125868) (Ma et al., 2023). Therefore, based on both morphological and molecular data, we identify our new isolate as a known species, *Pseudotubeufia laxispora*.

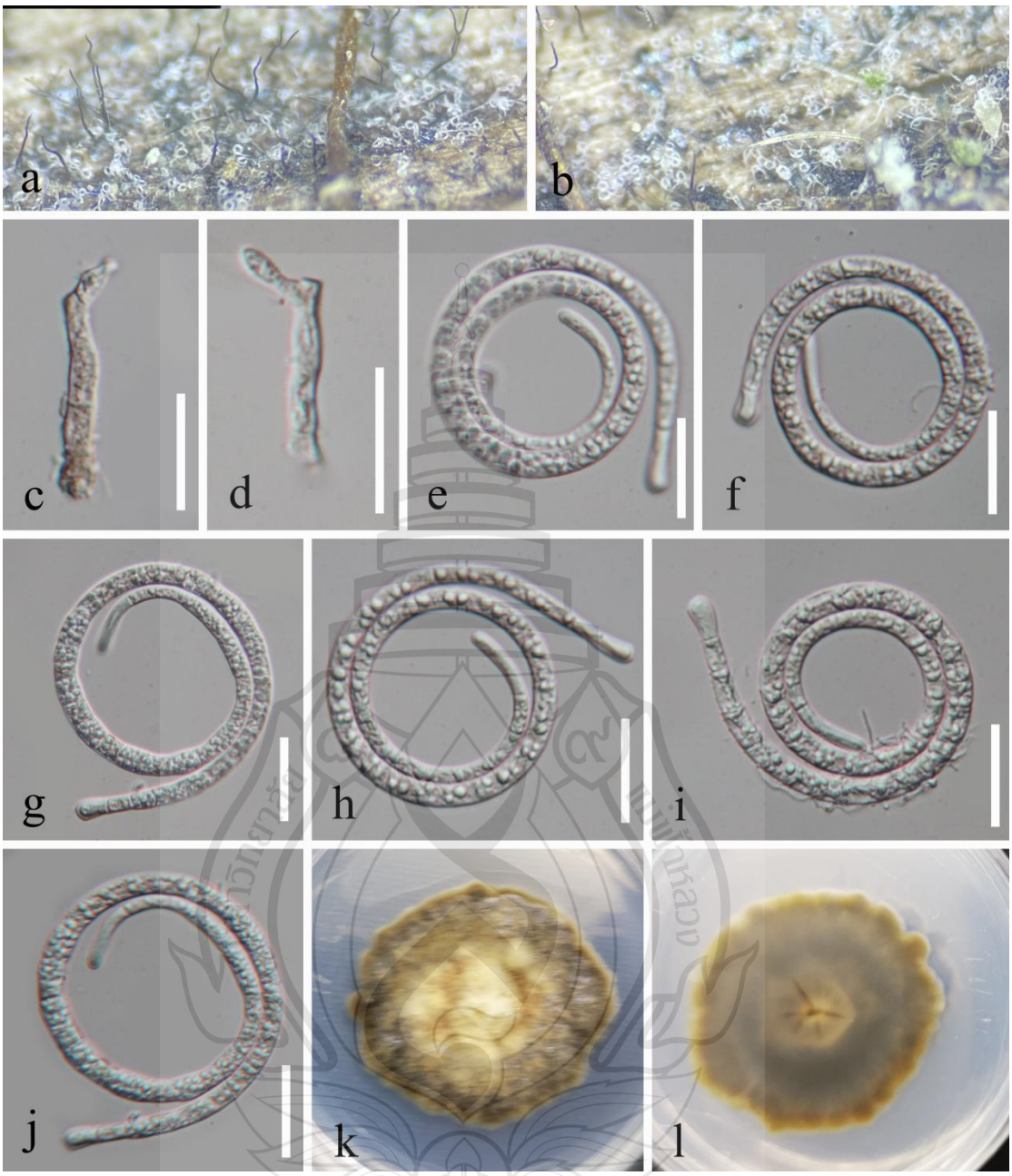

Figure 3.76 *Pseudotubeufia laxispora* (GZAAS 25-0687, new collection)

Figure 3.76 a, b Colonies on submerged decaying wood. c, d Conidiophores and conidiogenous cells. e–j Conidia. k, l Colonies on PDA from above and below. Scale bars: c–j = 20 µm.

Thaxteriellopsis Sivan., Panwar & S.J. Kaur, Kavaka 4: 39 (1976)

Index Fungorum number: IF 5409; *Facesoffungi number*: FoF 01866

Notes: *Thaxteriellopsis* was introduced by Sivanesan et al. (1976) with *T. lignicola* as the type species. Currently, *Thaxteriellopsis* comprises two species: *T. lignicola* and *T. obliqua*, found from freshwater and terrestrial habitats (Ma et al., 2024). Thaxteriellopsis is characterized by macronematous, mononematous, erect, cylindrical, branched or unbranched, septate, pale brown to dark brown conidiophores, holoblastic, mono- to poly-blastic, integrated, sympodial, intercalary or terminal, cylindrical conidiogenous cells, and solitary, acropleurogenous, helicoid, multi-septate, and hyaline conidia that taper towards the apex, usually rounded at the tips (Ma et al., 2024).

Thaxteriellopsis lignicola Sivan., Panwar & S.J. Kaur, Kavaka 4: 39 (1976); Figure 3.77

Saprobic on decaying wood in a terrestrial habitat. **Sexual morph**: Undetermined. **Asexual morph**: Hyphomycetous, helicosporous. *Conidiophores* 243–308 µm long, 6.5–7.5 µm wide, micronematous, mononematous, erect, cylindrical, arising as lateral branches from creeping hyphae, branched or unbranched, septate, slightly constricted at septa to give a monilioid appearance, the lower part brown and the upper part pale brown, smooth-walled. *Conidiogenous cells* 6–12.5 µm long, 4–5 µm wide, holoblastic, mono- to polyblastic, integrated, sympodial, terminal, cylindrical, pale brown, smooth-walled. *Conidia* solitary, acropleurogenous, helicoid, solitary, 14–15 µm diam. and conidial filament 4.5–7 µm wide in the broadest part, 16–17 µm long ($\bar{x}$ = 16.5 µm, n = 30), tightly coiled up to 11/2 times, not becoming loose in water, rounded at tip, up to 5-septate, guttulate, hyaline, smooth-walled.

Culture characteristics: Conidia germinated on PDA and produced germ tubes within 11 hrs. Colonies on PDA reached 31 mm diam. after 40 days of incubation at 25°C and had a circular shape with a flat surface and entire margin. They are pale brown to brown in PDA medium.

Material examined: China, Guizhou Province, Tongren City, Jiangkou County, Mamagou, on decaying wood in a terrestrial habitat, 6 December 2024, Xia Tang, GX2 (GZAAS 25-0688), living culture GZCC 25-0658.

Known distribution: China (this study); India (Sivanesan et al., 1976); Thailand (Boonmee et al., 2011; Doilom et al., 2017; Lu et al., 2018b).

Known hosts: on dead wood of *Lingo emortuo* (Sivanesan et al., 1976); on dead wood of *Zizyphus mauritiana* (Boonmee et al., 2011); on decaying wood of unidentified trees (Boonmee et al., 2011, this study); on dried bark of unidentified trees (Boonmee et al., 2011); on decaying inner-surface of bark of *Tectona grandis* (Doilom et al., 2017); on decaying wood in a freshwater stream (Lu et al., 2018b).

Notes: In our phylogenetic tree (Figure 3.64), our isolates (GZCC 25-0658) formed a sister clade to *Thaxteriellopsis lignicola* (MFLUCC 10-0121 and MFLUCC 10-0122) with 97% ML and 1.00 BYPP support, indicating that they belong to the same species. Our new isolate shares the same conidial features with the species *T. lignicola* (Boonmee et al., 2011; Doilom et al., 2017; Lu et al., 2018b). Thus, we identify our isolates as a known species, *T. lignicola*. This is the first time we report this species in a terrestrial habitat in China.

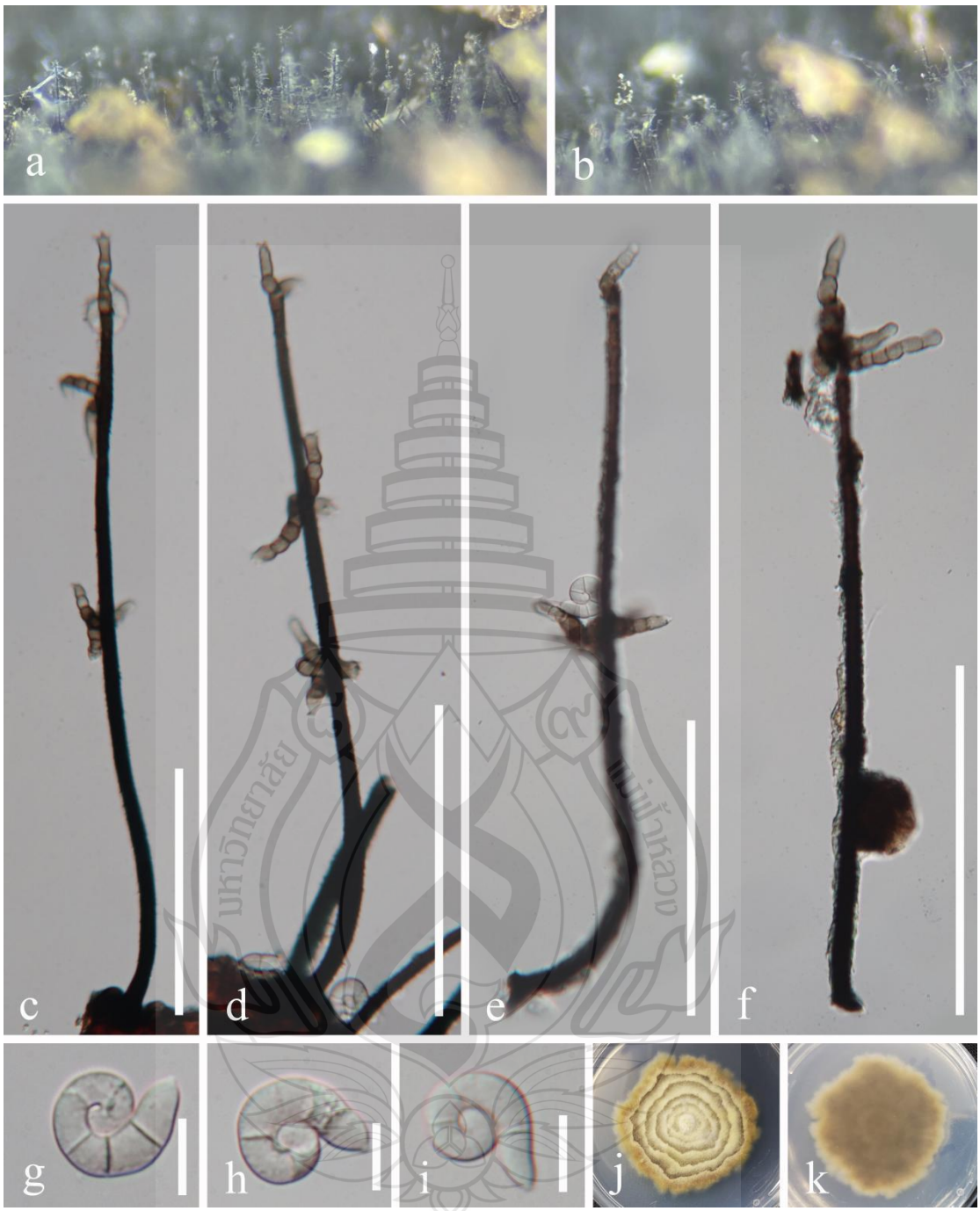

Figure 3.77 *Thaxteriellopsis lignicola* (GZAAS 25-0688, new geographical record)

Figure 3.77 a, b Colonies on submerged decaying wood. c–f Conidiophores and conidiogenous cells. g–i Conidia. j, k Colonies on PDA from above and below. Scale bars: c–f = 100 µm, g–i = 10 µm.

Tubeufia Penz. & Sacc., Malpighia 11: 517 (1898)

Index Fungorum number: IF 5635; *Facesoffungi number*: FoF 00063

Notes: *Tubeufia* was established by Penzig (1897) with *T. javanica* as the type species. At present, the genus comprises 88 species, including 29 from freshwater habitats, 44 from terrestrial habitats, and 15 occurring in both (Ma et al., 2025c). These species are typically saprobic on dead wood in freshwater and terrestrial environments and have been reported from diverse regions worldwide, such as Austria, Bermuda, Brazil, Canada, China, Colombia, Cuba, India, New Zealand, Panama, Peru, South Africa, Sri Lanka, Tanzania, Thailand, Trinidad, Uganda, Venezuela, and the USA (Ma et al., 2025c). Notably, the asexual morph of *Tubeufia* is regarded as the most morphologically diverse among helicosporous hyphomycetes (Ma et al., 2025c).

Tubeufia nigroseptum H.W. Shen, L.L. Li, H.Y. Su & Z.L. Luo (2022); Figure 3.78

Saprobic on submerged decaying wood in a freshwater stream. **Sexual morph**: Undetermined. **Asexual morph**: Hyphomycetous, helicosporous. *Colonies* on natural substrate superficial, effuse, gregarious, with masses of crowded conidia, pale brown to brown. *Mycelium* partly immersed, partly superficial, composed of pale brown to brown, branched, septate, smooth hyphae. *Conidiophores* 15–33 × 5–6.5 µm ($\bar{x}$ = 27 × 5.5 µm, n = 20), macronematous, mononematous, erect, cylindrical, straight or flexuous, unbranched, septate, pale brown to brown, thick-walled. Conidiogenous cells 11.5–13.5 × 4.5–5 µm ($\bar{x}$ = 12.5 × 4.8 µm, n = 25), holoblastic, monoblastic, integrated, terminal, cylindrical, truncate at apex after conidial secession, pale brown to brown, smooth-walled. *Conidia* solitary, acrogenous, helicoid, tapering towards the rounded ends, 35–40.5 µm diam. and conidial filament 5.5–7.5 µm wide ($\bar{x}$ = 37.5 × 6.5 µm, n = 20), 167.5–198.5 µm long ($\bar{x}$ = 184.5 µm, n = 30), tightly coiled up to 3 times, not becoming loose in water, septate, slightly constricted at septa, verrucose, guttulate, subhyaline when young, pale brown to brown when aged, smooth-walled.

Culture characteristics: Conidia germinating on PDA and producing germ tubes within 14 hrs. Colonies on PDA reaching 28 mm diam. after 28 days of incubation at 25°C and had a circular shape with a raised surface and entire margin, pale brown to brown in PDA medium.

Material examined: China, Guizhou Province, Tongren City, Jiangkou County, Mamagou, on decaying wood in a terrestrial habitat, 6 December 2024, Xia Tang, GF37 (GZAAS 25-0689), living culture GZCC 25-0659.

Known distribution: China (Li et al., 2022b; this study).

Known hosts: on submerged decaying wood (Li et al., 2022b); on decaying wood in a terrestrial habitat (this study).

Notes: *Tubeufia nigroseptum* was originally described by Li et al. (2022b) from submerged decaying wood in a freshwater stream in Yunnan, China. In our phylogenetic analyses, the newly obtained strains (GZCC 25-0659) clustered with the ex-type strain of *T. nigroseptum* (CGMCC 3.20430) with 100% ML bootstrap support and 1.00 Bayesian posterior probability (Figure 3.64), indicating that they belong to the same species. Morphologically, the new isolates were indistinguishable from the holotype of *T. nigroseptum* (HKAS 115528). Therefore, based on both molecular and morphological evidence, we identify these three strains (GZCC 25-0659) as a same species of *Tubeufia nigroseptum*. For our collection, this represents the first record of *T. nigroseptum* from a terrestrial habitat in China.

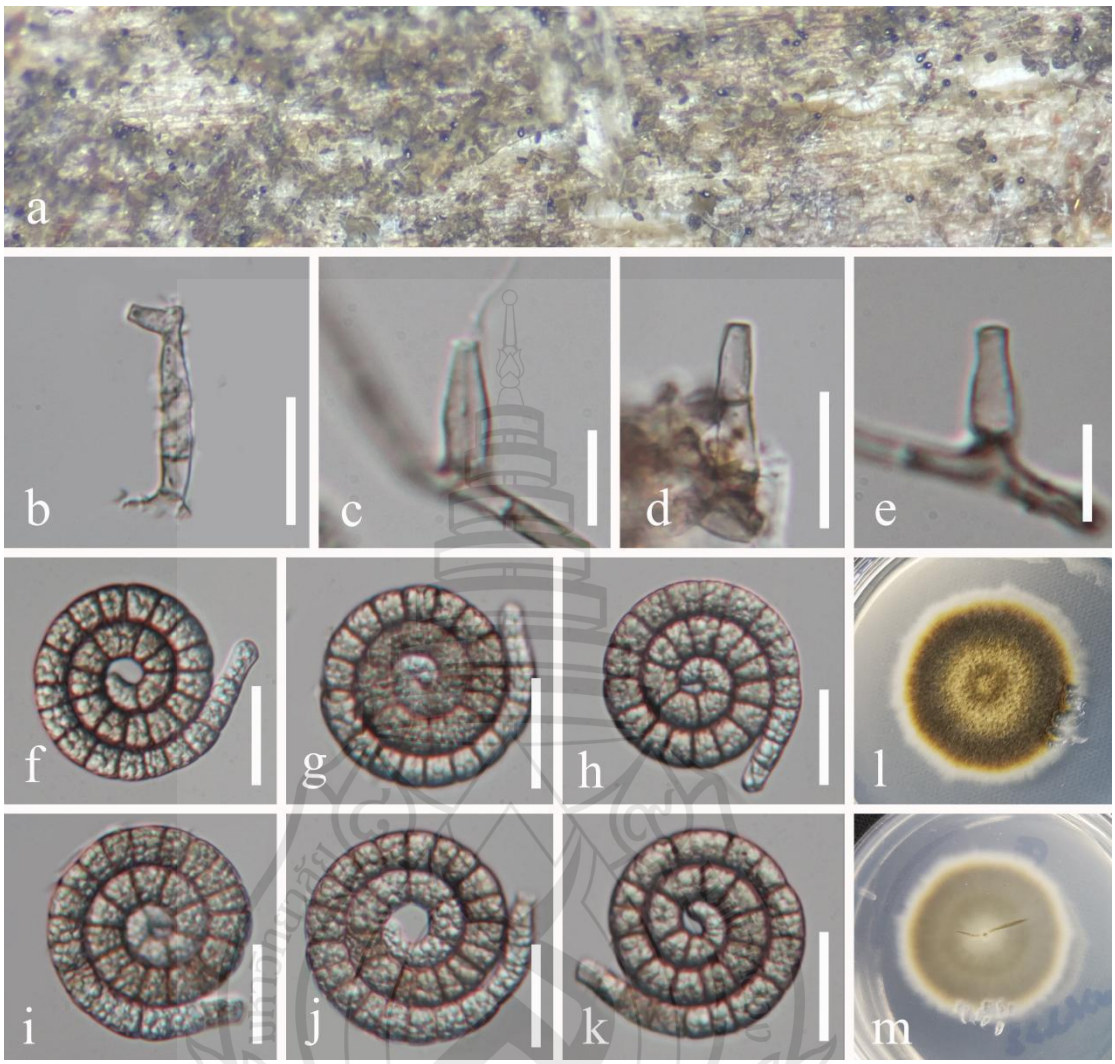

Figure 3.78 *Tubeufia nigroseptum* (GZAAS 25-0689, new habitat record)

Figure 3.78 a Colonies on submerged decaying wood. b–e Conidiophores and conidiogenous cells. f–k Conidia. l, m Colonies on PDA from above and below. Scale bars: b, d, f–k = 20 µm, c, e = 10 µm.

Pleosporales *genera incertae sedis* Luttr. ex M.E. Barr, Prodromus to class Loculoascomycetes: 67 (1987)

Asteromassaria Höhn., Sitzungsber. Kaiserl. Akad. Wiss., Wien. Math.-Naturwiss. Cl., Abt. 1 126: 368 (1917)

Index Fungorum number: IF 422; *Facesoffungi number*: FoF 06604

Notes: *Asteromassaria* was introduced by Höhnel (1917) and is typifies by *Asteromassaria macrospora* (= *Sphaeria macrospora* Desm.). The genus was initially accommodated in *Pleomassariaceae* by Lumbsch and Huhndorf (2010). It was then transferred to *Morosphaeriaceae* by Zhang et al. (2012). However, the genus was finally moved to *Dothideomycetes* genera incertae sedis based on morphology (Hyde et al., 2013; Kirk et al., 2013; Wijayawardene et al., 2014, 2018). Pem et al., (2019) re-examined the holotype specimen of *Asteromassaria macrospora* and concluded that the taxon was distinct from *Pleomassariaceae* based on morphology. Molecular data are currently lacking for the type species. DNA sequence data are available for *Asteromassaria berberidicola* (ITS), and *Asteromassaria pulchra* (SSU, LSU, *tef-α*, *rpb2*). Interestingly, these two taxa do not cluster together in the phylogenetic tree (Figure 3.2.72). *Asteromassaria berberidicola* CBS 125282 clusters with *Splanchnonema pupula* MFU 14-0807, while *Asteromassaria pulchra* forms a distinct lineage, basal to *Morosphaeriaceae* (Figure 3.2.72). Until sequence data for the type species is obtained, we retain *Asteromassaria* as incertae sedis in *Massarineae* (*Pleosporales*).

Most taxa of *Asteromassaria* have been described in their sexual morph. They are characterised by solitary, immersed to erumpent, depressed globose or subglobose, ostiolate ascomata. The pseudoparaphyses are cellular, filiform, septate. Asci are 8-spored, broadly cylindrical to broadly cylindro-clavate, short-pedicellate and apically rounded with a small ocular chamber. Ascospores are hyaline, 1-(eu)septate, constricted at the septum, with smooth or verrucose wall, and usually without any mucilaginous sheath (Pem et al., 2019). *Scolicosporium macrosporium* has been reported as the asexual state of *Asteromassaria macrospora* due to their occurrence on the same host; however, this has yet to be proven by molecular data (Spooner & Kirk, 1982; Sivanesan, 1984; Pem et al., 2019). *Asteromassaria* species are saprobic, foliicolous, or associated with blighted plant substrates in the terrestrial habitat (Mehrotra & Sivanesan, 1989; Tanaka et al., 2005; Pem et al., 2019). There are currently eleven species in the genus (Species Fungorum, 2025).

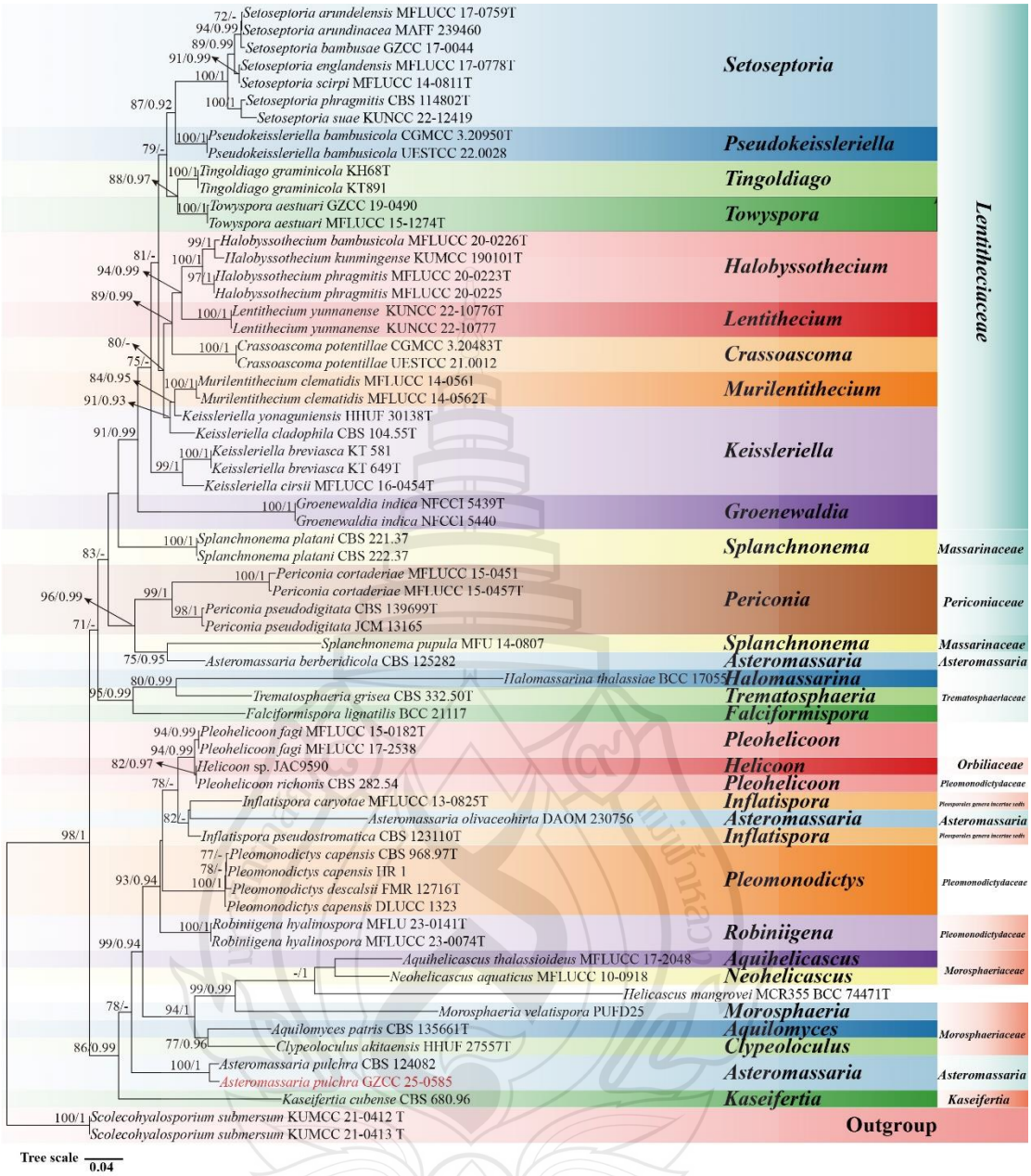

Figure 3.79 Phylogenetic analysis of *Asteromassaria*

Figure 3.79 Phylogenetic analysis of *Asteromassaria* was conducted using RAxML-based maximum likelihood analysis of a combined LSU and ITS sequence dataset. Bootstrap support values for maximum likelihood (ML) equal to or greater than 70% and Bayesian posterior probabilities (PP) equal to or greater than 0.95 are shown above the nodes. The tree is rooted with *Scolecohyalosporium submersum* (KUMCC 21 0412 and KUMCC 21 0413). Newly generated strains are highlighted in red, and type strains are indicated with a superscript 'T'.

Asteromassaria pulchra (Harkn.) Shoemaker & P.M. LeClair, Canad. J. Bot. 53 (15): 1588 (1975) Figure 3.80

= *Massaria pulchra* Harkness, Bull. Calif. Acad. Sci. l(1): 44. 1884.

Saprobic on unidentified decaying wood in the forest. **Sexual morph**: *Ascomata* 568–1062 ×353–1000 µm ($\bar{x}$ = 796 × 672 µm, n = 20), perithecial, erumpent, immersed, scattered to gregarious, coriaceous, globose to subglobose, uniloculate to multiloculate, centrally ostiolate, with a minute papilla, dark brown to black. Ostioles central, papillate, with a short canal. *Peridium* 29–95.5 µm ($\bar{x}$ = 56.8, n = 20) composed two layers, outer layers of thin, dark brown, inner layer of thick-walled, brown, composed of textura angularis cells. *Hamathecium* consisting of cylindrical, unbranched, smooth, hyaline, septate, straight to flexuous, slightly constricted at the septa, tapering toward the apex, exceeding the asci, *pseudoparaphyses* with anastomosing hyphae 2–3 µm ($\bar{x}$ = 2.6, n = 25) wide. *Asci* 89–393 × 29.5–76 µm ($\bar{x}$ = 295.5 × 64 µm, n = 10), 8-spored, bitunicate, fissitunicate, cylindrical to clavate, short-pedicellate, apically rounded with an indistinct ocular chamber. *Ascospores* 70–99 × 22–33 µm ($\bar{x}$ = 84.5 × 27.4 µm, n = 30), biseriate, ellipsoidal to fusiform to slightly reniform, 2-celled, hyaline, smooth-and thick walled, 1-septate, slightly constricted at the septa, sometimes strongly constricted, straight to slightly curved, both ends rounded, guttulate, each cell containing one to two large guttulate, surrounded by a prominent mucilaginous sheath.

Culture characteristics: Colonies on PDA at 25°C germinate from both end of ascospores, circular, crateriform, with undulate margins; mycelium compact in the center, becoming progressively looser towards the margin, thick, floccose to cottony, and soft in texture. The colony surface is centrally dark grey to blackish, outer region greyish white, with faint concentric zonation; The colony reverse is centrally dark brown to black, surrounded by a distinct pale brown marginal zone, with sharp color contrast.

Material examined: China, Guizhou province, Liupanshui City, Yushe National Forest Park, on unidentified decaying wood, 27 November 2024, Xia Tang, LS197 (GZAAS25-0615), holotype, ex-type living culture (GZCC 25-0585).

Known distribution: British (Tanaka et al., 2005); China (this study); Columbia (Tanaka et al., 2005); Canada (Tanaka et al., 2005); Japan (Tanaka et al.,

2005); USA (Tanaka et al., 2005).

Known hosts: *Acer* sp. (Tanaka et al., 2005); *Arbutus* sp. (Tanaka et al., 2005); *Holodiscus* sp. (Tanaka et al., 2005); on vines of *Berchemia racemosa* (Tanaka et al., 2005); on unidentified decaying wood (this study); *Quercus* sp. (Tanaka et al., 2005); *Salix* sp. (Tanaka et al., 2005); *Umbellularia californica* (Harkness et al., 1884).

Notes: Morphologically, our collection share the character with *Asteromassaria pulchra*, such as perithecial, globose to subglobose, uniloculate to multiloculate ascomata with centrally ostiolate; 8-spored, bitunicate, fissitunicate, cylindrical to clavate, short-pedicellate asci with an indistinct ocular chamber and biseriate, ellipsoidal to fusiform, 2-celled, hyaline, 1-septate, slightly constricted at the septa, sometimes strongly constricted, guttulate ascospores with each cell containing one to two large guttulate, surrounded by a prominent mucilaginous sheath.

In the phylogenetic analyses, our collection clusters with *Asteromassaria pulchra* (CBS 124082) (Figure 3.79) with support of 100% ML and 1.00 BYPP. Comparation of nucleotide sequence indicated that there is 0.5% (4/805) bp differences in LSU. Based on them resemble morphological character and phylogenetic analysis, we therefore identify our isolate as a known species, *Asteromassaria pulchra* following the guidelines of Jeewon and Hyde (2016) and Maharachchikumbura et al., (2021). *Asteromassaria pulchra*, originally recombined from *Massaria pulchra* Harkn. by Shoemaker and LeClair (1975), has since been documented in several countries and on diverse hosts, primarily through morphological observations (Harkness et al., 1884; Shoemaker & LeClair, 1975; Tanaka et al., 2005). Herein, we present the first record of *A. pulchra* in China, integrating detailed morphological characterization with robust phylogenetic analyses. This study not only provides novel sequence data but also significantly extends the known geographical distribution and enriches current understanding of the species' taxonomy and evolutionary relationships.

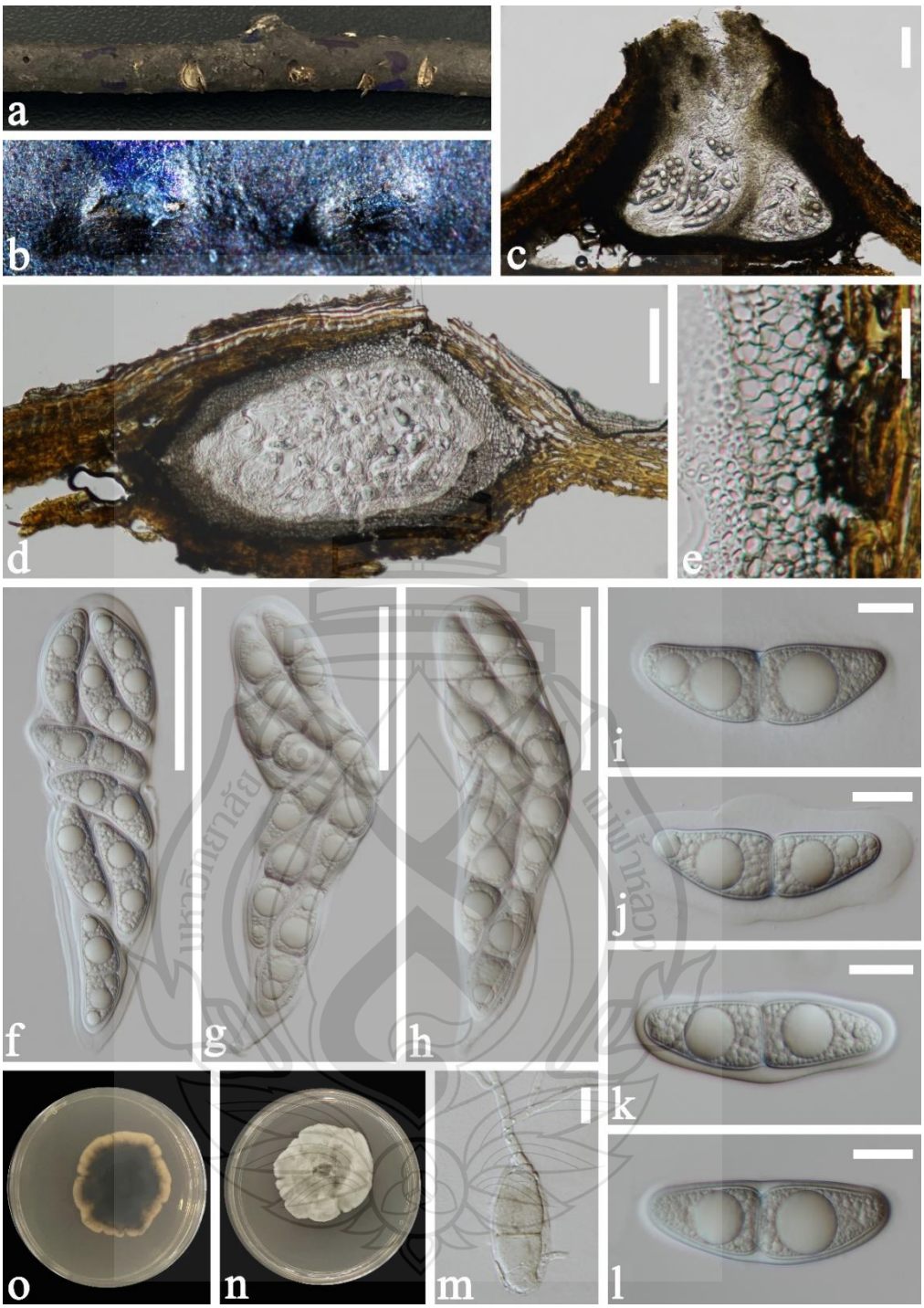

Figure 3.80 *Asteromassaria pulchra* (GZAAS25-0615, new geographical record)

Figure 3.80 a Host. b Appearance of ascomata on host substrate. c, d Section of an ascoma. e Peridium. f–h Asci in different stage. i–l Ascospores. m Germinated ascospore. n Colony on PDA (from front). o Colony on PDA (from reverse). Scale bars: c, d f–h = 100 µm, g–o = 20 µm.

3.3 Conclusion

The results of this chapter indicate that forest deadwood represents an important ecological niche for fungal diversity. From samples collected at ten sites across four provinces (Guizhou, Guangxi, Hainan and Yunnan), we described 55 taxa based on detailed morphological observations, illustrations and multi-gene phylogenetic analyses. These species belong to the classes Sordariomycetes and Dothideomycetes and include several novel taxa and new regional records, indicating that the taxonomic diversity of deadwood-inhabiting fungi in these regions remains far from fully documented. Within Sordariomycetes, four new species, *Arthrinium bambusicola*, *Cordana guizhouensis*, *C. liupanshuiensis* and *Sporidesmiella subellipsoidispora* were recovered, distributed in *Amphisphaeriales*, *Cordanales* and *Diaporthomycetidae families incertae sedis*, and assigned to the families *Apiosporaceae*, *Cordanacea*e and *Junewangiaceae*. *Dothideomycetes* comprised 23 new species, *Anteaglonium xingyiensis*, *Astrosphaeriella kangiana*, *Byssosphaeria guizhouensis*, *Hydellum hyalinum*, *Kirschsteiniothelia bulbosapicalis*, *K. dendryphioides*, *K. longirostrata, K. a mucilaginispora, K. subtruncatispora, Megacapitula guizhouensis, Neopleopunctum hydeanum, N. murisporum, Neohelicomyces congjiangensis, Ne. liuzhouensis, Neo. diaoluoshanense, Neo. xianhepingense, Pleocatenata chinensis, Polyplosphaeria guizhouensis, Po. hainanensis, Pseudotetraploa yunnanensis, Saprosporodochifer verrucosus, Tetraploa hainanensis, Te. Verrucosa*; two new genera, *Hydellum* and *Neohelicomyces*; 11 newly collected known species *Lophium arboricola, Astrosphaeriella roseobrunnea, Hermatomyces sphaericus, Helminthosporium velutinum, Lophiotrema hydei, L. neohysterioides, Pseudotubeufia laxispora, Roussoella bambusarum, Torula fici, T. mackenziei* and *Xylomyces chlamydosporu*; and 17 new host/ habit/ geographical records, *Acanthostigmina multiseptatum, Asteromassaria pulchra, Aquaphila albicans, Berkleasmium hydei, Camposporium lycopodiellae, Dictyosporium digitatum, D. tratense, Helicoma hydei, H. rugosa, Neopodoconis thailandica, Neohelicosporium griseum, Polyplosphaeria appendiculata, Parahelicomyces suae , Tetraploa aquatica, Thaxteriellopsis lignicola, Trichobotrys yunjushanensis accommodated* and *Tubeufia nigroseptum* in six orders *(Coniosporiales,*

Jahnulales, Kirschsteiniotheliales, Mytilinidiales, Pleosporales and Tubeufiales), 19 families (Aliquandostipitaceae, Anteagloniaceae, Astrosphaeriellaceae, *Coniosporiaceae*, *Dictyosporiaceae*, *Hermatomycetaceae*, *Kirschsteiniotheliaceae*, *Lophiotremataceae*, *Massarinaceae*, *Megacapitulaceae*, *Mytilinidiaceae*, *Melanommataceae*, *Pleosporaceae*, *Roussoellaceae*, *Pseudomassarinaceae*, *Sporormiaceae*, *Tetraplosphaeriaceae*, *Torulaceae* and *Tubeufiaceae*) and 33 genera. Notably, approximately 82% of all 55 taxa belong to Pleosporales and about 84% are asexual hyphomycetous fungi, with only eight taxa exhibiting sexual morphs. This pattern is consistent with previous findings that fungal communities on decaying wood are dominated by *Dothideomycetes*, particularly *Pleosporales*, and frequently occur in their asexual states. It also suggests that traditional taxonomy and sampling strategies focusing primarily on sexual morphs may underestimate both the true diversity and the functional importance of asexual fungi in forest wood decomposition. Through systematic sampling and multi-gene phylogenetic analyses, this study not only enriches the species inventory of deadwood-associated fungi, but also provides new data for understanding their ecological roles in the decomposition of woody debris and their phylogenetic placements, thereby underscoring the importance of continued investigations on fungal diversity and novel taxa in deadwood microhabitats.

CHAPTER 4

MICROFUNGI ASSOCIATED WITH *THVMELAEACEAE*

4.1 Endophytic Fungi Associated with *Thymelaeaceae*

4.1.1 Introduction

Fungal endophytes have been found in every plant species that have been examined so far, and they appear to be important. Endophytes are underappreciated in tropical forest trees, where they are thought to be the most common and varied. Several recent quantitative surveys of angiosperms have documented remarkable endophyte richness in individual leaves and trees (Lodge et al., 1996; Arnold et al., 2000; Froehlich & Petrini, 2000; Gamboa & Bayman, 2001). Saikkonen et al. (1998) reviewed multiple studies showing that individual temperate plants can harbor dozens of endophyte species. Endophytes, according to this research, may have a key impact on fungal diversity. Previous studies have documented endophytic fungi in tropical plants representing the families *Arecaceae* (Rodrigues & Samuels, 1990; Froehlich & Petrini, 2000), *Araceae*, *Bromeliaceae* and *Orchidaceae* (Petrini, 1981; Richardson & Currah, 1995), *Musaceae* (Brown et al., 1998; Photita et al., 2001), *Poaceae* (Danielsen & Jensen, 1999), *Piperaceae* and *Crassulaceae* (Dreyfuss & Petrini, 1984), *Meliaceae* (Rajagopal & Suryanarayanan, 2000; Gamboa & Bayman, 2001), *Acanthaceae*, *Chenopodiaceae* and *Aizoaceae* (Suryanarayanan & Kumaresan, 2000), *Rubiaceae* (Santamaría & Bayman, 2005), *Sapotaceae* (Lodge et al., 1996; Bayman et al., 1998), *Fabaceae* (Pereira et al., 1993), *Araliaceae* (Laessøe & Lodge, 1994), *Causarinaceae* (Bayman et al., 1998), and Arnold et al. (2001) isolated 418 endophytic fungi and document endophytic fungi in tropical representatives of the families *Anacardiaceae*, *Flacourtiaceae*, *Lecythidaceae*, *Melastomataceae*, and *Sterculiaceae*.

Bhattacharyya et al. (1952) first reported an endophytic fungus, *Epicoccum granulatum*, from *Aquilaria* trees, which induced agarwood formation in the trunk. Since then, several endophytic fungi have been isolated from *Aquilaria* species. Gong and Guo (2009) isolated endophytes from the leaves, roots, and stems of *A. sinensis*,

belonging to the genera *Calcarisporium*, *Cephalosporium*, *Epicoccum*, *Fusarium*, *Ovulariopsis*, and *Scytalidium*, with some mycelial isolates exhibiting antimicrobial activity. Mohamed et al. (2010) reported the presence of *Curvularia*, *Cunninghamella*, *Trichoderma*, and *Fusarium* species in the agarwood-associated fungal community in Malaysia. Cui et al. (2011) described 28 endophytic fungi from stem tissues of *A. sinensis*, representing 14 genera, including *Epicoccum*, *Cladosporium*, *Rhizomucor*, *Paraconiothyrium*, *Phaeoacremonium*, *Xylaria*, *Fusarium*, *Lasiodiplodia*, *Leptosphaerulina*, *Hypocrea*, *Phoma*, *Coniothyrium*, and *Chaetomium*. Tian et al. (2013) further reported *Phomopsis*, *Botryosphaeria*, *Cylindrocladium*, and *Colletotrichum gloeosporioides* in wounded *Aquilaria* trees, and *Alternaria*, *Mycosphaerella*, *Phoma*, *Ramichloridium*, and *Sagenomella* species in the internal tissues of non-resinous trees.

In this study, an investigation of endophytic fungi associated with *Thymelaeaceae* plants was conducted. Flower, leaf, stem, and root tissues were collected from six host species, *viz. Aquilaria* sp., *Daphne odora 'Aureomarginata'*, *Daphne papyracea*, *Edgeworthia chrysantha*, *Wikstroemia indica* and *Stellera chamaejasme*. Endophytic fungi were obtained using tissue isolation methods, induced to sporulate to reveal diagnostic morphological characteristics, and identified based on multilocus phylogenetic analyses (ITS, LSU, SSU, *tef1-α* and *rpb2*).

4.1.2 Results

By isolating endophytes from *Thymelaeaceae* plants, I obtained 616 endophytic fungal isolates from different organs of six host species, *viz. Aquilaria* sp., *Daphne odora 'Aureomarginata'*, *Daphne papyracea*, *Edgeworthia chrysantha*, *Wikstroemia indica* and *Stellera chamaejasme*. representing six classes (*Agaricomycetes*, *Dothideomycetes*, *Eurotiomycetes*, *Leotiomycetes*, *Mucoromycetes* and *Sordariomycetes*), 20 orders, 38 families, and 53 genera.

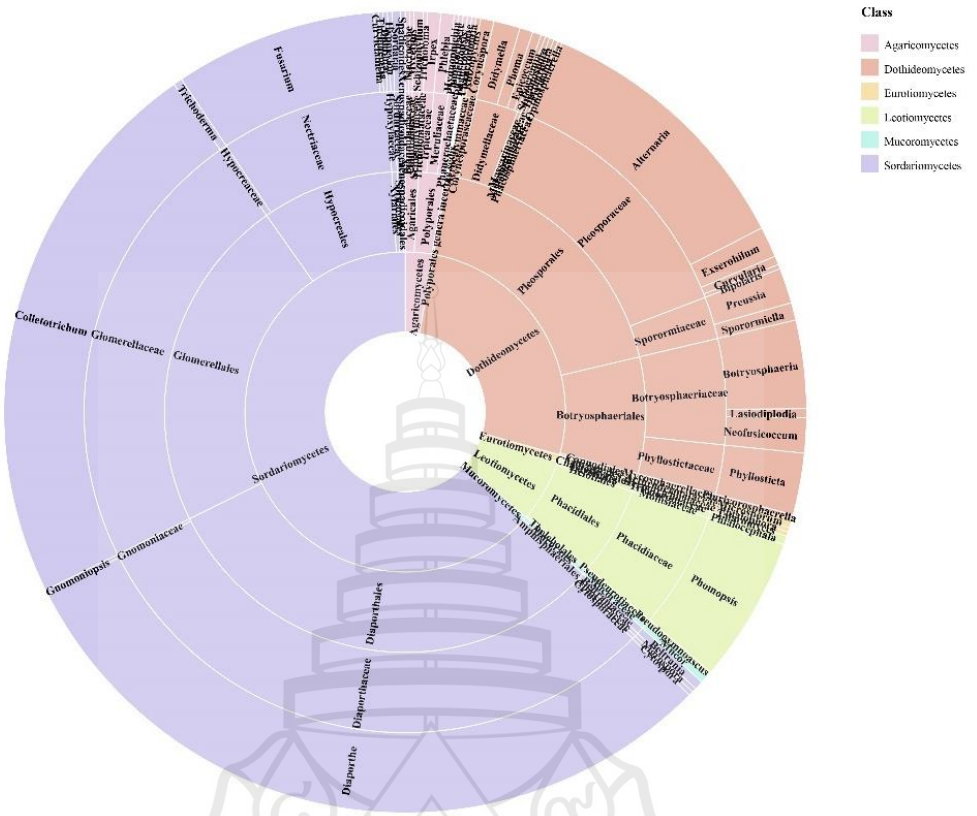

Figure 4.1 Distribution of 616 endophytic fungi in *Thymelaeaceae*

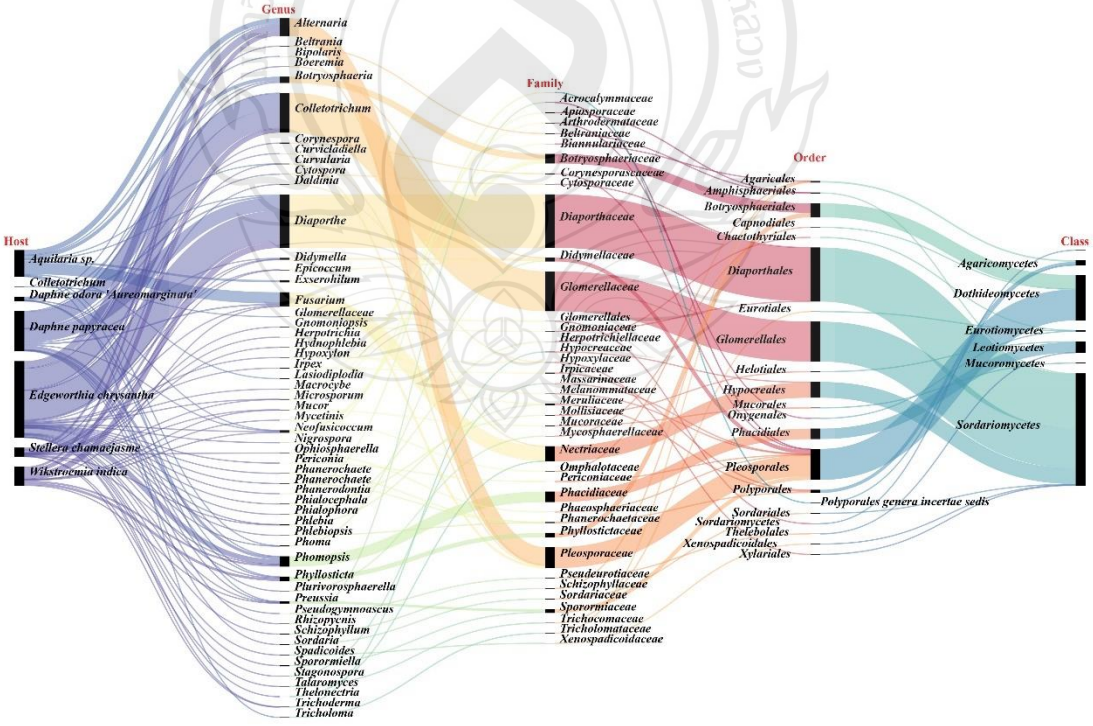

Figure 4.2 Visualization of host–taxonomy relationships of *Thymelaeaceae* endophytes

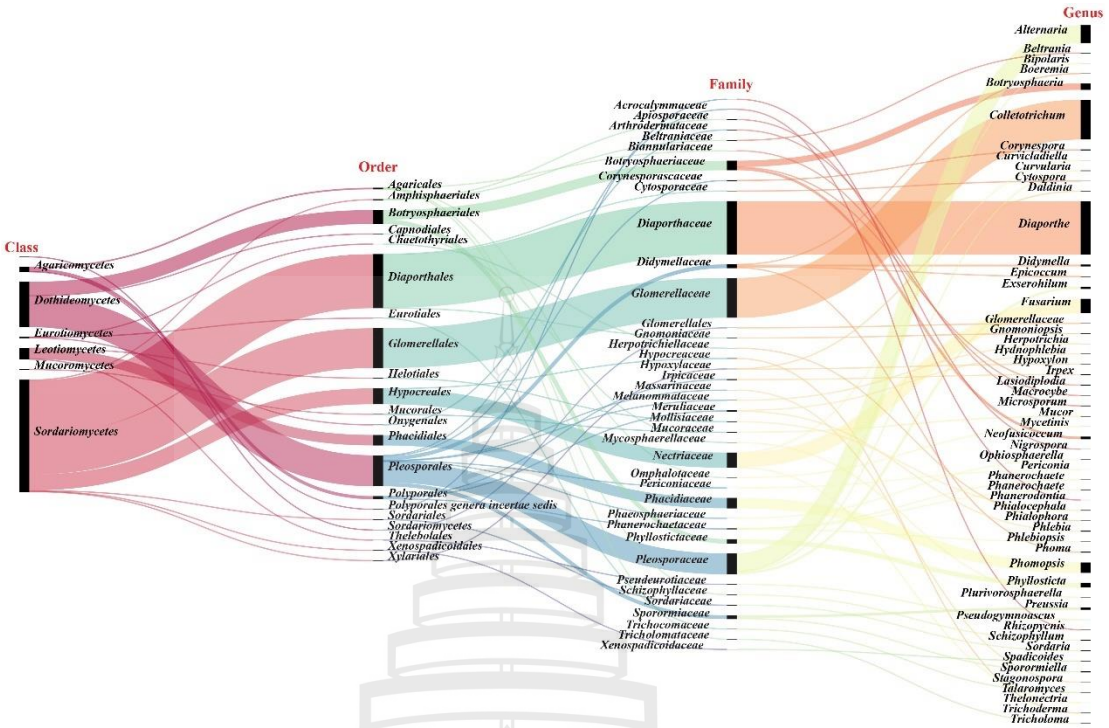

Figure 4.3 Visualization of endophytic fungal distribution from class to genus

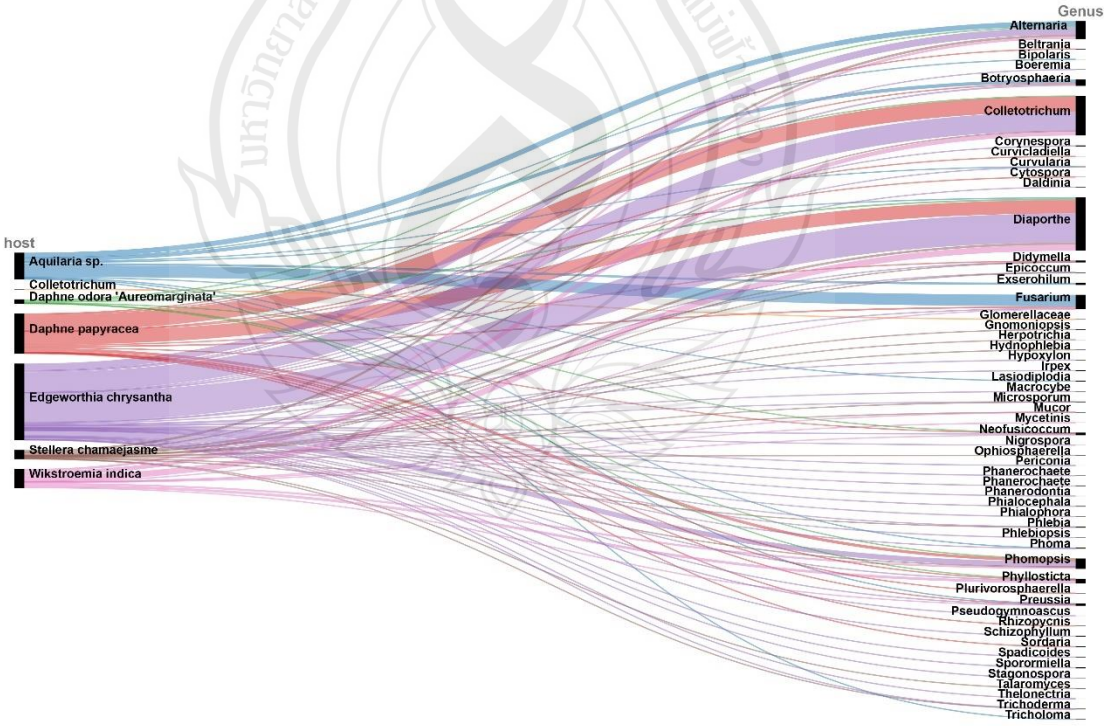

Figure 4.4 Visualization of endophytic fungal genera across *Thymelaeaceae* host

4.1.3 Taxonomy

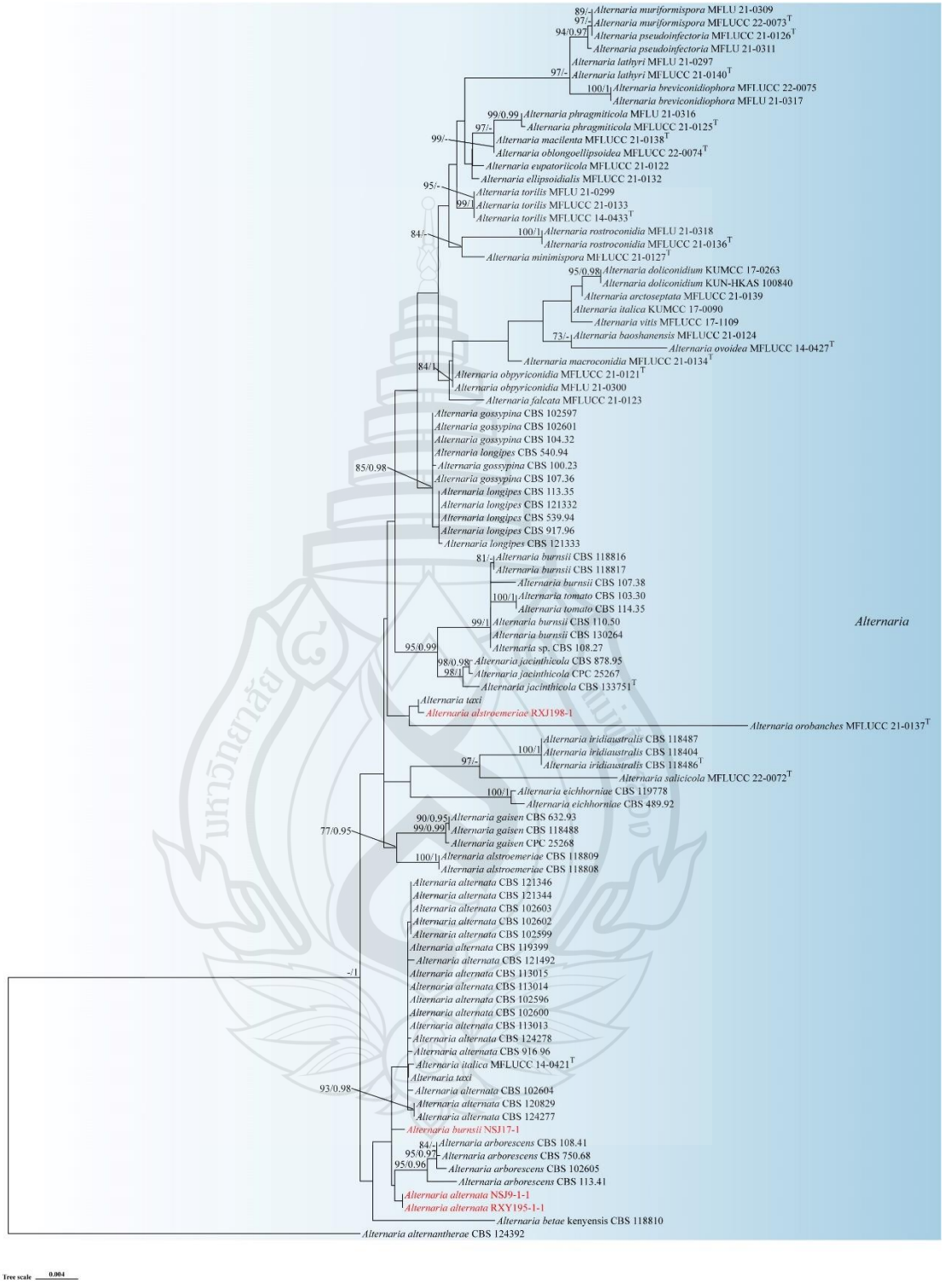

Figure 4.5 Phylogenetic analysis of *Alternaria*

Figure 4.5 Phylogenetic analysis of *Alternaria* was conducted using RAxML-based maximum likelihood analysis of a combined ITS, LSU, SSU, *rpb2*, *tef1-α*, *gapdh* and *Alt-al* sequence dataset. Bootstrap support values for maximum likelihood (ML) equal to or greater than 70% and Bayesian posterior probabilities (PP) equal to or greater than 0.95 are shown above the nodes. The tree is rooted with *Alternaria alternantherae* (CBS 124392). Newly generated strains are highlighted in red, and type strains are indicated with a superscript 'T'.

Dothideomycetes O.E. Erikss. & Winka, Myconet 1: 5 (1997)

Pleosporales Luttr. ex M.E. Barr, Prodromus to class Loculoascomycetes: 67 (1987)

Pleosporaceae Nitschke, Verh. naturh. Ver. preuss. Rheinl. 26: 74 (1869).

Alternaria Nees, Syst. Pilze (Würzburg): 72 (1816).

Index Fungorum number: IF 7106; *Facesoffungi number*: FoF 00501

Alternaria alstroemeriae E.G. Simmons & C.F. Hill, CBS Biodiversity Series 6: 444 (2007); Figure 4.6

Endophytes in *Stellera chamaejasme*. **Sexual morph**: Undetermined. **Asexual morph**: *Mycelium* superficial and immersed, composed of septate, branched, brown, smooth hyphae, 3.5–6 µm wide. *Conidiophores* solitary, arising directly from aerial hyphae, erect to slightly flexuous, with 1-6 septate, unbranched, subhyaline to brown, smooth. *Conidiogenous cells* 6–9.5 µm × 3–5.5 µm ($\overline{x}$ = 7.4 × 4.3 µm, n = 10) integrated, hyaline, smooth-walled, cylindrical or subglobose. *Conidia* 10–25.5 µm × 6–14 µm ($\overline{x}$ = 17.3 × 9.4 µm, n = 25) in simple short chains with up to 7 conidia, ovoid or subglobose, verrucose to tuberculate, brown, with some darkened middle transverse septa, 3–8 transverse septa, and 0–2 longitudinal or oblique septa per transverse segment, some primary conidia produce secondary conidiophores as lateral or terminal extensions from the conidial body, bearing conidia in short chains.

Culture characteristics: On WA (water agar), colonies reached 60 mm in diameter after 4 weeks at 25°C; surface irregular, floccose, dark brown to blackish.

Material examined: China, Guizhou Province, Guiyang City, from healthy stem of *Stellera chamaejasme* (*Thymelaeaceae*), 8 August 2022, Xia Tang; original isolate RXJ198-1 (193).

Note: *Alternaria alstroemeriae* was described by Simmons et al. (2007). Morphologically, the newly isolated strain conforms to the diagnostic characters of the type

of *A. alstroemeriae*. In the phylogenetic analyses (Figure 4.5), it clusters with *A. alstroemeriae*, forming a closely related lineage with strong support (99%). Based on combined morphological and phylogenetic evidence, we identify the isolate as *A. alstroemeriae*.

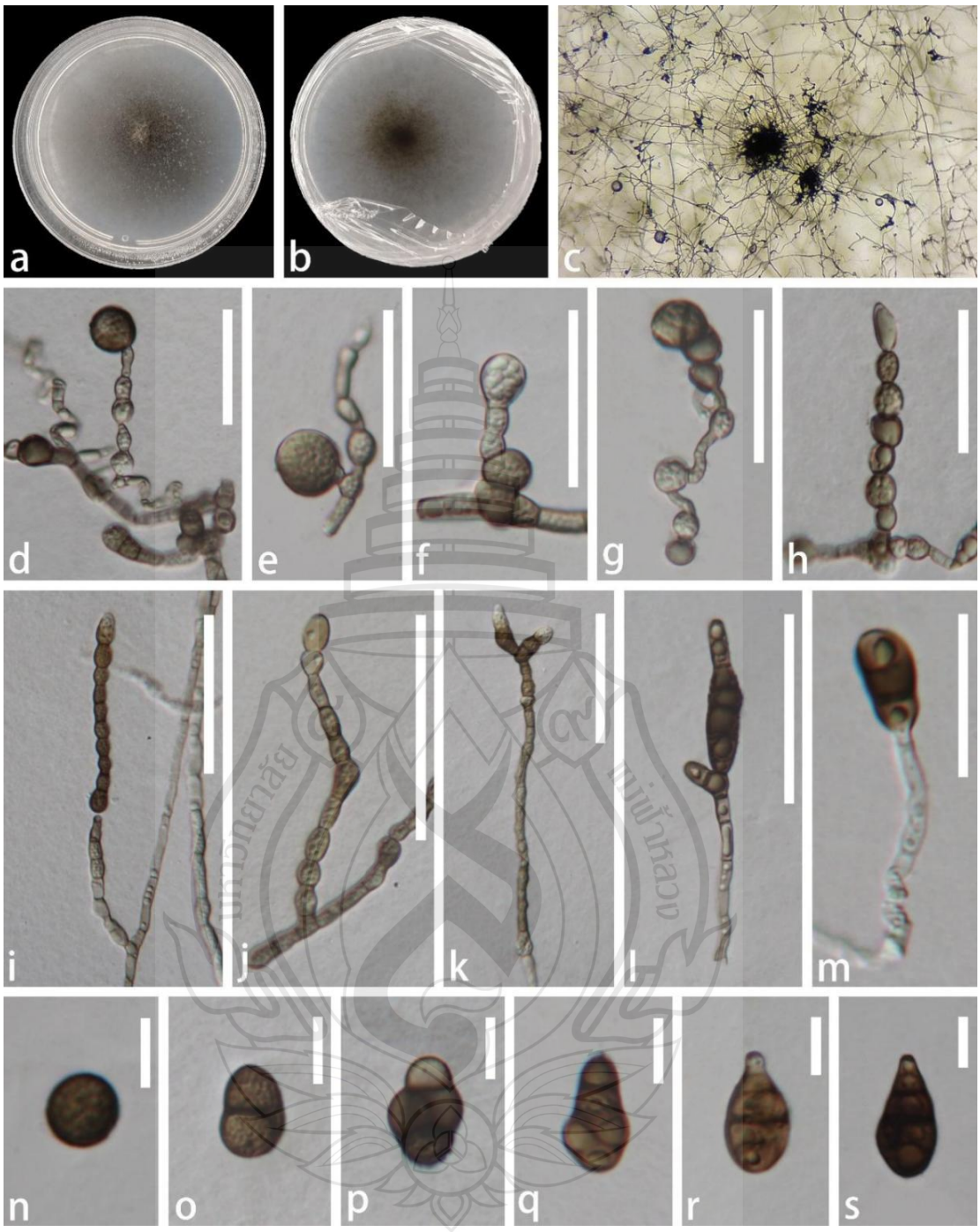

Figure 4.6 *Alternaria alstroemeriae* (RXJ198-1, new host record)

Figure 4.6 a–c: colonies on WA. d–k: Conidiophores, Conidiogenous cells baring conidia. o–s: Condia. Scale bar: i–l = 50 µm, d–h = 30 µm, m = 20 µm, n–s = 10 µm.

Alternaria alternata (Fr.) Keissl., Beih. Bot. Centralbl. 29: 433 (1912); Figure 4.7

Endophytes in *Edgeworthia chrysantha*. **Sexual morph**: Undetermined. **Asexual morph**: *Mycelium* 3–5.5 μm wide, superficial and immersed, composed of septate, branched, subhyaline to pale brown, smooth hyphae. *Conidiophores* 46–119.5 μm × 3.5–5.5 μm ($\overline{x}$ = 74.2 × 4.6 μm, n = 20) solitary, arising directly from aerial hyphae, erect to slightly flexuous, aseptate or septate, unbranched, subhyaline to brown, verruculose. *Conidiogenous cells* 6–17 μm × 4–6 μm ($\overline{x}$ = 9.5 × 4.8 μm, n = 10) integrated, cylindrical with guttulate, terminal, brown. *Conidia* 27.5–52 μm × 8.5–16 μm ($\overline{x}$ = 35.4 × 12.3 μm, n = 20) solitary or in simple short chains with up to 5 conidia, ovoid or obclavate, verrucose to tuberculate, brown, with some darkened middle transverse septa, 3–8 transverse septa, and 0–2 longitudinal some primary conidia produce secondary conidiophores as terminal extensions from the conidial body, bearing conidia in short chains.

Culture characteristics: On WA (water agar), colonies reached 50 mm in diameter after 4 weeks at 25°C; surface irregular, floccose (cottony), grey.

Material examined: China; Guizhou Province, Zunyi City, Suiyang County, specimen isolated from the healthy stem of *Edgeworthia chrysantha* (paperbush), 3 February 2023 by Xuemei Chen. Original specimen code: NSJ9-1-1.

Note: *Alternaria alternata* was first reported by Keissler et al. (1912). Morphologically, the newly isolated strain agrees with the descriptions of the type of *A. alternata*: chains of up to five conidia; in some cases, primary conidia extend from the apical end of the conidial body to produce secondary conidiophores; and conidiophores with verrucose (warty) apices. In phylogenetic analyses (Figure 4.5), the new isolate clusters with *A. alternata*, forming a closely related lineage with strong support. Based on morphology and phylogeny, we identify it as the known species *Alternaria alternata*.

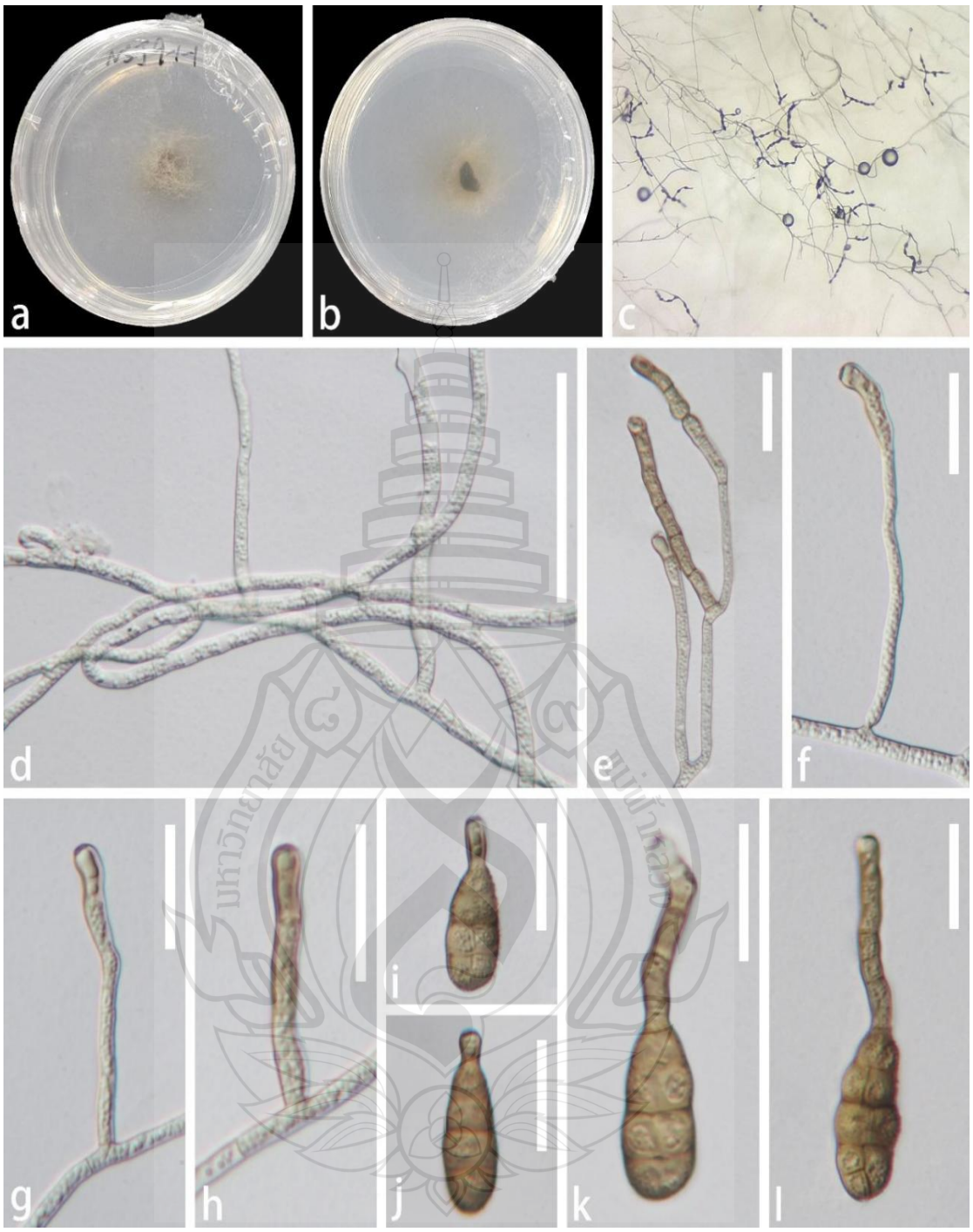

Figure 4.7 *Alternaria alternata* (NSJ9-1-1,new host rcord)

Figure 4.7 a–c Colonies on WA (water agar). d Vegetative hyphae. e–h Conidiophores. i–l conidia. Scale bars: d = 50 µm, e–l = 20 µm.

Alternaria alternata (Fr.) Keissl., Beih. Bot. Centralbl. 29: 433 (1912), Figure 4.8

Endophytes in *Stellera chamaejasme*. **Sexual morph**: Undetermined. **Asexual morph**: *Mycelium* superficial and immersed, composed of septate, guttulate, branched, brown, smooth hyphae, 4–6 μm wide. *Conidiophores* solitary, arising directly from aerial hyphae, erect to slightly flexuous, with 1–6 septate, guttulate, unbranched, subhyaline to brown, smooth, with 1 terminal conidiogenous locus. *Conidia* in simple short chains with up to 5 conidia, with guttulate when young, spherical or ovoid or obclavate, verrucose to tuberculate, brown, with some darkened middle transverse septa, 1–4 transverse septa, and 0–2 longitudinal or oblique septa per transverse segment, some primary conidia produce secondary conidiophores as lateral or terminal extensions from the conidial body, bearing conidia in short chains, 14.5–43 μm × 7–14.5 μm ($\overline{x}$ = 22.3 × 10.5 μm, n = 20).

Culture characteristics: On WA (water agar), colonies reached 60 mm in diameter after 2 weeks at 25 °C; surface irregular, raised, radiately furrowed, floccose, brown.

Material examined: China, Guizhou Province, Weining, from diseased leaf of *Stellera chamaejasme* (*Thymelaeaceae*), 8 August 2022, Xia Tang; original isolate RXY195-1-1 (518).

Notes: *Alternaria alternata* was first reported by Keissler et al. (1912). Morphologically, the newly isolated strain matches the descriptions of the type of *A. alternata*: chains of up to five conidia; in some cases, primary conidia extend from the apical end of the conidial body to produce secondary conidiogenous cells; and conidiophores with verrucose apices. In phylogenetic analyses (Figure 4.5), the isolate clusters with *A. alternata*, forming a closely related lineage with strong support. Based on combined morphological and phylogenetic evidence, we identify it as the known species *A. alternata*.

Figure 4.8 *Alternaria alternata* (RXY195-1-1, new host record)

Figure 4.8. a–c Colonies on WA (water agar). d–l Conidiophores with conidiogenous cells bearing conidia. m–y conidia. Scale bars: (e–o) = 30 µm; (d, p, q) = 20 µm; (r–u) = 10 µm, (v–y) = 5 µm.

Alternaria burnsii Uppal, Patel & Kamat, Indian J. Agric. Sci. 8: 61 (1938), Figure 4.9

= *Alternaria rhizophorae* E.G. Simmons, CBS Biodiversity Ser. (Utrecht) 6: 510. 2007.

Endophytes in *Edgeworthia chrysantha*. **Sexual morph**: Undetermined. **Asexual morph**: *Mycelium* superficial and immersed, composed of septate, branched, subhyaline to pale brown, smooth hyphae, 3-5 µm wide. *Conidiophores* 14–64.5 µm × 2.5–5.5 µm ($\overline{x}$ = 41.2 × 4 µm, n = 15) solitary, arising directly from aerial hyphae, erect to slightly flexuous, with 1-6 septate, unbranched, subhyaline to brown, smooth, with 1 terminal conidiogenous locus. *Conidiogenous cells* 5–10.5 µm × 2.5–5.5 µm ($\overline{x}$ = 7.5 × 4 µm, n = 10) integrated, terminal, cylindrical, brown. *Conidia* 18.5–51 µm × 9.5–18.5 µm ($\overline{x}$ = 32.1 × 12.7 µm, n = 25) in simple short chains with up to 5 conidia, ovoid or obclavate, verrucose to tuberculate, brown, with some darkened middle transverse septa, 3–6 transverse septa, and 0–2 longitudinal or oblique septa per transverse segment, some primary conidia produce secondary conidiophores as lateral or terminal extensions from the conidial body, bearing conidia in short chains.

Culture characteristics: On WA (water agar), colonies reached 50 mm in diameter after 4 weeks at 25°C; surface irregular, raised, floccose, dark brown to blackish.

Material examined: China, Guizhou Province, Zunyi City, Suiyang County, from healthy stem of *Edgeworthia chrysantha* (*Thymelaeaceae*), 13 February 2023, Xuemei Chen, original isolate NSJ17-1.

Notes: *Alternaria burnsii* was reported by Uppal et al. (1938). Morphologically, the newly isolated strain conforms to the diagnostic features of the type of *A. burnsii*. In the phylogenetic analyses (Figure 4.5), it clusters with *A. burnsii*, forming a closely related lineage with strong support (99%). Based on combined morphological and phylogenetic evidence, we identify the isolate as *Alternaria burnsii*.

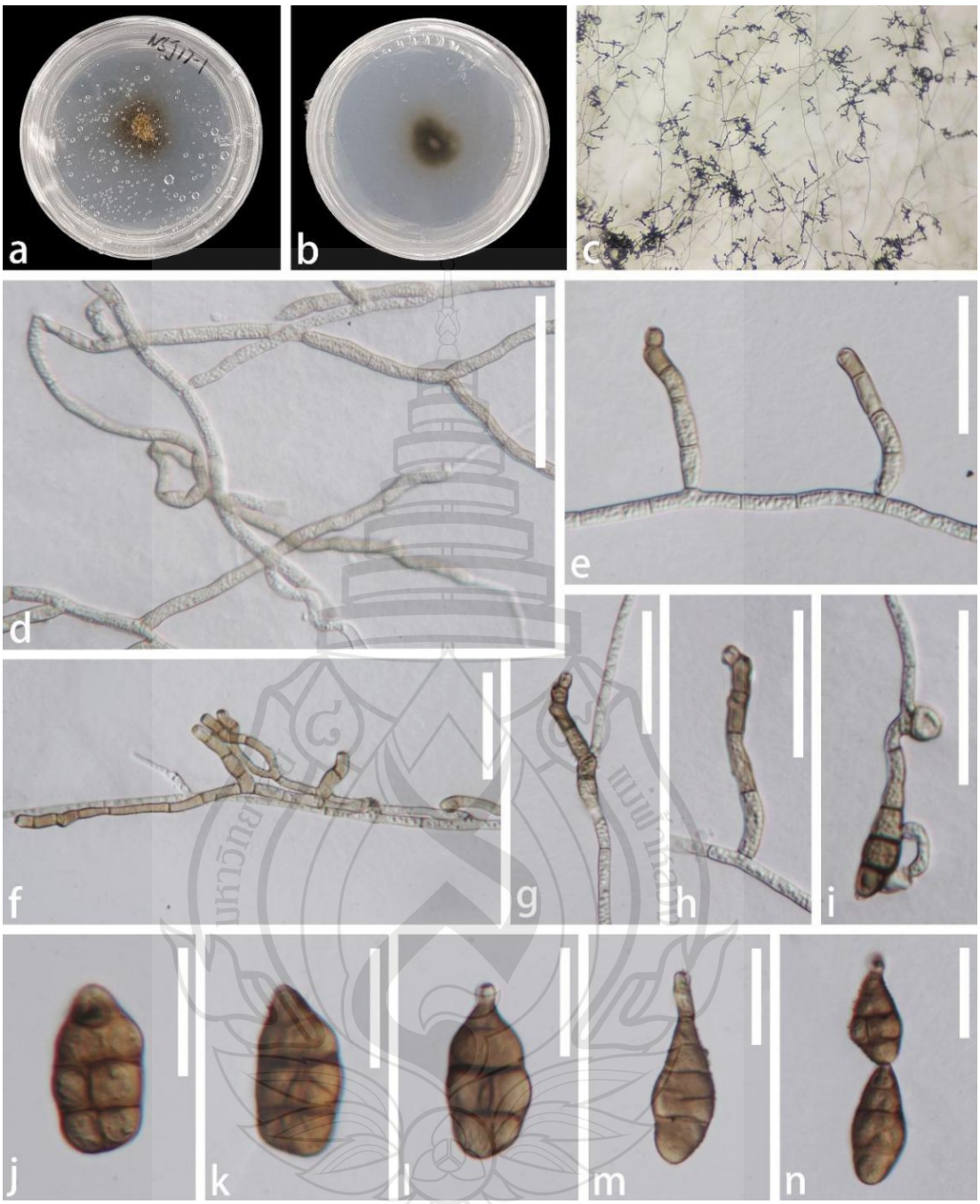

Figure 4.9 *Alternaria burnsii* (NSJ17-1, new host record)

Figure 4.9 a–c Colonies on WA (water agar). d Vegetative hyphae. e–h Conidiophores with conidiogenous cells bearing conidia i–n Conidia. Scale bars: d = 50 µm, e–i = 30 µm, j–n = 20 µm.

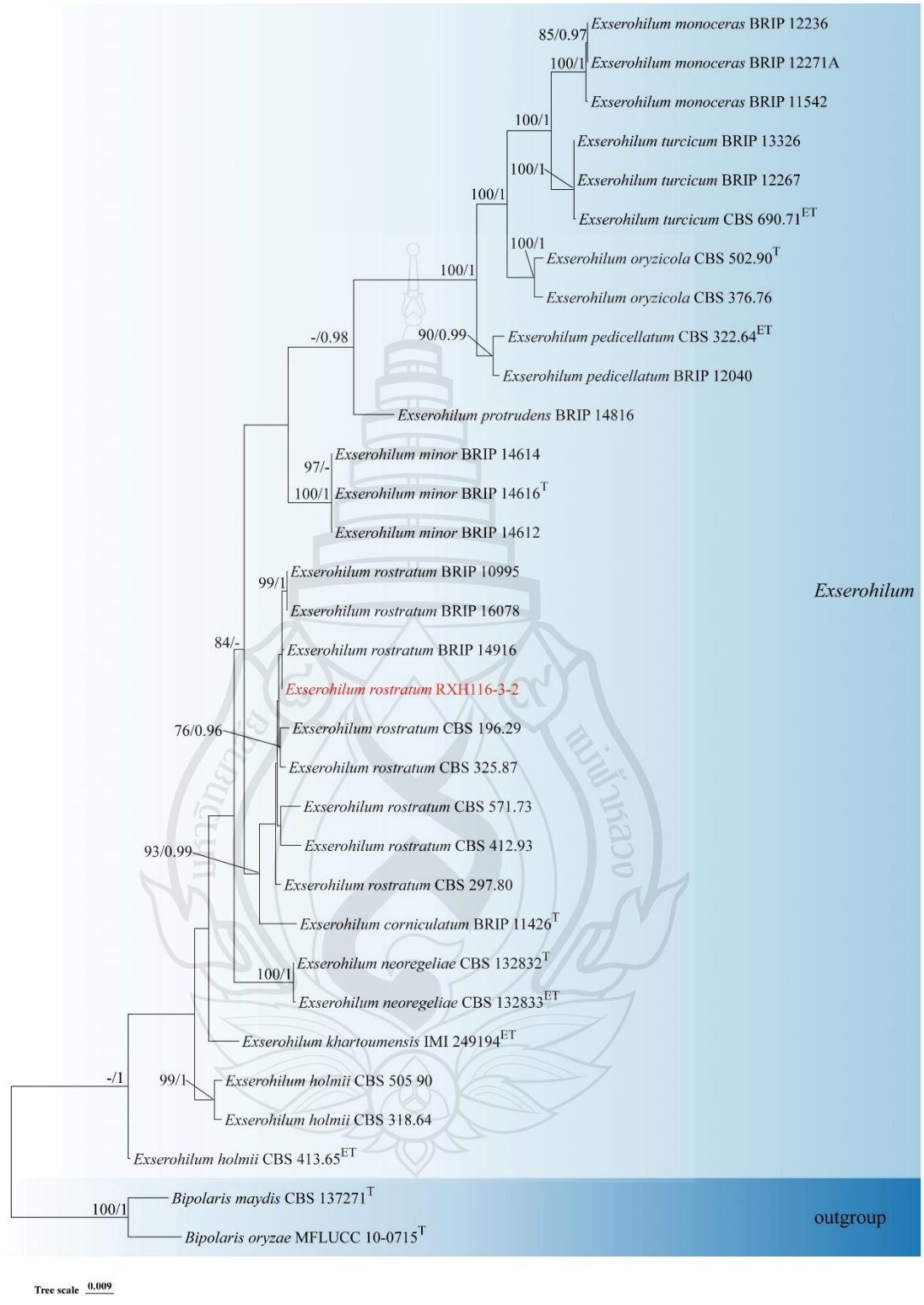

Figure 4.10 Phylogenetic analysis of *Exserohilum*

Figure 4.10 Phylogenetic analysis of *Exserohilum* was conducted using RAxML-

based maximum likelihood analysis of a combined ITS and LSU sequence dataset. Bootstrap support values for maximum likelihood (ML) equal to or greater than 70% and Bayesian posterior probabilities (PP) equal to or greater than 0.95 are shown above the nodes. The tree is rooted with *Bipolaris maydis* (CBS 137271) and *B. oryzae* (MFLUCC 10-0715). Newly generated strains are highlighted in red, and type strains are indicated with a superscript 'T'.

Exserohilum K.J. Leonard & Suggs, Mycologia 66: 289 (1974)

Exserohilum rostratum (Drechsler) K.J. Leonard & Suggs, Mycologia 66: 290 (1974), Figure 4.11

= *Helminthosporium rostratum* Drechs., 1923, J. Agric. Res. 24: 724.

= *Bipolaris rostrata* (Drechs.) Shoemaker, 1959, Canad. J. Bot. 37: 883.

= *Drechslera rostrata* (Drechs.) Richardson & Fraser, 1968, Trans. Brit. Mycol. Soc. 51: 148.

Endophytes in *Daphne papyracea*. **Sexual morph**: Undetermined. **Asexual morph**: *Vegetative* hyphae septate, branched, smooth, guttulate, subhyaline when young, pale olivaceous brown at maturity, 3–6 µm wide. *Conidiophores* macronematous, mononematous, straight to flexuous, sometimes geniculate towards the apex, septate, unbranched, subcylindrical, brown, smooth-walled, up to 7 µm wide. But sometimes becoming finely verruculose near the conidiogenous loci, with cell walls usually thicker than those of the vegetative hyphae, with occasional subnodulose to nodulose swellings. *Conidiogenous cells* 6–21 µm × 4–10 µm ($\bar{x}$ = 11.6 × 6.2 µm, n = 10) integrated, terminal and intercalary, mostly subcylindrical, mono- to polytretic, proliferating sympodially. *Conidia* 33–79.5 µm × 10.5–23.5 µm ($\bar{x}$ = 59.6 × 16.3 µm, n = 30) mostly subcylindrical to fusiform, straight to slightly curved, pale olivaceous brown to dark olivaceous brown, smooth to irregularly verruculose, 2–8-septate, thick-walled, sometimes with accentuated septa delimiting the basal cell or both the basal and apical cells, often becoming rostrate by means of a narrow apical extension, with a strongly protruding hilum.

Culture characteristics: On WA (water agar), colonies covered the 60-mm plate after 4 weeks at 25°C; surface irregular, raised, floccose, brown.

Material examined: China, Guizhou Province, from healthy petals of *Daphne papyracea* (*Thymelaeaceae*), 10 August 2022, Xia Tang; original isolate RXH116-3-2 (142).

Note: *Exserohilum rostratum* was transferred from *Drechslera* by Leonard and Suggs (1974). The present isolate was obtained from healthy flowers of *Daphne papyracea*. Morphologically, it conforms to the diagnostic characters of *E. rostratum* (e.g., distoseptate, rostrate conidia with a protruding basal hilum; sympodially proliferating, often geniculate conidiophores). In the phylogenetic analyses (Figure 4.10), the isolate clusters with *E. rostratum* without discernible divergence. Based on combined morphological and phylogenetic evidence, we identify it as *Exserohilum rostratum*.

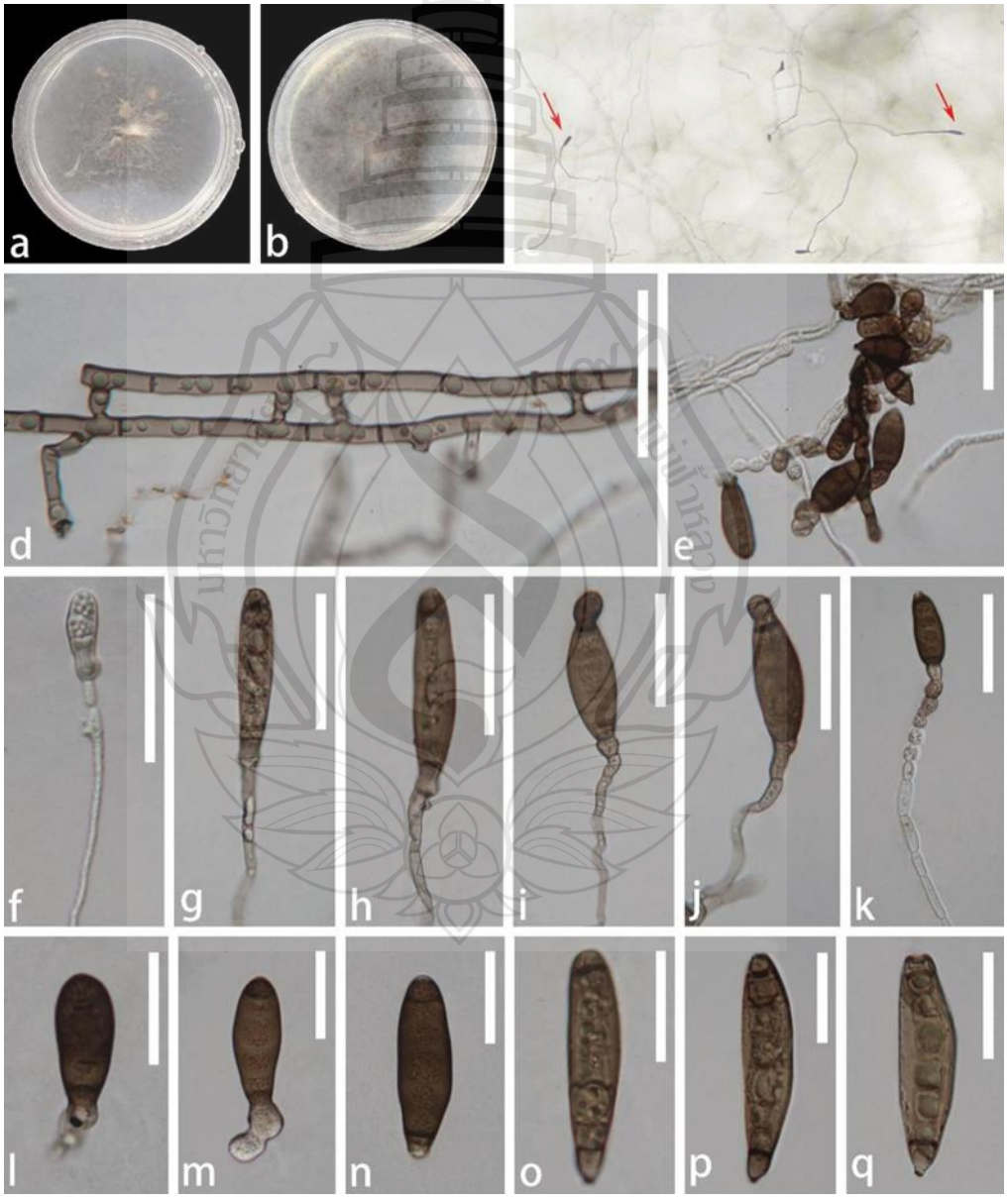

Figure 4.11 *Exserohilum rostratum* (RXH116-3-2 (142), new host record)

Figure 4.11 a–c Colonies on WA (water agar). d Vegetative hyphae. e–k Conidiophores with conidiogenous cells bearing conidia. l–q Conidia. Scale bars: d–k = 50 µm, l–q = 30 µm.

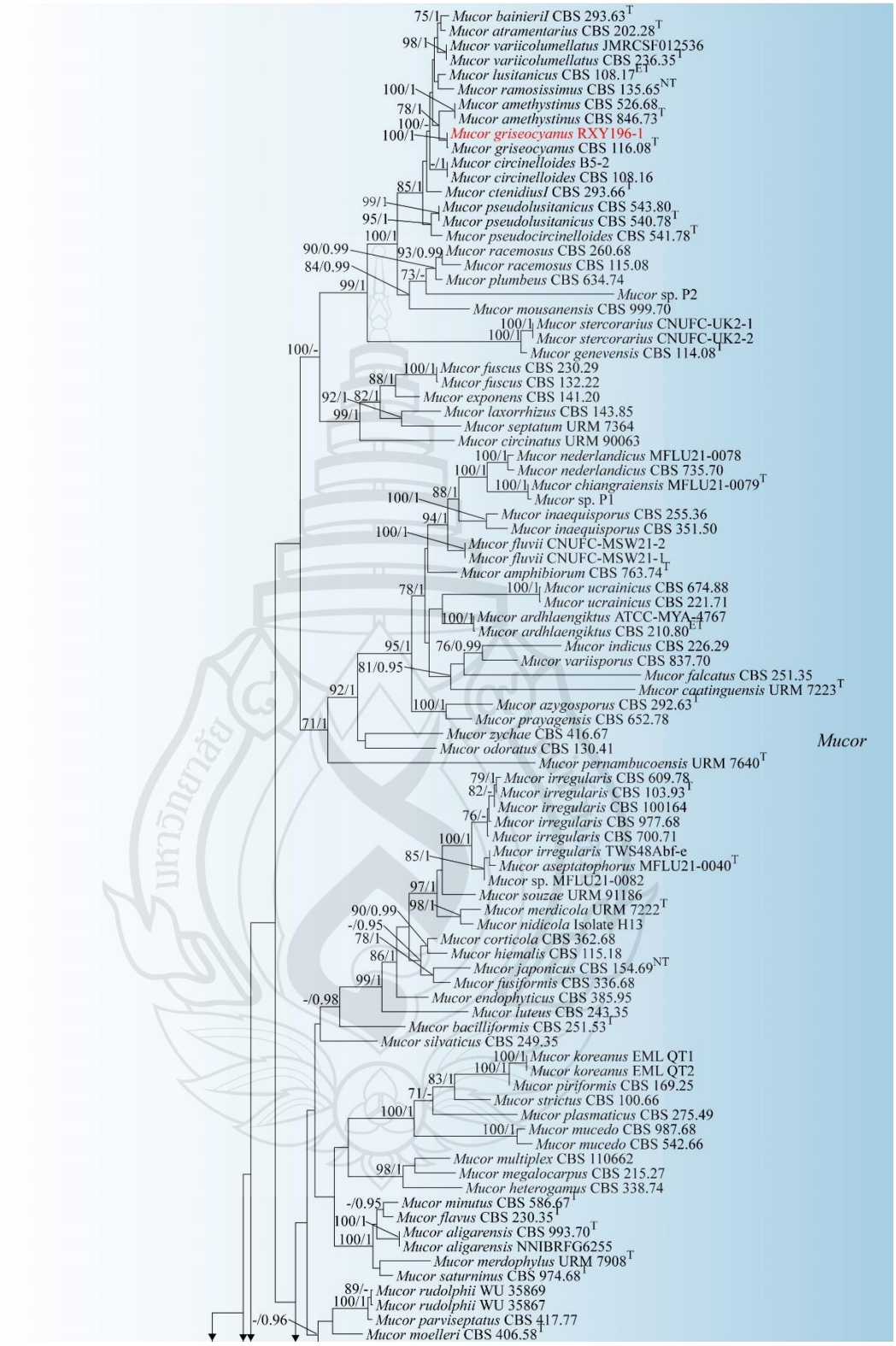

Figure 4.12 Phylogenetic analysis of *Mucor*

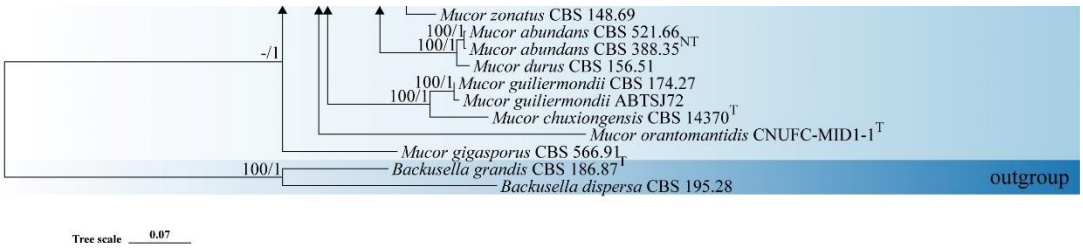

Figure 4.12 (continued)

Figure 4.12 Phylogenetic analysis of *Mucor* was conducted using RAxML-based maximum likelihood analysis of a combined ITS and LSU sequence dataset. Bootstrap support values for maximum likelihood (ML) equal to or greater than 70% and Bayesian posterior probabilities (PP) equal to or greater than 0.95 are shown above the nodes. The tree is rooted with *Backusella grandis* (CBS 186.87) and *B. dispersa* (CBS 195.28). Newly generated strains are highlighted in red, and type strains are indicated with a superscript 'T'.

Mucoromycetes Doweld, Prosyllabus Tracheophytorum, Tentamen systematis plantarum vascularium (Tracheophyta): LXXVII (2001)

Mucorales B.C. Dumortier, Analyse des familles des plantes, avec l'indication des principaux genres qui s'y rattachent: 73 (1829)

Mucoraceae Dumort., Commentationes botanicae: 69, 81 (1822)

Mucor Fresen., Beiträge zur Mykologie 1: 7 (1850)

Index Fungorum number: IF 25484; *Facesoffungi number*: FoF

Mucor griseocyanus Hagem, Skr. Vidensk.-Selsk. Christiana Math.-Nat. Kl. 1907 (no. 7): 28 (1908), Fig. 4.13

Endophytes in *Stellera chamaejasme*. **Sexual morph**: Undetermined. **Asexual morph**: *Vegetative* hyphae, hyaline, smooth-walled, septate, branched, guttulate, and the vegetative hyphae are enlarged, 3.5–6.5 µm wide. *Conidiophores* hyaline, smooth-walled, erect to slightly flexuous, aseptate, thin-walled, branched, cylindrical, sometimes tapering at the ends, 24.5–123.5 µm × 3.5–8 µm ($\overline{x}$ = 57.8 × 5.4 µm, n = 5). *Conidiogenous cells* integrated, hyaline, smooth-walled. *Sporangiophores* 11.5–18 µm ($\overline{x}$ = 14.1 µm, n = 20) diam brown, globose, thick-walled and with granular contents when young, thin-walled and granular contents gradually grow into conidia at maturity. *Conidia* 4.5–6 µm × 2.5–4.5 µm ($\overline{x}$ = 5.2 × 3.7 µm, n = 25) pale brown, subglobose or ellipsoid, smooth-walled, aseptate, with guttulate content.

Culture characteristics: On WA (water agar), colonies reached 40 mm in diameter after 4 weeks at 25°C; colony outline elliptical; surface irregular, grey-white.

Material examined: China, Guizhou Province, Weining, from healthy leaf of *Stellera chamaejasme* (*Thymelaeaceae*), 8 August 2022, Xia Tang; original isolate RXY196-1.

Note: Mucor griseocyanus was reported by Hagem (1908). Morphologically, the new isolate accords with the type descriptions of *M. griseocyanus*: hyaline, smooth-walled sporangiophores; black sporangia; and ovoid sporangiospores. In the phylogenetic analyses (Figure 4.12), the isolate clusters with *M. griseocyanu*s without appreciable branch-length divergence. Based on combined morphological and phylogenetic evidence, we identify it as *Mucor griseocyanus*. To our knowledge, this represents the first record of *M. griseocyanus* from *Stellera chamaejasme*.

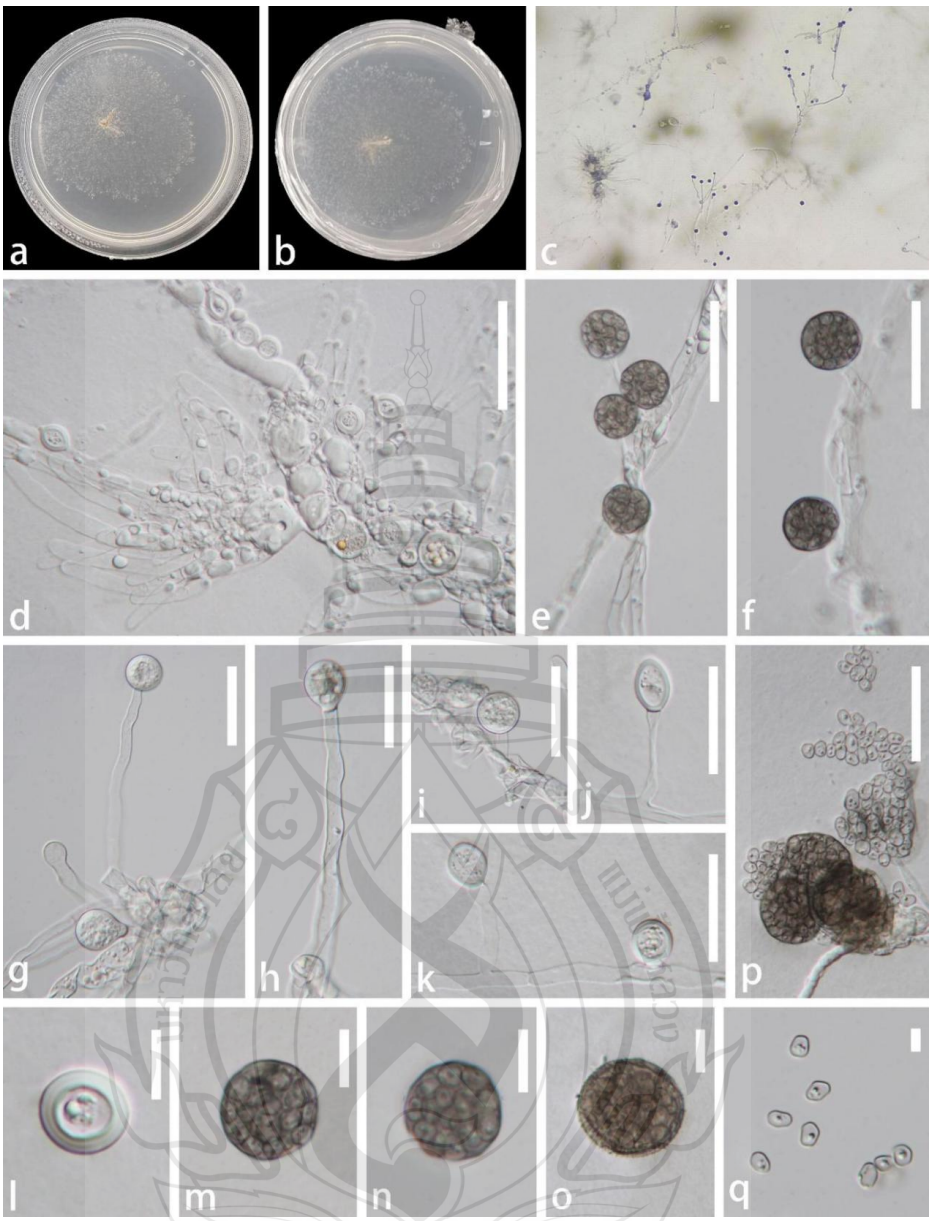

Figure 4.13 *Mucor griseocyanus* (RXY196-1, 197, new host record)

Figure 4.13 a, b Sporulating colonies on WA (water agar), obverse and reverse. c colony on WA. d mycelium with sporangia. e–k, p Columellae with sporangia. l–o sporangia; (q) Sporangiospores. Scale bars: d = 50 µm, e–k, p = 30 µm, l–o = 10 µm, q = 5 µm.

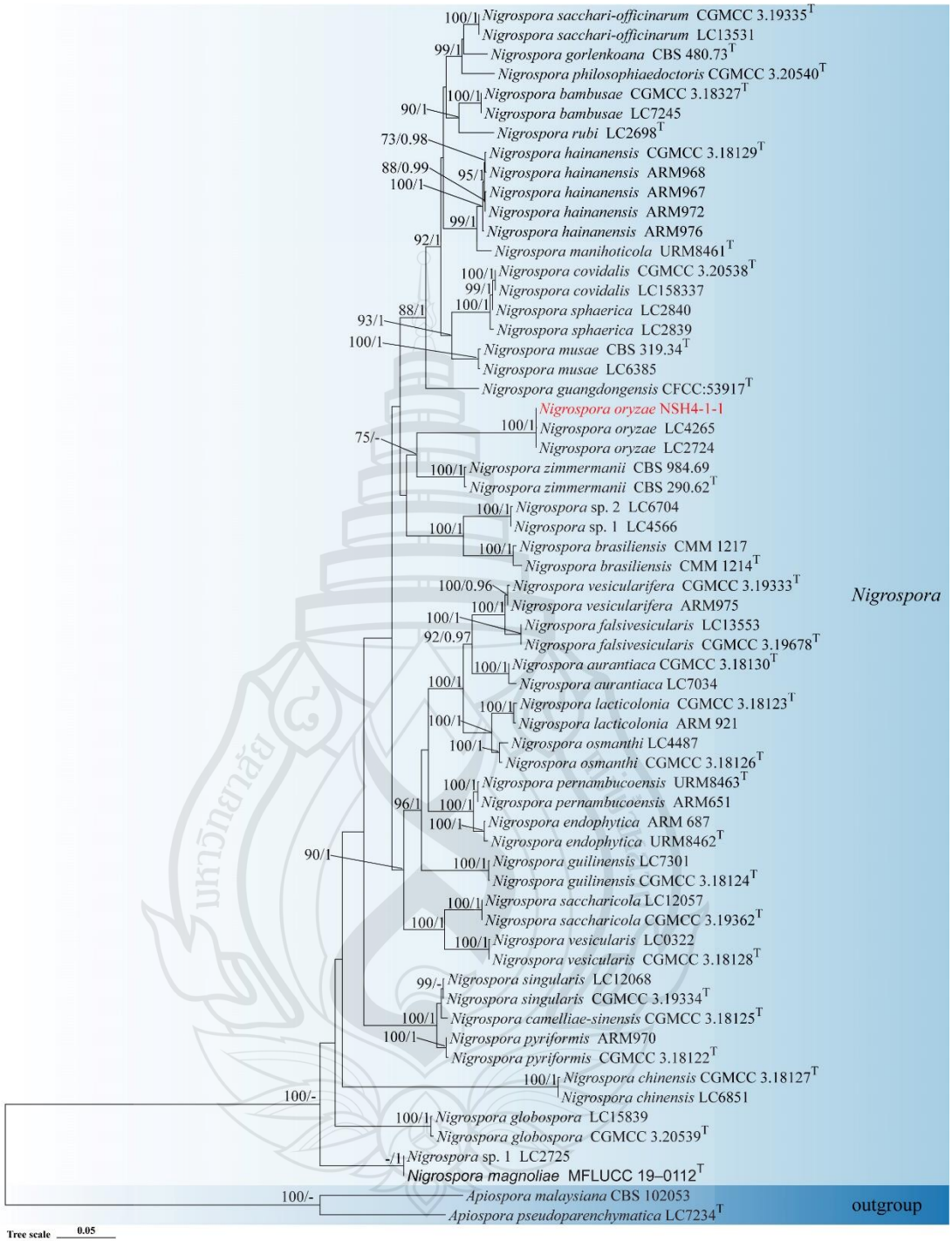

Figure 4.14 Phylogenetic analysis of *Nigrospora*

Figure 4.14 Phylogenetic analysis of *Nigrospora* was conducted using RAxML-based maximum likelihood analysis of a combined ITS and LSU sequence dataset. Bootstrap support values for maximum likelihood (ML) equal to or greater than 70% and Bayesian posterior probabilities (PP) equal to or greater than 0.95 are shown above the nodes. The tree is rooted with *Apiospora apseudoparenchymatica* (LC 7234) and *A. malaysiana* (CBS 102053). Newly generated strains are highlighted in red, and type strains are indicated with a superscript 'T'.

Sordariomycetes O.E. Erikss. & Winka, Myconet 1: 10 (1997)

Amphisphaeriales D. Hawksw. & O.E. Erikss., Syst. Ascomycetum 5: 177 (1986)

Nigrospora Zimm., Centralbl. Bakteriol. Parasitenk., 2. Abth. 8: 220 (1902)

Index Fungorum number: IF 9124; *Facesoffungi number*: FoF 14273

Nigrospora oryzae (Berk. & Broome) Petch, J. Indian Bot. Soc. 4: 24 (1924); Fig. 4.15

Endophytes in *Edgeworthia chrysantha*. **Sexual morph**: Undetermined. **Asexual morph**: *Mycelium* superficial and immersed, branched, septate, guttulate, hyaline to pale brown, 4–6.5 µm diam. *Conidiophores* 16.5–146 µm × 3.5–5.5 µm ($\overline{x}$ = 75.1 × 4.1 µm, n = 20) arising laterally from hyphae, occasionally branched, septate, guttulate, hyaline, cylindrical, some reduced to conidiogenous cells. *Conidiogenous cells* 4.5–13 µm × 3.5–5.5 µm ($\overline{x}$ = 7.1 × 4.5 µm, n = 15) pale brown, straight or flexuous, subspherical or cylindrical. *Conidia* 7.5–13 µm × 5.5–9 µm ($\overline{x}$ = 10.1 × 7.4 µm, n = 30) solitary or polyspores, straight or flexuous, globose or subglobose, pale brown, smooth, sometimes formed directly from the mycelia, aseptate.

Culture characteristics: On WA (water agar), colonies reached 40 mm in diameter after 2 weeks at 25°C; surface irregular, floccose, grey-brown.

Material examined: China, Guizhou Province, Zunyi City, Suiyang County, from healthy petals of *Edgeworthia chrysantha* (*Thymelaeaceae*), 13 February 2023, Xuemei Chen; original isolate NSH4-1-1.

Note: *Nigrospora oryzae* was reported by Petch (1924). Morphologically, the new isolate differs from the type in having longer conidiophores (16.5–146 × 3.5–5.5 µm) and shorter conidiogenous cells (4.5–13 × 3.5–5.5 µm), while conidial characters are similar. In phylogenetic analyses (Figure 4.14), the isolate clusters with *N. oryzae*. Based on combined morphological and phylogenetic evidence, we identify it as *Nigrospora oryzae*.

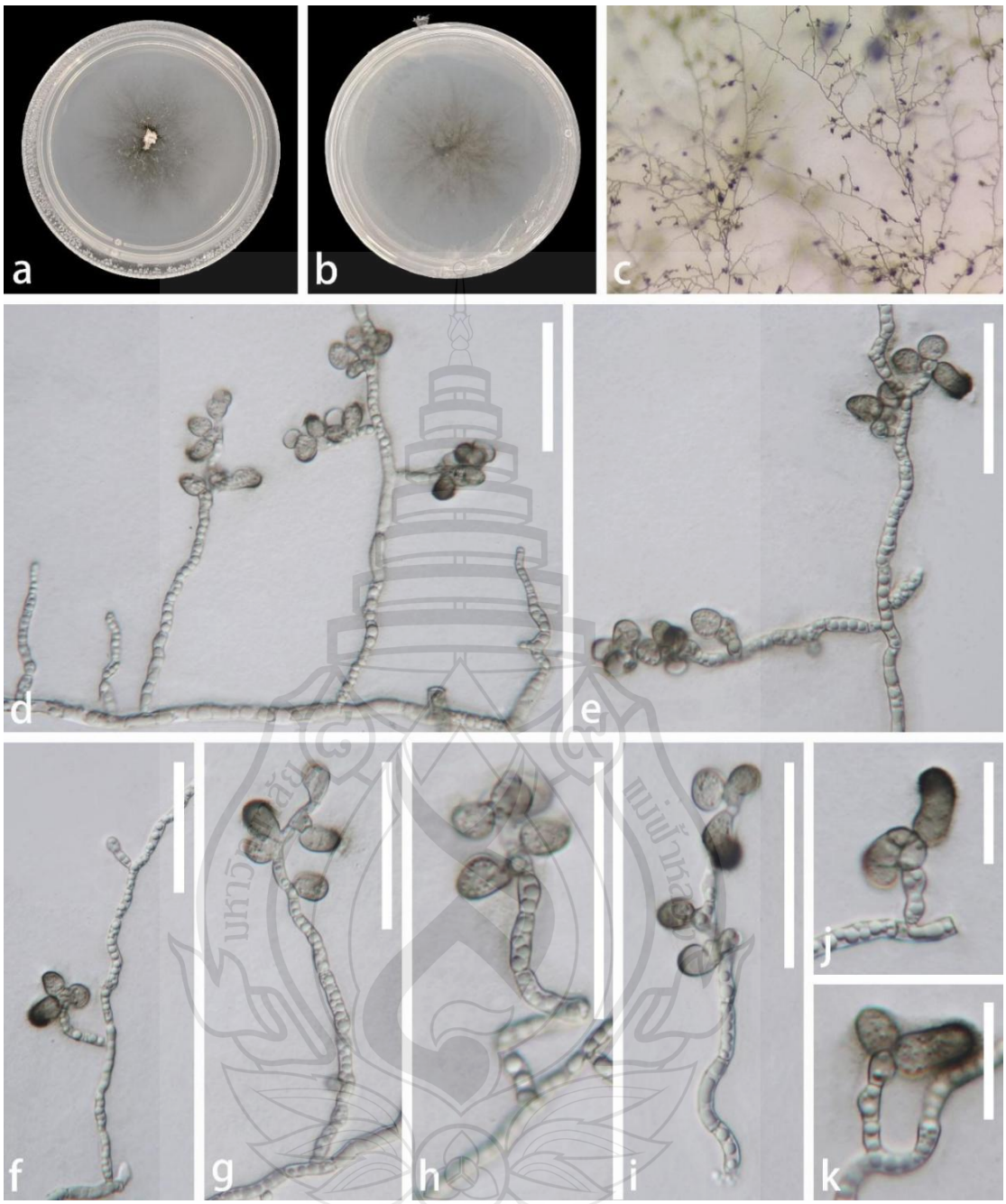

Figure 4.15 *Nigrospora oryzae* (NSH4-1-1, new host record)

Figure 4.15 a–c Colonies on WA (water agar). d Vegetative hyphae. e–k Conidiophores with conidiogenous cells bearing conidia. l–q Conidia. Scale bars: d–k = 50 µm, l–q = 30 µm.

4.2 Saprobic Fungi Associated with *Thymelaeaceae*

4.2.1 Introduction

Microfungi associated with forest plants are most frequently reported as saprobes. Prior work in forest ecosystems consistently shows that saprobic microfungi dominate and harbor substantial cryptic diversity; for example, Polishook et al. (1996) surveyed leaf litter of *Guarea guidonia* and *Manilkara bidentata* in the Luquillo Mountains (Puerto Rico) and obtained 3,337 isolates, which incuded spanning rare litter hyphomycetes, coelomycetes as well. Sutton (1969) described and illustrated two new species of *Acrodictys* from rotting *Populus* bark. Subsequently, 184 fungal species were reported from Tai National Park, a 360,000-ha park covered by native forest and representative of a subhygrophilous "Eremospato Mabetum" vegetation type (Rambelli et al., 2004). In Australian tropical rain forest, work on fallen leaves of *Ficus pleurocarpa* (*Moraceae*) yielded 562 cultures via indirect isolation, of which 265 (47%) sporulated and represented 53 taxa; the remaining 297 sterile cultures comprised 100 morphotaxa (Paulus et al., 2006). Surveys of bark from healthy and injured American beech, Fraser fir, and eastern hemlock recovered 94 fungal species, while along a transect from Kanyakumari (Tamil Nadu) to Mahabaleshwar (Maharashtra) via Kerala, 81 forest microfungi were reported; using a standardized isolation medium, 93 distinct bark-associated species were identified across three tree species (Baird et al., 2007; Bhat, 2008). The saprobic studies numerous studies from China and Thailand have likewise focused on saprobic fungi, collectively corroborating that forest ecosystems harbor a substantial reservoir of cryptic saprobic microfungal diversity. For instance, 239 fungi (including 92 ascomycetes) were identified from Thai woody litter (Kodsueb et al., 2008), and numerous saprobic hyphomycetes and allied taxa have been documented from tropical/subtropical forests of southern China (Zhang et al., 2009; Ma et al., 2010, 2011; Zhang et al., 2011; Ma et al., 2012; Ren et al., 2012). As an important lineage of forest hosts, the family *Thymelaeaceae* (e.g., *Aquilaria*, *Daphne*, *Edgeworthia*, *Wikstroemia*) provides a rich and heterogeneous array of substrates (dead twigs, leaf litter, decaying wood, and fissured bark) that support saprobic microfungi and likely harbor high taxonomic and functional diversity. However, compared with

more widely studied forest host lineages, research on saprobic microfungi associated with *Thymelaeaceae* remains limited and fragmented, with notable gaps in systematic sampling and molecular phylogenetic support.

Based on this backdrop, a targeted, systematic investigation of saprobic microfungi associated with *Thymelaeaceae* is both necessary to fill taxonomic and phylogenetic gaps and valuable for clarifying the role of these hosts within forest decomposition networks and biogeochemical cycling. Accordingly, the present study focuses on *Thymelaeaceae* substrates (dead twigs, leaf litter, and decaying wood), applying standardized isolation and morphological characterization, together with multi-locus phylogenetic analyses, phylogenetic placement, and host-association patterns of saprobic microfungi on *Thymelaeaceae*. This framework provides reproducible, comparable baseline data for subsequent work on ecological function and regional diversity synthesis.

4.2.2 Results

In this study, saprobic twig samples on *Thymelaeaceae* plants, including *Stellera chamaejasme* and *Edgeworthia chrysantha*, were collected from Weining and Zunyi in Guizhou Province, China. Based on morphological and phylogenetic analysis, seven species were obtained, belonging to two classes (*Dothideomycetes*, *Lecanoromycetes*), four orders (*Botryosphaeriales*, *Kirschsteiniotheliales*, *Pleosporales*, *Ostropales*), seven families (*Botryosphaeriaceae*, *Kirschsteiniotheliaceae*, *Corynesporascaceae*, *Phaeoseptaceae*, *Thyridariaceae*, *Torulaceae*, *Stictidaceae*) and seven genera (*Lasiodiplodia*, *Kirschsteiniothelia*, *Corynespora*, *Pleopunctum*, *Thyridaria*, *Neopodoconis*, *Fitzroyomyces*).

4.2.3 Taxomy

Dothideomycetes O.E. Erikss. & Winka, Myconet 1: 5 (1997)

Botryosphaeriales C.L. Schoch, Crous & Shoemaker, Mycologia 98 (6): 1050 (2007)

Botryosphaeriaceae Theiss. & P. Syd., Ann. Mycol. 16 (1-2): 16 (1918)

Lasiodiplodia Ellis & Everh., Bot. Gaz. 21: 92 (1896)

Index Fungorum number: IF 843438; *Facesoffungi number*: FoF 17612

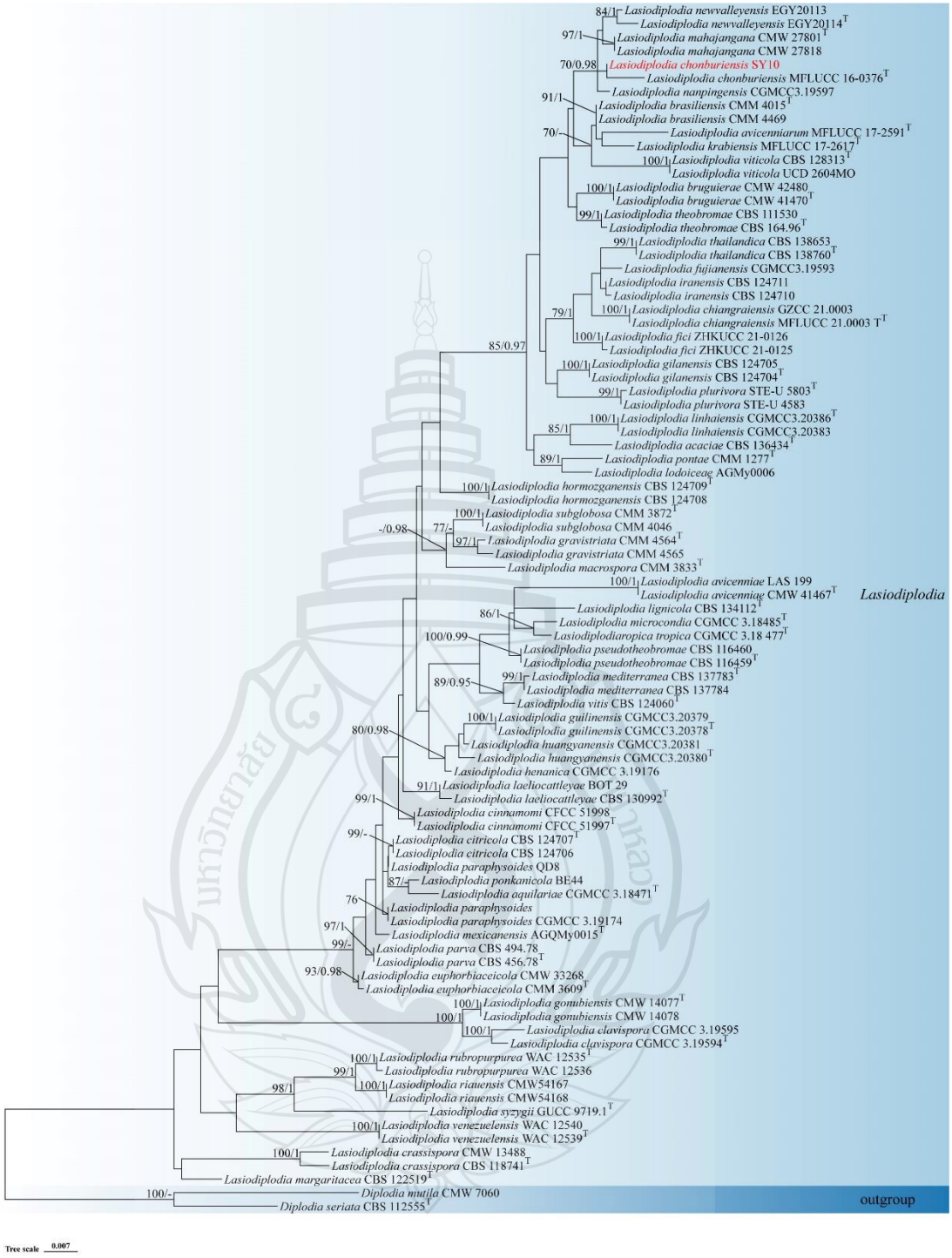

Figure 4.16 Phylogenetic analysis of *Lasiodiplodia*

Figure 4.16 Phylogenetic analysis of *Lasiodiplodia* was conducted using RAxML-based maximum likelihood analysis of a combined ITS *tef1-α* and *tub2* sequence dataset. Bootstrap support values for maximum likelihood (ML) equal to or greater than 70% and Bayesian posterior probabilities (PP) equal to or greater than 0.95 are shown above the nodes. The tree is rooted with *Diplodia mutila* (CMW 7060) and *D. seriata* (CBS 112555). Newly generated strains are highlighted in red, and type strains are indicated with a superscript 'T'.

Lasiodiplodia chonburiensis Tibpromma & K.D. Hyde, Fungal Diversity 93: 54 (2018); Figure 4.17

Saprobic on *Edgeworthia chrysantha*. **Sexual morph**: undetermined. **Asexual morph**: *Colonies* on natural substratum are effuse, gray and hairy. *Conidiomata* pycnidial, unilocular, immersed in substrate, globose to subglobose, ostiolate, thick-wall composed of several layers of black textura angularis. *Peridium* composed of walled, brown-black cells of textura angularis, thin inner wall. *Conidiophores* cylindrical, septate, unbranched, ends rounded, formed among conidiogenous cells. *Conidiogenous cells* hyaline, annellidic, cylindrical, thick-walled, smooth. *Conidia* 23.5–31 µm × 12.5–15 µm ($\bar{x}$ = 26.9 × 13.7 µm, n = 30), subglobose to oval, aseptate, hyaline to subhyaline with age, guttulate, without longitu-dinal striations and mucil.

Culture characteristics: On PDA, conidia germinated after 10 h. When transferred aseptically to fresh PDA and incubated at 25°C for 4 weeks, colonies covered the 60-mm plate; surface uneven, velvety, grey.

Material examined: China, Guizhou Province, Zunyi City, Suiyang County, Wangcao Town, Luobo Village, from decayed branches of *Edgeworthia chrysantha* (*Thymelaeaceae*), 13 February 2023, Xuemei Chen; original isolate SY10.

Note: *Lasiodiplodia chonburiensis* was described from dead leaves of Pandanus in Thailand by Tibpromma et al. (2018). Morphologically, our collection closely matches the type. In the phylogenetic tree (Figure 4.16), it clusters with *L. chonburiensis* without evident separation. Pairwise comparisons showed that there is 0.64% (3/469 bp) difference in ITS; 0.80% (2/249 bp) difference in *tef1-α*, and no difference (0/385 bp) in *tub2*. Based on combined morphological characters and multilocus phylogeny, we identified our collection as the known species, *Lasiodiplodia chonburiensis*. This is the first record of *L. chonburiensis* from decayed wood of *Edgeworthia chrysantha* in Guizhou, China.

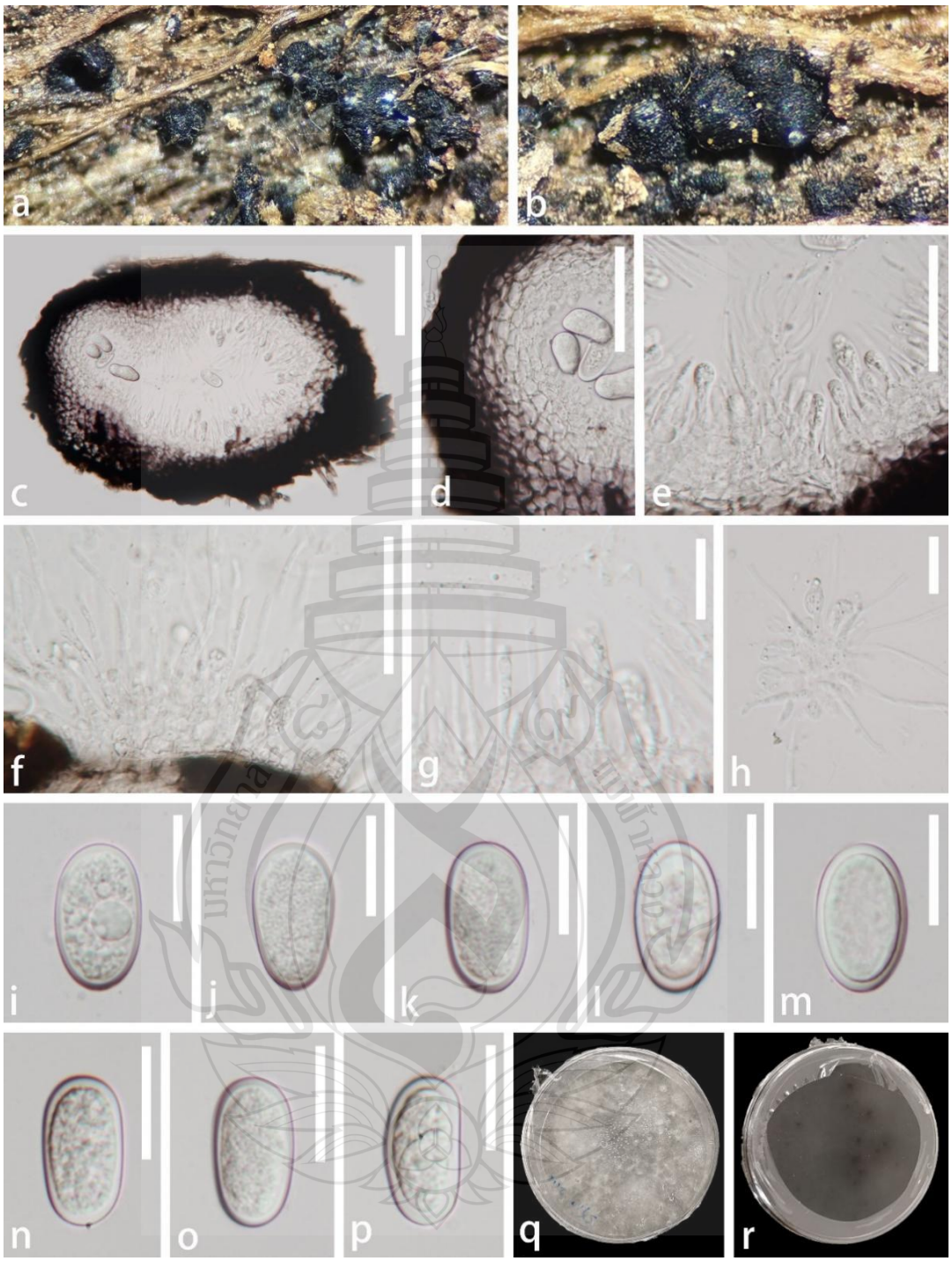

Figure 4.17 *Lasiodiplodia chonburiensis* (SY10, new host record)

Figure 4.17 a, b Conidiomata on dead branch of *Edgeworthia chrysantha*. c Vertical section of a conidioma. d Peridium. e–g Conidiophores bearing conidia. h Paraphyses. i–p Conidia. q colony on PDA, forward. r colony on PDA, reverse. Scale bars: c = 100 µm, d–f = 50 µm, g, p = 20 µm.

Kirschsteiniotheliales Hern.-Restr., R.F. Castañeda, Gené & Crous, Stud. Mycol. 86: 72 (2017)

Kirschsteiniotheliaceae Boonmee & K.D. Hyde, Mycologia 104 (3): 705 (2012)

Kirschsteiniothelia D. Hawksw., Bot. J. Linn. Soc. 91: 182 (1985)

Index Fungorum number: IF 25723; *Facesoffungi number*: FoF 08040

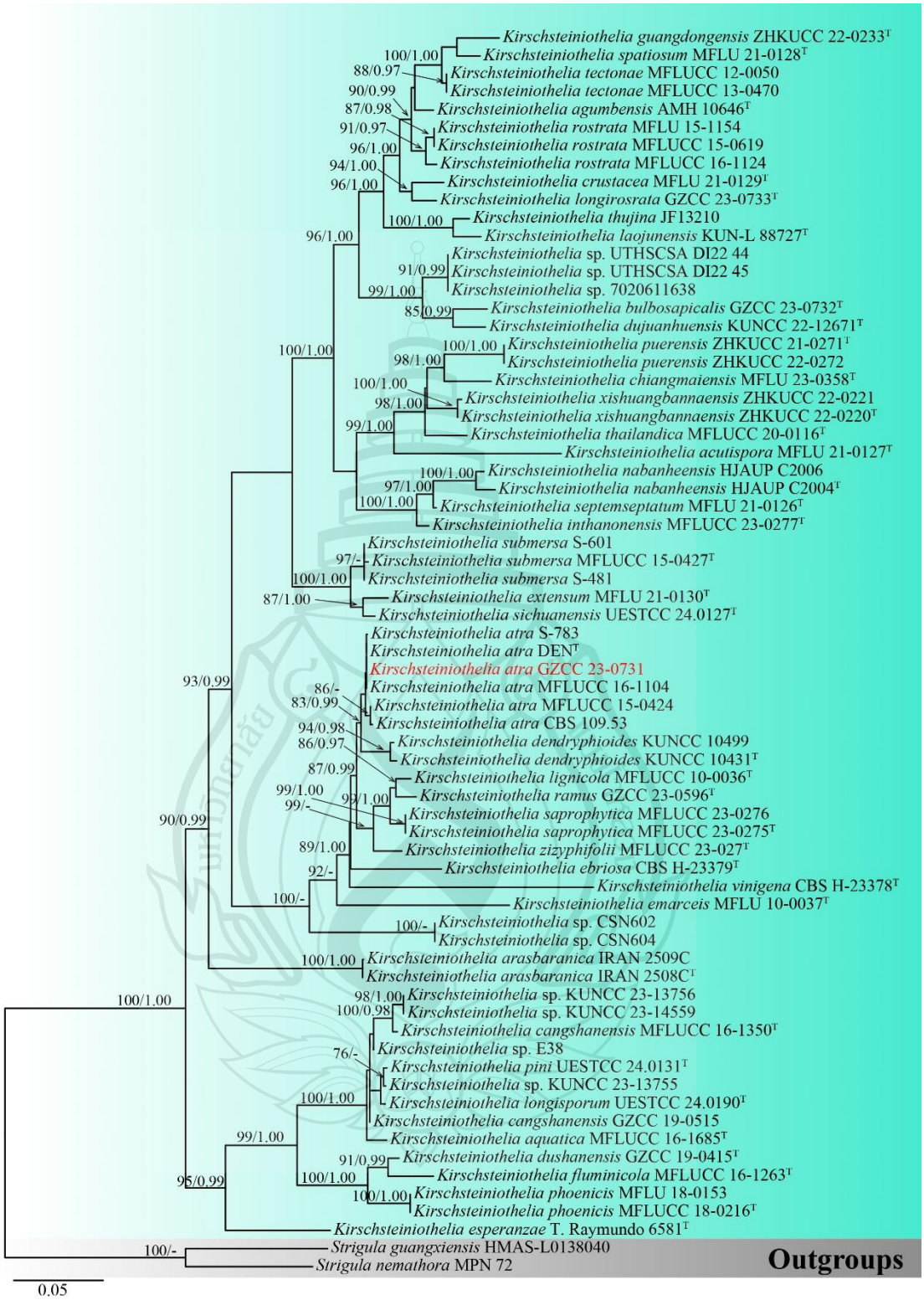

Figure 4.18 Phylogram of *Kirschsteiniothelia*

Figure 4.18 Phylogram of *Kirschsteiniothelia* taxa, based on the RAxML analysis of the combined ITS, LSU and SSU rDNA sequence dataset. Bootstrap support values for Maximum Likelihood (ML) equal to or greater than 75% and Bayesian posterior probabilities (PP) equal to or greater than 0.95 are shown above the nodes. The tree is rooted with *Strigula guangxiensis* (HMAS-L0138040) and *S. nemathora* (MPN 72). Newly-generated strains are denoted in red and type strains are indicated with a superscript 'T'.

Kirschsteiniothelia atra (Corda) D. Hawksw., Fungal Diversity 69: 37 (2014); Figure 4.19

≡ *Amphisphaeria aethiops* Sacc., Syll. fung. (Abellini) 1: 722 (1882)

= *Dendryphiopsis atra* (Corda) S. Hughes, Can. J. Bot. 31: 655 (1953)

≡*Dendryphion atrum* Corda, Icon. fung. (Prague) 4: 33 (1840)

≡*Kirschsteiniothelia aethiops* (Sacc.) D. Hawksw., J. Linn. Soc., Bot. 91(1–2): 185 (1985)

Saprobic on decaying wood of *Edgeworthia chrysantha*. **Sexual morph**: see Hawksworth (1985). **Asexual morph**: *Colonies* on the natural substrate superficial, effuse, gregarious, dark brown to black, glistening. *Mycelium* immersed, composed of branched, septate, thin-walled, smooth, brown hyphae. *Conidiophores* 253–396 × 8–15.5 µm ($\overline{x}$ = 334.6 × 11.7 µm, n = 20), macronematous, mononematous, erect, straight or flexuous, cylindrical, septate, smooth, brown to dark brown, becoming paler towards the apex and comprising numerous short branches. *Conidiogenous cells* 14.5–29 × 5–10 µm ($\overline{x}$ = 20.6 × 6.8 µm, n = 30), tretic, integrated, sometimes percurrent, terminal, doliiform or lageniform, subhyaline to pale brown, with new cells developing from the apical or subapical part of the subtending cells. *Conidia* 32–56.5 × 11–19.5 µm ($\overline{x}$ = 42.3 × 14.5 µm, n = 30), solitary, acrogenous, cylindrical, sometimes clavate, 3–4-septate, con-stricted and darker at the septa, smooth, brown and rounded at the apex.

Culture characteristics: Conidia germinating on Potato Dextrose Agar (PDA) within 24 h, and pro-ducing germ tubes either from the apex or base. Colonies circular, flat, dense, radial sulcate, edge entire, pearl-gray on the surface, dark brown on the reverse and becoming grey-white along the margin.

Material examined: China, Guizhou Province, Zunyi City, Suiyang County, saprobic on decaying branches of *Edgeworthia chrysantha*, 13 February 2023, Xue-

Mei Chen, SY12 (GZAAS 23-0807), living culture GZCC 23-0731.

Note: Morphologically, our collection matches the characteristics of *Kirschsteiniothelia atra*, including macronematous, mononematous conidiophores with numerous short branches; tretic, doliiform, or lagen-iform conidiogenous cells that develop new cells from the apical or subapical part of the subtending cells; and cylindrical, occasionally clavate conidia that are 3–4-septate, constricted and darker at the septa, which are rounded at the apex (Su et al., 2016). In the phylogenetic analyses, our collection (GZCC 23-0731) clusters with *Kirschsteiniothelia atra* (CBS 109.53, DEN, MFLUCC 15-0424, MFLUCC 16-1104 and S–783) (Figure 4.18). Excluding gaps, no difference was observed in the comparison of nucleotides across the ITS (491 bp), LSU (788 bp) and SSU (844 bp) regions between our collection and Kirschsteiniothelia atra (MFLUCC 16-1104). Based on these findings, we identify our isolate as *Kirschsteiniothelia atra*, following the guide-lines established by Jeewon and Hyde (2016) and Maharachchikumbura et al. (2021). This is the first time *Kirschsteiniothelia atra* has been reported from *Edgeworthia chrysantha*.

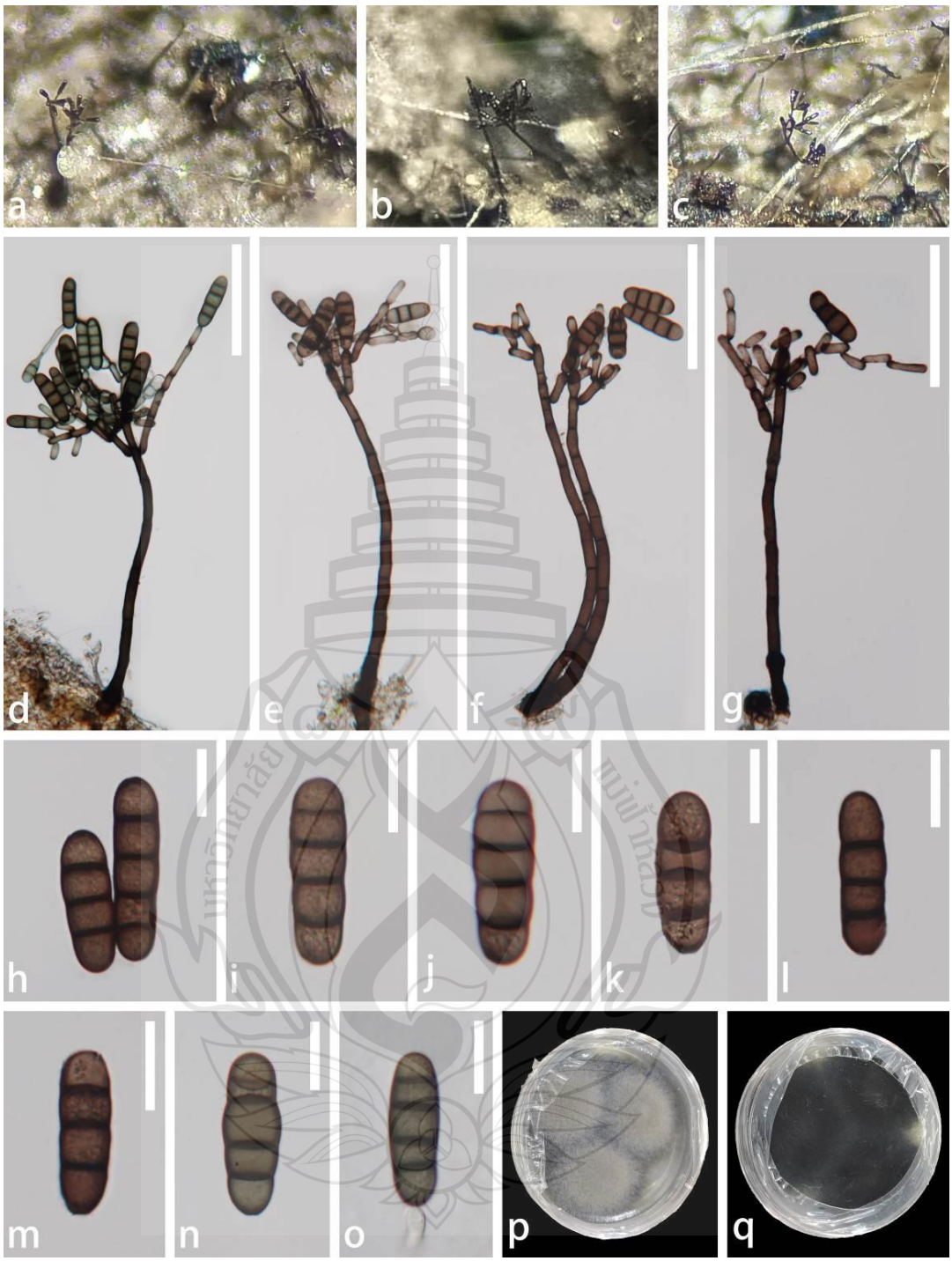

Figure 4.19 *Kirschsteiniothelia atra* (GZAAS 23-0807, new host record)

Figure 4.19 a–c Colonies on natural substrate. d–g Conidiophores and conidiogenous cells bearing conidia. h–n Conidia. o A germinated conidium. p Upper surface view of culture. q Lower surface view of culture. Scale bars: (d–g) = 100, (h–o) = 20 μm.

Pleosporales Luttr. ex M.E. Barr, Prodromus to class Loculoascomycetes: 67 (1987)

Corynesporascaceae Sivan., Mycol. Res. 100: 786 (1996)

Corynespora Güssow, J. Roy. Agric. Soc. England 65: 272 (1905)

Index Fungorum number: IF 92201; *Facesoffungi number*: FoF 06663

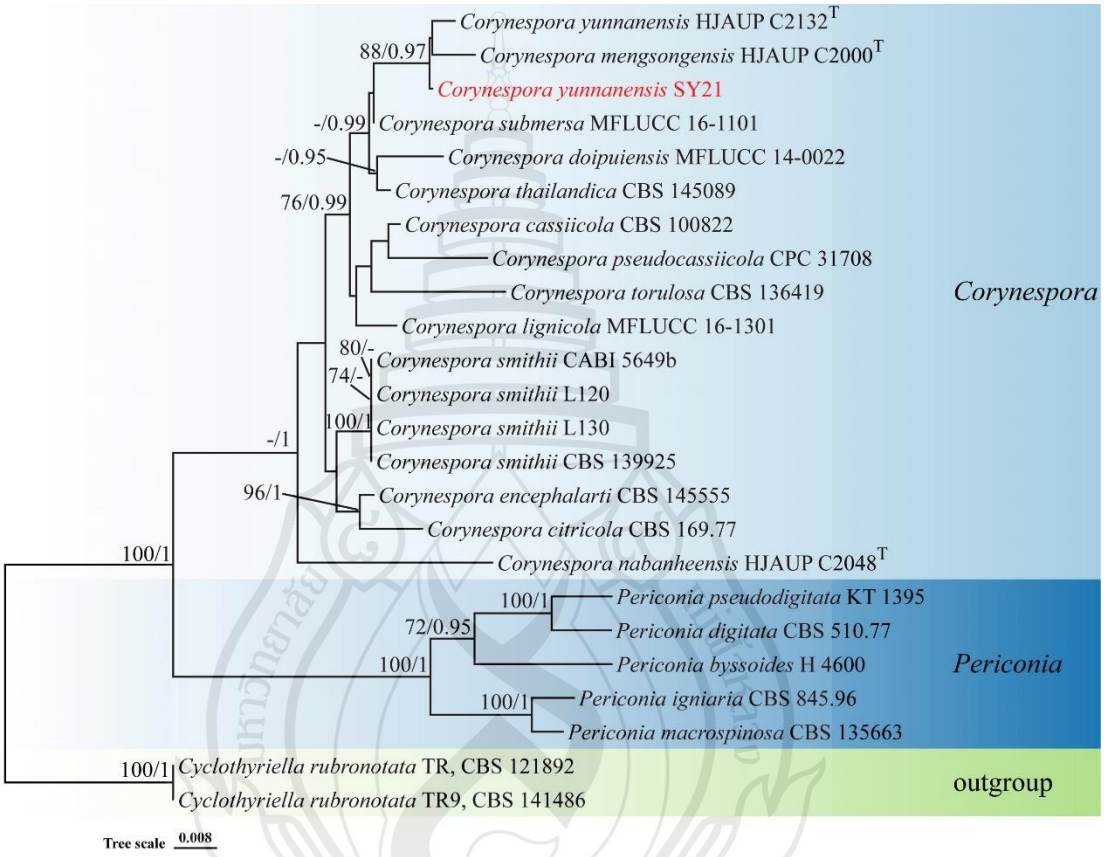

Figure 4.20 Phylogenetic analysis of *Corynespora*

Figure 4.20 Phylogenetic analysis of *Corynespora* was conducted using RAxML-based maximum likelihood analysis of a combined ITS and LSU sequence dataset. Bootstrap support values for maximum likelihood (ML) equal to or greater than 70% and Bayesian posterior probabilities (PP) equal to or greater than 0.95 are shown above the nodes. The tree is rooted with *Cyclothyriella rubronotata* (CBS 121892 and CBS 141486). Newly generated strains are highlighted in red, and type strains are indicated with a superscript ‘T’.

Corynespora yunnanensis Jing W. Liu & Jian Ma, J. Fungi 9 (1, no. 107): 11 (2023), Figure 4.21

Saprobic on *Edgeworthia chrysantha*. **Sexual morph**: undetermined. **Asexual morph**: Hyphomycete. *Colonies* on natural substratum are effuse, off white to pale brown and hairy. *Mycelium* are superficial and immersed, composed of branched, septate, pale green to brown, smooth-walled hyphae. *Conidiophores*178–445 µm × 8.5–17 µm ($\overline{x}$ = 302.1 × 12.1 µm, n = 30) macronematous, mononematous, unbranched, erect, straight or flexuous, cylindrical, smooth, septate and brown to dark brown, with 1–2 successive cylindrical extensions. *Conidiogenous cells* 14.5–49 µm × 7.5–12.5 µm ($\overline{x}$ = 26.4 × 10.3 µm, n = 30) are integrated, terminal, smooth, cylindrical and pale brown to brown. *Conidia* 106–180.5 µm × 11.5–23 µm ($\overline{x}$ = 145.1 × 18.6 µm, n = 20) acrogenous, solitary, obclavate, rostrate, rounded at the apex, straight or slightly curved, 0–23-distoseptate, pale green to brown and smooth, tapering near the apex, and truncated at the base with a protuberant dark brown hilum at the base.

Culture characteristics: On PDA, conidia germinated after 10 h. When transferred aseptically to fresh PDA and incubated at 25°C for 4 weeks, colonies reached 35 mm in diameter; colony outline elliptical; surface even, margin entire, velvety; colony grey-white.

Material examined: China, Guizhou Province, Zunyi City, Suiyang County, from decayed twigs of *Edgeworthia chrysantha* (*Thymelaeaceae*), 13 February 2023, Xuemei Chen; original isolate SY21.

Note: *Corynespora yunnanensis* was described by Liu et al. (2023) from decorticated dead branches of an unidentified broad-leaved tree in Yunnan, China. Morphologically, our isolate ressemble with *C. yunnanensis*: conidiophores straight to curved, unbranched, bearing 1–2 cylindrical apical extensions with terminal conidiogenous cells; conidia solitary, obclavate. In the phylogenetic analyses (Figure 4.20), the isolate clusters with *C. yunnanensis*, with no pairwise differences of ITS (555 bp) and SSU (907 bp) and LSU 1/546 bp (0.18%). Based on combined morphological and phylogenetic evidence, we identify the fungus as *Corynespora yunnanensis*. This is the first record of *C. yunnanensis* from decayed wood of *Edgeworthia chrysantha* in Guizhou, China.

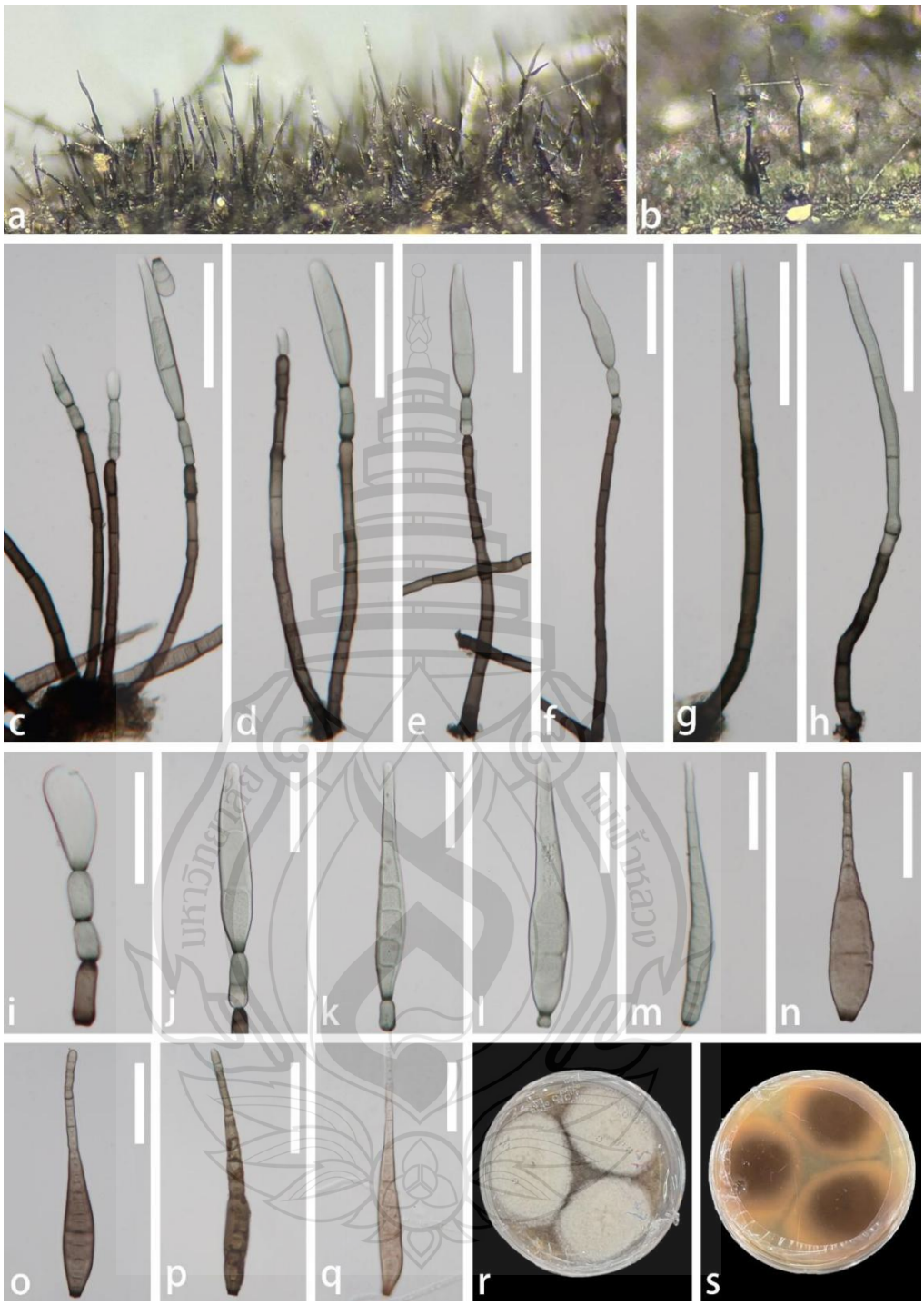

Figure 4.21 *Corynespora yunnanensis* (SY21, new host record)

Figure 4.21 a, b Colonies on natural substrate. c–h Conidiophores with conidiogenous cells bearing conidia. i–p Conidiogenous cells and conidia. q Germinated conidium. r Colony on PDA, forward. s Colony on PDA, reverse. Scale bars: c–h = 100 µm, i–q = 50 µm.

Phaeoseptaceae Boonmee, Thambug. & K.D. Hyde, Mycosphere 9 (2): 323 (2018)

Pleopunctum N.G. Liu, K.D. Hyde & Jian K. Liu, Mycosphere 10 (1): 767 (2019)

Index Fungorum number: IF 556522; *Facesoffungi number*: FoF 06113

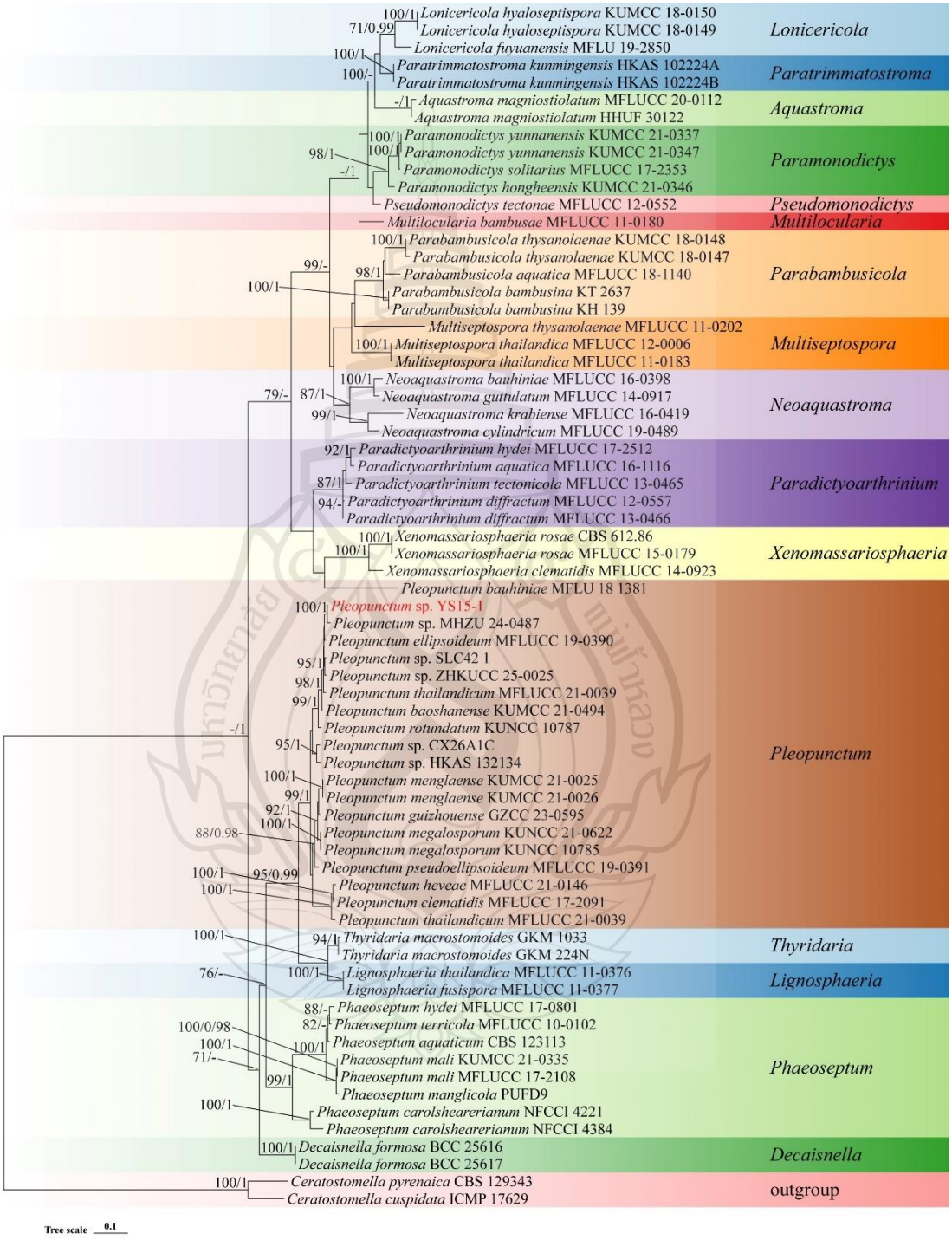

Figure 4.22 Phylogenetic analysis of *Pleopunctum*

Figure 4.22 Phylogenetic analysis of *Pleopunctum* was conducted using RAxML-

based maximum likelihood analysis of a combined ITS and LSU sequence dataset. Bootstrap support values for maximum likelihood (ML) equal to or greater than 70% and Bayesian posterior probabilities (PP) equal to or greater than 0.95 are shown above the nodes. The tree is rooted with *Ceratostomella cuspidata* (ICMP 17629) and *C. pyrenaica* (CBS 129343). Newly generated strains are highlighted in red, and type strains are indicated with a superscript 'T'.

Pleopunctum sp. MHZU 24-0487 Figure 4.23

Saprobic on dead wood of *Edgeworthia chrysantha*. **Sexual morph**: Undetermined. **Asexual morph**: Hyphomycetous. *Colonies* on natural substrate superficial, brown, scattered, gregarious, punctiform. *Mycelium* superficial, composed of septate, branched, greyish brown hyphae. *Conidiophores* 6.5–23 µm × 1.5–3 µm wide ($\overline{x}$ = 18.4 × 2 µm, n = 20), macronematous, mononematous, cylindrical, branched, septate, pale brown, smooth-walled, thick-walled. *Conidiogenous cells* monoblastic, terminal, integrated, brown. *Conidia* 41–59 × 22–32.5 µm ($\overline{x}$ = 50 × 26.5 µm, n = 30), acrogenous, solitary, muriform, constricted at septa, oval to ellipsoidal, smooth-walled, pale green to brown, broadly obtuse at apex and dark brown, truncate at base, often with a hyaline, elliptical to globose basal cell 8–19 µm × 12–19 µm ($\overline{x}$ = 13.8 × 16.1 µm, n = 30).

Culture characteristics: On PDA, conidia germinated after 10 h. When transferred aseptically to fresh PDA and incubated at 25 °C for 4 weeks, colonies reached 15 mm in diameter; colony circular, surface raised, margin entire; colony yellow-brown.

Material examined: China, Guizhou Province, Zunyi City, Suiyang County, from decayed branches of *Edgeworthia chrysantha* (*Thymelaeaceae*), 13 February 2023, Xuemei Chen; original isolate SY15.1.

Note: The new isolate clusters with *Pleopunctum* sp. MHZU 24-0487 with 100% statistical support in the LSU-ITS phylogenetic analyses (Figure 4.22). There are 0.3% and 1.3% base pair differences between the two strains with regards to LSU and ITS respectively, indicating insignificant genetic variation to differentiate the two strains as different species. *Pleopunctum* sp. MHZU 24-0487 has been isolated from *Livistona chinensis* in Jiangxi Province, China (REF). The present strain was isolated from *Edgeworthia chrysantha* in Guizhou Province, China. The isolate is therefore herein reported as a new host record from a different province in China.

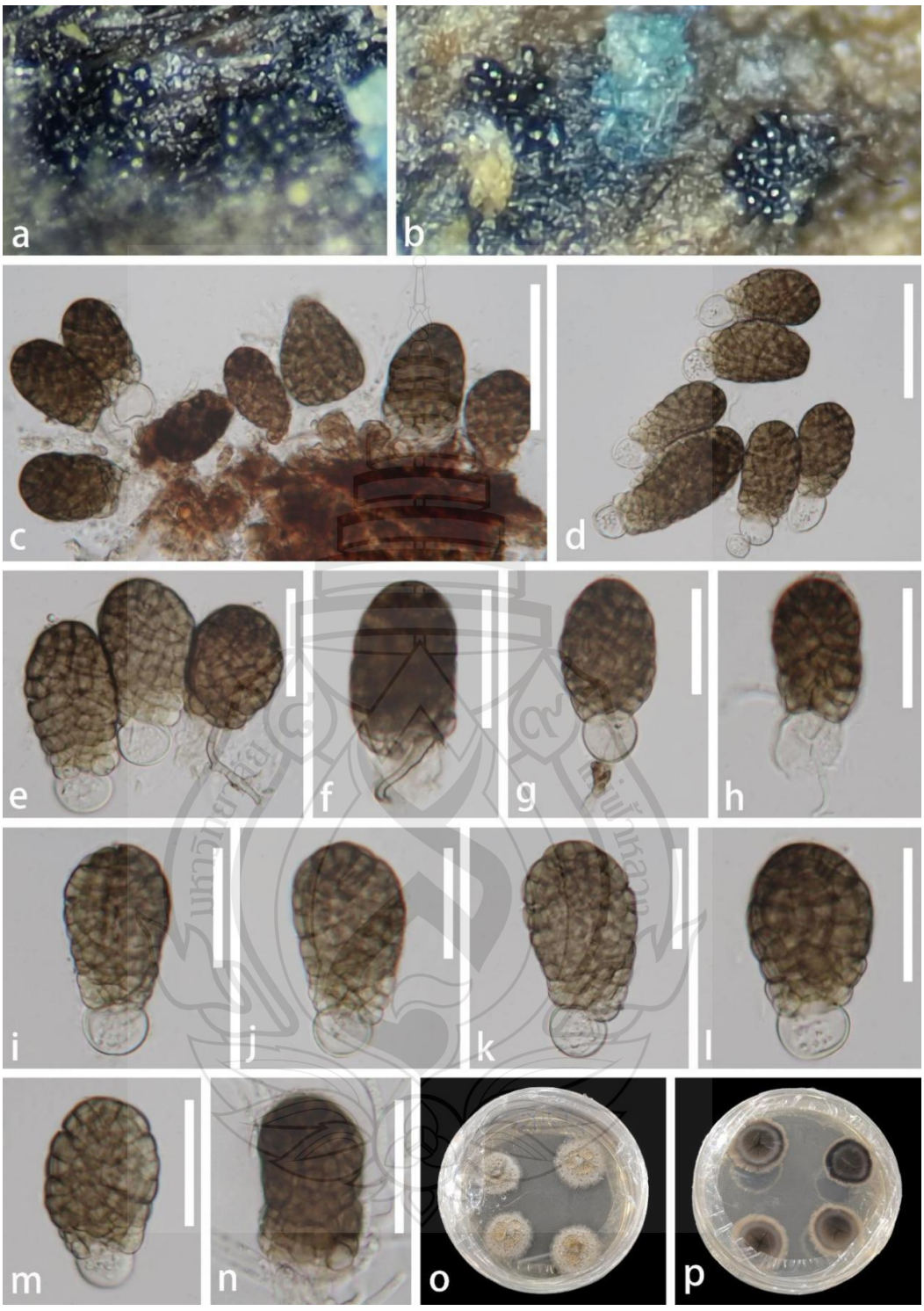

Figure 4.23 Pleopunctum sp. (SY15.1, new host record)

Figure 4.23 a, b Colonies on natural substrate. c, d, i–m Conidia and basal hyaline cells. e–h Conidiophores and conidia. n Germinating conidia. o Colony on PDA (obverse) p Colony on PDA (reverse). Scale bars: c, d = 50 µm, e–n = 20 µm.

Thyridariaceae Q. Tian & K.D. Hyde, Fungal Diversity 63 (1): 254 (2013)

Thyridaria Sacc., Mycoth. Ven. Cent. II: 21 (1875)

Index Fungorum number: IF 5463*; Facesoffungi number*: FoF 08375

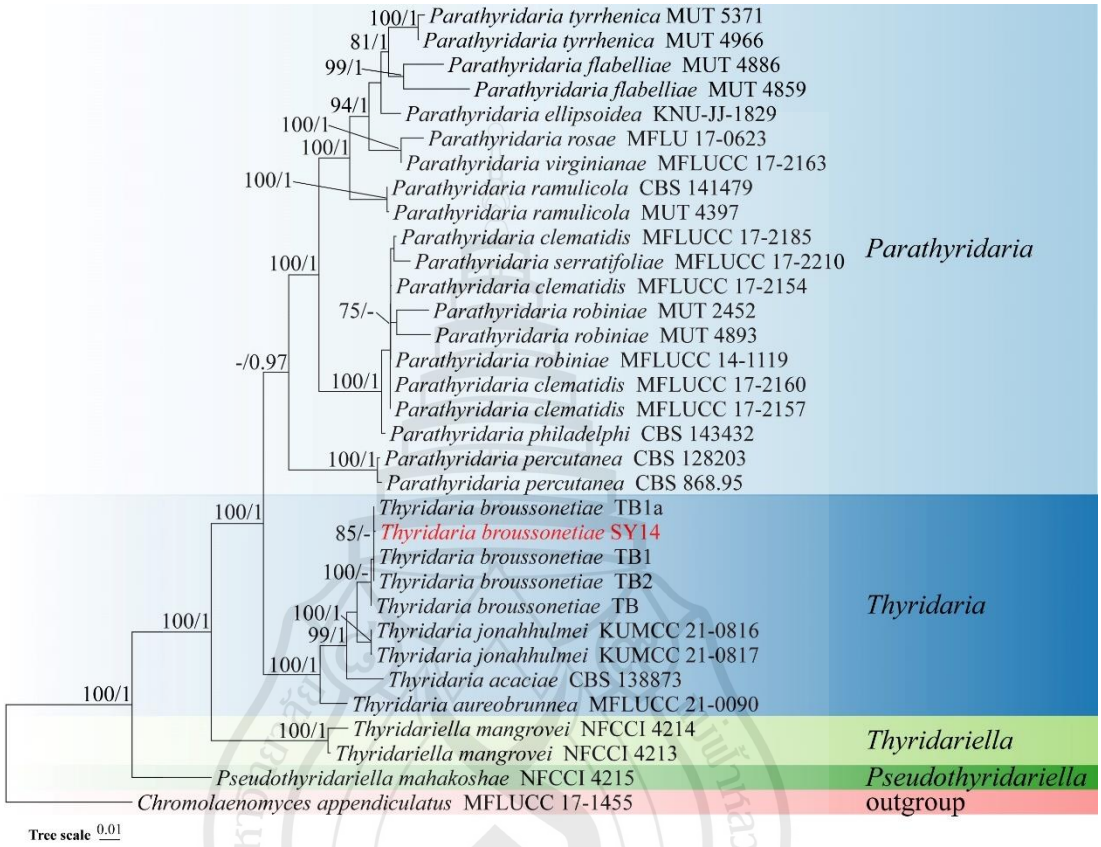

Figure 4.24 Phylogenetic analysis of *Thyridaria*

Figure 4.24 Phylogenetic analysis of *Thyridaria* was conducted using RAxML-based maximum likelihood analysis of a combined ITS, LSU, SSU, *tef1-α* and *rpb2* sequence dataset. Bootstrap support values for maximum likelihood (ML) equal to or greater than 70% and Bayesian posterior probabilities (PP) equal to or greater than 0.95 are shown above the nodes. The tree is rooted with *Chromolaenomtces appendiculatus* (MFLUCC 17-1455). Newly generated strains are highlighted in red, and type strains are indicated with a superscript 'T'.

Thyridaria broussonetiae (Sacc.) Traverso, Flora Italica Cryptogama 1(1): 301 (1906), Figure 4.25

Saprobic on *Edgeworthia chrysantha*. **Sexual morph**: Colonies on natural substratum are effuse, white and hairy. *Ascomata*, solitary or gregarious, immersed, coriaceous, black, globose to subglobose, ostiolate. *Peridium* 25–56 µm wide, wider at the apex, composed with two layers, with outer stratum comprising black, compressed, thick-walled cells of textura angularis, and inner stratum multi-layered and dark brown cells of textura angularis. *Hamathecium* 55–78 µm × 2–3.5 µm ($\overline{x}$ = 72.2 × 3.6µm, n = 5), comprised of branched, septate, cellular pseudoparaphyses, embedded in a gelatinous matrix. *Asci* 92.5–184.5 µm × 13–18 µm ($\overline{x}$ = 126.1×15.1 µm, n = 30), 8-spored, bitunicate, cylindrical to cylindric-clavate, long pedicellate (30–55 µm), and apex rounded with an ocular chamber. *Ascospores* 17–25.5 µm × 6.5–9 µm ($\overline{x}$ = 21.5 × 7.8 µm, n = 30), one-to-two-seriate, overlapping, and pale yellowish brown or dark green when young, turning yellowish brown to black at maturity, narrowly ellipsoid to fusoid, ends narrowly rounded (sometimes pointed), straight or curved, one-to-three-transversely septate, with median euseptum, slightly constricted at the septa, containing several guttules, with surface finely punctate. Asexual morph: undetermined.

Culture characteristics: On PDA, conidia germinated after 10 h. When transferred aseptically to fresh PDA and incubated at 25 °C for 4 weeks, colonies reached 25 mm in diameter; colony circular with an even, raised surface and entire margin; colony white.

Material examined: China, Guizhou Province, Zunyi City, Suiyang County, from decayed branches of *Edgeworthia chrysantha* (*Thymelaeaceae*), 13 February 2023, Xuemei Chen; original isolate SY14.

Note: *Thyridaria broussonetiae* was described by Traverso (1906) from Spain. Morphologically, our collection resembles the type material of *T. broussonetiae*. In phylogenetic analyses (Figure 4.24), our collection clusters with *T. broussonetiae* (TB1a, TB1, TB2, TB) with maximal support (ML = 100%). Pairwise comparisons between our collection and *T. broussonetiae* (TB1a) show 0.2% (2/863 bp) divergence in ITS, no differences in LSU and SSU, 0.5% (5/1045 bp) in rpb2, and 0.4% (3/709 bp) in *tef1-α*. Based on this evidence, we identify our material as *Thyridaria broussonetiae*. This represents the first record of *T. broussonetiae* from decayed wood of *Edgeworthia*

chrysantha in Guizhou, China.

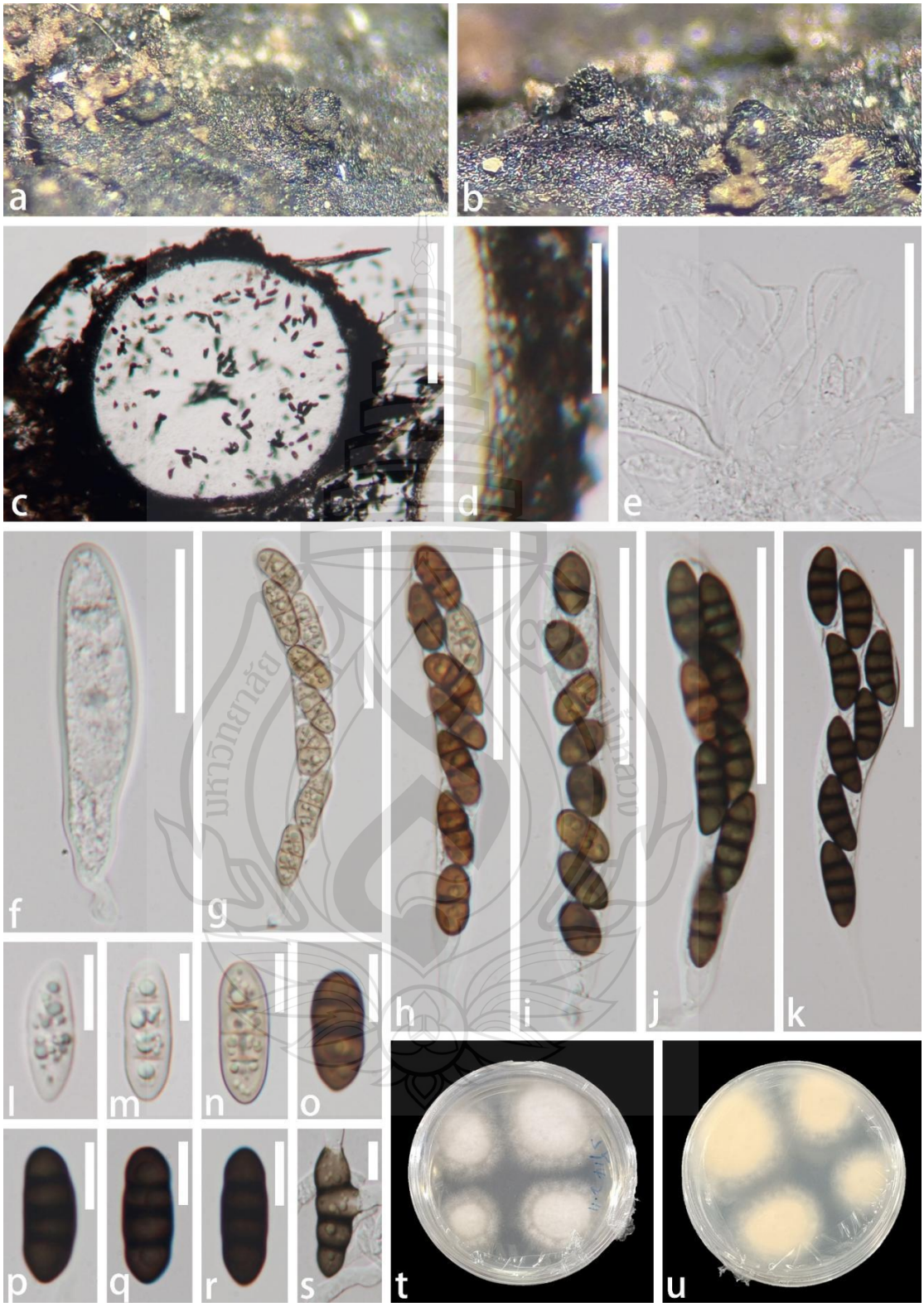

Figure 4.25 *Thyridaria broussonetiae* (SY14, new host record)

Figure 4.25 a–b Ascomata on natural substrate. c Vertical section of the ascoma. d Peridium. e Pseudoparaphyses. f–k Asci. l–s Ascospores. t Colony on PDA, surface view. u Colony on PDA, reverse view. Scale bars: c = 200 µm, d, e, g–k = 50 µm, f = 20 µm, l, s = 10 µm.

Torulaceae Corda, Deutschlands Flora, Abt. III. Die Pilze Deutschlands 2: 71 (1829)

Neopodoconis Rifai, Reinwardtia 12 (4): 277 (2008)

Index Fungorum number: IF 569714; *Facesoffungi number*: FoF 17030

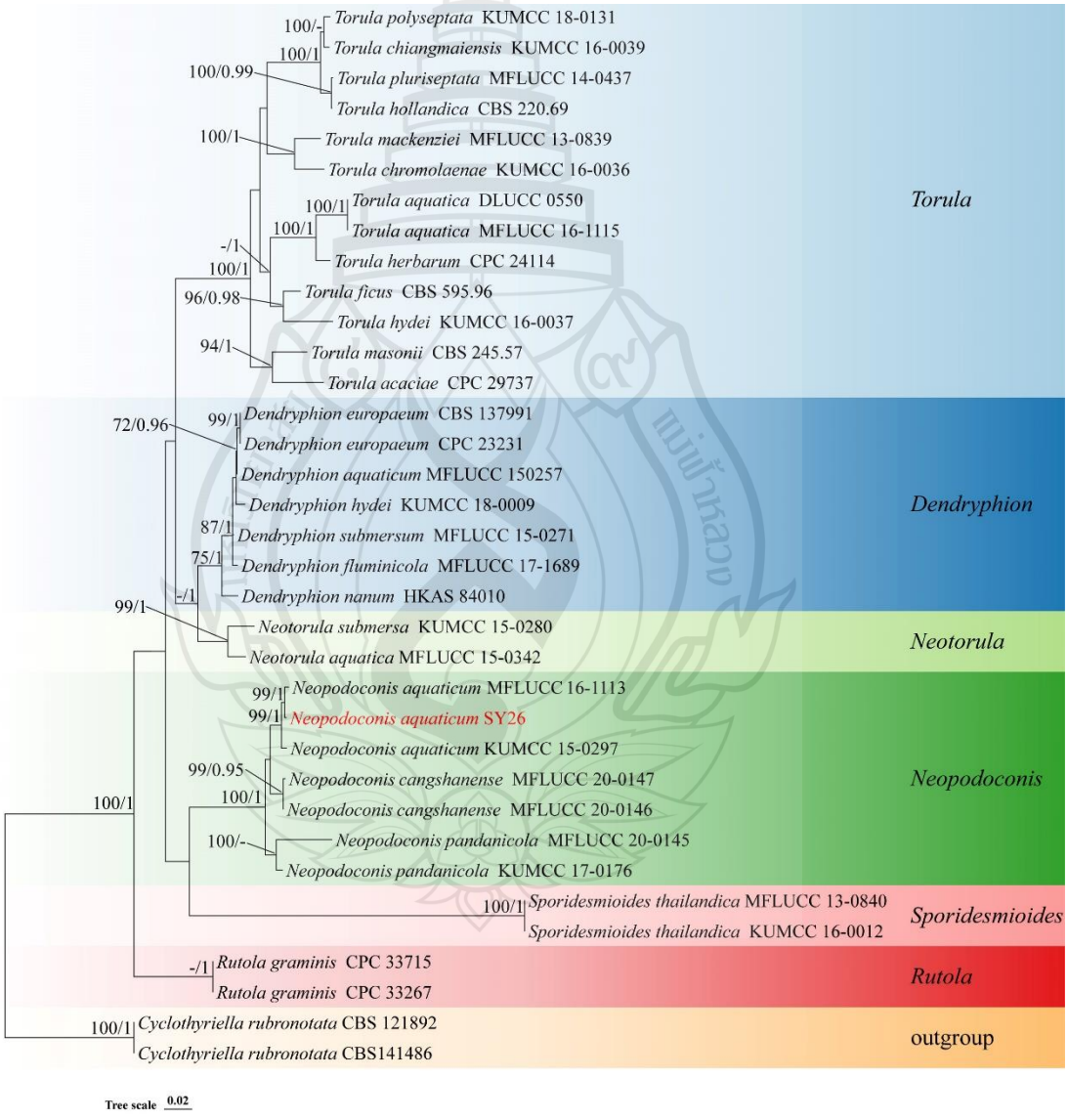

Figure 4.26 Phylogenetic analysis of *Neopodoconis*

Figure 4.26 Phylogenetic analysis of *Neopodoconis* was conducted using RAxML-based maximum likelihood analysis of a combined ITS, LSU, SSU, *tef1-α* and *rpb2* sequence dataset. Bootstrap support values for maximum likelihood (ML) equal to or greater than 70% and Bayesian posterior probabilities (PP) equal to or greater than 0.95 are shown above the nodes. The tree is rooted with *Cyclothyriella rubronotata* (CBS 121892 and CBS 141486). Newly generated strains are highlighted in red, and type strains are indicated with a superscript 'T'.

Neopodoconis aquaticum (Z.L. Luo, K.D. Hyde & H.Y. Su) Y.F. Hu, L. Qiu, R.F. Castañeda & Jian Ma, (2022); Figure 4. 27

Saprobic on *Edgeworthia chrysantha*. **Sexual morph**: Undetermined. **Asexual morph**: *Colonies* effuse on natural substrate, scattered, white. *Mycelium* immersed in the substrate, composed of white, septate, unbranched hyphae. *Conidiophores* 276–393.5 × 9.5–14 µm ($\overline{x}$ = 329.8 × 11.5 µm, n = 20) macronematous, mononematous, erect, septate, smooth, straight or slightly flexuous, pale brown to brown, paler at apex. *Conidiogenous cells* 20.5–56 × 9.5–17 µm ($\overline{x}$ = 35.6 × 12.2 µm, n = 20) monotretic or polytretic, sympodial, integrated, terminal, cylindrical, with 1 successive cylindrical extensions, brown. *Conidia* 94.5–160 µm × 18–29 µm ($\overline{x}$ = 116.4 × 23.4 µm, n = 20) solitary, dry, fusiform to pyriform, rostrate at maturity, yellowish brown to black, with guttulate cells, thickly cicatrized at the base, with a thick, black truncate scar at base and pale pigment cell above the scar, wide in the middle, narrowly cylindrical, obtuse, and subhyaline at apex, 7–9-septate, slightly constricted at some septa, smooth.

Culture characteristics: On PDA, conidia germinated after 10 h. When transferred aseptically to fresh PDA and incubated at 25°C for 4 weeks, colonies reached 40 mm in diameter; colony circular with even surface and entire margin; centre creamy white, margin translucent white.

Material examined: China, Guizhou Province, Zunyi City, Suiyang County, from decayed branches of *Edgewortia chrysantha* (*Thymelaeaceae*), 13 February 2023, coll. Xuemei Chen; original isolate SY26.

Note: *Neopodoconis aquaticum* was previously described by Su et al. (2018) from decaying wood in Yunnan, China and named *Rostriconidium aquaticum*; later it was transferred to *Neopodoconis* by Qiu et al. (2022). Morphologically, our collection ressamble to *N. aquaticum,* such as fusiform to pyriform conidia with a black, truncate

basal scar and pale pigmented cells, and conidiophores with continuous cylindrical apical extensions. In phylogenetic analyses (Figure 4.27), our collection is sister to *N. aquaticum* (MFLUCC 16-1113 and KUMCC 15-0297). The comparision of nuclieted between them shouwed there is 0.2% (1/540 bp) difference in ITS, no difference (540 bp) in LSU and 0.6% (4/686 bp) difference in *rpb2*. Based on the finds, we therefore identified it as the known species, *N. aquaticum*. This represents the first record of *N. aquaticum* from decayed wood of *Edgeworthia chrysantha*.

Figure 4.27 *Neopodoconis. aquaticum* (SY26, new host record)

Figure 4.27 a–b Colonies on natural substrate. c Conidiophore with conidiogenous cells bearing conidia. d–e Conidiophores. f–h Conidiogenous cells. i, o Conidia. p Colony on PDA (surface view). q Colony on PDA (reverse view). Scale bars: c–e = 100 µm, f–h = 50 µm, i–o = 20 µm.

Lecanoromycetes O.E. Erikss. & Winka, Myconet 1: 7 (1997)

Ostropales Nannf., Nova Acta Regiae Soc. Sci. Upsal. Ser. 4, 8 (2): 68 (1932)

Stictidaceae Fr., Summa vegetabilium Scandinaviae 2: 345, 372 (1849)

Fitzroyomyces Crous, Persoonia 39: 389 (2017)

Index Fungorum number: IF 823395

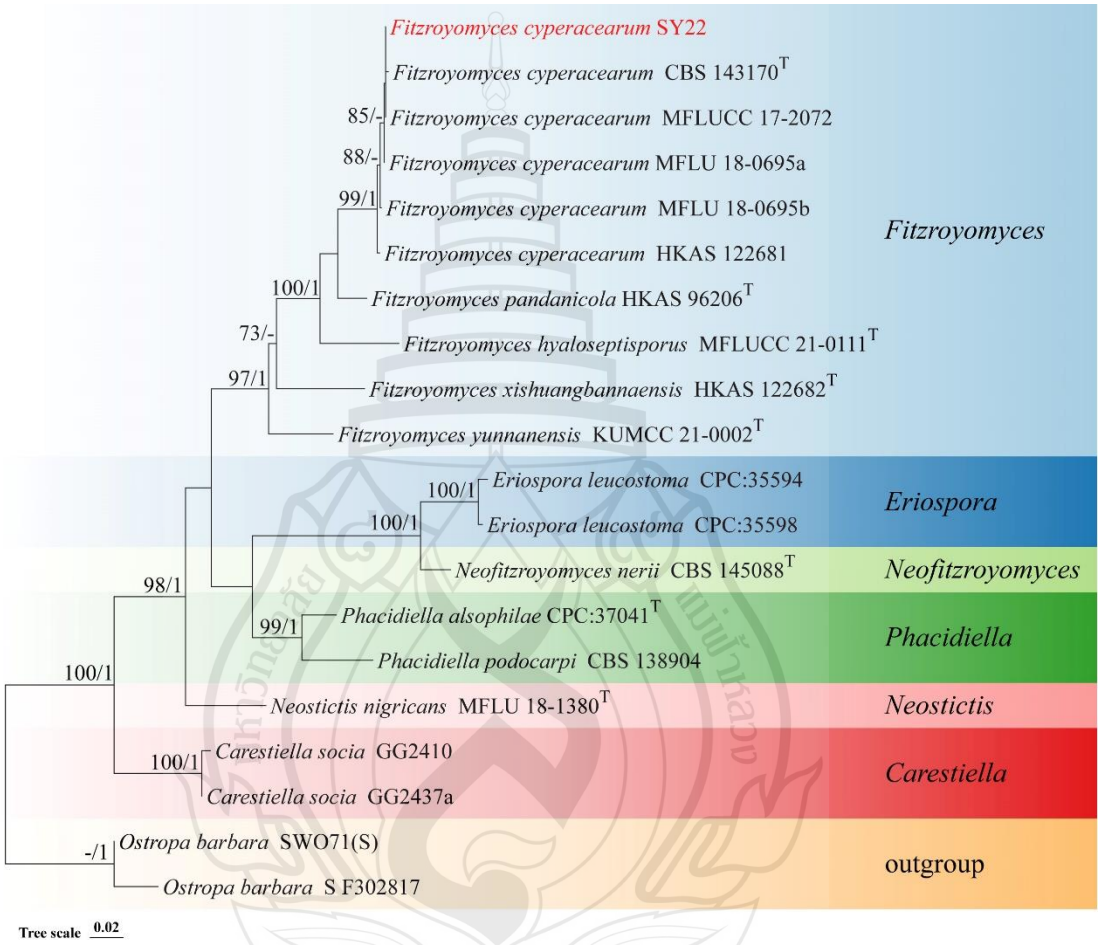

Figure 4.28 Phylogenetic analysis of *Fitzroyomyces*

Figure 4.28 Phylogenetic analysis of *Fitzroyomyces* was conducted using RAxML-based maximum likelihood analysis of a combined LSU and ITS sequence dataset. Bootstrap support values for maximum likelihood (ML) equal to or greater than 70% and Bayesian posterior probabilities (PP) equal to or greater than 0.95 are shown above the nodes. The tree is rooted with *Ostropa barbara* (SWO 71-S and S-F302817). Newly generated strains are highlighted in red, and type strains are indicated with a superscript ‘T’.

Fitzroyomyces cyperacearum Crous, Persoonia 39: 389 (2017); Figure 4.29

Saprobic on *Edgeworthia chrysantha*. **Sexual morph**: *Colonies* on natural substratum are effuse, white and hairy. *Apothecial* 380 µm high, 540 µm wide, subglobose, immersed in the substrate at first and opening by entire pore at maturity. Hypothecium convex. *Disc* deeply cupulate, whitish to cream, Margins white. Hymenium hyaline, enclosed in a thick gelatinous matrix. *Epithecium* absent. *Excipulum* composed of cells of textura intricata. *Paraphyses* 150 µm long, 1.5 µm wide, numerous, filiform, septate, wide at the apex, unbranched. *Asci* 162–200.5 µm × 9–16.5 µm ($\overline{x}$ = 186.1 × 12.7 µm, n = 10), 8-spored, unitunicate, cylindric-clavate and broadest at the middle, short sessile, rounded at the apex. *Ascospores* 111–224 µm × 2.5–4 µm ($\overline{x}$ = 150.1 × 3.2 µm, n = 10), filiform, multiseptate, hyaline, guttulate when immature. **Asexual morph**: Undetermined.

Culture characteristics: On PDA, conidia germinated after 10 h. When transferred aseptically to fresh PDA and incubated at 25°C for 4 weeks, colonies reached 15 mm in diameter; colony circular; surface uneven and raised, margin entire, floccose; colony white.

Material examined: China, Guizhou Province, Zunyi City, Suiyang County, from rotten branches of *Edgeworthia chrysantha* (*Thymelaeaceae*), 13 February 2023, Xuemei Chen; original isolate SY22.

Note: *Fitzroyomyces cyperacearum* was introduced by Crous et al. (2017) from unidentified decaying wood in Yunnan, China. Morphologically, our collection was similar to the type species, *F. cyperacearum*. In the phylogenetic analyses (Figure 4.28), our collection clusters with *F. cyperacearum* with support of 85% in ML and xx in BYPP. Based on combined morphological and phylogenetic evidence, we identify our isolate as *Fitzroyomyces cyperacearum*. This represents the first report of *F. cyperacearum* from decayed wood of *Edgeworthia chrysantha*.

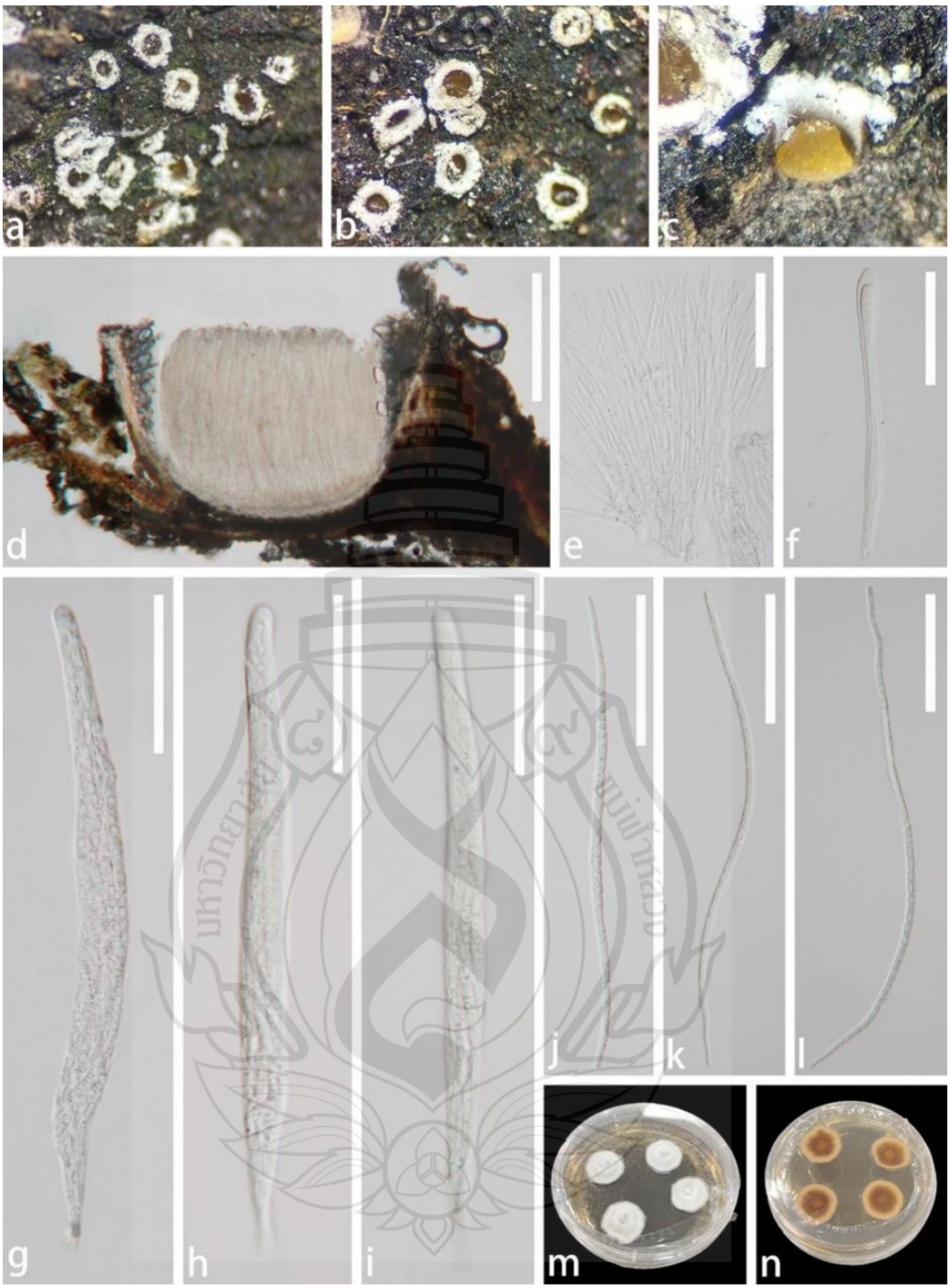

Figure 4.29 *Fitzroyomyces cyperacearum* (SY22, new host record)

Figure 4.29 a–c Colonies on natural substrate. d Vertical section of an apothecium. e Paraphyses. f–i Asci. j–l Ascospores. m Colony on PDA, obverse. n Colony on PDA, reverse. Scale bars: d = 200 µm, e–l = 50 µm.

4.3 Checklist of Fungi Associated with *Thymelaeaceae*

In this part, I present a checklist of fungi associated with *Thymelaeaceae* plants in China. In total, fungi are now known from seven host species in this family, and most of the recorded taxa are endophytes. Previous studies reported 92 fungal genera from *Aquilaria sinensis*, 2 genera from *Daphne odora*, 4 genera from *Edgeworthia chrysantha* and 18 genera from *Stellera chamaejasme*. In our study, we isolated 11 genera from *A. sinensis*, 7 of which, *Alternaria*, *Botryosphaeria*, *Curvularia*, *Diaporthe*, *Fusarium*, *Lasiodiplodia*, *Phoma* overlap with previously reported genera. From *E. chrysantha* we obtained 34 genera, with only one genus, *Fusarium*, overlapping with earlier studies. From *S. chamaejasme* I isolated 15 genera, including 2 genera, *Alternaria* and *Mucor* that were already known from this host. Before our work, three *Thymelaeaceae* species had not been investigated for their fungal communities: *Daphne odora 'Aureomarginata'*, *Daphne papyracea* and *Wikstroemia indica*. Our study therefore substantially expands the known fungal diversity associated with *Thymelaeaceae*. The number of host species examined for their fungal communities has increased from four to six, and we identified 80 fungal genera from different *Thymelaeaceae* hosts. As a result, the total number of genera reported from *A. sinensis* has increased to 96 genera from 92 genera, from *E. chrysantha* to 37 genera from 4 genera, and from *S. chamaejasme* to 31 from 18 genera, greatly enriching our understanding of fungal diversity and plant–fungus interactions within this family.

Table 4.1 Checklist of microfungi associated with Thymelaeaceae plants in China

Host species	Host genus	fungal Species/Genus	Substrate	Location	Reference
Aquilaria sinensis	*Aquilaria*	*Acrocalymma*, *Allophoma*, *Alternaria*, *Annulohypoxylon*, *Aspergillus*, *Aureobasidium*, *Banksiophoma*, *Bipolaris*, *Biscogniauxia*, *Botryosphaeria*, *Cephalosporium* sp., *Chaetomium*, *Cladophialophora* sp., *Cladorrhinum*, *Cladosporium*, *Colletotrichum*, *Coniella*, *Coniothyrium* sp., *Coprinopsis* sp., *Corynespora*, *Crassiparies*, *Curvularia*, *Cylindrocladium*, *Daldinia*, *Deniquelata*, *Diaporthe*, *Didymella*, *Epicoccum*, *Exophiala*, *Exserohilum*, *Fimetariella*, *Fomitiporia*, *Fomitopsis*, *Fonsecaea*, *Fusarium*, *Glomerularia*, *Guignardia*, *Hermatomyces*, *Hypocrea*, *Hypoxylon*, *Lasiodiplodia*, *Leptosphaerulina*, *Loculosulcatispora*, *Massaria*, *Medicopsis*, *Megacapitula*, *Meyerozyma*, *Monilia*, *Montagnula*, *Mortierella*, *Mucor*, *Mycelia*, *Mycosphaerella*, *Nectria*, *Nemania*, *Neodeightoni*a, *Neofusicoccum*, *Neopestalotiopsi*, *Neoscytalidium*, *Nigrograna*, *Nodulisporium*, *Ovulariopsis* sp., *Paracamarosporium*, *Paraconiothyrium*, *Paradictyoarthrinium*, *Penicillium*, *Periconia*, *Pestalotiopsis*, *Phaeoacremonium*, *Phanerochaetella*, *Phlebiopsis*, *Phoma*, *Phomopsis* sp., *Phyllosticta*, *Pichia*, *Pithomyces*, *Pleospora*, *Preussia*, *Pseudofusicoccum*, *Pseudopithomyces*, *Pseudorobillard*, *Purpureocillium*, *Ramichloridium*, *Rhinocladiella*, *Rhizomucor*, *Rhytidhysteron*, *Rigidoporus*, *Sagenomella*, *Scytalidium*, *Spergillus*, *Talaromyces*, *Trichoderma*, *Tricholoma*, *Trichosporon*, *Veronaea*, *Verticillium*, *Xenoroussoella*, *Xylaria*	low altitude mountains, hills and roadside sunny areas	Fujian, Guangdong, Guangxi, Hainan	Cui et al. (2011, 2013); Du et al. (2022a, 2022b); Liu et al. (2019); Wu et al. (2010); Tao et al. (2011); Li et al. (2011, 2022)

Table 4.1 (continued)

Host species	Host genus	fungal Species/Genus	Substrate	Location	Reference
Daphne odora 'Aureomarginata'	*Daphne*	*Alternaria, Colletotrichum, DiaportheNeofusicoccum, Phomopsis, Phyllosticta*	It usually occurs along forest margins, shaded mountain slopes, and moist, semi-shaded woodland edges.	mainly distributed in low-mountain and hilly areas along the Yangtze River Basin and regions to the south.	This study
Daphne odora	*Daphne*	*Phytophthora nicotianae*, *Phyllosticta capitalensis*	It occurs in warm, humid subtropical regions. It naturally occurs along forest margins, shaded or semi-shaded mountain slopes, shrublands, and moist woodland edges in low-mountain and hilly areas.	It is distributed in major cities of China	Cui et al. (2023); Hu et al. (2023)
Daphne papyracea	*Daphne*	*Beltrania*, *Botryosphaeria*, *Colletotrichum*, *Curvicladiella*, *Cytospora*, *Diaporthe*, *Didymella*, *Fusarium*, *Neofusicoccum*, *Phomopsis*, *Phyllosticta*, *Plurivorosphaerella*, *Preussia*, *Rhizopycnis*, *Sordaria*	It is a fertile, moist mountain that grows under dense forests or shrubs at an altitude of 700-2000 meters.	Guangdong, Guangxi, Guizhou, Hunan, Hubei, Sichuan, Yunnan and other provinces and regions	This study
Edgeworthia chrysantha	*Edgeworthia*	*Alternaria*, *Aspergillus* sp., *Boeremia*, *Botryosphaeria*, *Byssochlamys spectabilis*, *Colletotrichum*, *Corynespora*, *Curvularia*, *Daldinia*, *Diaporthe*, *Didymella*, *Epicoccum*, *Fitzroyomyces*, *Fusarium oxysporum*, *Fusarium* sp., *Hypoxylon*, *Irpex*, *Kirschsteiniothelia*, *Lasiodiplodia*, *Macrocybe*, *Microsporum*, *Neofusicoccum*, *Neopodoconis*, *Nigrospora*, *Penicillium purpurogenum*, P*ericonia*, *Phanerochaete*, *Phialocephala*, *Phialophora*, *Phlebia*, *Phlebiopsis*, *Phoma*, *Phomopsis*, *Phyllosticta*, P*leopunctum*, *Preussia*, *Pseudogymnoascus*, *Schizophyllum*, *Spadicoides*, *Sporormiella*, *Stagonospora*, *Thelonectria*, *Thyridaria*, *Trichoderma*	It is grown in moist fertile land.	Henan, Shaanxi and provinces south of the Yangtze River basin.	Zhang et al. (2015, 2016), Wu et al. (2018), Wang et al. (2022), This study

Table 4.1 (continued)

Host species	Host genus	fungal Species/Genus	Substrate	Location	Reference
Wikstroemia nutans var. nutans	*Wikstroemia*	*Coelomycetes*, *Hyphomycetes*	evergreen broad-leaved forest at 300-800-1650 meters above sea level	Fujian, Guangdong, Guangxi, Hainan, Hunan, Taiwan	Tang et al. (2003)
Wikstroemia indica	*Wikstroemia*	*Alternaria*, *Colletotrichum*, *Diaporthe*, *Fusarium*, *Mucor*, *Mycetinis*, *Neofusicoccum*, *Phomopsis*, *Phyllosticta*, *Preussia*, *Stenella wikslroemiae*, *Phaeoisariopsis williamsiae var. williamsiae*	open forests or on stony mountains in areas below 1500 meters above sea level	Fujian, Guangdong, Guangxi, Guizhou, Hunan, Hainan, Sichuan, Taiwan,Yunnan, Zhejiang and other provinces	Walker and White (1991); This study
Stellera chamaejasme	*Stellera*	*Acremonium exuviarum*, *Alternaria alternata*, *Alternaria brassicae*, *Alternaria solani*, *Alternaria tenuissima*, *Aporospora terricola*, *Ascomycota sp*., *Bionectria ochroleuca*, *Botryotinia fuckeliana*, *Cadophora malorum*, *Cadophora sp*., *Colletotrichum*, *Diaporthe*, *Didymella*, *Dothideomycetes* sp., *Dothiorella iberica*, *Epicoccum*, *Eucasphaeria capensis*, *Eupenicillium* sp., *Fusarium acuminatum*, *Fusarium avenaceum*, *Fusarium oxysporum*, *Fusarium sporotrichioides*, *Fusarium torulosum*, *Geomyces* sp., *Gnomoniopsis*, *Herpotrichia*, *Hydnophlebia*, *Ilyonectria* sp., *Microsporum*, *Mucor hiemalis*, *Mucor griseocyanus*, *Penicillium chrysogenum*, *Penicillium commune*, *Penicillium lanosum*, *phiosphaerella*, *Phlebia*, *Phomopsis*, *Schizophyllum commune*, *Scytalidium circinatum*, *Sordaria lappae*, *Sporormiella* sp., *Talaromyces*, *Trichoderma*	It is grown at an altitude of 2600 to 4200 meters above sea level, dry and sunny alpine grass slopes, lawns or river flats.	The provinces of northern and southwest regions of China	Jin et al. (2013); This study

CHAPTER 5

MICROFUNGI ASSOCIATED WITH DIPTEROCARPACEAE IN THAILAND

5.1 Introduction

As part of the core eudicots in the rosid II group, the order *Malvales* comprises ten families, many of which include commercially important species (Berry and Bates 2010). *Dipterocarpaceae* Blume is widely distributed throughout the tropical belt, with approximately 510 species in 16 genera occurring across Asia, Africa and South America, of which 13 genera and about 470 species are concentrated in Asia (Maury-Lechon & Curtet, 1998). In Asia, dipterocarps are mainly restricted to South and Southeast Asia and occupy a wide range of habitats (Wyatt-Smith, 1963; Maury-Lechon & Curtet, 1998), from coastal to inland, riverine to swamp and dry land, on undulating to level terrain, ridges, slopes and valley bottoms, in soils ranging from deeply weathered to shallow, well-drained to poorly drained, and nutrient-rich to nutrient-poor (Maury-Lechon & Curtet, 1998).

Dipterocarpaceae is a family of an important economical trees and the main element of Southeast Asian Forest. It provides significant economic resources, for instant, timber, camphor, oils, nuts, and resins (Shiva & Jantan, 1998; Maury-Lechon & Curtet, 1998), such as *Dipterocarpus alatus* (*Dipterocarpaceae*), it is an important timber tree that plays a dominant role in the ecology and economics of riparian forests in Thailand (Asanok et al., 2017).

Dipterocarpaceae is associated with a wide diversity of fungi, including both beneficial symbionts and pathogenic species. Most studies have focused on ectomycorrhizal (ECM) fungi, which are regarded as key mutualists of dipterocarps (Yuwa-Amornpitak et al. 2006; Hong, 1976). Due to their high economic value, many *Dipterocarpaceae*-dominated forests in tropical Asia have been heavily logged and degraded, leading to increasing interest in dipterocarp plantation establishment and, correspondingly, in the role of mycorrhizae in seedling establishment and forest

restoration (Maury-Lechon & Curtet, 1998). Mycorrhizas are intimate symbiotic associations between specialized root-inhabiting fungi and the roots of living plants, generally considered mutualistic because both partners benefit (Brearley, 2012). The host plant provides the fungus with carbon derived from photosynthesis, while the fungus enhances nutrient uptake, growth, water relations, and resistance to pathogens and heavy metals (van der Heijden & Sanders, 2002; Smith & Read, 2008; Brearley, 2012). Harley and Smith (1983) recognized seven mycorrhizal types, but only two, ectomycorrhizas and arbuscular mycorrhizas, have been reported in *Dipterocarpaceae* (Maury-Lechon & Curtet, 1998). Ectomycorrhizal fungi associated with dipterocarp roots protect against root pathogens, improve mineral nutrition, and promote early seedling growth (Yuwa-Amornpitak et al. 2006; Phosri et al., 2012). Ectomycorrhizal associations have been documented in numerous dipterocarp genera, including *Anisoptera*, *Cotylelobium*, *Dipterocarpus*, *Dryobalanops*, *Hopea*, *Marquesia*, *Monotes*, *Neobalanocarpus*, P*arashorea, Pentacme*, *Shorea*, *Vatica*, *Vateria*, *Vateriopsis* and *Upuna* (Chalermpongse, 1987; Hong, 1979; Singh, 1966; Högberg & Piearce, 1986; Tupas & Sajise, 1976; Ogawa, 1992; Alexander & Högberg, 1986; Maury-Lechon & Curtet, 1998; Sirikantaramas et al., 2003). These symbioses mainly involve basidiomycetous and ascomycetous fungi, with occasional reports from zygomycetous lineages (Chalermpongse, 1987; Smits, 1994; Trappe, 1962; Harley & Smith, 1983; Lee et al., 1997; Dell et al., 2005; Brearley, 2012). The basidiomycetous ECM fungi recorded from *Dipterocarpaceae* belong to several families, including *Russulaceae*, *Boletaceae*, *Cortinariaceae*, *Thelephoraceae*, *Hygrophoraceae*, *Sclerodermataceae*, *Cantharellaceae* and *Amanitaceae* (Sirikantaramas et al., 2003), with dominant taxa primarily distributed in the orders *Boletales*, *Agaricales* and *Thelephorales* (Maury-Lechon & Curtet, 1998; Chalermpongse 1987; Lee et al., 2002; Watling et al., 2001; Sirikantaramas et al., 2003).

In addition, fungi that associated with *Dipterocarpaceae* species also have negative effects, although there are many factors negative to cause the disease of the Dipterocarpaceae species, such as, bacteria, viruses, and fungal pathogen, the most effective one is a fungal pathogen (Maury-Lechon & Curtet, 1998). The infection occurs on the tree, during the flowering and/or development of the fruit, on the ground at the fruit fall, and during the period from harvesting to sowing in the nursery, and the

pathogens infect different parts of *Dipterocarpaceae* species in a different stage of growth, from the seeds to Seedlings and Saplings, the leaves and trees (Maury-Lechon & Curtet, 1998). For instant, the *Schyzophyllum commune* (*Basidiomyceteae*) has been observed on several *Dipterocarpaceae* species, such as causing die-back of young saplings of *Shorea robusta*, cankers caused by frost or fire providing the route of entry (Bagchee, 1954; Elouard & Philip, 1994; Hong, 1976; Vijayan & Rehill, 1990), infection developing on the cotyledons and embryo and finally covering the whole seed and producing carpophores (Maury-Lechon & Curtet, 1998). The pathogens also have been reported to the trees of *Dipterocarpaceae* species, which caused cankers and rots on the tree of *Dipterocarpaceae* species from Peninsular Malaysia, Thailand, Singapore, Indonesia and India (Bagchee, 1954; Bakshi, 1957; Hong, 1976; Charlempongse, 1985; Kamnerdratana et al., 1987). Infection leads to high levels of mortality: 70% of *Shorea leprosula* and *S. ovalis* seeds were rotted by a *Fusarium* species and 90% of *Shorea glauca* seeds were destroyed by *Schyzophyllum commune* (Elouard, 1998).

In this study, we collected five interesting species from dead twigs and fruits of *Dipterocarpaceae* sp. from Thailand. The morphological characteristics indicated that these five taxa belong to the order *Diaporthales*. Furthermore, a phylogenetic analysis using a combination of ITS, LSU, *tef1-α*, and *rpb2* sequence data confirmed them as distinct lineages within *Diaporthales*. Therefore, Two new genera, *Pulvinaticonidioma*, *Subellipsoidispora* and three new species, *Pseudoplagiostoma dipterocarpicola* (*Pseudoplagiostomaceae*), *Pulvinaticonidioma hyalinum* (*Cryphonectriaceae*) and *Subellipsoidispora guttulate* (*Coryneaceae*) from the order *Diaporthales* with detailed descriptions and illustrations.

Diaporthales is an order of ascomycetous fungi belonging to the subclass *Diaporthomycetidae* (*Sordariomycete*s) that dwell on terrestrial or aquatic taxa of plants, animals, and in soil (Senanayake et al., 2017, 2018; Wijayawardene et al., 2022). Senanayake et al. (2017, 2018) provided a recent treatment of the order and examined, described, and illustrated worldwide specimens and listed 27 families in *Diaporthale*s. Many studies of this order have led to an explosion of species, including a total of 29 families (Crous et al., 2019; Guterres et al., 2019). Jiang et al. (2020) redefined the family *Cryphonectriaceae* and established two new families for the order, with a total

of 31 families in *Diaporthales.* In the latest outline of the fungi and fungus-like taxa, Wijayawardene et al. (2022) accepted 32 families in the order.

Diaporthales contains both sexual and asexual morphs. The sexual morph is characterized by immersed stromata or substrata, brown or black perithecial ascomata with elongated beaks, sometimes with long papilla, deliquescent paraphyses at maturity, commonly unitunicate, thick-walled asci that are either evanescent with short stalks or intact, often floating free within the centrum at maturity, and have a refractive ring at the apex, containing 2–32 spores (Alexopoulus & Mims, 1978; Watling et al., 1996; Castlebury et al., 2002; Rossman et al., 2007; Fan et al., 2018b; Senanayake et al., 2018; Hyde et al., 2020b; Jiang et al., 2020). The asexual morph of *Diaporthales* is generally coelomycetous, rarely hyphomycetous, bearing their phialidic, rarely annellidic, conidiogenous cells, and conidia in acervuli or pycnidia with or without well-developed stromata. Since it has fewer distinguishing traits, proper identification at the genus and species levels is typically dependent on sequence data (Castlebury et al., 2002; Jiang et al., 2020).

5.2 Results

5.2.1 Phylogenetic Analyses

For the phylogenetic analyses, a combined dataset of ITS, LSU, *tef1-α*, and *rpb2* sequences was used. The dataset of *Cryphonectriaceae* included 70 taxa, with *Foliocryphia eucalypti* (CBS 124779) and *F. eucalyptorum* (CBS 142536) as outgroups. The data matrix comprised 2,860 total characteristics, including gaps (ITS: 1–481 bp, LSU: 482–1,290 bp, *tef1-α*: 1,291–1,858 bp, and *rpb2*: 1,859–2,564 bp). Phylogenetic reconstructions with broadly comparable topologies were produced by the combined dataset of ML, MP, and BI analyses. The top-scoring ML tree with a final ML optimization likelihood value of −16,383.140512 (ln) is shown in Figure 5.1. In the ML analysis, the GTRGAMMA + I-Invar model was used, and the results showed 1,022 unique alignment patterns and 27.97% of indeterminate characteristics or gaps. Base frequency estimates were as follows: A = 0.229377, C = 0.266423, G = 0.271764, and T = 0.232436; substitution rates were as follows: AC = 1.760988, AG = 4.032209, AT

= 1.914644, CG = 1.261342, CT = 8.527324, and GT = 1.000000; gamma distribution shape parameter alpha = 0.176927; and the tree length was 1.784127. The findings of the MP analysis showed that 2,564 characteristics remained unchanged, 103 were changeable but parsimoniously uninformative, and 733 were parsimoniously informative. The following values were displayed by the most parsimonious tree: TL = 2693, CI = 0.494, RI = 0.779, RC = 0.385, and HI = 0.506. The best-fit models for the BI analysis were GTR + I + G for ITS, LSU, tef1-α, and rpb2. With a final average standard deviation of split frequencies of 0.009895, Bayesian posterior probabilities (BYPP) from MCMC were analyzed. A new taxon correlated with the *Cryphonectriaceae* clade and is sister to *Chrysomorbus*. It is distinct from all other *Cryphonectriaceae* genera sampled herein, although with no support (Figure 5.1).

For the tree of *Coryneaceae,* the combined sequence dataset of 33 taxa was used with *Neopestalotiopsis protearum* (CBS 114178) and *N. rosae* (CBS 101057) as the outgroups. The data matrix comprised 2,977 total characteristics, including gaps (ITS: 1–597 bp, LSU: 598–1,426 bp, *tef1-α*: 1,427–2,123 bp, and *rpb2*: 2,124–3,151 bp). Based on the results of phylogenetic analysis, the top-scoring RAxML tree with a final ML optimization likelihood value of −19,448.697623 (ln) is shown in Figure 5.4. The GTRGAMMA+I-Invar model was applied to the RAxML analysis, and the findings revealed 1,332 distinct alignment patterns and 33.88% of ambiguous characteristics or gaps. The following were the base frequency estimates: A = 0.237835, C = 0.267649, G = 0.278605, and T = 0.215911; the substitution rates: AC = 1.607401, AG = 1.967526, AT = 1.403753, CG = 1.150806, CT = 5.717313, and GT = 1.000000; the gamma distribution shape parameter alpha = 0.260733; and the tree length = 3.464265. The results of the MP analysis revealed that 3,151 characteristics remained constant, 271 were variable and parsimoniously uninformative, and 1,142 were parsimoniously informative. The most frugal tree resulted in TL = 3,542, CI = 0.636, RI = 0.684, RC = 0.435, and HI = 0.364 as its values. For the BI analysis, the bestfit models were GTR+G for ITS, tef1-α, and rpb2 and SYM + I + G for LSU. The BYPP from MCMC were examined with a final average standard deviation of split frequencies of 0.009847. Based on the results of phylogenetic analysis of the combined ITS, LSU, *tef1-α*, and *rpb2* sequencing data, the new taxon is related to *Coryneum*, *Hyaloterminalis*, and *Talekpea* within *Coryneaceae*, with statistical support of 72% ML and 1 BYPP. It differs

from any other *Coryneaceae* genus sampled here (Figure 5.4).

For the species, *Pseudoplagiostoma dipterocarpicola* in *Pseudoplagiostomataceae*, a combined sequence dataset of ITS, LSU, *tef1-α* and *tub2* consisted of 52 taxa, with *Togninia minima* (AE-F56), *T. novae-zealandiae* (CBS 110156) and *Phaeoacremonium hungaricum* (CBS 123036) as the outgroups. The data matrix consisted of 2710 total characters including gaps (ITS: 1–597 bp, LSU: 598–1436 bp, tef1-α: 1437–1909 bp, tub2: 1910–2710 bp). The ML, MP and BYPP analyses of the combined dataset resulted in phylogenetic reconstructions with largely similar topologies. The best scoring RAxML tree with a final ML optimization likelihood value of -19772.417736 (ln) is presented in Figure 5.6. The GTRGAMMA+I-Invar model was used in a RaxML analysis which resulted in 1386 distinct alignment patterns and 45.48% of undetermined characters or gaps. The estimated values of the base frequencies were A = 0.240288, C = 0.265747, G = 0.259699, T = 0.234266, with substitution rates AC = 1.563097, AG = 2.754583, AT = 1.453344, CG = 1.064699, CT = 5.521478, GT = 1.000000, the gamma distribution shape parameter alpha = 0.309484 and the Tree-Length = 3.104519. For the MP analysis, 2710 characters remained unchanged, 191 were variable and parsimoniously uninformative, while 1048 were parsimoniously informative. The most parsimonious tree showed the following values: TL = 3757, CI = 0.578, RI = 0.805, RC = 0.465, HI = 0.422. For BYPP analysis, the best-fit models were selected as GTR + I + gamma for ITS and LSU, and HKY + I + gamma for *tef1-α* and *tub2*. Bayesian posterior probabilities from MCMC were evaluated with a final average standard deviation of split frequencies of 0.009856. Based on the results of the combined ITS, LSU, *tef1-α* and *tub2* sequence data analyses, the new taxon falls within the *Pseudoplagiostoma* clade, as sister to *P. mangiferae* (KUMCC 18-0197) with a statistic support of 78% ML, 68% MP and 1 BYPP.

5.2.2 Taxonomy

Sordariomycetes O.E. Erikss. & Winka, Myconet 1: 10 (1997)

Diaporthales Nannf., Nova Acta Regiae Soc. Sci. Upsal., Ser. 4, 8 (2): 53 (1932)

Cryphonectriaceae Gryzenh. & M.J. Wingf., Mycologia 98: 246. 2006

Index Fungorum number: IF510585; *Facesoffungi number*: FoF03455

Pulvinaticonidioma X. Tang, Jayaward, J.C. Kang & K.D. Hyde, gen. nov.

Index Fungorum number: IF900388; *Faceoffungi number*: FOF 13992

Etymology: The generic name refers to the pulvinate conidiomata.

Type species: Pulvinaticonidioma hyalinum X. Tang, Jayaward, J.C. Kang & K.D. Hyde.

Saprobic on *Dipterocarpaceae* sp. **Sexual morph**: not observed. **Asexual morph**: Coelomycetous. *Conidiomata* immersed to semiimmersed in the substrate, solitary, glabrous or rough, pycnidial, subglobose, unilocular, thick-walled, ostiolate, brown to dark brown. *Ostiole* central, single with slightly protruding ostiolar papilla. *Conidiomata* wall composed of thick-walled, pale brown to dark brown cells of textura angularis at the exterior, and convex and pulvinate at the base. *Conidiophores* hyaline reduced to conidiogenous cells. *Conidiogenous cells* phialidic, cylindrical to ampulliform, determinate, smooth-walled, hyaline. *Conidia* hyaline, cylindrical, with obtuse ends, straight, unicellular, aseptate, thick- and smooth-walled.

Notes: *Pulvinaticonidioma* is characterized by solitary, subglobose, pycnidial conidiomata, phialidic, conidiogenous cells, and aseptate hyaline conidia. This matches with the morphological characteristics of *Cryphonectriaceae* (Jiang et al., 2020). Phylogenetically, *Pulvinaticonidioma* clusters with *Chrysomorbus* (Figure 5.1). Both *Pulvinaticonidioma* and *Chrysomorbus* have a coelomycetous asexual morph (Chen et al., 2018). The former differs from the species in *Chrysomorbus* in having unilocular, glabrous or rough, thick-walled, ostiolate conidiomata with hyaline cells of textura angularis at the exterior, convex and pulvinate at the base; aseptate, straight, cylindrical, unicellular, and hyaline conidia with obtuse ends. After the comprehensive consideration based on the morphological and phylogenetic analysis, we, herein, introduce *Pulvinaticonidioma* as a new genus in *Cryphonectriaceae*, with *Pulvinaticonidioma hyalinum* as the type.

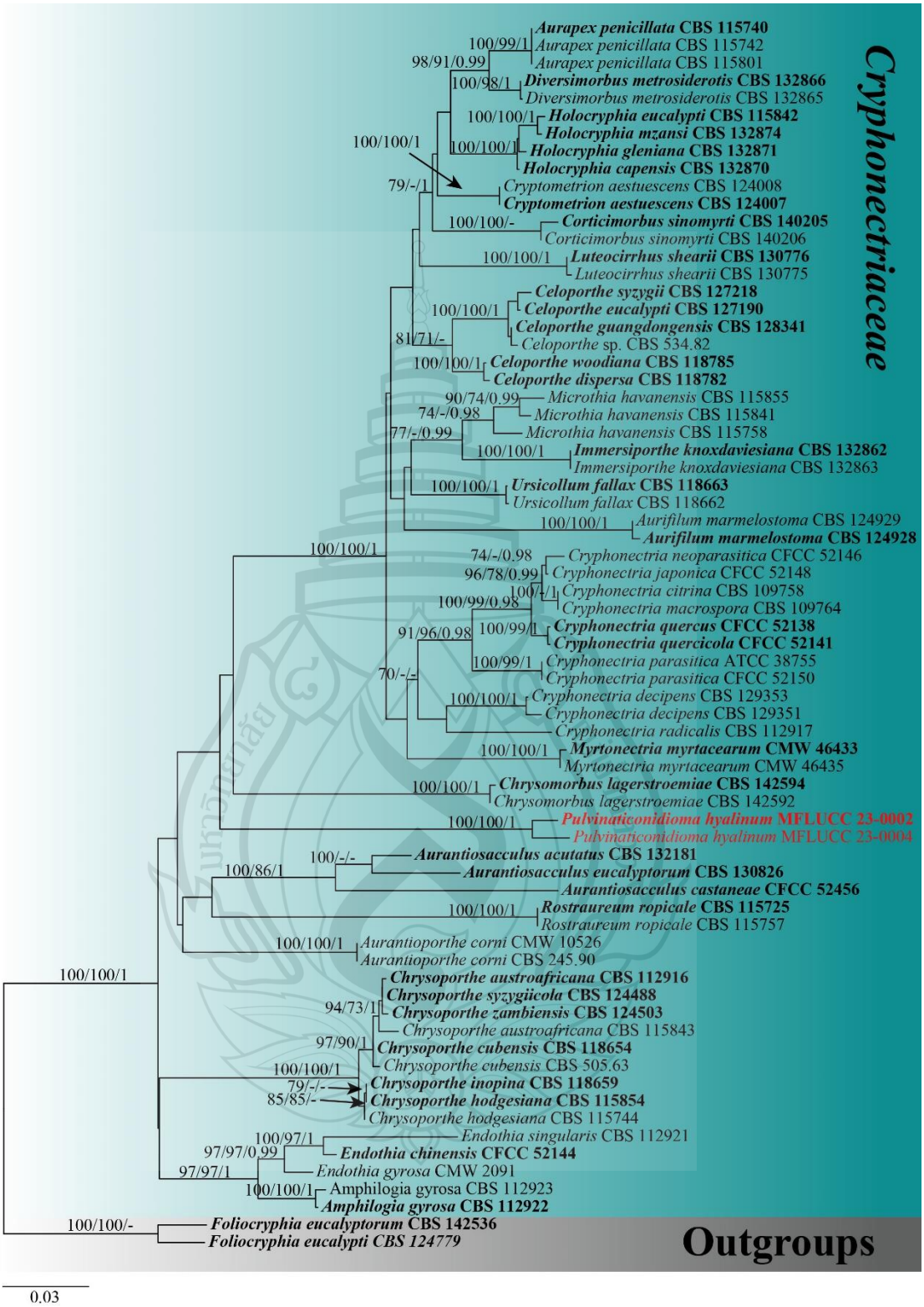

Figure 5.1 Phylogenetic tree of *Cryphonectriaceae*

Figure 5.1 Maximum likelihood (RAxML) tree, based on analysis of a combined dataset of ITS, LSU, *tef1-α* and *rpb2* sequence data. The tree is rooted with *Foliocryphia eucalypt*i (CBS 124779) and *F. eucalyptorum* (CBS 142536). Bootstrap support values for ML and MP greater than or equal to 70% and Bayesian posterior probabilities (BYPP) greater than or equal to 0.95 are given near the nodes, respectively. Ex-type strains are in bold, the new isolates are in red.

Pulvinaticonidioma hyalinum X. Tang, Jayaward, J.C. Kang & K.D. Hyde, sp. nov. Figure 5.2, 5.3

Etymology: The epithet refers to the hyaline conidia.

Holotype: MFLU 23-0052

Saprobic on *Dipterocarpaceae* sp. **Sexual morph**: not observed. **Asexual morph**: Coelomycetous. *Conidiomata* 297–473 × 211– 316μm ($\overline{x}$ = 375 × 267μm, n = 20), immersed to semi-immersed in substrate, solitary, glabrous or rough, pycnidial, subglobose, unilocular, thick-walled, ostiolate, brown to dark brown. *Ostiole* 51–65 × 34–48μm ($\overline{x}$ = 58 × 42μm, n = 10), central, single with slightly protruding ostiolar papilla. *Conidiomata* wall 50–88μm ($\overline{x}$ = 70μm, n = 20) wide, composed of thick-walled, pale brown to dark brown cells of textura angularis at the exterior, convex and pulvinate at the base 103–202μm high ($\overline{x}$ = 144μm, n = 20). *Conidiophores* hyaline, reduced to conidiogenous cells. *Conidiogenous cells* 6–11.5 × 1.8–3.4μm ($\overline{x}$ = 7 × 2.5μm, n = 20), phialidic, cylindrical to ampulliform, determinate, smooth-walled, hyaline. *Conidia* 15–20 × 2–3μm ($\overline{x}$ = 17 × 2.5μm, n = 20) hyaline, cylindrical, with obtuse ends, straight, unicellular, aseptate, thick- and smooth-walled.

Culture characters: Conidia germinated on PDA within 24 h, and germ tubes produced from one end. The culture was incubated at room temperature. Colonies reached 45mm diameter after 15 days, flat, spreading, fluffy colonies, circular with irregular lightly orange outer ring, cottony. The surface is lightly rough, with orange-red colonies, cream-colored hyphae attached to the center of the colony, with an irregular orange-yellow edge. The reverse orange-red, more orange-yellow at the margins, not pigmented.

Material examined: Thailand, Chiang Mai province, Mae Taeng District, on the fruits (pericarp and wings of the pod) of *Dipterocarpaceae*, 8 August 2019, Xia Tang, Dip17 (MFLU 23-0052, holotype; ex-type living culture, MFLUCC 23-0002), on the fruits of *Dipterocarpaceae*, 23 October 2020, Xia Tang, Dip41 (MFLU 23-0053, paratype; ex-

paratype living culture, MFLUCC 23-0004).

Notes: The two *Pulvinaticonidioma hyalinum* collections, showing similar morphology clustered together with ML = 100, MP = 100, and BYPP = 1 support (Figure 5.1). The base pair differences between the two strains were as follows: ITS = 0.7% (4/557), LSU = 0% (0/811), *tef1-α* = 6.2% (38/613), and *rpb2* = 1% (11/983), respectively, and we identified them as the same species following the guidelines for species delineation proposed by Chethana et al. (2021a). *Pulvinaticonidioma hyalinum* matches the characteristics of *Cryphonectriaceae* and is similar in having unilocular conidiomata without necks and conidiomata walls made of cells of textura globulosa (Jiang et al., 2020). However, *P. hyalinum* differs from the type species of *Cryphonectriaceae*, *Chrysomorbus lagerstroemiae* in their fruiting body, conidiomata wall, conidiophores, and conidia. *Pulvinaticonidioma hyalinum* has brown to dark brown conidiomata with slightly protruding ostiolar papilla, hyaline cells of textura angularis at the exterior, interior layers that are convex and pulvinate at the base, and unbranched conidiophores, while *Ch. lagerstroemiae* has unito multilocular, conidiomata lacking ostioles, with convoluted locules, and occasionally aseptate conidia with separating septa and branching conidiophores. The conidiogenous cells in *P. hyalinum* are phialidic, cylindrical to ampulliform with hyaline, straight, aseptate, unicellular, conidia with obtuse ends, while *Ch. lagerstroemiae* has flask-shaped conidiogenous cells with attenuated apices and minute, cylindrical conidia with obtuse ends, that are hyaline, fusoid to oval, aseptate, and exuded as orange droplets (Chen et al., 2018). The phylogenetic analysis of the combined ITS, LSU, *tef1-α*, and *rpb2* sequence data showed that *P. hyalinum* belongs to *Cryphonectriaceae* and forms a separate lineage sister to *Chrysomorbus*. Although the bootstrap values are low, the phylogenetic analysis supports the placement of our new taxa in *Cryphonectriaceae*, as well as the possibility of other close relatives that have not yet been discovered; hence, their placement within the family is subjected to change. The base pair differences between *P. hyalinum* and the type species of *Chrysomorbus*, *viz. Ch. lagerstroemiae* were as follows: ITS = 5% (27/539), LSU = 1.4% (11/811), and *tef1-α* = 26.5% (151/569), respectively. Based on the phylogenetic analysis and morphological comparison of the nearest genus, we, herein, introduce *Pulvinaticonidioma* as a new genus to accommodate the new collection, *P. hyalinum*.

Figure 5.2 *Pulvinaticonidioma hyalinum* (MFLU 23-0052, Holotype)

Figure 5.2 a Fallen pod of *Dipterocarpaceae* sp.. b Conidiomata on *Dipterocarpaceae* sp.. c Section of conidioma. d Conidioma wall e Ostiole. f Conidiogenous cells. g–i Conidia. j Germinated conidium. k Colonies on PDA. l Reverse of culture. Scale bars: b = 500 µm, c,d = 100 µm, e, g–j = 20 µm, f = 10 µm.

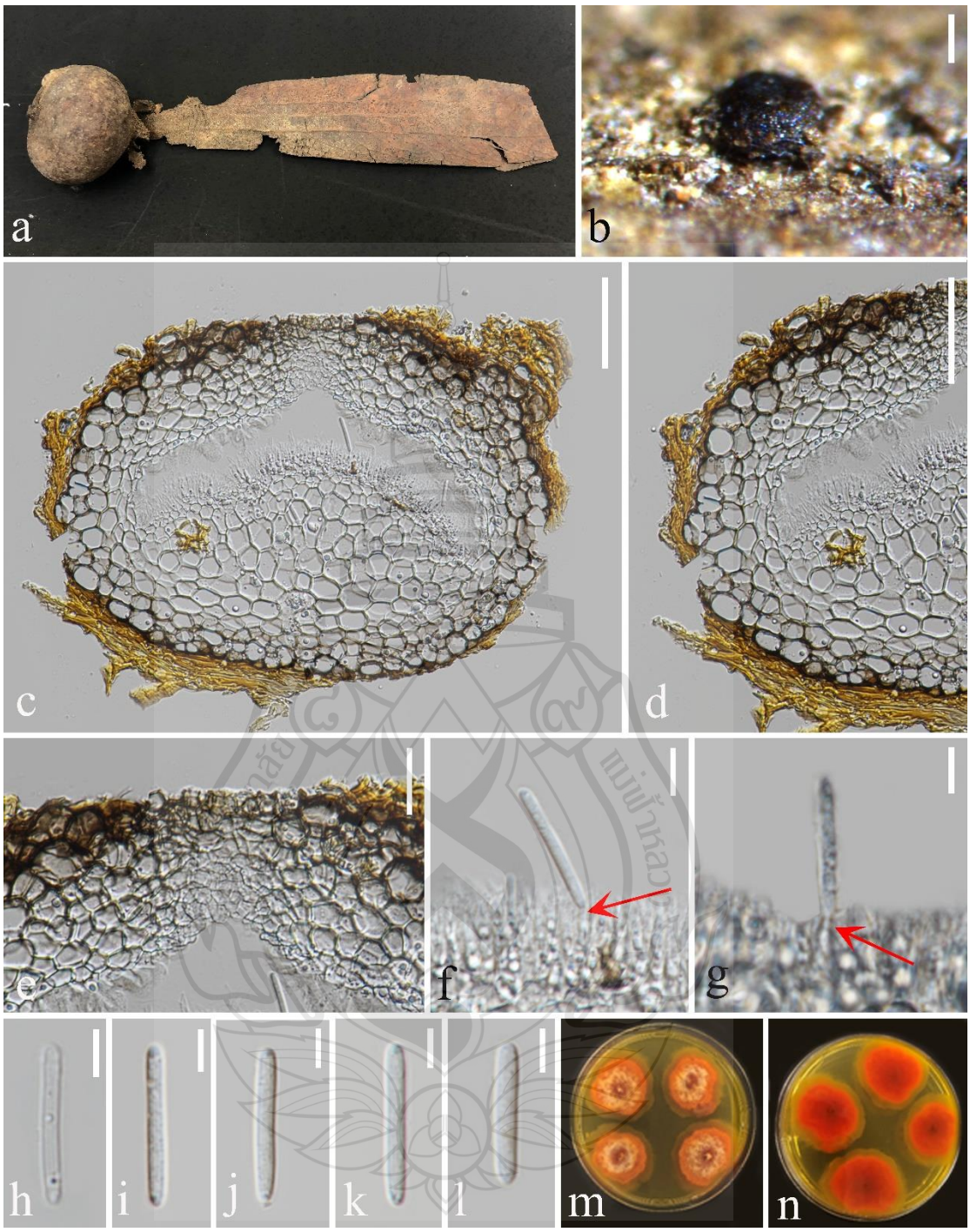

Figure 5.3 *Pulvinaticonidioma hyalinum* (MFLU 23-0053, Paratype)

Figure 5.3 a Fallen pod of *Dipterocarpaceae* sp.. b Conidiomata on *Dipterocarpaceae* sp.. c Section of conidioma. d Conidioma wall. e Ostiole. f, g Conidiogenous cells. h–l Conidia. m Colonies from above. n Reverse of culture. Scale bars: b = 200 µm, c, d = 50 µm, e = 20 µm, f–l = 5 µm.

Coryneaceae Corda, Icon. fung. (Prague) 3: 36 (1839) amend.

Subellipsoidispora X. Tang, Jayaward, J.C. Kang & K.D. Hyde, gen. nov.

Index Fungorum number: IF900389; *Faceoffungi number*: FOF 13994

Etymology: The epithet refers to the subellipsoidal ascospores.

Type species: *Subellipsoidispora guttulata* X. Tang, Jayaward, J.C. Kang and K.D. Hyde

Saprobic on *Dipterocarpaceae* sp.. **Asexual morph**: Not observed. **Sexual morph**: *Ascomata* perithecial, erumpent, scattered, solitary, coriaceous, immersed, globose to subglobose, papillate, ostiolate, dark brown to black. The *Ostiole* canal narrowing toward the base, internally covered by hyaline periphyses, cells around the base small, thick-walled, and brown. *Peridium* comprising brown, compressed, cells of textura angularis. *Hamathecium* composed of cylindrical, unbranched, straight to flexible, smooth, hyaline, septate paraphyses slightly constricted at the septa, tapering toward to end, longer than asci. *Asci* 8-spored, unitunicate, clavate to broadly fusoid, short pedicellate, apex blunt, with an indistinct, J- apical ring, evanescent. *Ascospores* overlapping uniseriate to biseriate, biturbinate to subellipsoidal, 1-septate, slightly constricted at the septa, guttulate, smooth, hyaline to pale brown.

Notes: *Subellipsoidispora* share characteristics with *Coryneaceae*, such as perithecial, coriaceous, ostiolate, brown to black ascomata; with thick-walled peridium having outer and inner brown cells of textura angularis and hyaline, compressed cells of textura angularis, respectively; paraphyses are longer than asci; clavate to broadly fusoid, 8-spored asci with J- apical ring; guttulate and smooth, hyaline to pale brown and straight ascospores (Hyde et al., 2020b). *Coryneaceae* contains three genera, *viz.* *Coryneum*, *Hyaloterminalis*, and *Talekpea* (Rathnayaka et al., 2020). Both *Subellipsoidispora* and *Coryneum* have the ascomycetous sexual morph, while *Talekpea* and *Hyaloterminalis* have a hyphomycetous asexual morph (Senanayake et al., 2017, 2018). *Subellipsoidispora* differs from the species in *Coryneum* in having scattered, solitary ascomata; a thick-walled ostiolar canal narrowing toward the base, internally covered by hyaline periphyses, a peridium of brown-walled, compressed, cells of textura angularis, clavate to broadly fusoid, short pedicellate asci and biturbinate to subellipsoidal, 1-septate, guttulate ascospores, slightly constricted at the septa. In the phylogenetic analysis, *Subellipsoidispora* clusters in *Coryneaceae* and

forms a separate lineage sister to *Hyaloterminalis* and *Talekpea* (Figure 5.4). Based on its unique morphology (Figure 5.5) and phylogenetic evidence (Figure 5.4), *Subellipsoidispora* is introduced as a new genus of *Coryneaceae*, and the sexual morph is described in this study, awaiting the discovery of its asexual morph.

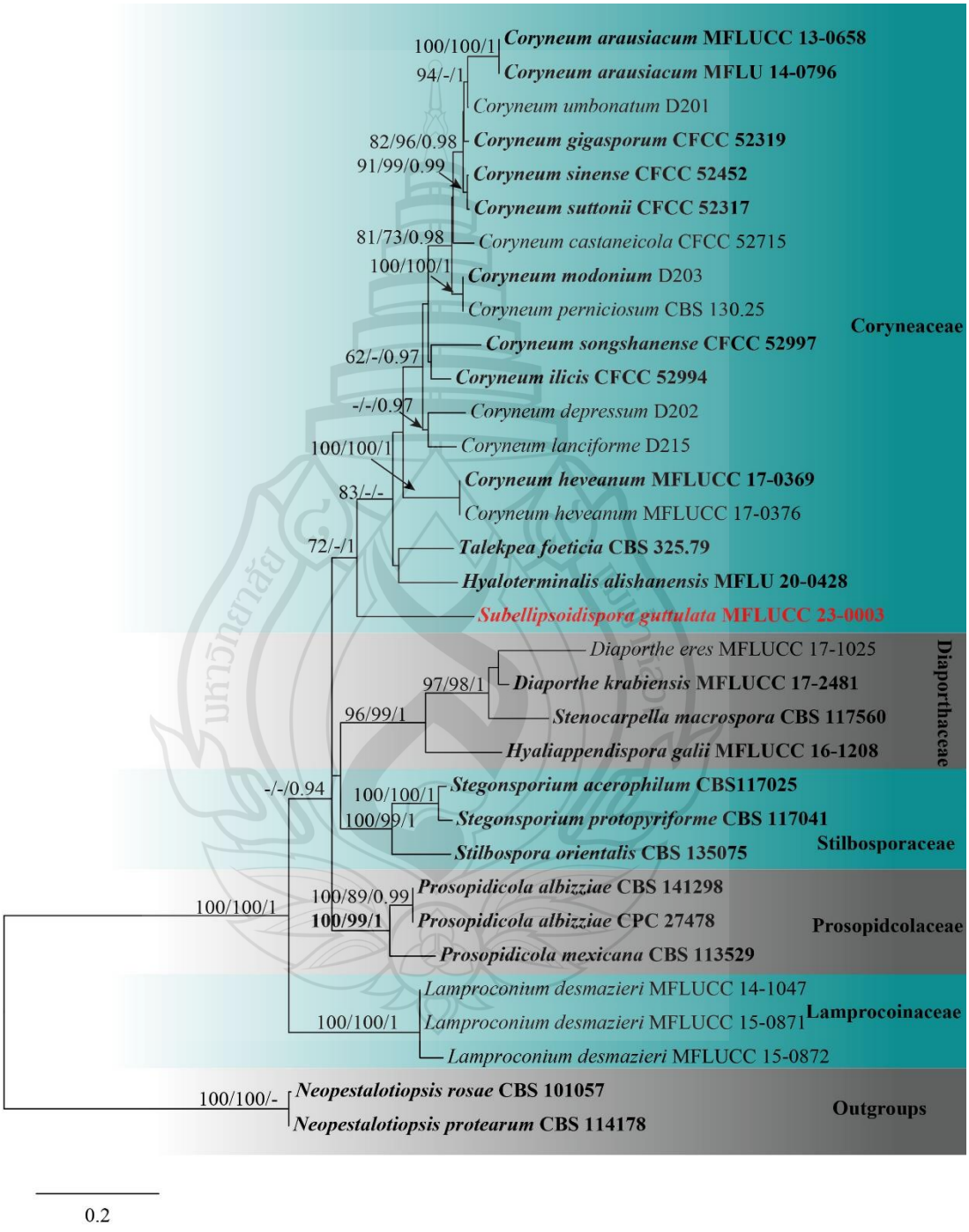

Figure 5.4 Phylogenetic tree of *Coryneaceae*

Figure 5.4 Maximum likelihood (RAxML) tree, based on analysis of a combined dataset of ITS, LSU, *tef1-α* and *rpb2* sequence data. The tree is rooted with *Neopestalotiopsis protearum* (CBS 114178) and *N. rosae* (CBS 101057). Bootstrap support values for ML and MP greater than or equal to 70% and Bayesian posterior probabilities (BYPP) greater than or equal to than 0.95 are given near the nodes, respectively. Ex-type strains are in bold, the new isolates are in red.

Subellipsoidispora guttulata X. Tang, Jayaward, J.C. Kang & K.D. Hyde, sp. nov.; Figure 5.5

Etmology: Name referring to the hyaline ascospores.

Holotype: MFLU 23-0054

Saprobic on dead barks of *Dipterocarpaceae* sp.. **Sexual morph**: *Ascomata* 117–270 × 71–155µm ($\bar{x}$ = 199 × 105µm, n = 20), immersed, scattered, solitary, globose to subglobose, dark brown to black, coriaceous, ostiolate, papillate. The *Ostiole* canal narrowing toward the base, internally covered by hyaline periphyses, cells around the base small, thick-walled, and brown. *Peridium* 8–28µm wide ($\bar{x}$ = 18µm, n = 20), comprising brown, compressed, cells of textura angularis. *Paraphyses* 3–6µm wide ($\bar{x}$ = 5.5µm, n = 30), cylindrical, unbranched, straight to flexible, smooth, hyaline, septate, slightly constricted at the septa, tapering toward to end, longer than asci. *Asci* 67–90 × 13–24µm ($\bar{x}$ = 79 × 19µm, n = 20), 8-spored, unitunicate, clavate to broadly fusoid, short pedicellate, apex blunt, with an indistinct, J- apical ring, evanescent. *Ascospores* 13–16 × 5–9µm ($\bar{x}$ = 14 × 7µm, n = 20), overlapping uniseriate to biseriate, biturbinate to subellipsoidal, 1-septate, slightly constricted at the septa rounded at both ends, guttulate, smooth-walled, hyaline to pale brown. Asexual morph: not observed.

Culture characters: Colonies grown on PDA and incubated at 25◦C reached a diameter of 40mm after 2 weeks, flat, spreading, fluffy, with a pale brown ring interlaced in the colonies. Surface lightly rough with brown mycelium, colonies somewhat raised in the middle, and with an irregular edge. The reverse side dark brown with an irregular, penniform, brown edge, and not pigmented.

Material examined: Thailand, Chiang Mai Province, Mae Taeng district, on dead bark of *Dipterocarpaceae* sp., 15 July 2020, Xia Tang, Dip25 (MFLU 23-0054, holotype; ex-type living culture, MFLUCC 23-0003).

Notes: *Subellipsoidispora guttulata* is similar to *Coryneum umbonatum* in

having immersed, coriaceous, brown to black ascomata, and unitunicate asci with an indistinct J- apical ring. However, *S. guttulata* differs from *C. umbonatum* in having clavate to broadly fusoid, short pedicellate asci and subellipsoidal, 1-septate, guttulate, hyaline to pale brown ascospores, while *C. umbonatum* has ellipsoid to cylindrical, stalk pedicellate asci, and ellipsoid, fusoid or elongate, distoseptate, straight or curved spores that are brown at maturity (Senanayake et al., 2018). Phylogenetic analysis showed that *S. guttulata* belongs to Coryneaceae and forms a basal lineage sister to *Coryneum*, an ascomycetous genus, *Hyaloterminalis* and *Talekpea*, a hyphomycetous and monotypic genus. The base pair differences between *S. guttulata* and *C. umbonatum* were as follows: ITS = 7.7% (45/581), LSU = 3.2% (26/842), and *rpb2* = 21.7% (223/1029), and the differences between *S. guttulata* and *Talekpea foeticia* were as follows: ITS = 12.5% (65/520) and LSU = 2% (17/843). Based on its phylogenetic and morphological analyses, we place *S. guttulata* as the type species of *Subellipsoidispora* in *Coryneaceae*.

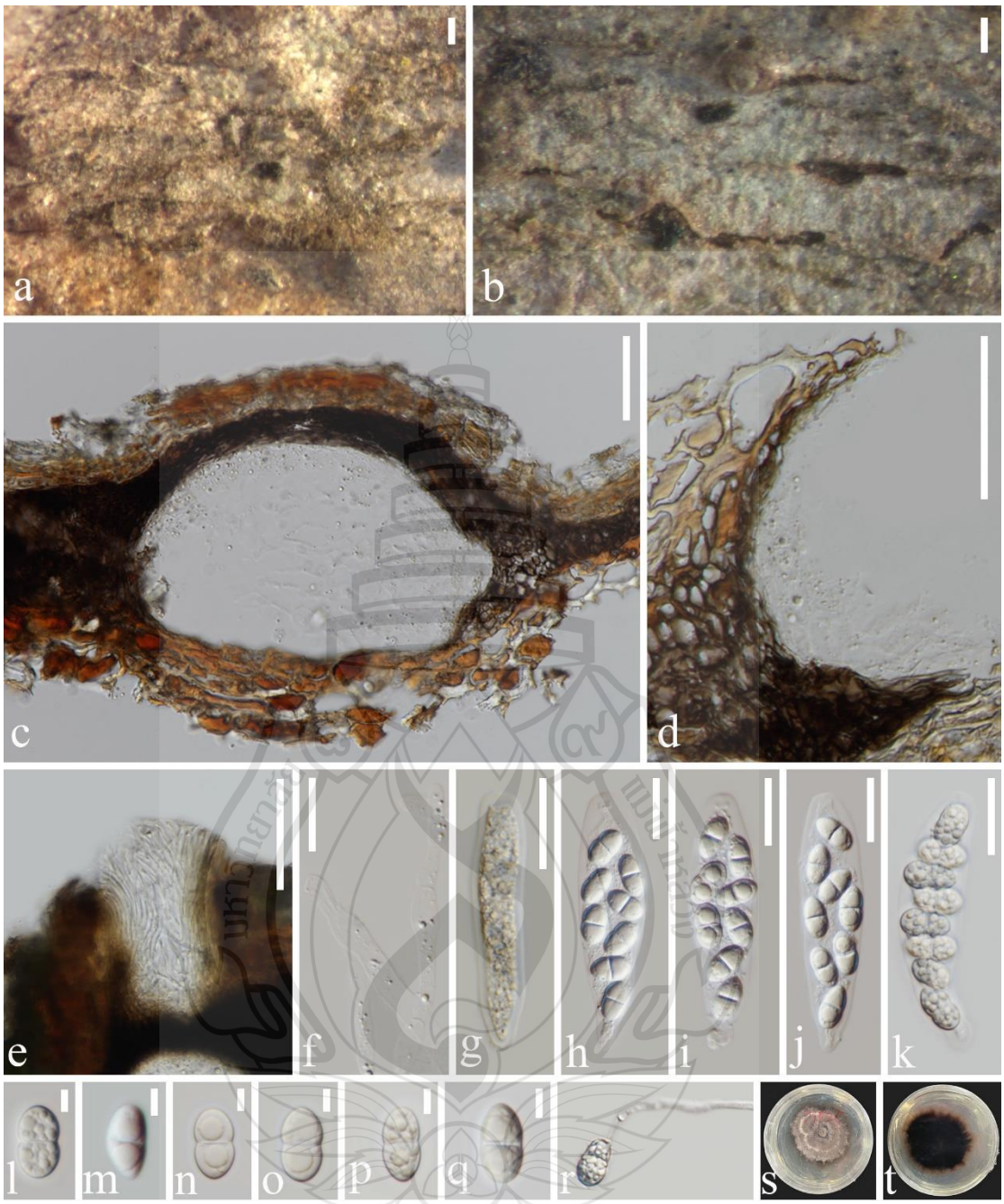

Figure 5.5 *Subellipsoidispora guttulata* (MFLU 23-0054, holotype)

Figure 5.5 a, b Appearance of ascomata on host substrate. c Section of an ascoma. d Peridium. e Ostiole. f Paraphyses. g–k Asci from immature to mature. l–q Ascospores. r Germinated ascospore. s Colony on PDA. t Reverse of culture. Scale bars: a, b = 200 µm, c–e = 50µm, f–k = 20 µm, l–q = 5 µm.

Pseudoplagiostomataceae Cheew., M.J. Wingf. & Crous, Fungal Diversity 44: 95 (2010)

Pseudoplagiostoma Cheew., M.J. Wingf. & Crous, Fungal Diversity 44: 96 (2010)

Index Fungorum number: IF 516496; *Facesoffungi number*: FoF10497

Note: *Pseudoplagiostoma* was established by Cheewangkoon et al. (2010) with *P. eucalypti*, *P. eucalypti* as the type species in *Pseudoplagiostomataceae*. As a monotypic family, *Pseudoplagiostomataceae* accommodates a cryptosporiopsis-like fungus, represented by *P. eucalypti*, isolated from *Eucalyptus* and characterized by immersed, subglobose or elliptical perithecia, an acentric or lateral beak, unitunicate asci with a subapical nonamyloid ring, an aparaphysate condition, uniseptate, hyaline ascospores with elongated hyaline terminal appendages (Cheewangkoon et al., 2010). *Pseudoplagiostoma* contains 35 species (Index Fungorum, 2025) which are mostly associated with the leaves of plants (Cheewangkoon et al., 2010; Crous et al., 2012a; Suwannarach et al., 2016; Crous et al., 2018b; Bezerra et al., 2019; Phookamsak et al., 2019; Gomdola et al., 2023; Hittanadurage et al., 2023; Zhang et al., 2023b, 2025; Wu et al., 2024), only *P. wuyishanense* was reported on both deacaying branches and leaf diseases of *Ilex chinensis* (Mu et al., 2024; Jiang et al., 2025), and *P. dipterocarpicola* was reported on deacaying twigs and fruits of *Dipterocarpus* sp. (Tang et al., 2022). The morphology of *Pseudoplagiostoma* was described as coelomycetous (Alvarez et al., 2016; Fan et al., 2018a; Guarnaccia et al., 2018; Senanayake et al., 2018; Bezerra et al., 2019), with the type species (*P. eucalypti*) described on the basis of its sexual and asexual morphs.

The sexual morph is characterized by immersed, beaked, ostiole ascomata, unitunicate asci, a non-amyloid subapical ring, hyaline ascospores that are 1-septate near the middle, with terminal, elongated hyaline appendages. The asexual morph is characterized by acervular to pycnidial, superficial and immersed conidiomata with masses of apically proliferous conidiogenous cells and hyaline, ellipsoidal conidia but with no conidiophores (Cheewangkoon et al., 2010). *Pseudoplagiostoma* is primarily described as a pathogen, and a few species have been classified as saprobes and endophytes. These were recorded on plant leaves from Australia, Brazil, China, Uruguay, Thailand and Venezuela (Cheewangkoon et al., 2010; Crous et al., 2012a;

Suwannarach et al., 2016; Crous et al., 2018; Bezerra et al., 2019; Phookamsak et al., 2019; Hyde et al., 2020b).

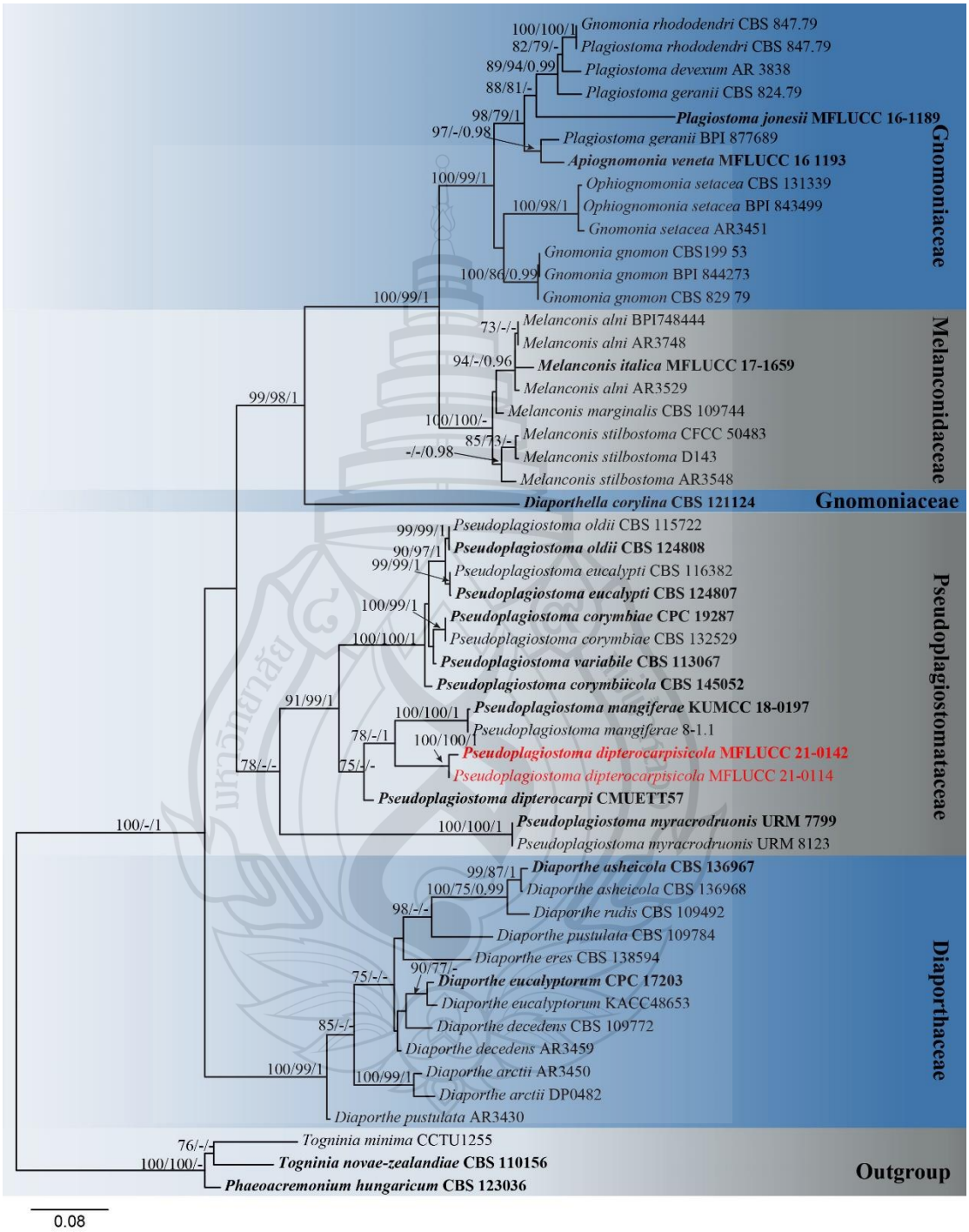

Figure 5.6 Phylogenetic tree of *Pseudoplagiostomataceae*

Figure 5.6 The best scoring RAxML tree obtained using a combined dataset of ITS, LSU, *tef1-α* and *tub2* sequences. The tree is rooted to *Togninia minima* (AE F56),

T. novae-zealandiae (CBS 110156) and *Phaeoacremonium hungaricum* (CBS 123036). ML and MP bootstrap values equal to or greater than 70% and BYPP equal to or greater than 0.95 are given at the nodes (ML/MP/BYPP). Ex-type strains are in black bold and the newly generated sequences are in red bold.

Pseudoplagiostoma dipterocarpicola X. Tang, R.S. Jayaward., K.D. Hyde, & J.C. Kang, sp. nov.; Figure 5.7

Etymology: The epithet refers to the genus of the host plant, *Dipterocarpus*.

Holotype: MFLU 21-0177

Associated with the twigs and fruits of *Dipterocarpus* sp.. **Sexual morph**: Undetermined. **Asexual morph**: Associated with the twigs of *Dipterocarpus* sp., coelomycetous. *Conidiomata* 63–153 μm long × 113–288 μm diam. ($\overline{x}$ = 109 μm × 203 μm, n = 25) immersed in the twigs of the host, medium brown to dark brown, pycnidia with pale yellow cylindrical strips of exuding conidia, subglobose, subcuticular to epidermal, unilocular, and irregularly breaking through plant tissue at the centre. *Conidiomata wall* 6–23 μm wide, thin-walled, composed of 2–5 dark brown layers, thickest near the base of the conidiomata, pseudoparenchymatous cells textura angularis, intermixed with the host cells at the base and on the sides. *Conidiophores* reduced to conidiogenous cells. *Conidiogenous cells* 5–11 μm × 1–2.5 μm ($\overline{x}$ = 9 × 2 μm, n = 25), proliferating enteroblastically, appearing as phialides with thickenings and collarette or with a percurrent proliferation in the apical portion, discrete, arising from the inner cell layer, hyaline, smooth, ranging from cylindrical with a long, slimy cylindrical neck to ampulliform, straight and short when wider at the base. *Conidia* 9.0–22 μm × 4–7.5 μm ($\overline{x}$ = 16 × 6 μm, n = 35), hyaline, ellipsoidal to elongated ellipsoidal, guttulate, smooth, thick-walled (0.5–1.5 μm), aseptate, apex broadly obtuse, straight or lightly curved at the base, with a prominent hilum or the hilum absent, frequently slightly narrow at the middle, the base tapering to a flat protruding scar.

Culture characteristics: Colonies developing on PDA are incubated at room temperature and reach a diameter of 30 mm after 15 days, flat, spreading, with a fluffy, moderately mouse-gray mycelium. Surface lightly rough with pale gray hyphae, colonies somewhat sunken in the middle, and with an irregular edge. The reverse side dark brown but pale brown at the margins, lobate at the center and not pigmented.

Material examined: Thailand, Chiang Mai Province, Mushroom Research Center, on dead twigs of *Dipterocarpus* sp., 08 August 2019, Xia Tang, Dip 31 (holotype: MFLU 21-0177; ex-type living culture: MFLUCC 21-0142), on dead fruits of *Dipterocarpus* sp., 08 August 2019, Xia Tang, Dip 16 (paratype: MFLU 21-0260; ex- paratype living culture: MFLUCC 21-0114).

Notes: *Pseudoplagiostoma dipterocarpicola* forms a clade with *P. mangiferae* with highly support (78% ML, 68% MP and 1 BYPP), but *P. dipterocarpicola* can be easily distinguished from *P. mangiferae*. *Pseudoplagiostoma dipterocarpicola* has dark brown, conidiomata with a thick wall at the base, two types of conidiogenous cells, these ranging from cylindrical with a long, slimy cylindrical neck to ampulliform and wider at the base, straight, short and without paraphyses, whereas *P. mangiferae* has a yellowish brown conidiomata wall, cylindrical to ampulliform conidiomata that are wider at the base, straight conidiogenous cells and paraphyses (Cheewangkoon et al., 2010).

Based on pairwise nucleotide comparisons, *P. dipterocarpicola* is different from *P. mangiferae* in 31/620 bp (3%) in ITS, 7/814 (0.98%) in LSU, 63/410 bp (15%) in *tef1-α* and 87/450 (19%) in *tub2*. Based on the combination of morphological characters and multigene phylogeny, we describe *P. dipterocarpicola* herein as a distinct species according to the guidelines of Jeewon and Hyde (2016).

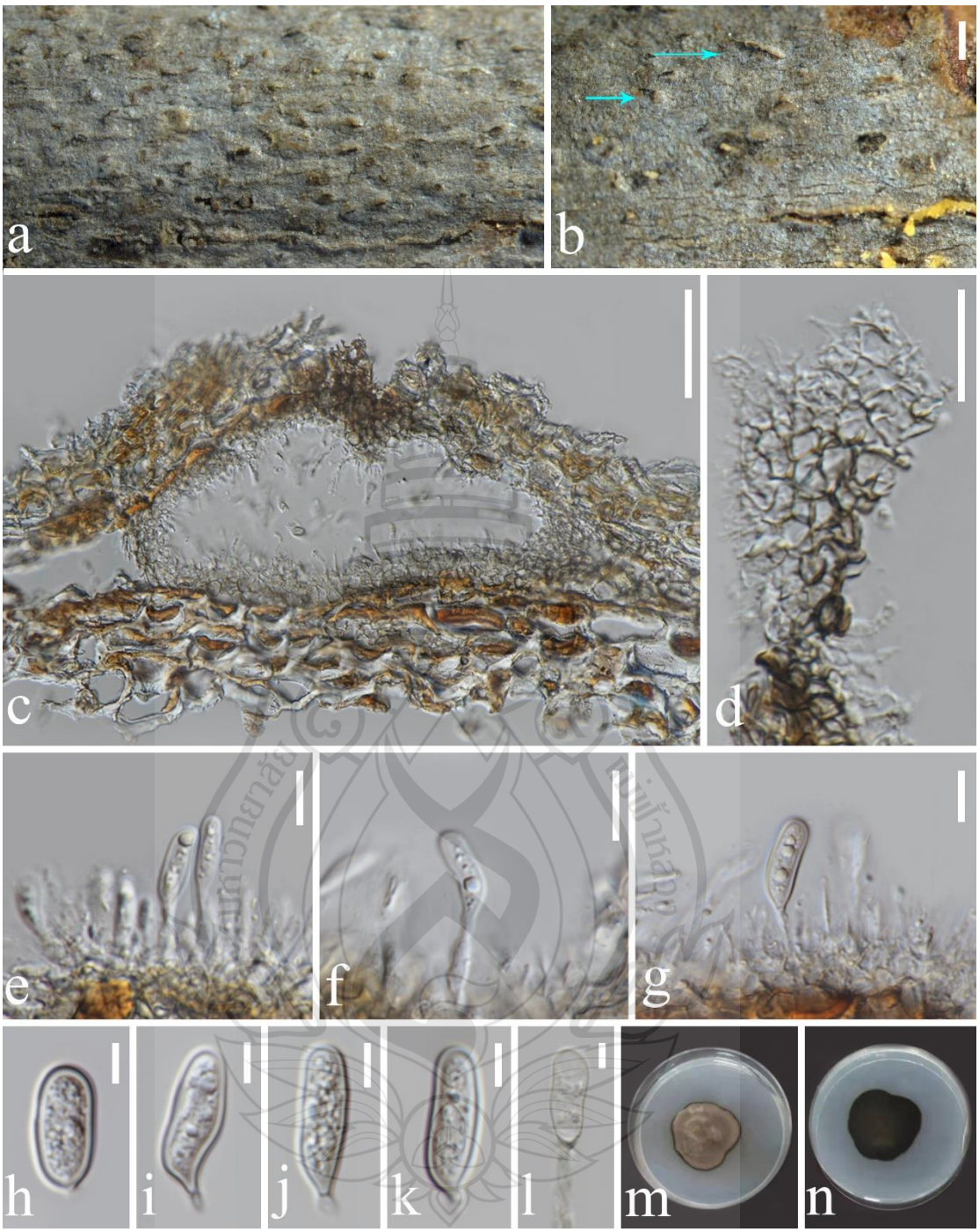

Figure 5.7 *Pseudoplagiostoma dipterocarpicola* (MFLU 21-0177, holotype)

Figure 5.7 a Host. b Specimen with conidiomata. c Vertical section of a conidioma. d Peridium. e–g Conidiogenous cells. h–k Conidia. l Germinated conidium. m, n Colony on PDA, obverse and reverse. Scale bars: b = 500 µm, c = 50 µm, d = 20 µm, e–g = 10 µm, h–l = 5 µm.

5.3 Discussion

Diaporthales (*Sordariomycetes*) is an order that contains saprobic, endophytic, and pathogenic taxa with a wide distribution on a variety of hosts (Barr, 1978; Castlebury et al., 2002; Rossman et al., 2007; Senanayake et al., 2017, 2018; Fan et al., 2018; Jiang et al., 2020). The pathogenic members cause great economic losses, such as chestnut blight, caused by *Cryphonectria parasitica* (*Cryphonectriaceae*) (Gryzenhout et al., 2006; Rigling & Prospero, 2018; Gomdola et al., 2022), polar and willow canker on *Populus* and *Salix*, caused by *Cytospora chrysosperma* (*Cytosporaceae*) (Fan et al., 2014, 2020; Wang et al., 2015), and stem-end rot of citrus fruits infected by *Diaporthe citri* (Huang et al., 2013). Researchers have carried out their research on secondary metabolites in *Diaporthaceae* and *Gnomoniaceae* (Chepkirui & Stadler, 2017; Wu et al., 2019). As saprobes, they cause the degradation of wood, such as *Apiosporopsis carpinea* (*Apiosporopsidaceae*) on the overwintered leaves of *Carpinus betulus* (Senanayake et al., 2017) and *Pseudoplagiostoma dipterocarpicola* on the decaying wood of *Dipterocarpaceae* (Tang et al., 2022). As endophytes, they live in medicinal plants and are used for studies that investigate antimicrobial activities, e.g., *Diaporthe* spp., which were isolated from the hosts *Copaifera langsdorffii* and *C. pubiflora* (de Carvalho et al., 2021). Antibacterial activity has been demonstrated using extracts of two unidentified *Diaporthe* spp. and *D. miriciae* (Carvalho et al., 2018). As more taxonomic studies of fungi are being conducted, the focus has steadily shifted from morphology to a combination of molecular phylogeny and morphology, serving as the foundation for the mainstream approach (Senanayake et al., 2017, 2018; Jiang et al., 2020; Chethana et al., 2021a; Maharachchikumbura et al., 2021). Initially, Castlebury et al. (2002) accepted *Cytosporaceae*, *Diaporthaceae*, *Gnomoniaceae*, and *Melanconidaceae* in *Diaporthales* by using LSU sequence data. Réblová et al. (2004) established a new family *Togniniaceae* to accommodate *Togninia* and its *Phaeoacremonium* anamorphs using LSU and SSU sequence data. Later, the family *Togniniaceae* was transferred into *Togniniales* from *Diaporthales* using LSU, SSU, *tef1-α*, and *rpb2* sequence data (Gramaje et al., 2015; Maharachchikumbura et al., 2015, 2016). The use of multi-gene

analysis for the identification of *Diaporthales* species was seen in subsequent studies, such as the combination of ITS-beta-tubulin (*tub2*) and ITS-LSU (Gryzenhout et al., 2006; Mostert et al., 2006; Cheewangkoon et al., 2010; Crous et al., 2012b; Voglmayr et al., 2012, 2017; Suetrong et al., 2015; Réblová et al., 2016b; Du et al., 2017; Yang et al., 2018; Maharachchikumbura et al., 2021). Voglmayr and Jaklitsch (2014) demonstrated through the evaluation of *Stegonsporium* and *Stilbospora* that LSU alone did not always contain sufficient phylogenetic resolution to identify consistently well-supported phylogenetic relationships at the generic level, and our research results matched this as well. Subsequently, *Schizoparmaceae* was revised using a combination of LSU, *rpb2*, ITS, and *tef1-α* (Alvarez et al., 2016). Combining DNA sequence data of ITS, LSU, *tef1-α*, and *rpb2* is advised by Senanayake et al. (2017, 2018) and Fan et al. (2018) to evaluate the phylogenetic relationships of diaporthalean families. Jiang et al. (2020) used the combination of ITS, LSU, *tef1-α*, and *rpb2* to redefine the family *Cryphonectriaceae* and to describe two new families, *viz. Foliocryphiaceae* and *Mastigosporellaceae*. With the increasing number of studies and knowledge on the diversity of lifestyles in *Diaporthales*, identifying its species has become difficult. The utilization of protein genes makes it possible to have a precise placement in *Diaporthales*, as proven in recent studies (Senanayake et al., 2017, 2018; Jiang et al., 2020). Thus, we suggest analyzing the families in *Diaporthales* via both morphological and molecular traits and the specific genes of each family for multigene phylogenetic analysis.

Members of the *Dipterocarpaceae* are economically significant trees generating lumber, camphor, and resin and are common in Southeast Asia (Maury-Lechon & Curtet, 1998). In this study, two new genera, namely *Pulvinaticonidioma* and *Subellipsoidispora*, were found on *Dipterocarpaceae* species in Thailand and were introduced. We introduce our collections as new genera based on unique features, such as the characteristics of the conidiomata, conidiogenous cells, and conidial appearance, as observed in the new taxon, *Pulvinaticonidioma hyalinum* when compared with other known genera in *Cryphonectriacea*. The results of the ML, MP, and MrBayes analyses also support that this is a new genus in *Cryphonectriaceae* and (Figure 5.1). Similarly, the second collection *Subellipsoidispora guttulata* is morphologically distinct from other known genera in *Coryneaceae* in having unique characteristics in their asci and

the shape of ascospores, and the phylogeny supports it as a new genus in *Coryneaceae* (Figure 5.4).

For our another new species *Ps. dipterocarpicola*, although it is mostly similar to *Plagiostoma* (*Gnomoniaceae*) and the two share some similar characters with respect to their morphology, the former has its own unique characters, including a truly lateral neck and appendages on both ends of its ascospores. At the level of phylogenetics, *Pseudoplagiostoma* is closer to the group of taxa with well-developed stromatic tissue but possessing both stromatic and non-stromatic tissues. The results of phylogenetic analyses showed that *Pseudoplagiostoma* differs from *Plagiostoma* and other families in the *Diaporthales* (Cheewangkoon et al., 2010). In this study, we provided two strains for the new species, *Ps. dipterocarpicola*, which cluster together with a highly support. The morphology of the paratype (MFLUCC 21-0114) is not available, as the herbarium specimen was too dry, but based on pairwise nucleotide comparisons, the two strains are similar (4/585 bp (0.6%) in ITS, 6/814 (0.7%) in LSU, 4/209 (1.9%) in *tef1-α* and 1/457 (0.2%) in *tub2*. We therefore identify these two strains as representing the same species, *Ps. dipterocarpicola*. In addition to the phylogenetic analysis in the text that links to a combined dataset of ITS, LSU, *tef1-α* and *tub2* sequences (Figure 5.6). The comparison results of these two phylogenetic analyses indicated that our new taxa belong to the genus *Pseudoplagiostoma*.

To date, eight species of microfungi on *Dipterocarpaceae* have been described from Thailand, *viz. Hermatomyces thailandica*, *Lauriomyces sakaeratensis*, *Lembosia xyliae*, *Pseudoplagiostoma dipterocarpi*, *Ps. dipterocarpicola*, *Pestalotiopsis shoreae*, *Pulvinaticonidioma hyalinum*, and *Subellipsoidispora guttulata* (Suwannarach et al., 2016; Chethana et al., 2021b; Farr & Rossman, 2025; Tang et al., 2022; This study). Among these species, *Pseudoplagiostoma dipterocarpi* is an endophyte, while the rest are saprobes. It is remarkable that in this study, we found two new genera in a family that has been relatively well studied but on lesser studied hosts. This indicates that many more taxa will be discovered with further surveys on *Dipterocarpaceae* and other poorly studied hosts (Hyde et al., 2020a; Bhunjun et al., 2022).

CHAPTER 6

CONCLUSIONS

6.1 Overall Conclusion

This study focuses on saprobic fungi associated with forest plants and members of *Thymelaeaceae*, with complementary sampling of endophytic fungi from *Thymelaeaceae*. Specimens were collected in Guizhou, Hainan, Guangxi and Yunnan (China) and Chiang Rai (Thailand) from substrates including decayed wood, *Juglans*, *Camptotheca*, *Edgeworthia*, *Stellera*, *Wikstroemia*, *Daphne*, bamboo, and *Dipterocarpus* in Thailand. A total of 72 strains were isolated and identified systematically, belonging to 44 genera, 28 families, 11 orders and 4 classes, mainly *Dothideomycetes* and *Sordariomycetes*, with a few classifieds in *Lecanoromycetes* and *Mucoromycetes*. Among them, 4 new genera and 30 new species, 31 new records and 11 new collections were included. This study provides standardized morphological descriptions, photoplates and multi-gene phylogenetic evidence to clarify their systematic positions. Meanwhile, a total of 557 endophytic fungi were isolated from Thymelaeaceae plants, distributed in 6 classes, Agaricomycetes, Dothideomycetes, Eurotiomycetes, Leotiomycetes, Mucoromycetes, and Sordariomycetes, 20 orders, 38 families, and 53 genrea, the correspondence between different organs/tissues of the Thymelaeaceae and fungal groups was analyzed, and the distribution information of microfungi of each genus and species of the Thymelaeaceae in China was compiled.

When we examined the specimens we collected, we discovered an interesting issue. Among the 72 fungal species we obtained, 90% were hyphomycetes, while only about 10% were performed as sexual of ascomycetes. When we reviewed our sampling locations, times, and specimens, we found the following: (1) The sampling locations were all in the deep forest, rich in decomposing rotten wood; (2) The sampling times were concentrated in March, May, September, October, and November, during which the rainfall was sufficient; (3) The trees at the collection sites were dense, and the light under the forest was insufficient; (4) During the isolation process, we mainly used PDA

medium, and some sexual of ascomycetes were not easy to germinate on PDA, despite multiple attempts, it was still difficult to obtain the cultures, resulting in a further reduction of sexual strains; (5) The collected samples mostly came from surface decaying wood, and it was speculated to be mostly newly fallen and in the early stage of decomposition. Considering all these factors, the reason for this phenomenon might be (i) the deep forest, humid and rich in decomposing wood substrate, together with the seasonal rainfall, provided a long-term high humidity/(semi-)waterlogged microenvironment, promoting the rapid colonization and frequent spore production of hygrophilous and (hydrophilic) ascomycetes on the recently fallen or early decomposed wood and leaf litter; such fungi have been repeatedly reported to be dominant in the decomposition process and community in the moist ecological niche (in streams/semi-humid environments, ascomycetes are the key drivers of litter decomposition and spore flux). (ii) The culture process we adopted was mainly rich in nutrients, at 25–28°C and with a shorter culture period, making it easier to "screen" fast-growing and easily spore-producing asexual basidiomycetes, while many slow-growing or requiring specific induction conditions groups (including some basidiomycete sexual forms and ascomycetes) were not easy to germinate/spore-produce on PDA, resulting in a bias towards ascomycetes in the culturable results; morphological induction and humid chamber methods, etc., with low nutrition/light treatment, are more conducive to detecting these "difficult-to-grow" groups. (iii) The samples were mostly taken from surface, early-decomposition stage decaying wood and litter, which was already in the "pioneer occupation" window of ascomycetes; during this time window, the colonization and spore production rates of ascomycetes were often higher than other functional groups, thus showing an increase in proportion at the isolation level. At the same time, some previous literature has also reported this.

6.2 Research Advantages

6.2.1 In this survey of saprobic fungi associated with forest plants, we discovered and described a number of previously unreported new species and new genera, along with several new country, habitat, and host records. For these taxa, we

provide detailed morphological descriptions, illustrations, and multi-gene phylogenetic analyses, thereby clarifying their accurate taxonomic placement. We also recovered several species that were described long ago; by comparing our material with historical morphological accounts and integrating molecular evidence, we resolved their relationships and bridged classical morphology-based taxonomy with modern phylogenetic frameworks. The new records further indicate that many saprobic fungi are not strictly host-specific but occur across multiple hosts and habitats, revealing greater ecological and systematic diversity. We also present complete specimen and collection data, thereby enriching the fungal biodiversity inventory of forest plants in Thailand and China and providing a solid foundation for subsequent taxonomic and ecological studies.

6.2.2 Most studies on the *Thymelaeaceae* have focused on agarwood-producing taxa, whereas fungi associated with other members of the family remain sparsely investigated. This study sampled multiple organs from species of *Daphne*, *Wikstroemia*, *Aquilaria*, and *Stellera*, and analyzed their endophytic fungi to explore organ-specific distribution patterns across *Thymelaeaceae* hosts. In addition, a checklist for the *Thymelaeaceae* species associated with microfungi in China were firstly provided.

6.2.3 An investigation of the microfungi associated with the surface decaying wood in subtropical and tropical forests. The results revealed that when branches fell and entered the early stage of decomposition, the community was dominated by functional groups such as rapid colonizing ascomycete/anamorphic ascomycetes, showing clear morphological-ecological preferences (such as exposed conidia and higher hyphal extension/spore production capabilities), corresponding to the pioneer stage of wood decomposition succession. This pattern is consistent with tropical/subtropical wood decomposition studies, the fungal community succession of dead wood and coarse woody debris (CWD), and the wood decomposition framework based on traits.

6.3 Future Work

6.3.1 Biodiversity Exploration

Future work should continue to focus on diversity surveys of saprobic fungi associated with forest plants and, on that basis, elucidate community structure, species interactions, and their roles and mechanisms in decomposition and nutrient (including carbon) cycling within forest ecosystems.

6.3.2 Distribution of Microfungi from Different Layers of Fallen Decaying Wood

By surveying the distribution of fungi across different layers of fallen coarse woody debris in forests (surface, interior, and the wood–soil interface) together with the surrounding soil microbiota, we elucidate the fungal community structure and successional dynamics at each stage of wood decomposition.

6.3.3 From Leaf to Root: Stratified Distribution of Endophytes from *Thymelaeaceae*

By systematically surveying and isolating endophytic fungi from different organs of Thymelaeaceae (e.g., leaves, twigs, bark, and roots), we characterize organ-specific community patterns and elucidate how endophytes influence host growth, stress tolerance, and nutrient acquisition.

6.3.4 Association between Fungal Community Distribution in *Stellera* sp. and Plant Toxicity

Our study shows that the roots of *Stellera* harbor lower endophytic fungal richness/abundance than other organs. Given that the plant's principal toxic constituents are concentrated in the roots—and that *Stellera* has been implicated in grassland degradation/desertification in some regions (potentially via toxicity, allelopathy, and livestock avoidance)—clarifying the organ-specific distribution patterns of its endophytes may inform risk assessment and management of grassland degradation (e.g., restoration actions and grazing management).

6.4 Publications

List of publications

6.4.1 First Author

Tang, X., Goonasekara, I. D., Jayawardena, R. S., Jiang, H. B., Li, J. F., Hyde, K. D., . . . Kang, J. C. (2020). *Arthrinium bambusicola* (Fungi, *Sordariomycetes*), a new species from Schizostachyum brachycladum in northern Thailand. *Biodiversity Data Journal, 8*, e58755. https://doi.org/10.3897/BDJ.8.e58755

Tang, X., Jayawardena, R. S., Stephenson, S. L., & Kang, J. C. (2022). A new species *Pseudoplagiostoma dipterocarpicola* (*Pseudoplagiostomataceae*, *Diaporthales*) found in northern Thailand on members of the *Dipterocarpaceae*. *Phytotaxa, 543*(4), 233-243.

Tang, X., Lu, Y. Z., Dissanayake, L. S., Goonasekara, I. D., Jayawardena, R. S., Xiao, Y. P., . . . Kang, J. C. (2023). Two new fungal genera (*Diaporthales*) found on *Dipterocarpaceae* in Thailand. *Frontiers in Microbiology, 14*, 1169052. https://doi.org/10.3389/fmicb.2023.1169052

Tang, X., Jeewon, R., Lu, Y. Z., Alrefaei, A. F., Jayawardena, R. S., Xu, R. J., . . . Kang, J. C. (2023). Morphophylogenetic evidence reveals four new fungal species within *Tetraplosphaeriaceae* (*Pleosporales*, *Ascomycota*) from tropical and subtropical forest in China. *MycoKeys, 100*, 171-204. https://doi.org/10.3897/mycokeys.100.113141

Tang, X., Jeewon, R., Jayawardena, R. S., Gomdola, D., Lu, Y. Z., Xu, R. J., . . . Kang, J. C. (2024). Additions to the genus *Kirschsteiniothelia* (*Dothideomycetes*); Three novel species and a new host record, based on morphology and phylogeny. *MycoKeys, 110*, 35-66. https://doi.org/10.3897/mycokeys.110.133450

Tang, X., Lu, Y. Z., Jayawardena, R. S., Kang, J. C., & Hyde, K. D. Taxonomic and phylogenetic evidence reveals two novel asexual species of *Strossmayeria* (*Leotiomycetes*) from the subtropical forests of China. [Manuscript preparation]

Tang, X., Lu, Y. Z., Jayawardena, R. S., Kang, J. C., & Hyde, K. D. Discovery of two novel fungal species and one new host record from C. in tropical and subtropical forests of China. [Manuscript preparation]

Tang, X., Jayawardena, R. S., Lu, Y. Z., Jeewon R., Kang, J. C., & Hyde, K. D. (2025) Discovery of a novel fungal species, *Periconia xishuiensis* from *Periconia* in subtropical forests of China. [Manuscript preparation]

Tang, X., Jayawardena, R. S., Jeewon R., Lu, Y. Z., Kang, J. C., & Hyde, K. D. (2025). Unravelling new taxa of *Dothideomycetes* associated with forest plants in China (at least 60 species, in which of 28 new species). [Manuscript preparation]

6.4.2 Co-author

Chen, X. M., Tang, X., Du, T. Y., Lu, Y. Z., Suwannarach, N., Xu, R. F., . . . Karunarathna, S. C. (2024). Two new species of *Rhodoveronaea* (*Rhamphoriales, Ascomycota*) from terrestrial habitats in China. *Phytotaxa, 638*(1), 49-60.

Chen, X. M., Tang, X., Ma, J., Liu, N. G., Tibpromma, S., Karunarathna, S. C., . . . Lu, Y. Z. (2024). Identification of two new species and a new host record of *Distoseptispora* (*Distoseptisporaceae, Distoseptisporales, Sordariomycetes*) from terrestrial and freshwater habitats in Southern China. *MycoKeys, 102*, 83-105. https://doi.org/10.3897/mycokeys.102.115452

Chethana, K. W. T., Niranjan, M., Dong, W., Samarakoon, M. C., Bao, D. F., Calabon, M. S., . . . Hyde, K. D. (2021). AJOM new records and collections of fungi: 101–150. *Asian Journal of Mycology, 4*(1), 113–260. https://doi.org/10.5943/ajom/4/1/8

Chethana, K. W., Jayawardena, R. S., Chen, Y. J., Konta, S., Tibpromma, S., Phukhamsakda, C., . . . Hyde, K. D. (2021). Appressorial interactions with host and their evolution. Fungal Diversity, 110(1), 75–107. https://doi.org/10.1007/s13225-021-00487-5

Dissanayake, L. S., Samarakoon, M. S., Maharachchikumbura, S. S., Hyde, K. D., Tang, X., Li, Q. R., . . . Wanasinghe, D. N. (2024). Exploring the taxonomy and phylogeny of Sordariomycetes taxa emphasizing Xylariomycetidae in Southwestern China. *Mycosphere, 15*(1), 1675-1793.

Dong, W., Hyde, K. D., Jeewon, R., Karunarathna, S. C., Zhang, H., Rossi, W., . . .Doilom, M. (2025). Fungal diversity notes 2017–2122: Taxonomic and phylogenetic contributions to freshwater fungi and other fungal taxa. *Fungal Diversity, 134*, 185-459. https://doi.org/10.1007/s13225-025-00560-3

Gomdola, D., Jeewon, R., McKenzie, E. H., Jayawardena, R. S., Al-Otibi, F., Tang, X., . . . Fu, L. (2025). Phylogenetic diversity of Colletotrichum species (Sordariomycetes, Glomerellales, Glomerellaceae) associated with plant diseases in Thailand. *MycoKeys, 119*, 137-195.

Hyde et al., next families of sordariomycetes (2025?). [Unpublished manuscript].

Hyde, K. D., Noorabadi, M. T., Thiyagaraja, V., He, M. Q., Johnston, P. R., Wijesinghe, S. N., . . . Radek, R. (2024). The 2024 outline of fungi and fungus-like taxa. *Mycosphere, 15*, 5146-6239. https://doi.org/10.5943/mycosphere/15/1/25

Hyde, K. D., Norphanphoun, C., Ma, J., Yang, H. D., Zhang, J. Y., Du, T. Y., . . . Zhao, Q. (2023). Mycosphere notes 387–412 – novel species of fungal taxa from around the world. *Mycosphere 14*(1), 663–744. https://doi.org/10.5943/mycosphere/14/1/8

Hyde, K. D., Suwannarach, N., Jayawardena, R. S., Manawasinghe, I. S., Liao, C. F., Doilom, M., . . . Bao, D. F. (2021). Mycosphere notes 325–344–Novel species and records of fungal taxa from around the world. *Mycosphere, 12*(1), 1101-1156. https://doi.org/10.5943/mycosphere/12/1/14

Hyde, K. D.,et al., ….AJOM (2025?). [Unpublished manuscript].

Hyde, K. D.,et al., ….CREAM (2025?). [Unpublished manuscript].

Hyde, K. D.,et al., ….Fungalpedia (2025?). [Unpublished manuscript].

Hyde, K., D., et al., 2025……fungal diversity notes Unpublished.

Jayawardena, R. S., Hyde, K. D., de Farias, A. R. G., Bhunjun, C. S., Ferdinandez, H. S., Manamgoda, D. S., . . . Thines, M. (2021). What is a species in fungal plant pathogens?. *Fungal Diversity, 109*, 239–266. https://doi.org/10.1007/s13225-021-00484-8

Jayawardena, R. S., Hyde, K. D., Wang, S., Sun, Y. R., Suwannarach, N., Sysouphanthong, P., . . . Wang, Y. (2022). Fungal diversity notes 1512–1610: Taxonomic and phylogenetic contributions on genera and species of fungal taxa. *Fungal Diversity, 117*(1), 1-272. https://doi.org/10.1007/s13225-022-00513-0

Jayawardena, R. S., Xia Tang et al., One stop shop VI. (?) Fungal diversity. (two genera). [Unpublished manuscript].

Lu, Q. T., Zhang, J. Y., Sun, Y. R., Tang, X., Lu, Y. Z., & Zhang, Z. (2022). *Diaporthe orixae* sp. nov., an endophytic species isolated from Orixa japonica in southern China. *Phytotaxa, 544*(1), 37-51.

Ma, J., Gomdola, D., Boonmee, S., Shen, H. W., Tang, X., Zhang, L. J., . . . Hyde, K. D. (2024). Three new species of *Neohelicomyces* (*Tubeufiales, Tubeufiaceae*) from freshwater and terrestrial habitats in China. *MycoKeys, 105*, 317.

Ma, J., Liu, N. G., Tang, X., Xiao, X. J., Chen, X. M., Xiao, Y. P., . . . Boonmee, S. (2023). Sclerococcum pseudobactrodesmium sp. nov. from a terrestrial habitat in China. *Phytotaxa, 630*(1), 69-79.

Ma, J., Zhang, J. Y., Xiao, X. J., Xiao, Y. P., Tang, X., Boonmee, S., . . . Lu, Y. Z. (2022). Multi-gene phylogenetic analyses revealed five new species and two new records of Distoseptisporales from China. *Journal of Fungi, 8*(11), 1202.

Mi et al., fungalpedia (2025?). [Unpublished manuscript].

Oom et al., (2025) fungalpedia. [Unpublished manuscript].

Yang, M., Lu, Y., Han, L., He, Z., Tang, X., & Kang, J. (2025). A novel endophytic fungus, alternaria semiverrucosa, and its ethyl acetate extract inhibit the proliferation, migration, and invasion of cervical cancer cells. *Chemistry & Biodiversity, 6*, e00945. https://doi.org/10.1002/cbdv.202500945

REFERENCES

Abdelfattah, A., Li Destri Nicosia, M. G., Cacciola, S. O., Droby, S., & Schena, L. (2015). Metabarcoding analysis of fungal diversity in the phyllosphere and carposphere of olive (*Olea europaea*). *PLoS One*, *10*(7), e0131069. https://doi.org/10.1371/journal.pone.0131069

Abelho, M., & Descals, E. (2019). Litter movement pathways across terrestrial–aquatic ecosystem boundaries affect litter colonization and decomposition in streams. *Functional Ecology*, *33*(9), 1785–1797. https://doi.org/10.1111/1365-2435.13356

Abreu, V. P., Pereira, O. L., Hyde, K. D., Bazzicalupo, A., Chethana, K. W., Clericuzio, M., . . . Kušan, I. (2017). Fungal diversity notes 603–708: Taxonomic and phylogenetic notes on genera and species. *Fungal Diversity*, *87*, 1–235. https://doi.org/10.1007/s13225-017-0391-3

Adeleke, B. S., & Babalola, O. O. (2021). The plant endosphere-hidden treasures: A review of fungal endophytes. *Biotechnology and Genetic Engineering Reviews*, *37*(2), 154–177. https://doi.org/10.1080/02648725.2021.1991714

Agut, M., & Calvo, M. Á. (2004). In vitro conidial germination in *Arthrinium aureum* and A*rthrinium phaeospermum*. *Mycopathologia*, *157*(4), 363–367. https://doi.org/10.1023/B:MYCO.0000030432.08860.f3

Ai, C. C., Ma, J., Zhang, K., Castañeda-Ruíz, R. F., & Zhang, X. G. (2019). *Cordana meilingensis* and *C. lushanensis* spp. nov. from Jiangxi, China. *Mycotaxon*, *134*(2), 329–334. https://doi.org/10.5248/134.329

Alexander, I. J., & Högberg, P. (1986). Ectomycorrhizas of tropical angiosperm trees. *New Phytologist*, *102*, 541–549.

Alexopoulus, C. J., & Mims, C. W. (1978). *Introductory mycology* (3rd ed.). Wiley.

Alvarez, L. V., Groenewald, J. Z., & Crous, P. W. (2016). Revising the *Schizoparmaceae*: Coniella and its synonyms *Pilidiella* and *Schizoparme*. *Studies in Mycology*, *85*, 1–34. https://doi.org/10.1016/j.simyco.2016.09.001

Alves, V. S., & Gusmão, L. F. P. (2024). *Xylomyces* (*Aliquandostipitaceae*, *Jahnulales*) freshwater hyphomycetes from the Brazilian Amazon. *Nova Hedwigia*, *111*, 187–197.

Ando, K. (1992). A study of terrestrial aquatic hyphomycetes. *Trans Mycol Soc Jpn*, *33*, 415–425.

Arnold, A. E., Maynard, Z., & Gilbert, G. S. (2001). Fungal endophytes in dicotyledonous neotropical trees: patterns of abundance and diversity. *Mycological research*, *105*(12), 1502–1507.

Arnold, A. E., Maynard, Z., Gilbert, G. S., Coley, P. D., & Kursar, T. A. (2000). Are tropical fungal endophytes hyperdiverse?. *Ecology letters*, *3*(4), 267–274.

Aryal, G. M., Kandel, K. P., Bhattarai, R. K., Giri, B., Adhikari, M., Ware, A., . . . Neupane, B. B. (2022). Material properties of traditional handmade paper samples fabricated from cellulosic fiber of lokta bushes. *ACS omega*, *7*(36), 32717–32726. https://doi.org/10.1021/acsomega.2c04398

Asanok, L., Kamyo, T., Norsaengsri, M., Salinla-um, P., Rodrungruang, K., Karnasuta, N., . . . Kutintara, U. (2017). Vegetation community and factors that affect the woody species composition of riparian forests growing in an urbanizing landscape along the Chao Phraya River, central Thailand. *Urban Forestry & Urban Greening*, *28*, 138–149. https://doi.org/10.1016/j.ufug.2017.10.013

Aschehoug, E. T., Callaway, R. M., Newcombe, G., Tharayil, N., & Chen, S. (2014). Fungal endophyte increases the allelopathic effects of an invasive forb. *Oecologia*, *175*(1), 285–291. https://doi.org/10.1007/s00442-014-2891-0

Bagchee, K. D. (1954). The fungal diseases of Sal (*Shorea robusta* Gaertn. f.). Indian Forest Records (New Series), *Mycology*, *1*, 97–184.

Baird, R. E., Watson, C. E., & Woolfolk, S. (2007). Microfungi from bark of healthy and damaged American beech, fraser fir, and eastern hemlock trees during an all taxa biodiversity inventory in forests of the Great Smoky Mountains National Park. *Southeastern Naturalist*, *6*(1), 67–82. https://doi.org/10.1656/1528-7092(2007)6[67:MFBOHA]2.0.CO;2

Bakshi, B. K. (1957). Fungi causing diseases of forest plants in India. *Indian Forest Records (New Series), Pathology*, *2*, 1–39.

Bao, D. F., Hyde, K. D., Maharachchikumbura, S. S., Perera, R. H., Thiyagaraja, V., Hongsanan, S., . . . Luo, Z. L. (2023). Taxonomy, phylogeny and evolution of freshwater *Hypocreomycetidae* (*Sordariomycetes*). *Fungal Diversity*, *121*(1), 1–94. https://doi.org/10.1007/s13225-023-00521-8

Bao, D. F., Zhang, J. Y., Lu, Y. Z., Tian, X. G., Hyde, K. D., Liu, N. G., . . . Kang, J. C. (2025). Endophytic fungi associated with medicinal ferns in Guizhou Province, China I: Morpho-molecular characterization of culturable endophytic fungi associated with *Dicranopteris* spp. *Mycosphere*, *16*(1), 2259–2455. https://doi.org/10.5943/mycosphere/16/1/13

Barnés-Guirado, M., Stchigel, A. M., & Cano-Lira, J. F. (2024). A new genus of the *Microascaceae* (*Ascomycota*) family from a hypersaline lagoon in Spain and the delimitation of the genus *Wardomyces*. *Journal of Fungi*, *10*(4), 236. https://doi.org/10.3390/jof10040236

Barr, M. E. (1978). The *Diaporthales* in North America: with emphasis on *Gnomonia* and its segregates. *Mycologia Memoir*.

Barr, M. E. (2000). Notes on coprophilous bitunicate *Ascomycetes*. *Mycotaxon*, *76*, 105–112.

Barr, M. E., & Huhndorf, S. M. (2001). *Loculoascomycetes*. In Systematics and Evolution: Part A (pp. 283–305). *Springer Berlin Heidelberg.* https://doi.org/10.1007/978-3-662-10376-0_13

Bayman, P., Angulo-Sandoval, P., Báez-Ortiz, Z., & Lodge, D. J. (1998). Distribution and dispersal of *Xylaria* endophytes in two tree species in Puerto Rico. *Mycological Research*, *102*(8), 944–948.

Berry, P. E., & Bates, D. M. (2010, August 30). *Malvales*. In Encyclopaedia Britannica. *Encyclopaedia Britannica*. https://www.britannica.com/plant/Malvales

Bezerra, J. D. P., Pádua, A. P. S. L., Oliveira, T. G. L., Paiva, L. M., Guarnaccia, V., & Souza-Motta, C. M. (2019). *Pseudoplagiostoma myracrodruonis* (*Pseudoplagiostomataceae*, *Diaporthales*): a new endophytic species from Brazil. *Mycological Progress*, *18*, 1329–1339. https://doi.org/10.1007/s11557-019-01531-0

Bhattacharyya, B., Datta, A., & Baruah, H. K. (1952). On the formation and development of agaru in *Aquilaria agallocha*. *Science and Culture*, *18*(5), 240–241.

Bhunjun, C. S., Niskanen, T., Suwannarach, N., Wannathes, N., Chen, Y. J., McKenzie, E. H. C., . . . Lumyong, S. (2022). The numbers of fungi: are the most speciose genera truly diverse? *Fungal Diversity*, *114*, 387–462. https://doi.org/10.1007/s13225-022-00501-4

Bills, G. F., & Polishook, J. D. (1994). Abundance and diversity of microfungi in leaf litter of a lowland rain forest in Costa Rica. *Mycologia*, *86*(2), 187–198. https://doi.org/10.1080/00275514.1994.12026393

Black, W. D. (2020). A comparison of several media types and basic techniques used to assess outdoor airborne fungi in *Melbourne*, Australia. *PLoS One*, *15*(12), e0238901. https://doi.org/10.1371/journal.pone.0238901

Boehm, E. W. A., Mugambi, G. K., Miller, A. N., Huhndorf, S. M., Marincowitz, S., Spatafora, J. W., . . . Schoch, C. L. (2009). A molecular phylogenetic reappraisal of the *Hysteriaceae*, *Mytilinidiaceae* and *Gloniaceae* (*Pleosporomycetidae*, *Dothideomycetes*) with keys to world species. *Studies in Mycology*, *64*(1), 49–83. https://doi.org/10.3114/sim.2009.64.03

Boehm, E. W., Schoch, C. L., & Spatafora, J. W. (2009). On the evolution of the *Hysteriaceae* and *Mytilinidiaceae* (*Pleosporomycetidae*, *Dothideomycetes*, *Ascomycota*) using four nuclear genes. *Mycological Research*, *113*(4), 461–479. https://doi.org/10.1016/j.mycres.2008.12.001

Bonan, G. B. (2008). Forests and climate change: Forcings, feedbacks, and the climate benefits of forests. *Science*, *320*(5882), 1444–1449. https://doi.org/10.1126/science.1155121

Boonmee, S., D'souza, M. J., Luo, Z., Pinruan, U., Tanaka, K., Su, H., . . . Hyde, K. D. (2016). *Dictyosporiaceae* fam. nov. *Fungal Diversity*, *80*(1), 457–482. https://doi.org/10.1007/s13225-016-0363-z

Boonmee, S., Ko, T. W. K., Chukeatirote, E., Hyde, K. D., Chen, H., Cai, L., . . . Hassan, B. A. (2012). Two new *Kirschsteiniothelia* species with *Dendryphiopsis* anamorphs cluster in *Kirschsteiniotheliaceae* fam. nov. *Mycologia*, *104*(3), 698–714. https://doi.org/10.3852/11-089

Boonmee, S., Wanasinghe, D. N., Calabon, M. S., Huanraluek, N., Chandrasiri, S. K., Jones, G. E., . . . Hyde, K. D. (2021). Fungal diversity notes 1387–1511: Taxonomic and phylogenetic contributions on genera and species of fungal taxa. *Fungal Diversity*, *111*(1), 1–335. https://doi.org/10.1007/s13225-021-00489-3

Boonmee, S., Zhang, Y., Chomnunti, P., Chukeatirote, E., Tsui, C. K., Bahkali, A. H., & Hyde, K. D. (2011). Revision of lignicolous *Tubeufiaceae* based on morphological reexamination and phylogenetic analysis. *Fungal Diversity*, *51*(1), 63–102. https://doi.org/10.1007/s13225-011-0147-4

Braun, U., & Heuchert, B. (2010). *Sporidesmiella lichenophila* sp. nov.—A new lichenicolous hyphomycete. *Herzogia*, *23*(1), 69–74. https://doi.org/10.13158/heia.23.1.2010.69

Brearley, F. Q. (2012). Ectomycorrhizal associations of the *Dipterocarpaceae*. *Biotropica*, *44*(5), 637–648. https://doi.org/10.1111/j.1744-7429.2012.00862.x

Brown, K. B., Hyde, K. D., & Guest, D. I. (1998). Preliminary studies on endophytic fungal communities of Musa acuminata species complex in Hong Kong and Australia. *Fungal Diversity*, *1*, 27–51.

Calabon, M. S., Hyde, K. D., Jones, E. G., Luo, Z. L., Dong, W., Hurdeal, V. G., . . . Zeng, M. (2022). Freshwater fungal numbers. *Fungal Diversity*, *114*(1), 3–235. https://doi.org/10.1007/s13225-022-00503-2

Calduch, M., Gené, J., Guarro, J., Mercado-Sierra, A., & Castañeda-Ruíz, R. F. (2002). Hyphomycetes from Nigerian rain forests. *Mycologia*, *94*(1), 127–135. https://doi.org/10.1080/15572536.2003.11833255

Calvo, A., & Guarro, J. (1980). *Arthrinium aureum* sp. nov. from Spain. *Transactions of the British Mycological Society*, *75*(1), 156–157.

Capella-Gutiérrez, S., Silla-Martínez, J. M., & Gabaldón, T. (2009). trimAl: a tool for automated alignment trimming in large-scale phylogenetic analyses. *Bioinformatics*, *25*, 1972–1973. https://doi.org/10.1093/bioinformatics/btp348

Capital, V., & Lao, P. (2020). AJOM new records and collections of fungi: 1–100. *Asian Journal of Mycology*, *3*, 22–294. https://doi.org/10.5943/ajom/3/1/3

Carbone, I., & Kohn, L. M. (1999). A method for designing primer sets for speciation studies in filamentous ascomycetes. *Mycologia*, *91*, 553–556. https://doi.org/10.1080/00275514.1999.12061051

Carvalho, C. D., Ferreira-D'Silva, A., Wedge, D. E., Cantrell, C. L., & Rosa, L. H. (2018). Antifungal activities of cytochalasins produced by *Diaporthe miriciae*, an endophytic fungus associated with tropical medicinal plants. *Canadian Journal of Microbiology*, *64,* 835–843. https://doi.org/10.1139/cjm-2018-0131

Castañeda, R. F., & Kendrick, B. (1990). Conidial fungi from Cuba: II. *Department of Biology, University of Waterloo*.

Castañeda-Ruiz, R. F., Iturriaga, T., & Guarro, J. (1999). A new species of *Cordana* from Venezuela. *Mycotaxon*, *73*, 1–8.

Castañeda-Ruiz, R. F., Li, D. W., Zhang, X. G., Kendrick, B., Ramos-García, B., Pérez-Martínez, S., . . . Sosa, D. (2018). *Ellismarsporium* gen. nov. and *Stanhughesiella* gen. nov. to accommodate atypical *Helminthosporium* and *Corynesporella* species. *Mycotaxon*, *132*(4), 759–766. https://doi.org/10.5248/132.759

Castlebury, L. A., Rossman, A. Y., Jaklitsch, W. J., & Vasilyeva, L. N. (2002). A preliminary overview of the *Diaporthales* based on large subunit nuclear ribosomal DNA sequences. *Mycologia*, *94*, 1017–1031. https://doi.org/10.1080/15572536.2003.11833157

Chalermpongse, A. (1987). Mycorrhizal survey of dry-deciduous and semi-evergreen dipterocarp forest ecosystems in Thailand. In *Proceedings third round table conference on dipterocarps* (pp. 81–102). UNESCO.

Chang, H. S. (1995). Some dematiaceous hyphomycetes from Taiwan. *Fungal Science*, *10*, 1–11.

Chauvet, E., & Suberkropp, K. (1998). Temperature and sporulation of aquatic hyphomycetes. *Applied and Environmental Microbiology*, *64*(4), 1522–1525. https://doi.org/10.1128/AEM.64.4.1522-1525.1998

Cheewangkoon, R., Groenewald, J. Z., Verkley, G. J. M., Hyde, K. D., Wingfield, M. J., Gryzenhout, M., . . . Crous, P. W. (2010). Re-evaluation of *Cryptosporiopsis eucalypti* and *Cryptosporiopsis*-like species occurring on *Eucalyptus* leaves. *Fungal diversity*, *44*(1), 89–105. https://doi.org/10.1007/s13225-010-0041-5

Chen, C. Y., & Hsieh, W. H. (2004). *Byssosphaeria* and *Herpotrichia* from Taiwan, with notes on the taxonomic relationship between these two genera. *Sydowia*, *56*(1), 24–38.

Chen, J. L., & Tzean, S. S. (1993). *Megacapitula villosa* gen. et sp. nov. from Taiwan. *Mycological Research*, *97*, 347–350.

Chen, J. L., Hwang, C. H., & Tzean, S. S. (1991). *Dictyosporium digitatum*, a new hyphomycete from Taiwan. *Mycological Research*, *95*(9), 1145–1149. https://doi.org/10.1016/S0953-7562(09)80565-0

Chen, S. F., Liu, Q. L., Li, G. Q., Wingfield, M. J., & Roux, J. (2018). A new genus of *Cryphonectriaceae* isolated from *Lagerstroemia speciosa* in southern China. *Plant Pathology*, *67*, 107–123. https://doi.org/10.1111/ppa.12723

Chen, Y. Y., Dissanayake, A. J., Liu, Z. Y., & Liu, J. K. J. (2020). Additions to Karst Fungi 4: *Botryosphaeria* spp. associated with woody hosts in Guizhou province, China including *B. guttulata* sp. nov. *Phytotaxa*, *454*(3), 186–202. https://doi.org/10.11646/phytotaxa.454.3.2

Chen, Y., Tian, W., Guo, Y., Madrid, H., & Maharachchikumbura, S. S. (2022). *Synhelminthosporium* gen. et sp. nov. and two new species of *Helminthosporium* (*Massarinaceae*, *Pleosporales*) from Sichuan Province, China. *Journal of Fungi*, *8*(7), 712. https://doi.org/10.3390/jof8070712

Chepkirui, C., & Stadler, M. (2017). The genus *Diaporthe*: a rich source of diverse and bioactive metabolites. *Mycological Progress*, *16*, 477–494. https://doi.org/10.1007/s11557-017-1288-y

Chethana, K. T., Manawasinghe, I. S., Hurdeal, V. G., Bhunjun, C. S., Appadoo, M. A., Gentekaki, E., . . . Hyde, K. D. (2021a). What are fungal species and how to delineate them?. *Fungal Diversity*, *109*(1), 1–25. https://doi.org/10.1007/s13225-021-00483-9

Chethana, K. W. T., Niranjan, M., Dong, W., Samarakoon, M. C., Bao, D. F., Calabon, M. S., . . . Hyde, K. D. (2021b). AJOM new records and collections of fungi: 101–150. *Asian Journal of Mycology*, *4*, 113–260. https://doi.org/10.5943/ajom/4/1/8

Chhipa, H., Chowdhary, K., & Kaushik, N. (2017). Artificial production of agarwood oil in *Aquilaria* sp. by fungi: A review. P*hytochemistry Reviews*, *16*(5), 835–860. https://doi.org/10.1007/s11101-017-9492-6

CITES. (2022). *Agarwood-producing genera (Aquilaria, Gyrinops)—review and trade documentation (SC/Annex reports)*. International Tropical Timber Organization (ITTO); CITES Secretariat.

Cobos-Villagrán, A., Pérez-Valdespino, A., Valenzuela, R., Martínez-González, C. R., Luna-Vega, I., Villa-Tanaca, L., . . . Raymundo, T. (2025). New Species of *Byssosphaeria* (*Melanommataceae*, *Pleosporales*) from the Mexican Tropical Montane Cloud Forest. *Journal of Fungi*, *11*(2), 89. https://doi.org/10.3390/jof11020089

Collinge D. B., Jensen, B., & Jørgensen, H. J. L. (2022). Fungal endophytes in plants and their relationship to plant health: progress and challenges. *Current Opinion in Plant Biology*, *67*, 102247. https://doi.org/10.1016/j.mib.2022.102177

Comita, L. S., Queenborough, S. A., Murphy, S. J., Eck, J. L., Xu, K., Krishnadas, M., . . . Zhu, Y. (2014). Testing predictions of the J anzen-C onnell hypothesis: A meta-analysis of experimental evidence for distance-and density-dependent seed and seedling survival. *Journal of Ecology*, *102*(4), 845–856. https://doi.org/10.1111/1365-2745.12232

Cooke, M. C., & Plowright, C. B. (1879). British Sphaeriacei. *Grevillea*, *7*, 77–89.

Corda, A. C. J. (1837). *Icones fungorum hucusque cognitorum* (Vol. 1). JG Calve.

Crous, P. W., & Groenewald, J. Z. (2013). A phylogenetic re-evaluation of *Arthrinium*. *IMA fungus*, *4*(1), 133–154. https://doi.org/10.5598/imafungus.2013.04.01.13

Crous, P. W., Carris, L. M., Giraldo, A., Groenewald, J. Z., Hawksworth, D. L., Hemández-Restrepo, M., . . . Wood, A. R. (2015). The genera of fungi-fixing the application of the type species of generic names-G 2: *Allantophomopsis*, *Latorua*, *Macrodiplodiopsis*, *Macrohilum*, *Milospium*, *Protostegia*, *Pyricularia*, *Robillarda*, *Rotula*, *Septoriella*, *Torula*, and *Wojnowicia*. *IMA fungus*, *6*(1), 163–198. https://doi.org/10.5598/imafungus.2015.06.01.11

Crous, P. W., Luangsa-Ard, J. J., Wingfield, M. J., Carnegie, A. J., Hernández-Restrepo, M., Lombard, L., . . . Groenewald, J. Z. (2018a). Fungal Planet description sheets: 785–867. *Persoonia-Molecular Phylogeny and Evolution of Fungi*, *41*(1), 238–417. https://doi.org/10.3767/persoonia.2018.41.12

Crous, P. W., Schoch, C. L., Hyde, K. D., Wood, A. R., Gueidan, C., De Hoog, G. S., . . . Groenewald, J. Z. (2009). Phylogenetic lineages in the *Capnodiales*. *Studies in mycology*, *64*(1), 17–47. https://doi.org/10.3114/sim.2009.64.02

Crous, P. W., Schumacher, R. K., Akulov, A., Thangavel, R., Hernández-Restrepo, M., Carnegie, A. J., . . . Groenewald, J. Z. (2019). New and interesting fungi. 2. *Fungal Systematics and Evolution*, *3*, 57–134. https://doi.org/10.3114/fuse.2019.03.06

Crous, P. W., Schumacher, R. K., Wingfield, M. J., Akulov, A., Denman, S., Roux, J., . . . Groenewald, J. Z. (2018b). New and interesting fungi. 1. *Fungal Systematics and Evolution*, *1*(1), 169–215. https://doi.org/10.3114/fuse.2018.01.08

Crous, P. W., Summerell, B. A., Alfenas, A. C., Edwards, J., Pascoe, I. G., Porter, I. J., & Groenewald, J. Z. (2012a). Genera of diaporthalean coelomycetes associated with leaf spots of tree hosts. *Persoonia-Molecular Phylogeny and Evolution of Fungi*, *28*(1), 66–75. https://doi.org/10.3767/003158512X642030

Crous, P. W., Summerell, B. A., Shivas, R. G., Burgess, T. I., Decock, C. A., Dreyer, L. L., . . . Groenewald, J. Z. (2012). Fungal Planet description sheets: 107–127. *Persoonia-Molecular Phylogeny and Evolution of Fungi*, *28*(1), 138–182. https://doi.org/10.3767/003158512X652633

Crous, P. W., Wingfield, M. J., Burgess, T. I., Carnegie, A. J., Hardy, G., Smith, D., . . . Rodríguez-Andrade, E. (2017). Fungal Planet description sheets: 625–715. *Persoonia: Molecular Phylogeny and Evolution of Fungi*, *39*, 270. https://doi.org/10.3767/persoonia.2017.39.11

Crous, P. W., Wingfield, M. J., Le Roux, J. J., Richardson, D. M., Strasberg, D., Shivas, R. G., . . . Groenewald, J. Z. (2015). Fungal Planet description sheets: 371-399. *Persoonia-Molecular Phylogeny and Evolution of Fungi*, *35*(1), 264–327. https://doi.org/10.3767/003158515X690269

Crous, P. W., Wingfield, M. J., Schumacher, R. K., Akulov, A., Bulgakov, T. S., Carnegie, A. J., . . . Groenewald, J. Z. (2020). New and interesting fungi. 3. *Fungal Systematics and Evolution*, *6*, 157. https://doi.org/10.3114/fuse.2020.06.09

Cubeta, M. A., Echandi, E., Abernethy, T., & Vilgalys, R. (1991). Characterization of anastomosis groups of binucleate *Rhizoctonia* species using restriction analysis of an amplified ribosomal RNA gene. *Phytopathology*, *81*, 1395–1400. https://doi.org/10.1094/Phyto-81-1395

Cui, C., Zeng, L., Xiao, Y., Yang, C., & Huo, G. (2023). First Report of Leaf Blotch Caused by *Phyllosticta capitalensis* on *Daphne odora* in China. *Plant Disease*, *107*(9), 2883. https://doi.org/10.1094/PDIS-11-22-2722-PDN

Cui, J. L., Guo, S. X., & Xiao, P. G. (2011). Antitumor and antimicrobial activities of endophytic fungi from medicinal parts of *Aquilaria sinensis*. *Journal of Zhejiang University Science B*, *12*(5), 385–392. https://doi.org/10.1631/jzus.B1000330

Cui, J., Wang, C., Guo, S., Yang, L., Xiao, P., & Wang, M. (2013). Evaluation of fungus-induced agilawood from *Aquilaria sinensis* in China. *Symbiosis*, *60*(1), 37–44. https://doi.org/10.1007/s13199-013-0237-z

Czachura, P., & Janik, P. (2024). *Lophium arboricola* (*Mytilinidiales*, *Ascomycota*) from conifer resins. *Plant and Fungal Systematics*, *69*(1), 1–6. https://doi.org/10.35535/pfsyst-2024-0001

da Silva, H. F., Menezes, R. F., Costa, L. A., Felix, J. R. B., Barbosa, F. R., & Fiuza, P. O. (2024). Environmental drivers and sampling techniques influence neotropical hyphomycetes composition in lakes and streams. *Fungal Biology*, *128*(8), 2274–2284. https://doi.org/10.1016/j.funbio.2024.10.003

Dai, D. Q., Phookamsak, R., Wijayawardene, N. N., Li, W. J., Bhat, D. J., Xu, J. C., . . . Chukeatirote, E. (2017). Bambusicolous fungi. *Fungal Diversity*, *82*(1), 1–105. https://doi.org/10.1007/s13225-016-0367-8

Dai, D. Q., Wijayawardene, N. N., Dayarathne, M. C., Kumla, J., Han, L. S., Zhang, G. Q., . . . Chen, H. H. (2022). Taxonomic and phylogenetic characterizations reveal four new species, two new asexual morph reports, and six new country records of bambusicolous *Roussoella* from China. *Journal of Fungi*, *8*(5), 532. https://doi.org/10.3390/jof8050532

Danielsen, S., & Jensen, D. F. (1999). Fungal endophytes from stalks of tropical maize and grasses: isolation, identification, and screening for antagonism against Fusarium verticillioides in maize stalks. *Biocontrol Science and Technology*, *9*(4), 545–553. https://doi.org/10.1080/09583159929505

de Bary, A. (1866). *Morphologie und physiologie der pilze, flechten und myxomyceten* (Vol. 1). Engelmann.

de Carvalho, C. R., Maia, M. Q., Sobral, M., Pereira, G. M. D., da Silva, K., Vital, M. J. S., . . . Rosa, L. H. (2021). Diversity and antimicrobial activity of culturable endophytic fungi associated with the neotropical ethnomedicinal plants Copaifera langsdorffii and Copaifera pubiflora. *South African Journal of Botany*, *142*, 305–315. https://doi.org/10.1016/j.sajb.2021.06.021

de Farias, A. R. G., Afshari, N., Silva, V. S. H., Louangphan, J., Karimi, O., & Boonmee, S. (2024). Three novel species and new records of *Kirschsteiniothelia* (*Kirschsteiniotheliales*) from northern Thailand. *MycoKeys*, *101*, 347. https://doi.org/10.3897/mycokeys.101.115286

De Hoog, G. S. (1973). A new species of *Cordana* (*Dematiaceae*, Hyphomycetes). Acta Botanica *Neerlandica*, *22*(3), 209–212. https://doi.org/10.1111/j.1438-8677.1973.tb00834.x

De Silva, N. I., Hyde, K. D., Lumyong, S., Phillips, A. J. L., Bhat, D. J., Maharachchikumbura, S. S. N., . . . Karunarathna, S. C. (2022). Morphology, phylogeny, host association and geography of fungi associated with plants of *Annonaceae*, *Apocynaceae* and *Magnoliaceae*. *Mycosphere*, *13*(1), 955–1076. https://doi.org/10.5943/mycosphere/13/1/12

Dell, B. (2002). Role of mycorrhizal fungi in ecosystems. *Chiang Mai University Journal of Natural Sciences*, *1*(1), 47–60.

Deng, H., Wang, Y., Lei, J. R., Chen, Z. Z., Liang, Z. Q., & Zeng, N. K. (2023). Four new species of Strobilomyces (Boletaceae, Boletales) from Hainan island, tropical China. *Journal of Fungi*, *9*(12), 1128. https://doi.org/10.3390/jof9121128

Deng, P. T., Liu, X. F., Yan, J., Chen, Z. H., & Zhang, P. (2024). Update on the taxonomy of *Clavulina* in China II: description of four new species from Hainan Island. *Mycological Progress*, *23*(1), 48. https://doi.org/10.1007/s11557-024-01988-8

Diene, O., Takahashi, T., Yonekura, A., Nitta, Y., & Narisawa, K. (2010). A new fungal endophyte, *Helminthosporium velutinum*, promoting growth of a bioalcohol plant, sweet sorghum. *Microbes and Environments*, *25*(3), 216–219. https://doi.org/10.1264/jsme2.ME09165

Dissanayake, A. J., Chen, Y. Y., & Liu, J. K. (2020). Unravelling *Diaporthe* species associated with woody hosts from karst formations (Guizhou) in China. *Journal of Fungi*, *6*(4), 251. https://doi.org/10.3390/jof6040251

Doilom, M., Dissanayake, A. J., Wanasinghe, D. N., Boonmee, S., Liu, J. K., Bhat, D. J., . . . Hyde, K. D. (2017). Microfungi on Tectona grandis (teak) in Northern Thailand. *Fungal Diversity*, *82*(1), 107–182. https://doi.org/10.1007/s13225-016-0368-7

Dong, W., Hyde, K. D., Jeewon, R., Doilom, M., Yu, X. D., Wang, G. N., . . . Zhang, H. (2021). Towards a natural classification of annulatascaceae-like taxa II: introducing five new genera and eighteen new species from freshwater. *Mycosphere*, *12*(1), 1–88. https://doi.org/10.5943/mycosphere/12/1/1

Dong, W., Wang, B., Hyde, K. D., McKenzie, E. H., Raja, H. A., Tanaka, K., . . . Zhang, H. (2020). Freshwater dothideomycetes. *Fungal Diversity*, *105*(1), 319–575. https://doi.org/10.1007/s13225-020-00463-5

Dreyfuss, M., & Petrini, O. (1984). Further investigations on the occurrence and distribution of endophytic fungi in tropical plants. *Botanica Helvetica*, *94*, 33–40.

Du, H., Chi, M., Wu, N., Dissanayake, A., Liu, N., Cheewangkoon, R., & Liu, J. (2025). Taxonomic and phylogenetic insights to *Dothideomycetes* and *Sordariomycetes* associated with medicinal plants in Southwestern China. *Mycosphere*, *16*(2), 179–343. https://doi.org/10.5943/mycosphere/16/2/2

Du, T. Y., Dao, C. J., Mapook, A., Stephenson, S. L., Elgorban, A. M., Al-Rejaie, S., . . . Tibpromma, S. (2022a). Diversity and biosynthetic activities of agarwood associated fungi. *Diversity*, *14*(3), 211. https://doi.org/10.3390/d14030211

Du, T. Y., Karunarathna, S. C., Hyde, K. D., Mapook, A., Wariss, H. M., Aluthwattha, S. T., . . . Tibpromma, S. (2022b). The endophytic fungi of *Aquilaria sinensis* from southern China. *Fungal Biotec*, *2*(2), 1–15. https://doi.org/10.5943/FunBiotec/2/2/1

Du, Z., Hyde, K. D., Yang, Q., Liang, Y. M., & Tian, C. M. (2017). *Melansporellaceae*: A novel family of *Diaporthales* (*Ascomycota*). *Phytotaxa*, *305*, 191–200. https://doi.org/10.11646/phytotaxa.305.3.6

Duarte, S., Bärlocher, F., Pascoal, C., & Cássio, F. (2016). Biogeography of aquatic hyphomycetes: current knowledge and future perspectives. *Fungal Ecology*, *19*, 169-181. https://doi.org/10.1016/j.funeco.2015.06.002

Durán, M., San Emeterio, L., & Canals, R. M. (2021). Comparison of culturing and metabarcoding methods to describe the fungal endophytic assemblage of Brachypodium rupestre growing in a range of anthropized disturbance regimes. *Biology*, *10*(12), Article 1246. https://doi.org/10.3390/biology10121246

Dyko, B. J., & Sutton, B. C. (1979). New and interesting Dematiaceous hyphomycetes from Florida. *Mycotaxon*, *8*, 119-124.

Eisvand, P., & Mehrabi-Koushki, M. (2025). Additional new species of *Preussia* from forest trees in Iran. *Antonie van Leeuwenhoek*, *118(*3), 1–16. https://doi.org/10.1007/s10482-025-02064-1

El-Elimat, T., Raja, H. A., Figueroa, M., Al Sharie, A. H., Bunch, R. L., & Oberlies, N. H. (2021). Freshwater fungi as a source of chemical diversity: A review. *Journal of Natural Products*, *84*(3), 898–916. https://doi.org/10.1021/acs.jnatprod.0c01340

Ellis, M. B. (1949). *Tetraploa*. *Transactions of the British Mycological Society*, *32*, 246–251.

Ellis, M. B. (1961). Dematiaceous Hyphomycetes III. *Mycological Papers*, *82*, 1–55.

Ellis, M. B. (1963). Dematiaceous Hyphomycetes: IV. *Commonwealth Mycological Institute*.

Ellis, M. B. (1976). More dematiaceous hyphomycetes. *Commonwealth Mycological Institute*.

Ellison, D., Morris, C. E., Locatelli, B., Sheil, D., Cohen, J., Murdiyarso, D., . . . Sullivan, C. A. (2017). Trees, forests and water: Cool insights for a hot world. *Global Environmental Change*, *43*, 51-61. https://doi.org/10.1016/j.gloenvcha.2017.01.002

Elouard, C. (1998). Pests and diseases of *Dipterocarpaceae*. A Review of *Dipterocarps*: Taxonomy, Ecology and Silviculture. *Center for International Forestry Research*, *Bogor*, 115–131.

Eriksson, O. (1981). The families of bitunicate ascomycetes. *Nordic Journal of Botany*, *1*(6), 800. https://doi.org/10.1111/j.1756-1051.1981.tb01167.x

Eriksson, O. E., & Winka, K. (1997). Supraordinal taxa of Ascomycota. *Myconet*, *1*(1), 1–16.

Errampalli, D., Saunders, J. M., & Holley, J. D. (2001). Emergence of silver scurf (*Helminthosporium solani*) as an economically important disease of potato. *Plant Pathology*, *50*(2), 141–153. https://doi.org/10.1046/j.1365-3059.2001.00555.x

Etxano, I., & Villalba-Eguiluz, U. (2021). Twenty-five years of social multi-criteria evaluation (SMCE) in the search for sustainability: Analysis of case studies. *Ecological Economics*, *188*, 107131. https://doi.org/10.1016/j.ecolecon.2021.107131

European Environment Agency. (n.d.). *Ecosystem services*. Forest Information System for Europe. Retrieved October 28, 2025, from https://forest.eea.europa.eu/topics/society/ecosystem-services

Falcon, F. D., Felicen, F. F., Balanon, B. C., Refuerzo, A., & Garcia, J. (2025). Chemical induction for agarwood formation: A recent review. *Discover Plants*, *2*(1), 1–27. https://doi.org/10.1007/s44372-025-00308-y

Fan, X. L., Bezerra, J. D., Tian, C. M., & Crous, P. W. (2018b). Families and genera of diaporthalean fungi associated with canker and dieback of tree hosts. *Persoonia*, *40*, 119–134. https://doi.org/10.3767/persoonia.2018.40.05

Fan, X. L., Bezerra, J. D., Tian, C. M., & Crous, P. W. (2020). *Cytospora* (*Diaporthales*) in China. *Persoonia*, *45*, 1–45. https://doi.org/10.3767/persoonia.2020.45.01

Fan, X. L., Du, Z., Bezerra, J. D. P., & Tian, C. M. (2018a). Taxonomic circumscription of Melanconis-like fungi causing canker disease in China. *MycoKeys*, *42*, 89–124. https://doi.org/10.3897/mycokeys.42.29634

Fan, X. L., Tian, C. M., Yang, Q., Liang, Y. M., You, C. J., & Zhang, Y. B. (2014). *Cytospora f*rom *Salix* in northern China. *Mycotaxon*, *129*, 303–315. https://doi.org/10.5248/129.303

FAO. (2023). Non-wood forest products—*Policy/Regional briefs*. FAO.

Farr, D. F., & Rossman, A. Y. (2025). Fungal databases. U.S. National Fungus Collections, ARS, USDA. Retrieved November 11, 2025, from https://nt.ars-grin.gov/fungaldatabases/

Fernandez, C. W., & Kennedy, P. G. (2016). Revisiting the 'Gadgil effect': Do interguild fungal interactions control carbon cycling in forest soils?. *New Phytologist*, *209*(4), 1382–1394. https://doi.org/10.1111/nph.13648

Food and Agriculture Organization of the United Nations. (2022). *The state of the world's forests 2022: Forest pathways for green recovery and building inclusive, resilient and sustainable economies*. Food and Agriculture Organization of the United Nations. https://doi.org/10.4060/cb9360en

Frank, B. (1885). Über die auf Wurzelsymbiose beruhende Ernährung gewisser Bäume durch unterirdische Pilze. *Berichte der Deutschen Botanischen Gesellschaft*, *3*, 128–145.

Frank, B. (2005). On the nutritional dependence of certain trees on root symbiosis with belowground fungi (An English translation of A. B. Frank's classic paper of 1885). *Mycorrhiza*, *15*(4), 267–275. https://doi.org/10.1007/s00572-004-0329-y

Fries, E. M. (1818). Uppställning af de i Sverige funne Vårtsvampar (Scleromyci). *Kongliga Vetenskaps Academiens Handlingar. 1818*(1), 100-120.

Fries, E. M. (1818). *Observationes Mycologicae*. *2*, 1–376.

Fries, E. M. (1823). *Systema mycologicum* (Vol. 2). Ex Officina Berlingiana.

Froehlich, J., & Petrini, O. (2000). Endophytic fungi associated with palms. *Mycological Research*, *104*(10), 1202–1212.

Fu, C. C., Huang, B. X., Wang, S. S., Song, Y. C., Metok, D., Tan, Y. X., . . . Zhu, F. Y. (2024). Deciphering the roles of bacterial and fungal communities in the formation and quality of agarwood. *Stress Biology*, *4*(1), 40. https://doi.org/10.1007/s44154-024-00179-5

Gamboa, M. A., & Bayman, P. (2001). Communities of endophytic fungi in leaves of a tropical timber tree (*Guarea guidonia*: *Meliaceae*) 1. *Biotropica*, *33*(2), 352–360. https://doi.org/10.1111/j.1744-7429.2001.tb00187.x

Gao, C., Shi, N. N., Liu, Y. X., Peay, K. G., Zheng, Y., Ding, Q., . . . Guo, L. D. (2013). Host plant genus-level diversity is the best predictor of ectomycorrhizal fungal diversity in a Chinese subtropical forest. *Molecular Ecology*, *22*(12), 3403–3414. https://doi.org/10.1111/mec.12297

Gao, M., Liu, B., Li, J., Deng, Y., Zhang, Y., Zhang, N., . . . Hu, Z. (2024). Diversity and distribution of fungi in the marine sediments of Zhanjiang Bay, China. *Journal of Fungi*, *10*(12), 867. https://doi.org/10.3390/jof10120867

Gao, Y., Zhong, T., Bhat, J. D., de Farias, A. R. G., Dawoud, T. M., Hyde, K. D., . . . Wanasinghe, D. N. (2023). Pleomorphic *Dematiomelanomma yunnanense* gen. et sp. nov. (*Ascomycota*, *Melanommataceae*) from grassland vegetation in Yunnan, China. *MycoKeys*, *98*, 273–288. https://doi.org/10.3897/mycokeys.98.107093

Gibson, I. A. S. (1977). The role of fungi in the origin of oleoresin deposits (agaru) in the wood of *Aquilaria agallocha* Roxb. *Bano Biggyan Patrika*, *6*(1), 16–26.

Gibson, I. A. S., Christensen, P. S., & Munga, F. M. (1964). First observations in Kenya of a foliage disease of pines caused by *Dothistroma pini* Hulbary. *The Commonwealth Forestry Review*, 31–48.

Glass, D. J., Taylor, A. D., Herriott, I. C., Ruess, R. W., & Taylor, D. L. (2014). Habitat preferences, distribution, and temporal persistence of a novel fungal taxon in Alaskan boreal forest soils. *Fungal Ecology*, *12*, 70–77. https://doi.org/10.1016/j.funeco.2014.03.001

Glass, N. L., & Donaldson, G. C. (1995). Development of primer sets designed for use with the PCR to amplify conserved genes from filamentous ascomycetes. *Applied and Environmental Microbiology*, *61*, 1323–1330. https://doi.org/10.1128/aem.61.4.1323-1330.1995

Goh, T. K., Ho, W. H., Hyde, K. D., & Tsui, K. M. (1997). Four new species of *Xylomyces* from submerged wood. *Mycological Research*, *101*(11), 1323–1328. https://doi.org/10.1017/S0953756297004164

Goh, T. K., Hyde, K. D., & Ho, W. H. (1999). A revision of the genus *Dictyosporium*, with descriptions of three new species. *Fungal Diversity*, *2*, 65–100.

Gomdola, D., Bhunjun, C. S., Hyde, K. D., Jeewon, R., Pem, D. & Jayawardena, R. S. (2022). Ten important forest fungal pathogens: a review on their emergence and biology. *Mycosphere*, *13*, 612–671. https://doi.org/10.5943/mycosphere/13/1/6

Gomdola, D., McKenzie, E. H., Hyde, K. D., Bundhun, D., & Jayawardena, R. S. (2023). Appressoria-producing *Sordariomycetes* taxa associated with Jasminum species. *Pathogens*, *12*(12), 1407. https://doi.org/10.3390/pathogens12121407

Gong, L., & Guo, S. (2009). Endophytic fungi from *Dracaena cambodiana* and *Aquilaria sinensis* and their antimicrobial activity. *African Journal of Biotechnology*, *8*(5). https://doi.org/10.4314/ajb.v8i5.59937

Goos, R. D., Brooks, R. D., & Lamore, B. J. (1977). An undescribed hyphomycete from wood submerged in a Rhode Island stream. *Mycologia*, *69*(2), 280–286. https://doi.org/10.1080/00275514.1977.12020059

Gottschall, F., Cesarz, S., Auge, H., Kovach, K. R., Mori, A. S., Nock, C. A., . . . Eisenhauer, N. (2022). Spatiotemporal dynamics of abiotic and biotic properties explain biodiversity–ecosystem-functioning relationships. *Ecological Monographs*, *92*(1), e01490. https://doi.org/10.1002/ecm.1490

Graça, M. A., Hyde, K., & Chauvet, E. (2016). Aquatic hyphomycetes and litter decomposition in tropical–subtropical low order streams. *Fungal Ecology*, *19*, 182–189. https://doi.org/10.1016/j.funeco.2015.08.001

Gramaje, D., Mostert, L., Groenewald, J. Z., & Crous, P. W. (2015). *Phaeoacremonium*: From esca disease to phaeohyphomycosis. *Fungal Biology*, *119*, 759–783. https://doi.org/10.1016/j.funbio.2015.06.004

Grove, W.B. 1886. New or noteworthy fungi: - Part III. *The Journal of Botany, British and Foreign*, *24*, 129–137.

Gryzenhout, M., Myburg, H., & Wingfield, B. D. (2006). *Cryphonectriaceae* (*Diaporthales*), a new family including *Cryphonectria*, *Chrysoporthe*, *Endothia* and allied genera. *Mycologia*, *98*, 239–249. https://doi.org/10.1080/15572536.2006.11832696

Guarnaccia, V., Groenewald, J. Z., Woodhall, J., Armengol, J., Cinelli, T., Eichmeier, A., . . . Crous, P. W. (2018). *Diaporthe* diversity and pathogenicity revealed from a broad survey of grapevine diseases in Europe. *Persoonia*, *40*, 135–153. https://doi.org/10.3767/persoonia.2018.40.06

Gusmao, L. F. P., Grandi, R. A. P., & Milanez, A. I. (2001). Hyphomycetes from leaf litter of *Miconia cabussu* in a Brazilian Atlantic rain forest. *Mycotaxon*, *79*, 201–214.

Guterres, D. C., Galvão-Elias, S., Dos Santos, M. D. D. M., de Souza, B. C. P., de Almeida, C. P., Pinho, D. B., . . . Dianese, J. C. (2019). Phylogenetic relationships of P*haeochorella parinarii* and recognition of a new family, *Phaeochorellaceae* (*Diaporthales*). *Mycologia*, *111*(4), 660–675. https://doi.org/10.1080/00275514.2019.1603025

Habib, K., Li, W. H., Ren, Y. L., Liu, L. L., Lu, C. T., Zhang, Q. F., . . . Li, Q. R. (2025). Exploration of ascomycetous fungi revealing novel taxa in Southwestern China. *Mycosphere*, *16*(1), 1412–1529. https://doi.org/10.5943/mycosphere/16/1/9

Hagem, O. (1908). Untersuchungen über norwegische Mucorineen. I. Skrifter utgitt av Videnskabsselskapet i Christiania. *Matematisk-Naturvidenskabelig Klasse*, *1908*(7), 1–28.

Han, S., Li, L. Z., & Song, S. J. (2020). *Daphne giraldii* Nitsche (*Thymelaeaceae*): Phytochemistry, pharmacology and medicinal uses. *Phytochemistry*, *171*, 112231. https://doi.org/10.1016/j.phytochem.2019.112231

Hansen, M. C., Potapov, P. V., Moore, R., Hancher, M., Turubanova, S. A., Tyukavina, A., . . . Townshend, J. R. (2013). High-resolution global maps of 21st-century forest cover change. *Science*, *342*(6160), 850–853. https://doi.org/10.1126/science.1244693

Hardoim, P. R., Van Overbeek, L. S., Berg, G., Pirttilä, A. M., Compant, S., Campisano, A., . . . Sessitsch, A. (2015). The hidden world within plants: Ecological and evolutionary considerations for defining functioning of microbial endophytes. *Microbiology and Molecular Biology Reviews*, *79*(3), 293–320. https://doi.org/10.1128/mmbr.00050-14

Haridas, S., Albert, R., Binder, M., Bloem, J., LaButti, K., Salamov, A., . . . Grigoriev, I. V. (2020).101 *Dothideomycetes* genomes: A test case for predicting lifestyles and emergence of pathogens. *Studies in Mycology*, *96*(1), 141–153. https://doi.org/10.1016/j.simyco.2020.01.003

Harkness, H. W. (1884). New species of Californian fungi. *Bulletin of the California Academy of Sciences*, *1*, 29–47.

Harley, J. L., & Smith, S. E. (1983). Mycorrhizal symbiosis. *Academic Press*.

Hashimoto, A., Matsumura, M., Hirayama, K., & Tanaka, K. (2017). Revision of *Lophiotremataceae* (*Pleosporales*, *Dothideomycetes*): *Aquasubmersaceae*, *Cryptocoryneaceae*, and *Hermatomycetaceae* fam. nov. *Persoonia: Molecular Phylogeny and Evolution of Fungi*, *39*(1), 51–73. https://doi.org/10.3767/persoonia.2017.39.03

Hatakeyama, S., Tanaka, K., & Harada, Y. (2005). Bambusicolous fungi in Japan (5): Three species of *Tetraploa*. *Mycoscience*, *46*(3), 196–200. https://doi.org/10.1007/s10267-005-0233-0

Hawksworth, D. L. (1985). *Kirschsteiniothelia*, a new genus for the Microthelia incrustans-group (*Dothideales*). *Botanical Journal of the Linnean Society*, *91*(1–2), 181–202. https://doi.org/10.1111/j.1095-8339.1985.tb01144.x

Hawksworth, D. L., Crous, P. W., Redhead, S. A., Reynolds, D. R., Samson, R. A., Seifert, K. A., . . . Zhang, N. (2011). The Amsterdam declaration on fungal nomenclature. *IMA Fungus*, *2*(1), 105–111. https://doi.org/10.5598/imafungus.2011.02.01.14

He, M. L., Qi, S. Y., & Hu, L. J. (2005). Rapid in vitro propagation of medicinally important *Aquilaria agallocha*. *Journal of Zhejiang University Science B*, *6*(8), 849–852. https://doi.org/10.1631/jzus.2005.B0849

He, S. C., Hyde, K. D., Jayawardena, R. S., Thiyagaraja, V., Wanasinghe, D. N., Zhao, Y. W., . . . Zhao, Q. (2025). Taxonomic contributions to *Pleosporales* and *Kirschsteiniotheliales* from the Xizang Autonomous Region, China. *Mycology*, 1–38. https://doi.org/10.1080/21501203.2025.2493072

Hernández-Restrepo, M., Gené, J., Mena-Portales, J., Cano, J., Madrid, H., Castañeda-Ruiz, R. F., . . . Guarro, J. (2014). New species of *Cordana* and epitypification of the genus. *Mycologia*, *106*(4), 723–734. https://doi.org/10.3852/13-122

Hernández-Restrepo, M., Schumacher, R. K., Wingfield, M. J., Ahmad, I., Cai, L., Duong, T. A., . . . Crous, P. W. (2016). Fungal systematics and evolution: FUSE 2. *Sydowia*, *68*, 193–230. https://doi.org/10.12905/0380.sydowia68-2016-0193

Heywood, V. H. (1996). *Flowering plants of the world* (2nd ed.). Oxford University Press.

Hibbett, D. S., Binder, M., Bischoff, J. F., Blackwell, M., Cannon, P. F., Eriksson, O. E., . . . Zhang, N. (2007). A higher-level phylogenetic classification of the Fungi. *Mycological Research*, *111*(5), 509–547. https://doi.org/10.1016/j.mycres.2007.03.004

Hillis, D. M., & Bull, J. J. (1993). An empirical test of bootstrapping as a method for assessing confidence in phylogenetic analysis. *Systematic Biology*, *42*(2), 182–192. https://doi.org/10.1093/sysbio/42.2.182

Hirayama, K., & Tanaka, K. (2011). Taxonomic revision of *Lophiostoma* and *Lophiotrema* based on reevaluation of morphological characters and molecular analyses. *Mycoscience*, *52*(6), 401–412. https://doi.org/10.1007/s10267-011-0126-3

Högberg, P., & Piearce, G. D. (1986). Mycorrhizas in Zambian trees in relation to host taxonomy, vegetation type and successional patterns. *The Journal of Ecology*, *74*(3), 775–785.

Höhnel, F. V. (1917). Fragmente zur Mykologie (XX Mitteilung, Nr. 1031 bis 1057). Sitzungsberichte der kaiserlichen akademie der wissenschaften math.-naturw. *Klasse Abt. I*, *126*, 353–399.

Holubová-Jechová, V. (1987). Studies on hyphomycetes from Cuba. V. Six new species of dematiaceous hyphomycetes from Havana province. *Česká Mykologie*, *41*, 29–36.

Hong, L. T. (1979). A note on dipterocarp mycorrhizal fungi. *The Malaysian Forester*, *42*, 280–283.

Hongsanan, S., Hyde, K. D., Phookamsak, R., Wanasinghe, D. N., McKenzie, E. H. C., Sarma, V. V., . . . Xie, N. (2020a). Refined families of *Dothideomycetes*: *Dothideomycetidae* and *Pleosporomycetidae*. *Mycosphere*, *11*(1), 1553–2107. https://doi.org/10.5943/mycosphere/11/1/13

Hongsanan, S., Hyde, K. D., Phookamsak, R., Wanasinghe, D. N., McKenzie, E. H. C., Sarma, V. V., . . . Xie, N. (2020b). Refined families of *Dothideomycetes*: Orders and families incertae sedis in *Dothideomycetes*. *Fungal Diversity*, *105*(1), 17–318. https://doi.org/10.1007/s13225-020-00462-6

Hongsanan, S., Khuna, S., Manawasinghe, I. S., Tibpromma, S., Chethana, K. W. T., Xie, N., . . . Karunarathna, S. C. (2025). Mycosphere Notes 521–571: A special edition of fungal biodiversity to celebrate Kevin D. Hyde's 70th birthday and his exceptional contributions to Mycology. *Mycosphere*, *16*(2), 2002–2180. https://doi.org/10.5943/mycosphere/16/2/1

Hongsanan, S., Maharachchikumbura, S. S., Hyde, K. D., Samarakoon, M. C., Jeewon, R., Zhao, Q., . . . Bahkali, A. H. (2017). An updated phylogeny of *Sordariomycetes* based on phylogenetic and molecular clock evidence. *Fungal Diversity*, *84*(1), 25–41. https://doi.org/10.1007/s13225-017-0384-2

Hou, L. W., Groenewald, J. Z., Pfenning, L. H., Yarden, O., Crous, P. W., & Cai, L. (2020). The phoma-like dilemma. *Studies in Mycology*, *96*, 309–396. https://doi.org/10.1016/j.simyco.2020.05.001

Hsieh, S. Y., Goh, T. K., & Kuo, C. H. (2021). New species and records of *Helicosporium* sensu lato from Taiwan, with a reflection on current generic circumscription. *Mycological Progress*, *20*(2), 169–190. https://doi.org/10.1007/s11557-020-01663-8

Hu, H. M., Liu, L. L., Zhang, X., Lin, Y., Shen, X. C., Long, S. H., . . . De Long, Q. (2022). New species and records of *Neomassaria*, *Oxydothis* and *Roussoella* (*Pezizomycotina*, *Ascomycota*) associated with palm and bamboo from China. *MycoKeys*, *93*, 165. https://doi.org/10.3897/mycokeys.93.89888

Hu, Y. F., Liu, J. W., Xu, Z. H., Castañeda-Ruíz, R. F., Zhang, K., & Ma, J. (2023). Morphology and multigene phylogeny revealed three new species of *Helminthosporium* (*Massarinaceae*, *Pleosporales*) from China. *Journal of Fungi*, *9*(2), 280. https://doi.org/10.3390/jof9020280

Huang, F., Hou, X., Dewdney, M. M., Fu, Y., Chen, G., Hyde, K. D., & Li, H. (2013). *Diaporthe* species occurring on citrus in China. *Fungal Diversity*, *61*, 237–250. https://doi.org/10.1007/s13225-013-0245-6

Huang, T., Su, L. J., Zeng, N. K., Lee, S. M., Lee, S. S., Thi, B. K., . . . Tang, L. P. (2023). Notes on *Amanita* section *Validae* in Hainan Island, China. *Frontiers in Microbiology*, *13*, 1087756. https://doi.org/10.3389/fmicb.2022.1087756

Huelsenbeck, J. P., & Ronquist, F. (2001). MRBAYES: Bayesian inference of phylogenetic trees. *Bioinformatics*, *17*(8), 754–755. https://doi.org/10.1093/bioinformatics/17.8.754

Hughes, S. J. (1953). Fungi from the Gold Coast. II. *Mycological Papers*, *50*, 1–104.

Hughes, S. J. (1955). Microfungi. I. *Cordana*, *Brachysporium*, *Phragmocephala*. *Canadian Journal of Botany*, *33*, 259–268.

Hughes, S. J. (1958). Revisiones hyphomycetum aliquot cum appendice de nominibus rejiciendis. *Canadian Journal of Botany*, *36(*6), 727–836. https://doi.org/10.1139/b58-067

Hughes, S. J. (1978). New Zealand fungi 25. Miscellaneous species. *New Zealand Journal of Botany*, *16*(3), 311–370. https://doi.org/10.1080/0028825X.1978.10425143

Hughes, S. J. (1983). *Cordana inaequalis*. Fungi Canadenses.

Hyde, K. D. (2022). The numbers of fungi. *Fungal Diversity*, *114*(1), 1–16. https://doi.org/10.1007/s13225-022-00507-y

Hyde, K. D., & Goh, T. K. (1999). Fungi on submerged wood from the River Coln, England. *Mycological Research*, *103*(12), 1561–1574. https://doi.org/10.1017/S0953756299008989

Hyde, K. D., & Soytong, K. (2008). The fungal endophyte dilemma. *Fungal Diversity*, *33*(163), e173.

Hyde, K. D., Dong, Y., Phookamsak, R., Jeewon, R., Bhat, D. J., Jones, E. G., . . . Sheng, J. (2020). Fungal diversity notes 1151–1276: Taxonomic and phylogenetic contributions on genera and species of fungal taxa. *Fungal Diversity*, *100*(1), 5–277. https://doi.org/10.1007/s13225-020-00439-5

Hyde, K. D., Fröhlich, J., & Taylor, J. E. (1998). Fungi from palms. XXXVI. Reflections on unitunicate ascomycetes with apiospores. *Sydowia*, *50*(1), 21–80.

Hyde, K. D., Hongsanan, S., Jeewon, R., Bhat, D. J., McKenzie, E. H. C., Jones, E. B. G., . . . Zhu, L. (2016). Fungal diversity notes 367–490: Taxonomic and phylogenetic contributions to fungal taxa. *Fungal Diversity*, *80*(1), 1–270. https://doi.org/10.1007/s13225-016-0373-x

Hyde, K. D., Jeewon, R., Chen, Y. J., Bhunjun, C. S., Calabon, M. S., Jiang, H. B., . . . Lumyong, S. (2020a). The numbers of fungi: is the descriptive curve flattening?. *Fungal Diversity*, *103*, 219–271. https://doi.org/10.1007/s13225-020-00458-2

Hyde, K. D., Jones, E. G., Liu, J. K., Ariyawansa, H., Boehm, E., Boonmee, S., . . . Zhang, M. (2013). Families of *Dothideomycetes*: In loving memory of Majorie Phyllis Hyde (29 August 1921–18 January 2013). *Fungal Diversity*, *63*(1), 1–313. https://doi.org/10.1007/s13225-013-0263-4

Hyde, K. D., McKenzie, E. H. C., & KoKo, T. W. (2011). Towards incorporating anamorphic fungi in a natural classification—Checklist and notes for 2010. *Mycosphere, 2*(1), 1–88.

Hyde, K. D., Noorabadi, M. T., Thiyagaraja, V., He, M. Q., Johnston, P. R., Wijesinghe, S. N., . . . Dissanayake, L. S. (2024). The 2024 outline of fungi and fungus-like taxa. *Mycosphere*, *15*(1), 5146–6239. https://doi.org/10.5943/mycosphere/15/1/25

Hyde, K. D., Norphanphoun, C., Ma, J., Yang, H. D., Zhang, J. Y., Du, T. Y., . . . Zhao, Q. (2023). Mycosphere notes 387–412 – Novel species of fungal taxa from around the world. *Mycosphere*, *14*(1), 663–744. https://doi.org/10.5943/mycosphere/14/1/8

Hyde, K. D., Norphanphoun, C., Maharachchikumbura, S. S. N., Bhat, D. J., Jones, E., Bundhun, D., . . . Xiang, M. M. (2020b). Refined families of *Sordariomycetes*. *Mycosphere*, *11*(1), 305–1059. https://doi.org/10.5943/mycosphere/11/1/7

Index Fungorum. (2025). Retrieved September 12, 2025, from http://www.indexfungorum.org/Names/Names.asp

IPBES. (2019). *Global assessment report on biodiversity and ecosystem services*. Intergovernmental Science-Policy Platform on Biodiversity and Ecosystem Services.

Isola, D., & Prenafeta-Boldú, F. X. (2025). Diversity and ecology of fungi from underexplored and extreme environments. *Journal of Fungi*, *11*(5), 343. https://doi.org/10.3390/jof11050343

Jayasiri, S. C., Hyde, K. D., Ariyawansa, H. A., Bhat, J., Buyck, B., Cai, L., . . . Promputtha, I. (2015). The Faces of Fungi database: fungal names linked with morphology, phylogeny and human impacts. *Fungal Diversity*, *74*, 3–18. https://doi.org/10.1007/s13225-015-0351-8

Jayasiri, S. C., Jones, E. G., Kang, J. C., Promputtha, I., Bahkali, A. H., & Hyde, K. D. (2016). A new species of genus *Anteaglonium* (*Anteagloniaceae*, *Pleosporales*) with its asexual morph. *Phytotaxa*, *263*(3), 233–244. https://doi.org/10.11646/phytotaxa.263.3.4

Jayawardena, R. S., Hyde, K. D., Wang, S., Sun, Y. R., Suwannarach, N., Sysouphanthong, P., . . . Wang, Y. (2022). Fungal diversity notes 1512–1610: Taxonomic and phylogenetic contributions on genera and species of fungal taxa. *Fungal Diversity*, *117*(1), 1–272. https://doi.org/10.1007/s13225-022-00513-0

Jeewon, R., & Hyde, K. D. (2016). Establishing species boundaries and new taxa among fungi: recommendations to resolve taxonomic ambiguities. *Mycosphere*, *7*, 1669–1677. https://doi.org/10.5943/mycosphere/7/11/4

Jiang, H. B., Hyde, K. D., Doilom, M., Karunarathna, S. C., Xu, J. C., & Phookamsak, R. (2019). *Arthrinium setostromum* (*Apiosporaceae*, *Xylariales*), a novel species associated with dead bamboo from Yunnan, China. *Asian Journal of Mycology*, *2*(1), 254–268. https://doi.org/10.5943/ajom/2/1/16

Jiang, N., Fan, X., Tian, C., & Crous, P. W. (2020). Reevaluating *Cryphonectriaceae* and allied families in *Diaporthales*. *Mycologia*, *112*, 267–292. https://doi.org/10.1080/00275514.2019.1698925

Jiang, N., Li, J., & Tian, C. M. (2018). *Arthrinium* species associated with bamboo and reed plants in China. *Fungal Systematics and Evolution*, *2*(1), 1–9. https://doi.org/10.3114/fuse.2018.02.01

Jiang, N., Xue, H., & Li, Y. (2025). Species diversity of *Pseudoplagiostoma* and *Pyrispora* (*Diaporthales*) from *Fagaceae* hosts in China. *IMA Fungus*, *16*, e153782. https://doi.org/10.3897/imafungus.16.153782

Jin, H., Yan, Z., Liu, Q., Yang, X., Chen, J., & Qin, B. (2013). Diversity and dynamics of fungal endophytes in leaves, stems and roots of *Stellera chamaejasme* L. in northwestern China. *Antonie Van Leeuwenhoek*, *104*(6), 949–963. https://doi.org/10.1007/s10482-013-0014-2

Johnson, N. C., Graham, J. H., & Smith, F. A. (1997). Functioning of mycorrhizal associations along the mutualism–parasitism continuum. *New Phytologist*, *135*(4), 575–585. https://doi.org/10.1046/j.1469-8137.1997.00729.x

Johnston, P. R., Johansen, R. B., Williams, A. F., Wikie, J. P., & Park, D. (2012). Patterns of fungal diversity in New Zealand Nothofagus forests. *Fungal Biology*, *116*(3), 401–412. https://doi.org/10.1016/j.funbio.2011.12.010

Jones, E. G., Pang, K. L., Abdel-Wahab, M. A., Scholz, B., Hyde, K. D., Boekhout, T., . . . Norphanphoun, C. (2019). An online resource for marine fungi. *Fungal Diversity*, *96*(1), 347–433. https://doi.org/10.1007/s13225-019-00426-5

KA, P. (1972). Microfungi of Tanzania. I. Miscellaneous fungi on oil palm. II. New Hyphomycetes. *Mycological Papers*, *129*, 1–64.

Kamnerdratana, B., Suriyajantratong, W., & Charlempongse, A. (1987). Seed-borne fungi of *Dipterocarpaceae* in Thailand. *Thai Journal of Forestry*, *6*, 15–27.

Karimi, O., Hyde, K. D., Asghari, R., Chethana, K. W. T., Kaewchai, S., Al-Otibi, F., . . . Li, Q. R. (2025). Peat swamp *Ascomycota* associated with palms (*Arecaceae*) from Narathiwat, Thailand. *Mycosphere*, *16*(1), 2456–2575. https://doi.org/10.5943/mycosphere/16/1/14

Karunarathna, S. C. (2025). Fungal community composition associated with the agarwood-producing tree, *Aquilaria sinensis*. *Mycosphere*, *16*(1), 2776–2847. https://doi.org/10.5943/mycosphere/16/1/18

Katoch, M., Khajuria, A., Sharma, P. R., & Saxena, A. K. (2015). Immunosuppressive potential of *Botryosphaeria dothidea*, an endophyte isolated from *Kigelia africana*. *Pharmaceutical Biology*, *53*(1), 85–91. https://doi.org/10.3109/13880209.2014.910673

Katoh, K., Rozewicki, J., & Yamada, K. D. (2017). MAFFT online service: multiple sequence alignment, interactive sequence choice and visualization. *Briefings in Bioinformatics*, *20*, 1160–1166. https://doi.org/10.1093/bib/bbx108

Keissler, K. (1912). Zur Kenntnis der Pilzflora Krains. *Beihefte zum Botanischen Centralblatt*, *29*, 395–440.

Kim, G. H., Hur, J. S., Choi, W. B., & Koh, Y. J. (2005). *Fusarium* Wilt of Winter *Daphne* (*Daphne odora* Thunb.) Caused by *Fusarium oxysporum*. *Plant Pathology Journal*, *21*(2), 102–105. https://doi.org/10.5423/PPJ.2005.21.2.102

Kim, Y. C., Lee, E. H., Lee, Y. M., Kim, H. K., Song, B. K., Lee, E. J., & Kim, H. M. (1997). Effect of the aqueous extract of *Aquilaria agallocha* stems on the immediate hypersensitivity reactions. *Journal of ethnopharmacology*, *58*(1), 31–38.

Kirk, P. M. (1982). New or interesting microfungi VI. *Sporidesmiella* gen. nov. (Hyphomycetes). *Transactions of the British Mycological Society*, *79*(3), 479–489. https://doi.org/10.1016/S0007-1536(82)80040-5

Kirk, P. M., & Spooner, B. (1984). An account of the fungi of Arran, Gigha and Kintyre. *Kew Bulletin*, *38*, 503–597. https://doi.org/10.2307/4108573

Kirk, P. M., Stalpers, J. A., Braun, U., Crous, P. W., Hansen, K., Hawksworth, D. L., . . . Stadler, M. (2013). A without-prejudice list of generic names of fungi for protection under the International Code of Nomenclature for algae, fungi, and plants. *IMA fungus*, *4*(2), 381–443. https://doi.org/10.5598/imafungus.2013.04.02.17

Kodsueb, R., McKenzie, E. H. C., Lumyong, S., & Hyde, K. D. (2008). Diversity of saprobic fungi on *Magnoliaceae*. *Fungal Diversity*, *30*(1), 37–53.

Kohlmeyer, J., & Volkmann-Kohlmeyer, B. (1998). A new marine *Xylomyces* on Rhizophora from the Caribbean and Hawaii. *Fungal Diversity*, *1*, 159–164.

Konta, S., Hyde, K. D., Karunarathna, S. C., Mapook, A., Senwanna, C., Dauner, L. A., . . . Lumyong, S. (2021). Multi-gene phylogeny and morphology reveal *Haplohelminthosporium* gen. nov. and *Helminthosporiella* gen. nov. associated with palms in Thailand, and a checklist for *Helminthosporium* worldwide. *Life*, *11*(5), 454. https://doi.org/10.3390/life11050454

Koukol, O., & Delgado, G. (2019). Do not forget Africa – revision of fungarium collections at Kew revealed a new species of *Hermatomyces* (*Hermatomycetaceae*, *Pleosporales*). *Nova Hedwigia*, *109*, 413–423. https://doi.org/10.1127/nova_hedwigia/2019/0559

Koukol, O., & Delgado, G. (2021). Why morphology matters: The negative consequences of hasty descriptions of putative novelties in asexual ascomycetes. *IMA Fungus*, *12*(1), 26. https://doi.org/10.1186/s43008-021-00073-z

Koukol, O., Delgado, G., Hofmann, T. A., & Piepenbring, M. (2018). Panama, a hot spot for *Hermatomyces* (*Hermatomycetaceae*, *Pleosporales*) with five new species, and a critical synopsis of the genus. I*nternational Mycological Association*, *9*, 107–141. https://doi.org/10.5598/imafungus.2018.09.01.08

Kristanti, A. N., Tanjung, M., & Aminah, N. S. (2018). Secondary metabolites of *Aquilaria*, a *Thymelaeaceae* genus. *Mini-reviews in organic chemistry*, *15*(1), 36–55. https://doi.org/10.2174/1570193X14666170721143041

Kruys, A., & Wedin, M. (2009). Phylogenetic relationships and an assessment of traditionally used taxonomic characters in the *Sporormiaceae* (*Pleosporales*, *Dothideomycetes*, *Ascomycota*), utilising multi-gene phylogenies. *Systematics and Biodiversity*, *7*(4), 465–478. https://doi.org/10.1017/S1477200009990119

Kunze, G. (1817). Zehn neue Pilzgattungen. *Mykologische Hefte*, *1*, 1–18.

Laessøe, T., & Lodge, D. J. (1994). Three host-specific *Xylaria* species. *Mycologia*, *86*(3), 436–446. https://doi.org/10.1080/00275514.1994.12026431

Lai, K. W., Zhang, H., Yang, F., & Gale, S. W. (2025). Using global trade data to identify priorities for agarwood conservation and trade management. *Global Ecology and Conservation*, *59*, e03560. https://doi.org/10.1016/j.gecco.2025.e03560

Lee, S. S., Alexander, I. J., & Watling, R. (1997). Ectomycorrhizas and putative ectomycorrhizal fungi of *Shorea leprosula* Miq. (*Dipterocarpaceae*). *Mycorrhiza*, *7*, 63–81. https://doi.org/10.1007/s005720050165

Lee, S. S., Watling, R., & Noraini Sikin, Y. (2002). Ectomycorrhizal basidiomata fruiting in lowland rain forests of Peninsular Malaysia. *Bois et Forêts des Tropiques*, *274*(4), 33–43.

Leonard, K. J., & Suggs, E. G. (1974). *Setosphaeria prolata*, the ascigerous state of *Exserohilum prolatum*. *Mycologia*, *66*(2), 281–297. https://doi.org/10.1080/00275514.1974.12019603

Li, B. J., Liu, P. Q., Jiang, Y., Weng, Q. Y., & Chen, Q. H. (2016). First report of culm rot caused by *Arthrinium phaeospermum* on *Phyllostachys viridis* in China. *Plant Disease*, *100*(5), 1013. https://doi.org/10.1094/PDIS-08-15-0901-PDN

Li, D., Wu, Z., Chen, Y., Tao, M., & Zhang, W. (2011). Chemical constituents of endophytic fungus *Nodulisporium* sp. A4 from *Aquilaria sinensis*. *China Journal of Chinese Materia Medica*, *36*(23), 3276–3280.

Li, J. F., Phookamsak, R., Jeewon, R., Bhat, D. J., Mapook, A., Camporesi, E., . . . Hyde, K. D. (2017) Molecular taxonomy and morphological characterization reveal new species and new host records of *Torula* species (*Torulaceae*, *Pleosporales*). *Mycological progress*, *16*(4), 447–461. https://doi.org/10.1007/s11557-017-1292-2

Li, L. L., Shen, H. W., Bao, D. F., Lu, Y. Z., Su, H. Y., & Luo, Z. L. (2022b). New species, *Parahelicomyces yunnanensis* sp. nov. and *Tubeufia nigroseptum* sp. nov. from freshwater habitats in Yunnan, China. *Phytotaxa*, *530*(1), 21–37. https://doi.org/10.11646/phytotaxa.530.1.2

Li, L. L., Shen, H. W., Bao, D. F., Wanasinghe, D. N., Lu, Y. Z., Feng, Y., & Luo, Z. L. (2022a). The plethora of *Tubeufiaceae* in lakes of the northwestern Yunnan plateau, China. *Frontiers in Microbiology*, *13*, 1056669. https://doi.org/10.3389/fmicb.2022.1056669

Li, T., Qiu, Z., Lee, S. Y., Li, X., Gao, J., Jiang, C., . . . Liu, J. (2023). Biodiversity and application prospects of fungal endophytes in the agarwood-producing genera, *Aquilaria* and *Gyrinops* (*Thymelaeaceae*): A review. *Arabian Journal of Chemistry*, *16*(1), 104435. https://doi.org/10.1016/j.arabjc.2022.104435

Li, W. L., Bao, D. F., Bhat, D. J., & Su, H. Y. (2020). *Tetraploa aquatica* (*Tetraplosphaeriaceae*), a new freshwater fungal species from Yunnan Province, China. *Phytotaxa*, *459*(2), 181–189. https://doi.org/10.11646/phytotaxa.459.2.8

Li, W. L., Liang, R. R., Dissanayake, A. J., & Liu, J. K. (2023). Mycosphere Notes 413–448: *Dothideomycetes* associated with woody oil plants in China. *Mycosphere*, *14*(1), 1436–1529. https://doi.org/10.5943/mycosphere/14/1/16

Li, X. H., Phookamsak, R., Sun, F. Q., Jiang, H. B., Xu, J. C., & Li, J. F. (2024). *Torula aquilariae* sp. nov.(*Torulaceae*, *Pleosporales*), a new species associated with A*quilaria sinensis* from Yunnan, China. *Studies in Fungi*, *9*(1), e020. https://doi.org/10.48130/sif-0024-0019

Liang, J., Crowther, T. W., Picard, N., Wiser, S., Zhou, M., Alberti, G., . . . Reich, P. B. (2016). Positive biodiversity-productivity relationship predominant in global forests. *Science*, *354*(6309), aaf8957. https://doi.org/10.1126/science.aaf8957

Liao, C. F., Dong, W., Chethana, K. T., Pem, D., Phookamsak, R., Suwannarach, N., & Doilom, M. (2022). Morphological and phylogenetic evidence reveal *Tetraploa cylindrica* sp. nov.(*Tetraplosphaeriaceae*, *Pleosporales*) from *Saccharum arundinaceum* (*Poaceae*) in Yunnan Province, China. *Phytotaxa*, *554*(2), 189–200. https://doi.org/10.11646/phytotaxa.554.2.7

Liao, M. G., Luo, X. X., Xia, J. W., Hu, Y. F., Zhang, X. G., Zhang, L. H., . . . Ma, J. (2025). Six novel species of *Distoseptispora* (*Distoseptisporaceae*, *Distoseptisporales*) and *Helminthosporium* (*Massarinaceae*, *Pleosporales*) isolated from terrestrial habitats in southern China. *Journal of Fungi*, *11*(7), 494. https://doi.org/10.3390/jof11070494

Link, H. F. (1809). Observationes in *Ordines plantarum* naturales: dissertatio I.ma complectens Anandrarum ordines Epiphytas, Mucedines Gastromycos et Fungos. *Der Gesellschaft Naturforschender Freunde zu Berlin*.

Liu, J., Hu, Y., Luo, X., Castañeda-Ruíz, R. F., Xia, J., Xu, Z., . . . Ma, J. (2023). Molecular phylogeny and morphology reveal four novel species of *Corynespora* and *Kirschsteiniothelia* (*Dothideomycetes*, *Ascomycota*) from China: A checklist for *Corynespora* reported worldwide. *Journal of Fungi*, *9*(1), 107. https://doi.org/10.3390/jof9010107

Liu, J., Zhang, X., Yang, J., Zhou, J., Yuan, Y., Jiang, C., . . . Huang, L. (2019). Agarwood wound locations provide insight into the association between fungal diversity and volatile compounds in *Aquilaria sinensis*. *Royal Society Open Science*, *6*(7), 190211. https://doi.org/10.1098/rsos.190211

Liu, L. L., Liu, Y. X., Chen, Y. Y., Gou, J. L., Chi, F., Liu, Y., . . . Zhou, S. (2025). Freshwater fungi in the karst plateau wetlands from Guizhou Province, China: taxonomic novelties in *Melanommataceae* (*Pleosporales*). *MycoKeys*, *113*, 209. https://doi.org/10.3897/mycokeys.113.140684

Liu, N. G., Hyde, K. D., Sun, Y. R., Bhat, D. J., Jones, E. G., Jumpathong, J., . . . Liu, J. K. (2024). Notes, outline, taxonomy and phylogeny of brown-spored hyphomycetes. *Fungal Diversity*, *129*(1), 1–281. https://doi.org/10.1007/s13225-024-00539-6

Liu, N. G., Lu, Y. Z., Bhat, D. J., McKenzie, E. H., Lumyong, S., Jumpathong, J., & Liu, J. K. (2019). *Kevinhydea brevistipitata* gen. et sp. nov. and *Helicoma hydei* sp. nov.,(*Tubeufiaceae*) from decaying wood habitats. *Mycological progress*, *18*(5), 671–682. https://doi.org/10.1007/s11557-019-01480-8

Liu, S., García-Palacios, P., Tedersoo, L., Guirado, E., van der Heijden, M. G., Wagg, C., . . . Delgado-Baquerizo, M. (2022). Phylotype diversity within soil fungal functional groups drives ecosystem stability. *Nature Ecology & Evolution*, *6*(7), 900–909. https://doi.org/10.1038/s41559-022-01756-5

Liu, Y. J., Whelen, S., & Hall, B. D. (1999). Phylogenetic relationships among ascomycetes: Evidence from an RNA polymerase II subunit. *Molecular Biology and Evolution*, *16*(12), 1799–1808. https://doi.org/10.1093/oxfordjournals.molbev.a026092

Liu, Y., Chen, H., Yang, Y., Zhang, Z., Wei, J., Meng, H., . . . Chen, H. (2013). Whole-tree agarwood-inducing technique: An efficient novel technique for producing high-quality agarwood in cultivated *Aquilaria sinensis* trees. *Molecules*, *18*(3), 3086–3106. https://doi.org/10.3390/molecules18033086

Locquin-Linard, M. (1977). *Chaetopreussia chadefaudii* n.g., n. sp. *Revue de Mycologie* (*Paris*), *41*(2), 181–187.

Lodge, D. J. (1997). Factors related to diversity of decomposer fungi in tropical forests. *Biodiversity & Conservation*, *6*(5), 681–688. https://doi.org/10.1023/A:1018314219111

Lodge, D. J., & Cantrell, S. (1995a). Diversity of litter agarics at Cuyabeno, Ecuador: Calibrating sampling efforts in tropical rainforest. *Mycologist*, *9*(4), 149–151.

Lodge, D. J., & Cantrell, S. (1995b). Fungal communities in wet tropical forests: Variation in time and space. *Canadian Journal of Botany*, *73*(S1), 1391–1398. https://doi.org/10.1139/b95-402

Lodge, D. J., & Laessøe, T. (1995). Host preference in *Camillea verruculospora*. *Mycologist*, *9*(4), 152–153.

Lodge, D. J., Fisher, P. J., & Sutton, B. C. (1996). Endophytic fungi of *Manilkara bidentata* leaves in Puerto Rico. *Mycologia*, *88*(5), 733–738.

Lofgren, L. A., & Stajich, J. E. (2021). Fungal biodiversity and conservation mycology in light of new technology, big data, and changing attitudes. *Current Biology*, *31*(19), R1312–R1325. https://doi.org/10.1016/j.cub.2021.06.083

Lu, B., & Hyde, K. D. (2000). *Checklist of Hong Kong Fungi*. Fungal Diversity Press.

Lu, Y. Z., Ma, J., Xiao, X. J., Zhang, L. J., Xiao, Y. P., & Kang, J. C. (2023). Morphology and phylogeny of *Tubeufia liyui* sp. nov. J*ournal of Fungal Research*, 21(1/2/3), 14–23. https://doi.org/10.13341/j.jfr.2023.1582

Lu, Y. Z., Liu, J. K., Hyde, K. D., Jeewon, R., Kang, J. C., Fan, C., . . . Eungwanichayapant, P. D. (2018b). A taxonomic reassessment of *Tubeufiales* based on multi-locus phylogeny and morphology. *Fungal Diversity*, *92*, 131–344. https://doi.org/10.1007/s13225-018-0411-y

Lumbsch, H. T., & Huhndorf, S. M. (2009). Outline of Ascomycota—2009. *Myconet / Field Museum, 14*.

Lumbsch, H. T., & Huhndorf, S. M. (2010). Myconet volume 14. Part one. Outline of Ascomycota—2009. Part two. Notes on ascomycete systematics. Nos. 4751–5113. *Fieldiana Life and Earth Sciences*, *2010*(1), 1–64. https://doi.org/10.3158/1557.1

Luo, Z. L., Bhat, D. J., Jeewon, R., Boonmee, S., Bao, D. F., Zhao, Y. C., . . . Hyde, K. D. (2017). Molecular phylogeny and morphological characterization of asexual fungi (*Tubeufiaceae*) from freshwater habitats in Yunnan, China. *Cryptogamie, Mycologie*, *38*(1), 27–53. https://doi.org/10.7872/crym/v38.iss1.2017.27

Luo, Z. L., Hyde, K. D., Liu, J. K., Maharachchikumbura, S. S., Jeewon, R., Bao, D. F., . . . Su, H. Y. (2019). Freshwater *Sordariomycetes*. *Fungal Diversity*, *99*(1), 451–660. https://doi.org/10.1007/s13225-019-00438-1

Luttrell, E. S. (1955). The ascostromatic ascomycetes. *Mycologia*, *47*(4), 511–532. https://doi.org/10.1080/00275514.1955.12024473

Luttrell, E. S. (1964). Parasitism of fungi on vascular plants. *Mycologia*, *56*(1), 2–15.

Ma, J. (2016). *Sporidesmiella lushanensis* and *S. jiulianshanensis* spp. nov. and a new record from China. *Mycotaxon*, *131*(3), 575–581. https://doi.org/10.5248/131.575

Ma, J., Hyde, K. D., Tibpromma, S., Gomdola, D., Liu, N. G., Norphanphoun, C., . . . Lu, Y. Z. (2024). Taxonomy and systematics of lignicolous helicosporous hyphomycetes. *Fungal Diversity*, *129*(1), 365–653. https://doi.org/10.1007/s13225-024-00544-9

Ma, J., Wang, Y., Ma, L. G., Zhang, Y. D., Castañeda-Ruíz, R. F., & Zhang, X. G. (2011). Three new species of *Neosporidesmium* from Hainan, China. *Mycological Progress*, *10*, 157–162. https://doi.org/10.1007/s11557-010-0685-2

Ma, J., Xia, J. W., Castañeda-Ruíz, R. F., & Zhang, X. G. (2015). Two new species of *Sporidesmiella* from southern China. *Nova Hedwigia*, *101*(1-2), 131–137. https://doi.org/10.1127/nova_hedwigia/2015/0254

Ma, J., Xiao, X. J., Liu, N. G., Boonmee, S., Xiao, Y. P., & Lu, Y. Z. (2023). Morphological and multi-gene phylogenetic analyses reveal *Pseudotubeufia* gen. nov. and two new species in *Tubeufiaceae* from China. *Journal of Fungi*, *9*(7), 742. https://doi.org/10.3390/jof9070742

Ma, J., Zhang, Y. D., Ma, L. G., Castañeda-Ruíz, R. F., & Zhang, X. G. (2012). Three new species of *Sporidesmiella* from southern China. *Mycoscience*, *53*(3), 187–193. https://doi.org/10.1007/s10267-011-0152-1

Ma, L. G., Ma, J., Zhang, Y. D., & Zhang, X. G. (2010). A new species of *Spadicoides* from Yunnan, China. *Mycotaxon*, *113*, 255–258. https://doi.org/10.5248/113.255

Ma, X. Y., Lu, Y. Z., He, L., Song, D. D., & Ma, J. (2025b). Two new species of *Neohelicosporium* (*Tubeufiaceae*, *Tubeufiales*) from freshwater and terrestrial habitats in China. *MycoKeys*, *118*, 1. https://doi.org/10.3897/mycokeys.118.151514

Ma, X. Y., Song, D. D., & Ma, J. (2025a). Morphological and phylogenetic analyses reveal two new species of *Neohelicomyces* (*Tubeufiales*, *Tubeufiaceae*) from China. *MycoKeys*, *121*, 237. https://doi.org/10.3897/mycokeys.121.158721

Ma, X. Y., Tian, F., Feng, J. F., Wang, M. M., Shi, H. H., & Ma, J. (2025c). Morphological and phylogenetic analyses reveal two new species of *Tubeufia* (*Tubeufiales*, *Tubeufiaceae*) from freshwater habitats in China. *MycoKeys*, *121*, 93. https://doi.org/10.3897/mycokeys.121.158724

Maharachchikumbura, S. S., Chen, Y., Ariyawansa, H. A., Hyde, K. D., Haelewaters, D., Perera, R. H., . . . Stadler, M. (2021). Integrative approaches for species delimitation in *Ascomycota*. *Fungal Diversity*, *109*, 155–179. https://doi.org/10.1007/s13225-021-00486-6

Maharachchikumbura, S. S., Hyde, K. D., Jones, E. G., McKenzie, E. H. C., Bhat, J. D., Dayarathne, M. C., . . . Wijayawardene, N. N. (2016). Families of *Sordariomycetes*. *Fungal Diversity*, *79*, 1–317. https://doi.org/10.1007/s13225-016-0369-6

Maharachchikumbura, S. S., Hyde, K. D., Jones, E. G., McKenzie, E. H., Huang, S. K., Abdel-Wahab, M. A., . . . Xu, J. (2015). Towards a natural classification and backbone tree for *Sordariomycetes*. *Fungal Diversity*, *72*(1), 199–301. https://doi.org/10.1007/s13225-015-0331-z

Mapook, A., Hyde, K. D., McKenzie, E. H., Jones, E. G., Bhat, D. J., Jeewon, R., . . . Purahong, W. (2020). Taxonomic and phylogenetic contributions to fungi associated with the invasive weed *Chromolaena odorata* (Siam weed). *Fungal Diversity*, *101*(1), 1–175. https://doi.org/10.1007/s13225-020-00444-8

Marcot, B. G. (2017). *A review of the role of fungi in wood decay of forest ecosystems* (Res. Note PNW RN 575). U.S. Department of Agriculture, Forest Service, Pacific Northwest Research Station. https://doi.org/10.2737/PNW-RN-575

Markham, W. D., Key, R. D., Padhye, A. A., & Ajello, L. (1990). Phaeohyphomycotic cyst caused by *Tetraploa aristata*. *Journal of Medical and Veterinary Mycology*, *28*(2), 147–150.

Markovskaja, S. (2003). A new species of *Cordana* from *Lithuania*. *Mycotaxon*, *87*, 179–185.

Matsushima, T. (1971). *Microfungi of the Solomon Islands and Papua-New Guinea*. Published by the author.

Matsushima, T. (1975). *Icones Microfungorum a Matsushima lectorum*. Published by the author.

Matsushima, T. (1980). *Matsushima mycological memoirs No. 1*. Matsushima Fungus Collection.

Matsushima, T. (1981). *Matsushima mycological memoirs No. 2*. Matsushima Fungus Collection.

Matsushima, T. (1996). *Matsushima mycological memoirs No. 9*. Matsushima Fungus Collection.

Maury-Lechon, G., & Curtet, L. (1998). Biogeography and evolutionary systematics of *Dipterocarpaceae*. In S. Appanah & J. M. Turnbull (Eds.), *A review of dipterocarps: Taxonomy, ecology and silviculture* (pp. 5–44). Center for International Forestry Research.

Mehrotra, M. D., & Sivanesan, A. (1989). *Asteromassaria tetraspora* sp. nov., a new ascomycete from India. *Mycological Research*, *93*(4), 557–558. https://doi.org/10.1016/S0953-7562(89)80055-3

Menéndez, P., Losada, I. J., Torres-Ortega, S., Narayan, S., & Beck, M. W. (2020). The global flood protection benefits of mangroves. *Scientific Reports*, *10*(1), 4404. https://doi.org/10.1038/s41598-020-61136-6

Mercado, A., Holubová-Ječhová, V., & Mena Portales, J. (1997). *Hifomicetes demaciáceos de Cuba. Monografie, Museo Regionale di Scienze Naturali* (Turin, Italy). Museo regionale di scienze naturali.

Micheli, P. A. (1729). *Nova plantarum genera. Florentiae: Typis Bernardi Paperinii*. Typis Bernardi Paperinii.

Miller, M. A., Pfeiffer, W., & Schwartz, T. (2010). Creating the CIPRES Science Gateway for inference of large phylogenetic trees. *In 2010 gateway computing environments workshop (GCE)*. https://doi.org/10.1109/GCE.2010.5676129

Ministry of Foreign Affairs of Japan (MOFA). (2023). *White paper on development cooperation—Takumi 04* (on mitsumata for banknote paper). Official Development Assistance (ODA).

Mohamed, R., Jong, P. L., & Zali, M. S. (2010). Fungal diversity in wounded stems of *Aquilaria malaccensis*. *Fungal Diversity*, *43*(1), 67–74. https://doi.org/10.1007/s13225-010-0039-z

Mongabay. (2025, June 4). *Resilient forests are key to ecological, economic and social resilience, report finds*. Mongabay. https://news.mongabay.com/2025/06/resilient-

Monteiro, J. S., Carmo, L. T. D., Fiúza, P. O., Ottoni, B. M. D. P., Gusmão, L. F. P., & Castañeda-Ruíz, R. F. (2014). New species of microfungi from Brazilian Amazon rainforests. *Mycotaxon*, *127*(1), 81–87. https://doi.org/10.5248/127.81

Moshiashvili, G., Tabatadze, N., & Mshvildadze, V. (2020). The genus *Daphne*: A review of its traditional uses, phytochemistry and pharmacology. *Fitoterapia*, *143*, 104540. https://doi.org/10.1016/j.fitote.2020.104540

Mostert, L., Groenewald, J. Z., Summerbell, R. C., Gams, W., & Crous, P. W. (2006). Taxonomy and pathology of *Togninia* (*Diaporthales*) and its *Phaeoacremonium* anamorphs. *Studies in Microbiology*, *54*, 1–115. https://doi.org/10.3114/sim.54.1.1

Mu, T., Lin, Y., Keyhani, N. O., Pu, H., Lv, Z., Lan, C., . . . Guan, X. (2024). Phylogenetic and morphological evidence for three new species of *Diaporthales* (*Ascomycota*) from Fujian Province, China. *Journal of Fungi*, *10*(6), 383. https://doi.org/10.3390/jof10060383

Mueller, G. M., Schmit, J. P., & Lodge, D. J. (2022). Reviewing the contributions of macrofungi to forest ecosystem processes and services. *Fungal Ecology*, *55*, 100970. https://doi.org/10.1016/j.funeco.2022.100970

Mugambi, G. K., & Huhndorf, S. M. (2009). Parallel evolution of hysterothecial ascomata in ascolocularous fungi (*Ascomycota*, Fungi). *Systematics and Biodiversity*, *7*(4), 453–464. https://doi.org/10.1017/S147720000999020X

Mulas, B., Pasqualetti, M., & Rambelli, A. (1995). Analysis of the litter microfungal communities in a Mediterranean maquis ecosystem. *Rendiconti Lincei*, *6*(1), 65–86. https://doi.org/10.1007/BF03001635

Mułenko, W., Majewski, T., & Ruszkiewicz-Michalska, M. (2008). *A preliminary checklist of micromycetes in Poland*. W. Szafer Institute of Botany, Polish Academy of Sciences.

MycoBank. (2025). *MycoBank: Fungal databases, nomenclature & species banks* [Database]. Westerdijk Fungal Biodiversity Institute. http://www.mycobank.org

Nannfeldt, J. A. (1932). Studien über die Morphologie und Systematik der nicht-lichenisierten inoperculaten Discomyceten. *Nova Acta Regiae Societatis Scientiarum Uppsaliensis, IV, 8*, 1–368.

Naranjo-Ortiz, M. A., & Gabaldón, T. (2019). Fungal evolution: Diversity, taxonomy and phylogeny of the Fungi. *Biological Reviews*, *94*(6), 2101–2137. https://doi.org/10.1111/brv.12550

Ngadiran, S., Baba, S., Nor, N. F. A., Yahayu, M., Muhamad, M. F., Kushairi, A. K. A., . . . Muhamad, I. I. (2023). The induction techniques of resinous agarwood formation: A review. *Bioresource Technology Reports*, *21*, 101337. https://doi.org/10.1016/j.biteb.2023.101337

Nguyen, T. T., & Lee, H. B. (2024). Descriptions of 19 unrecorded species belonging to *Sordariomycetes* in Korea. *Mycobiology*, *52*(6), 405–438. https://doi.org/10.1080/12298093.2024.2426840

Nóbrega, T. F., Ferreira, B. W., & Barreto, R. W. (2021). *Digitodesmium polybrachiatum* sp. nov., a new species of *Dictyosporiaceae* from Brazil. *Mycological Progress*, *20*(9), 1135–1144. https://doi.org/0.1007/s11557-021-01717-5

Noshad, D., Riseman, A., & Punja, Z. K. (2006). First report of *Thielaviopsis basicola* on *Daphne cneorum. Canadian Journal of Plant Pathology*, *28*(2), 310–312. https://doi.org/10.1080/07060660609507300

Nuñez Otaño, N. B., Bianchinotti, M. V., Romero, I. C., Perez Pincheira, E. V., Saxena, R. K., & Saparrat, M. C. N. (2022). Fossil *Tetraploa* redefinition and potential contribution of dark pigments for the preservation of its spores in the fossil record. *Mycosphere, 13*(2), 188–206.

Ogawa, M. (1992). Mycorrhiza of dipterocarps. In *Proceedings of the BIO-REFOR Tsukuba Workshop*, 19–21 May 1992 (pp. 55–58). BIO-REFOR, IUFRO-SPDC.

Oliveira, M. S., Malosso, E., Barbosa, M. A., Araújo, M. A., & Castañeda-Ruíz, R. F. (2015). *Xylomyces acerosisporus* sp. nov. from submerged leaves from Brazil. *Mycotaxon*, *130*(3), 875–878. https://doi.org/10.5248/130.875

Oyen, L. P. A., & Nguyễn, X. D. (Eds.). (1999). *Plant resources of South East Asia* (No. 19). Backhuys Publishers.

Pasqualetti, M., & Rambelli, A. (1999). Dactylaria asymmetrica, a new species of mitosporic fungi from Ivory Coast forest litter. *Mycotaxon*, *72*, 27–31.

Paulus, B., Gadek, P., & Hyde, K. (2006). Successional patterns of microfungi in fallen leaves of *Ficus pleurocarpa* (*Moraceae*) in an Australian tropical rain forest 1. *Biotropica: The Journal of Biology and Conservation*, *38*(1), 42–51. https://doi.org/10.1111/j.1744-7429.2006.00110.x

Pawar, V. H.; Mathur, P. N., Thirumalachar, M. J. (1967). Species of *Phoma* isolated from marine soils in India. *Transactions of the British Mycological Society*, *50*(2), 259–285.

Pem, D., Hongsanan, S., Doilom, M., Tibpromma, S., Wanasinghe, D. N., Dong, W., . . . Hyde, K. D. (2019). https://www.dothideomycetes.org: An online taxonomic resource for the classification, identification, and nomenclature of *Dothideomycetes*. *Asian Journal of Mycology*, *2*(1), 287–297. https://doi.org/10.5943/ajom/2/1/19

Pem, D., Jeewon, R., Chethana, K. W. T., Hongsanan, S., Doilom, M., Suwannarach, N., . . . Hyde, K. D. (2021). Species concepts of *Dothideomycetes*: Classification, phylogenetic inconsistencies and taxonomic standardization. *Fungal Diversity*, *109*(1), 283–319. https://doi.org/10.1007/s13225-021-00485-7

Penzig, A. J. O., & Saccardo, P. A. (1902). Diagnoses fungorum novorum in insula Java collectorum. *Series Tertia. Malpighia*, *15*(7–9), 201–260.

Penzig, O. (1897). *Fungi javanici. Pars secunda*. E. J. Brill.

Pereira, J. O., Azevedo, J. L., & Petrini, O. (1993). Endophytic fungi of *Stylosanthes*: A first report. *Mycologia*, *85*(3), 362–364. https://doi.org/10.1080/00275514.1993.12026286

Persoon, C. H. (1794). Dispositio methodica fungorum. *Neues Magazin für die Botanik in ihrem ganzen Umfange*, *1*, 81–128.

Petch, T. (1924). Journal of the Indian Botanical Society, 4.

Petrini, O. (1981). Endophytische pilze in epiphytischen *Araceae*, *Bromeliaceae* und *Orchidaceae*. *Sydowia*, *38*, 216–234.

Phookamsak, R., Hyde, K. D., Jeewon, R., Bhat, D. J., Jones, E. G., Maharachchikumbura, S. S., . . . Xu, J. (2019). Fungal diversity notes 929–1035: Taxonomic and phylogenetic contributions on genera and species of fungi. *Fungal Diversity*, *95*, 1–273. https://doi.org/10.1007/s13225-019-00421-w

Phookamsak, R., Norphanphoun, C., Tanaka, K., Dai, D. Q., Luo, Z. L., Liu, J. K., . . . Hyde, K. D. (2015). Towards a natural classification of Astrosphaeriella-like species: Introducing *Astrosphaeriellaceae* and *Pseudoastrosphaeriellaceae* fam. nov. and *Astrosphaeriellopsis* gen. nov. *Fungal Diversity*, *74*, 143–197. https://doi.org/10.1007/s13225-015-0352-7

Phosri, C., Polme, S., Taylor, A. F., Koljalg, U., Suwannasai, N., & Tedersoo, L. (2012). Diversity and community composition of ectomycorrhizal fungi in a dry deciduous dipterocarp forest in Thailand. *Biodiversity and Conservation*, *21*(9), 2287–2298. https://doi.org/10.1007/s10531-012-0250-1

Photita, W., Lumyong, S., Lumyong, P., & Hyde, K. D. (2001). Endophytic fungi of wild banana (Musa acuminata) at doi Suthep Pui National Park, Thailand. *Mycological Research*, *105*(12), 1508–1513. https://doi.org/10.1017/S0953756201004968

Phurbu, D., Huang, J. E., Song, S., Ni, Z., Zhou, X., Li, S., . . . Liu, F. (2025). Diversity of culturable fungi in six Tibetan Plateau lakes, with descriptions of eight new taxa. *Mycology*, *16*(2), 670–689. https://doi.org/10.1080/21501203.2024.2333300

Pinruan, U., Hyde, K. D., Lumyong, S., McKenzie, E. H. C., & Jones, E. B. G. (2007). Occurrence of fungi on tissues of the peat swamp palm *Licuala longicalycata*. *Fungal Diversity*, *25*(1), 157–173.

Pintos, Á., Alvarado, P., Planas, J., & Jarling, R. (2019). Six new species of *Arthrinium* from Europe and notes about *A. caricicola* and other species found in *Carex* spp. hosts. *MycoKeys*, *49*, 15–48. https://doi.org/10.3897/mycokeys.49.32115

Polishook, J. D., Bills, G. F., & Lodge, D. J. (1996). Microfungi from decaying leaves of two rain forest trees in Puerto Rico. *Journal of industrial microbiology and biotechnology*, *17*(3), 284–294. https://doi.org/10.1007/BF01574703

Prabhugaonkar, A., & Bhat, D. J. (2011). New record of *Megacapitula villosa* and *Paradictyoarthrinium diffractum* from India. *Mycosphere*, *2*(4), 463–467.

Preuss, C. G. T. (1852). Uebersicht untersuchter Pilze, besonders aus der Umgegend von Hoyerswerda (Fortsetzung). *Linnaea*, *25*, 723–742.

Preuss, G. T. (1851). Uebersicht untersuchter Pilze besonders aus der Umgegend von *Hoyerswerda*.

Promputtha, I., & Miller, A. N. (2010). Three new species of *Acanthostigma* (*Tubeufiaceae, Dothideomycetes*) from Great Smoky Mountains National Park. *Mycologia, 102*(3), 574–587.

Qiu, L., Hu, Y. F., Liu, J. W., Xia, J. W., Castañeda-Ruíz, R. F., Xu, Z. H., . . . Ma, J. (2022). Phylogenetic placement of new species and combinations of *Neopodoconis* within *Torulaceae*. Research Square. https://doi.org/10.21203/rs.3.rs-1755529/v1

Qiu, L., Zhang, K., Xu, Z. H., Castañeda-Ruíz, R. F., & Ma, J. (2021). *Cordana sinensis* sp. nov. from southern China. *Mycotaxon*, *136*(3), 553–562. https://doi.org/10.5248/136.553

Quaedvlieg, W. G. J. M., Verkley, G. J. M., Shin, H. D., Barreto, R. W., Alfenas, A. C., Swart, W. J., . . . Crous, P. W. (2013). Sizing up septoria. *Studies in Mycology*, *75*(1), 307–390. https://doi.org/10.3114/sim0017

Rajagopal, K., & Suryanarayanan, T. S. (2000). Isolation of endophytic fungi from leaves of neem (*Azadirachta indica* A. Juss.). *Current Science*, *78*(11), 1375–1378.

Rajeshkumar, K. C., Paraparath, S. O., Harikrishnan, K., Hongsanan, S., Ansil, P. S., Karunarathna, S. C., . . . Jeewon, R. (2024). *Megacapitulaceae*, a new family of *Pleosporales* through epitypification and multigene phylogeny based on fresh material from India. *Kavaka*, *60*(4), 1–12. https://doi.org/10.36460/Kavaka/60/4/2024/1-12

Rambelli, A. (1991). Comparative studies on microfungi in tropical ecosystems: Conclusive mycological studies in South-Western Ivory Coast forest litter (Report No. 3). *Università della Tuscia*.

Rambelli, A., Lunghini, D., Onofri, S., & Vagnozzi, A. (2004). Fungal biodiversity of leaf litter in the Taï National Park (Côte d'Ivoire). In G. M. Gadd (Ed.), Fungi in biogeochemical cycles (pp. 269–286). *Cambridge University Press*.

Rambelli, A., Mulas, B., & Pasqualetti, M. (1983). Comparative studies on microfungi in tropical ecosystems in Ivory Coast forest litter: behaviour on different substrata. *Mycological Research*, *108*(3), 325-336. https://doi.org/10.1017/S0953756204009396

Rambelli, A., Persiani, A. M., Maggi, O., Onofri, S., Riess, S., Dowgiallo, G., . . . Zucconi, L. (1984). Comparative studies on microfungi in tropical ecosystems. Further mycological studies in South Western Ivory Coast forest. *Plant Biosystem*, *118*(5–6), 201–243. https://doi.org/10.1080/11263508409426674

Rao, V. (1986). New or critical hyphomycetes from India. *Studies in Mycology*, *28*, 6–9.

Rashmi, M., Kushveer, J. S., & Sarma, V. V. (2019). A worldwide list of endophytic fungi with notes on ecology and diversity. *Mycosphere*, *10*(1), 798–1079. https://doi.org/10.5943/mycosphere/10/1/19

Rasool, S., & Mohamed, R. (2016). Understanding agarwood formation and its challenges. In R. Mohamed (Ed.), *Agarwood: Science behind the fragrance* (pp. 39–56). Springer Singapore. https://doi.org/10.1007/978-981-10-0833-7_3

Rathnayaka, A. R., Wanasinghe, D. N., Dayarathne, M. C., Chethana, K. T., Bhat, D. J., Kuo, C. H., . . . Hyde, K. D. (2020). *Hyaloterminalis*, a novel genus of *Coryneaceae* in order *Diaporthales*. *Phytotaxa*, *474*, 132–144. https://doi.org/10.11646/phytotaxa.474.2.3

Rayner, R. W. (1970). A mycological colour chart. *Mycologia*, *64*, 230–233. https://doi.org/10.2307/3758035

Réblová, M., Miller, A. N., Rossman, A. Y., Seifert, K. A., Crous, P. W., Hawksworth, D. L., . . . Wijayawarden, N. N. (2016a). Recommendations for competing sexual-asexually typified generic names in *Sordariomycetes* (except *Diaporthales*, *Hypocreales*, and *Magnaporthales*). *IMA Fungus*, *7*, 131–153. https://doi.org/10.5598/imafungus.2016.07.01.08

Réblová, M., Mostert, L., Gams, W., & Crous, P. W. (2004). New genera in the *Calosphaeriales*: *Togniniella* and its anamorph *Phaeocrella*, and *Calosphaeriophora* as anamorph of *Calosphaeria*. *Studies in Microbiology*, *50*, 533–550.

Réblová, M., Seifert, K. A., Fournier, J., & Štěpánek, V. (2016b). Newly recognised lineages of perithecial ascomycetes: The new orders *Conioscyphales* and Pleurotheciales. *Persoonia: Molecular Phylogeny and Evolution of Fungi*, *37*(1), 57–81. https://doi.org/10.3767/003158516X689819

Rehner, S. A., & Buckley, E. (2005). A Beauveria phylogeny inferred from nuclear ITS and *EF1-α* sequences: Evidence for cryptic diversification and links to *Cordyceps* teleomorphs. *Mycologia*, *97*(1), 84–98. https://doi.org/10.1080/15572536.2006.11832842

Ren, G. C., Wanasinghe, D. N., Monkai, J., Mortimer, P. E., Hyde, K. D., Xu, J. C., . . . Gui, H. (2021). Novel saprobic *Hermatomyces* species (*Hermatomycetaceae*, *Pleosporales*) from China (Yunnan Province) and Thailand. *MycoKeys*, *82*, 57. https://doi.org/10.3897/mycokeys.82.67973

Ren, S. C., Ma, J., Ma, L. G., Zhang, Y. D., & Zhang, X. G. (2012). *Sativumoides* and *Cladosporiopsis*, two new genera of hyphomycetes from China. *Mycological Progress*, *11*(2), 443–448. https://doi.org/10.1007/s11557-011-0759-9

Richardson, K. A., & Currah, R. S. (1995). The fungal community associated with the roots of some rainforest epiphytes of Costa Rica. *Selbyana, 16*(1), 49–73.

Rifai, M. A. (2008). Another note on podoconis megasperma boedijn (Hyphomycetes). *Reinwardtia*, *12*(4), 277–279.

Rigling, D., & Prospero, S. (2018). *Cryphonectria parasitica*, the causal agent of chestnut blight: invasion history, population biology and disease control. *Molecular Plant Pathology*, *19*(1), 7–20. https://doi.org/10.1111/mpp.12542

Rillig, M. C., & Mummey, D. L. (2006). Mycorrhizas and soil structure. *New Phytologist*, *171*(1), 41–53. https://doi.org/10.1111/j.1469-8137.2006.01750.x

Rodrigues, K. F., & Samuels, G. J. (1990). Preliminary study of endophytic fungi in a tropical palm. *Mycological Research, 94*(6), 827-830. https://doi.org/10.1016/S0953-7562(09)81386-5

Rodriguez, R. J., White, J. F. Jr, Arnold, A. E., & Redman, A. R. (2009). Fungal endophytes: Diversity and functional roles. *New Phytologist*, *182*(2), 314–330. https://doi.org/10.1111/j.1469-8137.2009.02773.x

Ronquist, F., Teslenko, M., Van Der Mark, P., Ayres, D. L., Darling, A., Höhna, S., . . . Huelsenbeck, J. P. (2012). MrBayes 3.2: efficient Bayesian Phylogenetic Inference and model choice across a large model space. *Systematic Biology*, *61*(3), 539–542. https://doi.org/10.1093/sysbio/sys029

Rossman, A. Y., Farr, D. F., & Castlebury, L. A. (2007). A review of the phylogeny and biology of the *Diaporthales*. *Mycoscience*, *48*(3), 135–144. https://doi.org/10.47371/mycosci.MYC48135

Ruíz, R. C., Saikawa, M., & Guarro, J. (1999). A new species of *Heteroconium* from a tropical rainforest. *Mycotaxon*, *71*, 295–300.

Saccardo, P. A. (1877). Fungi italici autographice delineati. *Hyphomycetes*, *23*, 124.

Saccardo, P. A. (1886). Sylloge fungorum omnium hucusque cognitorum (Vol. 4). Padova, Italy: Typis Seminarii.

Saccardo, P. A., & Paoletti, G. (1888). Mycetes Malacenses. Funghi della penisola di Malacca raccolti nel 1885 dell. *Ab Benedetto Scortechini*, *6*, 387–428.

Saikkonen, K., Faeth, S. H., Helander, M., & Sullivan, T. J. (1998). Fungal endophytes: A continuum of interactions with host plants. *Annual Review of Ecology and Systematics*, *29*(1), 319–343. https://doi.org/10.1146/annurev.ecolsys.29.1.319

Samarakoon, B. C., Phookamsak, R., Karunarathna, S. C., Jeewon, R., Chomnunti, P., Xu, J. C., & Li, Y. J. (2021). New host and geographic records of five pleosporalean hyphomycetes associated with *Musa* spp. (Banana). *Studies in Fungi*, *6*(1), 92–115. https://doi.org/10.5943/sif/6/1/5

Sánchez-Ramírez, S., Tulloss, R. E., Amalfi, M., & Moncalvo, J. M. (2015). Palaeotropical origins, boreotropical distribution and increased rates of diversification in a clade of edible ectomycorrhizal mushrooms (*Amanita* section *Caesareae*). *Journal of Biogeography*, *42*(2), 351–363. https://doi.org/10.1111/jbi.12402

Sandberg, D. C., Battista, L. J., & Arnold, A. E. (2014). Fungal endophytes of aquatic macrophytes: Diverse host-generalists characterized by tissue preferences and geographic structure. *Microbial Ecology*, *67*(4), 735–747. https://doi.org/10.1007/s00248-013-0324-y

Santamaría, J., & Bayman, P. (2005). Fungal epiphytes and endophytes of coffee leaves (Coffea arabica). *Microbial Ecology*, *38*(3), 310–321. https://doi.org/10.1007/s00248-004-0002-1

Saxena, R. K., Wijayawardene, N. N., Dai, D. Q., Hyde, K. D., & Kirk, P. M. (2021). Diversity in fossil fungal spores. *Mycosphere*, *12*(1), 670–874. https://doi.org/10.5943/mycosphere/12/1/8

Schoch, C. L., Crous, P. W., Groenewald, J. Z., Boehm, E. W. A., Burgess, T. I., De Gruyter, J., . . . Spatafora, J. W. (2009). A class-wide phylogenetic assessment of Dothideomycetes. *Studies in Mycology*, *64*(1), 1–15. https://doi.org/10.3114/sim.2009.64.01

Schoch, C. L., Shoemaker, R. A., Seifert, K. A., Hambleton, S., Spatafora, J. W., & Crous, P. W. (2006). A multigene phylogeny of the *Dothideomycetes* using four nuclear loci. *Mycologia*, *98*(6), 1041–1052. https://doi.org/10.1080/15572536.2006.11832632

Schulz, B., Wanke, U., Draeger, S., & Aust, H. J. (1993). Endophytes from herbaceous plants and shrubs: effectiveness of surface sterilization methods. *Mycological Research*, *97*(12), 1447–1450.

Senanayake, I. C., Crous, P. W., Groenewald, J. Z., Maharachchikumbura, S. S., Jeewon, R., Phillips, A. J., . . . Hyde, K. D. (2017). Families of *Diaporthales* based on morphological and Phylogenetic evidence. *Studies in Microbiology*, *86*, 217–296. https://doi.org/10.1016/j.simyco.2017.07.003

Senanayake, I. C., Jeewon, R., Chomnunti, P., Wanasinghe, D. N., Norphanphoun, C., Karunarathna, A., . . . Karunarathna, S. C. (2018). Taxonomic circumscription of *Diaporthales* based on multigene phylogeny and morphology. *Fungal Diversity*, *93*, 241–443. https://doi.org/10.1007/s13225-018-0410-z

Senanayake, I. C., Maharachchikumbura, S. S., Hyde, K. D., Bhat, J. D., Jones, E. G., McKenzie, E. H., . . . Camporesi, E. (2015). Towards unraveling relationships in *Xylariomycetidae* (*Sordariomycetes*). *Fungal Diversity*, *73*(1), 73–144. https://doi.org/10.1007/s13225-015-0340-y

Senanayake, I. C., Rathnayaka, A. R., Marasinghe, D. S., Calabon, M. S., Gentekaki, E., Lee, H. B., . . . Xiang, M. M. (2020). Morphological approaches in studying fungi: Collection, examination, isolation, sporulation and preservation. *Mycosphere*, *11*(1), 2678–2754. https://doi.org/10.5943/mycosphere/11/1/20

Senanayake, I. C., Rossi, W., Leonardi, M., Weir, A., McHugh, M., Rajeshkumar, K. C., . . . Song, J. (2023). Fungal diversity notes 1611–1716: Taxonomic and phylogenetic contributions on fungal genera and species emphasis in south China. *Fungal Diversity*, *122*(1), 161–403. https://doi.org/10.1007/s13225-023-00523-6

Shackleton, C. M., Adeyemi, O., & Setty, S. (2024). Why are non-wood forest products still the poor relative in Global Forest Resources Assessments?. *Forest Policy and Economics*, *163*, 103232. https://doi.org/10.1016/j.forpol.2024.103232

Sharma, R. P., Bhandari, S. K., & Bk, R. B. (2017). Allometric bark biomass model for *Daphne bholua* in the mid-hills of Nepal. *Mountain Research and Development*, *37*(2), 206–215. https://doi.org/10.1659/MRD-JOURNAL-D-16-00052.1

Sharma, R., Kulkarni, G., Sonawane, M. S., & Shouche, Y. S. (2014). A new endophytic species of *Arthrinium* (*Apiosporaceae*) from Jatropha podagrica. *Mycoscience*, *55*(2), 118–123. https://doi.org/10.1016/j.myc.2013.06.004

Shearer, C. A., Pang, K. L., Suetrong, S., & Raja, H. A. (2014). *Phylogeny of the Dothideomycetes and other classes of freshwater fissitunicate Ascomycota*. Mushroom Research Foundation.

Shen, H. W., Bao, D. F., Su, H. Y., Boonmee, S., & Luo, Z. L. (2021). *Rostriconidium cangshanense* sp. nov. and a new record *R. pandanicola* (*Torulaceae*) in Yunnan Province, China. *Mycosystema*, *40*(6), 1259–1273. https://doi.org/10.13346/j.mycosystema.200306

Shen, H. W., Luo, Z. L., Bao, D. F., Luan, S., Bhat, D. J., Boonmee, S., . . . Hyde, K. D. (2024). Lignicolous freshwater fungi from China IV: Morphology and phylogeny reveal new species of *Pleosporales* from plateau lakes in Yunnan Province, China. *Mycosphere*, *15*(1), 6439–6524. https://doi.org/10.5943/mycosphere/15/1/28

Sheng, Y., Cong, W., Yang, L., Liu, Q., & Zhang, Y. (2019). Forest soil fungal community elevational distribution pattern and their ecological assembly processes. *Frontiers in Microbiology*, *10*, 2226. https://doi.org/10.3389/fmicb.2019.02226

Shiva, M. P., & Jantan, I. (1998). Non-timber forest products from dipterocarps. A review of *Dipterocarps*. In S. Appanah & J. M. Turnbull (Eds.), *Taxonomy, ecology and silviculture CIFOR/FRIM* (pp. 187–197). Centre for International Forest Research.

Shivanand, P., Arbie, N. F., Krishnamoorthy, S., & Ahmad, N. (2022). Agarwood—the fragrant molecules of a wounded tree. *Molecules*, *27*(11), 3386. https://doi.org/10.3390/molecules27113386

Shoemaker, R. A. (2006). Nomenclature of *Drechslera* and *Bipolaris*, grass parasites segregated from '*Helminthosporium*'. *Canadian Journal of Plant Pathology*, *28*, S212–S220. https://doi.org/10.1080/07060660609507377

Shu, Y. X., Doilom, M., Boonmee, S., Xu, B., & Dong, W. (2024). Three novel cheiroid hyphomycetes in *Dictyocheirospora* and *Dictyosporium* (*Dictyosporiaceae*) from freshwater habitats in Guangdong and Guizhou Provinces, China. J*ournal of Fungi*, *10*(4), 259. https://doi.org/10.3390/jof10040259

Siboe, G. M., Kirk, P. M., & Cannon, P. F. (1999). New dematiaceous hyphomycetes from Kenyan rare plants. *Mycotaxon*, *73*, 283–302.

Sierra, Á. M. (1984). *Hifomicetes demaciáceos de Sierra del Rosario, Cuba*. Editorial Academia.

Silva, V. S. H., Perera, R. H., & De Farias, A. R. G. (2023). Addition to *Pseudoplagiostomataceae*: *Pseudoplagiostoma inthanonense* sp. nov. from Doi Inthanon National Park, Northern Thailand. *Phytotaxa*, *625*(1), 66–76. https://doi.org/10.11646/phytotaxa.625.1.4

Simmons, E. G. (2007). *Alternaria: an identification manual*. CBS Biodiversity Series.

Singh, S. (1966). Ectotrophic mycorrhiza in equatorial rain forests. *The Malayan Forester*, *29*, 13–18.

Sirikantaramas, S., Sugioka, N., Lee, S. S., Mohamed, L. A., Lee, H. S., Szmidt, A. E., & Yamazaki, T. (2003). Molecular identification of ectomycorrhizal fungi associated with *Dipterocarpaceae*. *Tropics*, *13*(2), 69–77. https://doi.org/10.3759/tropics.13.69

Sivanesan A, Panwar K, Kaur S (1976) *Thaxteriellopsis lignicola*, gen et sp nov, a new *Loculoascomycete* from India. *Kavaka*, *4*, 39–42.

Sivanesan, A. (1984). *The bitunicate ascomycetes and their anamorphs*. J. Cramer.

Sivanesan, A. (1987). *Graminicolous* species of *Bipolaris*, *Curvularia*, *Drechslera*, *Exserohilum* and their teleomorphs. *CAB International Mycological Institute*.

Slippers, B., & Wingfield, M. J. (2007). *Botryosphaeriaceae* as endophytes and latent pathogens of woody plants: Diversity, ecology and impact. *Fungal Biology Reviews*, *21*(2–3), 90–106. https://doi.org/10.1016/j.fbr.2007.06.002

Smith, S. E., & Read, D. J. (2008). *Mycorrhizal symbiosis*. Academic Press.

Smith, S. E., & Read, D. J. (2010). *Mycorrhizal symbiosis* (3rd ed.). Academic Press.

Smits, W. T. (1994). *Dipterocarpaceae*: *Mycorrhizae and regeneration*. Wageningen University and Research.

Song, H. Y., El Sheikha, A. F., Zhong, P. A., Liao, J. L., Wang, Z. H., Huang, Y. J., . . . Hu, D. M. (2020). *Westerdykella aquatica* sp. nov., producing phytase. *Mycotaxon*, *135*(2), 281–292. https://doi.org/10.5248/135.281

Sorrenti, S. (2017). *Non-wood forest products in international statistical systems*. Food and Agriculture Organzation of the United Nations.

Sosef, M. S. M., Hong, L. T., & Prawirohatmodjo, S. (Eds.). (1998). *Plant resources of South-East Asia (PROSEA) No. 5(3): Timber Trees — Lesser-Known Timbers*. PROSEA Foundation & Backhuys Publishers.

Species Fungorum. (2025). *Species Fungorum* [Online database]. Royal Botanic Gardens. https://www.speciesfungorum.org

Spegazzini, C. (1910). Mycetes Argentinenses (Series V). *Anales del Museo Nacional de Buenos Aires. ser. 3*, 13, 329–467.

Spooner, B. M., & Kirk, P. M. (1982). Taxonomic notes on *Excipularia* and *Scolicosporium*. *Transactions of the British Mycological Society*, *78*(2), 247–257. https://doi.org/10.1016/S0007-1536(82)80007-7

Sruthi, O. P., Rajeshkumar, K. C., Gowrav, S. M., Ansil, P. A., & Ashtamoorthy, S. K. (2024). Morphological and phylogenetic evidence for recognition of a new species of *Kirschsteiniothelia*, *K. agumbensis* and validation of five new combinations in *Kirschsteiniotheliaceae*. *Phytotaxa*, *649*(2), 159–181. https://doi.org/10.11646/phytotaxa.649.2.2

Stamatakis, A., Hoover, P., & Rougemont, J. (2008). A rapid bootstrap algorithm for the RAxML Web servers. *Systematic Biology*, *57*(5), 758–771. https://doi.org/10.1080/10635150802429642

Su, H., Hyde, K. D., Maharachchikumbura, S. S., Ariyawansa, H. A., Luo, Z., Promputtha, I., . . . Zhou, D. (2016). The families *Distoseptisporaceae* fam. nov., *Kirschsteiniotheliaceae*, *Sporormiaceae* and *Torulaceae*, with new species from freshwater in Yunnan Province, China. *Fungal Diversity*, *80*(1), 375–409. https://doi.org/10.1007/s13225-016-0362-0

Su, X. J., Luo, Z. L., Jeewon, R., Bhat, D. J., Bao, D. F., Li, W. L., . . . Hyde, K. D. (2018). Morphology and multigene phylogeny reveal a new genus and species of *Torulaceae* from freshwater habitats in northwestern Yunnan, China. *Mycological Progress*, *17*(5), 531–545. https://doi.org/10.1007/s11557-018-1388-3

Subramanian, C. V., & Vittal, B. P. R. (1974). Hyphomycetes on litter from India—1. In *Proceedings of the Indian Academy of Sciences, Section B* (Vol. 80, No. 5, pp. 216–221). Springer India. https://doi.org/10.1007/BF03050667

Subramanian, C. V., & Vittal, B. P. R. (1979). Studies on litter fungi. II. Fungal colonization of Atlantia monophylla leaves and litter. *Nova Hedwigia*, *63*, 361–369.

Subramanian, C. V., & Vittal, B. P. R. (1980). Studies on litter fungi. IV. Fungal colonization of *Gymnosporia emarginata* leaves and litter. *Transactions of the Mycological Society of Japan*, *21*, 339–344.

Suetrong, S., Boonyuen, N., Pang, K. L., Ueapattanakit, J., Klaysuban, A., Sri-Indrasutdhi, V., . . . Jones, E. G. (2011). A taxonomic revision and phylogenetic reconstruction of the *Jahnulales* (*Dothideomycetes*), and the new family *Manglicolaceae*. *Fungal Diversity*, *51*(1), 163–188. https://doi.org/10.1007/s13225-011-0138-5

Suetrong, S., Klaysuban, A., Sakayaroj, J., Preedanon, S., Ruang-Areerate, P., Phongpaichit, S., . . . Jones, E. G. (2015). *Tirisporellaceae*, a new family in the order *Diaporthales* (*Sordariomycetes*, *Ascomycota*). *Cryptogamie*, *Mycologie*, *36*, 319–330. https://doi.org/10.7872/crym/v36.iss3.2015.319

Sun, Y. R., Hyde, K. D., Liu, N. G., Jayawardena, R. S., Wijayawardene, N. N., Ma, J., . . . Wang, Y. (2025). Micro-fungi in southern China and northern Thailand: emphasis on medicinal plants. *Fungal Diversity*, *131*, 99–299. https://doi.org/10.1007/s13225-024-00549-4

Sun, Y. R., Jayawardena, R. S., Hyde, K. D., & Wang, Y. (2021). *Kirschsteiniothelia thailandica* sp. nov. (*Kirschsteiniotheliaceae*) from Thailand. *Phytotaxa*, *490*(2), 172–182. https://doi.org/10.11646/phytotaxa.490.2.3

Sun, Y. R., Liu, N. G., Hyde, K. D., Jayawardena, R. S., & Wang, Y. (2022). *Pleocatenata chiangraiensis* gen. et. sp. nov. (*Pleosporales*, *Dothideomycetes*) from medicinal plants in northern Thailand. *MycoKeys*, *88*(1), 77–99. https://doi.org/10.3897/mycokeys.87.79433

Sun, X., & Guo, L. D. (2012). Endophytic fungal diversity: review of traditional and molecular techniques. *Mycology*, *3*(1), 65–76. https://doi.org/10.1080/21501203.2012.656724

Suryanarayanan, T. S., & Kumaresan, V. (2000). Endophytic fungi of some halophytes from an estuarine mangrove forest. *Mycological Research*, *104*(12), 1465–1467. https://doi.org/10.1017/S0953756200002859

Sutton, B. C. (1969). Forest microfungi. II. Additions to *Acrodictys*. *Canadian Journal of Botany*, *47*(6), 853–858.

Suwannarach, N., Kumla, J., & Lumyong, S. (2016). *Pseudoplagiostoma dipterocarpi* sp. nov., a new endophytic fungus from Thailand. *Mycoscience*, *57*(2), 118–122. https://doi.org/10.1016/j.myc.2015.12.002

Suwannarach, N., Kumla, J., Khuna, S., Thitla, T., Senwanna, C., Hongsanan, S., . . . Lumyong, S. (2023). *Anteaglonium saxicola* (*Anteagloniaceae*, *Pleosporales*), a new species isolated from rocks in northern Thailand. *Phytotaxa*, *629*(1), 75–84. https://doi.org/10.11646/phytotaxa.629.1.6

Swofford, D. L. (1993). PAUP, phylogenetic analysis using parsimony. version 3.1. Computer program distributed by the Illinois Natural History Survey.

Sydow, H., & Sydow, P. (1913). Novae fungorum species – XV. *Annales Mycologici*, *11*(3), 254–271.

Tanaka, K., Hirayama, K., Yonezawa, H., Hatakeyama, S., Harada, Y., Sano, T., . . . Hosoya, T. (2009). Molecular taxonomy of bambusicolous fungi: *Tetraplosphaeriaceae*, a new *pleosporalean* family with Tetraploa-like anamorphs. *Studies in mycology*, *64*(1), 175–209. https://doi.org/10.3114/sim.2009.64.10

Tanaka, K., Hirayama, K., Yonezawa, H., Sato, G., Toriyabe, A., Kudo, H., . . . Hosoya, T. (2015). Revision of the *Massarineae* (*Pleosporales*, *Dothideomycetes*). *Studies in Mycology*, *82*, 75–136. https://doi.org/10.1016/j.simyco.2015.10.002

Tanaka, K., Ooki, Y., Hatakeyama, S., Harada, Y., & Barr, M. E. (2005). *Pleosporales* in Japan (5): *Pleomassaria*, *Asteromassaria*, and *Splanchnonema*. *Mycoscience*, *46*(4), 248–260. https://doi.org/10.1007/S10267-005-0245-9

Tang, A. M., Hyde, K. D., & Corlett, R. T. (2003). Diversity of fungi on wild fruits in Hong Kong. *Fungal Diversity*, *14*, 165–185.

Tang, X., Goonasekara, I. D., Jayawardena, R. S., Jiang, H. B., Li, J. F., Hyde, K. D., & Kang, J. C. (2020). *Arthrinium bambusicola* (Fungi, *Sordariomycetes*), a new species from *Schizostachyum brachycladum* in northern Thailand. *Biodiversity Data Journal*, *8*, e58755. https://doi.org/10.3897/BDJ.8.e58755

Tang, X., Jayawardena, R. S., Stephenson, S. L., & Kang, J. C. (2022). A new species *Pseudoplagiostoma dipterocarpicola* (*Pseudoplagiostomataceae*, *Diaporthales*) found in northern Thailand on members of the *Dipterocarpaceae*. *Phytotaxa*, *543*(4), 233–243. https://doi.org/10.11646/phytotaxa.543.4.3

Tao, M. H., Yan, J., Wei, X. Y., Li, D. L., Zhang, W. M., & Tan, J. W. (2011). A novel sesquiterpene alcohol from *Fimetariella rabenhorstii*, an endophytic fungus of *Aquilaria sinensis*. *Natural product communications*, *6*(6), 1934578X1100600605.

Taylor, D. L., Herriott, I. C., Stone, K. E., McFarland, J. W., Booth, M. G., & Leigh, M. B. (2010). Structure and resilience of fungal communities in Alaskan boreal forest soils. *Canadian Journal of Forest Research*, *40*(7), 1288–1301. https://doi.org/10.1139/X10-081

Tedersoo, L., Bahram, M., Põlme, S., Kõljalg, U., Yorou, N. S., Wijesundera, R., . . . Abarenkov, K. (2014). Global diversity and geography of soil fungi. *Science*, *346*(6213), 1256688. https://doi.org/10.1126/science.1256688

Tennakoon, D. S., de Silva, N. I., Maharachchikumbura, S. S., Bhat, D. J., Kumla, J., Suwannarach, N., . . . Lumyong, S. (2023). Exploring more on *Dictyosporiaceae*: The species geographical distribution and intriguing novel additions from plant litter. *Diversity*, *15*(3), 410. https://doi.org/10.3390/d15030410

Tennakoon, D. S., Kuo, C. H., Purahong, W., Gentekaki, E., Pumas, C., Promputtha, I., . . . Hyde, K. D. (2022b). Fungal community succession on decomposing leaf litter across five phylogenetically related tree species in a subtropical forest. *Fungal Diversity*, *115*(1), 73–103. https://doi.org/10.1007/s13225-022-00508-x

Tennakoon, D. S., Thambugala, K. M., de Silva, N. I., Song, H. Y., Suwannarach, N., Chen, F. S., . . . Hu, D. M. (2024). An overview of *Melanommataceae* (*Pleosporales*, *Dothideomycetes*): Current insight into the host associations and geographical distribution with some interesting novel additions from plant litter. *MycoKeys*, *106*, 43. https://doi.org/10.3897/mycokeys.106.125044

Tennakoon, D. S., Thambugala, K. M., Silva, N. I. D., Suwannarach, N., & Lumyong, S. (2022a). A taxonomic assessment of novel and remarkable fungal species in *Didymosphaeriaceae* (*Pleosporales*, *Dothideomycetes*) from plant litter. *Frontiers in Microbiology*, *13*, 1016285. https://doi.org/10.3389/fmicb.2022.1016285

Tian, J. J., Gao, X. X., Zhang, W. M., Wang, L., & Qu, L. H. (2013). Molecular identification of endophytic fungi from *Aquilaria sinensis* and artificial agarwood induced by pinholes-infusion technique. *African Journal of Biotechnology*, *12*(21), 3115–3131. https://doi.org/10.5897/AJB11.3159

Tian, S. M., Chen, Y. C., Zou, M. Q., & Xue, Q. (2007). First report of *Helminthosporium solani* causing silver scurf of potato in Hebei Province, North China. *Plant Disease*, *91*(4), 460. https://doi.org/10.1094/PDIS-91-4-0460B

Tian, W. H., Jin, Y., Liao, Y. C., Faraj, T. K., Guo, X. Y., & Maharachchikumbura, S. S. (2024). Phylogenetic insights reveal new taxa in *Thyridariaceae* and *Massarinaceae*. *Journal of Fungi*, *10*(8), 542. https://doi.org/10.3390/jof10080542

Tian, W., Su, P., Chen, Y., & Maharachchikumbura, S. S. N. (2023). Four new species of *Torula* (*Torulaceae*, *Pleosporales*) from Sichuan, China. J*ournal of Fungi*, *9* (2), 150. https://doi.org/10.3390/jof9020150

Tibpromma, S., Bhat, J., Doilom, M., Lumyong, S., Nontachaiyapoom, S., Yang, J. B., . . . Hyde, K. D. (2016). Three new *Hermatomyces* species (*Lophiotremataceae*) on *Pandanus odorifer* from southern Thailand. *Phytotaxa*, 275(2), 127–139. https://doi.org/10.11646/phytotaxa.275.2.4

Tibpromma, S., Hyde, K. D., McKenzie, E. H., Bhat, D. J., Phillips, A. J., Wanasinghe, D. N., . . . Karunarathna, S. C. (2018). Fungal diversity notes 840–928: micro-fungi associated with *Pandanaceae*. *Fungal Diversity*, *93*(1), 1–160. https://doi.org/10.1007/s13225-018-0408-6

Tóth, S. (1975). Some new microscopic fungi, III. *Annales Historico-naturales Musei Nationalis Hungarici*, *67*, 31–35.

Trappe, J. M. (1962). Fungus associates of ectotrophic mycorrhizae. *The Botanical Review*, *28*(4), 538–606.

Traverso, G. B. (1905). *Flora Italica Cryptogama: Pars 1: Fungi*. Società Botanica Italiana.

Tsuda, M., Ueyama, A., & Nishihara, N. (1977). *Pseudocochliobolus nisikadoi*, the perfect state of *Helminthosporium coicis*. *Mycologia*, *69*(6), 1109–1120. https://doi.org/10.1080/00275514.1977.12020169

Tupas, G. L., & Sajise, P. E. (1976). Mycorrhizal associations in some savanna and reforestation trees. *Kalikasan: Philippine Journal of Biology*, *5*, 235–240.

Turjaman, M., Tamai, Y., Santoso, E., Osaki, M., & Tawaraya, K. (2006). Arbuscular mycorrhizal fungi increased early growth of two nontimber forest product species *Dyera polyphylla* and *Aquilaria filaria* under greenhouse conditions. *Mycorrhiza*, *16*(7), 459–464. https://doi.org/10.1007/s00572-006-0059-4

Uppal, B. N., Patel, M. K., & Kamat, M. N. (1938). Alternaria blight of cumin. *Indian Journal of Agricultural Sciences*, *8*, 49-62.

Urooj, F. A. I. Z. A. H., Farhat, H. A. F. I. Z. A., Ali, S. A., Ahmed, M., Sultana, V., Shams, Z. I., . . . Ehteshamul-Haque, S. (2018). Role of endophytic *Penicillium* species in suppressing the root rotting fungi of sunflower. *Pak. J. Bot*, *50*(4), 1621–1628.

Vaidya, G., Lohman, D. J., & Meier, R. (2011). SequenceMatrix: concatenation software for the fast assembly of multi-gene datasets with character set and codon information. *Cladistics*, *27*, 171–180. https://doi.org/10.1111/j.1096-0031.2010.00329.x

Van der Heijden, M. G., & Sanders, I. R. (2002). Mycorrhizal ecology: synthesis and perspectives. In Mycorrhizal ecology (pp. 441-456). *Berlin, Heidelberg: Springer Berlin Heidelberg*. https://doi.org/10.1007/978-3-540-38364-2_17

van der Heijden, M. G., Martin, F. M., Selosse, M. A., & Sanders, I. R. (2015). Mycorrhizal ecology and evolution: The past, the present, and the future. *New Phytologist*, *205*(4), 1406–1423. https://doi.org/10.1111/nph.13288

Větrovský, T., Kohout, P., Kopecký, M., Machác, A., Man, M., Bahnmann, B. D., . . . Baldrian, P. (2019). A meta-analysis of global fungal distribution reveals climate-driven patterns. *Nature Communications*, *10*(1), 5142. https://doi.org/10.1038/s41467-019-13164-8

Viégas, A.P. 1943. Notas sôbre uma nova espécie de Sporormia. *Bragantia*, *3*(7), 155–164.

Vijayan, A. K., & Rehill, P. S. (1990). Schyzophyllum commune Fr. – First record on seeds of forest trees from India. *Indian Journal of Forestry*, *13*, 67–68.

Vilgalys, R., & Hester, M. (1990). Rapid genetic identification and mapping of enzymatically amplified ribosomal DNA from several *Cryptococcus* species. *Journal of Bacteriology*, *172*, 4238–4246. https://doi.org/10.1128/jb.172.8.4238-4246.1990

Voglmayr, H., & Jaklitsch, W. M. (2014). *Stilbosporaceae* resurrected: generic reclassification and speciation. *Persoonia: Molecular Phylogeny and Evolution of Fungi*, *33*, 61–82. https://doi.org/10.3767/003158514X684212

Voglmayr, H., & Jaklitsch, W. M. (2017). *Corynespora*, *Exosporium* and *Helminthosporium* revisited — new species and generic reclassification. *Studies in Mycology, 87*(1), 43–76. https://doi.org/10.1016/j.simyco.2017.05.001

Voglmayr, H., Gardiennet, A., & Jaklitsch, W. M. (2016). *Asterodiscus* and *Stigmatodiscus*, two new apothecial dothideomycete genera and the new order *Stigmatodiscales*. *Fungal Diversity*, *80*(1), 271–284. https://doi.org/10.1007/s13225-016-0356-y

Voglmayr, H., Rossman, A. Y., Castlebury, L. A., & Jaklitsch, W. M. (2012). Multigene phylogeny and taxonomy of the genus *Melanconiella* (*Diaporthales*). *Fungal Diversity*, *57*, 1–44. https://doi.org/10.1007/s13225-012-0175-8

Von Arx, J. A. (1981). *The genera of fungi sporulating in pure culture*, Vol. 3. Cramer, Lehre.

Von Höhnel, F. (1909). Fragmente zur Mykologie. XV. Mitteilung, Nr. 407 bis 467. *Math Naturw Kl, Abt*, *1*, 1461–1552.

Walker, J., & White, N. H. (1991). Species of *Phaeoisariopsis* and *Stenella* (Hyphomycetes) on W*ikstroemia* (*Thymelaeaceae*). *Mycological Research*, *95*(8), 1005–1013.

Wanasinghe, D. N., Phukhamsakda, C., Hyde, K. D., Jeewon, R., Lee, H. B., Gareth Jones, E. B., . . . Karunarathna, S. C. (2018). Fungal diversity notes 709–839: taxonomic and phylogenetic contributions to fungal taxa with an emphasis on fungi on *Rosaceae*. *Fungal diversity*, *89*(1), 1–236. https://doi.org/10.1007/s13225-018-0395-7

Wang, L. Y., Xia, G. Y., Wang, M., Wu, Y. Z., Wang, Y. N., Chai, L. M., & Lin, S. (2022). Penicipurate A, a new polyketide derivative from the endophytic fungus *Penicillium purpurogenum*. *Journal of Asian Natural Products Research*, *24*(11), 1086–1092. https://doi.org/10.1080/10286020.2022.2094786

Wang, M., Tan, X. M., Liu, F., & Cai, L. (2018). Eight new *Arthrinium* species from China. *MycoKeys*, *34*, 1–27. https://doi.org/10.3897/mycokeys.34.24221

Wang, W. P., Hyde, K. D., Bao, D. F., Wanasinghe, D. N., Lin, C. G., Shen, H. W., . . . Luo, Z. L. (2024). Lignicolous freshwater fungi from karst landscapes in Yunnan Province, China. *Mycosphere*, *15*(1), 6525–6640. https://doi.org/10.5943/mycosphere/15/1/29

Wang, Y. L., Lu, Q., Decock, C., Li, Y. X., & Zhang, X. Y. (2015). *Cytospora* species from *Populus* and *Salix* in China with *C. davidiana* sp. nov. *Fungal Biology*, *119*, 420–432. https://doi.org/10.1016/j.funbio.2015.01.005

Wang, Y. Z., Aptroot, A., & Hyde, K. D. (2004). Revision of the *Ascomycete* genus *Amphisphaeria*. *Fungal Diversity Research Series*, *13*, 1–168.

Wang, Z., Kim, W., Wang, Y. W., Yakubovich, E., Dong, C., Trail, F., . . . Yarden, O. (2023). The *Sordariomycetes*: An expanding resource with Big Data for mining in evolutionary genomics and transcriptomics. Front. *Fungal Biol.*, *4*, 1214537. https://doi.org/10.3389/ffunb.2023.1214537

Watling, R., Hawksworth, D. L., Kirk, P. M., Sutton, B. C., & Pegler, D. N. (1996). Ainsworth and Bisby's Dictionary of the Fungi. *Journal of Ecology*, *84*(5), 787.

White, T. J., Bruns, T., Lee, S. J. W. T., & Taylor, J. (1990). Amplification and direct sequencing of fungal ribosomal RNA genes for phylogenetics. In M. A. Innis, D. H. Gelfand, J. J. Sninsky & T, J. White (Eds.), PCR protocols: A guide to methods and applications (Vol. 18, pp. 315–322). Academic Press.

Whitton, S. R., McKenzie, E. H. C., & Hyde, K. D. (2012). Fungi associated with *Pandanaceae*. *Springer*.

Wijayawardene, N. N., Crous, P. W., Kirk, P. M., Hawksworth, D. L., Boonmee, S., Braun, U., . . . Hyde, K. D. (2014). Naming and outline of *Dothideomycetes* – 2014 including proposals for the protection or suppression of generic names. *Fungal Diversity*, *69*(1), 1–55. https://doi.org/10.1007/s13225-014-0309-2

Wijayawardene, N. N., Dissanayake, L. S., Li, Q. R., Dai, D. Q., Xiao, Y., Wen, T. C., . . . Kang, Y. (2021). Yunnan-Guizhou Plateau: A mycological hotspot. *Phytotaxa*, *523*(1), 1–31. https://doi.org/10.11646/phytotaxa.523.1.1

Wijayawardene, N. N., Hyde, K. D., Dai, D. Q., Sánchez-García, M., Goto, B. T., Saxena, R. K., . . . Thines, M. (2022). Outline of Fungi and fungus-like taxa – 2021. *Mycosphere*, *13*(1), 53–453. https://doi.org/10.5943/mycosphere/13/1/2

Wijayawardene, N. N., Hyde, K. D., Lumbsch, H. T., Liu, J. K., Maharachchikumbura, S. S., Ekanayaka, A. H., . . . Phookamsak, R. (2018) (2018). Outline of ascomycota: 2017. *Fungal diversity*, *88*(1), 167–263. https://doi.org/10.1007/s13225-018-0394-8

Wijayawardene, N. N., Hyde, K. D., Rajeshkumar, K. C., Hawksworth, D. L., Madrid, H., Kirk, P. M., . . . Karunarathna, S. C. (2017). Notes for genera: *Ascomycota*. *Fungal Diversity*, *86*(1), 1–594. https://doi.org/10.1007/s13225-017-0386-0

Wingfield, M. J., Slippers, B., Roux, J., & Wingfield, B. D. (2001). Worldwide movement of exotic forest fungi, especially in the tropics and the southern hemisphere: This article examines the impact of fungal pathogens introduced in plantation forestry. *Bioscience*, *51*(2), 134–140.

Winter, G. (1885). Pilze-Ascomyceten. In G. L. Rabenhorst (Ed.), *Kryptogamen-Flora von Deutschland, Österreich und der Schweiz* (Vol. 1, pp. 65–528). E. Kummer.

Witenweber, W. R. (1836). *Beiträge zur gesammten Natur- und Heilwissenschaften*. Kronberg.

Wu, C. J., Chen, J. L., Tzean, S. S., & Ni, H. F. (2024). Pseudoplagiostoma perseae sp. nov. causes leaf spot disease on avocado leaves in Taiwan. *European Journal of Plant Pathology*, *170*(3), 617–629. https://doi.org/10.1007/s10658-024-02921-1

Wu, G., Schuelke, T. A., & Broders, K. (2019). The genome of the butternut canker pathogen, *Ophiognomonia clavigignenti-juglandacearum* shows an elevated number of genes associated with secondary metabolism and protection from host resistance responses in comparison with other members of the *Diaporthales*. bioRxiv, 820977. https://doi.org/10.1101/820977

Wu, N., Chi, M. F., Du, H. Z., Chethana, K. T., Khongphinitbunjong, K., Chen, Y. Y., . . . Liu, J. K. (2025). Morpho-phylogenetic evidence reveals novel species and new records of *Torula* (*Torulaceae*, *Pleosporales*) from medicinal plants in China. *MycoKeys*, *122*, 169–196. https://doi.org/10.3897/mycokeys.122.161816

Wu, Y. Z., Zhang, H. W., Sun, Z. H., Dai, J. G., Hu, Y. C., Li, R., . . . Lin, S. (2018). Bysspectin A, an unusual octaketide dimer and the precursor derivatives from the endophytic fungus Byssochlamys spectabilis IMM0002 and their biological activities. *European Journal of Medicinal Chemistry*, *145*, 717–725. https://doi.org/10.1016/j.ejmech.2018.01.030

Wu, Z. C., Li, D. L., Chen, Y. C., & Zhang, W. M. (2010). A new isofuranonaphthalenone and benzopyrans from the endophytic fungus *Nodulisporium* sp. A4 from *Aquilaria sinensis*. *Helvetica Chimica Acta*, *93*(5), 920–924. https://doi.org/10.1002/hlca.200900307

Wyatt-Smith, J. (1963). Manual of Malayan silviculture for inland forests (Vols. 1–2; Malayan Forest Records No. 23). *Forest Department, Kuala Lumpur*, *Malaysia*.

Xiao, X. J., Liu, N. G., Ma, J., Zhang, L. J., Bao, D. F., Bai, S., . . . Lu, Y. Z. (2025). Three new asexual *Kirschsteiniothelia* species from Guizhou Province, China. *MycoKeys*, *113*, 147. https://doi.org/10.3897/mycokeys.113.139427

Xiong, Y. C., Xu, R. J., Luo, Z. L., Gao, Q., & Zhao, Q. (2024). *Sporidesmiella motuoensis*, a new freshwater fungus from Tibetan Plateau, China. *Phytotaxa*, *635*(1), 105–112. https://doi.org/10.11646/phytotaxa.635.1.7

Xu, R. F., Phukhamsakda, C., Dai, D. Q., Karunarathna, S. C., & Tibpromma, S. (2023). *Kirschsteiniothelia xishuangbannaensis* sp. nov. from Pará rubber (*Hevea brasiliensis*) in Yunnan, China. *Current Research in Environmental & Applied Mycology*, *13*(1), 34–56. https://doi.org/10.5943/cream/13/1/3

Xu, R. J., Thiyagaraja, V., Li, Y., Zhou, D. Q., Boonmee, S., & Zhao, Q. (2024). Two novel lignicolous freshwater fungi, *Conioscypha xizangensis* and *Cordana linzhiensis*, from the Tibetan Plateau, China. *New Zealand Journal of Botany*, *62*(2-3), 426–442. https://doi.org/10.1080/0028825X.2024.2336044

Xu, R., Zhang, Y., Su, W., & Li, Y. (2025) New Species, New Record, and Antagonistic Potential of *Torula* (*Torulaceae*, *Pleosporales*) from Jilin Province, China. *Microorganisms*, *13*(7), 1459. https://doi.org/10.3390/microorganisms13071459

Xu, X. L., Wang, F. H., Liu, C., Yang, H. B., Zeng, Z., Wang, B. X., . . . Yang, C. L. (2022). Morphology and phylogeny of ascomycetes associated with walnut trees (*Juglans regia*) in Sichuan province, China. *Frontiers in Microbiology*, *13*, 1016548. https://doi.org/10.3389/fmicb.2022.1016548

Xu, Y., Zhang, Z., Wang, M., Wei, J., Chen, H., Gao, Z., . . . Li, W. (2013). Identification of genes related to agarwood formation: Transcriptome analysis of healthy and wounded tissues of *Aquilaria sinensis*. *BMC Genomics*, *14*(1), 227. https://doi.org/10.1186/1471-2164-14-227

Xu, Z. H., Qiu, L., Kuang, W. G., Shi, X. G., Zhang, X. G., Castañeda-Ruíz, R. F., . . . Ma, J. (2020). *Varioseptispora chinensis* gen. & sp. nov., *V. apicalis* nom. nov., *V. hodgkissii* comb. nov., and *V. versiseptatis* comb. nov. *Mycotaxon*, *135*(4), 753–759. https://doi.org/10.5248/135.753

Yagura, T., Ito, M., Kiuchi, F., Honda, G., & Shimada, Y. (2003). Four new 2-(2-phenylethy) chromone derivatives from withered wood of Aquilaria sinensis. *Chemical and pharmaceutical bulletin*, *51*(5), 560–564. https://doi.org/10.1248/cpb.51.560

Yan, H., Jiang, N., Liang, L. Y., Yang, Q., & Tian, C. M. (2019). *Arthrinium trachycarpum* sp. nov. from *Trachycarpus fortunei* in China. *Phytotaxa*, *400*(3), 203–210. https://doi.org/10.11646/phytotaxa.400.3.7

Yang, C. L., Li, X. Y., Xiang, S. S., Xu, X. L., Zeng, Q., Sun, Q. R., . . . Liu, Y. G. (2025). Microfungi associated with plant diseases on horticultural vegetation in southwestern China. *Mycosphere*, *16*(1), 1861–2001. https://doi.org/10.5943/mycosphere/16/1/11

Yang, C. L., Xu, X. L., Dong, W., Wanasinghe, D. N., Liu, Y. G., & Hyde, K. D. (2019). Introducing *Arthrinium phyllostachium* sp. nov. (*Apiosporaceae*, *Xylariales*) on *Phyllostachys heteroclada* from Sichuan province, China. *Phytotaxa*, *406*(2), 91–110. https://doi.org/10.11646/phytotaxa.406.2.2

Yang, J., Liu, J. K., Hyde, K. D., Jones, E. G., & Liu, Z. Y. (2018). New species in *Dictyosporium*, new combinations in *Dictyocheirospora* and an updated backbone tree for *Dictyosporiaceae*. MycoKeys, *36*, 83. https://doi.org/10.3897/mycokeys.36.27051

Yang, J., Liu, L. L., Jones, E. G., Hyde, K. D., Liu, Z. Y., Bao, D. F., . . . Liu, J. K. (2023). Freshwater fungi from karst landscapes in China and Thailand. *Fungal Diversity*, *119*(1), 1–212. https://doi.org/10.1007/s13225-023-00514-7

Yang, Q., Fan, X. L., Du, Z., & Tian, C. M. (2018). *Diaporthosporellaceae*, a novel family of *Diaporthales* (*Sordariomycetes*, *Ascomycota*). *Mycoscience*, *59*(3), 229–235. https://doi.org/10.1016/j.myc.2017.11.005

Yang, T., Tedersoo, L., Liu, X., Gao, G. F., Dong, K., Adams, J. M., & Chu, H. (2022). Fungi stabilize multi-kingdom community in a high elevation timberline ecosystem. *iMeta*, *1*(4), e49. https://doi.org/10.1002/imt2.49

Yang, X., Lv, R., Yu, Z., Li, J., & Qiao, M. (2022). *Cordana yunnanensis* sp. nov., isolated from desertified rocky soil in southwest China. *Current Microbiology*, *79*(6), 183. https://doi.org/10.1007/s00284-022-02871-z

Yang, Y. Y., Thiyagaraja, V., Wanasinghe, D. N., de Farias, A., & Zhao, Q. (2024). Phylogenetic and taxonomic appraisal of *Neomanoharachariella xizangensis* sp. nov. and the first asexual report of *Acanthostigmina* (*Tubeufiaceae*, *Tubeufiales*) from Xizang Autonomous Region, China. *Phytotaxa*, *642*(2), 127–140. https://doi.org/10.11646/phytotaxa.642.2.2

Yasanthika, W. A. E., Chethana, K. W. T., Fatimah, A. O., Wanasinghe, D. N., Tennakoon, D. S., Samarakoon, M. C., . . . Hyde, K. D. (2025). Genera of soil *Ascomycot*a and an account on soil-inhabiting species isolated from Thailand. *Mycosphere*, *16*(1), 1530–1860. https://doi.org/10.5943/mycosphere/16/1/10

Yu, X. D., Zhang, S. N., & Liu, J. K. (2022). Morpho-phylogenetic evidence reveals novel Pleosporalean taxa from Sichuan Province, China. *Journal of Fungi*, *8*(7), 720. https://doi.org/10.3390/jof8070720

Yu, Y. X., Lu, Y. H., Tian, Q., & Dissanayake, A. J. (2025). *Byssosphaeria vaginata*, a new species of *Melanommataceae* from *Magnolia officinali*s in Sichuan Province, China. *Phytotaxa*, *705*(1), 35–49. https://doi.org/10.11646/phytotaxa.705.1.3

Yuan, H. S., Lu, X., Dai, Y. C., Hyde, K. D., Kan, Y. H., Kušan, I., . . . Zhou, L. W. (2020). Fungal diversity notes 1277–1386: taxonomic and phylogenetic contributions to fungal taxa. *Fungal Diversity*, *104*(1), 1–266. https://doi.org/10.1007/s13225-020-00461-7

Zakaria, L., & Aziz, W. N. W. (2018). Molecular identification of endophytic fungi from banana leaves (*Musa* spp.). *Tropical Life Sciences Research*, *29*(2), 201. https://doi.org/10.21315/tlsr2018.29.2.14

Zhang, H., Ruan, C., & Bai, X. (2015). Isolation and antimicrobial effects of endophytic fungi from *Edgeworthia chrysantha*. *Bangladesh Journal of Pharmacology*, *10*(3), 529–532. https://doi.org/10.3329/bjp.v10i3.23575

Zhang, H., Ruan, C., Bai, X., Zhang, M., Zhu, S., & Jiang, Y. (2016). Isolation and Identification of the Antimicrobial Agent Beauvericin from the Endophytic *Fusarium oxysporum* 5-19 with NMR and ESI-MS/MS. *BioMed research international*, *2016*(1), 1084670. https://doi.org/10.1155/2016/1084670

Zhang, J. F., Liu, J. K. J., Ran, H. Y., Khongphinitbunjong, K., & Liu, Z. Y. (2018). A new species and new record of *Lophiotrema* (*Lophiotremataceae*, *Dothideomycetes*) from karst landforms in southwest China. *Phytotaxa*, *379*(2), 169–179. https://doi.org/10.11646/phytotaxa.379.2.5

Zhang, J. F., Liu, J. K., Hyde, K. D., Chen, Y. Y., Ran, H. Y., & Liu, Z. Y. (2023). Ascomycetes from karst landscapes of Guizhou Province, China. *Fungal Diversity*, *122*(1), 1–160. https://doi.org/10.1007/s13225-023-00524-5

Zhang, J. Y., Hyde, K. D., Bao, D. F., Hongsanan, S., Liu, Y. X., Kang, J. C., . . . Lu, Y. Z. (2025). A worldwide checklist and morpho-molecular systematics of fungi associated with pteridophytes. *Fungal Diversity*, *132*, 151–423. https://doi.org/10.1007/s13225-025-00554-1

Zhang, K., Zhang, H., Li, D. W., & Castañeda-Ruíz, R. F. (2020). *Mirohelminthosporium* gen. nov. for an atypical *Helminthosporium* species and *H. matsushimae* nom. nov. *Mycotaxon, 135*, 777–783. https://doi.org/10.5248/135.777

Zhang, M., Wu, H. Y., & Wang, Z. Y. (2010). Taxonomic studies of *Helminthosporium* from China 5: Two new species from Hunan and Sichuan Province. *Mycotaxon*, *113*(1), 95–99. https://doi.org/10.5248/113.95

Zhang, M., Zhang, T. Y., & Wu, W. P. (2007). Taxonomic studies of *Helminthosporium* from China III: Three new species in Guangdong Province. *Mycotaxon*, *99*, 137–142.

Zhang, M., Zhang, T. Y., & Wu, W. W. (2004). Taxonomic studies of *Helminthosporium* from China II: Two new species in Sichuan Province. *Mycosystema*, *23*, 179–182.

Zhang, N., Castlebury, L. A., Miller, A. N., Huhndorf, S. M., Schoch, C. L., Seifert, K. A., . . . Sung, G. H. (2006). An overview of the systematics of the *Sordariomycetes* based on a four-gene phylogeny. *Mycologia*, *98*(6), 1076–1087. https://doi.org/10.1080/15572536.2006.11832635

Zhang, T. Y., Zhao, G., Zhang, X., Liu, H., & Wu, Y. (2009). Genera of Dematiaceous *Dictyosporous* Hyphomycetes excluding *Alternaria*. *Flora Fungorum Sinicorum*, *31*, 231.

Zhang, W. J., Xu, G. P., Liu, Y., Gao, Y., Song, H. Y., Hu, H. J., . . . Zhai, Z. J. (2024). Multi-gene phylogenetic analyses revealed two novel species and one new record of *Trichobotrys* (*Pleosporales*, *Dictyosporiaceae*) from China. *MycoKeys*, *106*, 117. https://doi.org/10.3897/mycokeys.106.123279

Zhang, Y. D., Ma, J., Wang, Y., Ma, L. G., Castañeda-Ruíz, R. F., & Zhang, X. G. (2011). New species and record of *Pseudoacrodictys* from southern China. *Mycological Progress*, *10*(3), 261–265. https://doi.org/10.1007/s11557-010-0696-z

Zhang, Y. Z., Chen, Q. L., Ma, J., Lu, Y. Z., Chen, H. B., & Liu, N. G. (2023a). Morphological and multi-gene phylogenetic analyses reveal five new hyphomycetes from freshwater habitats. *Frontiers in Microbiology*, *14*, 1253239. https://doi.org/10.3389/fmicb.2023.1253239

Zhang, Y., Crous, P. W., Schoch, C. L., & Hyde, K. D. (2012). *Pleosporales*. *Fungal Diversity*, *53*(1), 1–221. https://doi.org/10.1007/s13225-011-0117-x

Zhang, Z. X., Shang, Y. X., Liu, Q. Y., Li, D. H., Yin, C. Z., Liu, X. Y., . . . Zhang, X. G. (2025). Deciphering the evolutionary and taxonomic complexity of *Diaporthales* (*Sordariomycetes*, *Ascomycota*) through integrated phylogenomic and divergence time estimation. *Fungal Diversity*, 1–125. https://doi.org/10.1007/s13225-025-00551-4

Zhang, Z., Liu, X., Tao, M., Liu, X., Xia, J., Zhang, X., . . . Meng, Z. (2023b). Taxonomy, phylogeny, divergence time estimation, and biogeography of the family *Pseudoplagiostomataceae* (*Ascomycota*, *Diaporthales*). J*ournal of Fungi*, *9*(1), 82. https://doi.org/10.3390/jof9010082

Zhao, P., Crous, P. W., Hou, L. W., Duan, W. J., Cai, L., Ma, Z. Y., . . . Liu, F. (2021). Fungi of quarantine concern for China I: *Dothideomycetes*. *Persoonia – Molecular Phylogeny and Evolution of Fungi*, *47*(1), 45–105. https://doi.org/10.3767/persoonia.2021.47.02

Zhao, Y. Z., Zhang, Z. F., Cai, L., Peng, W. J., & Liu, F. (2018). Four new filamentous fungal species from newly-collected and hive-stored bee pollen. *Mycosphere*, *9*(6), 1089–1116. https://doi.org/10.5943/mycosphere/9/6/3

Zhou, M., Wang, H., Kou, J., & Yu, B. (2008). Antinociceptive and anti-inflammatory activities of *Aquilaria sinensis* (Lour.) Gilg. Leaves extract. *Journal of ethnopharmacology*, *117*(2), 345–350. https://doi.org/10.1016/j.jep.2008.02.005

Zhu, D., Luo, Z. L., Bhat, D. J., McKenzie, E. H., Bahkali, A. H., Zhou, D. Q., . . . Hyde, K. D. (2016). *Helminthosporium velutinum* and *H. aquaticum* sp. nov. from aquatic habitats in Yunnan Province, China. *Phytotaxa*, *253*(3), 179–190. https://doi.org/10.11646/phytotaxa.253.3.1

Zhuang, W. (Ed.). (2001). Higher fungi of tropical China. *Mycotaxon* Limited.

Zhuhui, L., Chunling, W., Yanli, W., Cuiling, L., Ling, W., & Qiong, D. (2024). Effects of host identity and leaf traits on foliar endophytic fungal communities in *Lauraceae* and *Fagaceae* plants of tropical montane rainforest of Hainan Island. *Acta Tropicalis*, *15*(1), 52–59. https://doi.org/10.15886/j.cnki.rdswxb.20220109

APPENDIX A

MEDIA AND CHEMICAL REAGENTS

1. Malt Extract Agar (MEA) used for fungal cultivation

Agar 15 g

Peptone 0.78 g

Glycerol 2.35 g

Dextrin 2.75 g

Maltose, Technical 12.75 g

Suspend 33.6 g of malt extract agar in distilled water and mix thoroughly. Heat with frequent agitation and boil for 1 minute to completely dissolve the power and bring volume to 1000 ml. Autoclave at 121oC for 20 minutes.

2. Potato dextrose agar (PDA) used for fungal cultivation

Potato starch (from the infusion) 4 g

Dextrose 20 g

Agar 15 g

Suspend 39 g of Potato dextrose agar in distilled water and mix thoroughly. Heat with frequent agitation and boil for 1 minute to completely dissolve the powder and bring volume to 1000 ml. Autoclave at 121oC for 20 minutes.

3. Water Agar (WA) used for Fungal Isolation and Sporulation

Agar 15 g

Suspend 15 g of agar in distilled water and mix thoroughly. Heat with frequent agitation and boil for 1 minute to completely dissolve the powder and bring volume to 1000 ml. Autoclave at 121°C for 20 minutes.

4. Indian ink used for observing gelatinous appendages of ascospores in some species.

APPENDIX B

ABSTRACT OF PUBLICATIONS

Biodiversity Data Journal 8: e58755
doi: 10.3897/BDJ.8.e58755

Taxonomic Paper

Arthrinium bambusicola (Fungi, Sordariomycetes), a new species from *Schizostachyum brachycladum* in northern Thailand

Xia Tang[‡,§,|], Ishani D. Goonasekara[§,|,¶], Ruvishika S. Jayawardena[§,|], Hong Bo Jiang[§,|,¶], Jun F. Li[§,|,¶], Kevin D. Hyde[§,|], Ji C. Kang[‡]

‡ Engineering and Research Center for Southwest Biopharmaceutical Resource of National Education Ministry of China, Guizhou University, Guiyang 550025, Guizhou, P.R. China, Guiyang, China
§ Centre of Excellence in Fungal Research, Mae Fah Luang University, Chiang Rai 57100, Thailand, Chiang Rai, Thailand
| School of science, Mae Fah Luang University, Chiang Rai 57100, Thailand, Chiang Rai, Thailand
¶ Key Laboratory for Plant Diversity and Biogeography of East Asia, Kunming Institute of Botany, Chinese Academy of Science, Kunming 650201, Yunnan, P.R. China, Kunming, China

Corresponding author: Ji C. Kang (jckang@gzu.edu.cn)

Academic editor: Danny Haelewaters

Received: 17 Sep 2020 | Accepted: 23 Nov 2020 | Published: 14 Dec 2020

Citation: Tang X, Goonasekara ID, Jayawardena RS, Jiang HB, Li JF, Hyde KD, Kang JC (2020) *Arthrinium bambusicola* (Fungi, Sordariomycetes), a new species from *Schizostachyum brachycladum* in northern Thailand. Biodiversity Data Journal 8: e58755. https://doi.org/10.3897/BDJ.8.e58755

Abstract

Background

Species of the fungal genus *Arthrinium* (Sordariomycetes, Amphisphaeriales, Apiosporaceae) are often found on bamboo in Asia. They are endophytes, saprobes and important plant pathogens. The genus *Arthrinium* currently contains 92 species and is widely distributed in North and South America, Europe, Africa, Asia and Oceania.

Phytotaxa 543 (4): 233–243
https://www.mapress.com/pt/

Article

ISSN 1179-3155 (print edition)
PHYTOTAXA
ISSN 1179-3163 (online edition)

https://doi.org/10.11646/phytotaxa.543.4.3

A new species *Pseudoplagiostoma dipterocarpicola* (Pseudoplagiostomataceae, Diaporthales) found in northern Thailand on members of the Dipterocarpaceae

XIA TANG[1,2,3,5], RUVISHIKA S. JAYAWARDENA[2,3,6], STEVEN L. STEPHENSON[4,7] & JI-CHUAN KANG[1,8]*

[1] *Engineering and Research Center for Southwest Biopharmaceutical Resource of National Education Ministry of China, Guizhou University, Guiyang, 550025, Guizhou Province, People's Republic of China*
[2] *Center of Excellence in Fungal Research, Mae Fah Luang University, Chiang Rai, 57100, Thailand*
[3] *School of science, Mae Fah Luang University, Chiang Rai, 57100, Thailand*
[4] *Department of Biological Sciences University of Arkansas Fayetteville AR 72701, USA*
[5] *bella19580412@gmail.com; https://orcid.org/0000-0003-2705-604X*
[6] *ruvi.jaya@yahoo.com; https://orcid.org/0000-0001-7702-4885*
[7] *slsteph@uark.edu; https://orcid.org/0000-0002-9207-8037*
[8] *jckang@gzu.edu.cn; https://orcid.org/0000-0002-6294-5793*
**Corresponding author: jckang@gzu.edu.cn*

Abstract

Pseudoplagiostoma dipterocarpicola sp. nov. is described herein on the basis material collected from twigs and fruits of *Dipterocarpus* sp. from Chiang Mai, Thailand. Phylogenetic analyses based on ITS, LSU, *tef1-α* and *tub2* DNA sequence data revealed this new species with a distinct asexual morph belongs to the family Pseudoplagiostomataceae. *Pseudoplagiostoma dipterocarpicola* is closely related to *P. mangiferae* but differs in the thick wall present at near the base of the conidiomata, with two types of conidiogenous cells, these ranging from cylindrical with an elongated slimy neck to ampulliform and having a wider base, and lacking paraphyses. The morphology of this new species is described and illustrated.

Keywords: New species, Coelomycetous fungus, Sordariomycetes, *Dipterocarpus*, Multi-locus phylogeny, Taxonomy

Introduction

Pseudoplagiostomataceae Cheewangkoon, M.J. Wingf. & Crous was introduced by Cheewangkoon *et al.* (2010) with *Pseudoplagiostoma* Cheewangkoon, M.J. Wingf. & Crous as the type genus. As a monotypic family, Pseudoplagiostomataceae accommodates a cryptosporiopsis-like fungus, represented by *P. eucalypti*, isolated from *Eucalyptus* and characterized by immersed, subglobose or elliptical perithecia, an acentric or lateral beak, unitunicate asci with a subapical nonamyloid ring, an aparaphysate condition, uniseptate, hyaline ascospores with elongated hyaline terminal appendages (Cheewangkoon *et al.* 2010). *Pseudoplagiostoma* contains eight species (Index Fungorum 2021) which are all associated with the leaves of plants (Cheewangkoon *et al.* 2010, Crous *et al.* 2012, Suwannarach *et al.* 2016, Crous *et al.* 2018, Bezerra *et al.* 2019, Phookamsak *et al.* 2019). The morphology of *Pseudoplagiostoma* was described as coelomycetous (Alvarez *et al.* 2016, Fan *et al.* 2018, Guarnaccia *et al.* 2018, Senanayake *et al.* 2018, Bezerra *et al.* 2019), with the type species (*P. eucalypti*) described on the basis of its sexual and asexual morphs. The sexual morph is characterized by immersed, beaked, ostiole ascomata, unitunicate asci, a non-amyloid subapical ring, hyaline ascospores that are 1-septate near the middle, with terminal, elongated hyaline appendages. The asexual morph is characterized by acervular to pycnidial, superficial and immersed conidiomata with masses of apically proliferous conidiogenous cells and hyaline, ellipsoidal conidia but with no conidiophores (Cheewangkoon *et al.* 2010). *Pseudoplagiostoma* is primarily described as a pathogen, and a few species have been classified as saprobes and endophytes. These were recorded on plant leaves from Australia, Brazil, China, Uruguay, Thailand and Venezuela (Cheewangkoon *et al.* 2010, Crous *et al.* 2012, Suwannarach *et al.* 2016, Crous *et al.* 2018, Bezerra *et al.* 2019, Phookamsak *et al.* 2019, Hyde *et al.* 2020).

In this study, we collected interesting example of *Pseudoplagiostoma* from dead twigs and fruits of *Dipterocarpus* sp. The morphological characters indicated that this was similar to *Pseudoplagiostoma*. In addition, a phylogenetic

Accepted by Sajeewa Maharachchikumbura: 30 Mar. 2022; published: 20 Apr. 2022

frontiers | Frontiers in Microbiology

TYPE Original Research
PUBLISHED 05 June 2023
DOI 10.3389/fmicb.2023.1169052

OPEN ACCESS

EDITED BY
Anna Gałązka,
Institute of Soil Science and Plant Cultivation, Poland

REVIEWED BY
Samantha Chandranath Karunarathna, Qujing Normal University, China
Rajesh Jeewon,
University of Mauritius, Mauritius

*CORRESPONDENCE
Ji-Chuan Kang
✉ jckang@gzu.edu.cn

RECEIVED 18 February 2023
ACCEPTED 09 May 2023
PUBLISHED 05 June 2023

CITATION
Tang X, Lu Y-Z, Dissanayake LS, Goonasekara ID, Jayawardena RS, Xiao Y-P, Hyde KD, Chen X-M and Kang J-C (2023) Two new fungal genera (*Diaporthales*) found on *Dipterocarpaceae* in Thailand. *Front. Microbiol.* 14:1169052. doi: 10.3389/fmicb.2023.1169052

Two new fungal genera (*Diaporthales*) found on *Dipterocarpaceae* in Thailand

Xia Tang[1,2,3], Yong-Zhong Lu[1,4], Lakmali S. Dissanayake[1], Ishani D. Goonasekara[2,5], Ruvishika S. Jayawardena[2,3], Yuan-Pin Xiao[4], Kevin D. Hyde[2,3], Xue-Mei Chen[4] and Ji-Chuan Kang[1]*

[1]Engineering and Research Center for Southwest Biopharmaceutical Resource of National Education Ministry of China, Guizhou University, Guiyang, Guizhou, China, [2]Center of Excellence in Fungal Research, Mae Fah Luang University, Chiang Rai, Thailand, [3]School of Science, Mae Fah Luang University, Chiang Rai, Thailand, [4]School of Food and Pharmaceutical Engineering, Guizhou Institute of Technology, Guiyang, Guizhou, China, [5]International Relations Unit, The Open University of Sri Lanka, Nawala, Nugegoda, Sri Lanka

Diaporthales is a species-rich order of fungi that includes endophytes, saprobes, and pathogens associated with forest plants and crops. They may also occur as parasites or secondary invaders of plant tissues injured or infected by other organisms or inhabit living animal and human tissues, as well as soil. Meanwhile, some severe pathogens wipe out large-scale cultivations of profitable crops, timber monocultures, and forests. Based on morphological and phylogenetic analyses of combined ITS, LSU, *tef1-α*, and *rpb2* sequence data, generated using maximum likelihood (ML), maximum parsimony (MP), and MrBayes (BI), we introduce two new genera of *Diaporthales* found in *Dipterocarpaceae* in Thailand, namely *Pulvinaticonidioma* and *Subellipsoidispora*. *Pulvinaticonidioma* is characterized by solitary, subglobose, pycnidial, unilocular conidiomata with the internal layers convex and pulvinate at the base; hyaline, unbranched, septate conidiophores; hyaline, phialidic, cylindrical to ampulliform, determinate conidiogenous cells and hyaline, cylindrical, straight, unicellular, and aseptate conidia with obtuse ends. *Subellipsoidispora* has clavate to broadly fusoid, short pedicellate asci with an indistinct J- apical ring; biturbinate to subellipsoidal, hyaline to pale brown, smooth, guttulate ascospores that are 1-septate and slightly constricted at the septa. Detailed morphological and phylogenetic comparisons of these two new genera are provided in this study.

KEYWORDS

2 new taxa, morphology, multi-gene phylogeny, saprophytic fungi, *Sordariomycetes*, taxonomy

Introduction

Diaporthales is an order of ascomycetous fungi belonging to the subclass *Diaporthomycetidae* (*Sordariomycetes*) that dwell on terrestrial or aquatic taxa of plants, animals, and in soil (Senanayake et al., 2017, 2018; Wijayawardene et al., 2022). Senanayake et al. (2017, 2018) provided a recent treatment of the order and examined, described, and illustrated worldwide specimens and listed 27 families in *Diaporthales*. Many studies of

MycoKeys

MycoKeys 100: 171–204 (2023)
DOI: 10.3897/mycokeys.100.113141

Research Article

Morphophylogenetic evidence reveals four new fungal species within Tetraplosphaeriaceae (Pleosporales, Ascomycota) from tropical and subtropical forest in China

Xia Tang[1,2,3], Rajesh Jeewon[4,5], Yong-Zhong Lu[1,6], Abdulwahed Fahad Alrefaei[5], Ruvishika S. Jayawardena[2,3], Rong-Ju Xu[2,3], Jian Ma[2,3], Xue-Mei Chen[7], Ji-Chuan Kang[1]

1 *Engineering and Research Center for Southwest Biopharmaceutical Resource of National Education Ministry of China, Guizhou University, Guiyang, 550025, Guizhou Province, China*
2 *Center of Excellence in Fungal Research, Mae Fah Luang University, Chiang Rai, 57100, Thailand*
3 *School of Science, Mae Fah Luang University, Chiang Rai, 57100, Thailand*
4 *Department of Health Sciences, Faculty of Medicine and Health Sciences, University of Mauritius, Reduit, Mauritius*
5 *Department of Zoology, College of Science, King Saud University, P.O. Box 2455, Riyadh 11451, Saudi Arabia*
6 *School of Food and Pharmaceutical Engineering, Guizhou Institute of Technology, Guiyang, Guizhou Province550003, China*
7 *Center for Yunnan Plateau Biological Resources Protection and Utilization, College of Biological Resource and Food Engineering, Qujing Normal University, Qujing 655011, China*

Corresponding authors: Rajesh Jeewon (r.jeewon@uom.ac.mu); Ji-Chuan Kang (jckang@gzu.edu.cn)

Abstract

Tetraplosphaeriaceae (Pleosporales, Ascomycota) is a family with many saprobes recorded from various hosts, especially bamboo and grasses. During a taxonomic investigation of microfungi in tropical and subtropical forest regions of Guizhou, Hainan and Yunnan provinces, China, several plant samples were collected and examined for fungi. Four newly discovered species are described based on morphology and evolutionary relationships with their allies inferred from phylogenetic analyses derived from a combined dataset of LSU, ITS, SSU, and *tub2* DNA sequence data. Detailed illustrations, descriptions and taxonomic notes are provided for each species. The four new species of Tetraplosphaeriaceae reported herein are *Polyplosphaeria guizhouensis*, *Polyplosphaeria hainanensis*, *Pseudotetraploa yunnanensis*, and *Tetraploa hainanensis*. A checklist of Tetraplosphaeriaceae species with available details on their ecology is also provided.

Key words: Anamorphic fungi, checklist, Dothideomycetes, ribosomal genes, species diversity, taxonomy

OPEN ACCESS

Academic editor: C. S. Bhunjun
Received: 22 September 2023
Accepted: 9 November 2023
Published: 6 December 2023

Citation: Tang X, Jeewon R, Lu Y-Z, Alrefaei AF, Jayawardena RS, Xu R-J, Ma J, Chen X-M, Kang J-C (2023) Morphophylogenetic evidence reveals four new fungal species within Tetraplosphaeriaceae (Pleosporales, Ascomycota) from tropical and subtropical forest in China. MycoKeys 100: 171–204. https://doi.org/10.3897/mycokeys.100.113141

Introduction

The Southwestern part of China is characterised by a tropical to subtropical climate and several provinces are well known for their high diversity of plants as well as fungi (Feng and Yang 2018; Hyde et al. 2020b; Bao et al. 2021; Yang et al. 2023). Yunnan province, for example, is considered a hotspot for species diversity. Over the last few decades, there has been a number of studies that have reported novel fungal species from this region (Jeewon et al. 2003; Luo et al. 2017, 2018; Huang et al. 2018; Su et al. 2018; Yang et al. 2019; Hyde et al. 2020b;

MycoKeys

MycoKeys 110: 35–66 (2024)
DOI: 10.3897/mycokeys.110.133450

Research Article

Additions to the genus *Kirschsteiniothelia* (Dothideomycetes); Three novel species and a new host record, based on morphology and phylogeny

Xia Tang[1,2,3], Rajesh Jeewon[4], Ruvishika S. Jayawardena[2,3], Deecksha Gomdola[2,3], Yong-Zhong Lu[5], Rong-Ju Xu[2,3], Abdulwahed Fahad Alrefaei[6], Fatimah Alotibi[7], Kevin D. Hyde[2,3,7], Ji-Chuan Kang[1]

1 *Engineering and Research Center for Southwest Biopharmaceutical Resource of National Education Ministry of China, Guizhou University, Guiyang, 550025, Guizhou Province, China*
2 *Center of Excellence in Fungal Research, Mae Fah Luang University, Chiang Rai, 57100, Thailand*
3 *School of Science, Mae Fah Luang University, Chiang Rai, 57100, Thailand*
4 *Department of Health Sciences, Faculty of Medicine and Health Sciences, University of Mauritius, Reduit, Mauritius*
5 *School of Food and Pharmaceutical Engineering, Guizhou Institute of Technology, Guiyang, Guizhou Province 550003, China*
6 *Department of Zoology, College of Science, King Saud University, P.O. Box 2455, Riyadh 11451, Saudi Arabia*
7 *Department of Botany and Microbiology, College of Science, King Saud University, P.O. Box 22452, 11495 Riyadh, Saudi Arabia*

Corresponding authors: Ji-Chuan Kang (jckang@gzu.edu.cn); Kevin D. Hyde (kdhyde3@gmail.com)

This article is part of:
Exploring the Hidden Fungal Diversity: Biodiversity, Taxonomy, and Phylogeny of Saprobic Fungi
Edited by Samantha C. Karunarathna, Danushka Sandaruwan Tennakoon, Ajay Kumar Gautam

Academic editor:
Danushka Sandaruwan Tennakoon
Received: 30 July 2024
Accepted: 1 October 2024
Published: 28 October 2024

Citation: Tang X, Jeewon R, Jayawardena RS, Gomdola D, Lu Y-Z, Xu R-J, Alrefaei AF, Alotibi F, Hyde KD, Kang J-C (2024) Additions to the genus *Kirschsteiniothelia* (Dothideomycetes); Three novel species and a new host record, based on morphology and phylogeny. MycoKeys 110: 35–66. https://doi.org/10.3897/mycokeys.110.133450

Abstract

During a survey of microfungi associated with forest plants, four specimens related to *Kirschsteiniothelia* were collected from decaying wood in Guizhou, Hainan and Yunnan Provinces, China. *Kirschsteiniothelia* species have sexual and asexual forms. They are commonly found as saprophytes on decaying wood and have been reported as disease-causing pathogens in humans as well. In this study, we introduce three novel *Kirschsteiniothelia* species (*K. bulbosapicalis*, *K. dendryphioides* and *K. longirostrata*) and describe a new host record for *K. atra*, based on morphology and multi-gene phylogenetic analyses of a concatenated ITS, LSU and SSU rDNA sequence data. These taxa produced a dendryphiopsis- or sporidesmium-like asexual morph and detailed descriptions and micromorphological illustrations are provided. Furthermore, we provide a checklist for the accepted *Kirschsteiniothelia* species, including detailed host information, habitat preferences, molecular data, existing morphological type, country of origin and corresponding references.

Key words: Checklist, diversity, Dothideomycetes, Kirschsteiniotheliales, one new host record, taxonomy, three new taxa

Introduction

Kirschsteiniothelia was introduced by Hawksworth (1985) and typified by *K. aethiops*, based on morphological observation, linking it to its asexual genus, *Dendryphiopsis* S. Hughes. Later, the type species was reclassified with its asexual morph, *K. atra* (Hyde et al 2011; Wijayawardene et al. 2014). The connection between the sexual morphs of *Kirschsteiniothelia atra* (characterised by cylindrical-clavate, bitunicate, 8-spored or rarely 4-spored asci and ellipsoidal verruculose or smooth ascospores with 1–2 septa, lacking a distinct gelatinous sheath) and the asexual morphs (characterised by macronematous, mononematous and

CURRICULUM VITAE

NAME Xia Tang

EDUCATIONAL BACKGROUND

2017 Bachelor of School of Food and Pharmaceutical Engineering, Guizhou Institute of Technology, China

PUBLICATION

First Author Publications

Tang, X., Goonasekara, I. D., Jayawardena, R. S., Jiang, H. B., Li, J. F., Hyde, K. D., . . . Kang, J. C. (2020). *Arthrinium bambusicola* (Fungi, *Sordariomycetes*), a new species from Schizostachyum brachycladum in northern Thailand. *Biodiversity Data Journal, 8*, e58755. https://doi.org/10.3897/BDJ.8.e58755

Tang, X., Jayawardena, R. S., Stephenson, S. L., & Kang, J. C. (2022). A new species *Pseudoplagiostoma dipterocarpicola* (*Pseudoplagiostomataceae*, *Diaporthales*) found in northern Thailand on members of the *Dipterocarpaceae*. *Phytotaxa, 543*(4), 233-243.

Tang, X., Lu, Y. Z., Dissanayake, L. S., Goonasekara, I. D., Jayawardena, R. S., Xiao, Y. P., . . . Kang, J. C. (2023). Two new fungal genera (*Diaporthales*) found on *Dipterocarpaceae* in Thailand. *Frontiers in Microbiology, 14*, 1169052. https://doi.org/10.3389/fmicb.2023.1169052

Tang, X., Jeewon, R., Lu, Y. Z., Alrefaei, A. F., Jayawardena, R. S., Xu, R. J., . . . Kang, J. C. (2023). Morphophylogenetic evidence reveals four new fungal species within *Tetraplosphaeriaceae* (*Pleosporales*, *Ascomycota*) from tropical and subtropical forest in China. *MycoKeys, 100*, 171-204. https://doi.org/10.3897/mycokeys.100.113141

Tang, X., Jeewon, R., Jayawardena, R. S., Gomdola, D., Lu, Y. Z., Xu, R. J., . . . Kang, J. C. (2024). Additions to the genus *Kirschsteiniothelia* (*Dothideomycetes*); Three novel species and a new host record, based on morphology and phylogeny. *MycoKeys, 110*, 35-66. https://doi.org/10.3897/mycokeys.110.133450

Tang, X., Lu, Y. Z., Jayawardena, R. S., Kang, J. C., & Hyde, K. D. Taxonomic and phylogenetic evidence reveals two novel asexual species of *Strossmayeria* (*Leotiomycetes*) from the subtropical forests of China. [Manuscript preparation]

Tang, X., Lu, Y. Z., Jayawardena, R. S., Kang, J. C., & Hyde, K. D. Discovery of two novel fungal species and one new host record from C. in tropical and subtropical forests of China. [Manuscript preparation]

Tang, X., Jayawardena, R. S., Lu, Y. Z., Jeewon R., Kang, J. C., & Hyde, K. D. (2025) Discovery of a novel fungal species, *Periconia xishuiensis* from *Periconia* in subtropical forests of China. [Manuscript preparation]

Tang, X., Jayawardena, R. S., Jeewon R., Lu, Y. Z., Kang, J. C., & Hyde, K. D. (2025). Unravelling new taxa of *Dothideomycetes* associated with forest plants in China (at least 60 species, in which of 28 new species). [Manuscript preparation]

Co-author

Chen, X. M., Tang, X., Du, T. Y., Lu, Y. Z., Suwannarach, N., Xu, R. F., . . . Karunarathna, S. C. (2024). Two new species of *Rhodoveronaea* (*Rhamphoriales, Ascomycota*) from terrestrial habitats in China. *Phytotaxa, 638*(1), 49-60.

Chen, X. M., Tang, X., Ma, J., Liu, N. G., Tibpromma, S., Karunarathna, S. C., . . . Lu, Y. Z. (2024). Identification of two new species and a new host record of *Distoseptispora* (*Distoseptisporaceae, Distoseptisporales, Sordariomycetes*) from terrestrial and freshwater habitats in Southern China. *MycoKeys, 102*, 83-105. https://doi.org/10.3897/mycokeys.102.115452

Chethana, K. W. T., Niranjan, M., Dong, W., Samarakoon, M. C., Bao, D. F., Calabon, M. S., . . . Hyde, K. D. (2021). AJOM new records and collections of fungi: 101–150. *Asian Journal of Mycology, 4*(1), 113–260. https://doi.org/10.5943/ajom/4/1/8

Chethana, K. W., Jayawardena, R. S., Chen, Y. J., Konta, S., Tibpromma, S., Phukhamsakda, C., . . . Hyde, K. D. (2021). Appressorial interactions with host and their evolution. Fungal Diversity, 110(1), 75–107. https://doi.org/10.1007/s13225-021-00487-5

Dissanayake, L. S., Samarakoon, M. S., Maharachchikumbura, S. S., Hyde, K. D., Tang, X., Li, Q. R., . . . Wanasinghe, D. N. (2024). Exploring the taxonomy and phylogeny of Sordariomycetes taxa emphasizing Xylariomycetidae in Southwestern China. *Mycosphere, 15*(1), 1675-1793.

Dong W., FDN (2025). Fungal diversity notes 2020–2125: Taxonomic and phylogenetic contributions to freshwater fungi and other fungal taxa.

Gomdola, D., Jeewon, R., McKenzie, E. H., Jayawardena, R. S., Al-Otibi, F., Tang, X., . . . Fu, L. (2025). Phylogenetic diversity of Colletotrichum species (Sordariomycetes, Glomerellales, Glomerellaceae) associated with plant diseases in Thailand. *MycoKeys, 119*, 137-195.

Hyde et al., next families of sordariomycetes (2025?). [Unpublished manuscript].

Hyde, K. D., Noorabadi, M. T., Thiyagaraja, V., He, M. Q., Johnston, P. R., Wijesinghe, S. N., . . . Radek, R. (2024). The 2024 outline of fungi and fungus-like taxa. *Mycosphere, 15*, 5146-6239. https://doi.org/10.5943/mycosphere/15/1/25

Hyde, K. D., Norphanphoun, C., Ma, J., Yang, H. D., Zhang, J. Y., Du, T. Y., . . . Zhao, Q. (2023). Mycosphere notes 387–412 – novel species of fungal taxa from around the world. *Mycosphere 14*(1), 663–744. https://doi.org/10.5943/mycosphere/14/1/8

Hyde, K. D., Suwannarach, N., Jayawardena, R. S., Manawasinghe, I. S., Liao, C. F., Doilom, M., . . . Bao, D. F. (2021). Mycosphere notes 325–344–Novel species and records of fungal taxa from around the world. *Mycosphere, 12*(1), 1101-1156. https://doi.org/10.5943/mycosphere/12/1/14

Hyde, K. D.,et al., ….AJOM (2025?). [Unpublished manuscript].

Hyde, K. D.,et al., ….CREAM (2025?). [Unpublished manuscript].

Hyde, K. D.,et al., ….Fungalpedia (2025?). [Unpublished manuscript].

Hyde, K., D., et al., 2025……fungal diversity notes Unpublished.

Jayawardena, R. S., Hyde, K. D., de Farias, A. R. G., Bhunjun, C. S., Ferdinandez, H. S., Manamgoda, D. S., . . . Thines, M. (2021). What is a species in fungal plant pathogens?. *Fungal Diversity, 109*, 239–266. https://doi.org/10.1007/s13225-021-00484-8

Jayawardena, R. S., Hyde, K. D., Wang, S., Sun, Y. R., Suwannarach, N., Sysouphanthong, P., . . . Wang, Y. (2022). Fungal diversity notes 1512–1610: Taxonomic and phylogenetic contributions on genera and species of fungal taxa. *Fungal Diversity, 117*(1), 1-272. https://doi.org/10.1007/s13225-022-00513-0

Jayawardena, R. S., Xia Tang et al., One stop shop VI. (?) Fungal diversity. (two genera). [Unpublished manuscript].

Lu, Q. T., Zhang, J. Y., Sun, Y. R., Tang, X., Lu, Y. Z., & Zhang, Z. (2022). *Diaporthe orixae* sp. nov., an endophytic species isolated from Orixa japonica in southern China. *Phytotaxa, 544*(1), 37-51.

Ma, J., Gomdola, D., Boonmee, S., Shen, H. W., Tang, X., Zhang, L. J., . . . Hyde, K. D. (2024). Three new species of *Neohelicomyces* (*Tubeufiales, Tubeufiaceae*) from freshwater and terrestrial habitats in China. *MycoKeys, 105*, 317.

Ma, J., Liu, N. G., Tang, X., Xiao, X. J., Chen, X. M., Xiao, Y. P., . . . Boonmee, S. (2023). Sclerococcum pseudobactrodesmium sp. nov. from a terrestrial habitat in China. *Phytotaxa*, *630*(1), 69-79.

Ma, J., Zhang, J. Y., Xiao, X. J., Xiao, Y. P., Tang, X., Boonmee, S., . . . Lu, Y. Z. (2022). Multi-gene phylogenetic analyses revealed five new species and two new records of Distoseptisporales from China. *Journal of Fungi*, *8*(11), 1202.

Mi et al., fungalpedia (2025?). [Unpublished manuscript].

Oom et al., (2025) fungalpedia. [Unpublished manuscript].

Yang, M., Lu, Y., Han, L., He, Z., Tang, X., & Kang, J. (2025). A novel endophytic fungus, alternaria semiverrucosa, and its ethyl acetate extract inhibit the proliferation, migration, and invasion of cervical cancer cells. *Chemistry & Biodiversity, 6*, e00945. https://doi.org/10.1002/cbdv.202500945